Biomolecular Materials
Principal Investigators' Meeting–2011

October 23–26, 2011

Annapolis Westin Hotel, Annapolis, MD

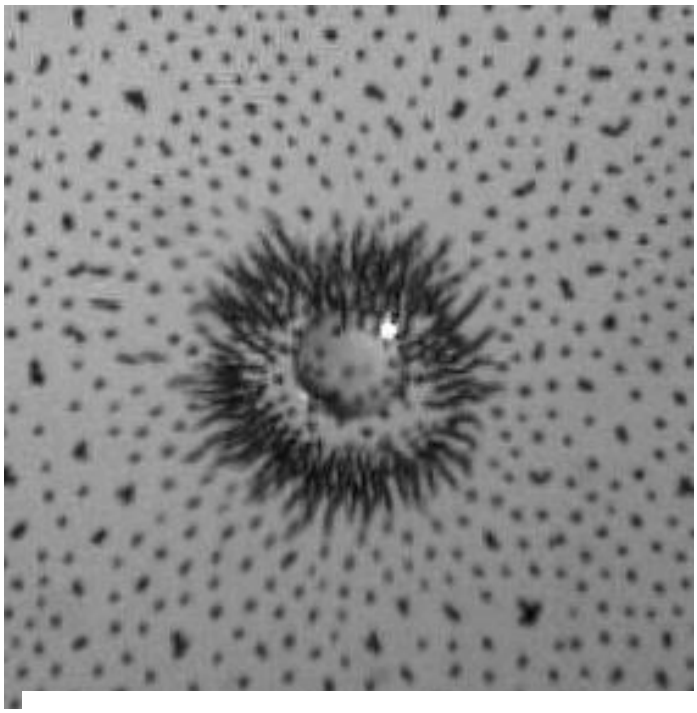

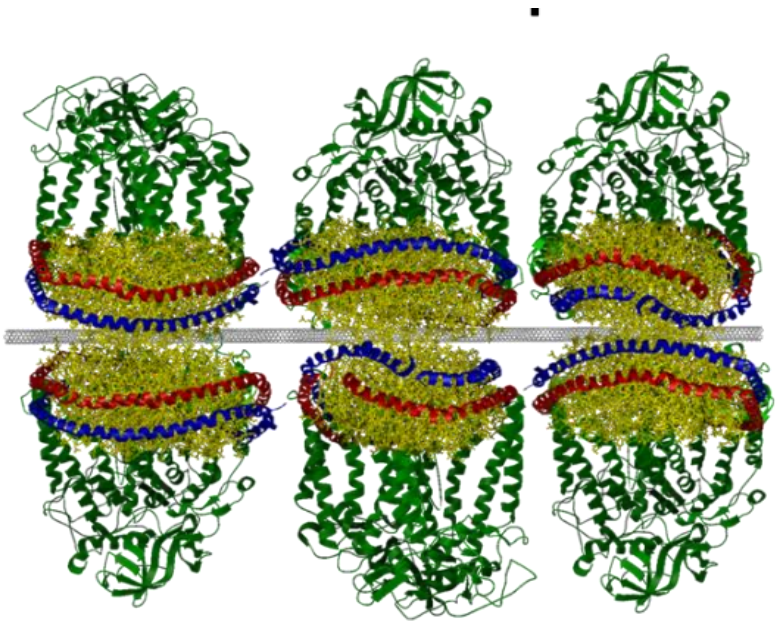

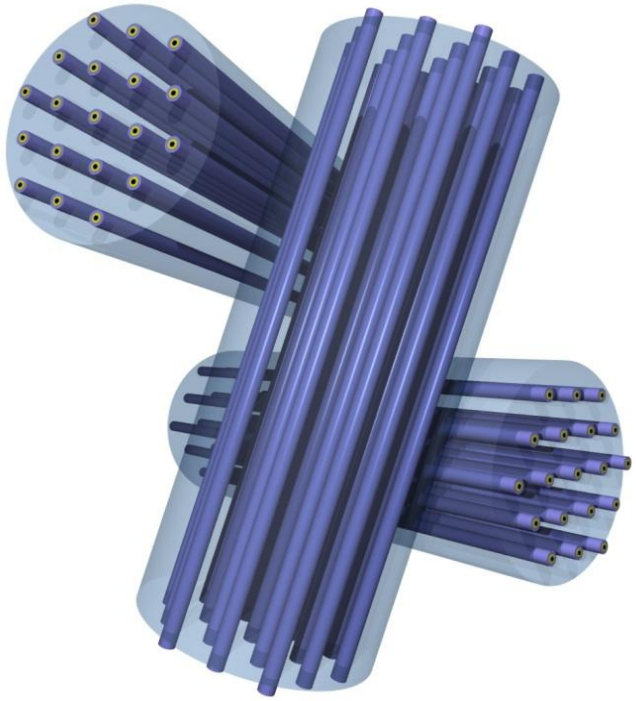

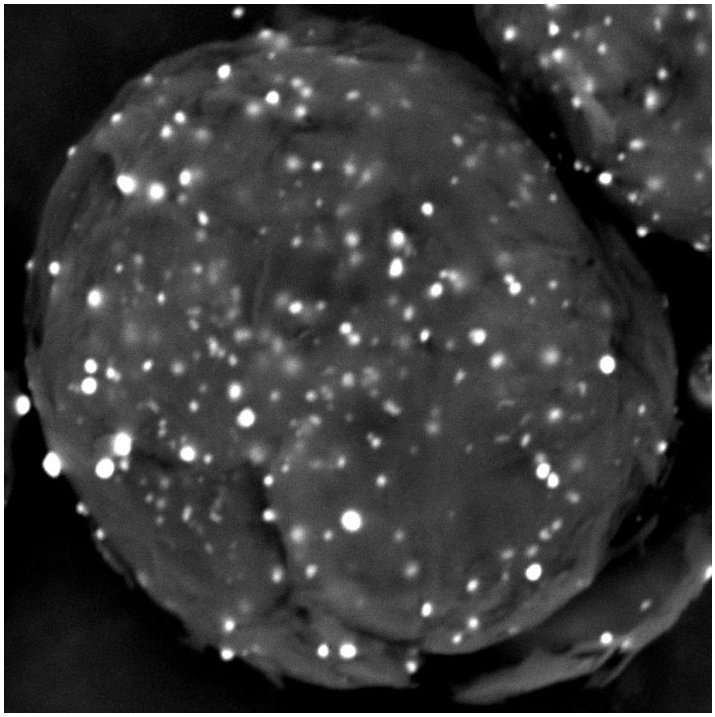

U.S. DEPARTMENT OF ENERGY

Office of Basic Energy Sciences

Materials Sciences and Engineering Division

On the Cover

Top Left: Transmission electron micrograph of magnetically directed capture of targeted particle by aster colloid assembly
Courtesy: *Igor Aranson, Argonne National Laboratory*
A. Snezhko and I. S. Aranson, *Nature Materials*, 2011, 10 (9), 698–703.

Top Right: Artificial photosynthetic system composed of an ordered structure of carbon nanotubes, proteins, lipids, and a bacterial photosynthetic reaction center that mimics the self-repair process used by plants as they convert light into energy.
Courtesy: *Michael Strano, Massachusetts Institute of Technology*
M. H. Ham et al., *Nature Chemistry*, 2010, 2(11), 929–936.

Bottom Left: Schematic of peptide filaments crystallize into a hexagonally ordered phase—rather than repel each other as expected—due to chemical changes when exposed to x-rays that result in highly charged filaments.
. `
Courtesy: *Samuel Stupp, Northwestern University*
H. Cui et al., *Science*, 2010, 327, 555–559.

Bottom Right: Tin-in graphite anode: uniform dispersion of Sn grown in situ throughout the graphite matrix using bioinspired kinetically controlled process.
Courtesy: *Daniel Morse, University of California at Santa Barbara*
Hong-Li Zhang and Daniel E. Morse, *J. Mater. Chem*., 2009, 19, 9006–9011.

This document was produced under contract number DE-AC05-06OR23100 between the U.S. Department of Energy and Oak Ridge Associated Universities.

The research grants and contracts described in this document are supported by the U.S. DOE Office of Science, Office of Basic Energy Sciences, Materials Sciences and Engineering Division.

Foreword

This volume comprises the scientific content of the 2011 Biomolecular Materials Principal Investigators' Meeting sponsored by the Materials Sciences and Engineering (MSE) Division in the Office of Basic Energy Sciences (BES) of the U. S. Department of Energy (DOE). The meeting, held on October 23–26, 2011 at the Westin Annapolis Hotel in Annapolis, MD, is the fourth such meeting on this topic, and is one of several research theme-based Principal Investigators' Meetings conducted by BES. The meeting's focus is on research at the intersection of materials sciences and biology, and it also features research that cuts across other MSE core research program areas where appropriate and relevant. The agenda at this year's meeting is representative of many of the major scientific areas supported by the Biomolecular Materials program. As has been the case for other BES Principal Investigators' Meetings, previous meetings have been highly valued and cherished by the participants for the opportunity to see the entire research program, learn about the latest results/advances, develop new ideas, and forge new collaborations. In addition, the meeting will also help MSE in assessing the state of the program, identifying new research directions and recognizing programmatic needs.

The Biomolecular Materials Core Research Activity (CRA) formally came into existence following the recommendations of a workshop sponsored by the Basic Energy Sciences Advisory Committee (BESAC) in 2002. In addition, recent BES workshops and The National Academies' reports have clearly identified mastering the capabilities of living systems as a Grand Challenge that could provide the knowledge base to discover, design, and synthesize new materials with totally new properties for next-generation energy technologies. To address these goals, the Biomolecular Materials program supports fundamental research in the discovery, design and synthesis of functional materials and complex structures based on principles and concepts of biology. The major programmatic focus is on the creation of robust, scalable, energy-relevant materials and systems with collective behavior, which rival or exceed biology's extraordinary effectiveness for controlling matter, energy, and information.

I genuinely look forward to this meeting and hope that it will be as fruitful as past BES Principal Investigators' Meetings. It is a great pleasure to express my sincere thanks to all of the attendees, including the invited plenary speakers, for their active participation and sharing their ideas and new research results. The advice and help of Meeting Chairs, Sharon Glotzer and Sam Stupp, in organizing this meeting are deeply appreciated. My hearty thanks also go to Teresa Crockett in MSE, Lee-Ann Talley and Joreé O'Neal at the Oak Ridge Institute for Science and Education (ORISE) for their outstanding work in taking care of all the logistical aspects of the meeting.

Mike Markowitz
Program Manager, Biomolecular Materials
Materials Sciences and Engineering Division
Office of Basic Energy Sciences
U.S. Department of Energy

Agenda

Meeting Chairs: **Samuel Stupp** and **Sharon Glotzer**
Northwestern University / University of Michigan

Agenda

Sunday, October 23, 2011

3:00 – 6:00 pm	Arrival and Registration
5:00 – 6:00 pm	Reception (No Host)
6:00 – 7:00 pm	*****Working Dinner*****
7:00 – 7:30 pm	*Introductory Remarks* **Linda Horton** Director, Materials Sciences and Engineering Division, Basic Energy Sciences
7:30 – 7:50 pm	**Mike Markowitz** Program Manager, Biomolecular Materials Meeting Chairs: **Samuel Stupp** and **Sharon Glotzer** Northwestern University/ University of Michigan
Session 1	**Bioinspired Directed Assembly** Chair: **Sharon Glotzer**, University of Michigan
7:50 – 8:20 pm	**Igor S. Aronson,** Argonne National Laboratory *Dynamics of Active Self-Assembled Materials*
8:20 – 8:50 pm	**David Erickson,** Cornell University *Directed Assembly of Hybrid Nanostructures using Optically Resonant Nanotweezers*
8:50 – 9:20 pm	**Darryl Y. Sasaki**, Sandia National Laboratories *Adaptive and Reconfigurable Nanocomposites*
9:20 – 11:00 pm	**Small Group Discussions**

Monday, October 24, 2011

7:00 – 8:00 am	***** Breakfast*****
Session 2	**Biology as Inspiration for Hybrid Systems** Chair: **Samuel Stupp**, Northwestern University
8:00 – 8:30 am	**Ada Yonath (Invited),** Weizmann Institute *From Basic Science to Attempts at Combating Antibiotics*

8:30 – 9:00 am	**John H. Golbeck**, Pennsylvania State University *A Hybrid Biological/Organic Photochemical Half-Cell for Generating Dihydrogen*
9:00 – 9:30 am	**Jim De Yoreo,** Lawrence Berkeley National Laboratory *Directed Organization of Functional Materials at Inorganic-Macromolecular Interfaces*
9:30 – 10:00 am	**Ravi Kane,** Rensselaer Polytechnic Institute *Engineering the Interface between Inorganic Materials and Cells*
10:00 – 10:30 am	***** Break *****
Session 3	**Dynamically Adaptive Materials** Chair: **Anna C. Balazs**, University of Pittsburgh
10:30 – 11:00 am	**Steve Granick**, University of Illinois at Urbana-Champaign *Phospholipid Vesicles in Materials Science*
11:00 – 11:30 am	**Cyrus Safinya**, University of California, Santa Barbara *Miniaturized Hybrid Materials Inspired by Nature*
11:30 – 12:00 pm	**Erik Spoerke**, Sandia National Laboratories *Microtubule Mimicry: Toward Biomolecular Self-Assembly in Synthetic Materials*
12:00 – 12:30 pm	**Juan de Pablo**, University of Wisconsin *Functional, Hierarchical Colloidal Liquid Crystal Gels and Liquid Crystal Elastomer Nanocomposites*
12:30 – 3:30 pm	***** Working Lunch/ Small Group Discussions *****
3:30 – 5:30 pm	***** Poster Session 1 *****
5:30 – 7:00 pm	***** Working Dinner/ Meeting Discussions *****
Session 4	**Biotemplated Synthesis** Chair: **C. Jeffrey Brinker**, Sandia National Laboratories
7:00 – 7:30 pm	**John Spencer Evans**, New York University *Material Lessons from Biology: Structure-Function Studies of Protein Sequences Involved in Inorganic-Organic Composite Material Formation*
7:30 – 8:00 pm	**Klaus Schmidt-Rohr**, Ames Laboratory *Solid-State NMR of Complex Materials*
8:00 – 8:30 pm	**Trevor Douglas**, Montana State University *Multicomponent Protein Cage Architectures for Photocatalysis*
8:30 – 10:30 pm	***** Poster Session 1 (Continues)*****

Tuesday, October 25, 2011

7:00 – 8:00 am	***** Breakfast*****
Session 5	**Bioinspired Catalysts** Chair: **Sarah Heilshorn**, SLAC National Accelerator Laboratory
8:00 – 8:30 am	**James Swartz**, Stanford University *Using In Vitro Maturation and Cell-Free Evolution to Understand [Fe-Fe]hydrogenase Activation and Active Site Constraints*

8:30 – 9:00 am	**Annabella Selloni**, Princeton University *Theoretical Research Program on Bioinspired Inorganic Hydrogen Generating Catalysts and Electrodes*
9:00 – 9:30 am	**Andrew A. Gewirth**, University of Illinois at Urbana-Champaign *Cathode Catalysis in Hydrogen/Oxygen Fuel Cells: New Catalysts, Mechanism, and Characterization*
9:30 –10:00 am	**Nils Kröger**, Georgia Institute of Technology *(Bio)Chemical Tailoring of Biogenic 3-D Nanopatterned Templates with Energy-Relevant Functionalities*
10:00 – 10:30 am	*****Break*****
Session 6	**Bioinspired Polymer and Peptide Materials** Chair: **Zhibin Guan**, University of California, Irvine
10:30 – 11:00 am	**Matthew Tirrell (Invited)**, University of Chicago and Argonne National Laboratory *Phase Behavior and Self-Assembly in Polyelectrolyte Complexes*
11:00 – 11:30 am	**John D. Tovar**, Johns Hopkins University *Self-Assembly of Pi-Conjugated Peptides in Aqueous Environments Leading to Energy-Transporting Bioelectronic Nanostructures*
11:30 – 12:00 pm	**F. Akif Tezcan**, University of California, San Diego *Inorganic Control of Biological Self-Assembly: Engineering Novel Biological Architectures and Redox-Active Protein Assemblies*
12:00 – 12:30 pm	**P. Leslie Dutton**, University of Pennsylvania *Modular Designed Protein Constructions for Solar Generated H_2 from Water*
12:30 – 3:30 pm	***** Working Lunch/ Small Group Discussions *****
3:30 – 5:30 pm	***** Poster Session 2 *****
5:30 – 7:00 pm	***** Working Dinner/ Meeting Discussions *****
Session 7	**Surface-Controlled Assembly and Behavior of Bioinspired Materials** Chair: **Y. Elaine Zhu**, University of Notre Dame
7:00 – 7:30 pm	**Benjamin Ocko**, Brookhaven National Laboratory *Soft-Matter Physics: Directed Self-Assembly of Soft-Matter and Biomolecular Materials*
7:30 – 8:00 pm	**Joanna Aizenberg**, Harvard University *Actuation of Bioinspired, Adaptive "HAIRS" Powered by Responsive Hydrogels*
8:00 – 8:30 pm	**Anand Jagota**, Lehigh University *Bioinspired Architectures for Controlled Adhesion, Friction, and Surface Compliance*
8:30 – 10:30 pm	***** Poster Session 2 (Continues) *****

Wednesday, October 26, 2011

7:00 – 8:00 am	***** Breakfast *****
Session 8	**Bioinspired Composite Materials** Chair: **Michael S. Strano**, Massachusetts Institute of Technology

8:00 – 8:30 am	**Vincent Rotello**, University of Massachusetts at Amherst *Hyperbranched Conjugated Polymers and Their Nanodot Composites as Universal Bioinspired Architectures*
8:30 – 9:00 am	**Ravi F. Saraf**, University of Nebraska - Lincoln *Electronic Interfacing between a Living Cell and a Nanodevice: A Bio-Nano Hybrid System*
9:00 – 9:30 am	**Padma Gopalan**, University of Wisconsin *Optical and Electro-optic Modulation of Biomimetically Functionalized Nanotubes*
9:30 – 10:00 am	**John A. Shelnutt**, Sandia National Laboratories *Molecular Nanocomposites: Cooperative Binary Ionic Solids, Nanostructures, and Nanocomposites*
10:00 – 10:30 am	***** Break *****
Session 9	**Bioinspired Materials Discovery** Chair: **Daniel Morse**, University of California, Santa Barbara
10:30 – 11:00 am	**Surya Mallapragada**, Ames Laboratory *Bioinspired Materials*
11:00 – 11:30 am	**Dan Feldheim**, University of Colorado *RNA-Mediated Evolution of Catalysts for the Production and Utilization of Alternative Fuels*
11:30 – 12:00 pm	**Troy Van Voorhis**, Massachusetts Institute of Technology *High Efficiency Biomimetic Organic Solar Cells*
12:00 – 12:30pm	*Remarks* **Sam Stupp** and **Sharon Glotzer**, Meeting Chairs **Mike Markowitz**, Program Manager, Biomolecular Materials
12:30 – 1:30pm	*****Lunch, Open Discussions and Adjourn***** (Optional box lunches available)

Table of Contents

Table of Contents

University Grant Projects

Invited Talks

LABORATORY PROJECTS

Program Title: Dynamics of Active Self-Assembled Materials

Principal Investigator: Igor S. Aronson, Co-Investigator: Alexey Snezhko
Mailing Address: Materials Science Division, Argonne National Laboratory, 9700 South Cass Avenue, Argonne, IL60439
E-mail: aronson@anl.gov

Program Scope

Self-assembly, a natural tendency of simple building blocks to organize into complex architectures, is a unique opportunity for materials science. In-depth understanding of self-assembly paves the way for design of tailored smart materials for emerging energy technologies. Self-assembled materials pose a formidable challenge: they are intrinsically complex, with an often hierarchical organization occurring on many nested length and time scales. This program combines in-depth theoretical and experimental studies of the dynamics of active self-assembled materials, such as magnetic colloids, suspensions of motile bacteria and synthetic swimmers, for the purpose of control, prediction, and design of novel bio-inspired materials for energy applications. Examples are reconfigurable self-repairing materials for soft robotics, self-assembled sensors that can detect, trap, and dispose of pathogens; materials that can self-regulate porosity, strength, water or air resistance, viscosity, or conductivity. We have chosen these seemingly different model systems for the following reasons: they are relatively simple yet non-trivial, with primary physical/biological mechanisms well characterized, and amendable to in-depth investigation using methods of non-equilibrium statistical physics.

In the past two years our program yielded discoveries of drastic reduction of viscosity in suspensions of swimming bacteria, extraction of useful energy from chaotic movement of swimmers [1], correlations in active transport of cargo along cytoskeletal networks [6], and self-assembled colloidal structures performing simple robotic functions [10]. For all these model systems we have developed theoretical descriptions leading to prediction and control of the emergent self-assembled structures.

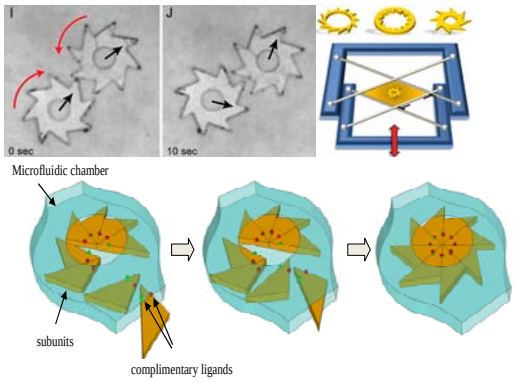

Figure 1. Top: Two 0.5 mm microgears rotated by motile bacteria in a freely suspended liquid film [1]. Bottom: Bacteria-assisted synthesis: triangular building blocks are transported into a microfluidic chamber by swimming bacteria. They are functionalized with complimentary ligands (red and green dots) to ensure the desired assembly pattern. The assembled gears are powered by bacterial motion, rectified by ratchet geometry.

In the next three years we plan to explore a broad range of self-assembled bio-inspired materials stemming from the advancement of our program: functional 2D and 3D dynamic colloidal structures built from elementary functionalized sub-units that are transported into place and assembled by self-propelled autonomous agents such as swimming bacteria or synthetic swimmers

and controlled by electric or magnetic fields.

Recent progress

Swimming Bacteria Power Microscopic Gears. A suspension of self-propelled swimmers is the simplest example of active matter. We have designed a hybrid bio-mechanical system in which common aerobic bacteria *Bacillus subtilis*, swimming in a free-standing fluid film, power sub-millimeter gears decorated with asymmetric teeth [1]. The resulting rotational velocities of the gears are controlled by the amount of oxygen and nitrogen available to the bacteria and depend on the concentration of bacteria. As shown in Figure 1, bacteria can assemble primitive machines: a system of two engaged gears rotating in opposite direction. The ability to harness and control the power of collective motions appears an important requirement for further development of hybrid bio-mechanical systems driven by microorganisms and design of self-assembled functional materials capable of extracting energy from the environment, repair damage, and adapt to new conditions.

Self-Assembled Colloidal Asters Perform Simple Robotic Functions. Recently, we discovered that active functional machines could be self-assembled from a dispersion of magnetic colloidal particles at the interface between two immiscible isotropic fluids, energized by an alternating magnetic field applied perpendicular to the interface. Dynamic self-assembled structures, which we term localized asters and tunable clusters of asters, exhibit locomotion, shape change, and even self-repair [10]. The asters and arrays of asters perform simple robotic functions such as capture, transport, and positioning of target particles, see Figure 2. The size of these aster-microrobots can be further tuned by the frequency of an applied magnetic field, as well as density and surface tension of the liquids. Via this demonstration of emerging functionality in a seemingly simple active colloidal system, our work hints at the process to create precisely designed functional materials in ways not currently available. Possible applications include self-assembled grippers or tweezers for the manipulation of microparticles on the surfaces of liquids.

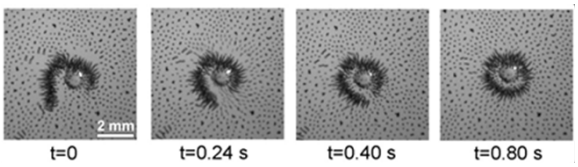

Figure 2. Self-assembled colloidal robot-aster, made of 80 μm magnetic Ni microparticles suspended at the interface between two immiscible liquids (water/silicon oil). The aster, remotely controlled by a small magnetic field applied parallel to the interface between two liquids, performs simple robotic functions: grip, moves and position non-magnetic particles [10].

Future Plans

With these inspirations in mind, we propose a new approach for creation of dynamic structures, in which the building units are transported into place and assembled by preprogrammed active matter, such as swimming bacteria or synthetic swimmers. The

concept of the swimmer-assisted assembly is illustrated in Figure 1. All these agents move collectively, form dynamic structures and shapes by assembling and latching onto each other. Functionalization of the building blocks by complimentary polymers, peptides and/or proteins will allow us to control the response to external stimuli such as light, field, chemical gradients, shearing, and, thus perform useful functions, e.g., as a micro-sensor or mixer.

Specifically, since swimming bacteria, such as *Bacillus subtilis*, can convert chemical energy from nutrients into mechanical energy sufficient to move submillimeter objects, these bacteria could act as agents or "workers" assembling new materials and micro-systems from small functionalized blocks. The building blocks will be designed in such a way that the bacteria are able to transport and place them in desired locations. To complete the assembly process, complimentary recognition properties of surface-attached functionalities can be used. The first route we will try will be to employ the biotin-avidin interaction, which is very strong and well-characterized. Another strategy to be explored involves attachment of complimentary antibodies (for example, immunoglobulins IgE or IgG or complimentary proteins) to specific particles and proper antigens to other particles. Formation of specific antibody-antigen cross-links between the particles will result in formation of an array of particles defined by the geometrical shape of the sub-units and methods of assembly. Having more than one pair of complementary interactions will enable the simultaneous assembly of more than one kind of object, thereby producing multiple functions in the same medium. Motion of the sub-units can be suddenly stopped when needed, by filling the assembly chamber with nitrogen, which temporally immobilizes the bacteria [1]. If necessary, the motion can be resumed by refilling the chamber with oxygen. As an example, the bacteria can assemble a gear inside of a microfluidic chamber into which the gear parts can be delivered one by one. Then, the gear powered by the same bacteria can pump the fluid through the device or perform useful work, see Figure 1. This bio-inspired active matter approach will potentially allow us to position and control simultaneously thousands of micro-objects. This "parallelism" will significantly decrease the time of assembly compared to conventional micromanipulators/3D lithography techniques.

Another promising direction of research is self-assembled reconfigurable materials for microrobotics [10]. We plan to pursue significant size reduction of these microrobots via modification of the properties of liquids, and via shape and molecular functionalization of the magnetic particles. Functionalization of the particles will allow self-assembly of a new generation of robots, capable, for example, of recognition and selective attachment to particles or cells of interest. In addition, new functionality can be achieved by using instead of spherical magnetic particles shape-anisotropic magnetic particles, such as large aspect ratio magnetic rods. Different parts of the rods can be functionalized with specific ligands responding on desired chemical stimuli. This approach may potentially lead to a new generation of self-assembled robots with rich functionality.

In addition to experimental research, we will conduct theoretical studies and large-scale simulations focused on elaboration of fundamental mechanisms of active self-assembly [3,8]. We will implement massive parallel algorithm for simulation of suspensions of active swimmers/floaters on Graphic Processing Units (GPU). The simulations will be

carried out on the GPUs (42 Fermi GPU cards) cluster acquired by Argonne's Materials Science Division in 2010. The main focus will be the interactions between swimmers with functionalized units and predictive modeling of active magnetic colloids using hybrid discrete particles/fluid dynamics algorithm [3].

References (which acknowledge DOE support).

1. Andrey Sokolov, Mario Apadoca, Bartosz A. Grzybowski, Igor S. Aranson, "Swimming bacteria power microscopic gears", *Proc National Acad. Sci*, **107**, 969- 974 (2010), featured in New Your Times, 22 Dec 2009, p D3; Forbes /www.forbes.com/2009/12/19/physics-gears-energy-technologybreakthroughs-bacteria.html
2. Vitaliy Gyrya, Igor S. Aranson, Leonid V. Berlaynd, Dmitrii Karpeev, "A model of hydrodynamic interaction between swimming bacteria", *Bulletin of Mathematical Biology*, **72**, 148-183 (2010)
3. Maxim Belkin, Andreas Glatz, Alexey Snezhko, and Igor S Aranson, " Model for dynamic self-assembled magnetic surface structures", *Physical Review E* **82**, 015301 (2010)
4. Sumanth Swaminathan, Falko Ziebert, Igor S Aranson, and Dmitry Karpeev, "Patterns and intrinsic fluctuations in semi-dilute motor-filament systems", *Europhysics Letters*, **90**, 28001 (2010)
5. Vitaliy Gyrya, Konstantin Lipnikov, Igor S Aranson, and Leonid Berlyand, "Effective shear viscosity and dynamics of suspensions of micro-swimmers: from small to moderate concentrations", *Journal of Math Biology*, **62**, 707 (2010)
6. Alexey Snezhko, Kari Barlan, Vladimir I. Gelfand, and Igor S Aranson, "Statistics of Active Transport in Xenopus Melanophores Cells", *Biophysical Journal*, **99**(10) pp. 3216 – 3223, (2010)
7. Sumanth Swaminathan, Falko Ziebert, Igor S. Aranson, Dmitrii Karpeev, "Motor-Mediated Microtubule Self-Organization in Dilute and Semi-Dilute Filament Solutions", *Math. Modeling Nat. Phen*, **6** , 119-137 (2011)
8. Shawn D Ryan, Brain M. Haines, Leonid Berlyand, Falko Ziebert, Igor S. Aranson, "Viscosity of bacterial suspensions: Hydrodynamic interactions and self-induced noise", *Physical Review E*, **83**, 050904 (2011)
9. Andreas Glatz, Igor S. Aranson, Tatiana I. Baturina, Nikolay M. Chtchelkatchev, Valerii M. Vinokur, "Self-organized superconducting textures in thin films", *Physical Review B*, **84** 024508 (2011)
10. Alexey Snezhko and Igor S. Aranson, "Magnetic Manipulation of Colloidal Asters", *Nature Materials*, doi:10.1038/nmat3083, 2011; featured in R&D Magazine, New Scientist, and DOE Energy blog http://energy.gov/articles/tiny-terminators-new-micro-robots-assemble-repair-themselves-and-are-surprisingly-strong
11. German V. Kolmakov, Alexander Schaefer, Igor S. Aranson and Anna C. Balazs, Designing Mechano-responsive Microcapsules that Undergo Self-propelled Motion, submitted to *Soft Matter*, 2011

Toward Capturing Soft Molecular Material Dynamics

Dominik Ziegler*, Babak Sanii[*], Andreas Frank[#], Sindy Frank[#], Alex Chen[††], Travis Meyer[††], Rodrigo Farnham[†], Nen Huynh[†], Jim DeYoreo[*], Ivo Rangelow[#], Jen-Mei Chang[†], Andrea Bertozzi[††], Paul Ashby[*+]

[*]Imaging and Manipulation Facility, Molecular Foundry, Lawrence Berkeley National Laboratory, Berkeley, California, USA, 94720.
[#]Institut für Mikro- und Nano-Elektronik, Technical University Ilmenau, Ilmenau, Germany, 98684.
[††] Department of Mathematics, University California Los Angeles, Los Angeles, California, USA, 90095.
[†]Department of Mathematics, California State University Long Beach, Long Beach, California, USA, 90840.
[+]pdashby@lbl.gov

Biological Atomic Force Microscopy

Scientific Challenge

Many soft materials readily deform under the minimum force required to perform an AFM measurement precluding imaging at high temporal and spatial resolution. Methods to reduce significantly the minimum detectable force and increase imaging rate are required.

Research Achievement

Although quite fashionable, attempts to use feedback methods such as Q-control and frequency modulation have failed to improve the image quality when in solution. Q-control amplifies weak tip-sample interactions and the thermal noise equally providing no overall advantage.[1] Frequency modulation also amplifies weak tip-sample interactions but controls the amplitude noise. However, the feedback shifts the amplitude noise to the time domain precluding a precise measurement of frequency providing no overall advantage either.[2] Instead, the thermal force-noise of the cantilever is the principal limitation to reducing sample deformation. Minimizing a cantilever's cross- section reduces its noise significantly and the minimum size of the cantilever is currently limited by a conventional deflection detection scheme, which requires

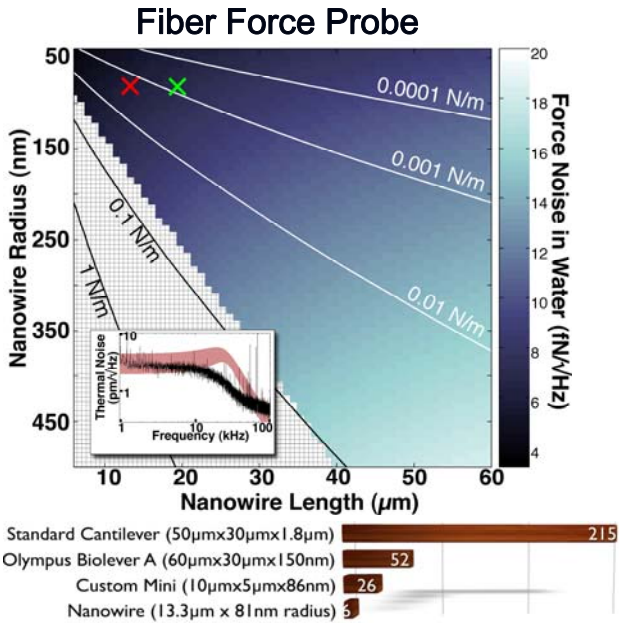

Figure 1 - The calculated force noises of nanowires as a function of their radii and lengths, in water. Contour lines denote cantilever stiffnesses, and the hashed region corresponds to thermal fluctuations that are too small to be detected with our system, with 5 mW of laser power. Inset figure is the measured thermal noise spectrum of the 2±1 mN/m stiff nanowire marked with a red × (force noise of 6±3 fN/√Hz), as well as a theoretical prediction based on its dimensions and material properties. The green × is a measured 19:4 μm by 82.5 nm nanowire (force noise of 7±4 fN/√Hz). The bar chart shows Fiber Force Probe force noise relative to other AFM cantilevers. The Fiber Force Probe has record low force noise in solution.

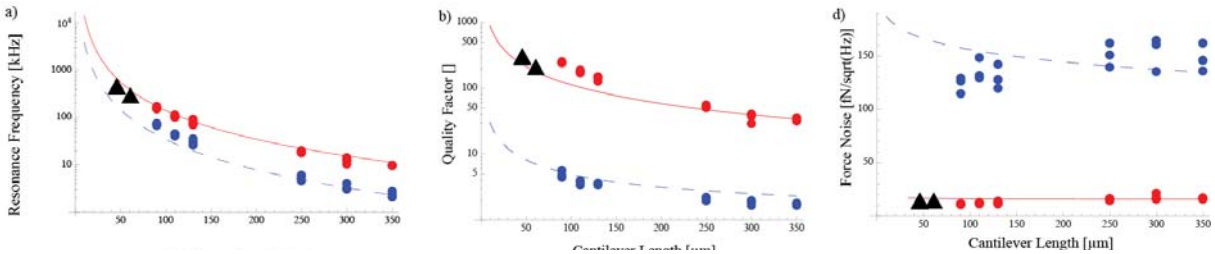

Figure 2 - Resonance frequency, quality factor, and force noise as a function of cantilever length for normal cantilevers in air (●) and in water (●). The encased cantilevers (▲) in water have the same high-performance as normal cantilevers in air.

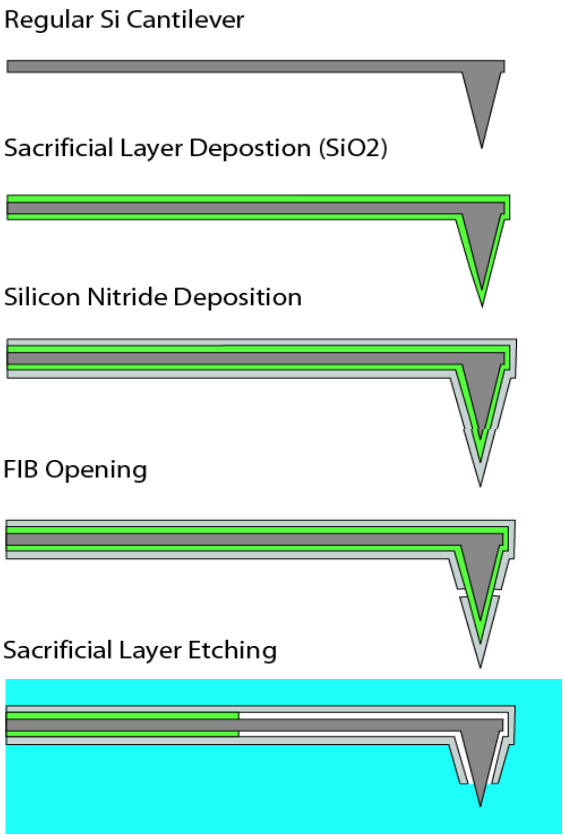

Figure 3 - Cartoon of encased cantilevers fabrication process. PE CVD is used to deposit a sacrificial layer and the encasement. The sacrificial layer is etched back from an opening at the probe apex. Surface tension prevents water from entering the encasement.

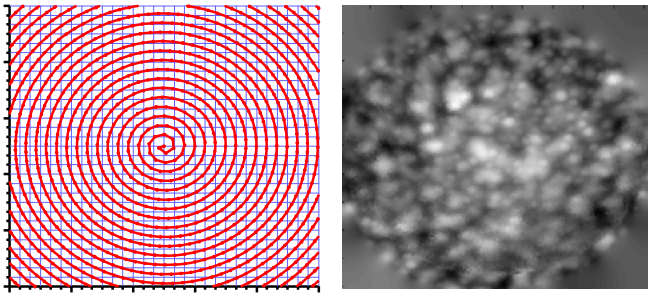

Figure 4 - spiral scans require lower acceleration and force them raster scanning enabling higher tip velocities and frame rates for the same scanner

a large surface area for laser specular reflection. A forward scattering optical deflection detection technique enables the use of nanowires as cantilevers. We achieved a force noise in water of 6 fN/√Hz that is orders of magnitude gentler than conventional AFM using the Fiber Force Probe AFM.[3] The Fiber Force Probe has a number of significant limitations such as slow scan speed, difficult sample geometry, and lack of robustness. To mitigate these challenges we reduced force noise by reducing the fluid viscosity with a protective encasement for the cantilever. The cantilever operates in air but the probe protrudes from the encasement through the solution to the sample. Encased cantilevers have exceptionally high resonance frequency, Q factor, and detection sensitivity and low force noise enabling gentle high speed imaging.[4] They also work in all commercial AFM systems without modification. These are significant milestones towards non-invasive scanning probe imaging of biological processes on the surfaces of vesicles and cell membranes.

Present raster scan techniques are poorly matched to the instrument limitations of Atomic Force Microscopy. Serial data collection from the local probe makes image collection slow and unable to match the timescales of many chemical and biological processes. One basic issue is the propensity of scientists to oversample data. We have used advanced image processing tools such as inpainting to recover high-resolution images from sparse quickly collected images to improve temporal resolution without applying more force or

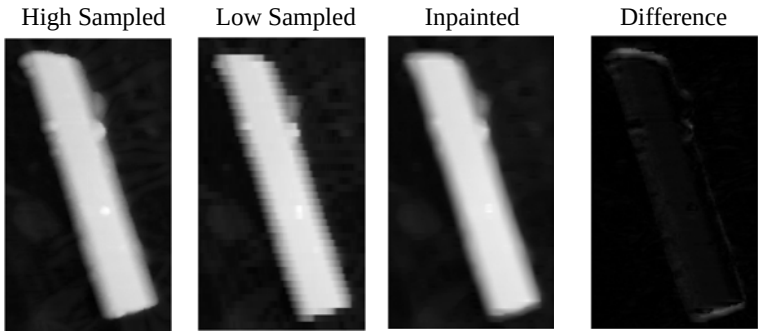

Figure 5 - inpainting diffuses data from known regions of an image to unknown regions by balancing fidelity to the original data and smooth connectedness of the resulting image. For simple images and edges quickly acquired low density data is all that is required enabling higher frame rates.

increasing bandwidth.[5] We are also using non-raster scan algorithms such as spiral and cyclic scanning to increase temporal resolution. Spiral scanning better matches the mechanical limitations of the AFM scanner and allows higher tip velocities without distortion. Inpainting or interpolation is used to quickly create images from the nongrided data.[6]

The use of gentle high bandwidth probes and fast scanning algorithms will enable Atomic Force Microscopy to probe soft materials with high resolution and capture dynamics of assembly and function.

References

[1] Paul D. Ashby, Gentle imaging of soft materials in solution with amplitude modulation atomic force microscopy: Q control and thermal noise, *Appl. Phys. Lett.*, **2007**, *91*, 254102.

[2] Paul D. Ashby, Impact force noise in Frequency Modulation Atomic Force Microscopy, in preparation.

[3] Babak Sanii, Paul D. Ashby, High Sensitivity Deflection Detection of Nanowires, Physical Review Letters, **2010**, *104*, 147203.

[4] Dominik Zieler, Paul D. Ashby, Encased Cantilevers for Ultra Sensitive Force and Mass Detection, in preparation .

[5] Alex Chen, Pascal Getreuer, Yifei Lou, Paul D. Ashby, Andrea Bertozzi, Enhancement and Recovery in Atomic Force Microscopy Images, submitted.

[6] Travis Meyer, Rodrigo Farnham, Nen Huynh, Alex Chen, Jen-Mei Chang, Paul D. Ashby, Andrea Bertozzi, Fast Atomic Force Microscopy Imaging using Self-Intersecting Scans and Inpainting, in preparation.

Dynamic Self-Assembly of Composite Nanomaterials

George Bachand, Marlene Bachand, Sergei von Hoyningen-Huene, Nathan Bouxsein, Erik Spoerke, Mark Stevens, and Bruce Bunker
Sandia National Laboratories, PO Box 5800, MS 1303, Albuquerque, NM 87185
Email: gdbacha@sandia.gov

Program Scope

Our project, *Active Assembly of Dynamic and Adaptable Materials,* examines fundamental materials science issues at the intersection of biology, nanomaterials, and hybrid interfaces. Unique attributes of living systems such as self-replication and adaptive/intelligent behaviors are commonly associated with dynamic self-assembly processes.[1] The interactions responsible for dynamic self-assembly occur only if the system is dissipating energy, which often occurs in living systems via enzymatic reactions that alter protein-protein interactions. Research activities within our project focus on the dynamic and adaptive assembly of hybrid nanomaterials through the application of energy-dissipative transport by motor proteins (e.g., kinesin) and cytoskeletal filaments (e.g., microtubules). Organisms use the cooperative behavior of kinesin and microtubules in a range of cellular processes including mitotic spindle formation during cell division, maintenance and rearrangement of the endoplasmic reticulum, and responsive reorganization of pigment-containing vesicles in melanophore cells.[2] A central goal of our work is to understand and exploit these energy-consuming proteins to self-assemble nanomaterials into complex structures that are not constrained by limitations associated thermal equilibrium.

We have previously demonstrated the application of energy dissipation via motor protein transport to dynamically self-assemble hybrid nanostructures (Fig. 1).[3] In this system, kinesin motor proteins actively assemble oligomeric complexes of microtubules and quantum dots into ring structures through the conversion of ATP into mechanical work. Our understanding of this system demonstrates how both thermodynamics and energy dissipation play critical roles in both the self-assembly and disassembly of these structures.[4, 5] In these studies, the kinesin motor proteins were solely responsible for energy dissipation as the microtubule filaments were stabilized to inhibit their intrinsic instability (see further discussion below). The dynamic nature of microtubule self-assembly, however, offers a unique means of assembling and organizing nanoscale materials. Thus, this abstract discusses our recent work on dynamic self-assembly of microtubule filaments and its application to assembling unique nanocomposite structures (in the absence of motor proteins).

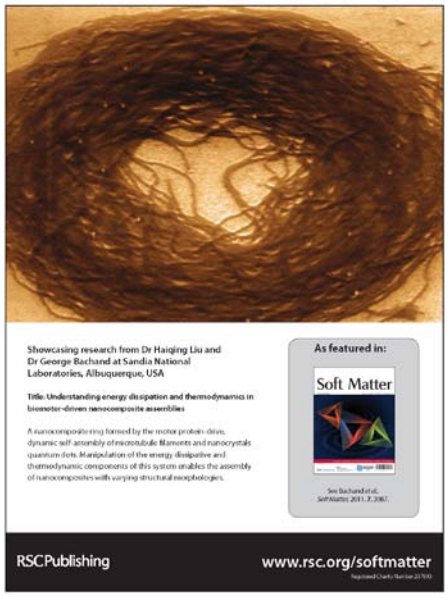

Fig. 1: Dynamic self-assembly of nano-composite rings. Microtubule filaments with attached quantum dots dynamically self-assemble into ordered ring structures through thermodynamic and energy dissipative processes (see Liu & Bachand 2011).

Recent Progress

As described above, MTs are cytoskeletal filaments that help maintain a cell's structure, as well as establish

a three-dimensional, intracellular transport network.[6] MT filaments are essentially a polymer of αβ tubulin dimers that self-assemble to form hollow filaments of 25 nm in diameter and 10s of microns in length. Because the building blocks are dimers, microtubules possess an intrinsic polarity with the "plus-end" capped by a β subunit, and the "minus-end" capped by an α subunit. The process of polymerization occurs via a biomolecular reaction in which dimers are added to the growing polymer through the hydrolysis of guanosine triphosphate (GTP). These chains of tubulin dimers, called proto-filaments, are then stabilized by weaker lateral interactions with adjacent filaments, forming a sheet that curls into the mature MT filament.

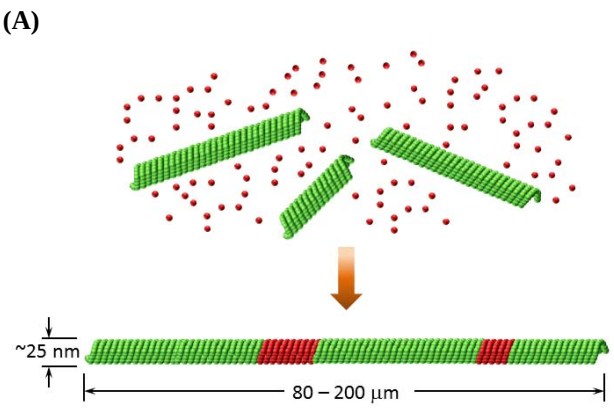

Fig.2: Models of tubulin polymerization suggest that growth occurs via sequentially addition of GTP-tubulin dimers to the ends of microtubule protofilaments. Our recent work, however, demonstrates a new process in which microtubule filaments may fuse over extended periods of time to form long, extended filaments.

Dynamic instability is a unique property of microtubules in which the filaments switch between growing and shrinking states.[7] While energetically expensive, cells rely on dynamic instability to search for, and subsequently move cellular components (e.g., chromosomal segregation during mitosis). The dynamic nature of polymerization/depolymerization has been characterized both *in vivo* and *in vitro*, and shown to be dependent on four critical factors: (1) tubulin concentration, (2) GTP hydrolysis, (3) temperature, and (4) stabilizing/destabilizing agents. In particular, inhibition of microtubule depolymerization by the anti-cancer drug taxol (paclitaxel) has been widely used in laboratory-based research to stabilize microtubules against dynamic instability.

Recently, we discovered a new mechanism for growth and stability of microtubules that does not involve normal microtubule polymerization dynamics. In this mechanism, existing microtubule segments are fused together end-to-end to form longer microtubules. The first step occurs when the plus-end of one microtubule encounters the minus-end of another microtubule and sticks to form a junction (Fig 2). However, this joint is likely imperfect as the microtubule ends may be blunt, tapered, or curved and lead to defects. Thus the second step involves rearrangement and/or additions of tubulin dimers near the junction in an "annealing" process that eliminates the defects. Annealing is facilitated by the presence of free GTP-tubulin dimers that can help fill in the imperfections. We have performed both experiments and simulations to confirm this hypothesis. In initial experiments, red- (rhodamine dye) and green- (HiLyte Fluor™ 488 dye) fluorescently labeled microtubules were mixed together, and the growth and stability of the microtubule population were characterized over time. If growth is due to polymerization, mosaic, red-green microtubules with either solid green or red central regions would be expected, based on the nucleated polymerization with free tubulin. Alternatively, fusion should result in alternating red-green segments where the segment lengths are approximately similar to their initial lengths following polymerization and stabilization. The total number of microtubule filaments in the population should also decrease as the length of the filaments increase due to fusion. One day after initiation of these experiments (i.e., rhodamine and HiLyte microtubules were mixed), the average filament length had increased from ~17 μm to 52 μm, while the length

of the individual rhodamine and HiLyte segments did not change. Fourteen days after initiation, the average filament length had increased to 160 μm with no significant change in the length of the individual rhodamine and HiLyte segments. The change in filament length over time over time followed a first-order exponential increase to a maximum (Fig. 3). Moreover, the number of microtubule per field of view followed a first-order exponential decay. The inverse correlation between microtubule length and the number of microtubules in the population is consistent with the proposed fusion mechanism. Tubulin polymerization, however, cannot be completely excluded as a proportion of tubulin in the initial sample remains unpolymerized. When free tubulin (and GTP) was removed by centrifugation, fusion was still observed, but the rate and extent of fusion was greatly reduced. Overall, these experiments demonstrate a novel process in which taxol-stabilized microtubule filaments may self-assemble in a directed, end-to-end manner to form long, extended filaments.

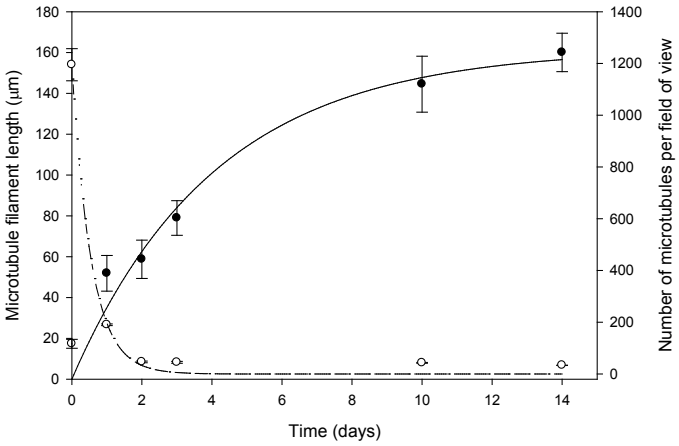

Fig. 3. The average length of microtubules (●–) and the number of microtubules per field of view (--○--) observed over time.

To better understand the role of free GTP-tubulin in the fusion process, unpolymerized GTP-rhodamine tubulin was combined with stabilized HiLyte microtubules that had been centrifuged to remove the unpolymerized HiLyte tubulin. We observe native HiLyte segments connected by short rhodamine segments within minutes after combining. This observation is consistent with fusion of short (~1 μm) microtubule fragments immediately after mechanical shearing.[8] In our experiments, however, the initial microtubule filaments were much larger (i.e., ~10 μm) and fused to form microtubule filaments in excess of 200 μm in length (Fig. 4). Moreover, the fusion continued to occur over a much longer time scale than previously reported (days vs. hours). Fused filaments under these conditions were observable even after 89 days post-polymerization (Fig. 4), which is considerably longer than prior reports.[9] These observations confirm the role of GTP-tubulin in the end-to-end fusion of microtubule filaments. Currently, we are evaluating the importance of the GTP nucleotide and its hydrolysis in the fusion process.

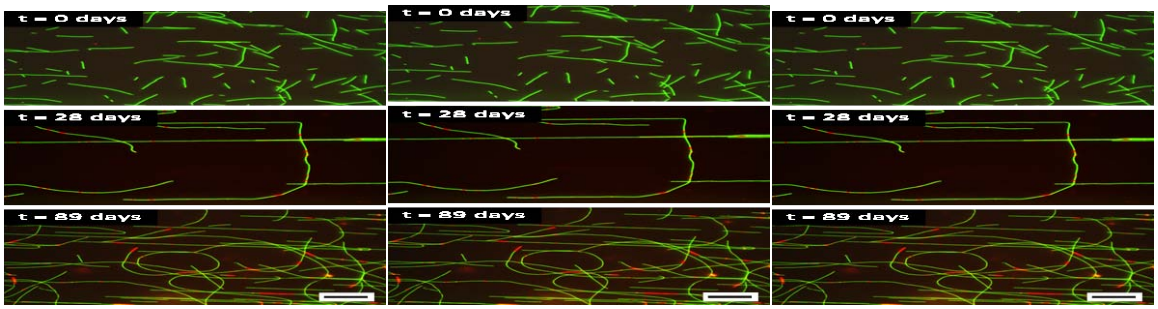

Fig. 4: Fluorescence photomicrographs of "microtubule annealing" in which rhodamine-tubulin dimers function as glue between annealed HiLyte filaments. Annealed filaments can achieve aspect ratios >4,000 : 1. Scale bar = 10 μm.

Future Plans

Whereas lateral assembly and organization of biopolymers has been well-documented,[10] the process of microtubule fusion offers a unique model system to study the end-to-end self-assembly of protein polymers. We are continuing to study the mechanism by which fusion occurs, particularly with respect to how the physiochemical properties of the microtubule drive self-assembly. For example, the microtubule surface charge density may be chemically altered to characterize the contribution of electrostatic repulsion on end-to-end assembly. In addition, the effect of microtubule ordering (e.g., isotropic vs. nematic) and changes in entropy on fusion kinetics will be characterized. We also plan on using microtubule fusion as a means to synthesize high aspect ratio nanowires and heterostructures via established electroless deposition methods.[11]

Acknowledgment

This research was supported by the U.S. Department of Energy, Office of Basic Energy Sciences, Division of Materials Sciences and Engineering, Project KC0203010. Sandia National Laboratories is a multi-program laboratory operated by Sandia Corporation, a wholly owned subsidiary of Lockheed Martin company, for the U.S. Department of Energy's National Nuclear Security Administration under contract DE-AC04-94AL85000

References

1. M. Fialkowski, K. J. M. Bishop, R. Klajn, S. K. Smoukov, C. J. Campbell and B. A. Grzybowski, *J. Phys. Chem. B*, 2006, **110**, 2482-2496.
2. L. S. B. Goldstein and Z. H. Yang, *Annu. Rev. Neurosci.*, 2000, **23**, 39-71.
3. M. Bachand, A. M. Trent, B. C. Bunker and G. D. Bachand, *J. Nanosci. Nanotechnol.*, 2005, **5**, 718-722.
4. H. Q. Liu and G. D. Bachand, *Soft Matter*, 2011, **7**, 3087-3091.
5. H. Q. Liu, E. D. Spoerke, M. Bachand, S. J. Koch, B. C. Bunker and G. D. Bachand, *Adv. Mater.*, 2008, **20**, 4476-4481.
6. J. Howard, *Mechanics of Motor Proteins and the Cytoskeleton*, Sinauer Press, Inc., Sunderland, MA, 2001.
7. A. Desai and T. J. Mitchison, *Annu Rev Cell Dev Bi*, 1997, **13**, 83-117.
8. S. W. Rothwell, W. A. Grasser and D. B. Murphy, *J Cell Biol*, 1986, **102**, 619-627.
9. A. Boal, H. Tellez, S. Rivera, N. Miller, G. Bachand and B. Bunker, *Small*, 2006, **2**, 793-803.
10. B. Brodsky, K. Kar, P. Amin, M. A. Bryan, A. V. Persikov, A. Mohs and Y. H. Wang, *J Biol Chem*, 2006, **281**, 33283-33290.
11. A. K. Boal, T. J. Headley, R. G. Tissot and B. C. Bunker, *Adv. Funct. Mater.*, 2004, **14**, 19-24.

DOE-Sponsored Publications (2010-2011)

- H. Liu, and G.D. Bachand, (2011). Understanding energy dissipation and thermodynamics in biomotor-driven nanocomposite assemblies. *Soft Matter* 7 (7): 3087-3091. (***Cover***)
- N.W. Polaske, D.V. McGrath, and J.R. McElhanon, (2011). Thermally reversible dendronized linear AB step-polymers via "Click" chemistry. *Macromolecules* 44 (9): 3203-3210.
- N.W. Polaske, D.V. McGrath, V. Dominic, and J.R. McElhanon, (2010). Thermally reversible dendronized step-polymers based on sequential Hulsgen 1,3-dipolar cycloaddition and Diels-Alder "Click" Reactions. *Macromolecules* 43 (3): 1270-1276.

Program Title: Molecular Nanocomposites

Principle Investigator: Andrew M. Dattelbaum
Mailing Address: MS K771, Los Alamos National Laboratory
Los Alamos, NM 87545
E-mail: amdattel@lanl.gov

Program Scope

The goal of this program is to establish the key scientific principles needed to design and fabricate molecular nanocomposite materials that integrate functional molecular and/or biomolecular components with rigid nanostructured inorganic architectures. To this end, our studies have previously been aimed at understanding the mechanisms of templated composite material formation, the development of methods to create patterned thin films with nanoporous architectures, and the creation of new material functionalities by incorporating active molecular and/or biomolecular components into patterned and templated oxide materials.

Our current efforts are focused on understanding interfacial issues between encapsulated nanomaterials and the surrounding matrix. This understanding will provide the fundamental knowledge needed to control the properties of encapsulated nanomaterials. Such studies will lead to new techniques for the characterization and preparation of functional composite materials with potential applications in molecular and biomolecular sensing, as well as next generation photovoltaic materials.

The key LANL investigator is Andrew M. Dattelbaum, who works in collaboration with a larger research team at Sandia National Laboratories (Albuquerque) led by James Voigt.

Recent Progress

1. Preparation of fluorescent single walled carbon nanotube (SWNT)-silica gels: We have investigated the relationship between photoluminescence (PL) intensity and environmental sensitivity of surfactant-wrapped single walled carbon nanotubes (SWNTs).[1,2] SWNTs were studied under a variety of conditions in suspension as well as encapsulated in silica nanocomposites, which were prepared by an efficient chemical vapor into liquids (CViL) sol-gel process, Figure 1. The dramatically improved silica encapsulation process described by us has several advantages, including fast preparation and high SWNT loading concentration, over other encapsulation methods used to prepare fluorescent SWNT/silica nanocomposites. Further, addition of glycerol to SWNT suspensions prior to performing the CViL sol-gel process allows for the preparation of freestanding fluorescent silica xerogels, which to the best of our knowledge is the first report of such nanocomposites.

Our spectroscopic data on SWNTs suspended in aqueous surfactants or encapsulated in silica show that achieving maximum PL intensity results in decreased sensitivity of SWNT emission response to changes imparted by the local environment. In addition, silica encapsulation can be used to "lock-in" a surfactant micelle structure surrounding SWNTs to minimize interactions between SWNTs and ions/small molecules. Ultimately, our work demonstrates that one should consider a balance between maximum PL intensity and the ability to sense environmental changes when designing new SWNT systems for future sensing applications.

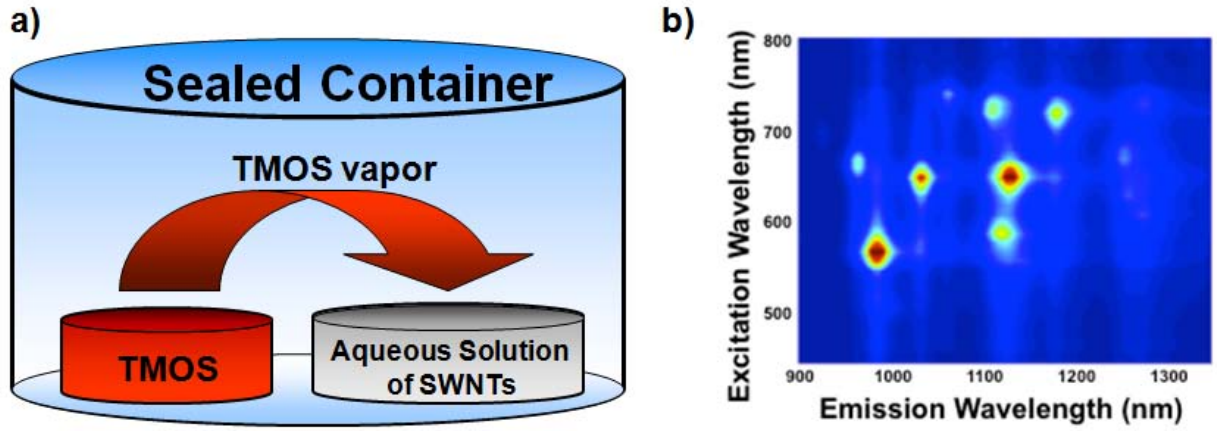

Figure 1. **a)** Schematic of the vapor transfer process used to prepare surfactant wrapped SWNT-silica gel nanocomposites. **b)** Photoluminescence excitation map of a SWNT-silica wet gel (prepared from a DOC-SWNT suspension).

2. Preparation of fluorescent single walled carbon nanotube (SWNT)-silica aerogels: A general challenge in generating functional materials from nanoscale components is integrating them into useful composites that retain or enhance the properties of interest. Development of single walled carbon nanotube (SWNT) materials for optoelectronics and sensing has been especially challenging in that SWNT optical and electronic properties are highly sensitive to environmental interactions, which can be particularly severe in composite matrices. Percolation of SWNTs into aqueous silica gels shows promise as an important route for exploiting their properties, but retention of the aqueous and surfactant environment still impacts and limits optical response, while also limiting the range of conditions in which these materials may be applied. We present for the first time an innovative approach to obtain highly fluorescent solution-free SWNT-silica aerogels, which provides access to novel photophysical properties.[2,3] Luminescence data from a typical SWNT-silica aerogel is shown in Figure 2. Strongly blue-shifted spectral features, revelation of new diameter-dependent gas-phase adsorption phenomena, and significant increase (~ 3× that at room-T) in photoluminescence intensities at croyogenic temperatures all indicate greatly reduced SWNT-matrix interactions consistent with the SWNTs experiencing a surfactant-free environment. The results demonstrate that this solid-state nanomaterial will play an important role in further revealing the true intrinsic SWNT chemical and photophysical behaviors and represents for the first time a promising new solution- and surfactant-free material for advancing SWNT applications in sensing, photonics, and optoelectronics.

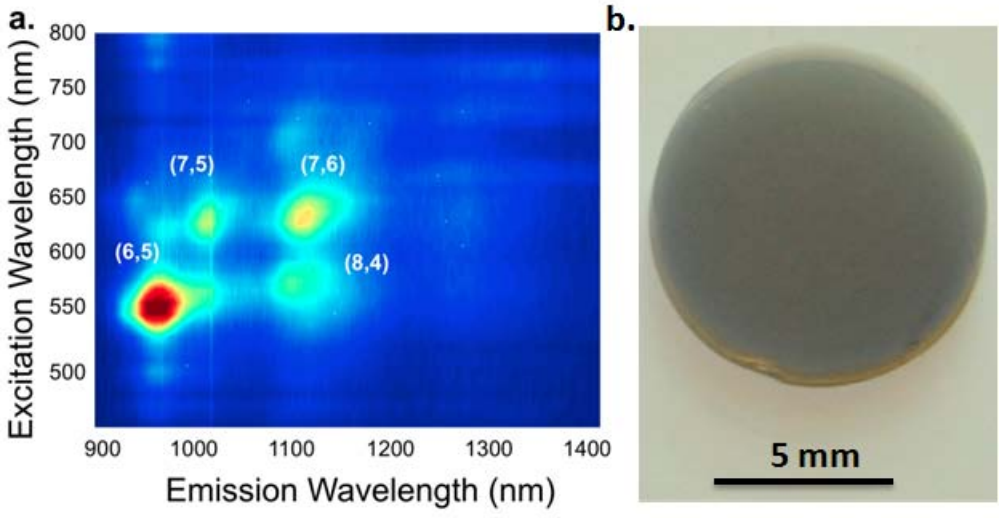

Figure 2. a) Photoluminescence excitation map of a SWNT-aerogel (prepared from a DOC-SWNT suspension) with *(n,m)* structural indices of specific features identified. b) Optical image of a SWNT-silica aerogel.

Future Plans

We plan to focus our future efforts on t he preparation and characterization of hybrid organic/inorganic materials. W e will continue to develop synthetic strategies to prepare new carbon nanotube-silica composite materials. We will use the SWNT/silica gels, as well as develop new routes towards SWNT/titania materials, to prepare novel luminescent aerogels. Both mechanical and photoluminescence properties will be studied in a variety of conditions, e.g., different gaseous media (Ar, CO_2, etc.) and solutions, to optimize the properties of the aerogel materials. Modification of the matrix building blocks using, for example, $RSi(OR)_3$, precursor molecules will lead to new robust materials. Future studies will also include the incorporation of natural light harvesting complexes, such as chlorosomes obtained from green sulfur bacteria, into inorganic matrices with carbon nanotubes. We will study the energy transfer from chlorosomes to the carbon nanotubes and the affect of the matrix on these properties. Such systems will be particularly useful for elucidating energy transfer pathways and may be useful for photovoltaic applications.

References (which acknowledge DOE support)

1. A New Route to Fluorescent SWNT/Silica Gels: Balancing Fluorescence Intensity and Environmental Sensitivity. J. G. Duque, G. Gupta, S. K. Doorn and A. M. Dattelbaum, *J. Phys Chem. C.* 2011,*115*, 15147–15153, DOI: 10.1021/jp2012107.

2. Stable and responsive fluorescent carbon nanotube silica gels. G. Gupta, J. G. Duque, S. K. Doorn A. M. Dattelbaum, *Mater. Res. Soc. Symp. Proc.*, 2010, DOI: 10.1557/PROC-1258-R12-07.

3. Fluorescent Single-Walled Carbon Nanotube Aerogels in Surfactant Free Environments. Juan G. Duque, Christopher E. Hamilton, Gautam Gupta, Scott A. Crooker, Jared. J. Crochet, Aditya Mohite, Sanjeev Singh, Han Htoon, Kimberly A. DeFriend Obrey, Andrew M. Dattelbaum and Stephen K. Doorn, *ACS Nano*, 2011, in press, DOI: 10.1021/nn202225k.

4. Carbon Nanomaterials in Silica Aerogel Matrices. C. E. Hamilton, M. E. Chavez, J. G. Duque, G. Gupta, S. K. Doorn, A. M. Dattelbaum and K. A. DeFriend-Obrey, *Mater. Res. Soc. Symp. Proc.*, **2010**, DOI: 10.1557/PROC-1258-R05-11.

Program Title: Directed Organization of Functional Materials at Inorganic-Macromolecular Interfaces

PI: *Tony Van Buuren*[1]; Co-Is: *Jim De Yoreo*[2], *Alex Noy*[1,3], *George Gilmer*[1] *and Matt Francis*[2]

Mailing address: [1]Physical & Life Sciences Directorate, Lawrence Livermore National Laboratory, Livermore, CA[2]; The Molecular Foundry, Lawrence Berkeley, National Laboratory, Berkeley, CA[3]; School of Natural Sciences, University of California Merced, Merced, CA

E-mail: *vanbuuren1@llnl.gov*

PROGRAM SCOPE

The purpose of this project is to develop a quantitative physical picture of macromolecular organization and its relationship to function, and to use macromolecular organization to derive new functionality. The research is divided into three tasks. In the first, we are fabricating bio-nanoelectronic devices in which phospholipids bilayers assembled on "1D" Si nanowires create an impermeable barrier against solution species transport to the nanowire surface. The bilayers serve as artificial environments for membrane pore proteins, thus creating a versatile structure for biomimetic control of ion transport to and from nanowire surfaces. In the second task, we are creating artificial light harvesting complexes using virus-DNA origami arrays assembled on "2D" chemical templates. MS2 viral capsids functionalized on their exterior surfaces with DNA linkers are modified to include light adsorbing centers that comprise FRET pairs. These are precisely assembled at the nm-scale scale using DNA origami tiles, which are in turn organized at μm-scale using strand complements patterned via scanned probe lithography. In the final task, we are investigating the mechanistic controls on formation of extended 2D macromolecular structures in which conformational transformations are an inherent feature of assembly and multiple order parameters evolve on distinct timescales. Using two self-organizing systems — S-layer tetramers and collagen triple helices — we are determining the dependence of assembly pathway, kinetics and morphology on the intermolecular and substrate interactions.

RECENT PROGRESS

(1) Bionanoelectronic Devices Based on 1D-Lipid Bilayers on Nanotube and Nanowire Templates.

One of the obstacles to achieving the vision of a bionanoelectronic circuit is the lack of a versatile interface that facilitates communication between biomolecules and electronic materials. To address this challenge, we have been developed a bionanoelectronic platform in which nanowires and nanotubes are covered by a lipid bilayer that serves both as a universal membrane protein matrix and an insulating shield (Fig. 1a). We used this platform to build prototype devices that incorporate self-assembled active and passive membrane proteins as integral parts of the circuit. In this way, we demonstrated the first example

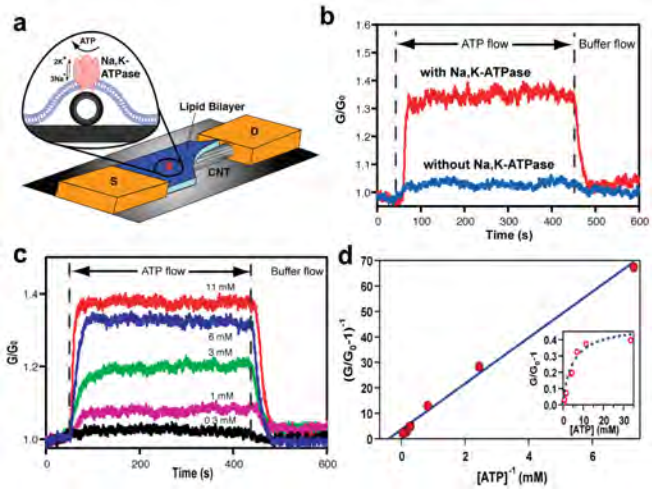

Fig. 1. Bionanoelectronic transistor gated by a biological ion pump. (a) Schematic of the experiment. (b) Time traces of normalized device conductance recorded for the device incorporating Na^+/K^+-ATPase (red trace) and a similar device that did not have protein in the lipid bilayers (blue). (c) Time traces of normalized conductance of the Na^+/K^+-ATPase containing CNT device recorded at different concentration of ATP as indicated on the plot. (d) Lineweaver–Burk (double reciprocal) plot of the device response as a function of the ATP concentration.

of a bioelectronics device that uses a protein ion pump, Na^+/K^+-ATPase, as a *biological gate* for a carbon nanotube transistor. For these experiments we incorporated Na^+/K^+-ATPase molecules in the lipid bilayers covering a microfabricated carbon nanotube transistor. When we added ATP to the solution flowing through the fluid cell covering the device that contained at most 10 individual ion pump proteins in the lipid layer, the nanotube conductance registered a sharp increase of ~ 35% (Fig. 1b). As expected, in absence of the ion pump the device was insensitive to the ATP concentration changes. Further investigation showed that the device response changed in clear ATP-dependent manner — higher "fuel" (i.e. ATP) concentration produced larger device conductance change (Fig. 1c). Not surprisingly, the device response follows the Michaelis-Menten enzyme kinetics (Fig. 1d) with the conductance increase saturating as the enzyme turnover rate saturate. Adding specific protein pump inhibitors to the testing cell also allowed us to prove that the device behavior was indeed controlled by the specific protein activity. Further analysis also revealed a fairly complicated gating mechanism where the ion pumping disturbed the pH equilibrium in the thin water layer under the lipid bilayer, and the pH change in turn modulated the nanowire conductance.

(2) Immobilization and organization of optically-active virus capsids with nanoscale precision using DNA origami.

Virus capsids are nanoscale objects with molecular-scale structure that present a high density of equivalent positions that can be exploited for making molecular-density arrays of active sites whose positions are precisely defined. We modified the interior of MS2 capsids with Oregon Green maleimide fluorescent dye to ~100% modification (180 copies), and modified the exterior with a 20-nt poly-T DNA sequence to ~11% modification, (20 copies). The capsids readily bound to DNA origami tiles bearing complementary probe strands for both 90 x 60 nm^2 rectangles and 120 nm equilateral triangles (Fig. 2A,B). In each case, we were able to alter the position of the capsids on the tiles by changing the locations of the probe strands. We also demonstrated formation of extended tile chains through addition of "staple strands" complementary to the DNA sequences along the tile edges (Fig. 2C), and showed that the capsids could themselves serve as the linking groups between the tiles (Fig. 2D).

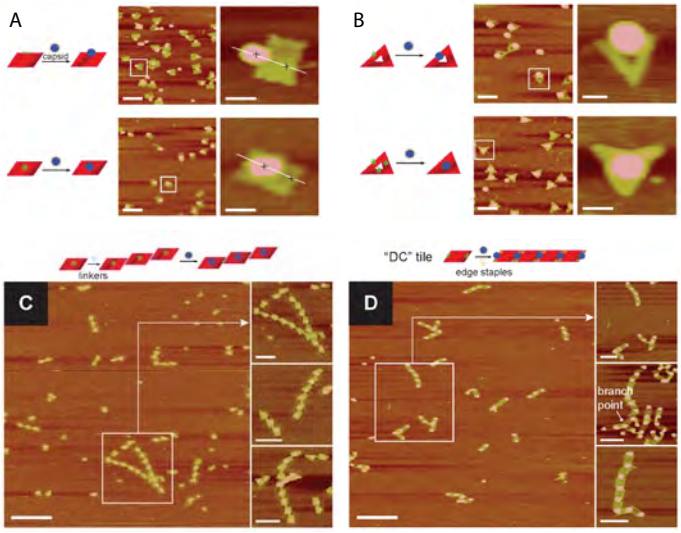

Fig. 2. Attachment of functionalized MS2 viral capsids to DNA origami tiles. By moving the location of the probe strands, capsids could be attached to the edges (top) and centers (bottom) of (A) rectangular and (B) triangular origami tiles. Zoom-out scale bars represent 200 nm, and zoom-in scale bars represent 50 nm. Through the addition of appropriate staple strands, the rectangular tiles could be connected into linear arrays, as shown in (C). Alternatively, the capsids themselves could serve to link the tiles, as shown in (D). In C and D, the zoom-out scale bars represent 500 nm, and the zoom-in scale bars represent 200 nm

To study enhancement of capsid fluorescence by Au nanoparticles, we used origami as a programmable template to control capsid-nanoparticle separation from ~0 to 70 nm. Comparison of confocal fluorescence maps and AFM maps of separation showed that indeed enhancement that was highly dependent on this separation. To study FRET efficiency, MS2 capsids were labeled with donor (interior) and acceptor (exterior) FRET chromophores. The

distances between dyes on individual protein subunits were < 3 Å, well below the Förster radius of the dye pair (~7.4 Å); numerous dyes on more distant subunits were located 3–5 Å apart, so multiple energy transfer pathways between donor and acceptor chromophores were predicted. Spectrofluorometry and surface confocal fluorometry from individual capsids and clusters of capsids demonstrated donor excitation resulted in energy transfer to the acceptor.

(3) 2D self-assembly of proteins with comformational transitions and substrate interactions.

Although the primary sequence of proteins dictates their governing interactions, function emerges from the nanoscale organization that arises out of self-assembly. S-layers proteins, which comprise the outermost cell envelope in many strains of bacteria, form compact 2D crystalline arrays and can be reconstituted *in vitro* in both bulk solutions and at surfaces. Because they exhibit large-scale order and periodicity commensurate with the dimensions of quantum dots and nanotubes, they were amongst the first protein structures to be exploited as scaffolds for organizing nanostructures. Here we used *in situ* AFM to follow 2D assembly of S-layers on supported lipid bilayers (Fig. 3). We obtained a molecular-scale picture of multi-stage self-assembly that revealed the importance of conformational transformations in directing the pathway. We found that monomers with an extended conformation first formed a mobile adsorbed phase, from which they condensed into amorphous clusters. These clusters underwent a phase transition through S-layer folding into crystalline clusters composed of compact tetramers. Growth then proceeded by formation of new tetramers exclusively at cluster edges, implying tetramer formation was auto-catalytic. Analysis of the growth kinetics led to a quantitative model in which tetramer creation was rate limiting. However, the estimated barrier was much smaller than expected for folding of isolated S-layer proteins, suggesting an energetic rationale for the auto-catalytic growth and the dominance of a multi-stage pathway.

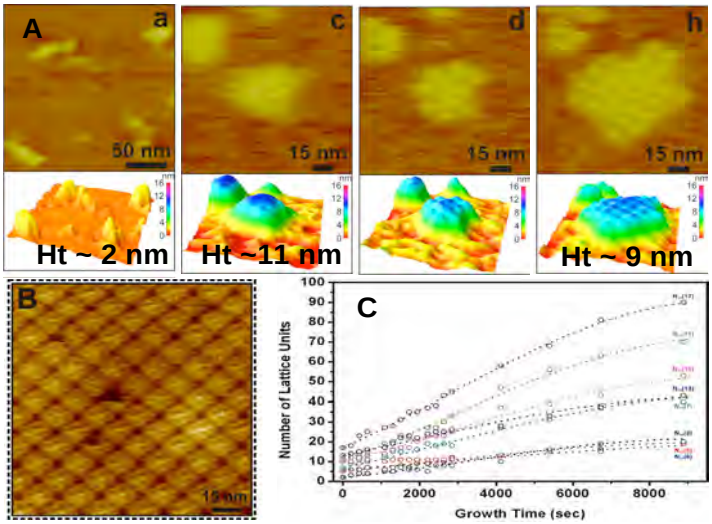

Fig. 3. (A) Sequence of *in situ* AFM images and 3D surface plots showing S-layer assembly into 2D crystals on supported lipid bilayer (SLB). (B) Higher resolution image of S-layer crystal on SLB revealing tetrameric arrangement of the four S-layer monomers comprising each lattice unit. (C) Time dependence of cluster size. Dotted lines are fits to model in which only adjustable parameter is rate coefficient for tetramer creation that yields the activation barrier. (See movie of S-layer self-assembly at: https://webspace.lbl.gov/xythoswfs/webui/_xy-8352525_1-t_VB2pJj9L)

FUTURE PLANS

Our work on lipid-nanowire bioelectronics devices will focus on integration of photo-induced proton transport into bionanoelectronic devices by inserting proteorhodopsin into our 1D lipid bi-layer platform. We will investigate the effect of membrane curvature and confinement on proton pumping and test the limits of sensitivity by trying to detect the signal from a single protein. In our research on organization of MS2 viruses using virus/DNA-origami heterostructures, we will use chemical patterning to create 2D arrays of FRET-active capsids complexes. Distances will be optimized for light harvesting based on our current experiments

with individual FRET pairs and FRET efficiency will be measured. For both systems, we will relate long-range order and atomic-scale structure to device function.

Finally, we will explore conformation-dependent assembly pathways and dynamics using S-layer proteins and collagen, both of which assemble into 2D architectures that are dependent on intermolecular and substrate interactions. For the third, we will characterize assembly dynamics and order using *in situ* AFM and SAXS, respectively, and test physical models of organization through MD and Monte Carlo simulations based on interaction energies determined from in situ dynamic force spectroscopy measurements.

PUBLICATIONS.

A. Noy, Force Spectroscopy 101: How to design, perform, and analyze an AFM-based single molecule force spectroscopy experiment, *Current Opinion in Chemical Biology* (invited), in press (**2011**)

A. Noy, Bionanoelectronics, *Advanced Materials* **23**, 807–820, **invited review** (2011) **Cover Article.**

R.W. Friddle, K. Battle, V. Trubetskoy, J. Tao, E.A. Salter, J.J. De Yoreo, A. Wierzbicki, Single-Molecule Determination of the Face-Specific Adsorption of Amelogenin's C-terminus on Hydroxyapatite, *Angewandte Chemie Int. Ed.* **50**, 7541 –7545 (2011).

V. Lulevich, S. Kim, C.P. Grigoropoulos, A. Noy, Frictionless sliding of ssDNA in a carbon nanotube pore observed by single molecule force spectroscopy, *Nano Letters*, **11**, 1171–1176 (2011)

J-B. In, C.P. Grigoropoulos, A. Chernov, A. Noy, Kinetics of Oxygen-Free CVD Growth of Vertically-Aligned Carbon Nanotube Arrays, *Applied Physics Letters***, 98**, 153102- 153104 (2011)

N. Stephanopoulos, M. Liu, G.J. Tong, Z. Li, Y. Liu, H. Yan, M.B. Francis, Immobilization and One-Dimensional Arrangement of Virus Capsids With Nanoscale Precision Using DNA Origami, *Nano Letters*, **10**, 2714–2720 (2010).

Chung, S., Shin, S-H., Bertozzi, C.R. and De Yoreo, J.J., Self-catalyzed growth of S layers via an amorphous-to-crystalline transition limited by folding kinetics**.** *Proc. Nat'l. Acad. Sci.* **107**, 16536-16541 (2010).

S.-C. J. Huang, A.B. Artyukhin, N. Misra, J.A. Martinez, P.A. Stroeve, C.P. Grigoropoulos, J.-W.W. Ju, A. Noy, Carbon nanotube devices controlled by an ion pump gate, *Nano Letters* **10**, 1812–1816 (2010).

P.G. Holder, D.T. Finley, D.S. Clark, M.B. Francis, Dramatic Thermal Stability of Virus-Polymer Conjugates in Hydrophobic Solvents, *Langmuir*, **26**, 7383-17388 (2010).

C.L. Cheung, A.I. Rubinstein, E.J. Peterson, A. Chatterji, R.F. Sabirianov, W-N. Mei, T. Lin, J.E. Johnson, and J.J. DeYoreo, Steric and Electrostatic Complementarity in the Assembly of Two-Dimensional Virus Arrays" *Langmuir* **26**, 3498-3505 (2010).

N. Stephanopoulos, Z.M. Carrico, M.B. Francis, Nanoscale Integration of Sensitizing Chromophores and Photocatalytic Groups Using Bacteriophage MS2, *Angewandte Chemie Int. Ed.*, **48**, 9498-9502 (2009**)**.

A. Noy, A. Artyukhin, N. Misra, NanoBioElectronics with 1D Materials, *Materials Today*, **12**, 22-31, **invited review** (2009).

O. Bakajin, A. Noy, Separation Materials: Proteins make for finer filters, (News and Views Feature) *Nature Nanotechnology*, **4**, 345 – 346 (2009).

Nanostructured Biocomposite Materials for Energy Transduction

Sungwon Lee, Scott M. Brombosz, Bryan S. Ringstrand, Alex Polozov, Simonida Grubjesic, Laurel S. Almer, and Millicent A. Firestone (PI)

Materials Science Division, Argonne National Laboratory, Argonne, IL 60439

Program Scope

The *Nanostructured Biocomposite Materials for Energy Transduction* research program has as its overarching goal the design, synthesis, and characterization of a new class of functional nanoscale materials that exploit the native capabilities of biological molecules to store and transduce energy. A major research thrust in this work is the development of biologically-inspired synthetic soft materials that stabilize, organize and regulate the activity of a wide variety of proteins. The work encompasses the design and synthesis of small organic molecules (e.g., amphiphiles, monomers) that constitute the fundamental building blocks used to fabricate these materials. The molecules are tailorable permitting re-programming their spontaneous organization into a variety of nanostructures. Chemical moieties are also added to allow for capture of the self-assembled architectures in a durable form by polymerization and / or crosslinking, rendering the materials environmentally stable and mechanically durable. A second thrust of the program is centered on synthetic modification of the soft materials to allow for successful biotic-abiotic functional integration. This component of the program seeks to develop functional electronic interfaces for harnessing protein output (e.g., light-generated electron flow).

Recent Progress

Proteo-compatible crosslinked complex fluid. Previously, we reported the development of biomimetic materials that self-assemble into three-dimensional matrices that allow for the compartmentalization and organization of a v ariety of membrane proteins and accessory molecules. During this funding period we have worked to chemically modify the composition of these materials so as to improve their mechanical properties.[1] A structurally reinforced hydrogel possessing a biomembrane mimicking architecture has been prepared. The introduction of a diacrylate end-derivatized PEO-PPO-PEO macromer, F98$(Acr)_2$, into a lamellar structured lipid-based complex fluid has been photocrosslinked with a water-soluble co-macromer, PEGDA, producing water layer confined intra- and interlamellar crosslinks between pendant acrylate moieties (Figure 1). X-ray scattering studies show that the self-assembled lamellar structure is successfully captured by photocrosslinking, converting the weak physical gel into a self-supporting chemical gel. Formation of the water channel confined crosslinks serves to reinforce and

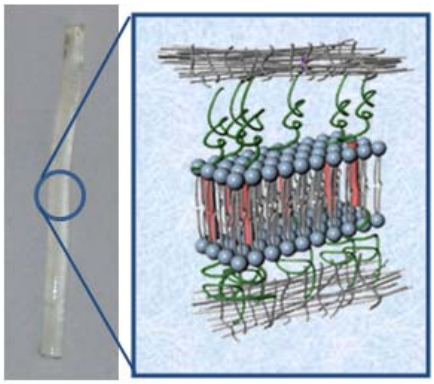

Figure 1. Photocrosslinking of water-channel confined acrylate moieties in a self-assembled complex fluid generates a structure stabilizing artificial cytoskeleton producing a mechanically robust hydrogel. Photo (left). Schematic illustration of SAXS determined structure (right).

stabilize the amphiphile bilayer, functioning as a primitive cytoskeleton mimic. The synthetic approach yields a material that possesses stacks of well-hydrated bilayers that have the thickness (~45 Å) suitable to accommodate the trans-insertion of membrane proteins. The facile production of a material that more closely resembles the chemical composition and internal architecture of natural biomembranes represents a key step towards producing an alternative to polymer hydrogels, produced by phase segregated block copolymers which have bilayers of considerably larger thickness (2 to 3 times that of a lipid bilayer). The crosslinked complex fluid can be readily handled, exhibiting improved stability of fragile solid supported lipid bilayers. The enhanced stability of the crosslinked complex fluids is further demonstrated by the ability to re-hydrate the gels with recovery of structure. The lamellar gel structure is also retained upon exposure to organic solvents that do not solubilize the lipid component. Lastly, unlike prior work exploring the crosslinking of self-assembled lipids that frequently suffer from alterations in the bilayer structure due to the local stresses imposed by covalent coupling within a nanoconfined space/geometry, the crosslinking strategy reported herein is found to successfully capture the physical gel lamellar architecture. Thus, our work shows that introduction of a chemically end-derivatized block copolymer intercalated within the organized lipid bilayer can successfully convert the labile architecture (i.e., the physical gel) into a more permanent material (i.e., chemical gel) without detriment to the self-assembled structure presumably by confinement of the crosslinks to within a large intervening water layers. The hierarchically structured hydrogel will offer opportunities for use as a durable platform for sequestering lipophilic and possibly water-soluble guests (proteins) into the segregated domains. The unperturbed lipid bilayer should readily permit transmembrane insertion of proteins.

Functional (electronic) coupling of proteins. A second thrust of the program is centered on synthetic modification of the soft materials to allow for successful biotic-abiotic functional integration. This component of the program seeks to develop functional electronic interfaces for harnessing protein output (e.g., light-generated electron flow). Two materials which achieve direct electronic communication to recessed protein prosthetic groups and function as bulk electronic conductors are under development[2-4]. The first material is a Au-nanoparticle (NP)-poly(ionogel), Au NP-poly[$C_{10}VIm^+$][Cl^-], composite that contains surface-exposed metal nanoparticles for facilitated direct electronic communication to buried redox centers of a protein [4]. The bulk, multidimensional Au NP-polymer composite was prepared by self-assembly of a vinyl ionic liquid monomer, [$C_{10}VIm^+$][Cl^-], in an aqueous solution of a Au ion precursor ($AuCl_4^-$), followed by UV irradiation.

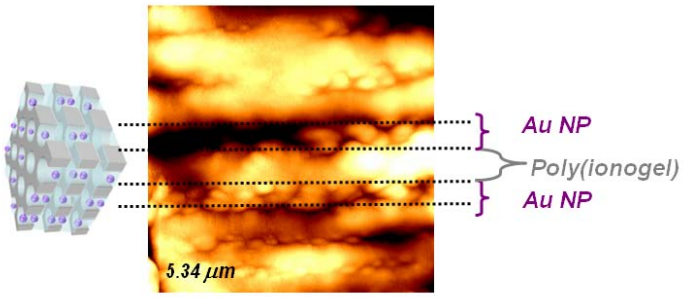

Figure 2. Au NP-poly(ionic liquid) composite. Schematic illustration of SAXS determined structure (left). Topographic AFM image of a composite prepared with low Au^{3+} concentration. Image shows incomplete filling of Au NPs within the water channels (right).

Topographic AFM images confirm the perforated lamellar composite architecture determined by SAXS and further show that the *in situ* synthesized Au NPs are localized within the hydrophilic (water) domains of the structure (Figure 2). At the highest Au NP content examined two component transport was observed, arising from a combination of ionic conduction from the IL polymer and electronic conduction mediated by the tightly-coupled, (packed) encapsulated Au nanoparticles. Electronic conduction due to aggregated Au NPs was further confirmed by dc conductivity measurements. In addition, the open porous structure allows for electrolyte accessibility and exposure of the Au nanoparticles thereby serving to facilitate direct electron transfer to the adsorbed electro-active proteins.

The second proteo-compatible electronic conductor was based upon a π-conjugated poly(ionogel) that contains a unique reactive moiety for site-specific electronic wiring to a protein. Specifically, electro-oxidative polymerization of a bifunctional monomer possessing both vinyl and thienyl groups appended to an alkylimidazolium-based ionic liquid yielded a liquid-crystalline, poly[3-VImC_{10}O-4-MThienyl$^+$][Br^-] polymer [2,3]. Cyclic voltammetry (CV) determined the polymer oxidation potential (1.66 V) and electrochemical band gap, E_g, (2.45 eV). The polymer was found to exhibit electrochromism, converting from yellow in the neutral form (λ_{max} = 380 nm) to blue in the polaronic state at 0.6 V (λ_{max} = 672 nm) and to blue-grey in the bipolaronic state at 1.2 V (λ_{max} > 800 nm). Topographic AFM images reveal isolated (separated) fibrils. Grazing incidence small-angle X-ray scattering (GISAXS) studies indicate a lamellar structure with a lattice spacing of 3.2 nm. Wide-angle X-ray diffraction studies further suggest that the polymerized thiophene sheets are oriented perpendicular to the polymerized vinylimidazolium. The electrical conductivity, as determined by four-probe d.c. conductivity measurements, was found to be 0.52 S/cm in the neutral form and 2.36 S/cm in the iodine-doped state, values higher than typically observed for polyalkylthiophenes. The structural ordering is believed to contribute to the observed enhancement of the electrical conductivity. A reactive moiety (haloalkane) for covalent coupling to a cysteine amino acid residue present on the exterior surface of a protein has been introduced onto poly[3-VImC_{10}O-4-MThienyl$^+$][Br^-] via a post-modification procedure. Specifically, an allylic bromine was installed at the methyl group position on the thiophene ring through a Wohl-Ziegler bromination reaction, producing poly[3-VImC_{10}O-4-MBrThienyl$^+$][Br^-]. The development of proteo-compatible electronic materials for charge / electron management between conventional materials and proteins is a critical step for harnessing a biomolecule's ability to perform efficient energy transduction.

Future Plans

Self-healing or repairable polymers is an area of growing research activity. During the next funding cycle we will direct significant effort to the development of synthetic strategies for incorporating reversible crosslinks that will allow for removal and replacement or repair of damaged (misfolded, denatured) proteins. It is well established that the functional lifetime of proteins are finite. In order to "repair" the materials it will be necessary to remove inactive protein from the bilayer and reconstitute with active protein. Our initial efforts will be directed at the development of reversibly crosslinked complex fluids under biological conditions (e.g., in water at mild temperatures, free of

metal catalyst and in presence of delicate proteins). As a starting point for these studies we will employ a modification of the synthetic strategy previously used to prepare the acrylate crosslinked complex fluids. For example, a furan end-derivatized PEO-PPO-PEO macromer will be synthesized and introduced into a lamellar structured lipid-based complex fluid. The thermally-initiated crosslinking of the appended furan moieties with a water-soluble co-macromer, bismaleimide PEG will be studied. Once conditions have been optimized to form a durable, self-supporting structured gel, evaluation of conditions for uncrosslinking (retro-Diels-Alder reaction) will be studied. Recent reports describing diene and dieneophile modifications that serve to significantly reduce the temperature requirements for thermoreversible bond formation as well as permit photoreversible linkages will be evaluated. This component of the research program seeks to introduce sophisticated biomimetic regenerative properties within soft materials. Ultimately, it may be possible to not only extract and replace inactive proteins but to also mimic the cell's elaborate machinery that detects and re-folds partially denatured proteins. This component of the research program is important for increasing the operational lifetime of protein-based materials for energy conversion.

DOE Sponsored Publications in 2011-2009

1. Grubjesic, S.; Lee, B.; Seifert, S.; Firestone, M.A. "*Preparation of a self-supporting cell architecture mimic by water channel confined photocrosslinking within a lamellar structured hydrogel*" *Soft Matter* invited for special issue on Biomimetic Soft Matter (2011) DOI:10.1039/c1sm06364b. In press.
2. Becht, G. A.; Sofos, M.; Seifert, S.; Firestone, M. A., "*Formation of a liquid-crystalline interpenetrating poly(ionic liquid) network hydrogel"*, *Macromolecules* (2011), 44(6), 1421-4128 .
3. Becht, G. A.; Lee, S.; Seifert, S.; Firestone, M. A. "*Solvent tunable optical properties of a polymerized vinyl and thienyl substituted ionic liquid*", *J. Phys. Chem. B* (2010), 114(45), 14703-14711.
4. Lee, S. Becht, G. A.; Lee, B.; Burns, C. T.; Firestone, M. A., "*Electropolymerization of a bi functional ionic liquid monomer yields an electroactive liquid-crystalline polymer*." *Adv. Func. Mater.* (2010), 20(13), 2063-2070. Cover of July 9, 2010 issue.
5. Green, O.; Grubjesic, S.; Lee, S.; Firestone, M. A. "*The design of polymeric ionic liquids for the preparation of functional materials*", *Polymer Reviews*. (2009), 49(4), 339-360. Invited review article.
6. Lee, S.; Cummins, M. D.; Willing, G. A.; Firestone, M. A. "*Conductivity of ionic liquid-derived polymers with internal gold nanoparticle conduits*". *J. Mater. Chem*. (2009), 19(43), 8092-8191. Cover of November 21, 2009 issue.
7. Crisci, A.; Hay, D. N. T.; Seifert, S.; Firestone, M. A. "*pH and ionic strength-induced structural changes in poly(acrylic acid)-lipid based self-assembled materials*, *Macromol. Symp*. (2009), 281(1), 126-134.
8. Grubjesic, S.; Seifert, S.; Firestone, M. A. "*Cytoskeleton mimetic reinforcement of a self-assembled N,N'-Dialkylimidazolium ionic liquid monomer by copolymerization*", *Macromolecules* (2009), 42(15), 5461-5470.

Task Title: Protein Biotemplates for Self-Assembly of Nanostructures

Investigators: Sarah Heilshorn, Nicholas Melosh, Seb Doniach, and Andrew Spakowitz
476 Lomita Mall, McCullough 246, Stanford University, Stanford, CA 94305. Heilshorn@stanford.edu

Program Scope: Self-assembly has become a powerful method to create highly-ordered structures with spatial and temporal patterning on two-dimensional substrates. However, the divide between our current technological capabilities and the power demonstrated by biological systems to assemble both organic and inorganic species into intricate three-dimensional structures is still vast. The ultimate goal of this program is to identify the necessary combination of assembly mechanisms and building-block properties for deterministic formation of complex three-dimensional organic/inorganic constructs. By appropriate selection of architecture, materials, and morphology; these materials will lead to fundamentally new designs for bio-inorganic devices for energy storage, catalysis, and fuel cells. This collaborative effort has focused on the remarkable self-assembling protein, clathrin. Clathrin is composed of three-armed "triskelion" monomers, with three-fold symmetry, semiflexible arms, and specific binding sites for adaptor peptide sequences. Clathrin is a highly unusual self-assembling material, as it occurs naturally in 2-D sheets, 3-D cubes, tetragons, and geodesic spheres. Because of the rich diversity of structure and dimensionality, clathrin is an ideal model for understanding how natural systems controllably transform from inherently two-dimensional materials into the third dimension. Our program is designed to demonstrate clathrin as a controllable 2-D and 3-D assembly system, identify the key self-assembly characteristics that make it successful, and finally template inorganic species to the clathrin networks.

Recent Progress:

1. Formation and characterization of two-dimensional clathrin assemblies at lipid monolayers. Clathrin assembly on 2-D surfaces is an important window into the design and organization principles of biologically-evolved self-assembling structures. In the cell, clathrin is recruited to the membrane, where it rapidly forms 2-D networks, which may rely solely upon clathrin triskelia as structure directing agents or involve an assembly promoter such as a rigid protein raft. Understanding clathrin network formation dynamics may yield new insights into rapid assembly of highly organized and self-healing systems. Through surface shear rheology and surface pressure measurements on clathrin at lipid monolayers, we discovered that clathrin is initially recruited to the lipid surface through interactions with PIP2 lipids, where it diffuses laterally. As more triskelia add to the lipid, the surface pressure increases while the shear modulus remains low, indicating the clathrin are either individual molecules or small, non-interconnected clusters, Fig 1. As the surface pressure passes a threshold value of ~65% of the maximum, the shear modulus increases rapidly. This observation fits well with percolation theories for hexagonal networks, which predict spanning clusters will form at a threshold concentration of 65%. A power-law percolation model fits the network viscoelasticity data quite well, indicating that in this ideal system, clathrin assembles by cluster formation and growth. This picture agrees with our simulations, which show similar cluster formation.

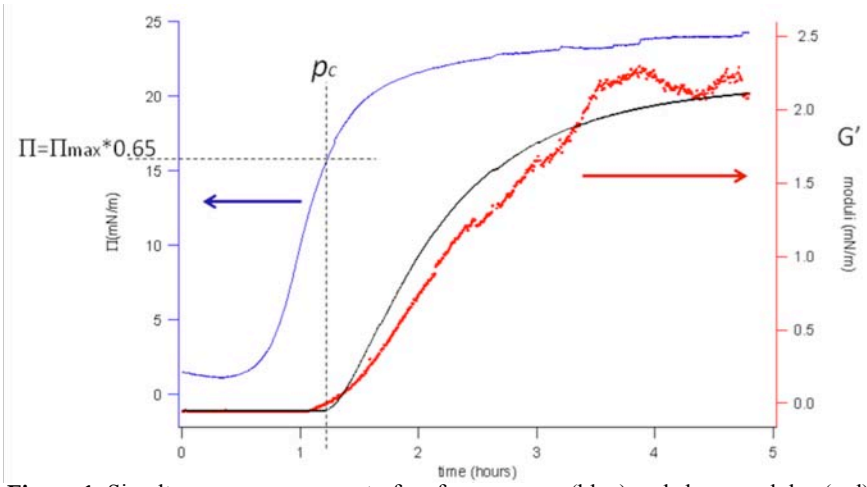

Figure 1. Simultaneous measurement of surface pressure (blue) and shear modulus (red) of clathrin at a lipid monolayer. The bond percolation threshold for a hexagonal network is marked p_c. Beyond this point, the surface moduli increases and can be approximated by simple percolation theory (black).

Clathrin interactions with a lipid monolayer were also studied using synchrotron x-ray liquid surface scattering techniques, aided by tagging clathrin with gold nanoparticles via the W-box binding domain, Fig 2. Reflectivity data showed protein binding induces membrane thickening and surface roughening as evidenced by fits to the reflectivity data and the increased fall-off against the Fresnel curve after addition of protein. This roughening is likely from clathrin induced membrane curvature and is also implicated by increased diffuse scattering from GIXD scans.

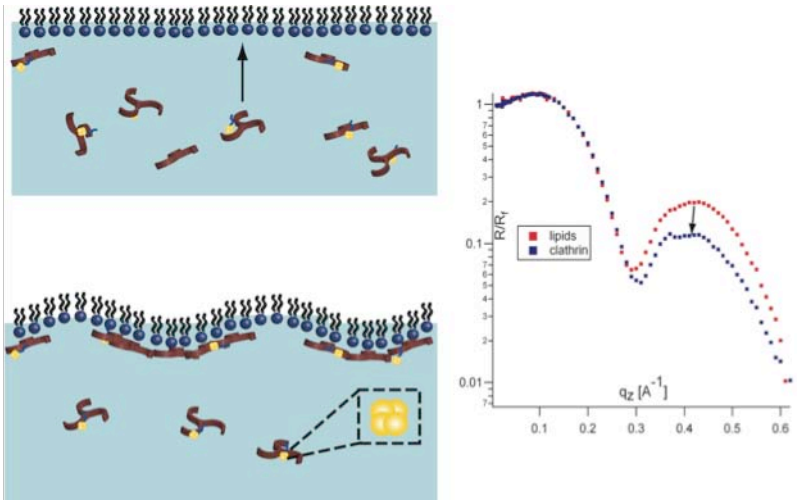

Figure 2. GIXD of 2-D clathrin assembly on lipid monolayers demonstrates membrane thickening upon clathrin binding.

2. Modeling of 2-D clathrin assemblies demonstrating the importance of molecular elasticity. We developed a detailed, mesoscale theoretical model that incorporates molecular flexibility of the clathrin triskelion to demonstrate thermodynamics and kinetics of clathrin self-assembly. The clathrin triskelia were modeled as flexible pinwheels that form leg-leg associations and resist bending and stretching deformations. We used our theoretical model in Brownian dynamics simulation to track the motion of clathrin pinwheels at sufficiently long time scales, and used Monte Carlo simulation to demonstrate clathrin self-assembly morphologies at thermodynamic equilibrium conditions, Fig 3. Invoking theories of dislocation-mediated melting in two dimensions, we illustrated the phase behavior for clathrin self-assembly. Our results show the pivotal role that molecular elasticity plays in the physical behavior of self-assembling and self-healing materials.

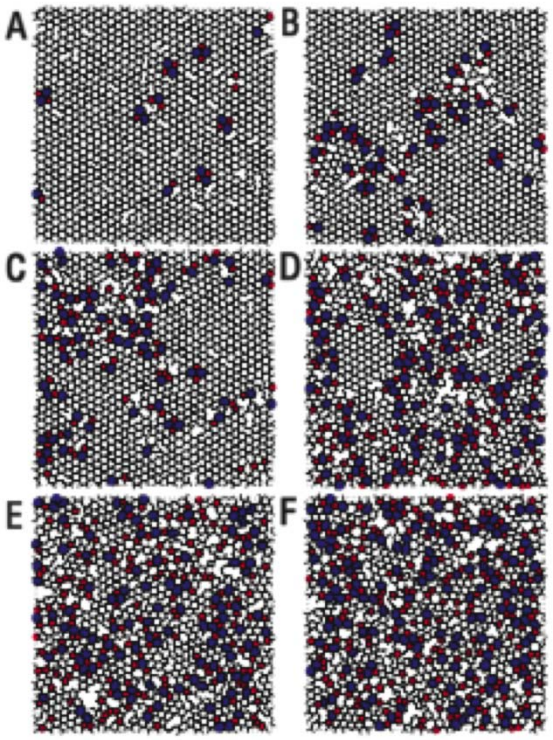

Figure 3. Monte Carlo simulation of a self-assembled clathrin lattice demonstrating the effect of elasticity on large-scale structural fluctuations. To locate defects, pentagons and heptagons are shown in red and blue, respectively. Here, bk_sr^2 = 85 (A), 75 (B), 70 (C), 65 (D), 60 (E), and 55 (F) and $bk_b = bk_sr^2 = 10$, where $b = 1/k_BT$. T is temperature, r is pinwheel leg length, and k_s and k_b are stretching and bending stiffness.

3. Formation and characterization of three-dimensional clathrin assemblies. We examined short-term kinetics and long-term stability of clathrin assemblies using a combination of dynamic light scattering (DLS) and cryo-transmission electron microscopy (TEM). A systematic DLS study of cage assembly dependence on pH and salt concentration has yielded results that can be directly compared with the 3-D model of clathrin assembly to generate a phase diagram for 3-D clathrin nanostructures, Fig 4a, b. In general, assembly induced by lower pH (5.1-5.4) results in larger assemblies that persist over 24 hours. These larger assemblies undergo remodeling to reach a stable assembly with hydrodynamic radius ~150

nm after 5 days. In contrast, solutions at higher pH (6.6-6.9) show negligible assembly after 24 hours, but reach a similarly-sized final assembly with hydrodynamic radius ~150 nm after 5 days.

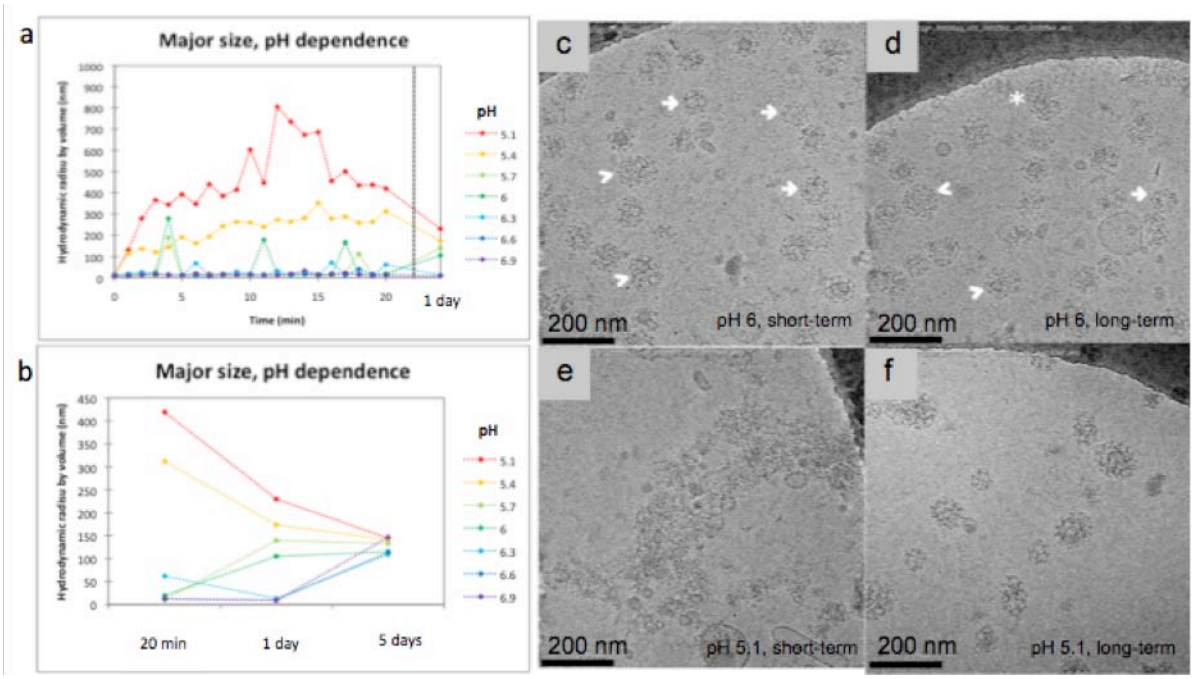

Figure 4. a) Short-term kinetics of clathrin cage assembly by dynamic light scattering. Radius of hydration (nm) is plotted versus time. b) Long-term stability of clathrin cage assemblies shown in a). Cryo-TEM images of clathrin assemblies at pH 6 (c,d) and pH 5.1 (e,f) at 20 minutes (c,e) and 4 days (d,f). Arrows, arrow heads, and asterisks in c) and d) indicate cages of different sizes.

Cryo-TEM experiments were carried out in collaboration with Prof. Roger Kornberg's laboratory to understand the aggregation states of clathrin at different pH. On initiating self-assembly of clathrin at pH 6, 65-95 nm clathrin cages were observed after 20 min and were stable over a period of days, Fig 4c, d. At pH 5.1, clathrin triskelia form very large aggregates greater than 200 nm in size, Fig 4e. After 4 days at room temperature, these large clathrin aggregates rearrange into smaller clathrin cages, Fig 4f. These results correspond nicely with the DLS observations and demonstrate that clathrin self-assembly is a highly dynamic process, opening up the possibility of tuning the assembly reaction to produce novel nanostructures that are kinetically trapped assemblies.

4. Modeling of three-dimensional clathrin assemblies. Our 3-D pinwheel model exhibits cage formation upon sudden increase of leg-leg associations showing a qualitative agreement between the size distribution of assembled cages obtained from simulation results and dynamic light scattering data. We have used our 3-D theoretical model in Brownian dynamics simulation to understand the thermodynamics and kinetics of self-assembly in 3-D, Fig 5. These simulations have been utilized to calculate the radius of gyration of assembled cages and to predict the kinetics and polydispersity of assemblies. Current efforts are underway to compare cage sizes obtained from simulation with experimental dynamic light scattering and cryo-TEM results. Further work will be done to determine appropriate experimental parameters for the formation of novel 3-D nanostructures and kinetically trapped states to guide additional DLS and cryo-TEM experiments.

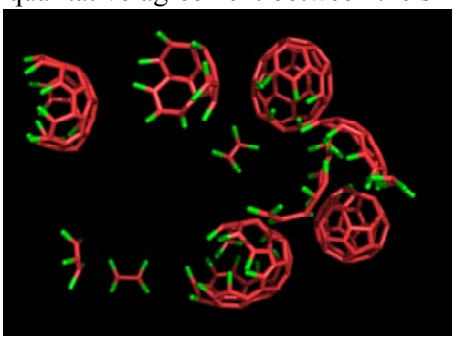

Figure 5. Snapshot from 3-D simulation of clathrin self-assembly. Bound clathrin legs are shown in red; free legs are in green.

5. Use of 3-D clathrin assemblies for inorganic templating. We designed bi-functional peptide linkers to functionalize clathrin molecules for interaction with inorganic materials through the clathrin box epitope recognition site on the clathrin N-terminal domain. We have demonstrated the flexibility of our novel non-covalent, site-specific method to bridge the interface between proteins and two classes of other materials: metal oxides and noble metals, including titanium dioxide, cobalt oxide, and gold.

Clathrin cage assemblies were covalently crosslinked with paraformaldehyde before incubation with an inorganic-nucleating peptide of choice. Mixing fixed clathrin cages with the titania-nucleating peptide and subsequent addition of titanium (IV) bis(ammonium lactato) dihydroxide (TiBALDH) generated crystalline nanoparticles of anatase titanium dioxide with an average diameter of 160 nm at ambient conditions, Fig. 6a. Addition of cobalt chloride and sodium borohydride as a reducing agent to a solution of cages and cobalt oxide-nucleating peptide resulted in amorphous cobalt oxide nanoparticles with a scalloped morphology and an average diameter of 55 nm, Fig 6b. To extend the demonstration to noble metals, chloroauric acid was added to a solution of cages and gold-nucleating peptide and the reaction proceeded overnight in the dark to prevent photoreduction. Without any added reducing agent, the reaction yielded polycrystalline, round gold nanoparticles with an average diameter of 20 nm, Fig 6c. Reaction products were analyzed using high resolution TEM, diffraction pattern analysis, and energy dispersive spectroscopy (EDS).

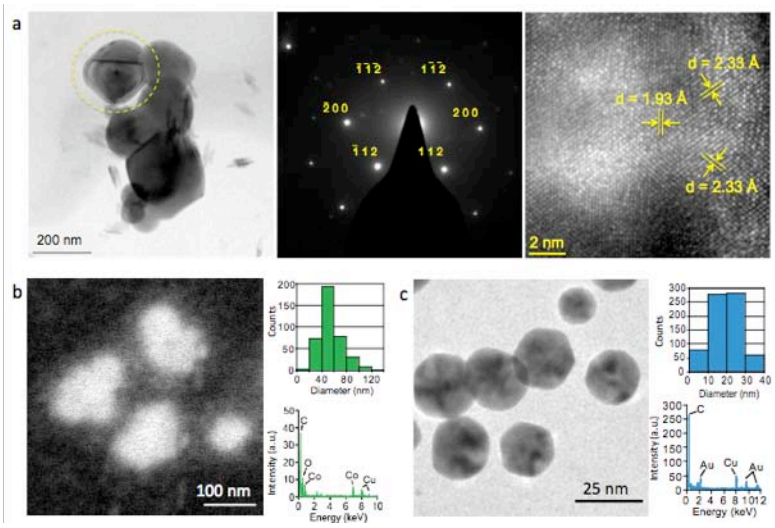

Figure 6. a) Bright field TEM, diffraction pattern analysis, and high-resolution TEM of templated single crystalline titanium dioxide nanoparticles. b) Scanning dark field TEM of templated cobalt oxide nanoparticles, size distribution, and EDS spectrum. c) Bright field TEM of templated gold nanoparticles, size distribution, and EDS spectrum.

Future Plans:

- Extend our 2-D clathrin model to address assembly on a f luctuating membrane. Goals include combining simulations and analytical theory to develop a phase diagram for interfacial assembly.
- Develop protocols for combined use of multiple peptide binding sites within clathrin cage assemblies to generate composite nanomaterials with site-specificity.
- Evaluate our 3-D clathrin simulations based on classical nucleation and growth theory, interpreting assembly-size distributions as kinetic trapping of clusters.
- Design hetero-assembling peptide linkers to induce hierarchical assembly of biologic/inorganic nanoparticles into self-healing networks.

Publications:

1. Mehraeen S, Cordella N, Yoo JS, Spakowitz AJ. *Impact of defect creation and motion on the thermodynamics and large-scale reorganization of self-assembled clathrin lattices*, **Soft Matter**, 2011, in press.
2. Schoen AP, Heilshorn SC. *TEThER: A flexible mix and match system for protein-based biotemplating.* **American Chemical Society Proceedings, Division of Polymer Chemistry**, 2010, POLY-126, August 22-26, Boston, MA.
3. Ali M, Lipfert J, Seifert S, Herschlag D, Doniach S. *The Ligand-Free State of the TPP Riboswitch: A Partially Folded RNA Structure.* **Journal of Molecular Biology**, 2010, 396(1): 153-165.

Molecular Nanocomposites
Biotic/Abiotic Interfaces, Materials, and Architectures

Bryan Kaehr[1,2], C. Jeffrey Brinker[1,2], Jason Townson[2], Eric C. Carnes[2], and Carlee Ashley[1]
[1] Sandia National Laboratories, [2] The University of New Mexico
Advanced Materials Lab, 1001 University Blvd SE, Albuquerque, NM 87106
cjbrink@sandia.gov
http://www.unm.edu/~solgel

Program Scope - Our bio-molecular nanocomposites research focuses on two complementary, interrelated goals: 1) the use of living cells and biomolecular-interfaces to direct the formation of new classes of complex, symbiotic, hierarchical materials with life-like functionality and 2) the use of cell-directed and lithographically defined biomolecular materials and architectures to understand and direct cellular behavior. Our work builds on three key biomolecular nano-to-micro fabrication strategies developed by our team: evaporation-induced self-assembly, its extension to cell directed assembly, and multi-photon protein lithography.

Recent Progress

Cell-Directed Integration into Three-Dimensional Lipid-Silica Nanostructured Matrices - We have continued to study a unique approach wherein living cells direct their integration into 3D solid-state nanostructures. Yeast cells deposited on a weakly condensed lipid/silica thin film mesophase are observed to actively reconstruct the surface to create a conformal, fully 3D bio/nano interface, composed of localized lipid bilayers enveloped by a lipid/silica mesophase. During the past year we demonstrated that this 'silicification' results via a self-catalyzed silica condensation process resulting from an osmotic stress response of the yeast that causes a localized pH gradient, along with cell surface protein-directed silica deposition. The role of proteins in silica deposition has been studied extensively in the context of biomineralization – our observation of cell-directed silica deposition prompted the recent follow-on study described below.

Cell Replication *in silico* - Natural bioinorganic composites as found in bone, shell, and diatoms have long been heralded as model functional materials that evolved over billions of years to optimize properties and property combinations. Often functionality derives from hierarchical architectures composed of hard and soft components organized according to multiple prioritized length scales. To date it has been difficult to mimic these multiscale designs in synthetic manmade materials. In our molecular nanocomposites program we have developed synthetic strategies that mimic features of the natural silica depositing system of diatoms, single celled organisms that are known to construct exquisite and elaborate silica composite exoskeletons. Although there has been significant progress towards an understanding of the molecular components involved in biogenic silica formation, the whole picture remains vague, as evidenced by a current inability to reproduce diatom-like silica features *in vitro* using synthetic or native silica-associated biomolecules. Diatom silica biosynthesis is clearly a process by

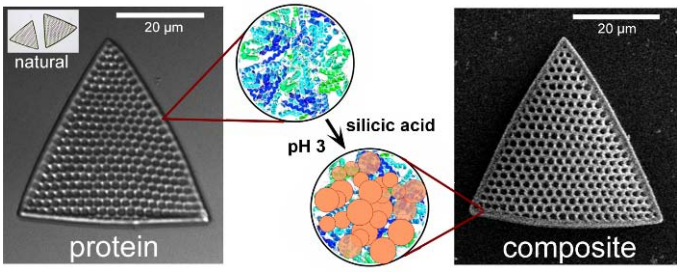

Fig. 1. Protein hydrogels comprised of cross-linked proteins were microfabricated using MPL. Incubation in silicic acid resulted in a c omposite that retained template features following calcination.

which the chemical microenvironment is tightly controlled through compartmentalization and transport. Taking lessons from nature concerning silica morphogenesis within the acidic diatom silica deposition vesicle (SDV), we wondered if a mildly acidic and highly crowded and confined macromolecular scaffold would prove sufficient for silica deposition.

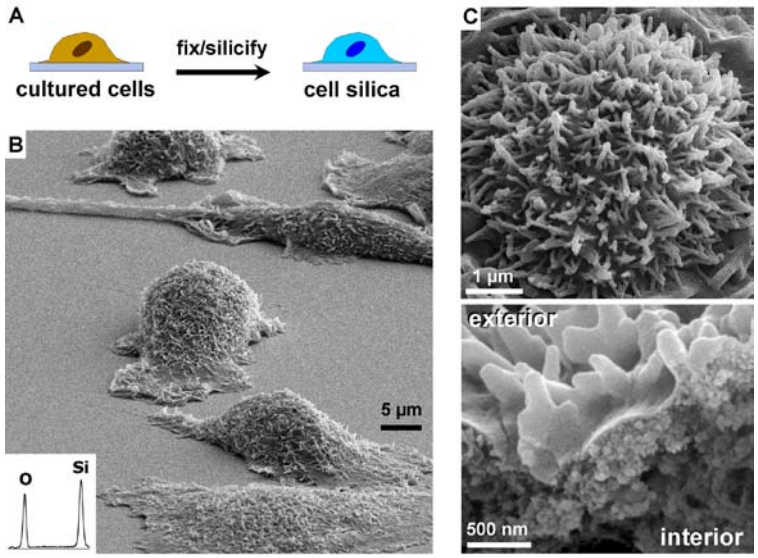

Fig. 2. (A, B) Cultured mammalian cells (ASPC1 pancreas cells) were found to undergo (intracellular) silicification (C) using methods similar to those used for protein hydrogels. Cell/silica composites (CSCs) retained cellular features even following calcination.

To test this hypothesis, we used multiphoton lithography (MPL) to fabricate protein hydrogel scaffolds. This technique enables microstructures comprised of proteins of choice to be fabricated with arbitrary 3D geometries. We observed that under dilute acidic conditions these scaffolds direct their precise replication to form silica/protein biocomposites with preserved feature sizes that survive calcination (Figure 1). Importantly, proteins of diverse properties (e.g., isoelectric point; pI) directed silica condensation under identical solution conditions, which is to some extent contrary to the existing paradigm that cationic species (e.g., proteins with pI > 7) are necessary for *in vitro* silica condensation/ deposition. These protein hydrogels are highly concentrated (> 40% protein by wt vol^{-1}) producing a locally crowded molecular environment, which acts to capture and concentrate silica precursors (mono-, oligo-silicic acid, and nanoparticles) via hydrogen bonding and other non-covalent interactions.

Based on these results, we considered that cells are composed of elaborate and functional protein scaffolds and surfaces that are organized over multiple length scales. Could these natural protein architectures also direct silica deposition under similar chemical conditions? To address this question we fixed cells (in this case a mammalian cancer cell line, but any cells can be used) and treated them with dilute acidic silica solutions as for proteins. We observed that all cellular features are preserved with very high fidelity under what appears to be a self-limiting process (Fig. 2).

The cell/silica composites (CSCs) preserve the original cellular structure upon evaporation (and calcination), whereas the parent cells without silica lose their shape and surface features upon drying (Fig. 3). Since cells when detached from the substrate are approximately spherical and monosized, silica cell composites can be prepared as nearly

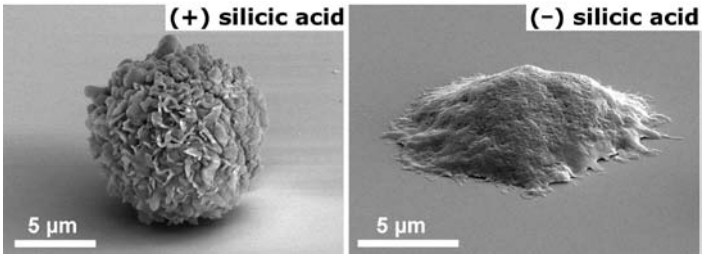

Fig. 3. Cell silicification (HTB77 ovarian cells) produces a mechanically stable composite resistant to deformation upon drying.

monodisperse powders in large scale batch operations (Fig. 4).

The silica condensation in CSCs is directed via hydrogen bonding and other non-covalent interactions with proteins organized throughout the cell. Thus the resultant biocomposite does not perturb the protein secondary and tertiary structure. This allows at least a subset of biocatalytic enzymatic activity to be preserved in CSCs. Additionally the silica cell surface can be reconstituted with a lipid bilayer membrane. Together this construct has a number of protocellular features. Fig. 4B shows enzymatic esterase activity can be monitored by fluorescence via a standard 'viability' probe.

We have shown both a manmade (lithographic) and a cell-directed approach to form hierarchical 3D bioinorganic composites. These approaches can be adapted to other chemistries (e.g. titania), and silica structures can be transformed to semiconductors (e.g. silicon). As in diatoms, the silica serves to protect the internal biomolecular components. Preserved and possibly enhanced enzymatic activity could be useful for sensing, catalysis, decontamination, and energy conversion, and the composite may exhibit combined toughness, hardness, and light weight associated with natural biocompositess like nacre.

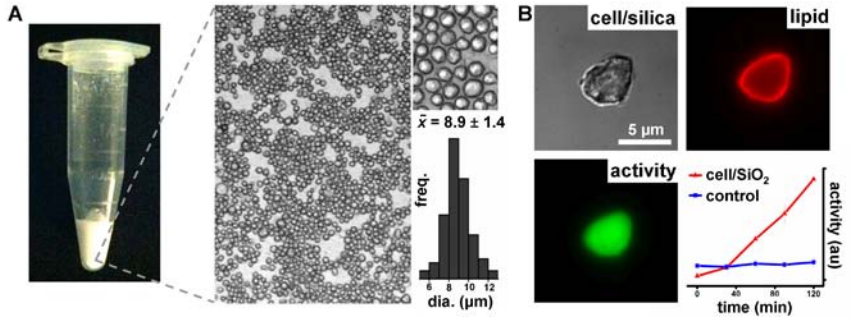

Fig. 4. (A) Silicification of cells (4T1 breast cells) in solution leads to monosized particles through a s calable process. (B) A lipid bilayer is reconstituted on a c ell/silica particle and shows accumulation of esterase fluorogenic products (red line). The blue line shows activity of calcined CSCs supporting lipid bilayers.

The high fidelity silica templating of the complete heterogeneity of surface and intracellular features via a s elf-limiting process shown here, to some extent, contradicts a general theme amongst the biomolecular community that molecular specificity is a key requirement for both directed *in vitro* and natural biomineralization processes. Based on our findings, we feel that the contribution of non-covalent (scaffolding) interactions governing silica biomineralization deserves greater attention.

Future Plans

CSCs represent a new and exciting discovery with implications for a spectrum of advanced materials as well as biopreservation. They should provide a foundation for biomineralization studies using tractable models. Multiple options of cell choice and silicification procedures remain to be explored in order to achieve maximum CSC functionality, environmental stability, and broad application. Customization of CSCs using genetic and chemical engineering will be explored to develop robust materials for desired applications. In an effort to extend preservation to multicellular systems (tissues, organs) and ultimately organisms, we will investigate SCR using model organisms (e.g., *C. elegans*) to understand the effects of precursor diffusion and cell-cell interactions on preservation and reactivation.

Publications

1. Zarzar LD, Kim P, Kolle M, Brinker CJ, Kaehr B. 2011. Direct Writing and Actuation of Three Dimensionally Patterned Hydrogel Pads on Micropillar Supports. Angewandte Chemie International Edition. DOI: 10.1002/anie.201102975

2. Xiong S, Molecke R, Bosch M, Schunk PR, Brinker CJ. 2011. Transformation of a Close-Packed Au Nanoparticle/Polymer Monolayer into a Large Area Array of Oriented Au Nanowires via E-beam Promoted Uniaxial Deformation and Room Temperature Sintering. Journal of the American Chemical Society 133: 11410-3
3. Khripin CY, Pristinski D, Dunphy DR, Brinker CJ, Kaehr B. 2011. Protein-Directed Assembly of Arbitrary Three-Dimensional Nanoporous Silica Architectures. ACS Nano 5: 1401-9
4. Harper JC, Lopez DM, Larkin EC, Economides MK, McIntyre SK, Alam TM, Tartis MS, Werner-Washburne M, Brinker CJ, Brozik SM, Wheeler DR. 2011. Encapsulation of S. cerevisiae in Poly(glycerol) Silicate Derived Matrices: Effect of Matrix Additives and Cell Metabolic Phase on Long-Term Viability and Rate of Gene Expression. Chemistry of Materials 23: 2555-64
5. Dunphy DR, Garcia FL, Kaehr B, Khripin CY, Collord AD, Baca HK, Tate MP, Hillhouse HW, Strzalka JW, Jiang Z, Wang J, Brinker CJ. 2011. Tricontinuous Cubic Nanostructure and Pore Size Patterning in Mesostructured Silica Films Templated with Glycerol Monooleate. Chemistry of Materials 23: 2107-12
6. Dunphy DR, Garcia FL, Jiang Z, Strzalka J, Wang J, Brinker CJ. 2011. X-Ray characterization of self-assembled long-chain phosphatidylcholine/bile salt/silica mesostructured films with nanoscale homogeneity. Chemical Communications 47: 1806-8
7. Baca HK, Carnes EC, Ashley CE, Lopez DM, Douthit C, Karlin S, Brinker CJ. 2011. Cell-directed-assembly: Directing the formation of nano/bio interfaces and architectures with living cells. Biochimica et Biophysica Acta (BBA) - General Subjects 1810: 259-67
8. Ashley CE, Dunphy DR, Jiang Z, Carnes EC, Yuan Z, Petsev DN, Atanassov PB, Velev OD, Sprung M, Wang J, Peabody DS, Brinker CJ. 2011. Convective Assembly of 2D Lattices of Virus-like Particles Visualized by In-Situ Grazing-Incidence Small-Angle X-Ray Scattering. Small 7: 1043-50
9. Ashley CE, Carnes EC, Phillips GK, Padilla D, Durfee PN, Brown PA, Hanna TN, Liu J, Phillips B, Carter MB, Carroll NJ, Jiang X, Dunphy DR, Willman CL, Petsev DN, Evans DG, Parikh AN, Chackerian B, Wharton W, Peabody DS, Brinker CJ. 2011. The targeted delivery of multicomponent cargos to cancer cells by nanoporous particle-supported lipid bilayers. Nat Mater 10: 389-97
10. Ashley CE, Carnes EC, Phillips GK, Durfee PN, Buley MD, Lino CA, Padilla DP, Phillips B, Carter MB, Willman CL, Brinker CJ, Caldeira JdC, Chackerian B, Wharton W, Peabody DS. 2011. Cell-Specific Delivery of Diverse Cargos by Bacteriophage MS2 Virus-like Particles. ACS Nano, 5, 5729–45
11. Xiong SS, Miao XY, Spencer J, Khripin C, Luk TS, Brinker CJ. 2010. Integration of a Close-Packed Quantum Dot Monolayer with a Photonic-Crystal Cavity Via Interfacial Self-Assembly and Transfer. Small 6: 2126-9
12. Moghaddam S, Pengwang E, Jiang YB, Garcia AR, Burnett DJ, Brinker CJ, Masel RI, Shannon MA. 2010. An inorganic-organic proton exchange membrane for fuel cells with a controlled nanoscale pore structure. Nature Nanotechnology 5: 230-6
13. Khripin CY, Brinker CJ, Kaehr B. 2010. Mechanically tunable multiphoton fabricated protein hydrogels investigated using atomic force microscopy. Soft Matter 6: 2842-8
14. Kendall EL, Mills E, Liu JW, Jiang XM, Brinker CJ, Parikh AN. 2010. Salt-induced lipid transfer between colloidal supported lipid bilayers. Soft Matter 6: 2628-32
15. Kaehr B, Brinker CJ. 2010. Using bacterial cell growth to template catalytic asymmetry. Chemical Communications 46: 5268-70
16. Jiang XM, Ward TL, Cheng YS, Liu JW, Brinker CJ. 2010. Aerosol fabrication of hollow mesoporous silica nanoparticles and encapsulation of L-methionine as a candidate drug cargo. Chemical Communications 46: 3019-21
17. Jiang XM, Brinker CJ. 2010. Rigid templating of high surface-area, mesoporous, nanocrystalline rutile using a polyether block amide copolymer template. Chemical Communications 46: 6123-5
18. Harper JC, Khirpin CY, Carnes EC, Ashley CE, Lopez DM, Savage T, Jones HDT, Davis RW, Nunez DE, Brinker LM, Kaehr B, Brozik SM, Brinker CJ. 2010. Cell-Directed Integration into Three-Dimensional Lipid-Silica Nanostructured Matrices. ACS Nano 4: 5539-50
19. Chen Z, Jiang YB, Dunphy DR, Adams DP, Hodges C, Liu NG, Zhang N, Xomeritakis G, Jin XZ, Aluru NR, Gaik SJ, Hillhouse HW, Brinker CJ. 2010. DNA translocation through an array of kinked nanopores. Nature Materials 9: 667-75
20. Carnes EC, Lopez DM, Donegan NP, Cheung A, Gresham H, Timmins GS, Brinker CJ. 2010. Confinement-induced quorum sensing of individual Staphylococcus aureus bacteria. Nat Chem Biol 6: 41-5

Program Title: Molecularly Organized Nanostructural Materials

Principal Investigators: Jun Liu, Gregory J. Exarhos, Maria Sushko, Praveen Thallapally, Birgit Schwenzer, Xiaolin Li
Mailing Address: Battelle Boulevard, Pacific Northwest National Laboratory
Richland, WA 99352
Email Address: Jun.liu@pnl.gov

Program Scope

Nanomaterials with controlled micro- and nanoporosities, crystalline phases and structural ordering are important for energy storage, catalysis, and many other energy related applications. Great progress has been made in the literature in understanding of the biomolecular controlled nucleation and mineralization processes, and extensive study has been conducted on nucleation on two-dimensional substrate. Still, synthesis of well-controlled three-dimensional architectures with the desired functionality is a great challenge. The overall goal of this project is to understand and manipulate the interfacial reactions to control self-assembly and nucleation of complex nanomaterials for energy applications. In this project, we investigate the fundamental interactions involved in the nucleation on well-defined nanoscale building blocks, and use such building blocks to direct the self-assembly of more complex nanostructures. The project contains the following components:

- Manipulation of the kinetics of competing self-assembly and precipitation reactions
- Use of molecular ligands and interfaces to control nucleation and growth
- Multiscale modeling of the self-assembly process in solution
- Structure-property relationships for energy applications

Recent Progress

We are developing a new strategy to take advantages of the interfacial reactions in well-defined nanoscale building blocks to construct complex three-dimensional structures. We use molecularly dispersed graphene sheets as the template and nanoscale building block. We demonstrate that functionalized graphene sheets can act as a molecular template to control nucleation and self-assembly. Depending on the surface chemistry of the graphene sheets and the interactions with other constituents, a wide range of complex nanostructures are developed. First, we take advantage of the defect chemistry and the associated functional groups on graphene surfaces. These functionalized graphene sheets are synthesized through thermal oxidation and expansion, and the density of the defects can be systematically controlled. Through extensive computer modeling and electron microscopy study, we found that the defect chemistry controls the nucleation and growth of metal oxides and metals on the graphene surface. The surface chemistry also determines which crystalline phases are stabilized. Graphene-metal-metal oxide nanocomposite can be constructed using this approach with the metal nanoparticles stabilized in the triple junction points between graphene and metal oxides. Furthermore, the functional graphene sheets can be assembled into 3D hierarchical porous electrode for high performance Li-air batteries with the defect structure controlling the nucleation of the reaction products.

Recently, we also demonstrated that the graphene template can direct the self-assembly of high ordered structures such as highly crystalline mesoporous TiO_2. This is a good example of using 2D chemistry to form 3D nanostructures that are otherwise very difficult to synthesize under normal experimental conditions.

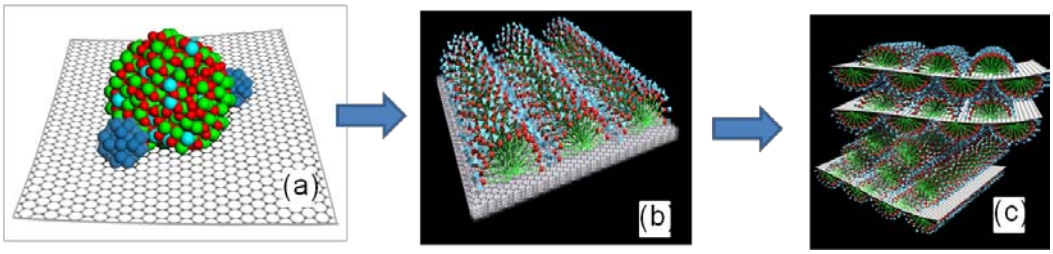

Figure 1. Functionalized graphene sheets as molecular directing template to control nucleation and self-assembly. (a) Defect controlled nucleation. (b) Surfactant self-assembly on garphene surfaces. (c) Three-dimensional self-assembly for functional nanocomposites.

Significance: The recent progress on this project has the potential to bridge the gap of two-dimensional crystallization and three-dimensional self-assembly, and the gap between microporous and nanoporous materials. First, we have proven that the surface chemistry (defects and functional groups) on the graphene surfaces controls nucleation and crystallization, as well the crystalline phases. We have further demonstrated that the 2d structures can be used as the building blocks to build complex 3D structures. In the past, self-assembled oxide materials are mostly limited to single phase materials and nanoparticle based systems. Our study points to a new direction for self-assembly using multiple phases and multilength building blocks. The materials developed under this project already demonstrated superior kinetics and stability for electrocatalysis in fuel cells, good performance in Li-ion and Na-ion batteries, and in Li-sulfur and Li-air batteries.

Future Plan: Our future plan will pursue further fundamental understanding of the molecular level interactions by developing and using state-of-the-art characterization and simulation tools. Specifically, we will use molecular simulation and surface sensitive spectroscopy techniques to investigate the molecular interaction of complex polymers and biomolecules such as DNA and protein molecules on graphene surfaces. The use of more complex molecules will provide more flexibility in synthesizing complex materials. Second, we will use DFT computer modeling and expand our recently developed in-situ transmission electron microscopy technique to investigate the nucleation mechanism of metal oxide, zeolite and nanoporous materials on graphene and other well-defined surfaces. Finally, we will greatly expand the range of complex materials that can be synthesized using our approach. Currently many other building blocks are available besides graphene sheets, such as carbon nanotubes, nanowires and nanorods, and ceramic nanoplates. Similar principles should apply for such nanoscale building blocks and will lead to truly multifunctional composite materials with controlled architectures.

Selected References (which acknowledge BES support):

1. J Tian, PK Thallapally, J Liu, GJ Exarhos, and JL Atwood. 2011. "Gas-Induced Solid State Transformation of an Organic Lattice: From Nonporous to Nanoporous." Chemical Communications 47(2):701-703.

2. Y Cao, L Xiao, W Wang, D Choi, Z Nie, J Yu, LV Saraf, Z Yang, J Liu, 2011, Reversible Sodium Ion Insertion in Single Crystalline Manganese Oxide Nanowires with Long Cycle Life, Advanced Materials, 23 (28) 3155-3160.
3. CM Wang, W Xu, J Liu, JG Zhang, LV Saraf, BW Arey, D Choi, ZG Yang, J Xiao, S Thevuthasan, DR Baer 2011. "In Situ Transmission Electron Microscopy Observation of Microstructure and Phase Evolution in a SnO_2 Nanowire during Lithium Intercalation." Nano Letters, 11 (5) 1874-1880.
4. Y Cao, X Li, IA Aksay, JP Lemmon, Z Nie, Z Yang, and J Liu. 2011. "Sandwich-Type Functionalized Graphene Sheet-Sulfur Nanocomposite for Rechargeable Lithium Batteries." Physical Chemistry Chemical Physics. PCCP, 13 (17) 7660-7665.
5. ML Sushko and J Liu. 2011. "Surfactant Two-Dimensional Self-Assembly under Confinement." Journal of Physical Chemistry B., 115 (15) 4322-4328.
6. DH Wang, R Kou, D Choi, ZG Yang, ZM Nie, J Li, LV Saraf, DH Hu, JG Zhang, GL Graff, J Liu, MA Pope and IA Aksay 2010. "Ternary Self-Assembly of Ordered Metal Oxide-Graphene Nanocomposites for Electrochemical Energy Storage." ACS Nano 4(3): 1587-1595.
7. SK Nune, PK Thallapally, A Dohnalkova, CM Wang, J Liu and GJ Exarhos 2010. "Synthesis and Properties of Nano Zeolitic Imidazolate Frameworks." Chemical Communications 46(27): 4878-4880.
8. ML Sushko and J Liu 2010. "Structural Rearrangements in Self-Assembled Surfactant Layers at Surfaces." Journal of Physical Chemistry B 114(11): 3847-3854.

Program Title: Bioinspired Materials

PIs: Surya Mallapragada (FWP leader), Mufit Akinc, David Vaknin, Marit Nilsen-Hamilton, Alex Travesset, Monica Lamm, and Tanya Prozorov. Collaborator: Klaus Schmidt-Rohr
Mailing Address: Division of Materials Sci. and Eng., Ames Laboratory, Ames, IA 50011
Email: suryakm@iastate.edu

Program Scope: The objective of the Bioinspired Materials FWP is to explore biomimetic mechanisms and routes for the growth of hierarchically self-assembled unique functional materials with fundamental new properties for a variety of energy applications. Our approach mimics Nature using organic templates coupled to mineralization proteins/peptides to control the growth of the inorganic phase to form self-assembled nanocomposites. Biological organisms such as magnetotactic bacteria, act as inspiration and a source of mineralization proteins that have the potential to control crystal formation, shape, size and function. The objective of this FWP is to unravel these mineralization mechanisms and to go further and employ the biomineralization principles *in vitro* to produce novel hierarchically assembled materials of energy relevance, and enable shape-selective fabrication of nanocrystals with sizes not easily realizable via conventional techniques.

This FWP focuses on the (i) development of multiscale self-assembling bioinspired hybrid materials using bottom-up approaches [1-6]; (ii) development of techniques understand the biomineralization mechanisms and to probe assembly at multiple length scales and properties of these nanocomposites [7-13]; and (iii) development of computational methods for understanding general design rules for self-assembled polymer nanocomposites [14-17]. Our future directions in the FWP are to build on our current successes to fabricate nanocomposites with complex inorganic nanocrystals of energy relevance, and to also control the hierarchical assembly/disassembly process to create nanocomposites with *dynamic nanostructures*. The ability of this approach to control the material structure at different length scales align well with the future directions outlined for "control science" by BESAC. This project utilizes the unique expertise in magnetotactic bacteria, and the interdisciplinary backgrounds of PIs at Ames Lab with complementary strengths in synthesis, molecular biology, characterization, and modeling.

Recent Progress: The focus in the last three years has been on self-assembling nanocomposites with three different inorganic phases - calcium phosphate, magnetite and zirconia. The initial approach was developed using bone as inspiration for the development of calcium phosphate nanocomposites, and magnetotactic bacteria as inspiration for the magnetite nanocomposites. More recently, zirconia nanocomposites are being explored using similar principles and approaches because of their relevance in solid-oxide fuel cells. Characterization techniques such as solid-state NMR and scattering methods have been developed to elucidate the hierarchical assembly and to understand the role of the mineralization proteins. The experimental techniques were complemented with computational methods to model the self-assembly processes of the templates in the presence of the mineralization proteins and the inorganic phases.

Synthesis: A family of hierarchically self-assembling pH and temperature-responsive block copolymers with different functional groups were synthesized and used as templates for mineralization. We have developed a novel, room-temperature bioinspired route to nanostructured magnetic materials, using the recombinant protein, Mms6, found in the

magnetotactic bacteria to promote shape-specific magnetite nanocrystal growth. To investigate the mineralization mechanism, mutants of Mms6 were developed. Control samples without protein, as well as mutants of the wild-type Mms6 showed only the small ill-shaped crystallites, while all of the protein-templated samples showed larger well-defined particles. We were able to template synthesis of more complex and highly magnetic nanocrystals in vitro that do not occur in living organisms, such as uniform platelet-shaped cobalt ferrite nanocrystals, and more recently gadolinium-containing magnetic nanoparticles (Fig. 1). For the first time, we have also demonstrated that the magnetic properties of nanocrystals in magnetotactic bacteria can be significantly altered by the incorporation of metal ions other than iron in the crystal structure, as seen by a major shift in the Verwey transition.

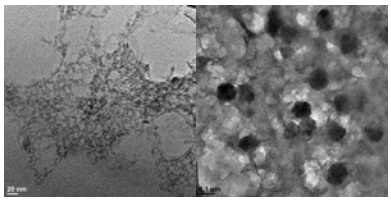

Fig 1. Gadolinium containing magnetic nanoparticles synthesized in the absence of (left) and in the presence of Mms6 (right)

We have also focused on bioinspired self-assembling calcium phosphate nanocomposites using block copolymers as templates attached to hydroxyapatite (HAp) nucleating peptides. This work demonstrated that trace quantities of specific additives have a profound effect on crystal size and morphology (as in native bone) that may be extended to other energy relevant materials. The results from XRD, FTIR, SAXS, TEM and ^{31}P NMR confirmed that the inorganic phase is carbonated HAp of nano-scale dimensions, with an elongated plate-like morphology, very similar to the mineral phase of natural bone. Overall, this approach allows a bioinspired bottom-up approach to self-assembled HAp nanocomposites using block copolypeptide templates. Inspired by these results, we used them as a template for synthesis of nanocrystalline ZrO_2. We believe this is the first demonstration of templated growth of mesoporous nanocrystalline ZrO_2 using entirely aqueous media. An open network structure of ZrO_2 and mesoporosity is retained even after heat treatment at 900˚C, making this material a potential candidate for various applications such as catalysts and anodes in solid oxide fuel cells.

Characterization: We have systematically established solid-state NMR as a tool for characterizing hierarchically assembled nanocomposites. The composition of the surface layers of both the inorganic phase and polymer templates, which are responsible for the interactions between the components, can be determined by selective NMR techniques. We have introduced several NMR methods (in collaboration with the *Solid State NMR* FWP) for proving the presence of a nanocomposite where standard electron microscopy fails to provide a specific signature. To understand the role of mineralization proteins, we have developed surface sensitive synchrotron X-ray scattering and spectroscopic techniques for determination of ion-specific distributions on molecular length scales at the surface of charged soft-matter templates. Using anomalous X-ray reflectivity, we determined the distributions of mono- and multivalent ions. We have expanded on the development of X-ray spectroscopic techniques, such as energy scans at fixed momentum-transfers under specular reflectivity conditions and fluorescence techniques. This allows us to distinguish the presence of solubilized Fe^{2+} vs. Fe^{3+} and Mms6 at the water-air interface.

In an ion-specific binding study at aqueous soft interfaces, we used X-ray reflectivity and spectroscopic techniques in combination with thermodynamic measurements and theoretical modeling to unravel the mechanism of specific ionic adsorption at vapor/solution interfaces. We found that ions with same charge, such as, Fe^{3+} and La^{3+}, respond dramatically differently when interacting with a charged template at the vapor/solution interface, demonstrating that classical

electrostatic interactions alone do not capture the binding mechanism of these ions at the interface. These results are directly relevant to a number of ongoing projects, such as, understanding how Mms6 induces crystal growth of magnetic nanocrystals. Synchrotron experiments performed on mixed-charge templates demonstrated that the molecules comprising the template are miscible on a molecular length scale.

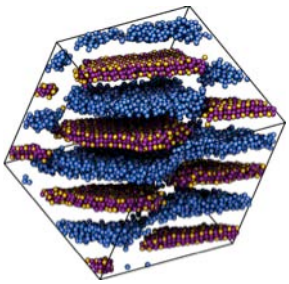

Fig. 2. Lamellar phase obtained with block copolymer/inorganic self-assembled nanocomposites

Computational: Our work has been focused on two main topics 1) Self-assembly of block-copolymer gels and nanoparticles and 2) Ionic specificity in the self-assembly process. In the process, we have pioneered the use of Graphic Processing Units (GPUs) for molecular dynamics (MD), resulting in HOOMD-blue the first general purpose MD. The self-assembly work has resulted in a detailed characterization of the phase diagram and the dynamics of equilibrium of block copolymer gels, and has provided general guidelines necessary for inorganic components (such as calcium phosphate or magnetite nanoparticles) to self-assembled polymer nanocomposites (Fig. 2) in solution [14-16].

Future Plans: We plan to focus on the synthesis and investigation of three classes of self-assembling bioinspired materials: 1) complex magnetic nanoparticles 2) zirconia nanocomposites and 3) calcium oxalate nanocrystals. The first two classes of materials build on our existing work. Calcium oxalate crystals assemble together as a druse or crystal sand in plant cells to collect and reflect light efficiently to the chloroplasts. Forming these bioinspired structures could help in the design of more efficient solar cells.

We have already demonstrated our ability to produce nanostructured inorganic materials and control their placement in an organic matrix through self-assembly. In this next phase of the work, we plan to fabricate *dynamic* structures with reversible assembly/disassembly of the magnetic nanocrystals in the organic matrix. This will enable the formation of tunable and dynamic "smart" structures with different hierarchical structures and magnetic properties in response to different environmental stimuli. It will further impart a new degree of functionality that cannot be obtained with materials fabricated using top-down approaches. Using the templates and mineralization proteins similar to those outlined above, three different strategies will be explored for the creation of dynamic hybrid materials that facilitate the reversible assembly/disassembly: 1) use of fusion proteins and leucine zipper pairs 2) use of complementary DNA strands attached to the ends of self-assembling polymers and 3) use of aptamers. We have synthesized the fusion proteins involving the leucine zipper pairs. The templates will be used for synthesis and dynamic site-specific localization of magnetic nanocrystals. Based on our previous theoretical work, we have provided a detailed theoretical understanding for the complementary DNA based experiments and we have predicted a new class of materials consisting of hybridization of nanoparticles with grafted ssDNA and linkers attached to hydrophobic blocks. Combinations of templating methods, mineralization proteins and nanocrystal systems will be explored.

We will continue to search for novel methods for comprehensive characterization of both inorganic and organic components of the nanocomposites and probe structure, composition and

function, as well as mechanisms of biomineralization. The computational/theoretical challenges address the problems of characterizing the design rules of polymer nanocomposites as well as the challenge to simulate biomineralization processes. The goal is to provide a theoretical framework for the proposed experiments and will build upon the success of the models and methods developed during in this program.

References (which acknowledge DOE support)

1. Y. Hu, Y. Yusufoglu, M. Kanapathipillai, C. Yang, Y. Wu, P. Thiyagarajan, T. Deming, M. Akinc, K. Schmidt-Rohr, and S. Mallapragada, "Self-Assembled Calcium Phosphate Nanocomposites Using Block Copolypeptide Templates," *Soft Matter*, 5, 4311 (2009).
2. M. Kanapathipillai, and S.K. Mallapragada, "Polymeric Nanomaterials as Templates for Biomineralization," *Int. J. Nanosci.*, **8**, 473 (2009).
3. Y.Y. Hu, X.P. Liu, X. Ma, A. Rawal, T. Prozorov, M. Akinc, S.K. Mallapragada, and K. Schmidt-Rohr, "Biomimetic Self-Assembling Copolymer-Hydroxyapatite Nanocomposites with the Nanocrystal Size Controlled by Citrate," *Chem. Mater.*, 23, 2481 (2011).
4. X.P. Liu, and S.K. Mallapragada, "Bioinspired Synthesis of Organic/Inorganic Nanocomposites", in Biomimetic, Ed. L. Pramatorova, Intech Publishers. (2011).
5. X. Wei, O. Ugurlu, A. Agarwal, H.Y. Acar, and M. Akinc, "Dissolution Behavior of Si, Zn-Modified Tricalcium Phosphates," *Mater. Sci. Eng. C,* **29,** 126–135 (2009).
6. C. Lefevre, R.B. Frankel, M. Posfai, T. Prozorov, and D.A. Bazylinski, "Isolation of Obligately Alkaliphilic Magnetotactic Bacteria from Extremely Alkaline Environments", *Env. Microbiol*., doi. 10.1111/j.1462-2920.2011.02505.x (2011).
7. W. Bu, K. Flores, J. Pleasants, and D. Vaknin, "Preferential Affinity of Calcium Ions to Charged Phosphatidic Acid Surface from a Mixed Calcium/Barium Solution: X-ray Reflectivity and Fluorescence Studies," *Langmuir*, **25,** 1068 (2009).
8. W. Bu and D. Vaknin, "X-ray Fluorescence Spectroscopy from Ions at Charged Interfaces," *J. Appl. Phys.*, **105**, 084911 (2009).
9. E.E. Kooijman, D. Vaknin, W. Bu, L. Joshi, S.W. Kang, A. Gericke, E.K. Mann, and S. Kumar, "Structure of Ceramide-1-Phosphate at the Air-Water Solution Interface in the Absence and Presence of Ca^{2+}," *Biophys. J.*, **96**, 2204 (2009).
10. S. Seok, T.J. Kim, S.Y. Hwang, Y.D. Kim, D. Vaknin, and D. Kim, "Imaging of Collapsed Fatty Acid Films at Air-Water Interfaces," *Langmuir*, **25**, 9262 (2009).
11. D. Vaknin, W. Bu, J. Sung and D. Kim, "Thermally Excited Capillary Waves at Vapor-Liquid Interfaces of Water-Alcohol Mixtures," *J. Phys: Cond. Mat.*, **21**, 115105 (2009).
12. D. Vaknin and W. Bu, "Neutrally Charged Gas/Liquid Interface by a Catanionic Langmuir Monolayer," *J. Phys. Chem. Lett.*, **1**, 1936 (2010).
13. W.J. Wang, R.Y. Park, A. Travesset, and D. Vaknin, "Ion-Specific Induced Charges at Aqueous Soft Interfaces," *Phys. Rev. Lett.*, **106**, 056102 (2011).
14. J.A. Anderson, R. Sknepnek, and A. Travesset, "Design of Polymer Nanocomposites in Solution by Polymer Functionalization," *Phys. Rev. E*, **82**, 021803 (2010).
15. C. Knorowski, S.Burleigh and A. Travesset, "Dynamics and Statics of DNA-Programmable Nanoparticle Self-Assembly and Crystallization", *Phys. Rev. Lett.*, 106, 215501 (2011).
16. C. Knowrowski and A. Travesset, "Materials Design by DNA Programmed Self-Assembly", *Cur. Opin. Cond. Matter Mater. Sci.* (in press).
17. W. Wang, R. Y. Park, D. H. Meyer, A. Travesset and D. Vaknin, "Ionic Specificity in pH Regulated Charged Interfaces: Fe^{3+} versus La^{3+}", *Langmuir* (in press).

Building Metamaterials Bottom-Up with Biological Nanotemplates

Marit Nilsen-Hamilton, Andrew Hillier, Lee Bendickson, Wei-Hsun Yeh, Supipi Auwardt, Surya Mallapragada, Thomas Koschny, Costas Soukoulis

Ames Laboratory, Division of Materials Science and Engineering, Ames, IA 50011

Mail: marit@iastate.edu

Complete control of an electromagnetic light wave requires the ability to directly manipulate its electric *and* magnetic vector components. This level of control has not been possible until the recent advent of metamaterials, which are tailored man-made materials composed of sub-wavelength metallic building blocks ("photonic atoms") that are densely packed into an effective material [1, 2]. A particularly important example of a photonic atom is the split-ring resonator (SRR), which is a tiny electromagnet that allows for artificial magnetism at elevated frequencies, thereby enabling the formerly missing control of the magnetic component of the light wave. The negative magnetic response (i.e., $\mu<0$) above the SRR Eigen frequency, combined with a more usual negative electric response from metal wires (i.e., $\varepsilon<0$), can lead to a negative index of refraction. Originally proposed theoretically in 1999 [3], negative refractive index metamaterials were realized at microwave frequencies by 2000 [4, 5] and almost entered the optical regime (few micrometers wavelength to the visible) in 2004 [1]. By 2007, by using variations of the SRR scheme, negative-index metamaterials were created that reached the red end of the visible spectrum [2]. Metamaterials that operate at optical, or near optical frequencies are referred to as "optical metamaterials". However, the fabrication of sub-wavelength building blocks requires advanced nanofabrication approaches and poses several challenges for quantitative calculations with *predictive* power.

Currently, metamaterials [6] are limited by two main factors: 1) The problem of high losses occurring at optical frequencies in the metallic resonators that constitute the metamaterial and 2) the challenge to fabricate, orient and align the microscopic structural elements that provide the electric and magnetic response of the metamaterial. While the first problem can be addressed by incorporating gain materials into the metamaterial and is subject to current research, the fabrication problem has been historically approached by scaling successful microware metamaterial designs down in size, and therefore up in operating frequency, to achieve optical metamaterials.

Metamaterials rely on artificial, usually metallic resonant structures to provide the material's electric and magnetic response. These resonators, usually arranged in a periodic fashion, can be designed to have a structural length scale that is much smaller than the wavelength of the incident wave at the operating frequency of the metamaterial. If the structural length scale is at least one order of magnitude smaller than the operating wavelength, the incident light experiences an averaged response over many unit cells of the metamaterial. In this desirable limit the metamaterial can be described as an effective homogeneous medium – in the same way as ordinary window glass can be treated as homogeneous with respect to the propagation of visible light, despite of its discrete molecular substructure. Examples of such resonators include 1) short metallic rods as electric resonators which provide a resonant electric dipole moment due to oscillation of the electric polarization along their long axis, and 2) Pendry's SRR as magnetic resonators, which (in their simplest form) are a conductive ring (providing inductance) interrupted by a gap (providing capacitance) such that they support an resonant, oscillating ring current analog to an LC oscillator. The magnetic moment associated with this resonant ring current is the source of the magnetic response. The response of the

electric resonators controls the effective permittivity and the response of the magnetic resonators controls the effective permeability of the metamaterials. The permittivity and response can vary spatially, which allows tailoring of electric and magnetic properties of the metamaterial independently of one another and as a function of spatial location. Thus, these metamaterials allow for ultimate control over the propagation of light in ways unimaginable in naturally occurring materials.

The spatial control over the electric permittivity, $\varepsilon(\omega)$, and magnetic permeability, $\mu(\omega)$, provided by metamaterials enables an entirely new class of applications based on transformation optics [7]. Transformation optics is based on the analogy of the effects of curvature and geometry of the configuration space and the spatial distribution of the permittivity and permeability tensors in Maxwell's equations, which govern the propagation of light. Light propagation in a complicated curved geometry, e.g. a geometry avoiding and channeling light around an enclosed "hidden" volume, can be mapped to a geometrically flat material with complicated space dependent on $\varepsilon(\omega)$ and $\mu(\omega)$. One popular example is the "cloaking" by a specially designed metamaterial shell [8, 9]. The exciting new applications promised by transformation optics are strictly contingent upon full spatial and spectral control of the permittivity and permeability tensors that can only be provided by a metamaterial.Metamaterials can also provide a chiral response with giant optical activity if composed of chiral microscopic resonators that cross-couple the local electric and magnetic polarizations [10-12]. Besides providing an alternative route to negative refractive index without simultaneous negative electric and magnetic response, optical chiral metamaterials may achieve a repulsive Casimir force and avoid stickiness and friction in micromechanical devices [13].

For optical metamaterials that operate in the visible the range (i.e. wavelengths of ~800 nm to 400 nm) the size of the metamaterial unit cell must be smaller than 40-80 nm, and the sizes of the resonators should be even smaller. In addition, realistic metamaterials need to be three-dimensional with full control over the orientation of the constituent resonators in all three directions. All existing designs for negative μ or negative n increase their operational frequency range towards the optical regime by reducing the size of the unit cell to about or below 100 nm [Fig. 1]. This is the top-down approach.

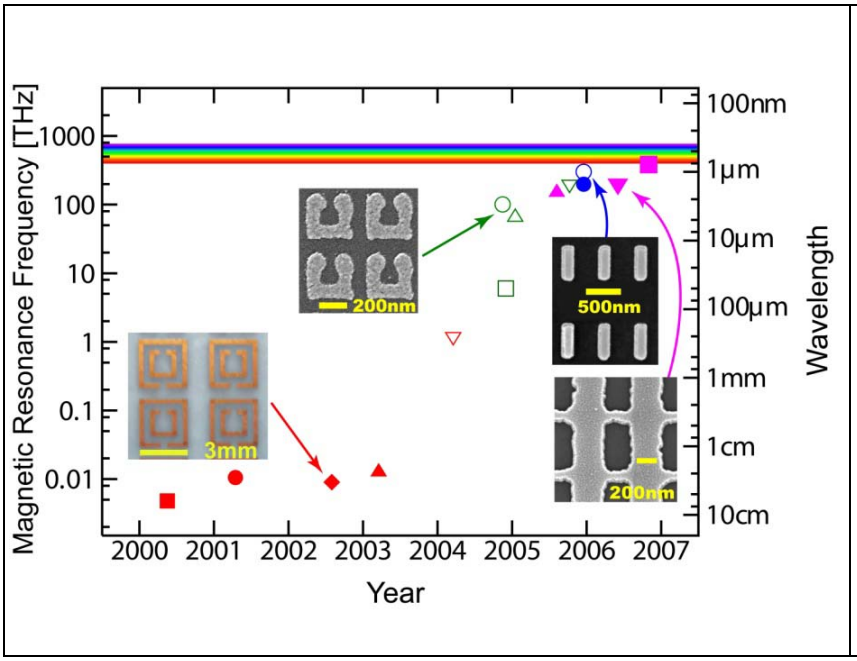

Figure 1. Advances in scaling and redesigning metamaterials with artificial negative magnetic permeability, μ, and/or negative refractive index, n. The solid symbols have $n<0$, while the open symbols only have $\mu<0$. The red color describes structures based on the double split-ring resonator (SRR), the green color describes the U-shape SRRs, the blue describes pairs of metallic nanorods and the magenta describes the "fishnet" structure. The four insets give pictures of fabricated structures in different frequency regions. The Ames Laboratory metamaterial group at ISU and their collaborators has played an important role in designing, fabricating and testing the negative index materials, from GHz frequencies to optical wavelengths (780 nm). This figure is from [2].

Although a magnetic response can be demonstrated at optical frequencies in metamaterials fabricated by lithographic techniques, these approaches suffer from some major limitations: 1) Limits to the minimum feature size with which metallic structures can be patterned. For instance, the width of metallic traces accessible by electron lithography is of the order of 50 nm, which is just at the size limit necessary for optical metamaterials, 2) Lithographic fabrication is expensive and does not allow for very large sample sizes. 3) Current lithographic fabrication methods for optical metamaterials are essentially limited to planar structures, or at the most, layered structures with a few functional layers. The resulting metamaterials are one-dimensional and therefore can only work for one direction of propagation.

Optical metamaterials can also be assembled from pre-existing metallic nanoparticles and clusters of nanoparticles of specific shapes. Examples include paired parallel nanorods of rings or cylindrical clusters made of metallic nano-spheres to serve as magnetic resonators, high aspect ratio metallic nanorods to serve as electric resonators, “tuning fork” shaped nanoparticles that simultaneously act as both electric and magnetic resonant elements, and chiral nanostructures made of chiral assemblies of nanoparticles such as rotated cross-wires or chiral nanoparticles. Here, in addition to the problem of fabricating the individual nanoparticles, the particles must be oriented, aligned and arranged at the nanoscale to form identical nano-resonator structures, which are the unit cells of the metamaterial.

An innovation in the production of nano-resonators being developed here is to assemble regularly structured biologically-based nanotemplates on which metals are deposited. This approach avoids the difficulty of organizing nanoparticles into larger, regular and coherent structures. Biology presents a rich range of possible templates and we propose to use biological templates as a novel means for building resonators. Many very regular biological structures exist at the nanometer to millimeter length scales required for effective macroscopic, three-dimensional metamaterials. Unlike metal-coated nanoparticles, biological building blocks are uniquely structured to fit within larger regular three-dimensional structures into which they are incorporated. The technologies of genetic engineering also provide for the opportunity to change the structural characteristics of the biological building blocks with the result that new nanostructures are created.

DNA origami is a relatively new approach to forming nanostructures. With this approach a DNA scaffold with known sequence is complemented with a series of smaller oligonucleotides with the appropriate sequences for hybridization. The strong propensity of DNA strands of complementary sequence to hybridize results in the reproducible formation of regular and stable structures. Proteins exist and can be designed that selectively recognize specific DNA sequences.

Our approach is to developing homogeneous split-ring resonators use a combination of DNA origami with DNA tiles and proteins that bind specific sequences to direct the locations of metallization on the DNA. In our preliminary experiments, DNA circles of various sizes have been

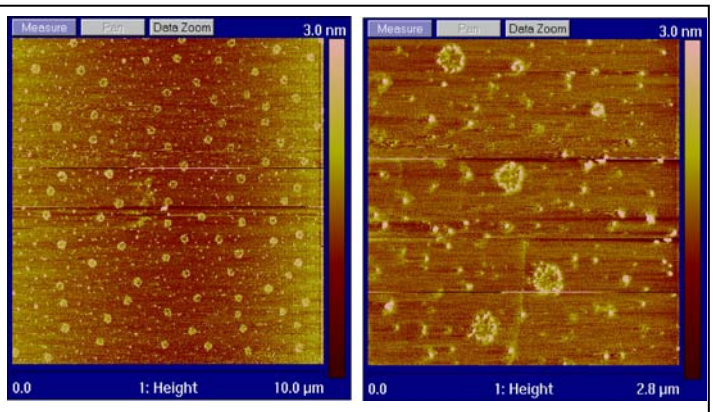

Figure 2. AFM images of homogeneous preparation of DNA circles decorated with gold nanoparticles.

created by DNA origami and m etallized by way of 1.4 nm diameter gold particles (Nanogold) functionalized with several cationic amine linkages followed by electroless deposition using either custom or commercial electrolytic deposition baths. Due to the presence of the gold nanoparticles, selective deposition onto the DNA was achieved (Fig. 2). In the subsequent examples, a c ommercial gold plating batch was used (GoldEnhance EM, Nanoprobes). This ELD bath consisted of a hexachloroaurate solution in the presence of a weak reducing agent, with deposition controlled by the deposition time. In addition to gold, silver is another potential candidate for metallization, which also exhibits many of the optical properties desired in a metamaterial. We have use a silver ELD bath (SilverEnhance EM, Nanoprobes) to coat our nanoparticle-DNA complex. Preliminary results suggest that this may be a route to a deposit that is even more continuous (Fig. 3).

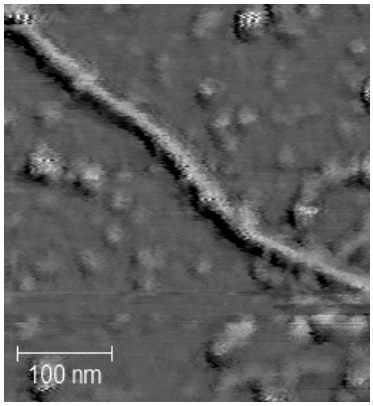

Figure 3. AFM image of silver-coated DNA following electroless silver deposition onto gold-tethered nanoparticles.

Literature Cited

1. Smith, D.R., J.B. Pendry, and M.C. Wiltshire, *Metamaterials and negative refractive index.* Science, 2004. **305**(5685): p. 788-92.
2. Soukoulis, C.M., S. Linden, and M. Wegener, *Physics. Negative refractive index at optical wavelengths.* Science, 2007. **315**(5808): p. 47-9.
3. Pendry, J., et al., *Magnetism from Conductors and Enhanced Nonlinear Phenomena.* IEEE Trans. Microwave Theory and Techniques, 1999. **47**: p. 2075.
4. Smith, D.R., et al., *Composite medium with simultaneously negative permeability and permittivity.* Phys Rev Lett, 2000. **84**(18): p. 4184-7.
5. Shelby, R.A., D.R. Smith, and S. Schultz, *Experimental verification of a negative index of refraction.* Science, 2001. **292**(5514): p. 77-9.
6. Soukoulis, C.M. and M. Wegener, *Optical Metamaterials—More Bulky and Less Lossy.* Science, 2010. **330**(6011): p. 1633-1634.
7. Leonhardt, U. and T. Tyc, *Broadband invisibility by non-Euclidean cloaking.* Science, 2009. **323**(5910): p. 110-2.
8. Pendry, J.B., D. Schurig, and D.R. Smith, *Controlling electromagnetic fields.* Science, 2006. **312**(5781): p. 1780-2.
9. Schurig, D., et al., *Metamaterial electromagnetic cloak at microwave frequencies.* Science, 2006. **314**(5801): p. 977-80.
10. Plum, E., et al., *Metamaterial with negative index due to chirality.* Phys. Rev. Lett., 2009. **79**: p. 035407.
11. Decker, M., et al., *Twisted split-ring-resonator photonic metamaterial with huge optical activity.* Optics Letters, 2010. **35** p. 1593-1595.
12. Decker, M., et al., *Strong optical activity from twisted-cross photonic metamaterials.* Optics Letters, 2009. **34**(2501-2503).
13. Zhao, R., et al., *Repulsive Casimir force in chiral metamaterials.* Phys Rev Lett, 2009. **103**(10): p. 103602.

Soft-Matter Physics: Directed Self-Assembly of Soft-Matter and Biomolecular Materials

Benjamin Ocko (ocko@bnl.gov), Antonio Checco (checco@bnl.gov) & Masa Fukuto (fukuto@bnl.gov), Brookhaven National Laboratory, Upton, NY 11973

Program Scope: The primary goal of the group is to understand the effects of nanoscale confinement and the role of self-assembly in soft and biomolecular materials through the use of patterned templates and well-defined interfaces. We use synchrotron x-ray scattering, scanning probe and optical microscopy techniques to study fundamental properties of complex fluids, simple liquids, macromolecular assemblies, liquid crystals, polymers, and biomolecular materials. The challenges are (1) to understand the behavior and structure of liquids under nano-confinement, (2) how templates and confinement can be used to direct the assembly of biomolecular materials and diblock copolymer thin films, (3) to gain a fundamental understanding of interactions which give rise to similar self-assembly behavior for a wide variety of systems, (4) how the order correlates with function. Understanding structural aspects of self-assembly at interfaces and in thin organic films underlies many emerging organic based devices and energy technologies. Our approach uses two complementary structural probes, x-ray scattering and AFM. An important aspect of our approach is to use nanopatterned surfaces to confine liquids and complex fluids. To accomplish this, we are using polymer based self-assembly techniques and AFM based local-oxidation nanolithography.

Recent Progress:

A. Biomolecular materials: One of our main efforts is focused on lipid-mediated assembly of biomolecular nanoparticles (BNPs) at liquid interfaces. A key challenge in nanoscience is to understand anisotropic interparticle interactions and exploit them in directed assembly, an issue of increasing importance due to the recent progress in the synthesis of anisotropic nanoparticles. Another challenge of longstanding interest has been to control the assembly of nano-objects in aqueous media, which is complicated by the interplay between various competing interactions (electrostatic, H-bonding, hydrophobic, van der Waals). Arrays of BNPs, i.e., proteins and viruses, formed at the lipid membrane-aqueous solution interface are well suited for addressing these issues in 2D because of the monodispersity and well-defined anisotropy of BNPs as model building blocks, the use of a fluid-phase lipid monolayer to promote the orientational order and mobility of interface-confined BNPs, and the ability to tune the BNP-BNP and BNP-surface interactions through chemical compositions in the buffer and in the lipid membrane. Our recent progress in this area includes:

• *Electrostatic 2D crystallization of icosahedral viruses.* Crystallization is often induced by increasing density. For charged nanoparticles, crystallization in 2D may be achieved through the adsorption of weakly charged particles onto an oppositely charged, planar interface with a high surface charge density. In order to test this approach, we investigated the assembly of cowpea mosaic virus (CPMV) and turnip yellow mosaic virus (TYMV) on positively charged lipid monolayers at the aqueous solution surface, by means of *in situ* grazing-incidence small-angle x-ray scattering (GISAXS) measurements at the liquid–vapor interface. The assembly was studied as a function of the solution pH,

which was used to vary the net charge on the virus, and of the mole fraction of the cationic lipid in the binary lipid monolayer, which set the interface charge density. The 2D crystallization of viruses occurred in a narrow pH range just above the particle's isoelectric point, where the particle charge was weakly negative, and only when the cationic-lipid fraction in the monolayer exceeded a threshold. The results demonstrate that the 2D crystallization is achieved in the region of phase space where the electrostatic interactions maximize the interfacial adsorption of virus particles.

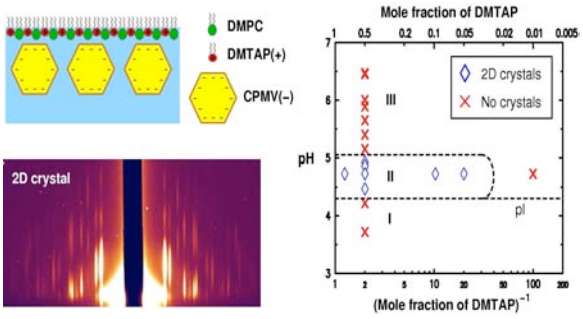

Fig. 1: (Top, left) Schematics for electrostatic 2D assembly of charged viruses on a cationic lipid monolayer. (Right) 2D assembly behavior as a function of pH and cationic lipid fraction. (Bottom, left) GISAXS pattern from 2D crystals of CPMV.

• *Role of anisotropic interactions in 2D assembly.* The above GISAXS results revealed two new forms of 2D crystals of TYMV, one consisting of a square array with a double-square rectangular unit cell and the other a centered-rectangular crystal. Comparison with the particle's shape and surface patchiness, deduced from the known atomic coordinates of the virus, indicate that these structures are stabilized by both hydrophobic patch-patch attractions and interparticle contacts that exhibit electrostatic and shape complementarity.

B. Surface induced order at liquid interfaces*:*

Understanding interface-induced order is relevant to many fields including those used in molecular electronic and photovoltaic devices. We have had a long-standing program to understand interface-induced ordering of simple molecular systems. One of the most elegant examples is surface freezingof alkanes at the liquid/vapor interface, discovered by our group, where a crystalline phase forms up to 3˚C above the bulk melting transition. Related phenomena, described below, is now observed at the solid/liquid and liquid/liquid interfaces:

• *Surface freezing of long-chain alcohols at the sapphire interface:* X-ray reflectivity measurements have been carried out to determine the structure at the solid/liquid (*s/l*) interface between a bulk alcohol (octadecanol: C18OH) and sapphire, (0001), a solid support. Over a range of temperature (about 30 ˚C) above the freezing point of the alcohol an extremely well defined monolayer is stable at the solid interface, with surface-normal, rather than surface-parallel, molecules. This reversible formation of an interfacial monolayer is reminiscent of surface freezing at the solid/vapor (*s/v*) interface where the much larger temperature range for the solid interface is

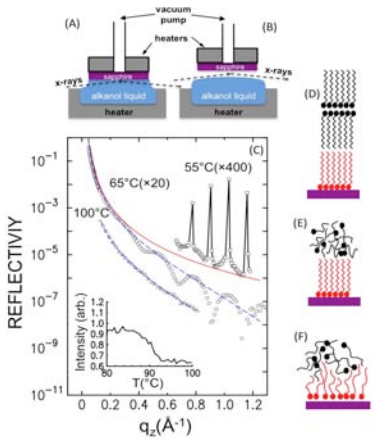

Fig. 2: (A) *s/l* and (B) *s/v* interface configurations. (C) X-ray reflectivity versus q_z at the *s/l* (sapphire/C18OH) interface at 55, 65 and 100˚C corresponding to the crystalline, monolayer and disordered phases. (inset) Intensity at q_z =0.55 Å^{-1} versus temperature. (D,E,F) Schematic descriptions of the crystalline (D), monolayer (E) and disordered (F) surface phases.

consistent with the much stronger surface interaction. We have also shown that the in-plane octadecanol order is commensurate with the sapphire.

• *Surface freezing at the oil/water interface:* We have investigated the liquid/liquid interface between aqueous solutions containing mM quantities of Cetyl trimethylammonium bromide (CTAB), a cationic surfactants, and n-alkanes. At high temperatures the surfactants form a thin liquid-like monolayer at the bulk alkane/water interface. Upon cooling, this layer undergoes a freezing transition well above the bulk freezing temperature of the alkanes, surfactant and water, forming a solid monolayer of densely-packed, extended, surface-normal-aligned molecules where the alkane and CTAB chains are interdigitated. This surface frozen state represents the first example of surface freezing at a liquid/liquid interface.

C. Nanoliquids: The effects of confinement and long-range interactions between the liquid and the nanostructured substrate may lead to substantial deviations from the macroscopic wetting behavior. In situ X-ray scattering and AFM are then used to study the morphology of the confined nanoliquids which are then compared to recent theoretical models. Recent progress includes work on nannobubbles and on the wetting of chemically nanopatterned surfaces.

• *Nanobubbles.* We have studied the trapping of air at the interface between water and a hydrophobic silicon surface decorated with hexagonal arrays of ~20 nm-sized parabolic cavities prepared using diblock-copolymer lithography. We have found that air nanobubbles form inside the cavities where the bubble's shape depends on the geometry and hydrophobicity of the cavity wall. These results improve our understanding of nanobubble formation and may guide the design of novel superhydrophobic nanostructured surfaces.

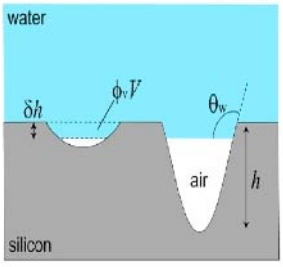

Fig. 3: Schematic shows nanobubbles that form inside parabolic cavities at the water surface. Water penetration into the cavities doesn't depend on their depth.

Future Plans: In addition to the projects discussed above, many of which are ongoing, we highlight some additional research plans below. In the area of biomolecular materials, we will extend the approach of the lipid-mediated 2D assembly to water-soluble inorganic nanoparticles and to graphoepitaxial assembly at chemically patterned substrate-liquid interfaces. In the area of surface induced ordering, we intend to study the surface freezing of alcohols at the sapphire interface to mixtures, both of alcohols of different length and fatty acids. Surface freezing studies will be extended to semi-fluorinated, diblock alkanes, where we have observed nano-dome formation in preliminary studies. In the area of nanoliquids, we will extend our studies to non-equilibrium wetting phenomena such as the dynamics of nanodroplet evaporation. The studies on the effect of lateral confinement on spreading will be extended to complex liquids (such as polymers and liquid crystals) where anomalous behavior is expected. We have started a program to improve our understanding of the structure and phase separation in organic electronic materials and organic photovoltaic devices using LDRD funds. Our initial studies of nanoimprint-induced orientation effects will be extended to new materials. Structural studies of conjugated polymers and semiconducting molecular systems will be carried out on a range of new materials. The Group has spearheaded the

proposal for the Soft Matter Interfaces (SMI) undulator beamline at NSLS II. This facility will be vital for the Group's future plans once the existing synchrotron is shuttered.

DOE Sponsored Publications (Sept. 2009-2011)

Grazing incident small angle x-ray scattering: a metrology to probe nanopatterned surfaces, Hofmann, T., Dobisz, E. and Ocko, B, J. Vac. Sci. Technol**. 27**, 3238 (2009).

Layering of [BMIM](+)-based ionic liquids at a charged sapphire interface, Mezger, M., Schramm, S., Schroder, H., Reichert, H., Deutsch, M., De Souza, E.J., Okasinski, J.S., Ocko, B.M., Honkimaki, V., and Dosch, H., J. Chem. Phys. **131**, 094701 (2009).

Structure and Interaction in 2D Assemblies of Tobacco Mosaic Viruses, L. Yang, S. T. Wang, M. Fukuto, A. Checco, Z. Niu, and Q. Wang, Soft Matter **5**, 4951 (2009).

Effects of Divalent Cations on Phase Behavior and Structure of a Zwitterionic Phospholipid (DMPC) Monolayer at the Air-Water Interface, Kewalramani, S., Hlaing H., Ocko, B.M. Kuzmenko, I., Fukuto, M., J. Phys. Chem. Lett. **1,** 489 (2010).

Atomic-Scale Structure of a Liquid Metal-Insulator Interface, Tamam, L., Pontoni, D., Ocko, B.M., Reichert, H. and Deutsch, M.D.. J. Phys. Chem. Lett. **1,** 1041 (2010).

Effects of surface ligand density on lipid-monolayer-mediated 2D assembly of proteins, Fukuto, M., Wang, S.T., Lohr, M.A., Kewalramani, S., and Yang. L, Soft Matter **6,** 1513 (2010).

Formation and Collapse of Poly(n-Butyl Acrylate) Homopolymer Monolayers at the Air-Water Interface, K. N. Witte, S. Kewalramani, I. Kuzmenko, W. Sun, M. Fukuto, and Y.-Y. Won, Macromolecules **43**, 2990 (2010).

Morphology of Air Nanobubbles *Trapped at Hydrophobic Nanopatterned Surfaces*, Checco, A., Hofmann, T., DiMasi, E.D., Black, C.T., and Ocko, B.M. Nano Letters **10**, 1354 (2010).

Direct self-assembly of Block copolymers in 2D chemical patterns fabricated from Electro-oxidation nanolithography, J. Xu, S. Park, T.P. Russell, A. Checco, and B.M. Ocko, Adv. Mat, **22**, 2268 (2010).

Surface Layering at the Mercury-Electrolyte Interface, Eisen, A., Murphy, B.M.. Ocko, B.M., Taman, L., Deutsch, M.D., Kuzmenko, I., and Magnussen, O.M. Phys. Rev. Lett. **104**, 105501 (2010).

Wetting of Nanopatterned Grooved Surfaces, Hofmann, T., Tasinkevych, M., Checco, A., Dobisz, E., Dietrich, S., and Ocko, B.M., Phys. Rev. Lett. **104**, 106102 (2010).

Charged diblock copolymers at interfaces: Micelle dissociation upon compression, Theodoly, O., Checco, A., and Muller, P., Europhys. Lett. **90**, 28004 (2010).

Systematic approach to electrostatically induced 2D crystallization of nanoparticles at liquid interfaces, Kewalramani, S., Wang, S.T., Lin, Y., Huong, G.N., Wang, Q., Fukuto, M., and Yang, L., Soft Matter **7**, 939 (2011).

Block copolymer self-assembly in chemically patterned squares, Xu, J., Russell, T.P., Ocko, B.M., and Checco, A., Soft Matter **7**, 3915 (2011).

Reversible uptake of water on NaCl nanoparticles at relative humidity below deliquescence point observed by noncontact environmental atomic force microscopy, Bruzewicz, D.A., Checco, A., Ocko, B.M., Lewis, E.R., McGraw, R.L., and Schwartz, S.E., J. Chem. Phys. **134**, 044702 (2011).

Unifying Interfacial Self-Assembly and Surface Freezing, Ocko, B.M., Hlaing, H., Jepsen, P.N., Kewalramani, S., Tkachenko, A., Pontoni, D., Reichert, H., and Deutsch, M., Phys. Rev. Lett. **106**, 137801 (2011).

Modification of deeply buried hydrophobic interfaces by ionic surfactants, Tamam, L., Pontoni, D., Sapir, Z., Yefet, S., Sloutskin, E., Ocko, B.M., Reichert, H., and Deutsch, M., Proc. Natl. Acad. Sci. USA **108**, 5522 (2011).

Checkerboard Self-Patterning of an Ionic Liquid Film on Mercury, Tamam, L., Ocko, B.M., Reichert, H., and Deutsch, M., Phys. Rev. Lett. **106**, 197801 (2011).

Role of electrostatic interactions in two-dimensional self-assembly of tobacco mosaic viruses on cationic lipid monolayers, Wang, S.T., Fukuto, M., Checco, A., Niu, Z.W., Wang, Q., and Yang, L., J. Colloid Interface Sci. **358**, 497 (2011).

Project: Emergent Atomic and Magnetic NanoStructures

PI: Tanya Prozorov

Collaborators: Surya K. Mallapragada, Marit Nilsen-Hamilton, Ruslan Prozorov, Monica Lamm, Damien Faivre, Dennis A. Bazylinski, Rchard B. Frankel, Mihály Pósfai, Michael Winklhofer, Rafal Dunin-Borkowski, Beena Kaliski, Concepcion Jimenez Lopez, Marcin Konczykowski.

Mailing Address: 108 Spedding Hall, Ames Laboratory, Division of Materials Science and Engineering, Ames, IA 50011

Email: tprozoro@ameslab.gov

Project Scope: The project is focused on direct visualization of *in-situ* growth of templated magnetic nanocrystals from the incipient nuclei to the fully developed crystalline and magnetic structures.

The objective of the newly formed Emergent Atomic and Magnetic NanoStructures Group is to deploy new characterization techniques based on the high-resolution TEM imaging of individual nanocrystals in real time by using continuous-flow fluid sample holder, as they are being formed. on a TEM grid. In addition, the "snapshots" of frozen specimen will be acquired with Cryo-TEM for the step-by-step study of growing nanostructures. The proposed research offers a unique opportunity for a real-time in-situ investigation of individual magnetic nanoparticle nucleation, growth, crystallization and development of the long-range order, as well as clustering and development of collective interactions. In biological systems, nucleation and crystallization of biogenic inorganic materials is usually controlled by diverse biomineralization proteins. Using the recombinant iron-binding protein, Mms6, and corresponding peptides, well-formed nanocrystals of magnetite and cobalt ferrite can be grown in polymeric matrices in a process that mimics the growth of magnetite in live magnetotactic bacteria [1,2]. However, neither the structure of Mms6, nor the detailed process of protein-assisted nanoparticle nucleation and growth are established. The major issue is that common characterization techniques only work with large, macroscopic assemblies of nanoparticles, so that interactions and collective effects mask the behavior of individual nanoparticles. Therefore, determining the mechanism of *individual particle* formation is the key for understanding the whole process. Once learned, this can be applied to the fabrication of various bio-compatible magnetic nanomaterials with controlled and well-defined properties.

The overall goal is to use the nanocrystals, templated by specific iron-binding proteins and synthetic peptides on the functionalized electron microscopy grids to study emergence of crystal structure and ferromagnetism in individual magnetic nanocrystals in real time by utilizing the advanced electron microscopy techniques. The approaches will include:

- developing a new in-situ, on-the-EM-grid, synthesis of nanocrystals as a tool of direct evaluation of nucleation and growth of nanocrystalline materials under precise temperature control, using various templating agents, free of artifacts associated with conventional TEM sample preparation, by employing recently developed microscopic continuous flow fluid sample holder;

- developing a novel Cryo-TEM method aimed at labeling and characterization of the specific bacterial proteins using their iron-binding ability, and to employ the iron self-staining for direct visualization of protein-rich areas of the vitrified samples;

- extending the developed methods to a real-time study of magnetic nanocrystal growth utilizing the integrated microfluidics system, developed for the nanometer scale imaging of materials in fluid environments, and advanced analytical EM tools, such as high angle annular dark field (HAADF) imaging in STEM mode for obtaining compositional and morphological information of the sample (Z-contrast imaging), phase contrast (electron holography) for visualization of magnetic fields to study evolving ferromagnetism in a single nanocrystalline particle as it grows, as well as spatial characterization (electron tomography) to understand the growth process, specifically at the particle-protein interface.

Preliminary Results: The first step was to test the *on-the grid* synthesis of biomacromolecule-templated magnetite nanocrystals and adapting the existing theories and methods to understand the specific behavior of materials at various stages of formation. In this synthesis, protein is printed directly on t he electron microscopy grid, as shown in Figure 1.

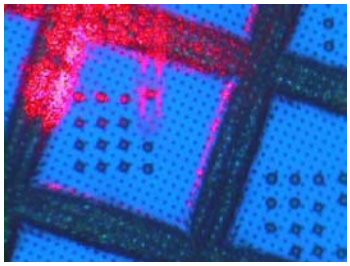

Figure 1. 2 μm protein printing on the surface of a QuantiFoil® Electron Microscopy grid.

These tests provide initial information needed to determine optimal temperature, reagents delivery, and overall chemical environment for these specimens. In a close collaboration with the Hummingbird Scientific we are working to customize the Continuous Flow Liquid Cell TEM holder to satisfy the specific requirements for the *in-situ* synthesis of the protein-templated nanocrystals.

Another aspect of the collaborative research included detailed electron microscopy examination of new magnetotactic bacteria. Novel greigite-producing magnetotactic bacterial strain, cultured in the laboratory of Dennis A. Bazylinski, was shown to produce a mixture of magnetite and greigite, and the publication describing this unusual finding was submitted to Science [3]. The magnetic properties of this strain cannot be measured due to the extremely low amount of specimen. We are attempting to use the electron holography to establish magnetic signatures of the individual nanocrystals in magnetosome chains.

References:

[1] Prozorov, T.; Mallapragada, S. M.; Narasimhan, B.; Wang, L.; Palo, P.; Nilsen-Hamilton, M.; Williams, T. J.; Bazylinski, D. A.; Prozorov, R.; Canfield, P. C. "Protein-Mediated Synthesis of Uniform Superparamagnetic Magnetite Nanocrystals", *Advanced Functional Materials 17*, 951 (2007).

[2] Prozorov, T.; Palo, P.; Wang, L.; Nilsen-Hamilton, M.; Jones, D.; Orr, D.; Mallapragada, S. K.; Narasimhan, B.; Canfield, P. C.; Prozorov, R. "Cobalt Ferrite Nanocrystals: Out- Performing Magnetotactic Bacteria", *ACS Nano 1*, 228 (2007).

[3] Lefèvre, C. T., Menguy, N., Abreu, F., Lins, U., Pósfai, M., Prozorov, T., Pignol, D., Frankel, R. B., Bazylinski, D. A. "A Cultured Greigite-Producing Magnetotactic Bacterium in a N ovel Group of Sulfate-Reducing Bacteria", *Science*, submitted (2011).

Program Title: Adaptive and Reconfigurable Nanocomposites

Molecular Nanocomposites Project - Subtask 1

Principal Investigators: J. A. Voigt, B. C. Bunker; Co PIs: D. R. Wheeler, D. L. Huber, M. J. Stevens, D. Y. Sasaki
Mailing Address: Sandia National Laboratories, P.O. Box 969, Livermore, CA 94551 & P.O. Box 5800 Albuquerque, NM 87185

Program Scope

The goal of this subtask is to explore the use of energy consuming, switchable, and/or responsive components to create programmable and/or reconfigurable composites. Our ultimate goal is to understand and mimic the complex, emergent, and self-healing behaviors exhibited by biological materials.

The classes of building blocks required to construct molecular nanocomposites that are truly adaptable and reconfigurable are: 1) elements that can be programmed using energy sources such as heat, light, host-guest complexation, or electric fields, and 2) responsive hosts that have sufficient mobility to allow components to reconfigure themselves in response to applied stimuli.

In terms of programmable elements, we have been exploring molecular units whose size, shape, charge, hydrophobic/hydrophilic character, and/or interaction potentials can be switched in a reversible fashion between at least two distinct states. In terms of responsive hosts, we are exploring fluid or viscous phases ranging from aqueous solutions to lipid bilayers to polymeric liquids and liquid crystals. For composite materials, we are investigating programmable elements, such as optically, electrically, or chemically-addressable molecules, to functionalize both hosts and active materials. In terms of behavior, we are observing how molecular programming controls the size, shape, oligomerization, transport, and phase behavior of molecular and nanoscale assemblies.

Here, we describe the use of phase separation in lipid membranes as a way to define regions of distinct mechanical, chemical, and physical properties that can be addressed by external stimuli. Using protein-membrane affinity on the phase-separated domain we demonstrate structural transformation of 2D planar membranes into 3D membrane tubules as a result of steric pressure by bound proteins. Interestingly, we find that the persistence length and dynamics of the tubule can be tuned by modulating the mechanics of the membrane phase. Since the phase-separated domain also defines a specific physical state (e.g., electrostatic charge) we also show that membrane can be addressed using an electric field to orient the domain in giant vesicles. These results represent our recent efforts in developing materials with addressable components for nanoscale structural assembly.

Recent Progress

Lipid tubules from planar domains

Recently, we have shown that lipid domains on giant unilamellar vesicles (GUVs) can be

transformed from planar assemblies into tubular structures of large persistence length [Stachowiak, *PNAS* **2010**]. The lipid domains were composed of iminodiacetic acid (IDA) functionalized lipids that exist as gel phase assemblies in the membrane at room temperature (DSIDA). The domains were then activated to exhibit strong and selective affinity for histidine-tagged proteins by the addition of $CuCl_2$ to form the Cu^{2+}-IDA complex [Hayden, *JACS* **2009**]. Upon the addition and binding of his-tagged proteins we observed the buckling and collapse of the lipid domains, ultimately resulting in the formation of long and rigid membrane nanotubes (Figure 1). The structural transformation is believed to be a result of cumulative forces that bend (i.e., steric pressure between bound proteins) and collapse the structure.

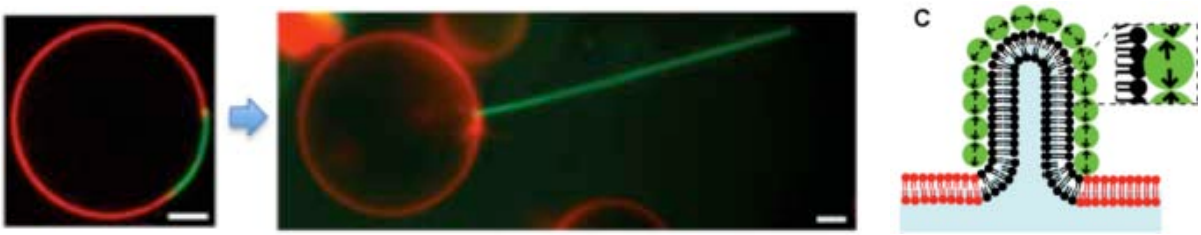

Figure 1. Lipid domain in a giant unilamellar vesicle undergoing nanotube formation. (Left) Fluorescence microscopic images of a GUV composed of 10% DSIDA/DPhPC before and after nanotube formation. Liquid disordered DPhPC membrane was labeled with red BODIPY 530/550 HPC and gel phase DSIDA domain was bound with his-tagged green fluorescent protein (GFP). (Right) Cartoon of domain undergoing tubulation as induced by steric pressure of bound proteins. (Scale bars, 2 μm).

Targeting proteins to liquid ordered domains

In the work mentioned above we demonstrated that host-guest complexation serves as a switch to reconfigure the structure of lipid membranes. In that initial effort the membrane domain consisted of a gel phase lipid that imparts high bending energy to that region of the membrane. Nanotubes that formed from these domains were straight and rigid suggesting that the persistence length may be coupled to the membrane mechanics. In an effort to show that it is possible to modulate the mechanics of membrane domains and thereby tune the physical behavior of reconfigured structures, we explored new lipid designs and compositions of varying phase behavior. Figure 2 shows some of the IDA lipids we have synthesized that partition to or form specific membrane phases.

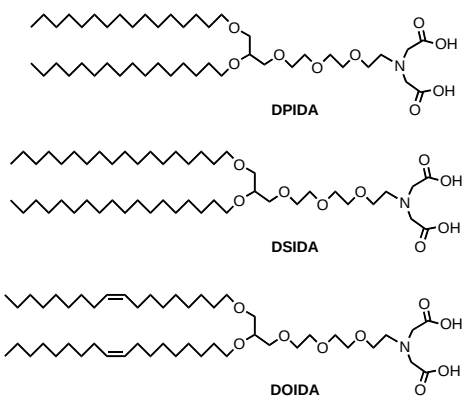

Figure 2. Protein affinity lipids designed for specific membrane phases: DSIDA - gel, DPIDA – L_o, DOIDA – L_d.

We recently showed that the lipid DPIDA partitions into the cholesterol-rich L_o phase of membranes and serves as a target for binding proteins to raft-like domains [Stachowiak, *Langmuir* **2011**]. DPIDA was designed to mimic the structure of DPPC (dipalmitoyl phosphatidylcholine), a lipid known to partition into liquid ordered (L_o) domains [Veatch,

Biophys. J. **2006**]. What is unique about the L_o phase is its high packing order but low bending energy compared to gel phase structures. In the absence of cholesterol, DPIDA forms gel phase domains in liquid disordered (L_d) phase membranes, while in the presence of cholesterol it partitions into the L_o phase. Both types of domains exhibit strong, selective affinity for his-tagged proteins in the presence of Cu^{2+}. Although both domains collapse into lipid tubules, those from gel phase domains possess large persistence length while those from the L_o phase form worm-like tubules of low persistence length (Figure 3). This work not only demonstrates the possibility of programming materials with specific mechanical behavior through molecular design, but also opens the possibility of modeling protein interactions and membrane curvature effects in raft-like structures.

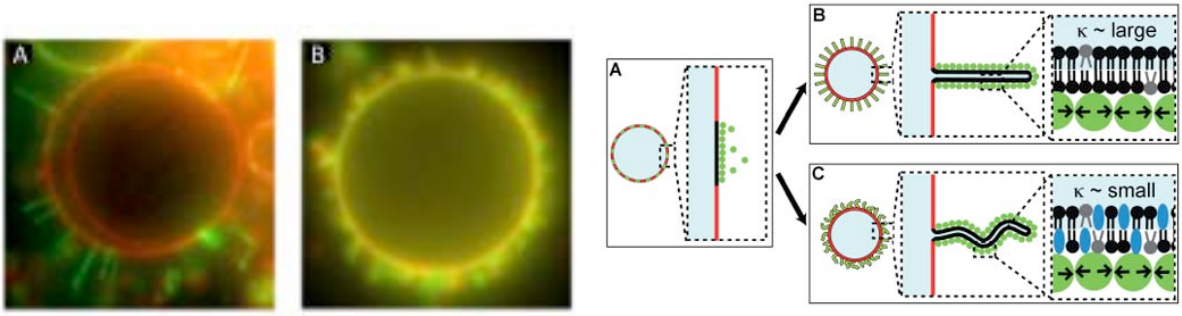

Figure 3. Lipid nanotube formation from domains of gel and liquid ordered phases. (Left) Fluorescence microscopic images of GUVs composed of (A) 20% DPIDA/DPhPC and (B) 12% DPIDA/8% DPPC/40% DPhPC/40% cholesterol both labeled with 0.3% BODIPY 530/550 HPC (red) and exposed to his-tagged GFP (green). Gel phase domains in (A) produce rigid rod nanotubes whereas the liquid ordered domains (B) yield worm-like nanotubes. (Right) Cartoon of nanotube formation upon protein binding that produce structures of either high or low persistence length depending on bending energy (κ) of the domain.

Orientation of lipid domains via electric field

In an effort attain a level of directional control over the formation of our reconfigurable assemblies we have examined the use of electric fields to orient lipid domains [Zendejas, *ChemComm* **2011**]. Phase separated domains of charged lipids in surface-bound GUVs were shown to orient in applied fields of < 2 V/cm in a matter of seconds. When an external electric field is applied across the GUVs, the charged domains in the buffer solution experience an electrostatic Coulomb force similar to a charged particle during electrophoresis [Chen, *J. Coll. Interf. Sci*. **2010**]. This force causes the domain to align towards the electrode of opposite charge. The GUVs composed of DSIDA/DPhPC produce slightly negatively charged domains that orient towards the positive electrode, whereas positively charged DSDAP in GUVs of POPC orient towards the negative electrode. Protein bound regions, such as GFP on Cu^{2+}-IDA domains, were also shown to orient in the electric field.

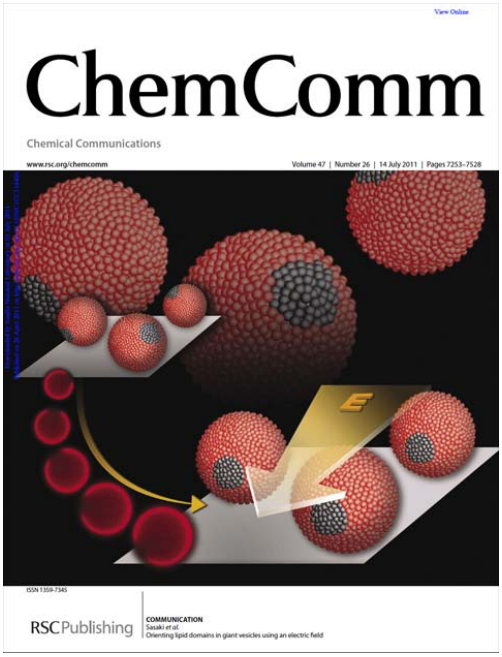

Future Plans

In other areas of this subtask researchers are exploring the use of temperature sensitive materials that reconfigure shape and physical behavior of self-assembled materials. For example, polyNIPAM surfactants are being studied as coatings on nanoparticles for heat-induced organization of hierarchical assemblies. Temperature sensitive systems are also being explored on lipid membrane systems to further understand the role of steric confinement on membrane curvature and structure deformation. Through an integrated approach of theory, simulations, and experiments we are investigating the relationship between the responsiveness of molecular structure and supramolecular organization to external stimuli. In addition to thermally-activated systems we are also examining light-activated (e.g., azobenzenes) and redox-activated (e.g., quinone) surfactants that would offer novel and orthogonal means to address highly functional composite architectures.

Acknowledgements

This research was supported by the Division of Materials Science and Engineering in the Department of Energy Office of Basic Energy Sciences. Sandia is a multiprogram laboratory operated by Sandia Corporation, a wholly owned subsidiary of Lockheed Martin Corp., for the U.S. Department of Energy NNSA under Contract DE-AC04-94AL85000.

Publications resulting from this subtask (2009 – 2011)

Lavin, J. M.; Huber, D. L.; Bunker, B. C. "Reconfigurable Gold Nanocomposites" submitted to *ACS Nano*.

Zendejas, F. J.; Meagher, R. J.; Stachowiak, J. C.; Hayden, C. C.; Sasaki, D. Y. "Orientation of Lipid Domains in Giant Vesicles Using an Electric Field" *ChemComm* **2011**, *47(26)*, 7320 – 7322.

Stachowiak, J. C.; Hayden, C. C.; Sanchez, M. A. A.; Wang, J.; Bunker, B. C.; Voigt, J. A.; Sasaki, D. Y. "Targeting Proteins to Liquid-Ordered Domains in Lipid Membranes" *Langmuir* **2011**, 27, 1457 – 1462.

Stachowiak, Jeanne C.; Hayden, Carl C.; Sasaki, Darryl Y., "Steric Confinement of Proteins on Lipid Membranes Can Drive Curvature and Tubulation" *Proceedings of the National Academy of Sciences of the United States of America*, **2010**, *107(17)*, 7781 – 7786.

Somin Eunice Lee, Darryl Y. Sasaki, Thomas D. Perroud, Daniel Yoo, Kamlesh D. Patel, and Luke P. Lee, "Biologically Functional Cationic Phospholipid-Gold Nanoplasmonic Carriers of RNA" *J. Am. Chem. Soc.* **2009**, *131(39)*, 14066 - 14074.

Orendorff, C. J., Huber, D. L., and Bunker, B. C., "Effects of Water and Temperature on Conformational Order in Model Nylon Thin Films," *J. Phys. Chem. C.*, **2009**, *113*, 13723.

Orendorff, C. J., T. M. Alam, D. Y. Sasaki, B. C. Bunker, and J. A. Voigt. 2009. "Phospholipid-Gold Nanorod Composites" *ACS Nano*, **2009**, *3*, 971 - 983.

Hayden, C. C., J. S. Hwang, E. A. Abate, M. S. Kent, and D. Y. Sasaki. "Directed Formation of Lipid Membrane Microdomains as High Affinity Sites for His-Tagged Proteins" *J. Am. Chem. Soc.*, **2009**, *131*, 8728 - 8729.

Other references

Chen, S. B. "Electrophoretic mobility of a spherical liposome" *J. Colloid Interf. Sci.* **2010**, *348*, 177

Veatch, S. L.; Gawrisch, K.; Keller, S. L. "Closed-Loop Miscibility Gap and Quantitative Tie-Lines in Ternary Membranes Containing Diphytanoyl PC" *Biophys. J.* **2006**, *90*, 4428

***Program Title*: Solid-State NMR of Complex Materials**

***Principal Investigators*:** Klaus Schmidt-Rohr (FWP leader), Mei Hong, E. M. Levin.
Mailing Address: Div. of Materials Science & Engineering, Ames Laboratory, Ames IA 50011

Coworkers: Dr. Aditya Rawal, Dr. Bosiljka Njegic, Ms. Jinfang "Jean" Cui, Mr. Robert Johnson, Mrs. Marilu Dick-Perez, Mr. Tuo Wang

Program Scope

We develop and apply solid-state nuclear magnetic resonance (NMR) methods for studying complex materials. In the context of biomolecular materials, we analyze the structure and composition of organic-inorganic biomaterials and of plant cell walls on the nanometer scale. Other parts of this FWP involve studies of the nanostructure of the Nafion fuel-cell membrane and of complex thermoelectric tellurides. In this Abstract, we will focus on the aspects of our program with bio-relevance. Part of this work has been tightly integrated with the FWP on *Bioinspired Materials* led by Dr. Surya Mallapragada.

Recent Progress

The organic-inorganic interface in bone. The stiff and tough load-bearing material in bone is a nanocomposite of calcium phosphate (apatite) nanocrystals imbedded in a matrix of the fibrous protein collagen, at a 45:45 volume ratio; water accounts for the remaining 10 vol%. As a target for biomimetic materials synthesis,[1,2] this nanocomposite needs to be characterized more accurately. We have shown that multinuclear (^{13}C, ^{1}H, ^{31}P) NMR can characterize many important aspects of this nanocomposite, in particular regarding the organic-inorganic interface. For instance, we have shown that two different layers of water are present near the interface, one of crystal-bound water and one forming a viscous monomolecular layer outside the crystals that may act as hydrogen-bonding "glue" between the components of the nanocomposite.

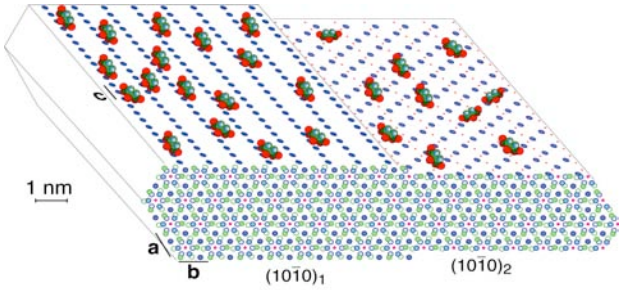

Figure 1. Schematic of apatite-bound citrate (oxygen of carboxylate groups in red) interacting with Ca^{2+} (blue circles) on two surfaces of high morphological importance of an idealized bone apatite nanocrystal, with the citrate orientation determined by NMR and at a realistic citrate surface density of 1/(2 nm)^2. [3]

Strongly bound citrate stabilizes the apatite nanocrystals in bone. The nanocrystals of apatitic calcium phosphate impart the organic-inorganic nanocomposite in bone with favorable mechanical properties, but the factors preventing crystal growth beyond the favorable thickness of ~3 nm had not been identified. We have shown [3] by multinuclear NMR, including ^{13}C{^{31}P} REDOR, ^{13}C{^{1}H} spectral editing, and chemical-shift anisotropy dephasing, that the nanocrystal surfaces in bone are studded with strongly bound citrate molecules, which have no large-amplitude mobility on the 10-s scale or below, and have characterized the density (0.25 nm^{-2}) and geometry of the bound citrate with the three carboxylate groups at distances of 0.3 to 0.45 nm from the apatite surface, see Figure 1. The structural analysis was facilitated by multispin analysis developed earlier in this program. Incorrect assignments of the citrate signals to polysaccharides presented in several papers in the literature, or to special hydroxyproline sidegroups (our earlier working model, fortunately never published), have been disproved by spectral editing. The peak assignment was further

confirmed by exchange of the native citrate with ^{13}C-labeled molecules, which also enhanced sensitivity 30-fold for detailed distance measurements.[3] Bound citrate is highly conserved, being found in fish, avian, and mammalian bone, which indicates its critical role in interfering with crystal thickening and stabilizing the apatite nanocrystals in bone.

Cell walls in higher plants are an energy-rich material important for the mechanical strength, protection against environmental stress, and growth and division of plants. Plant cell walls have recently gained economic importance as the source of lignocellulose-based biofuels due to their high content of energy-rich polysaccharides. However, biofuel production is hampered by the toughness of the cell wall, since cellulose is linked to hemicellulose, pectins, and lignin. Thus, understanding the structure and packing of cell wall biopolymers is important for developing new technologies to produce alternative bio-energy. Plants have a primary cell wall laid down by growing cells and a secondary wall produced after termination of cell growth. The major biopolymers common to both walls are cellulose, hemicellulose, pectins, and glycoproteins. Secondary cell walls also contain lignin, a highly branched aromatic-rich polymer. Most structural studies of cell walls so far have relied on extraction-based chemical analysis, which causes partial and non-specific bond cleavage, and on electron microscopy and X-ray diffraction, which mostly detect the crystalline cellulose but not the amorphous matrix polysaccharides. While solid-state NMR has been used to study cellulose as early as the 1980s, the studies relied on unlabeled materials with low sensitivity. More recent studies used specifically ^{13}C-labeled individual components of the cell wall. Thus, few studies have dealt with the native cell wall in its entirety.

We have completed a first, comprehensive, study of uniformly ^{13}C-labeled *Arabidopsis thaliana* using 2D and 3D MAS NMR.[4] With a suite of dipolar and scalar-coupling mediated polarization transfer techniques, we resolved and assigned the sugar resonances of all major polysaccharides in the intact cell wall (Figure 2a,b), including surface and interior cellulose, xyloglucan (XG), rhamnogalacturonan (RG), homogalacturonan (HGA), arabinan, and galactan. Further, using long spin diffusion times in a 3D ^{13}C-^{13}C-^{13}C experiment, we detected intermolecular cross peaks between the different polysaccharides, which directly revealed the spatial proximity of the wall polysaccharides (Figure 2c). The 3D spectra showed that cellulose microfibrils interact extensively with pectins, while the hemicellulosic XG exhibited only a few contacts with cellulose, mostly in the interior. The latter is interesting because it disagrees with the current paradigm of extensive surface coating of cellulose microfibrils by XG but suggests entrapment of a small number of XG segments in the fibrils.

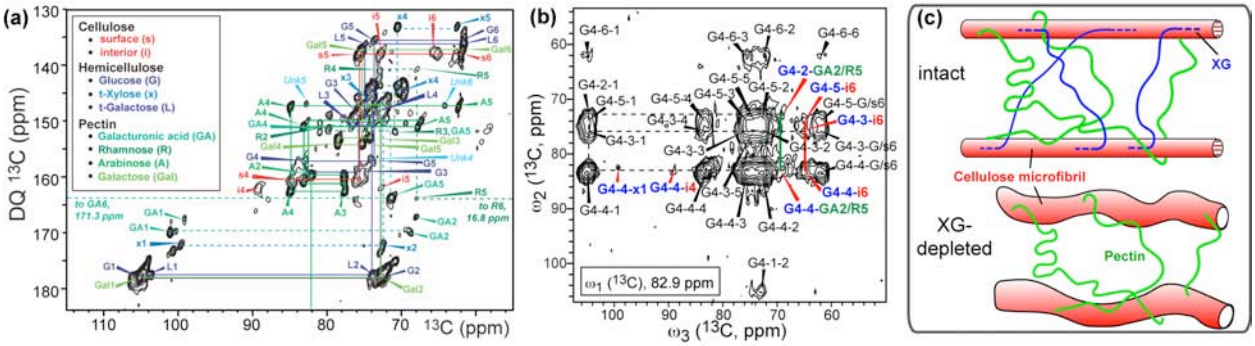

Figure 2. Representative 2D and 3D MAS ^{13}C NMR spectra of uniformly ^{13}C-labeled primary cell wall. (a) 2D J-INADEQUATE spectra showing one-bond ^{13}C cross peaks of mostly mobile polysaccharides. Assignments are color coded for the three major types of polysaccharides. (b) Example of a 2D plane of a 3D ^{13}C-^{13}C-^{13}C correlation spectrum, showing cellulose-hemicellulose (red and blue) and cellulose-pectin (red and green) cross peaks. (c) Structural models of intact and xyloglucan-depleted cell walls. The microfibrils are stabilized by semi-rigid hemicellulosic chains and interact extensively with pectins, which provide flexibility and porosity to the cell wall.

^{13}C T_1 and ^{1}H $T_{1\rho}$ relaxation times indicate that pectin is highly dynamic while cellulose is the most rigid, and XG exhibits intermediate motional rates and amplitudes. In a mutant plant where XG is enzymatically removed, all polysaccharides showed enhanced motion, indicating that XG helps to maintain the rigidity of the cell wall (Figure 2d). Taken together, these results provide the most definitive evidence so far that load bearing in cell walls is achieved by a single network of all three polysaccharides instead of a cellulose-XG network, thus revising the conventional model of cell wall structure. We further investigated the structural role of pectins using a depectinated cell wall sample, and found higher intermolecular cross peaks and longer relaxation times, indicating that the polysaccharides become more rigid and pack more tightly in the absence of pectins.

Future Plans

The nanostructure of bone. Various models of bone assume that apatite nanocrystals are concentrated in the "gap" regions of the collagen fibrils. This would require the presence of thick collagen layers in the apatite-poor regions. We will test these models by probing the thickness of the collagen layers in bone by long-range $^{13}C\{^{31}P\}$ NMR; thick layers would produce a nearly constant intensity at long dephasing times. We will also determine the nanoparticle size distribution in bone, based on heteronuclear NMR combined with quantitative scattering analysis. Further, we will try to determine to what extent the surface layer of biological apatite nanocrystals resembles octacalcium phosphate (OCP), by identifying the NMR and diffraction characteristics of OCP in nanocrystals. In the end, we should be able to present a well-founded comprehensive and detailed model of the local structure of the nanocomposite in bone.

Structure determination of cell wall materials. We will determine the specific residues that form intermolecular contacts between different polysaccharides in plant cell walls. For example, the hemicellulose xyloglucan (XG) is decorated with many sidechains such as xylose, fucose, and galactose. In the uniformly ^{13}C-labeled cell wall, the residues responsible for entrapment in the cellulose microfibrils are not fully clear due to remaining resonance overlap, especially among C2, C3 and C5 carbons, which cluster within a narrow range of 72-75 ppm. We will use site-specifically ^{13}C-labeled cell walls to address this question. C1-C2 labeling will allow unambiguous assignment of pectin Rha and GalA based on their C2 chemical shifts, whereas the C1 chemical shift distinguishes xylose from other sugars. The C4-C5 labeling will allow the assignment of Xyl and Ara through their 62 ppm peaks, without overlap from the C6 of cellulose and XG backbone. Specifically labeled plants have been produced using media supplemented with 1,2-^{13}C labeled glucose or 4,5-^{13}C labeled glucose. 2D and 3D MAS experiments will be performed to extract intermolecular contacts.

In collaboration with Seth DeBolt at the University of Kentucky, we will investigate cellulose biosynthesis in plants. Understanding the molecular machinery for cellulose synthesis is important because it may provide insights into how to increase the disorder of cellulose (while still having viable plants) to facilitate its deconstruction to produce fermentable sugars. Cellulose is synthesized by large plasma-membrane hexameric complexes of cellulose synthase (CESA). The precise structure and assembly of CESA proteins in these so-called particle rosettes is unknown. One model posits that each subunit of the hexameric array contains six CESA proteins from three different genes. Each CESA protein is thought to contain eight transmembrane (TM) helices that form a pore through which the growing glucan chains are extruded to reach the cell wall. In this model, the structure of each microfibril is directly correlated with the rosette structure and contains 36 glucan chains. DeBolt's laboratory has identified several mutations in the catalytic and TM domains of two CESA proteins that cause stunted plant growth. We will use multidimensional MAS NMR to study the structure, dynamics, and packing of cellulose and other polysaccharides in

these mutant cell walls and compare them with the wild-type cellulose structure.

Biological and biomimetic calcium-carbonate–polymer composites. By far the most abundant biogenic mineral is calcium carbonate, which exists in four structural forms: calcite, aragonite, vaterite, and amorphous, all of which are used by various organisms for a variety of purposes such as mechanical support, defense, feeding, and locomotion. While crystals embedded within an organic matrix have been well studied, organic molecules introduced within the crystals have been gaining attention only recently. Introducing macromolecules into calcite single crystals, which are often used as structural units by organisms, reduces their inherent brittleness, e.g. in sea-urchin skeletal parts and mollusk shells. Sea-urchin biogenic single crystals exhibit greater toughness than calcite crystals and conchoidal fracture surfaces instead of the typical cleavage planes. It is unclear whether the organics that incorporate into the calcite crystal without apparent disruption of the crystalline lattice are all found at mosaic block boundaries, in nanometer sized cavities, as lattice impurities, or in an entrapped 3-D nanofiber network.

We plan to study organic molecules occluded in calcium-carbonate crystals by NMR, to elucidate the molecular aggregation of the organic species, the organic-inorganic interface, and the influence of the organic moieties on the crystal growth and structure. We will study this both in nacre of abalone shells, as well as in ^{13}C-labeled calcite synthesized in the presence of possibly ^{13}C labeled organic molecules like citrate and agarose. Porous single crystals of calcite will be synthesized via the hydrogel process using $CaCl_2$ and NH_4CO_3 solutions to grow calcite monoliths in a manner that incorporates the hydrogel within the crystal. The calcite will also be synthesized with the hydrogel replaced by biologically important molecules such as citrate. 2D ^{13}C-^{1}H correlation NMR -spectroscopy will be employed to monitor the inclusion of the organic molecules into the calcite crystals. ^{13}C-^{13}C and ^{1}H-^{13}C-^{13}C spin exchange measured by NMR will enable estimation of the extent of organic inclusion within the crystal lattice. Long-range ^{13}C-^{1}H dipolar dephasing will allow estimation of the fraction of calcium carbonate in close proximity to the organic molecules. Finally, ^{13}C chemical shift analysis will allow determination of molecular conformation and estimation of the degree of structural disorder induced within the crystalline matrix.

Publications 2009-2011

Related to biomolecular systems:

[1] Y-Y. Hu, Y. Yusufoglu, M. Kanapathipillai, J. Yang, P. Thiyagarajan, T. Deming, M. Akinc, K. Schmidt-Rohr, S. Mallapragada, "Self-assembled calcium phosphate nanocomposites using block copolypeptide templates", *Soft Matter* **5**, 4311 (2009).

[2] Y-Y. Hu, X. Liu, X. Ma, J. Yang, A. Rawal, M. Akinc, T. Prozorov, S. Mallapragada, K. Schmidt-Rohr, "Biomimetic Self-assembling Copolymer–Hydroxyapatite Nanocomposites with the Nanocrystal Size Controlled by Citrate", *Chem. Mater.* **23**, 2481 (2011).

[3] Y.-Y. Hu, A. Rawal, and K. Schmidt-Rohr, "Strongly Bound Citrate Stabilizes the Apatite Nanocrystals in Bone," *Proceedings of the National Academy of Sciences*, **107,** 22425 (2010).

[4] M. Dick-Perez, Y.A. Zhang, J. Hayes, A. Salazar, O.A. Zabotina, and M. Hong, "Structure and Interactions of Plant Cell-Wall Polysaccharides by Two- and Three-Dimensional Magic-Angle-Spinning Solid-State NMR," *Biochemistry*, **50**, 989 (2011).

Y.Y. Hu and K. Schmidt-Rohr, "Effects of L-Spin Longitudinal Quadrupolar Relaxation in S{L} Heteronuclear Recoupling & S-Spin Magic-Angle Spinning NMR," *J. Magn. Reson.*, **197**, 193 (2009).

Plus 8 other DOE-supported publications, in J. Am. Chem. Soc., Adv. Funct. Mater., Macromolecules, Phys. Rev. B, Polymer, J. Magn. Magn. Mater., and Solid State NMR.

Molecular Nanocomposites
Cooperative Binary Ionic Solids, Nanostructures, and Nanocomposites

John A. Shelnutt[1,2], Frank van Swol[1,3], Craig J. Medforth[3], Yongming Tian[4], and Kathleen E. Martin[3]
[1]Sandia National Laboratories, [2]The University of Georgia, [3]The University of New Mexico, New Mexico Tech
Advanced Materials Lab, 1001 University Blvd SE, Albuquerque, NM 87106
jasheln@sandia.gov
http://jasheln.unm.edu/

Program Scope - Our nanocomposites research focuses on the use of analogs of biomolecular cofactors of proteins that perform electron transport, chemical sensing and signaling, catalysis, and photosynthetic light-harvesting to form new classes of complex, hierarchical nanomaterials with biomimetic functionalities related to renewable energy systems. Our synthesis of these nanocomposites and determination of their crystalline structures and morphologies are directly related to our efforts to utilize their unique photophysical, photochemical, and catalytic behaviors for artificial photosynthesis. The work builds on key bottom-up fabrication strategies developed by our team including ionic self-assembly, directed assembly, and photocatalytic metals nanostructuring.

Recent Progress

Synthesis and Morphological Characterization of Cooperative Binary Ionic (CBI) Solids - Recently, we discovered a new type of binary solid composed of ionically self-assembled organometallic anions and cations.[1,2] Crystalline solids self-assembled from ionic porphyrin molecules provide a multifunctional new class of optoelectronic micro- and nanoscale materials.[1-8] We call these new porphyrin-based materials *cooperative binary ionic* (CBI) solids because the cooperative interactions between the complementary functional porphyrin subunits of the solid lead to interesting emergent collective properties that are useful in a variety of opto-electronic and energy-related applications. Initially, these unique CBI materials came in the form of complex microscale morphologies, such as the four-leaf clover-like microstructures with nanoscale features shown in Fig. 1 that form by diffusion-limited crystallization of oppositely charged porphyrins. An important feature of these crystalline solids is that the metals in the porphyrin anions and cations can be chosen freely for their preferred metalloporphyin functionalities (*e.g.*, electron donor and acceptor abilities). This tunability is possible because, within limits, the metals do not significantly alter the crystal structure.[6] The ability to substitute a variety of metals in the two types of porphyrin chromophores without altering the crystal structure permits the functional properties of the solid to be altered and tuned systematically. For example, the commonality of the crystal structures of the solids formed with Zn and Sn metal ions in the porphyrins $TPPS^{4-}$ and $T(N\text{-}EtOH\text{-}4\text{-}Py)P^{+4}$ is reflected in their similar clover-like structures. The similarity of the crystal structure is confirmed by their XRD patterns.

We have platinized the photo-catalytically clovers shown in Fig. 1 and used them to photosensitize H_2 production for more than two weeks of continuous operation without degradation of the platinized clovers or decrease in

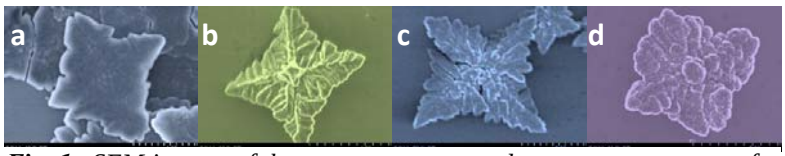

Fig. 1. *SEM images of the structures prepared at room temperature for all four combinations of Zn(II) and Sn(IV) in the porphyrins $TPPS^{4-}$ and $T(N\text{-}EtOH\text{-}4\text{-}Py)P^{+4}$. Zn/Sn (a), Sn/Zn (b), Zn/Zn (c), and Sn/Sn (d).*

their efficiency. We have also shown using conducting AFM that the Zn/Sn combination (Fig. 1a) gives photoconductive clovers.

Determination of the First X-ray Crystal Structure of a CBI Solid - We have utilized the ALS synchrotron X-ray source to determine the first crystal structure of a CBI crystalline solid,[9] namely, nanosheets formed from the pair of cationic (electron acceptor) and anionic (electron donor) porphyrins, dihydroxy tin(IV) tetra(N-methyl-4-pyridiniumyl)porphyrin^{4+} and aquo zinc(II) tetra(4-sulfonatophenyl)porphyrin^{4-}, respectively. We also investigated the Zn/Sn nanosheets by SEM, XRD, and UV-visible spectroscopy and microscopy. An SEM image and a view of the complex crystal structure of the nanosheets are shown in Fig. 2. The asymmetric unit cell contains one complete $Zn(H_2O)$-$TPPS^{4-}$ molecule and half of a second $Zn(H_2O)TPPS^{4-}$; the cell also contains three half $Sn(OH^-)_2TNMePyP^{4+}$ molecules thus balancing the charge without other non-porphyrinic counter-ions. In addition, the unit cell contains 20.4 water molecules in 47 partially occupied sites.

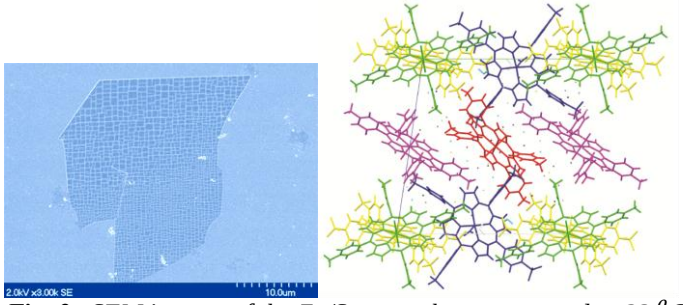

Fig. 2. *SEM images of the Zn/Sn nanosheets prepared at 23 ^{o}C with 210 μM initial total concentrations of ZnTPPS and SnTNMePyP, in equal proportion.*

Electronic properties of these nanosheets, determined by conducting AFM measurements, can be rationalized based on the observed crystal structure. The insulating nanosheets are not photoconducting, unlike the corresponding clovers. For the nanosheets, a photocurrent is not expected because of the lack of extended π–π stacking of porphyrin molecules in the crystal. Although the solid is formed from an equal proportion of electron donors (ZnTPPS) and acceptors (SnTNMePyP) and thus charge transfer is likely to occur within the solid, the lack of extended π–π porphyrin stacks limits the formation of mobile electrons and holes. Therefore, the structure explains of the lack of photoconductivity for the nanosheet and also the absence of J-aggregate bands in the optical spectra of the nanosheets. and conceivably their low H_2 generation rates (Fig. 3). The different crystal structure of the photoconductive Zn/Sn clovers admits J-aggregated bands that indicate stacking and may explain why they are more efficient at H_2 generation.

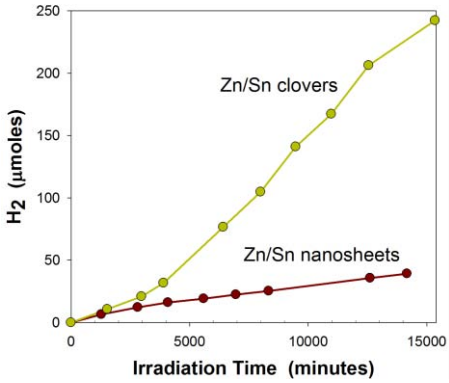

Fig. 3. *Hydrogen generated by platinized Zn/Sn nanosheets or Zn/Sn clovers as a function of irradiation time with visible light from an incandescent lamp (0.10 watt cm^{-2}). Triethanolamine was used as a sacrificial electron donor and methylviologen as an electron relay molecule.*

H_2 Generation by Zn/Sn Nanosheets and Clovers – The porphyrins used in the synthesis of the nanosheets and clover-like CBI nanomaterials and nanocomposites are analogs of the biological pigments of photosynthesis. Moreover, the morphologies produced by ionic self-assembly of porphyrins mimic naturally occurring light-harvesting structures such as the self-assembled bacteriochlorophyll-based chlorosomal nanorods of green bacteria. So, it is not surprising that these structures also can be utilized successfully in artificial photosynthetic systems. To date it has been difficult to mimic these light harvesting systems in a stable and efficient manner, but we have shown that platinized clover-like CBI nanocomposites efficiently

produce H_2 for weeks of continuous visible light irradiation. The analogous Zn/Sn nanosheets also act as light-harvesting structures for the steady generation of H_2 in the presence of sacrificial electron donor, electron relay, and platinum nanocatalyst photocatalytically deposited onto the nanosheet surface. However, the rate of hydrogen production by the Zn/Sn nanosheets is significantly lower than the analogous clovers (Fig. 3). The lower rate might be caused by differences in morphology and charge mobility between the platinized nanosheets and clovers.

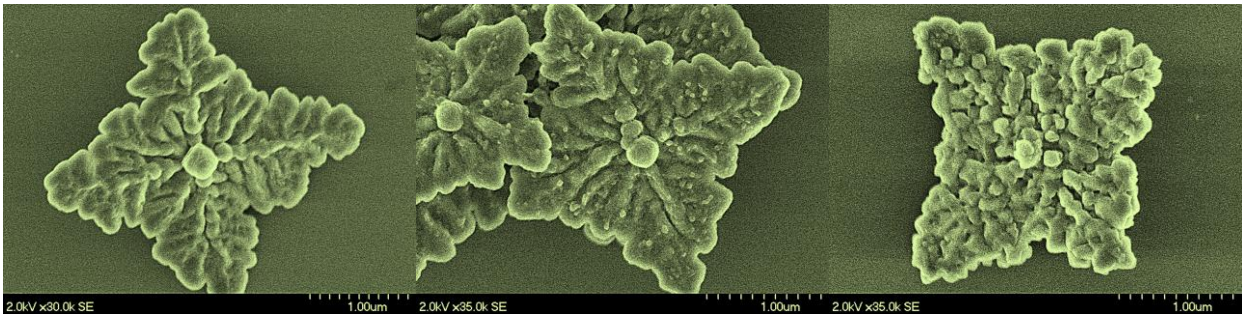

Fig. 4. *Nanocomposite structures designed for visible light-driven CO_2 reduction: (a) Sn/Zn clovers, (b) Sn/Zn clovers with 20% Sn/Co particles grown on surface, and (c) Sn/Zn clovers with 40% Sn/Co particles grown on surface. Notice the increasing size of the Sn/Co particles. Co porphyrins are known CO_2 reduction electrocatalysts and Sn porphyrin are known photocatalysts; the underlying Sn/Zn clovers are efficient and stable photocatalytic light-harvesting structures for artificial photosynthesis of H_2.*

Hierarchical Hybrid CBI Nanocomposites – In our molecular nanocomposites program, we have developed synthetic strategies for producing hierarchical hybrid CBI structures such as those shown in Fig. 4. Our goal is to produce hierarchical CBI nanocomposites that can carry out the multiple functions necessary for photosynthesis of carbon-based fuels using sunlight, including light-harvesting, charge separation and transport, and catalysis. The fabrication of these CBI nanocomposites relies on our ability to substitute different metals into the porphyrins of CBI solids without significantly altering their ionic crystal structure.[1,2,6-8] This makes it possible to graft one CBI structure onto another, possibly by epitaxial growth. The Sn/Zn-Sn/Co nanocomposite structures shown in the SEM images of Fig. 4 and 5 have been investigated by conventional SEM and high-resolution SEM with element mapping by EDS (Fig. 4), XRD, and confocal fluorescence microscopy. The selected-area EDS experiments show that the nanoparticles grafted onto the surface of the Sn/Zn clovers contain the Sn/Co solid, and the XRD measurements further show that the grafted Sn/Co CBI nanoparticles have the same basic crystal structure shared by the pure Sn/Zn and Sn/Co clovers. The latter result admits the possibility that the Sn/Co solid is

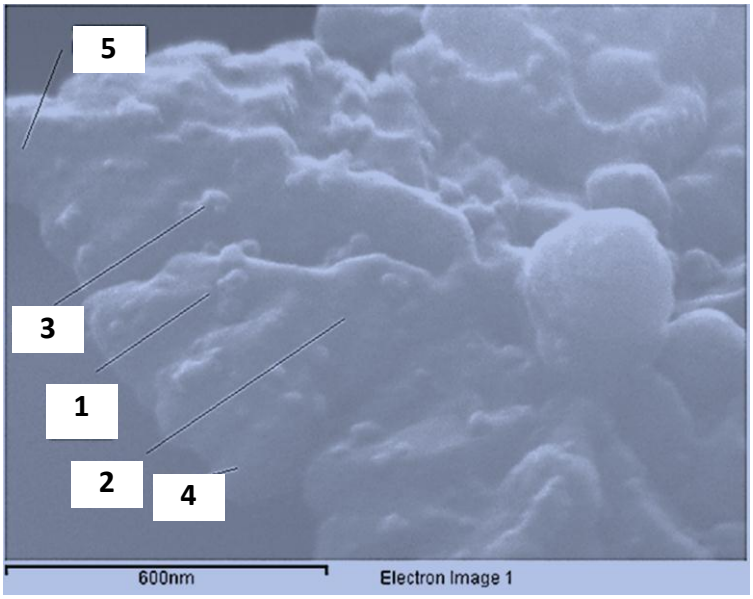

Fig. 5. *SEM image of a Sn/Zn-20% Sn/Co clover coated with a 4-nm thick Au/Pd layer. The lines indicate regions where the EDS analysis was performed. Co peaks are seen only in regions 1 and 3 that are occupied by particles of the Sn/Co clover CBI crystalline solid.*

epitaxially grown onto the Sn/Zn clover surface.

Although there has been significant progress towards an understanding of the molecular components involved in photosynthesis, the development of artificial photosynthetic systems directed toward carbon-based fuel products is largely undeveloped. Hierarchical nano-composites like those shown in Figs. 4 and 5 demonstrate grafting together structurally similar CBI solids. In this case, one solid consists of a catalyst for CO_2 reduction (Co porphyrin) and an electron acceptor (Sn porphyrin) and the other consists of an electron donor (Zn porphyrin) and an electron-acceptor, forming a photoconducting charge-transfer CBI clover that serves as a light-harvesting framework. Such bio-inspired constructs have the potential for performing light-driven CO_2 reduction to CO under visible light and ambient conditions.[10]

Future Plans

CBI solids represent a new and exciting discovery with implications for a spectrum of advanced materials with applications in opto-electronics and renewable energy. The preparation of mixed porphyrin and phthalocyanine CBI nanomaterials points to future synthetic strategies involving myriad other organic ions. The wide variety of CBI materials that can be synthesized provides a foundation for future studies of their opto-electronic, light-harvesting, non-linear optical, photochemical, and catalytic properties. Preliminary results from Monte Carlo simulations of ionic self-assembly, crystal growth studies, X-ray crystal structure determinations, and resonance Raman studies of CBI solids suggest that these experimental and computational approaches offer new opportunities for furthering our understanding of this new class of biomolecular materials. Such investigations of CBI nanomaterials will enable and provide the basis for exploring and customizing their development as robust materials for renewable energy and other applications.

Our References and Recent Publications[1,2,6-16]

1. Martin, K. E. *et al.* Donor-acceptor biomorphs from the ionic self-assembly of porphyrins. *J. Am. Chem. Soc.* **132**, 8194-8201 (2010).
2. Medforth, C. J. *et al.* Self-assembled Porphyrin Nanostructures. *Chem. Commun.*, 7261-7277 (2009).
3. Wang, Z., Medforth, C. J. & Shelnutt, J. A. Porphyrin nanotubes by ionic self-assembly. *J. Am. Chem. Soc.* **126**, 15954-15995 (2004).
4. Wang, Z., Li, Z., Medforth, C. J. & Shelnutt, J. A. Self-assembly and self-metallization of porphyrin nanosheets. *J. Am. Chem. Soc.* **129**, 2440-2441 (2007).
5. Wang, Z., Ho, K. J., Medforth, C. J. & Shelnutt, J. A. Porphyrin nanofiber bundles from phase-transfer ionic self-assembly and their photocatalytic self-metallization. *Adv. Mater.* **18**, 2557-2560 (2006).
6. Tian, Y. *et al.* Morphological families of self-assembled porphyrin structures and their photosensitization of hydrogen generation. *Chem. Commun.* **47**, 6069-6071 (2011).
7. Medforth, C. J. & Shelnutt, J. A. in *Handbook of Porphyrin Science* Vol. 11 (eds K. M. Kadish, K. M. Smith, & R. Guilard) Ch. 50, 181-222 (World Scientific Publishing, 2011).
8. Shelnutt, J. A. & Medforth, C. J. in *Organic Nanomaterials* (eds G. Bottari & T. Torres) in press (Wiley, 2011).
9. Tian, Y. *et al.* Crystal structure and properties of a porphyrin-based cooperative binary ionic solid. *Nature Chemistry*, submitted (2011).
10. Leung, K., Nielsen, I. M. B., Sai, N., Medforth, C. & Shelnutt, J. A. Cobalt-porphyrin catalyzed electrochemical reduction of carbon dioxide in water. 2. Mechanism from first principles. *J. Phys. Chem. A* **114**, 10174-10184 (2010).
11. Haddad, R. *et al.* Steric bulkiness of pyrrole substituents and the out-of-plane deformations of porphyrins: Nickel(II) octaisopropylporphyrin and its *meso*-nitro derivative. *J. Porphyrins Phthalocyanines* **15**, DOI No: 10.1142/S1088424611003707 (2011).
12. Garcia, R. M. *et al.* Templated growth of platinum nanowheels using the inhomogeneous reaction environment of bicelles. *Phys. Chem. Chem. Phys.* **13**, 4846-4852 (2011).
13. McIntyre, N. R., Franco, R., Shelnutt, J. A. & Ferreira, G. C. Nickel(II) Chelatase Variants Directly Evolved from Murine Ferrochelatase: Porphyrin Distortion and Kinetic Mechanism. *Biochemistry* **50**, 1535-1544 (2011).
14. Miranda, A. *et al.* One-pot synthesis of triangular gold nanoplates allowing broad and fine tuning of edge length. *Nanoscale* **2**, 2209-2216 (2010).
15. Franco, R. *et al.* Internal organization and electronic structure of porphyrin nanotubes revealed by resonance raman spectroscopy. *Phys. Chem. Chem. Phys.* **12**, 4072 (2010).
16. Challa, S. R., Song, Y., Shelnutt, J. A., Miller, J. E. & van Swol, F. Evolution of dendritic nanosheets into durable holey sheets: A lattice gas simulation study. *J. Porphyrins Phthalocyanines* **15**, 449-466 (2011).

Molecularly Engineered Biomimetic Nanoassemblies

Andrew P. Shreve (shreve@lanl.gov), Hsing-Lin Wang (hwang@lanl.gov), Jennifer S. Martinez (jenm@lanl.gov), Srinivas Iyer (siyer@lanl.gov), Reginaldo Rocha (rcrocha@lanl.gov),
Los Alamos National Laboratory;
James Brozik (brozik@wsu.edu), Washington State University;
Darryl Sasaki (dysasak@sandia.gov), Sandia National Laboratories;
Atul N. Parikh (anparikh@ucdavis.edu), University of California, Davis;
Sunil K. Sinha (ssinha@physics.ucsd.edu), University of California, San Diego.

Program Scope

The program aims to develop self-assembly and biologically-assisted assembly methods for the control of functional responses in complex, multi-component materials. The overall motivation is derived from an examination of natural systems that demonstrate exquisite manipulation and transduction of optical energy. We are interested in developing assemblies of nanomaterials that mimic two particular functions of natural systems, photo-induced charge separation and control of light-harvesting (or manipulation of electromagnetic fields). An important aspect of natural systems is their hierarchical organization, which allows for control and manipulation of energy across multiple length scales in a spatially directed manner. In many cases, this hierarchical organization is associated with complex membrane assemblies. Thus, we also explore the integration of functional synthetic nanomaterials with complex membrane-based architectures in order to generate materials with energy-relevant functions that demonstrate larger-scale organization similar to that found in natural systems. A general schematic that illustrates the approach we envision is shown in Figure 1. Functionally active synthetic materials under study include conjugated polymers and polyelectrolytes, carbon-based nanomaterials, and luminescent noble-metal nanoclusters. Approaches used include a co mbination of material synthesis and fabrication, static and time-resolved spectroscopies, optical and scanning probe microscopies, structural characterization, and modeling and analysis.

Recent Progress

We highlight here four areas of recent work that will form the basis of presentations. Progress in other areas related to the program scope is represented in the publication list.

Multiscale assemblies of conjugated polymers and carbon nanomaterials (Wang, Shreve). Blends of conjugated polymers and carbon nanomaterials such as functionalized fullerenes are the basis of many organic photovoltaic technologies. In the context of improving performance in such systems, an important challenge is understanding how to control the aggregation properties of polymers and fullerenes, and how to manipulate the interfaces between polymer- and fullerene-rich regions across multiple length scales in hierarchical assemblies. We have explored methods to introduce chemically tunable functionalization into conjugated polymers such as PPV (Wang *et al.* (2010)), and to assemble both polymers and polymer-fullerene composites on multiple scales. As an example, we have integrated one of these functionalized PPVs with functionalized fullerenes (Kokubo *et al.* (2010)), and patterned the resulting composite material over large scales using the so-called “breath figure method” of self-assembly (Figure 2; Tsai *et*

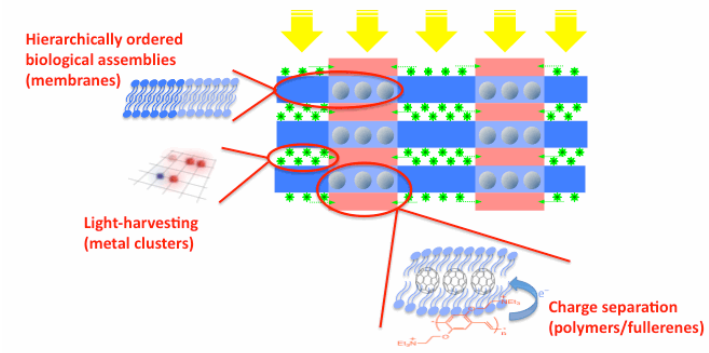

Figure 1. A schematic diagram of hierarchically organized lipid-based assemblies that incorporate synthetic nanomaterials to perform photo-induced charge separation or light-harvesting functions. In order to realize these types of assemblies, our efforts are focused on generating improved understanding of polymer assemblies, polymer-fullerene interactions, nanomaterial-membrane and membrane-surface interactions, and fluorescent nanocluster structure and properties.

al. (2011)). The resulting functional material demonstrates efficient photo-induced charge separation, and is amenable to being integrated with other large-scale assembly methods.

Co-assembly of conjugated polymers and membranes (Sasaki, Parikh, Shreve, Wang). An initial step in developing lipid-based methods for producing functional nanoassemblies is to understand and control the interactions of active materials with membranes. To that end, we have been investigating the interaction of conjugated polyelectrolytes with model membrane assemblies, both in solution and on surfaces (Figure 3). Significant enhancements of cationic polymer fluorescence are observed upon interaction with vesicles and other model membrane systems containing negatively charged lipids. Further, when using lipid compositions that demonstrate phase separation, one can identify spatial regions with which the conjugated polyelectrolytes preferentially interact. This result demonstrates the potential of using lipid phase-separation to spatially organize conjugated polymers and other active nanomaterials, a step toward the types of functional composite assemblies being targeted. Ongoing work in this area includes the extension of these studies to surfaces, in which the phase separation of lipids can be controlled through surface patterning techniques using tethered molecules (e.g., tethered, cushioned cholesterols), and the incorporation of fullerenes that are functionalized either to interact with lipid head groups or the hydrophobic membrane interior.

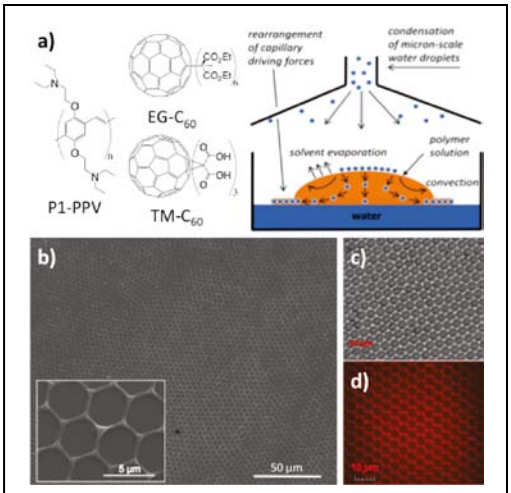

Figure 2. (a) Structures of P1, of water-soluble trismalonic fullerene (TM-C60) and emerald fullerene (EG-C60). Schematic illustration of the breath method used to deposit large area (up to 1 mm^2) P1-honeycombs. (b) SEM image and zoom of a P1-honeycomb deposited from chlorobenzene. (c, d) Optical bright-field and fluorescence images of a P1-honeycomb deposited on a coverglass.

Complex lipid assemblies and membrane-surface interactions (Parikh, Iyer, Shreve, Brozik, Sasaki, Sinha). Ultimately, in many important cases, functional materials assemblies will need to be integrated with solid substrates or other surfaces. In order to better understand relevant interfacial phenomena, we have studied complex structures that form within lipid assemblies on surfaces and how membranes interact with substrates. Recent efforts have included simulation studies of asymmetries in lipid bilayers that are induced

by interactions between membranes and surfaces in substrate-supported lipid assemblies (Hartshorn *et al.* (2010)), the development and characterization of multi-component, multi-layered bilayer assemblies on solid substrates (Poudel *et al.* (2011)), stabilization of membrane assemblies using trehalose, and the development of patterned, surface-tethered membrane architectures to control the spatial organization of phase-separated membranes.

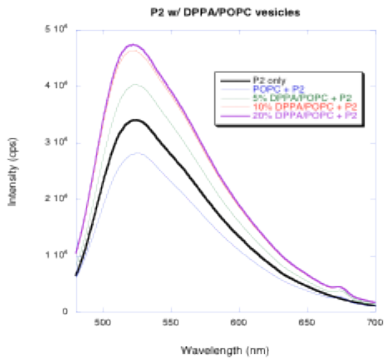

Figure 3. Fluorescence intensity after association of conjugated polyelectrolyte (P2) with vesicles containing negatively charged lipids. Microscopy of giant vesicles and substrate-supported model membrane systems has also been used to investigate how phase separation in lipid assemblies modulates polymer behavior.

Development and characterization of fluorescent noble metal nanoclusters (Martinez, Shreve, Rocha, Sinha). Noble metal nanoclusters (typically less than 1 nm in size) are synthesized and stabilized using a variety of small molecule and polymeric templates, including DNA. (Sharma *et al.* (2010); Bao *et al.* (2010); Yeh *et al.* (2010)) These materials have potential as a new type of active component in nanoassemblies with energy transfer or other light manipulation functions. (Sharma *et al.* (2011)) However, there is still a need for better understanding of structure-property relationships of individual clusters in order to enable longer-term applications that could involve multi-cluster assembly. We note that while assemblies of larger nanoparticles are well known, the assembly behavior of the much smaller nanoclusters being studied here is completely unexplored. Since DNA-based assembly methods provide a promising route for nanocluster assembly (or potentially *in-situ* synthesis of nanocluster arrays), we have been focusing on the development and characterization of DNA-templated silver nanoclusters. Clusters can be produced with sequence-specific tunable emission wavelengths (Figure 4; Sharma *et al.* (2010)). Recent characterization studies have used EXAFS (Extended X-Ray Fine Structure) analysis to provide the first direct confirmation of the presence of silver clusters in DNA-templated systems, to analyze silver-silver and silver-DNA interactions, and to obtain estimates of cluster size. (Neidig *et al.* (2011)) Work in progress includes spectroelectrochemical investigations of the role of redox processes in controlling luminescence and the use of small angle neutron and x-ray methods to investigate cluster size, and in the longer term, cluster-cluster interactions.

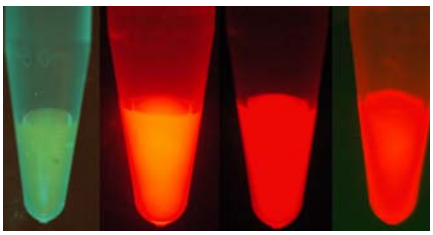

Figure 4. Spectrum of emission colors from sequence specific DNA-templated silver nanoclusters.

Future Plans

Future work will integrate active functional components into complex assemblies targeting photo-induced charge separation and light-harvesting functions. Characterization of assemblies and their functions using spectroscopic, scanning probe, electrochemical, imaging, and scattering methods will provide for improved understanding of how multi-scale and multi-component functional assemblies can be produced using the tools of self-assembly and biologically-assisted assembly.

Publications (2010-2011)

C.M. Hartshorn, C.M. Jewett, and J.A. Brozik, "Molecular Effects of a Nanocrystalline Quartz Support Upon Planar Lipid Bilayers," *Langmuir* **26** (2010) 2609.

J. Sharma, H.-C. Yeh, H. Yoo, J.H. Werner and J.S. Martinez, "A complementary palette of fluorescent silver nanoclusters," *Chem. Commun.* **46** (2010) 3280.

H. Yoo, J. Sharma, H.-C. Yeh, and J.S. Martinez, "Solution-phase synthesis of Au fibers using rod-shaped micelles as shape directing agents," *Chem. Commun.* **46** (2010) 6813.

Y.P. Bao, H.-C. Yeh, C. Zhong, S.A. Ivanov, J.K. Sharma, M.L. Neidig, D.M. Vu, A.P. Shreve, R.B. Dyer, J.H. Werner, and J.S. Martinez, "Formation and stabilization of fluorescent gold nanoclusters using small molecules," *J. Phys. Chem. C* **114** (2010) 15879.

S.H. Jeon, P. Xu, N.H. Mack, L.Y. Chiang, L. Brown and H.-L. Wang, "Understanding and controlled growth of silver nanoparticles using oxidized N-methyl-pyrrolidone as a r educing agent," *J. Phys. Chem. C* **114** (2010) 36.

P. Xu, N.H. Mack, S.H. Jeon, S.K. Doorn, X.J. Han and H.-L. Wang, "Facile fabrication of homogeneous 3D silver nanostructures on gold-supported polyaniline membranes as promising SERS substrates," *Langmuir* **26** (2010) 8882.

C.C. Wang, H.H. Tsai, H.H. Shih, S.H. Jeon, Z.H. Xu, D. Williams, S. Iyer, T.C. Sanchez, L. Wang, M. Cotlet and H.-L. Wang, "Synthesis and characterization of ethylene glycol substituted poly(phenylene vinylene) derivatives," *ACS Appl. Matls and Interfaces* **2** (2010) 738-747.

H.-C. Yeh, J. Sharma, H. Yoo, J.S. Martinez and J.H. Werner, "Photophysical characterization of fluorescent metal nanoclusters synthesized using oligonucleotides, proteins, and small molecule ligands," Proc. SPIE, **7576** (2010) 75760N-75761.

H. Siu, J. Duhamel, D.Y. Sasaki and J.L. Pincus, "Nanodomain formation in lipid membranes probed by time-resolved fluorescence," *Langmuir* **26** (2010) 10985.

K. Kokubo, R.S. Arastoo, T. Oshima, C.-C. Wang, Y. Gao, H.-L. Wang, H. Geng and L.Y. Chiang, "Synthesis and regiochemistry of [60]fullerenyl 2-methylmalonate bisadducts and their facile electron-accepting properties," *J. Org. Chem.* **75** (2010) 4574.

K.R. Poudel, D.J. Keller and J.A. Brozik, "Single particle tracking reveals corralling of a transmembrane protein in a double-cushioned lipid bilayer assembly," *Langmuir* **27** (2011) 320.

J. Sharma, H.-C. Yeh, H. Yoo, J.H. Werner, J.S. Martinez, "Silver nanocluster aptamers: in situ generation of intrinsically fluorescent recognition ligands for protein detection," *Chem. Commun.* **47** (2011) 2294.

H.H. Tsai, Z.H. Xu, R.K. Pai, L.Y. Wang, A.M. Dattelbaum, A.P. Shreve, H.-L. Wang and M. Cotlet, "Structural dynamics and charge transfer via complexation with fullerene in large area conjugated polymer honeycomb thin films," *Chem. Mater.* **23** (2011) 759.

M.L. Neidig, J. Sharma, H.-C. Yeh, J.S. Martinez, S.D. Conradson and A.P. Shreve, "Ag K-edge EXAFS analysis of DNA-templated fluorescent silver nanoclusters: Insight into the structural origins of emission tuning by DNA sequence variations," *J. Am. Chem. Soc.* **133** (2011) 11837.

H. Yoo, J. Sharma, J.K. Kim, A.P. Shreve, J.S. Martinez, "Tailored microcrystal growth: A facile solution-phase synthesis of gold rings," *Adv. Mater.* (2011)DOI:10.1002/adma.201101455.

Microtubule Mimicry: Toward Biomolecular Self-Assembly in Synthetic Materials

Erik Spoerke, Mark Stevens, James McElhanon, Dara Gough, and Bruce Bunker.

Sandia National Laboratories, Albuquerque, NM USA, Email: edspoer@sandia.gov

Sandia is a multiprogram laboratory operated by Sandia Corporation, a Lockheed Martin Company, for the United States Department of Energy's National Nuclear Security Administration under Contract DE-AC04-94AL85000.

Program Overview:

The following work represents efforts in the Artificial Microtubules subtask within the Active Assembly of Dynamic and Adaptable Materials program at Sandia. While the overall goal of the program is to explore how energy-consuming proteins such as tubulin and kinesin can be used to organize, assemble, and transport nanomaterials, the specific focus of the Artificial Microtubules effort is based on developing synthetic molecular materials whose assembly and structure mimic these natural biomolecular architectures.

Microtubules (MTs) are dynamic supramolecular protein nanofibers polymerized from dimers of alpha and beta tubulin. Only ~25 nm in diameter, but ranging in length from a less than a micrometer to more than a millimeter, MTs facilitate and direct a host of complex biological processes in cells ranging from chromosome separation during cell division to regulating cellular morphology and the trafficking of intracellular nanocargo.[1] In their native biological environments, MTs are polymerized and depolymerized "on-demand" to accommodate the diverse and evolving needs within a cell. Learning to translate the principles and properties of these versatile, multifunctional biological nanofibers to synthetic systems would create an opportunity to dramatically advance nanoscale materials assembly.

To meet this goal, we are focused on understanding MT polymerization and organization as nanomaterials assembly processes and developing synthetic materials and methods that mimic the self-assembly and structure of these remarkable biological models. Completely reproducing the remarkable sophistication and complexity of natural MTs, however, is a daunting challenge. Assembled MTs are elegant, multifunctional protein structures that interact selectively with a host of other biological agents, and the processes regulating the dynamic assembly and disassembly of these nanofibers are dominated by a complex series of interactions with accessory proteins, nucleotide binding, and hydrolysis.[2] To make our challenge more tractable, we have focused on replicating select key MT characteristics such as one-dimensional tubular MT structure, the thermally reversible nature of MT polymerization, and the asymmetric biochemical character of the tubulin assemblies. I will highlight here our recent chemical and computational efforts exploring synthetic supramolecular MT mimics.

Recent Progress

Thermally Responsive Dendritic Polymers

A key objective of our work is to develop an understanding of the reversible assembly of artificial systems and the macromolecular geometries that are formed. It is well established that dendritic macromolecules form dense bulk peripheries as generational size increases, while providing interior void space capable of host-

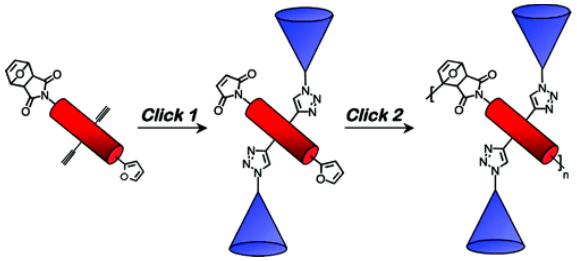

Fig. 1: Schematic depicting the thermally reversible polymerization of asymmetric dendrimer building blocks through click chemistry.[3]

guest interactions, encapsulation of small molecules, and energy transfer reactions. The ability to readily derivatize these compounds while fine tuning their properties is highly desirable as it offers the opportunity to tailor the form and function of assembled supramolecular MT mimics. We have developed a specific approach to synthesize *thermally reversible* linear polymers containing dendritic side groups. Our design is aimed at creating a completely reversible dendritic polymer assembly that contains a dense bulk periphery that surrounds a porous core, thus providing a thermally responsive tubular structure.

We have explored the synthesis, characterization, and polymerization behavior of thermally reversible AA-BB and AB step-polymer systems utilizing sequential CuAAC and furan-maleimide Diels Alder (DA) "click" reactions.[3,4] (Fig. 1) Not only are these systems thermally reversible, but the asymmetric nature of the monomer leads to a directional, linear polymerization, similar to that observed in the polar polymerization of MTs. After optimization of the retro-DA conditions using [G-1] dendritic monomers, each system was polymerized and the subsequent assembly, disassembly, and reassembly behaviors were monitored by gas permeation chromatography (GPC) and nuclear magnetic resonance spectroscopy (NMR). Both NMR and GPC studies demonstrated that dendritic monomers undergo assembly and disassembly cleanly and predictably using relatively mild temperature conditions. Atomic force microscopy (AFM) of cast thin films of [G-3] dendritic polymers, the largest system studied, revealed a highly ordered structure (Fig. 2).

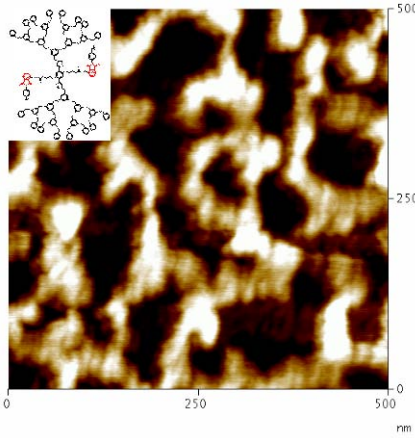

Fig. 2: AFM image of G-3 dendritic polymers. Inset shows molecular structure of G-3 polymer. Image is 500nm on each side.

Reversible Peptide Assemblies

We have also investigated several peptide-based supramolecular systems including engineered cyclic peptides. Various cyclic peptides have been shown capable of assembling into tubular structures[5] making this an attractive candidate class of materials for mimicking the linear tubular morphology of MTs. The cyclic peptides we have investigated are based on sequences related to the protein elastin. Polymers formed from pentapeptide repeats of elastin, such as valine-proline-glycine-valine-glycine or VPGVG, exhibit an inverse temperature transition of hydrophobic folding,[6] varied according to composition around approximately 35^{o}C, a temperature comparable to the temperature at which tubulin most often polymerizes. Using these elastin motifs introduces biomimetic thermal control over supramolecular assembly. Our cyclic peptides comprise 3-5 repeats of a modified VPGVG pentamer. By substituting into this sequence acidic residues in particular, we have created water soluble cyclic peptides whose assembly is moderated by the protonation of these electrostatically repulsive acidic residues. When dissolved in room temperature water at a pH above the pKa of the acid residues, the electrostatic repulsion of the carboxylic acids present keep the molecules dispersed. When the dissolved peptide is warmed to 37^{o}C, however, the molecule undergoes its inverse phase transition and the associated hydrophobic folding ultimately leads to the neutralization of the repulsive negative charges. As a result, hydrophobic interactions and hydrogen bonding drive the peptide rings to assemble into self-supporting network gels at concentrations as low as 1 weight percent! When the gels are cooled to 4^{o}C, the molecular phase transformation is reversed, the acidic residues regain their charge, and the self-assembled gel is dispersed. This

unique, thermally-reversible assembly process represents a promising analog to the temperature-sensitive assembly of MTs.

Theory and Modeling

The current emphasis of the theoretical component of the Artificial Microtubules task to understand the fundamental principles that direct how monomers can be programmed to create different polymerized structures, including MTs. Regardless of whether we are dealing with a dendrimer or a nanoparticle, the polymerization of these monomers into species such as MTs depends on monomer shapes as well as the strength and geometric distribution of interaction potentials or functional groups around each monomer. We are using molecular dynamics (MD) simulations to understand the minimal and most fundamental features of monomers that will yield the geometry and dynamic properties of interest. The initial focus involves determining the design rules for the assembly of tubular structures from monomers. Our model monomer (Fig. 3) is a wedge shaped particle that is designed to fit into a ring structure with 13 monomers (like MTs) with the rings stacking to form a tubular structure. To form rings there are complementary attractive sites (red and blue in Fig.1) on the sides. The two distinct sites are needed to break symmetry and force binding in a single orientation. Similarly the top and bottom have complementary attractive sites that promote filamentary growth or ring stacking.

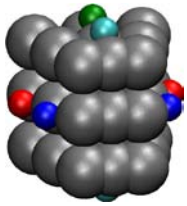

Fig. 3: Simulated wedge-shaped monomer comprising repulsive gray spheres and non-gray spheres represent sites attractive to other sites of the same color.

The potential used in these simulations is a simple cosine potential with a minimum energy of $-g$ at the site center going to zero at a cutoff distance r, defined as the size of the gray spheres diameter, d. The value of g for the lateral and vertical sides is set independently and labeled, g_L and g_V, respectively. Large values of g_L promote the formation of rings, while large values of g_V promote formation of filaments. We have calculated a phase diagram (Fig. 4) of the wide range of structures produced by varying these interaction parameters. Region A shows no assembly because of weak interaction strengths. Along the axis, $g_L = 0$, filaments form in region B. Along the axis, $g_V = 0$, partial rings form in region C and full rings form in region D. Increasing g_V from 0 yields region E, which is a mixture of rings and short tubes. Region F is where full tubes are found. Region G has curved sheets and tends to yield kinetically trapped structures. Interestingly, region G also shows the formation of helical tubules. This observation is unexpected given the design was for stacks; however, the energy difference between the two tubular structures is less than kT and therefore both structures occur.

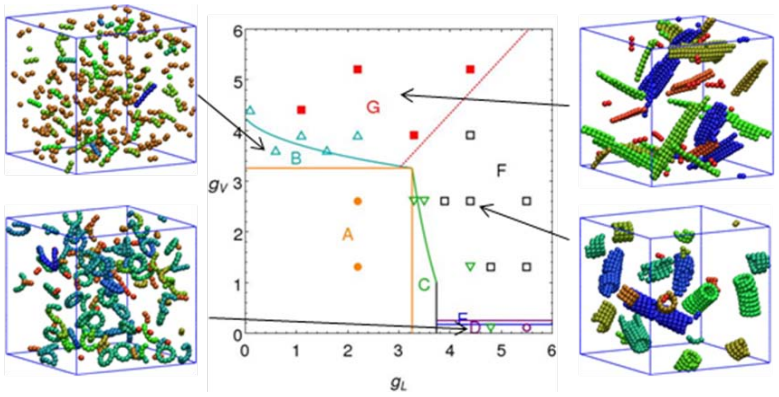

Fig. 4: Theoretical phase diagram with simulation data exhibits a variety of different structures. Wedge monomers are represented by a single sphere and the structures are colored based on the number of monomers in the cluster. In the image in the lower right, not only do tubules formed of stacked rings occur, but also helical tubules occur.

Even this simple monomer model shows the complex structures that can be

formed when the monomer is a macromolecule with multiple interaction sites. These simulations have provided important insight into both the nature of MT assemble and the design of synthetic supramolecular building blocks.

Future work:

Moving forward, the efforts on the thermally-responsive dendrimer work will focus on increasing polymer size, reaction rates, and water solubility of the dendron polymers as well as more extensively characterizing the nanoscale morphology of the assemblies. Work on peptide assembly will continue to explore the influences of peptide size and composition on the self-assembling behavior and structure of the peptides. We will also introduce ancillary molecules to moderate assembly and introduce more defined anisotropy to these building blocks. In addition, we will explore a recently synthesized series of wedge-shaped peptide dendrimers modeled after the building blocks simulated in the MD work described above (Fig.1). By controlling the strength and molecular positioning of asymmetric electrostatics, hydrogen bonding, and hydrophobicity we will attempt to empirically reproduce the predictions laid out by the MD simulations. In the molecular modeling work itself, we will continue to introduce additional traits of MTs to the model, potentially including simulated interactions with stabilizing or destabilizing bioagents. Following these exciting new directions, we expect to find even more rich supramolecular chemistries and enhance our growing understanding of the critical driving forces that may be used to mimic MTs.

References:

1. H. Lodish, et al. Cell Motility and Shape II: Microtubules and Intermediate Filaments. In *Molecular Cell Biology*, 4th ed.; W.H. Freeman and Co.: New York, NY, 1999; pp 795.
2. T.L. Karr, et al. J. Biol. Chem. (1980) **255**(18). 8560-8566.
3. N.W. Polaske, et al. *Macromolecules*. (2011) **44**(9). 3203-3210.
4. N.W. Polaske, et al. *Macromolecules.* (2010) **43**(3). 1270-1276.
5. C. Valery, et al. *Soft Matter*. (2011) DOI: 10.1039/c1sm05698k.
6. D.W. Urry, et al. *Biopolymers.* (1992) **32**, 373-379.

Program publications(2010-2011):

N.W. Polaske, D.V. McGrath, and J.R. McElhanon. "Thermally Reversible Dendronized Linear AB Step-Polymers via "Click" Chemistry." *Macromolecules* **44**(9), 3203-3210, (2011).

H. Liu and G.D. Bachand. "Understanding energy dissipation and thermodynamics in biomotor-driven nanocomposite assemblies." *Soft Matter* **7**, 3087-3091. (2011).

N.W. Polaske, D.V. McGrath, and J.R. McElhanon. "Thermally Reversible Dendronized Step-Polymers Based on Sequential Huisgen 1,3-Dipolar Cycloaddition and Diels-Alder "Click" Reactions." *Macromolecules* **43**(3), 1270-1276, (2010).

E.D. Spoerke, B. Connor, and B.C. Bunker. "Microtubule Templated CdS Semiconductor Nanowires," Submitted to *Small* (2011).

E.D. Spoerke, A.K. Boal, G.D. Bachand, and B.C. Bunker. "3-Dimensional Biodynamic Assembly of Fluorescent Nanocrystals." Submitted to *Langmuir*, (2011).

This work was supported by the U.S. Department of Energy, Office of Basic Energy Sciences, Division of Materials Sciences and Engineering.

Molecular Biomimicry with Information-Rich Polymers

Ronald N. Zuckermann
Molecular Foundry, Lawrence Berkeley National Laboratory
1 Cyclotron Rd., MS 67-5110, Berkeley, CA 94720
rnzuckermann@lbl.gov

Program Scope. Despite the fact that proteins and bulk polymers share a common linear polymeric architecture, the fields of Structural Biology and Polymer Science are presently separated by a great divide [1]. In fact, there are relatively few non-natural polymer systems that include even the most fundamental of biopolymer attributes: chemical diversity and sequence specificity. The chemical information encoded within the polypeptide chain, by virtue of its linear sequence of chemical functional groups, is sufficient to "instruct" it to fold into a precise 3D architecture, and to exhibit advanced properties, such as molecular recognition and catalysis [2]. We are exploring the concept of building analogous protein-mimetic materials from "information rich" synthetic polymers [3]. The solid-phase submonomer synthesis of *N*-substituted glycine peptoid oligomers has emerged as one of the most efficient ways to synthesize sequence-specific polymers from a highly chemically diverse monomer set [4-6]. We are applying fundamental rules that govern protein folding to the world of polypeptoids, with the aim of folding peptoid polymers into artificial protein-like structures to yield a new generation of robust protein-mimetic materials [7-11].

The *de novo* design of proteins remains a challenging problem despite the availability of a large database of protein structures and sophisticated computational tools. So where do we start when approaching the problem of folding non-natural polymers into atomically-defined architectures? We have simplified the problem by first focusing on mimicry of the two fundamental secondary structural units found in protein structure: alpha helices and beta sheets. We have shown that despite a lack of H-bond donors in the peptoid backbone, peptoids bearing alpha-chiral sidechains can fold into helices [12, 13]. This effect was first predicted in 1997, and then demonstrated experimentally in 1998. But the discovery of a peptoid beta-sheet mimetic was not discovered until over a decade later [10, 11]. This is because a helix involves only the local folding of a single chain, whereas folding into a sheet involves chain-chain interactions, a higher level of complexity [14]. Here, we explore the sequence requirements to fold a peptoid chain into an achiral, supramolecular nanosheet (Figure 1).

Figure 1. Peptoid structure, function and self-assembly research efforts presented at the 7th Peptoid Summit are featured in a special issue of *Biopolymers: Peptide Science* (September, 2011).

Recent Progress. We reasoned that the most fundamental rules that govern protein folding should also apply to peptoid polymers. We therefore began our search for peptoid beta-sheet mimetics by considering the visionary ideas of Ken Dill, Michael Hecht and others, who noted the overwhelming importance of the patterning of hydrophilic and hydrophobic groups within the polypeptide chain [15, 16]. It was demonstrated that the exact identity of an amino acid was not as important as whether it was polar or non-polar. It was also shown that helices and sheets also exhibit distinct sequence periodicities of polar and non-polar residues.

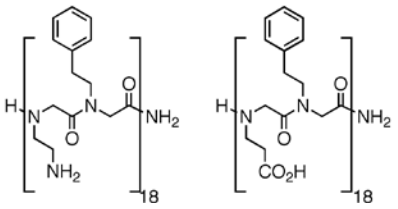

Figure 2. A 1:1 mixture of oppositely charged two-fold periodic peptoid 36mer amphiphiles forms nanosheets in dilute aqueous conditions at room temperature.

These observations inspired us to explore the impact of sequence periodicity on peptoid structure. We set out to synthesize repeating patterns of hydrophilic and hydrophobic peptoid sequences using our robotic parallel synthesizers. To enable such a study, we used a minimalist monomer set that included one hydrophobic monomer (*N*-2-phenylethylglycine), and a pair of polar monomers (*N*-2-aminoethylglycine and *N*-2-carboxyethylglycine). This way the number of possible sequence variants could be kept manageable. A systematic set of 36mer peptoids was synthesized consisting of different repeating patterns of these monomers (the two-fold periodic sequences are shown in Figure 2). The purified peptoids were then dissolved in dilute physiological buffers and examined by optical and electron microscopy.

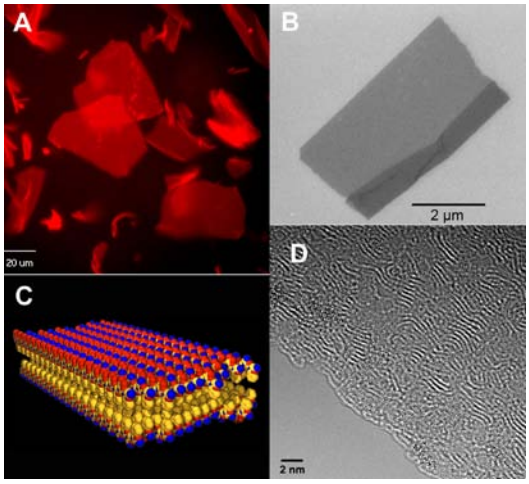

Figure 3. Two-dimensional crystalline nanosheets self assemble from an ionic and hydrophobic peptoid sequence. The peptoid nanosheets sheets: (a) as observed by fluorescence microscopy, (b) have very sharp, straight edges as observed by scanning electron microscopy, (c) are composed of fully extended polymer chains lined up side-by-side in a bilayer, and (d) individual polymer chains are directly observed by abberration-corrected TEM.

Peptoids containing an alternating two-fold repeating pattern of hydrophilic and hydrophobic sidechains assembled into micron-sized nanosheets in high yield (Figure 3) [10, 11]. The nanosheets were further characterized by atomic force microscopy, X-ray powder diffraction, and transmission electron microscopy, and found to be uniformly ~3 nm thick and highly ordered. The data are consistent with a bilayer model (Figure 1), where the hydrophobic groups are buried in the core, and the ionic groups are exposed to water. The nanosheets often have very straight edges, are stable over a broad pH range (3-11) and can survive in hot water and even drying under vacuum. They

spontaneously dissolve in the presence of >50% acetonitrile. Because the nanosheets are comprised of achiral peptoid polymers, the resulting planar structure shows no surface curvature, in contrast to peptidic beta sheets [17].

Future Plans. The peptoid nanosheet structure demonstrate that a non-natural polymer can be folded into a defined structure based on the monomer sequence pattern. The nanosheet structure itself is an excellent two-dimensional platform upon which to display functionality in a planar array in solution. Such a unique material is likely to find utility in a variety of applications. We will investigate the use of functionalized nanosheets as membrane mimetics, where the nanosheet structure can be fine-tuned to allow the selective transport and separation of ions, gases or fuel molecules. We will also investigate the ability of functionalized nanosheets to serve as molecular recognition elements for chemical and biological detection. We will also use them as templates for the growth of inorganic materials. More broadly, the ability to mimic one of the two fundamental secondary structural units found in nature, the beta sheet, lays the structural foundation upon which to build protein-like architectures of increased complexity.

References:

1. Jones, R.A.L., Biomimetic nanotechnology with synthetic macromolecules. *J. Polym. Sci. B* **2005**, *43*, 3367.
2. Anfinsen, C.B., Principles that Govern the Folding of Protein Chains. *Science* **1973**, *181*, 223.
3. Goodman, C.M.; Choi, S.; Shandler, S.; DeGrado, W.F., Foldamers as versatile frameworks for the design and evolution of function. *Nature Chem. Biol.* **2007**, *3*, 252.
4. Culf, A.S.; Ouellette, R.J., Solid-Phase Synthesis of N-Substituted Glycine Oligomers (α- Peptoids) and Derivatives. *Molecules* **2010**, *15*, 5282.
5. Fowler, S.A.; Blackwell, H.E., Structure-function relationships in peptoids: Recent advances toward deciphering the structural requirements for biological function. *Org. Biomol. Chem.* **2009**, *7*, 1508.
6. Yoo, B.; Kirshenbaum, K., Peptoid Architectures: Elaboration, Actuation, and Application. *Curr. Op. Chem. Biol.* **2008**, *12*, 714.
7. Burkoth, T.S.; Beausoleil, E.; Kaur, S.; Tang, D.Z.; Cohen, F.E.; Zuckermann, R.N., Toward the synthesis of artificial proteins: The discovery of an amphiphilic helical peptoid assembly. *Chemistry & Biology* **2002**, *9*, 647.
8. Lee, B.C.; Chu, T.K.; Ken A, D.; Zuckermann, R.N., Biomimetic nanostructures: Creating a high-affinity zinc-binding site in a folded nonbiological polymer. *J. Am. Chem. Soc.* **2008**, *130*, 8847.
9. Lee, B.C.; Zuckermann, R.N.; Dill, K.A., Folding a nonbiological polymer into a compact multihelical structure. *J. Am. Chem. Soc.* **2005**, *127*, 10999.
10. Nam, K.T.; Shelby, S.A.; Choi, P.H.; Marciel, A.B.; Chen, R.; Tan, L.; Chu, T.K.; Mesch, R.A.; Lee, B.C.; Connolly, M.D.; Kisielowski, C.; Zuckermann, R.N., Free-floating ultrathin two-dimensional crystals from sequence-specific peptoid polymers. *Nat. Mater.* **2010**, *9*, 454.
11. Kudirka, R.; Tran, H.; Sanii, B.; Nam, K.T.; Choi, P.H.; Venkateswaran, N.; Chen, R.; Whitelam, S.; Zuckermann., R.N., Folding of a single-chain, information-rich polypeptoid sequence into a highly-ordered nanosheet. *Peptide Sci.* **2011**, *96*, 586.
12. Armand, P.; Kirshenbaum, K.; Falicov, A.; Jr., R.L.D.; Dill, K.A.; Zuckermann, R.N.; Cohen, F.E., Chiral N-Substituted Glycines Can Form Stable Helical Conformations. *Folding and Design* **1997**, *2*, 369.

13. Kirshenbaum, K.; Barron, A.E.; Goldsmith, R.A.; Armand, P.; Bradley, E.K.; Truong, K.T.V.; Dill, K.A.; Cohen, F.E.; Zuckermann, R.N., Sequence-Specific Polypeptoids: A Diverse Family of Heteropolymers with Stable Secondary Structure. *Proc. Natl. Acad. Sci. U. S. A.* **1998**, *95*, 4303.
14. Minor, D.L.; Kim, P.S., Context is a major determinant of [beta]-sheet propensity. *Nature* **1994**, *371*, 264.
15. Dill, K.A., Dominant Forces in Protein Folding. *Biochemistry* **1990**, *29*, 7133.
16. Xiong, H.; Buckwalter, B.L.; Shieh, H.M.; Hecht, M.H., Periodicity of polar and nonpolar amino acids is the major determinant of secondary structure in self-assembling oligomeric peptides. *Proc. Natl. Acad. Sci. U. S. A.* **1995**, *92*, 6349.
17. Zhang, S., Fabrication of novel biomaterials through molecular self-assembly. *Nat. Biotech.* **2003**, *21*, 1171.

DOE funded publications (from past 2 years):

1. Zuckermann, R.N., Protein Mimicry with Bioinspired Peptoid Polymers. In *Proc. 22nd Amer. Pep. Symp.*, Lebl, M., Ed. American Peptide Society: San Diego, **2011**; pp 174-175.
2. Zuckermann, R.N., Peptoid Origins. *Peptide Science* **2011**, *96*, 545.
3. Seo, J.; Lee, B.-C.; Zuckermann, R.N., Peptoids - Synthesis, Characterization, and Nanostructures. In Comprehensive Biomaterials, Healy, K.E., Ed. Elsevier: 2011; p In press.
4. Robinson, D.B.; Buffleben, G.M.; Langham, M.E.; Zuckermann, R.N., Stabilization of nanoparticles under biological assembly conditions using peptoids. *Peptide Sci.* **2011**, *In press*.
5. Kudirka, R.; Tran, H.; Sanii, B.; Nam, K.T.; Choi, P.H.; Venkateswaran, N.; Chen, R.; Whitelam, S.; Zuckermann, R.N., Folding of a Single-Chain, Information-Rich Polypeptoid Sequence into a Highly-Ordered Nanosheet. *Peptide Sci.* **2011**, *96*, 586.
6. Chen, C.-L.; Qi, J.; Zuckermann, R.N.; DeYoreo, J.J., Engineered Biomimetic Polymers as Tunable Agents for Controlling CaCO3 Mineralization. *J. Am. Chem. Soc.* **2011**, *133*, 5214.
7. Seo, J.; Barron, A.E.; Zuckermann, R.N., Novel Peptoid Building Blocks: Synthesis of Functionalized Aromatic Helix-Inducing Submonomers. *Org. Lett.* **2010**, *12*, 492.
8. Rosales, A.M.; Murnen, H.K.; Zuckermann, R.N.; Segalman, R.A., Control of Crystallization and Melting Behavior in Sequence Specific Polypeptoids. *Macromolecules* **2010**, *43*, 5627.
9. Nam, K.T.; Shelby, S.A.; Marciel, A.B.; Choi, P.C.; Chen, R.; Tan, L.; Chu, T.K.; Mesch, R.A.; Lee, B.-C.; Connolly, M.D.; Kisielowski, C.; Zuckermann, R.N., Free-floating ultra-thin two-dimensional crystals from sequence-specific peptoid polymers. *Nature Mater.* **2010**, *9*, 454.
10. Murnen, H.K.; Rosales, A.M.; Jaworski, J.N.; Segalman, R.A.; Zuckermann, R.N., Hierarchical Self-Assembly of a Biomimetic Diblock Copolypeptoid into Homochiral Super Helices. *J. Am. Chem. Soc.* **2010**, *132*, 16112.
11. Lee, B.-C.; Zuckermann, R.N., Templated display of biomolecules and inorganic nanoparticles by metal ion-induced peptide nanofibers. *Chem. Comm.* **2010**, *46*, 1634.
12. Ding, B.; Deng, Z.; Yan, H.; Cabrini, S.; Zuckermann, R.N., Gold Nanoparticle Self-Similar Chain Structure Organized by DNA Origami. *J. Am. Chem. Soc.* **2010**, *132*, 3248.
13. Thakkar, A.; Cohen, A.S.; Connolly, M.D.; Zuckermann, R.N.; Pei, D., High-Throughput Sequencing of Peptoids and Peptide−Peptoid Hybrids by Partial Edman Degradation and Mass Spectrometry. *J. Comb. Chem.* **2009**, *11*, 294.
14. Dohm, M.T.; Seurynck-Servoss, S.L.; Seo, J.; Zuckermann, R.N.; Barron, A.E., Close mimicry of lung surfactant protein B by "clicked" dimers of helical, cationic peptoids. *Peptide Sci.* **2009**, *92*, 538.

UNIVERSITY GRANT PROJECTS

Program Title: Actuation of Bioinspired, Adaptive "HAIRS" Powered by Responsive Hydrogels

Principle Investigator: Joanna Aizenberg
Mailing Address: 29 Oxford St, Cambridge, MA 02138
Email: jaiz@seas.harvard.edu

Program Scope

The goal of this project is to develop materials, strategies, and architectures for hybrid nano/microstructured surfaces which sense and autonomously respond to a changing environment. We aim to generate 'smart' systems which serve to continuously adapt in ways allowing us to reduce energy consumption and increase functional efficiency. We undertake a bio-inspired approach to the design of such systems by combining the unique properties of nanoscale structures with the responsive behavior of hydrogels in order to create hybrid surfaces with tunable and dynamic properties; we have termed such surfaces hydrogel-actuated integrated responsive systems (HAIRS).[1] The design is analogous to living organisms: each consists of a variety of material elements which, only when integrated, are allowed to cooperatively function together in an adaptive and responsive system. In our hybrid approach, the nanostructures provide the system with surface properties uniquely associated with the nanoscale (e.g. wetting behavior or optical properties). The other component is the hydrogels providing environmental sensitivity and mechanical forces which bring about dynamically reconfiguring properties to the otherwise static nanostructures. We envision these design principles of responsive surfaces and dynamic systems to be remarkable progress towards the design of adaptive, energy harvesting, and sustainable building materials as well as for smart surfaces featuring anti-fouling properties, cargo transportation, flow generation, and reversible adhesion. For example, a light sensitive or heat sensitive system may autonomously change surface properties in order to reduce heat loss in a building during the winter but keep it cool during the summer, or a humidity responsive surface may become hydrophilic when water is scarce and hydrophobic when water is plentiful.

A unique characteristic of our approach is the nearly limitless number of combinations of nano or microstructures with tailored hydrogel response allowing us to select and program into an intelligent system a variety of customized structure/function/response relationships. In terms of the structure, we have been experimenting not only with geometric variance (size, shape, symmetry, etc.) but also material (e.g. silicon or polymer)[2,3] and material properties (e.g. modulus). Hydrogels in turn can be designed to respond to a variety of stimuli (temperature, pH, humidity, light, etc.), and have tunable swelling ratios.[4] Each combination provides distinct self-adapting and self-responsive properties. A change in the environment, whether it be a chemical change (such as pH) or a thermal or optical stimulus, is inherently a source of energy that we can harvest and use to drive the nano/microstructures to reconfigure thus allowing for tunable and adaptive surface properties.

Recent Progress

Submerged Hydrogel-Actuated Polymer Microstructures Operating in Response to pH[5]

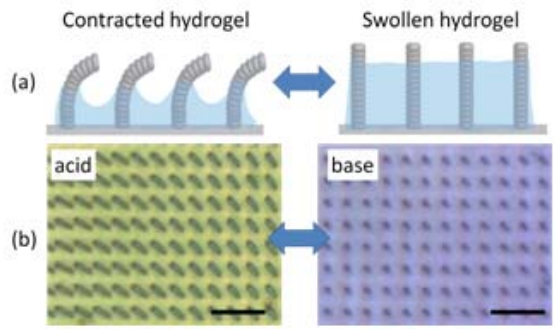

Figure 1: (a) Schematic of hydrogel-driven actuation. (b) Optical microscope images of pH-responsive actuation of microposts. Scale bar = 20 μm

Figure 1a outlines the general mechanism for hydrogel-driven surface actuation; surface-attached high-aspect-ratio structures embedded in hydrogel are initially in an unconstrained, upright orientation when the hydrogel in swollen and become bent when the hydrogel contracts imparting strain on the structures. Previously, HAIRS were only sensitive to humidity (wet/dry states) and thus could not function in a submerged environment.[2] To generate a HAIRS applicable in fluidic environments, we integrated a new hydrogel, pH-responsive poly(acrylic acid-*co*-acrylamide) with flexible, polymeric high-aspect-ratio microstructured surfaces. In this pH-responsive case, structures remained in the unconstrained conformation when the environmental pH > 4.3 and structures bent when the hydrogel contracted at pH < 4.3 (Figure 1b). We observed unique dynamics of response and actuation that had not been previously observed in a humidity-responsive system; differences in the kinetics of hydrogel swelling and contraction in a submerged environment generated spatio-temporal asymmetry in the actuation cycles thus generating an inherent asymmetric beating motion of the actuating microstructures. Such an asymmetric motion is a requirement for a surface designed to generate flow.[6]

We also demonstrated actuation of asymmetric fin-shaped structures which, due to their preferential bending direction, allow for the fabrication of large areas (cm^2) of highly uniform actuation. Additionally, toward the potential for integration with lab-on-a-chip devices, we have combined these microfin HAIRS with microfluidic channels and observed the actuation response to laminar flow of acid and base. We find that the actuation is highly sensitive and localized; the sharp interface between acid and base laminar flows in the microchannel is translated in terms of actuation response to the underlying surface with high fidelity (Figure 2).

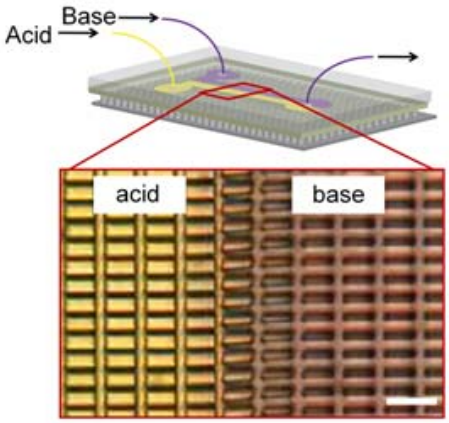

Figure 2: Asymmetric microfin structures have a preferred bending orientation allowing for large area, uniform actuation. We demonstrate control of actuation in a microfluidic channel. Scale bar = 20 μm

<u>Controlling the Stability and Reversibility of Micropillar Assembly by Surface Chemistry</u>[7]

Instead of using hydrogels as the force for structure actuation, here we use capillary forces to drive their initial self assembly. Importantly, we have examined how the surface chemistry of the structures affects the stability and reversibility of clustering as well as their adhesion in different solvents. The surface chemistry can be patterned, and we are able to generate reversible area-selective clustering. This study provides insight into the fundamental chemical interactions between the surface structures which may allow us to combine self-assembling characteristics with HAIRS.

Structural Transformation by Electrodeposition on Patterned Substrates (STEPS)[8]

STEPS allows us to systematically vary geometric characteristics of our structures that we use for HAIRS quickly and cheaply therefore letting us experiment with a wide range of geometries that would have otherwise been prohibitively expensive and time consuming to produce by traditional fabrication techniques. In STEPS, polypyrrole (PPy) is electrochemically grown to user-defined thicknesses on gold electrodes which are patterned on an original epoxy structure which we wish to modify. Depending on the method used for patterning electrodes, we are able to transform the original structure into a new set of structures by changing the feature size, creating asymmetric tapered shapes and overhanging features, and tilted geometries (Figure 3). We are able to create gradient samples (for example, a gradient of structure diameter) by slowly withdrawing samples from the electrochemical bath allowing us to create a large library of diverse features on a single surface. We are then able to make PDMS molds of the newly modified PPy-coated structures allowing us to replicate them many times over in a variety of polymers. These samples are ideal for screening surface structures for use in HAIRS.

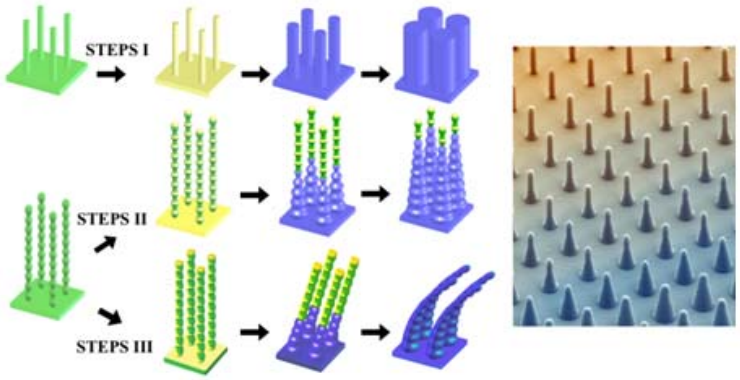

Figure 3: Schematics of various STEPS processes: STEPS I represents conformal growth of PPy on uniformly deposited metal; STEPS II represents stepwise growth of PPy converting a straight post to a tapered, cone shaped post (see the SEM image on the right) using evaporated metal at normal incidence; STEPS III represents anisotropic growth of PPy converting a straight post to a tilted post using evaporated metal at an angle.

Direct Writing and Actuation of 3D-Patterned Hydrogel Pads on Micropillar Supports[9]

We have developed methods for patterning pH-responsive poly(AAc-*co*-AAm) and temperature-responsive poly(*N*-isopropylacrylamide) (PNIPAM) hydrogels in three dimensions with microscale precision using multiphoton lithography (MPL). This method allows us to precisely place hydrogel 'muscle' of user-defined shapes anywhere on a sample thus enabling superior control over actuation of individual structures (Figure 4). Importantly, we are also able to fabricate hydrogel pads which are *not* surface attached but rather tethered to the middle or tips of the surface structures, a capability only

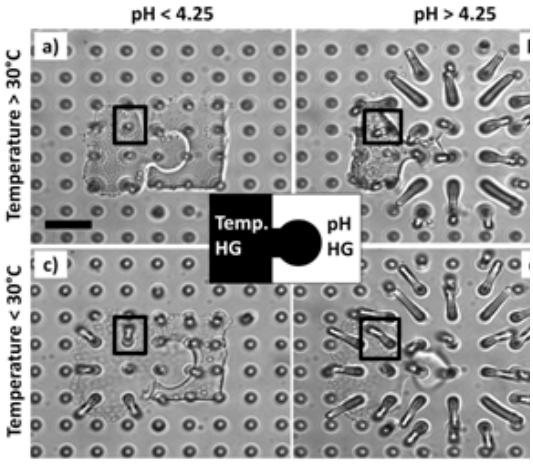

Figure 4: Temperature and pH-responsive hydrogel patterned in user-defined puzzle piece shapes. One post is highlighted which displays four different stable orientations (a-d) resulting from the four different combinations of stimuli. Scale bar = 10 μm

enabled by the 3D nature of MPL. In this case, even hydrogels of only a few microns in thickness are left relatively unconstrained and retain large swelling ratios (Figure 4). Further, we can pattern multiple kinds of gels in sequence with precise registration of materials; in a sense, we are now able to affect actuation of structures using not just one muscle, but two, meaning that surfaces can now respond to multiple combinations of independent stimuli.

Future Plans

We are currently exploring the use of temperature-responsive hydrogel to create surfaces with unique responsive optical and thermal properties. By coating the sides of the microstructures, we are able to create surfaces showing reversible reflection and transmission properties. We are now investigating the thermal properties of these surfaces for possible use in energy efficient windows. Additionally, we are continuing to investigate the use of HAIRS within microfluidic environments. Specifically, we aim to create a responsive system capable of a feedback mechanism which controls a chemical reaction in situ. We also are exploring the use of the HAIRS as anti-fouling surfaces and prevention of biofilm growth. Other stimuli, including light, redox states, and biological molecules are also of interest.

References

1. Kim, P.; Zarzar, L. D.; He, X.; Grinthal, A.; Aizenberg, J., Hydrogel-actuated integrated responsive systems (HAIRS): Moving towards adaptive materials. *Curr. Opin. Solid State Mater. Sci.* **2011**. DOI: 10.1016/j.cossms.2011.05.004.
2. Kim, P.; Zarzar, L. D.; Zhao, X.; Sidorenko, A.; Aizenberg, J., Microbristle in gels: Toward all-polymer reconfigurable hybrid surfaces. *Soft Matter* **2010,** *6*, 750-755.
3. Sidorenko, A.; Krupenkin, T.; Taylor, A.; Fratzl, P.; Aizenberg, J., Reversible Switching of Hydrogel-Actuated Nanostructures into Complex Micropatterns. *Science* **2007,** *315*, 487-490.
4. Nelson, A., Stimuli-responsive Polymers: Engineering Interactions. *Nature Materials* **2008,** *7*, 523-525.
5. Zarzar, L. D.; Kim, P.; Aizenberg, J., Bio-inspired Design of Submerged Hydrogel-Actuated Polymer Microstructures Operating in Response to pH. *Adv. Mater.* **2011,** *23*, 1442-1446.
6. Blake, J., Hydrodynamic Calculations on the Movements of Cilia and Flagella. *J. Theor. Biol.* **1974,** *45*, 183-203.
7. Matsunaga, M.; Aizenberg, M.; Aizenberg, J., Controlling the Stability and Reversibility of Micropillar Assembly by Surface Chemistry. *J. Am. Chem. Soc.* **2011,** *133*, 5545–5553.
8. Kim, P.; Epstein, A. K.; Khan, M.; Zarzar, L. D.; Lipomi, D. J.; Whitesides, G. M.; Aizenberg, J., Structural Transformation by Electrodeposition on Patterned Substrates (STEPS): A New Versatile Nanofabrication Method. *Nano Letters* **2011**. DOI: 10.1021/nl200426g. Research highlight in *Nature* **2011**, *472*, 8.
9. Zarzar, L. D.; Kim, P.; Kolle, M.; Brinker, C. J.; Aizenberg, J.; Kaehr, B., Direct Writing and Actuation of 3D-Patterned Hydrogel Pads on Micropillar Supports. *Angew. Chem. Int. Ed.* **2011**, in press.

Publications Resulting from DOE Support

References 1, 5, 7, 8, 9

Title: Designing Colonies of Communicating Microcapsules that Exhibit Collective Behavior

Principle Investigator: Anna C. Balazs, Chemical Engineering Department, University of Pittsburgh, Pittsburgh, PA 15261

E-mail: balazs@pitt.edu

Program Scope

Using theory and simulation, our goal is to design assemblies of active micro-scale structures that signal and communicate at the nano-scale and thereby, collectively perform a large-scale, concerted function. The nanoparticle-mediated interactions between the microcapsules involve complex couplings, feedback loops and noise. Thus, we anticipate that *multiple, interacting* microcapsules will exhibit remarkable forms of collective activity. Furthermore, the microcapsule colonies provide an ideal "laboratory" for uncovering the fundamental physics that governs the non-linear, dynamical behavior. The studies also allow us to establish routes for controlling the dynamic self-assembly of non-equilibrium systems.

Recent Progress

We designed colonies of biomimetic microcapsules that exploit chemical mechanisms to communicate and alter their local environment [1,2]. As a result, these synthetic objects can self-organize into various autonomously moving structures (see **Fig. 1**) and exhibit ant-like tracking behavior [1]. In the simulations, signaling microcapsules release agonist particles, while target microcapsules release antagonist particles and the permeabilities of both capsule types depend on the local particle concentration in the surrounding solution. Additionally, the released nanoscopic particles can bind to the underlying substrate and thereby create adhesion gradients that propel the microcapsules to move. (The self-imposed adhesion gradients provide an interaction energy that is then converted into kinetic energy as the capsules interact with the surfaces.) Hydrodynamic interactions and the feedback mechanism provided by the dissolved particles are both necessary to achieve the collective dynamics exhibited by these colonies.

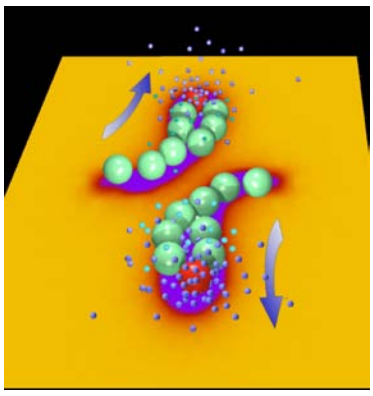

Fig. 1. Two self-organized, self-propelled "snakes" formed by the communicating capsules.

Our model provides a platform for integrating both the spatial and temporal behavior of assemblies of "artificial cells", and allows us to design a rich variety of structures capable of exhibiting complex, cooperative behavior. Due to the cell-like attributes of polymeric microcapsules and polymersomes, material systems are available for realizing our predictions. Importantly, these systems "generate" all the energy they need for their propulsion. They do not need an external input or energy source to drive their motion and collective behavior. The guidelines from these studies can facilitate the development of smart micro-machines or micro-robots that can be made to perform without an external energy supply. We note that our computational model also provides a new approach for simulating cell signaling processes and can yield greater insight into the interrelationships between the signaling events, the movement of compliant cells and hydrodynamic interactions.

The above study really captured peoples' imaginations and at one point, was reported on more than 800 web sites, including the Discovery Channel (news.discovery.com/tech/virtual-ants-slime-mold.html), MSNBC.com (http://www.msnbc.msn.com/id/38384798) and Science

Daily (www.sciencedaily.com/releases/2010/07/100719142452.htm). A video accompanying the paper were also posted to YouTube by one of the readers. (Can be found under "Artificial cell: dragon formation").

As an extension of the above studies, we designed a system of active polymeric microcapsules that pick-up, convey and drop-off a cargo between locations on a patterned surface [3]. To create this system, we harness the signaling and target capsules, which release nanoparticles into the surrounding solution. These nanoparticles bind to the underlying surface and thereby create adhesion gradients that trigger the spontaneous motion of the capsules. One signaling and two target capsules are found to form a stable triad, which can transport a cargo of four target capsules. Guided by an adhesive stripe on the surface, the triad and cargo form a "train" that moves autonomously along the substrate (see **Fig. 2**). The stripe is designed to encompass a small region with a lower adhesive strength. Through the aid of this patch, the triad can deposit its cargo and move on to potentially pick up a new payload at another location. Since the microcapsules can encase a wide variety of compounds, the system could provide an effective means of autonomously transporting a broad range of substances within microfluidic devices.

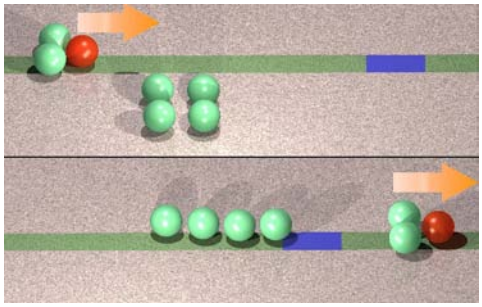

Fig. 2. The triad of capsules (initially on the left) acts as a mini-mover that picks up and delivers the four-capsule cargo.

In a different set of studies, we used both theoretical modeling and simulation to show how ordered arrays of microcapsules in solution can be harnessed to propagate chemical signals in directed and controllable ways, allowing the signals to be transmitted over macroscopic distances [4,5]. The system encompasses two types of capsules that are localized on an adhesive surface. The "signaling" capsules release inducer molecules, which trigger "targets" to release nanoparticles. The released nanoparticles can bind to the underlying surface and thus, create adhesion gradients, which then propel the signaling capsules to shuttle between neighboring targets. This arrangement acts like a relay, so that triggering target capsules at a particular location in the array also triggers target capsules in adjacent locations. For an array containing two target columns, our simulations and analysis show that steady input signal leads to a sustained periodic output (**Fig. 3**). For an array containing multiple target columns, we show that by introducing a prescribed ratio of nanoparticle release rates between successive target columns, a chemical signal can be propagated along the array without dissipation. We also demonstrate that similar signal transmission cannot be performed via diffusion alone. The *J. Mat. Chem*. paper describing these results [4] was designated a "Hot Article".

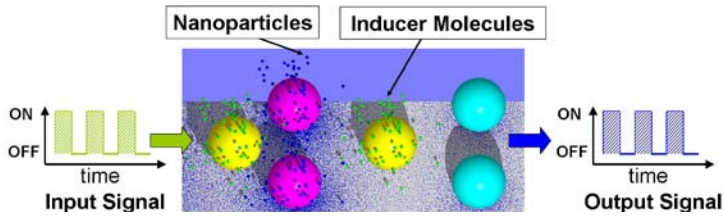

Fig. 3 An array of synthetic microcapsules is used to generate and transmit periodic chemical signals

We also simulated the behavior of nanoparticle-filled microcapsules that are propelled by an imposed shear to move over a substrate, which encompasses a microscopic crack [6]. When the microcapsules become localized in the crack, the nanoparticles can penetrate the capsule's shell to bind to and fill the damaged region. We isolated conditions where the microcapsules enter the cracks, deposit nanoparticles and then are driven to leave this region by the imposed flow (see **Fig. 4C**). In this manner, we determined optimal conditions for creating an effective "repair-and-go" system where the micro-carriers not only deliver a high volume fraction of particles into the crack, but also leave the fissure and thus, can potentially repair additional damage within the system. These studies also generated considerable interest. In particular, Scott R. White and Philippe H. Geubelle were commissioned to write a "News and Views" article for *Nature Nanotechnology* ("Self-healing materials: Get ready for repair-and-go" *Nat. Nano*. **2010**, *5* , 247)

Collaboration with T. Emrick, T. Russell and A. Crosby has lead to an experimental realization of the above system [7]. **Figure 4** summarizes the process of encapsulation, transport, and localized delivery of fluorescent nanoparticles into the cracked regions of the substrate. In particular, **Fig. 4D** shows the result of a repair-and-go experiment, in which the deposition of nanoparticles into the cracks is apparent from the fluorescence emanating from the cracked regions.

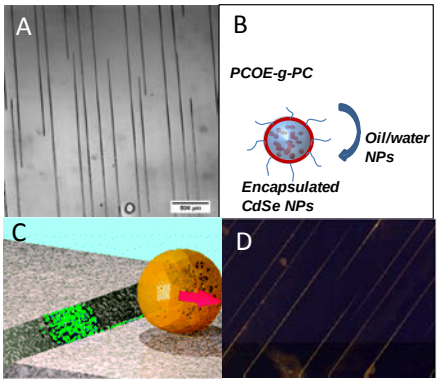

Fig. 4. (A) Optical micrograph of a cracked substrate (surface-oxidized PDMS) used for repair-and-go experiments; (B) copolymer used for droplet stabilization and nanoparticle encapsulation; (C) snapshot from simulation showing nanoparticles (in green) depositing in a crack, followed by rolling of the capsule to the next crack; (D) fluorescence micrograph of a substrate following nanoparticle deposition into the cracks.

Finally, we recently collaborated with Prof. Alan Russell's group at the University of Pittsburgh to experimentally realize our theoretical predictions on the behavior of capsules on striped surfaces [9] and thereby demonstrate that fluid-driven cells rolling on chemically patterned substrates can be readily sorted by their binding affinities [10]. Our results point to a low-cost means of performing efficient bio-assays.

Future Plans

We are attempting to design microcapsules systems that undergo self-propelled motion in response to mechanical deformation [11]. We will initially focus on a single nanoparticle-filled capsule; the diffusion of particles from the internal fluid to the external solution is proportional to the deformation of the capsule's shell. Here, we use the local curvature as the measure of deformation. The released nanoparticles that bound to the surface make this substrate less adhesive; hence, the capsule moves to regions of lower nanoparticles concentration. To break the initial symmetry, we deform the capsule asymmetrically by pressing on one side of the shell. Our preliminary results show that the capsule undergoes the sustained motion due to this initial mechanical deformation. This example provides an idea system for exploring the effects of inter-converting mechanical (the deformation of the shell), chemical (the formation of the gradients on the surface) and kinetic (the motion of the capsule) energy. Consequently, the studies provide guidelines for creating autonomously moving micro-machines or soft-robots that can be controlled by mechanical stimuli.

We will also expand the scope of the studies illustrated in Fig. 2 to consider a form of dynamic self-assembly where the triad capsules pick up different types of cargo in a controllable

manner. For example, there will be a number of different types of capsules that are located along the side of the adhesive track (green stripe in Fig. 2). For instance, there will be depots of A- and B-type capsules (i.e., these capsules will be decorated with different ligands). By picking up these capsules in a specific order, the triad will construct different "trains" or strands of information. For example, one four-capsule train can be composed of "ABAB" capsules, while another train might be an "AABB" arrangement. We will isolate conditions where the triads can construct longer trains with specific sequences, which constitute longer sentences of information. Through these studies, we will be creating a novel form of self-organization that operates in a purely autonomous manner.

We have also initiated a collaboration with Prof. Dan Hammer at UPenn; his group will be carrying out experimental studies to test our theoretical predictions. In the next year, we plan to work with Dan to facilitate their efforts in translating our findings into experimental observations.

Publications resulting from this project over the last two years

1. Kolmakov, G. V., Yashin, V.V., Levitan, S.P., Balazs, A.C., "Designing Communicating Colonies of Biomimetic Microcapsules", *PNAS*, 107 (2010) 12417-12422.
2. Kolmakov, G. V., Yashin, V.V., and Balazs, A.C., "Design Rules for Creating Sensing and Self-actuating Microcapsules", *Smart Structures and Systems*, 7 (2011) 199-211.
3. Kolmakov, G. V., Yashin, V.V., Levitan, S.P., Balazs, A.C "Designing Self-propelled Microcapsules for Pick-up and Delivery of Microscopic Cargo", *Soft Matter*, 7 (2011) 3168-3176.
4. Bhattacharya, A. and Balazs, A.C., "Biomimetic Chemical Signaling Across Synthetic Microcapsule Arrays" *J. Mat. Chem*., 20 (2010) 10384-10396.
5. Bhattacharya, A. and Balazs, A.C., "Chemical Signaling across an Array of Biomimetic Microcapsules" *Phys. Rev. E*., 82 (2010) 021801—021801-11.
6. Kolmakov, G. V., Revanur. R., Tangirala, R., Emrick, T., Russell, T.P., Crosby A. J., Balazs, A.C., "Using Nanoparticle-filled Microcapsules for Site-Specific Healing of Damaged Substrates: Creating a 'Repair and Go' System", *ACS Nano,* 4 (2010) 1115-1123.
7. Kratz, K., Narasimhan, A., Tangirala, R., Moon, S.C., Revanur, R., Kundu, S., Kim, H.S., Crosby, A.J. Russell, T.P., Emrick, T., Kolmakov, G. and Balazs, A.C. "Probing damaged substrates with 'repair-and-go' ", *Nature Nanotechnology*, submitted.
8. Maresov, E., Kolmakov, G. V., Yashin, V.V., Van Vliet, K. and Balazs, A.C "Modeling the Making and Breaking of Bonds as an Elastic Microcapsule Moves over a Compliant Substrate", *Soft Matter*, submitted.
9. Balazs, A.C and Alexeev, A., "Modeling the Interactions Between Compliant Microcapsules and Patterned Surfaces" in Multiscale Modeling of Paticle Interactions: Applications in Biology and Nanotechnology, MR King and DJ Gee, Eds, John Wiley, Chapter 7, (2010) 185-221.
10. Edington, C., Murata, H., Koepsel, R., Andersen, J., Eom, S., Kanade, T., Balazs, A.C., Kolmakov, G., Kline, C., McKeel, D., Liron, Z., and Russell, A.J., "Tailoring the Trajectory of Cell Rolling with Designer Surfaces", *PNAS*, submitted.
11. Kolmakov, G., Schaefer, A., Aronson, I. and Balazs, A.C. "Designing Mechano-responsive Microcapsules that Undergo Self-propelled Motion", *Soft Matter*, submitted.

High Efficiency Biomimetic Organic Solar Cells

Massachusetts Institute of Technology
77 Massachusetts Ave, Cambridge, MA 02139
PI: M.A. Baldo
Dept. of Electrical Engineering and Computer Science, Room 13-3053
Co-PI: T. Van Voorhis,
Dept. of Chemistry, Room 6-229

I Program Scope: Unlike conventional solar cell materials, organic semiconductors generate localized excitons when they absorb light. But the binding energy of these excitons is so large that they cannot be split into charge by the electric field inside a solar cell. Consequently, organic materials require a fundamentally different architecture. The donor-acceptor interface (Fig. A1) solves this problem by dissociating excitons into a hole in the donor and an electron in the acceptor. Recently, however, it has been recognized that the combination of the hole and electron at the donor-acceptor interface *also* forms a bound charge transfer (CT) state. Although smaller than the binding energy of an exciton, the CT binding energy is still likely much greater than the thermal energy (~ 0.1 eV).(*2*) The binding energy of a CT state opposes the generation of free charge, and encourages an important loss process – the recombination of the CT state into a neutral ground state. Thus, organic solar cells must overcome the binding energy of *both* the exciton and the CT state.

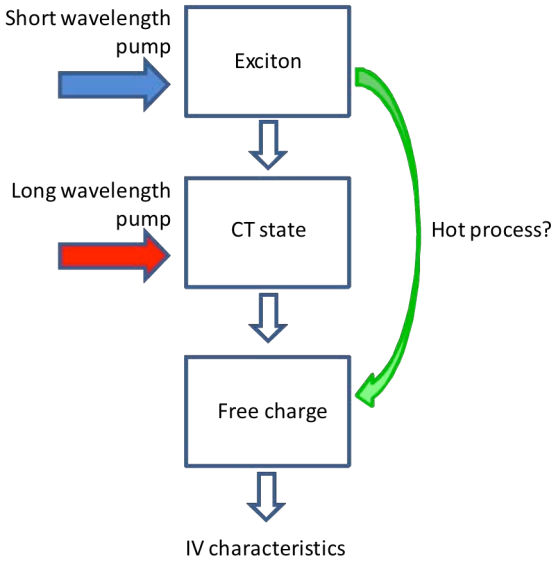

Fig. 1. We can probe the existence of a hot exciton dissociation process by comparing the output of solar cells under direct photoexcitation of either excitons CT states.

In this proposal we address two key questions: **1)*How do excitons and CT states dissociate in organic solar cells?*** *and* ***2)Will a biomimetic architecture help overcome the CT state binding energy?*** The biomimetic approach draws upon photosynthesis. In photosynthetic reaction centers, exciton dissociation is achieved through a multi-step electron transfer rather than a single donor-acceptor junction. A multi-step electron transfer can destabilize the CT states and rapidly separate the charge carriers. Indeed, the quantum efficiency of reaction centers is believed to exceed 95%.

II Recent Progress: Exciton and Charge Transfer state dissociation

Organic heterojunction PVs suffer from recombination of separated charges at the exciton-dissociation interface. Ultimately, this recombination limits the efficiency of organic PVs. Current understanding is that recombination is mediated by charge transfer (CT) states at the exciton dissociation interface. But the dynamics of CT states have been controversial.[1] While it is generally accepted that the binding energy of CT states is >> *kT*, it is also evident that the separation of CT states into charge can be very efficient. There are two main explanations for the apparent contradiction: (i) hot exciton dissociation, or (ii) slow recombination rates.

In a simple experiment, we have shown conclusively that there are no hot exciton effects. The implication is that CT state recombination is relatively slow.

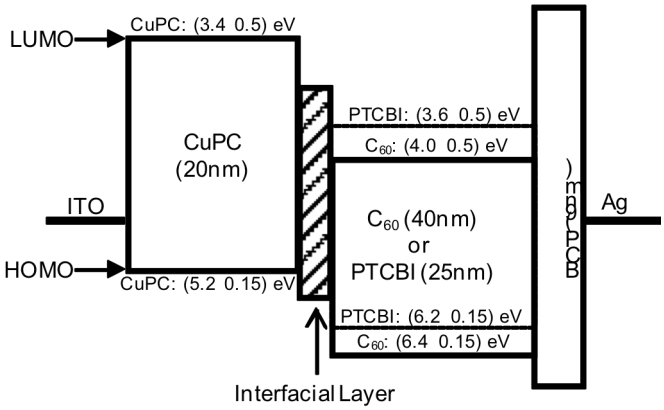

Fig. 2. Devices with thin interfacial layers exhibit higher external quantum efficiencies. The optimal layer thickness is approximately 15Å. The interfacial layer reduces recombination of separated charges at the exciton-dissociation interface.

II Recent Progress: Biomimetic multistep charge dissociation interfaces in organic PV cells

Organic heterojunction PVs suffer from recombination of separated charges at the exciton-dissociation interface. Ultimately, this recombination limits the efficiency of organic PVs. Device structure modifications represent one of the most promising routes to higher efficiency.

To reduce losses we have investigated an architecture is modeled on the multistep electron transfer cascade used in photosynthetic reaction centers. It creates a cascade energy structure at the exciton-dissociation interface as shown in Fig. 1. We have shown that both the voltage and current increase for solar cells of this structure. The voltage increase is expected because the charge transfer state energy at the dissociation interface increases. But the increase in photocurrent reflects a reduction in recombination losses.

III Future Work: Spin engineering of CT recombination dynamics

If the CT state recombination time is the primary determinant of the efficiency of free charge generation, we may be able to improve the efficiency of organic solar cells by spin engineering. The principle is that the ground state of a molecule is almost always a singlet (spin 0) state. Thus, recombination can be spin disallowed if the CT state is a triplet (spin 1). Indeed, in photosynthetic complexes, triplet CT states have been observed to live for several seconds at low temperature.[2]

Previously, our efforts at spin engineering have not been successful. We had focused on bilayer devices composed of the fullerene C60 and a metal free octaethylporphyrin (H_2OEP). These materials were chosen under the expectation that photoexcitation of fullerene would generate triplet excitons and hence triplet CT states [3], while H_2OEP would generate singlet excitons and hence singlet CT states . Device data shown

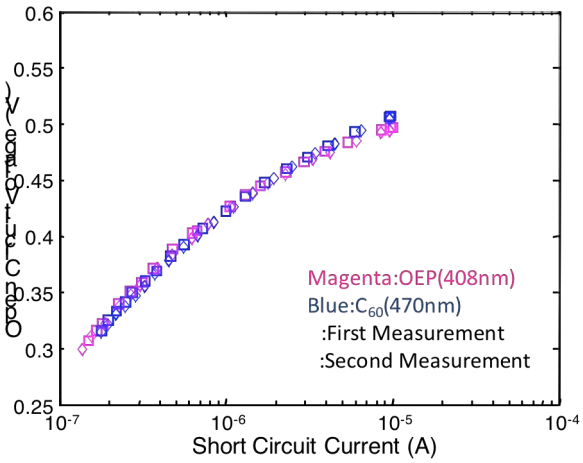

Fig. 3. Comparisons of the open circuit voltage upon direct excitation of either H_2OEP or C60 show no evidence for spin-induced modulation of CT state recombination times.

in Fig. 3, demonstrates, however, no observable difference in the open circuit voltage under specific photoexcitation of either singlet or triplet excitons.

Recently, we have modified the donor and acceptor layers to pentacene and PTCBI, respectively. Pentacene forms triplets at a very high yield via a fission process. Consequently, it contributes only minimal spin orbit coupling, which might alter CT mixing rates. PTCBI should generate singlet CT states. But we are still observing similar results to the H_2OEP/C60 system.

The preliminary conclusion is that the lifetime of CT states is sufficiently long for mixing to occur, even in the absence of notable spin orbit coupling. We plan to cool down the devices and introduce a magnetic field to quantify the mixing rates and perhaps observe a spin-dependent effect on recombination losses.

III Future Work: Dielectric screening and disorder at donor-acceptor interfaces

One conclusion of our earlier work on the apparent absence of hot exciton effects in organic PV is that the CT state dissociation process is barrierless. For example, the argument goes that: (i) we have shown that CT states definitely mediate exciton dissociation, but (ii) the efficiency of organic PV is relatively high even though CT states are involved. Thus, CT state dissociation cannot have a significant barrier, as this would lead to losses. This is in contrast to a molecular picture, which would suggest that at a distance of ~1 nm, the geminate electron hole pair should be bound by ~0.5 eV. If the latter were true, it would have a significant impact on device design.

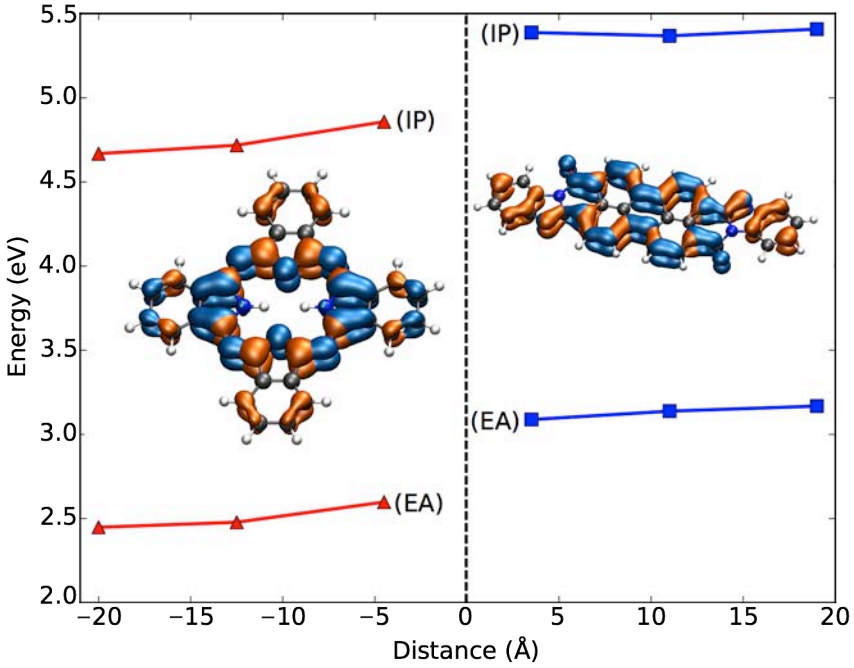

Fig 4. 'Band bending' at the donor acceptor interface can cause CT states to dissociate.

Through a combination of QM/MM simulations on a model H_2PC/PTCBI molecular interface, we have been able to demonstrate for the first time that geminate charge pairs are not bound. Rather, the Coulombic attraction of the positive and negative charge carriers is offset at the interface by a decrease in the dielectric screening. This reduced screening bends the bands of the electronic semiconductor in a manner reminiscent of their inorganic counterparts (see below). The result is that geminate electron/hole pairs have a thermodynamic driving force to separate,

so as to improve the dielectric screening. We expect this result to be quite general, as it results any time there is imperfect packing at the interface.

IV. References

[1] X. Y. Zhu, Q. Yang, and M. Muntwiler, Accounts of Chemical Research **42** (11), 1779 (2009).

[2] B. van Dijk, P. Gast, and A.J. Hoff, Phys. Rev. Lett. **77** (21), 4478 (1996).

[3] Nathan S. Lewis and George Crabtree, (U.S. Department of Energy, http://www.sc.doe.gov/bes/reports/files/SEU_rpt.pdf, 2005), p. 276.

V. List of Papers Published over the last two years

1. Mulder, Theogarajan, Currie, Maple, Baldo, and Vaughn. *" Luminescent solar concentrators employing phycobilisomes,"* Advanced Materials **21**, 1-5 (2009).
2. Lee, J., P. Jadhav, and M.A. Baldo, "*High efficiency organic multilayer photodetectors based on singlet exciton fission*," Applied Physics Letters, **95**, 033301 (2009).
3. Lee, Vandewal, Yost, Bahlke, Goris, Baldo, Manca, and Van Voorhis. *"Charge Transfer State Versus Hot Exciton Dissociation in Polymer-Fullerene Blended Solar Cells*." Journal of the American Chemical Society **132**(34): 11878-11880 (2010).
4. Heidel, Hochbaum, Sussman, Singh, Bahlke, Hiromi, Lee, and Baldo, *"Reducing recombination losses in planar organic photovoltaic cells using multiple step charge separation,"* Journal of Applied Physics, accepted for publication, (2011)
5. Difley, Wang, Yeganeh, Yost and Van Voorhis, "*Electronic Properties of Disordered Organic Semiconductors via QM/MM Simulations*," Acc. Chem. Res. **43**, 995 (2010).
6. Difley and Van Voorhis, "*Exciton/Charge Transfer Electronic Couplings in Organic Semiconductors,"* Journal of Chemical Theory and Computation, **7** 594-601 (2011).
7. Yost, Wang and Van Voorhis, "*Molecular Insight Into the Energy Levels at the Organic Donor/Acceptor Interface: A QM/MM Study*," J. Phys. Chem. C. **115**, 14431 (2011).

Optimizing immobilized enzyme performance in cell-free environments to produce liquid fuels

Joseph J. Grimaldi and Georges Belfort
Howard P Isermann Department of Chemical and Biological Engineering, and
Center of Biotechnology and Interdisciplinary Studies
Rensselaer Polytechnic Institute, Troy, NY 12180-3590

Active research to produce energy via biofuel cells or through the bioconversion of sugars to liquid fuels offers exciting new alternates to fossil fuel. We focus here on the bioconversion route that uses enzymes to convert sugars to butanol, for example. While these enzymatic routes offer great promise and excellent selectivity for the production of biofuels, enzymes exhibit slow kinetics, display low volume capacity in solution and exhibit product feed back inhibition. These limitations have to be overcome so that biofuels can be produced in an economically viable fashion.

Our approach is quite different to most others in that we produce the requisite enzymes via rDNA technology with *E. coli*, and then use these enzymes *in vitro* coupled with pervaporation to produce and continuously remove the desired butanol, respectively. Initially, we are interested in immobilizing a model enzyme, beta-galactosidase, and determining its reaction rates adsorbed on or tethered to flat convex or concave surfaces (AIM 1). These experiments are currently in progress. We plan to next study the separate reactions of immobilized keto acid decarboxylase (KDC) and alcohol dehdrogenase (ADH) (i.e. the product of the first enzyme is the substrate for the second one) on the best two surfaces (Aims 1 & 2) to produce long-chain alcohols. In collaboration with a molecular biologist, Dr. Cynthia Collins, Assistant Professor, Chemical and Biological Engineering, RPI, we have ordered the strain and DNA from NIZO of KDC, and plan to clone it into an *E. coli* expression vector with a His tag. ADH is available commercially. We are also planning to meet with our collaborator, Dr Sanat Kumar, Professor , Chemical Engineering, Columbia University, NY min order to initiate the modeling aspects of the research.

Biological and Synthetic Oligomers for Platinum Nanocrystal Synthesis

Lauren M. Forbes, Aoife M. O'Mahony, Sirilak Sattayasamitsathit, Joseph Wang*, Jennifer N. Cha*
University of California, San Diego; Email: jencha@ucsd.edu

Summary

In recent years, the design and synthesis of nanoscale platinum architectures have been explored extensively for applications ranging from heterogeneous catalysis to fuel cells. To obtain homogeneous catalytic activities while minimizing precious metal costs, research has focused on the development of efficient, facile methods to synthesize monodisperse sub-10nm nanocrystals while exercising accurate shape control. Platinum nanocrystals can be synthesized with relatively controlled sizes and morphologies through mediation by a surfactant or polymer. However, using ligands that show affinity for specific crystal plane may allow synthesis of more catalytically potent morphologies. Inorganic-binding biomolecules, such as peptides, have excellent potential as a class of morphology-specific ligands due to their variety of available amino acid sequences, but it has proven very difficult to controllably produce monodisperse and monomorphic nanocrystals from peptides with tunable size and shape. In the first half of the project report, we demonstrate the controlled synthesis of platinum nanocrystals with a variety of sizes and morphologies from a single peptide sequence at room temperature. After isolating a peptide designed to bind a specific crystal plane of platinum by phage display, we produced structures ranging from sub-2nm seed crystals to monodisperse 4 nm platinum polyhedra to 7-8 nm platinum cubes using simply by changing the rates of metal reduction. These peptides stabilized platinum nanoparticles were next tested for catalysis by running oxygen reduction reaction (ORR) studies. For this, both as-synthesized and acid washed particles were deposited on glassy carbon electrodes (GCE) but in all cases tested, the particles demonstrated extremely poor catalytic activity. As this was thought to be due to the strong interactions between the peptide and the platinum surfaces that could not be reversed in the acid electrolyte solutions, a systematic approach was taken to better understand the role of each amino acid toward particle synthesis and determine the final chemical nature of each amino acid after platinum synthesis. Since single amino acids could not be effective capping ligands and produce platinum particles of well-defined shape and size, we hypothesized that we could use peptide modified polymer scaffolds by chemically ligating single amino acids to the ends of short polymer chains. As a first step toward this, we studied the role of a water-soluble polymer, specifically polyethylene glycol for platinum nanoparticle synthesis and catalysis. Once we understood how the polymer alone behaved and found that the polymer backbone played no role toward platinum nanocrystal nucleation and growth, the idea was to attach single amino acid R groups to the ends of the short polyehthylene glycol (PEG) chains. In this simply polymer study, we demonstrate that 1) the backbone of PEG has little influence over crystal morphology but that the end groups can greatly influence crystal growth 2) the oxidation or reduction of the pendant end groups can dramatically affect catalysis and specifically ORR.

1. Investigations of platinum binding peptides for nanocrystal growth and catalysis

Peptides that bind a single crystal plane of platinum were isolated using a variant of phage display, a facile and oft-applied method to find peptides that bind specific substrates. The reason to screen against a single crystal plane of platinum was to obtain homologous sequences that would bind specifically to Pt (100), thereby providing a peptide sequence that would template specifically to this crystal plane. Solutions of the phage library (NEB, Ph.D. 12) composed of 10^9 different peptide sequences were carefully dropped onto the cleaned platinum nanocrystal substrates and incubated for 2h. Unbound phage were removed by careful washing and bound phage bound were eluted at pH 2 and amplified. After three consecutive rounds, the amino acid sequences of

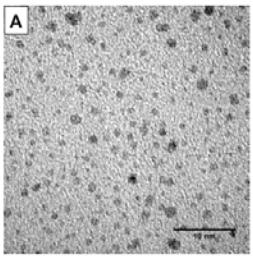

Figure 1. Pt NPs synthesized by Pt binding peptides. (A) with K_2PtCl_4 (B) with $Pt(NH_3)_{4(}(NO_3)_2$

the peptides that bound to the Pt (100) platinum nanocrystal substrates were determined through DNA extraction of select phage. Because the starting platinum substrates were highly crystalline and contained mostly a single crystal plane, significant amino acid homology between the sequences was observed, with a consensus sequence of Pro-Trp-X-X-Gln-Arg-Glu-Leu-Ser-Val (PWxxQRELSV).

Next, we explored the ability of the isolated peptides to mediate nanocrystal synthesis. First, the peptide sequence Tyr-Gln-Pro-Trp-Lys-Thr-Gln-Arg-Glu-Leu-Ser-Val (YQPWKTQRELSV) was chosen at random and obtained commercially. Varying concentrations of peptide and Pt^{2+} precursors (K_2PtCl_4 or $Pt(NH_3)_4(NO_3)_2$) were incubated in either deioinzed water or 20mM Tris buffer for 5-15 minutes at room temperature with constant stirring, followed by rapid addition of five molar equivalents of sodium borohydride ($NaBH_4$) to Pt^{2+}. Aliquots were removed at time intervals ranging from 10-30 minutes and analyzed by electron microscopy. As shown in Figure 2A, in the presence of K_2PtCl_4, fast reduction by $NaBH_4$ produced extremely small (1-2nm) platinum nuclei from the soluble platinum-binding peptides with no particles of any defined morphology (Fig. 1A). These nuclei were obtained almost irrespective of the molar ratio of K_2PtCl_4 to peptide (25:1 thru 250:1). In contrast to the K_2PtCl_4 reactions, when the Pt (100) platinum binding peptides were mixed with the less reactive $Pt(NH_3)_4(NO_3)_2$ at 25:1 Pt^{2+}:peptide ratios at pH 7 and reduced by $NaBH_4$, well-defined 3-4 nm platinum polyhedra nanocrystals were produced (Fig. 1B). The sizes and shape distributions remained consistent up to 250:1 $Pt(NH_3)_4(NO_3)_2$ to peptide ratios and the use of either 20mM Tris buffer (pH 7) or water did not affect particle synthesis. At higher molar ratios of $Pt(NH_3)_4(NO_3)_2$, particle formation was uncontrolled in both size and morphology and many particles aggregated. Using a different inorganic binding peptide, the silver binding NH_2-Asn-Pro-Ser-Ser-Leu-Phe-Arg-Tyr-Leu-Pro-Ser-Asp-COOH (NPSSLFRYLPSD), yielded bulk aggregates with no individual well-defined nanocrystals for both Pt^{2+} sources; these were similar to that observed when no peptides were used at all.

These peptide-Pt particles were next tested for ORR activity. As already stated however, in all cases, little or no ORR activity was detected. Although this was thought to be because of the strong binding between the peptide and the platinum surfaces, FTIR and NMR analyses could not elucidate which amino acids were most strongly bound to the Pt particles and whether the amino acid had either reduced or oxidized during the synthesis. The complex nature of the twelve amino acid peptide in terms of both sequence and secondary structure made it difficult to determine the role, if any, each amino acid had on platinum synthesis and catalysis. Although single amino acids were tried as potential ligands for particle synthesis, typical syntheses yielded only disordered or irregular shaped aggregates or particles.

2. Polymer mediated synthesis of Pt nanostructures

Since the twelve amino acid peptide was too complex and single amino acids yielded no controlled structure, polymers to which single amino acids could be attached were investigated. For this, it was important to use polymers whose pendant groups did not bind strongly to platinum surfaces so as to test only the role of the attached amino acid on platinum synthesis and catalysis. For this, we started with low molecular weight PEG. Although PEG has been shown to control gold or palladium[48] crystal growth, results with platinum have yielded mainly small spherical particles. To exert greater control over platinum nanocrystal synthesis from the polymer, different molecular weights of unmodified linear PEG (200, 8000, and 20,000 Da) were reacted at varying molar ratios with N_2-purged aged solutions of 1 x 10^{-4} M K_2PtCl_4 in water and reduced by bubbling H_2 through for 5 min and sealing overnight. As shown in Figure 2A, the shortest PEO (PEG200) chain at 1:1 PEG:Pt molar ratios generated well-defined 6.6 ± 1.0 nm platinum cubes and truncated cubes. As the PEG chain lengths increased (Fig. 2B, 2C), control over both crystal morphology and size also appeared to diminish, and using the longest PEG chain (PEG20K) produced largely spherical platinum particles of 4.5 +/- 1.1 nm (Fig. 2C). The longer polymer chains were thought to produce more ill-defined and spherical particles because of the larger effective volume a longer

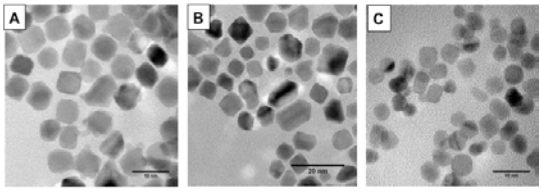

Figure 2. PEG synthesized Pt NPs using PEG molecular weights of (A) 200, (B) 8K, (C) 20K

PEG chain would occupy on a growing nanoparticle, which would prevent effective end-group stabilization of a growing particle face.

To determine the effect different end groups of PEG on p latinum synthesis, di-methoxy, methoxy-amine and methoxy-maleimide terminated PEG chains were reacted with aged and nitrogen-purged K_2PtCl_4 and reduced in H_2. In the case of the di-methoxy PEG, uncontrolled particle growth and mainly large aggregated clumps were observed, verifying the importance of the end groups on PEG for particle synthesis and ruling out the ethylene oxide backbone as a ligand for synthesis (Fig. 2). In the case of amine terminated PEG (PEG-amine), platinum nanostructures similar to those obtained using PEG200 were obtained, including cubes with size distributions of roughly 8-9 nm. While the maleimide functionalized PEG polymers (PEG-maleimide) demonstrated inferior overall control than either PEG200 or amine-PEG and produced particles of varying morphologies such as cubes and hexagons, to a large extent particle size and shape was relatively controlled.

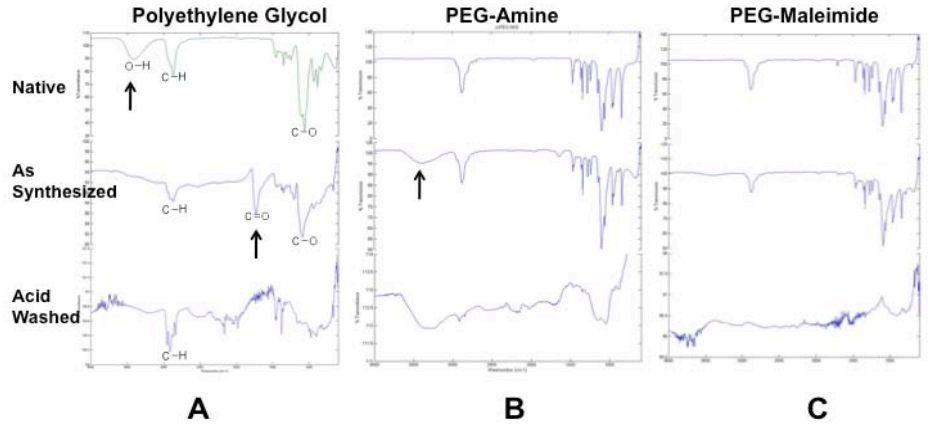

Figure 3. FTIR Spectra of polymer alone, as synthesized Pt NPs and acid washed Pt NPs.

The fates of the polymer end groups during particle synthesis were also studied by FTIR. While native PEG200 possesses a strong OH stretch, after synthesis this peak disappeared with the concurrent appearance of a strong carbonyl peak at 1728 cm^{-1} (Fig. 3A). The disappearance of the strong OH stretch in the PEG200-Pt samples indicated that the terminal hydroxyl groups play a significant role in binding to the platinum surface during particle growth. Second, the appearance of a carbonyl unit indicated that the hydroxyl group most likely became oxidized to aldehydes or carboxylic acids during the reaction or post-synthesis. FTIR analyses further showed that these weak carbonyl-platinum interactions could be dissociated by acids such as the electrolytes used for ORR since simple rinsing of the PEG-Pt particles in 0.5M H_2SO_4 caused the polymers to wash off (Fig. 3A). FTIR analyses of the PEG-amine particles showed the emergence of a new peak at 3391 cm^{-1} indicating that the amines may have oxidized to the N-oxide during or after synthesis (Fig. 3B). Although the polymer signals weakened substantially after washing the PEG-amine particles in H_2SO_4, some polymer still remained behind, indicating that unlike the more labile carbonyl-platinum interactions seen with the PEG200, the oxidized amine-platinum interactions were harder to dissociate. Previous work has also shown that electrochemical oxidation of aliphatic amines cause covalent attachment to platinum surfaces. FTIR analyses of the PEG-maleimide particles did not provide any peaks different than the polymers alone but the interactions with the platinum surface are presumably through the carbonyl units of the maleimide group, as the carbon-carbon double bond most likely becomes reduced during the platinum synthesis in hydrogen. Acid washing of the PEG-maleimide platinum particles showed that the polymers can be easily washed off.

Platinum Nanoparticles	Mass Activity/ μA μg^{-1}	$E_{1/2}$/ mV (*vs.* Ag/AgCl)
Pt Black	45	529
PEG200	50	487
PEG-maleimide	26	568
PEG-amine	26	421
PEG20K	22	340

Figure 4. Mass activities and half-wave potentials of the Pt NPs towards ORR.

The activity of the polymer-assisted Pt nanoparticles towards ORR was next tested (Figure 4). For this, ORR polarization curves were determined at Pt-modified glassy carbon electrodes (GCE) prepared using the polymer synthesizd nanoparticles (Fig. 4). In all cases, after synthesis the particles were collected by centrifugation and washed three times with 0.1M H_2SO_4, water and acetone. As a comparison, platinum black was also tested for ORR. The platinum nanoparticles were immobilized onto the GCE through evaporation and confined with 0.05% Nafion. For each of the species examined, an increase in current was observed with increasing rotation speed. The values of the peak currents were examined using the Koutecky-Levich equation, where the inverse of the square root of rotation speed was plotted *vs.* the inverse of the steady-state current and values for kinetic current. These values were used to calculate mass activity for each species, which are outlined in Fig. 4 and clearly show a difference in ORR catalytic activity for the different nanoparticles. As shown, the PEG200 platinum particles yielded the highest current output of all the polymer-assisted nanoparticles that was also strongly comparable to Pt Black. Figure 4 also shows a comparable mass activity of PEG200 with Pt black, showing the high surface area of the PEG200 nanoparticles exposed to O_2 for ORR. The half-wave potential value shown in Fig. 4 for PEG200 was also relatively high showing a high catalytic ability of this species towards ORR. The PEG-maleimide platinum nanoparticles also performed quite well compared to Pt black with the onset of ORR at a low overpotential and the half wave potential to be 568mV. The half-wave potential for the PEG-maleimide particles were actually more positive than that observed for Pt black, showing that these nanoparticles have a high catalytic ability towards ORR. The mass activity for PEG-maleimide, however, was less than that observed for PEG200 and Pt black, and this may have been due to two factors: (i) aggregation of the nanoparticles, which would decrease the overall surface area per mass of Pt; (ii) the presence of polymer still at the surface of the nanoparticles which would block active sites from ORR, thus having a similar effect to aggregation. Because the FTIR evidence showed that the PEG-maleimide polymers could be easily removed from the particles by a single acid wash however particle aggregation was more likely the explanation for lower mass activity. As had also been noted earlier, the PEG-maleimide also demonstrated less overall control than either PEG200 or amine-PEG. The catalysis towards ORR was also somewhat diminished for the PEG-amine platinum particles as observed in the voltammetry, where a significant decrease in peak current was observed as compared to the PEG200 and PEG-maleimide particles and with the onset of reduction of oxygen at a higher overpotential. The half-wave potential was significantly lower than the previous two species, showing a lower catalytic ability towards ORR. The mass activity was also lower than those of Pt Black and PEG200, but comparable to that of PEG-maleimide. While the lower mass activity of PEG-maleimide may be attributed to aggregation of the particles since FTIR showed facile removal of the polymer from the nanoparticles, since the FTIRs showed that PEG-amine remains behind even after acid washings, the low mass activity in this case may be attributed to the remaining presence of polymer at the Pt surface, thus blocking active sites from ORR. The least favorable catalytic reaction towards ORR proved to be the PEG20K platinum particles with a much more negative half-wave potential and a mass activity at 22 $\mu A\ \mu g^{-1}$, lower than that observed for the other platinum particles, in particular, PEG200. With the PEG20K platinum particles, the low ORR activity was most likely due to the fact that the polymer is 100 times larger in molecular weight than PEG200 and cannot therefore wash away from the platinum surfaces and escape through the porous Nafion coating on top, thus hindering ORR almost completely. The stability of the platinum nanoparticles prepared from PEG200 was tested using 1000 repetitive CV cycles over range 0 V to 1.0 V at 50 $mV\ s^{-1}$ in 0.1 M H_2SO_4. After an initial slight decay in current from cycles 1 to 300, the current remained stable thereafter up to 1000 repetitive CV cycles.

Publications: (1) L.M. Forbes, A.P. Goodwin, J.N.Cha*, "Controlled Nucleation of Platinum Nanocrystals from Peptides", *Chemistry of Materials* 22, 6524-6528 (2010)
(2) L.M. Forbes, A.M. O'Mahony, S. Sattayasamitsathit, J. Wang, J.N. Cha*, "Polymer End-Group Mediated Synthesis of Well-Defined Catalytically Active Platinum Nanoparticles", *J. Mater. Chem. In press* (2011)

Functional, Hierarchical Colloidal Liquid Crystal Gels and Liquid Crystal Elastomer Nanocomposites

PI: Juan de Pablo, co-PI: Nicholas Abbott
Address: University of Wisconsin - Madison
depablo@engr.wisc.edu

Program Scope

Liquid crystalline elastomers (LCEs) exhibit a number of unusual thermophysical properties that are not encountered in traditional elastomers or in simple liquid crystals. A key property of LCEs that we seek to exploit is their so-called "soft elasticity," through which a small applied stress can give rise to a large deformation of the material. Such a macroscopic deformation is accompanied by a change in the orientation of small liquid crystalline domains, and could in principle be quantified by optical means. While various aspects of LCEs have been studied in the past, the molecular origins of their behavior remain poorly understood. Furthermore, composites of LCEs with functionalized nanoparticles have not been considered before. LCE nanocomposites have the potential to display entirely new functionalities that arise naturally in biological systems, but that have not been realized in synthetic materials. Our efforts over the past year have sought to characterize the behavior of micro- and nano-particles dispersed in LCEs, and to develop a molecular model of LCE nanocomposites capable of predicting and explaining our experimental observations.

1) Investigation of the Influence of Strain on Ordering of Liquid Crystalline Elastomers about Silica Microparticles.

It is now broadly appreciated that microparticles dispersed in low molecular weight liquid crystals (LMWLCs) generate topological defects within the LC phase. The topological defects can be point, Saturn ring and boojum, depending upon factors such as the particle size and surface chemistry. It is also understood that the topological defects formed in the LC can mediate interparticle interactions that lead to formation of particle arrays and microparticles chaining. Whereas past studies have focused on LMWLCs, recent studies at UW-Madison have provided the first experimental characterization of an investigation of the orientational ordering liquid crystalline elastomers (LCEs) around microparticles.

LCEs are cross-linked polymer networks with either mesogenic main- or side-chains. A key property of LCEs is the strain of the polymer network and the orientational order of the mesogens, which leads to shape memory behaviors, and responsiveness to changes in temperature, light, pH, electric fields etc. Past studies have established that this coupling can give rise to unusual mechanical properties such as so-called "soft elasticity" where linear strain of the material

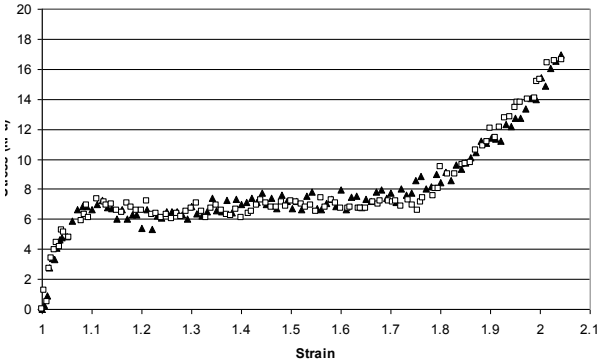

Figure 1. Stress-strain curve of perpendicular stretching of monodomain LCE films with (▲) or without (□) silica microparticles.

orthogonal to the director is accommodated by reorientation of the mesogens. Our initial experiments sought to confirm the presence of "soft elasticity" in the samples prepared at UW-Madison. This was successfully accomplished (see Figure 1). A key accomplishment of the UW-Madison research has been the development of an experimental procedure that allows the incorporation of microparticles in liquid crystalline elastomers (LCEs). We note that the initial attempts to incorporate microparticles into LCEs using previously reported methods of LCE preparation resulted in sedimentation of the particles to the interface of the LCE (very few particles were located in the bulk). As seen in Figure 1, we also observed the presence of "soft elasticity" in these particle-containing LCEs.

We performed experimental characterization of the optical signatures of the LCEs in the vicinity of the microparticles to determine if the ordering of LCEs is similar to those in LMWLCs system, including the influence of surface anchoring of the LCE on the microparticles and local orientation of LCEs. We also characterized the nature of the optical signatures around microparticles and how they respond to the strain-induced changes in the orientation of the LCEs. We hypothesized that the orientational order of mesogens near microparticles dispersed in LCEs would be likely different from that observed using LMWLCs because of local strain of the polymer network in the vicinity of the microparticles. Our results (Figure 2) support this proposition and suggest that the strong coupling of the mesogenic order to the local strain provides new ways to explore local deformations of polymer networks near inclusions. In order to provide insight into the origins of the optical signatures around microparticles in LCEs, we compared them with topological defects formed around microparticles in LMWLCs. Silica microparticles were functionalized with dimethyloctadecyl[3-(trimethoxysilyl)propyl] ammonium chloride (DMOAP), which caused perpendicular or homeotropic anchoring of 5CB.

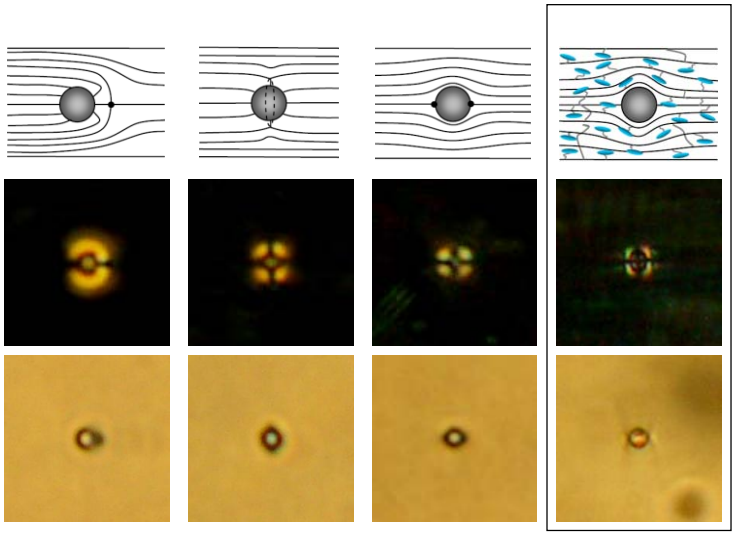

Figure 2. (A) Point defect; (B) Saturn ring defect; (C) boojum defect of silica microparticles in low molecular weight of liquid crystals (LMWLCs) (5CB) and (D) orientational ordering of LCEs around silica microparticles. Top row is the schematic illustration of director fields. The blue rods represent mesogens in LCEs. The size in the sketch is not to scale. Middle row is optical images (crossed polars). The double arrow in the middle row of (A-B) represents the polyimide rubbing direction, or director field of 5CB. The double arrow in the middle row of (D) represents the director of LCEs, **n0**. The bottom row is the bright field images. The scale bar represents 5 μm.

The DMOAP-functionalized silica microparticles with a diameter of 3 μm were introduced into a rubbed wedge cell, which induced parallel or planar orientation along the rubbing direction, denoted as double arrow in Figure 2A-C. In thicker parts of the cell (Figure 2A), above ~ 5 μm, the microparticles tended to form point defects (also called hyperbolic hedgehog defects) with dipolar symmetry, and a dark spot was evident in bright field image. The microparticle and the point defect aligned along the rubbing direction. The director field was distorted around the microparticles on a micrometer scale, therefore, the optical signatures in polarized image with a dimension of 7.0 μm × 8.0 μm were bigger than that of 3 μm × 3 μm in bright field image. In the thinner parts of the cell (Figure 2B), smaller than 5 μm, the microparticles tended to form Saturn ring defects with quadrupolar symmetry. The dark thin Saturn ring was around the equator of particle and perpendicular to the rubbing direction, see Figure 2B. The diameter ratio of the Saturn ring (3.3 μm) and microparticles (3 μm) in bright field image was ~ 1.1. Due to the distortion of director field around the equator of the particle, the optical signatures in polarized image showed 5.6 μm and 6.0 μm axis parallel and perpendicular to the director field, respectively. Another possible configuration is comprised of two boojum defects with four bright lobes around microparticles, see Figure 2C. In our experiment, the surfaces of the silica microparticles without any treatment caused parallel/planar anchoring of 5CB. The boojum defects in bright field showed two dark spots at the poles of the microparticle, which were parallel to the rubbing direction. The optical signatures in polarized image showed 5.2 μm and 4.5 μm axis parallel and perpendicular to the director field, respectively. For comparison, Figure 2D shows optical signatures of microparticles in LCEs. Compared to topological defects of microparticles in LMWLCs in Figure 2A-C, the optical signatures of microparticles in LCEs were clearly different from point defects. The former one had quadrupolar symmetry, and the latter one had dipolar symmetry. The optical signatures of microparticles in LCEs have similarities to boojum defects, with four bright lobes just off the microparticles, and the narrow dark gaps on the poles of the microparticles parallel to the director. The dimensions of optical signatures of microparticles in LCEs along and perpendicular to the director were 3.7 μm × 4.5 μm, which were smaller from Saturn defects (5.6 μm × 6.0 μm) or boojum (5.2 μm × 4.5 μm) defects. This difference is because relaxation is driven by strain of polymer network not elasticity of LCs. In addition, the bright field image of microparticles in LCEs did not show defect structure as normally observed in topological defects of microparticles in LMWLCs, suggesting the optical signatures of microparticles in LCEs cannot be simply explained by the same rules in LMWLCs. We conclude that the optical signatures do not depend on the surface chemistry of the silica microparticles, and the mesogenic ordering about the microparticles in the LCEs is not surface-induced in a manner comparable to LMWLCs. Instead, our results suggest that local mesogenic ordering is induced by the local strain of the polymer network of the LCE about the microparticles, and the strong coupling of the orientational order of the LCEs to that strain. This proposition was supported by experiments involving strain of the LCE.

2) Molecular Modeling of Liquid Crysalline Elastomers About Nanoparticles:

The experimental results outlined above require that new models be developed for liquid crystalline elastomers. There are no such models available in the literature. Our first step has been to develop a coarse grained representation of the elastomer in which the crosslinker molecules have been represented by either flexible or rigid oligomeric units.

In the latter case, crosslinker molecules enhance the anisotropic nature of the LCE sample and provide stability to the material. In the rigid case, the crosslinkers and the mesogens

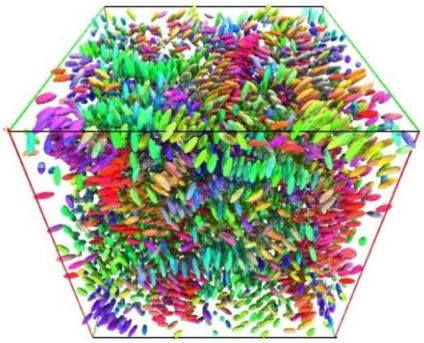

Figure 3. Representative configuration of model LCE at zero stress, in the polydomain state. Clusters of nematogens of different colors correspond to nematic domains with independent orientations.

(LC) molecules are represented by ellipsoidal particles. Flexible crosslinkers are represented as short polymer chains consisting of spherical particles. The interactions between mesogens and crosslinkers are described by a Gay-Berne potential energy function. To avoid any ambiguity in the interpretation of our results, our initial work has been focused on the study of defect-free networks with a diamond topology.

At equilibrium, in the absence of an applied stress, the LCE exhibits several nematic domains whose directors are independent of each other (Fig. 3). These results confirm that the proposed model is capable of describing a polydomain state, as observed in experimental studies. As an uniaxial stress is applied, the system initially remains in a polydomain state, but these domains rotate about themselves in order to accommodate the applied external stress at a local level. Above a critical, threshold value, the system exhibits a transition from a polydomain to a monodomain state. The monodomain system becomes uniformly nematic. The corresponding stress-strain curve for the model LCE depicted in Figure 3 is shown in Figure 4. Consistent with our experimental results (see Figure 1), our model elastomers also exhibit soft elasticity. We have also observed that the domains rotate with the application of stress, but they grow in size only marginally, indicating that the polydomain-to-monodomain transition occurs through a rotation of nematic domains, as opposed to their growth.

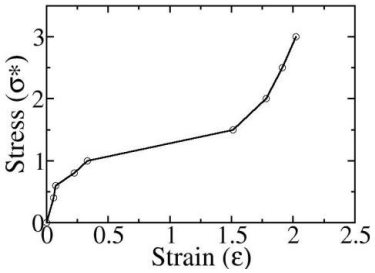

Figure 4. Stress-strain curve for model LCE. The stress is shown in dimensionless units. The strain response of the model LCE is consistent with observed in our experimental system (Figure 1). The model exhibits the sought-after soft elasticity behavior characteristic of LCEs.

Consistent with experimental observations, we find that nanoparticle addition does not influence the overall soft-elasticity behavior of the LCE. However, at a local level, the nanoparticles induce a strain in nearby mesogens that alters their orientation significantly. The LCE simulations described above have been enabled by development of novel simulations techniques that we refer to by "Flux Tempered Metadynamics."

Program Title: **Multicomponent Protein Cage Architectures for Photocatalysis**

Principal Investigator: T. Douglas; Co-PI: B. Kohler
Mailing Address: Department of Chemistry and Biochemistry, Montana State University, Bozeman, MT 59717
E-mail: tdouglas@chemistry.montana.edu

Program Scope

Virus capsids and other protein cage architectures exhibit a remarkable variety of sizes and can be produced in large quantities. Selective deposition of organic or inorganic materials, by design, at specific locations on the protein cage affords precise control over the size, spacing, and assembly of nanomaterials, resulting in uniform and reproducible nano-architectures. A simple approach is to genetically modify the protein subunits for the specific function of directing the growth of desired nanoparticles and polymers that can serve as basic building blocks for functional materials. This multidisciplinary effort was aimed towards the development of a biomimetic approach to materials synthesis that utilize protein-based templates for coupled light harvesting and hydrogen formation.

Recent Progress

Background

The central focus of this work is the development of protein architectures for the templated synthesis of light harvesting and catalytic nanoparticle hybrids. These include both inorganic nanoparticles as well as coordination polymers that incorporate light harvesting and catalytic sites, and linear and crosslinked polymers which can be modified to incorporate active sites. Using a bio-inspired approach, we have utilized a range of protein cage architectures to direct the nucleation, growth, and proximity of a range of component materials and investigated their structure and catalytic activity. These materials are highly homogeneous and in some instances are stable to temperatures in excess of 100ºC.

Discussion of Findings

1) Protein Cages as Templates for Encapsulated Nanoparticle Synthesis

We directed the synthesis of nanoparticles of TiO_2 within the cavity of the Cowpea chlorotic mottle virus (CCMV), a-Fe_2O_3 synthesized within a ferritin cage from the hyperthermophilic archeon *Pyrococcus furiosis*, and ultrasmall Pt-nanoparticles synthesized within the smaller Dps protein cage. These hybrid materials have been structurally characterized using TEM (electron diffraction) and PDF (pair distribution function) methods with high-energy X-ray scattering data, collected at APS. The syntheses of these nanoparticles utilized a biomimetic approach, where complexed anionic Ti(IV) bis-(ammonium lactato)-dihydroxide (Ti-BALDHI) was used for conversion to nanoparticulate TiO_2 (**Figure 1**), controlled oxidative hydrolysis of Fe(II) and polymorph transformation to form nanoparticulate hematite, and reduction of Pt ions to form highly active Pt clusters. In all cases the resultant nanoparticles were size and shape constrained by the interior surface of the protein cage. The

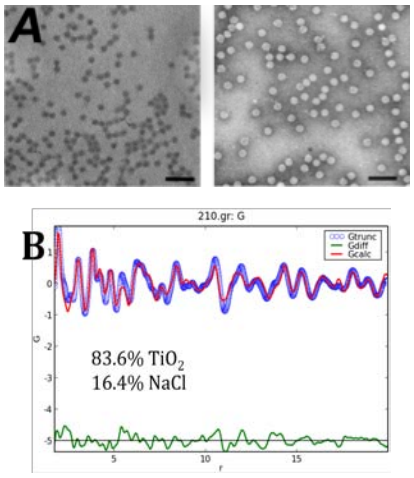

Figure 1. A. Transmission electron micrograph of unstained (right) and uraynl acetate stained (left) Cowpea chlorotic mottle virus reacted with Ti-BALDHI. The scale bars are 100 nm. **B.** PDF data and fit of β-TiO_2 formed within the CCMV capsid

TiO_2 reaction product had a diffraction pattern that could be indexed to β-TiO_2, which was confirmed by more extensive PDF analysis. The α-Fe_2O_3 was synthesized by initial deposition of the disordered iron oxide ferrihydrite and the subsequent transformation of this polymorph to hematite (α-Fe_2O_3) at elevated temperature (~100ºC, 12 hours). In addition, the growth of the Fe_2O_3 was monitored using mass spectrometry to establish the distribution of species present, especially at very early timepoints in the nucleation. This mass spectrometry methodology was also used to monitor the formation of ultrasmall Pt nanoparticles, within the Dps protein cage, with very high surface area and high catalytic activity.

We have measured the photocurrent generated from the TiO_2-virus materials using a coupled electrochemical system, with ethanol as sacrificial reductant and methyl viologen as electron transfer mediator. We utilized a transparent ITO working electrode, and ITO counter electrode and Ag pseudo reference and illuminated the sample with a Xe-arc lamp to mimic the solar spectrum. Similarly, the photocatalytic activity of the hematite encapsulated material, a visible band gap semiconductor, was measured using a coupled electrochemical system, in ethanol (as sacrificial reductant) and methyl viologen as electron transfer mediator, with a transparent ITO working electrode, and ITO counter electrode and a Ag pseudo reference (**Figure 2**) and a blue LED light source. The ability to reduce MV^{2+} under these conditions means we could couple this system to a number of redox enzyme systems that can use MV^{+} as a reducing agent.

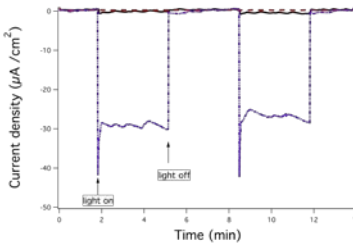

Figure 2. Photocurrent generated upon exposure of ferrihydrite in Pf_Fn (red dashed), Methyl viologen (black solid), and hematite Pf_Fn / Methyl viologen (blue dash-dotted) to a high intensity LED light.

We demonstrated efficient hydrogen production using the ultrasmall Pt^0 nanoparticles encapsulated with the protein cages using a coupled $Ru(bpy)_3^{2+}$/methyl viologen or $[Ir(ppy)_2(bpy)]^+$) (with no mediator) based photosystem. Reaction mixtures were illuminated at 25 ^oC and the hydrogen produced was monitored by gas chromatography (GC). While the Dps samples with theoretical loadings equal to or less than 45 Pt^0 produced hydrogen near at baseline levels, the 75 Pt^0 containing Dps generated approximately four times more hydrogen than the background level. This supports the idea that the 75 Pt atoms form a single nanocluster rather than multiple nanoclusters in the Dps. In contrast, the 45 Pt^0 or lower Pt^0 containing cages don't appear to form a sufficiently large cluster to catalyze hydrogen production.

2) Programmed co-assembly and e ncapsulation using the P22 protein cage. The bacteriophage P22 assembles with the assistance of a scaffold protein (SP) into a T=7 60 nm icosahedral shell with a 50 nm central cavity. Only the C termimal region of the SP is necessary for capsid assembly while the N-terminus can be truncated or fused to other proteins or polypeptides, with no effect on assembly. We have demonstrated the fusion of two different protein and polypeptides to the SP and demonstrated assembly of the

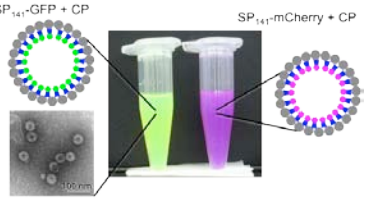

Figure 3. Truncated SP genetically fused with GFP or mCherry also templates the self-assembled with the coat protein subunit to form the icosahedral capsid as shown. TEM of the purified material is indistinguishable from P22 capsids assembled with full length SP.

P22 and encapsulation of the fusion product.

The fusion of green fluorescent protein and red fluorescent protein (mCherry) to the SP results in assembly of the P22 capsid with the GFP or RFP encapsulated on the inside (*8*) as shown in **Figure 3**. Co-encapsulation of a triple fusion SP-GFP-mCherry (with a variable length peptide linker between the two fluorescent proteins) results in very efficient energy transfer when forced into the crowded environment of the capsid but complete loss of FRET when these are released from the capsid. This clearly demonstrates the effects of molecular crowding of the properties of the encapsulated cargo.

The fusion of a polypeptide with a $(EA)_n$ repeat to the SP also results in directed encapsulation. Treatment of these EA-SP capsids with Fe(II) followed by air oxidation results in the homogeneous formation of Fe_2O_3 selectively within the capsid (**Figure 4**). The highly charged polypeptide acts as a nucleation template.

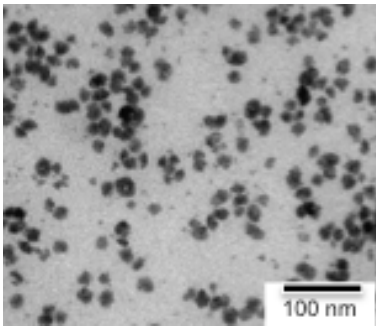

Figure 4. TEM of Fe_2O_3 synthesized inside the P22, nucleated on the SP-fusion to an (EA) repeat polypeptide.

Future Directions: We will explore the fusion and encapsulation of a range of polypeptides for the directed synthesis of nanomaterials for light harvesting and catalysis, including TiO_2, ZnO, ZnS(Se) and CdS(Se).

3) Templated Synthesis of Polymers within Protein Cage Architectures

We have demonstrated growth of a series of crosslinked and hyperbranched polymers within protein cages using either an alkyne-azide [3+2] cycloaddition "click-reaction" or ATRP (with methacrylate or acrylamide monomers) initiated in a site selective manner on the interior protein cage surface (**Figure 5**). We can control the growth of the polymer, the degree of crosslinking and importantly the functionality of the monomeric unit. The degree of crosslinking dramatically influences the degree of stiffness, and mechanical, chemical, and thermal stability of the overall PCN structure.

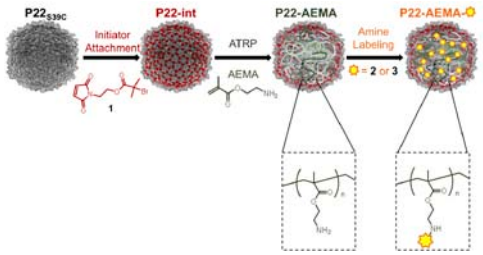

Figure 5. Assembly of the internal polymer P22 VLP. $P22_{S39C}$ modified with a cysteine reactive ATRP initiator (**1**) is used as macroinitiator and a size constrained reaction vessel for ATRP growth of poly(AEMA) strands inside the virus like particle. This introduced polymer scaffold can subsequently modified with primary amine reactive agents.

When grown inside the P22 capsid these hyper-branched, dendritic structures grow from the walls of the capsid towards the interior resulting in control over metal coordination adjacencies and a high degree of polymer crosslinking. In addition, using a range of straightforward synthetic coordination chemistries, we are able to control the stepwise connectivity between the monomers in this dendritic growth, which allows us to make both molecular systems and extended polymeric solids. We have the capacity to make small well-defined molecular coordination clusters with 2 different metals (in different ratios), which can be connected with control over the degree of conjugation in the polymer backbone and are also important for the photophysical studies of electron transfer between the light harvesting (Ru) center and the catalytic (Co) center.

Of particular interest are conjugated coordination polymers composed of $Ru(phen)_3^{2+}$ alone and controlled mixtures of Ru(II) and Co(II) phenanthroline (and other chelators) monomers for directed energy transfer for light harvesting and catalytic chemical reduction—both functions of great interest in solar energy conversion. We have demonstrated that $Co(phen)_3^{2+}$ and $Ru(phen)_3^{2+}$ mixed together as individual molecules will generate H_2 in a photochemical reaction.

Future Directions: Our expectation is that when coupled together into an extended and conjugated coordination polymer the efficiency of light harvesting and catalysis should increase. Alternatives to $Co(phen)_3^{2+}$ are the cobalt-glyoxime complexes, which have been shown to be excellent H_2 catalysts - and through modification of the dimethylglyoxime ligand can be incorporated into the polymerization scheme. These compounds will be studied by femtosecond transient absorption and emission spectroscopy in the Kohler Lab, which has expertise in the ultrafast photophysics of ruthenium photosensitizer compounds. When paired with transient absorption signals, emission lifetime measurements provide unambiguous assignment of rates of forward and back electron transfer.

References (which acknowledge DOE support)

(1) Kang, S., Jolley, C. C., Liepold, L. O., Young, M., and Douglas, T. (2009) From Metal Binding to Nanoparticle Formation: Monitoring Biomimetic Iron Oxide Synthesis within Protein Cages using Mass Spectrometry. *Angewandte Chemie 48*, 4772-4776.

(2) Klem, M. T., Suci, P., Britt, D. W., Young, M., and Douglas, T. (2009) In-Plane Ordering of a Genetically Engineered Viral Protein Cage. *Journal of Adhesion 85*, 69-77.

(3) Suci, P. A., Kang, S., Young, M., and Douglas, T. (2009) A Streptavidin-Protein Cage Janus Particle for Polarized Targeting and Modular Functionalization. *Journal of the American Chemical Society 131*, 9164-9165.

(4) Kang, S., Suci, P. A., Broomell, C. C., Iwahori, K., Kobayashi, M., Yamashita, I., Young, M., and Douglas, T. (2009) Janus-like Protein Cages. Spatially Controlled Dual-Functional Surface Modifications of Protein Cages. *Nano Letters 9*, 2360-2366.

(5) Jolley, C. C., Uchida, M., Reichhardt, C., Harrington, R., Kang, S., Klem, M. T., Parise, J. B., and Douglas, T. (2010) Size and Crystallinity in Protein-Templated Inorganic Nanoparticles. *Chemistry of Materials 22*, 4612-4618.

(6) Broomell, C. C., Birkedal, H., Oliveira, C. L. P., Pedersen, J. S., Gertenbach, J. A., Young, M., and Douglas, T. (2010) Protein cage nanoparticles as secondary building units for the synthesis of 3-dimensional coordination polymers. *Soft Matter 6*, 3167-3171.

(7) Kang, S., Uchida, M., O'Neil, A., Li, R., Prevelige, P. E., and Douglas, T. (2010) Implementation of P22 Viral Capsids as Nanoplatforms. *Biomacromolecules 11*, 2804-2809.

(8) Klem, M. T., Young, M., and Douglas, T. (2010) Biomimetic synthesis of photoactive alpha-Fe2O3 templated by the hyperthermophilic ferritin from Pyrococus furiosus. *Journal of Materials Chemistry 20*, 65-67.

(9) Lucon, J., Abedin, M. J., Uchida, M., Liepold, L., Jolley, C. C., Young, M., and Douglas, T. (2010) A click chemistry based coordination polymer inside small heat shock protein. *Chemical Communications 46*, 264-266.

(10) O'Neil, A., Reichhardt, C. R., Uchida, M., Prevelige, P. E., and Douglas, T. (2011) Programmed Encapsulation of Gene Products within the P22 Capsid. *Angewandte Chemie 50, 7425-7428.*

(11) Reichhardt, C. R., O'Neil, A., Uchida, M., Prevelige, P. E., and Douglas, T. (2011) Supramolceular Viral Architectures: Templates for Core Shell Iron Oxide Nanoparticle Synthesis. *Chem Commun 47, 6326-6328.*

(12) Jolley, C. C., Klem, M. T., Harrington, R., Parise, J. B., and Douglas, T. (2011) Structure and photoactivity of a virus capsid-TiO2 nanocomposite. *Nanoscale*, 3, 1004 – 1007.

Program Title: Modular Designed Protein Constructions for Solar Generated H_2 from Water

Principle Investigator: P. Leslie Dutton
Mailing address: Johnson Research Foundation, Department of Biochemistry and Biophysics, University of Pennsylvania, Philadelphia, PA
E-mail: dutton@mail.med.upenn.edu

Program Scope:

Overall research aims:
Abundance of solar power has turned attention toward engineering and constructing molecular devices that convert sunlight energy into stored chemical energy useful to mankind. This grant aims to engineer and construct from-scratch novel protein molecules equipped with light-absorbing pigments and redox cofactors organized to promote efficient light-driven splitting of water and catalyze the generation of hydrogen for fuel. The longer-term plans extend to the design of alternative reductive catalytic sites for reduction of carbon dioxide and nitrogen for fuels and valuable chemical resources.

Focus on the October Biomaterials Meeting presentation:
Progress toward creation of molecular systems that harvest sunlight for the generation of renewable fuels and green chemical resources has been hindered by the absence of a clear set of generally applicable guidelines for design, engineering and assembly. While biological photosystems continue to play important roles for inspiration and mimicry, they do not illustrate what are the most efficient designs for photochemical energy conversion. Here we use our principles of electron tunneling to create blueprints that demonstrate that photochemical efficiencies observed in existing natural photosynthetic reaction center proteins and their synthetic photochemical mimics can be dramatically improved in simple cofactor triads of electron donor, photoactive pigment and electron acceptor with prescribed inter-cofactor distances and selected relative redox potentials. Effective preservation of the absorbed photon energy in the redox energy of long-lasting charge-separated states by triads supported by the framework of simple protein constructions will facilitate the development of broad range of catalytic reactions.

Recent Progress:

Analytical treatment of photochemical charge separation in molecular systems:

At the time of writing, this comprehensive analytical treatment is completed for submission to Nature (1). The analysis we describe is made possible by application of our empirical electron tunneling expressions (7, 8), which have recently received further support (9) and prove applicable at the threshold of redox enzyme catalysis (2). The results are germane to all molecular photochemical systems and so include natural photosynthesis and designed protein reproductions and the many synthetic molecules that comprise a photo-pigment (P) and associated electron donor (D) and/or acceptors (A). To our knowledge no such analysis of this universal process has been undertaken.

Figure 1 shows an example of here a DPA triad, subjected to analytical treatment for optimized light-energy conversion efficiency (percentage free-energy between D and A retained versus energy of the activating photon) and lifetime of the charge-separated state. We consider the effect of varying photo-pigment and relevant tunneling parameters with the exception of the generic nuclear vibrational frequency (560 cm^{-1}).

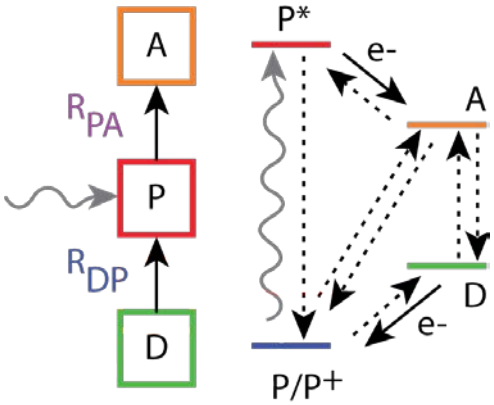

Figure 1. An example of the linear geometry of a triad of cofactors: electron donor, photo-pigment and acceptor. 8 electron-tunneling rates and one radiative decay rate (arrows) determine the time evolution of triad after light- induced formation of the excited state (dotted steps contribute to inefficiency

The main conclusions are briefly summarized:

1. Efficiency: The energetic efficiency of natural photosystems and existing synthetic dyads, triads, tetrads and beyond are far surpassed by optimized simple linear triads. With the right design, triad efficiency is sufficient to make possible the use of a *single* near-infrared 680nm photon for water splitting and H_2 production. This contrasts with green plants that use two 680/700nm photo-systems (PSII and PSI) operating in tandem for similar products.

2. Time: High efficiencies of the kind required for one-step water splitting are maintained for charge-separation lifetimes typical of natural photosynthetic rates. Slower catalysis that need longer charge separated lifetimes can be accommodated in larger intercofactor distances especially between P and D. Indeed triads can be designed with charge separation lifetimes that extend to hours with only modest loss of efficiency, good for difficult catalysis and even poor catalysis encountered during development.

3. Tolerances: In most time ranges, optimal triad designs maintain efficiency even when intercofactor distances are varied over several Å; on the other hand free energies are more constrained.

4. Size: Optimized triads are a significant improvement over dyads, but extending the chain to tetrads adds little. Dyads, triads and tetrads linked by covalent bridges that offer a lower tunneling barrier facilitate faster inter-cofactor electron tunneling. But because forward and back electron transfer is speeded up similarly, bridges offer no performance advantage and require that bridged molecules must be larger to compensate.

<u>Blueprints for protein maquettes equipped for binding cofactor triads:</u>

Synthetic protein maquettes provide an adaptable scaffold to accommodate high efficiency triads. Inter-cofactor distances prescribed in triad blueprints to support high efficiency multi-electron catalysis in the milliseconds or longer time-domain are larger than evident in most natural proteins and extend beyond our first generations of synthetic protein maquettes. The longer maquette example shown in Figure 2 is designed to be half as long again as current maquettes to accommodate triads separated sufficiently to generate hour-long charge separations while still maintain 30% efficiency even with non-optimal cofactor redox properties. These larger proteins have now been demonstrated to be expressible in *E. coli*.

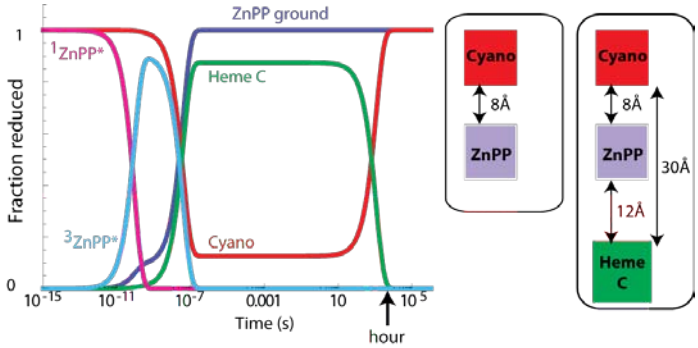

EIWKQHEDALQKFEEAHNQFEDNLQKLFEDALQKGGSGSGSGG
ECIACHEDALQKFEEALNQFEDNLQKLFEDALQKGGSGSGSGG
EIWKQHEDALQKFEEAANQFEDNLQKLFEDAKQLGGSGSGSGG
EIWKQHEDALQKFEEALNQFEDNLQKLFEDAKQL

Figure 2. An example of an extended maquette framework for a triad with D and A separated by 30Å. The overall length dimension of this 4-α-helix bundle accommodating a triad is 60Å verses the 40Å typical of maquettes made to date; shown to its left

The sequence for the long 4-α-helix bundle include a CXXCH pattern for heme C insertion, a single His site for ZnPPIX insertion and a bis-His site for cyanoheme insertion. In the left is a kinetic analysis of the long bundle which demonstrates that a lifetime of the charge separation on the hour timescale.

Covalent cofactor development for selected binding triads:

The long maquette shown in Figure 2 has already been expressed, although the yield of in vivo insertion of covalently linked heme C content is low. We have since overcome the issue of low heme C content in shorter maquettes (Anderson et al unpublished). In these maquettes, expressed heme C allows the HF treatment to replace the Fe with Zn (Kodali et al unpublished) to turn an otherwise strictly electron transfer active Donor or Acceptor into a photoactive P (center row of Figure 3). Other Fe- and Zn-porphyrins have been successfully synthesized by Tatiana Esipova under the guidance of collaborator Sergei Vinogradov. The one shown at the bottom left of Figure 3 is in the first set of greatly simplified porphyrins designed to bind to either bis-histidine (with Fe) or mono-histidine (with Zn) sites within the maquette bundle. The polar Newkome attachments prevent aggregation during the minutes required for binding.

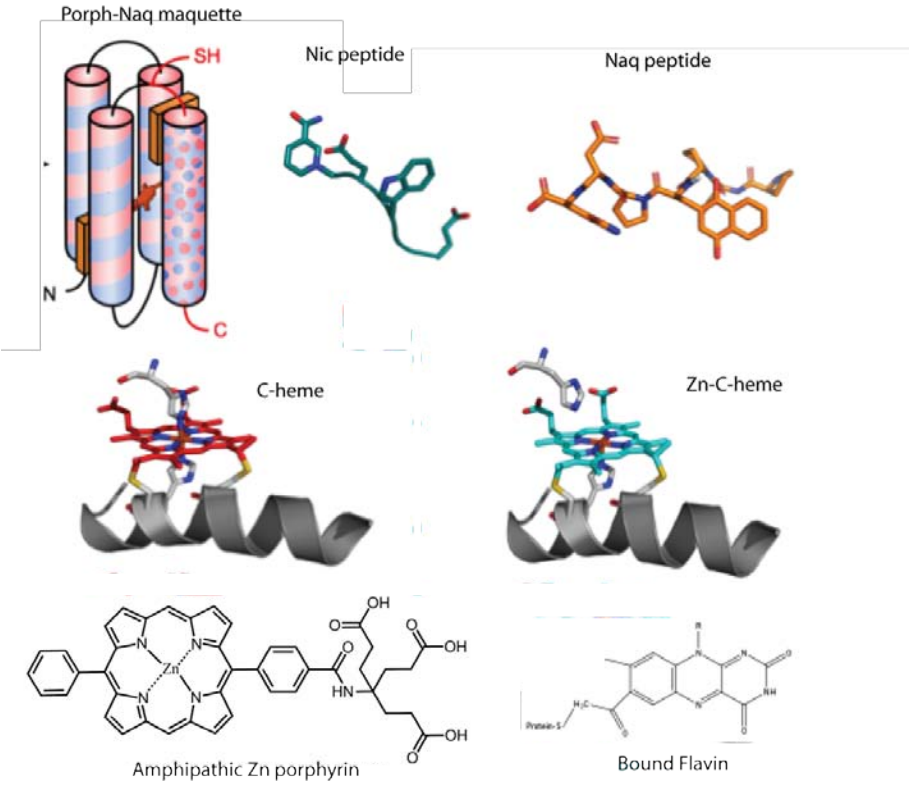

Figure 3 also shows completed work on two electron cofactors for covalent links to triad designs extending the range of redox midpoint potentials and accumulating oxidants and reductants for catalysis. The top left shows a naphthaquinone amino acid (6; top right) as part of a triad in the hydrophobic interior (see 4) of a maquette. Top center is a nicotinamide amino acid that had the redox and spectral properties of $NADH/NAD^{+}$. Covalently bound flavin is shown at the bottom right chains.

Future Plans

Maquette scaffolds

It is our intent to develop as robust and adaptable a work-horse maquette framework as possible to support light-activated charge separation. Testing of the blueprint prescriptions will take place within this robust framework. Cofactors equipped for covalent attachment will aid high fidelity assembly of triads in specified locations in maquettes. Synthetic Zn porphyrins will be modified to both raise (0.8 -1.3 V) and lower (0.4 - 0.8 V) the redox potential range of P/P* and P/P+ energies. A similar effort is being applied to several flavin cofactors.

Redox catalytic sites

Maquettes supporting light-activated charge separation at high efficiency with selected lifetimes are critical steppingstones to catalytic site design. We have designed a long maquette to group carboxylic amino acids with a view to promote light-driven assembly of oxy-metal clusters, as seen in natural PSII and pioneered with the bacterioferritin variant (5). Our intent is to explore the catalytic properties of these oxidative clusters and take steps towards oxygen evolution. At the reducing side our plans include work with collaborator John Golbeck to tether hydrogenase and other reductases to our maquettes in a fashion similar to that successful with natural PSI.

References over the past two years that acknowledge DOE support

1. Molecular Blueprints for Photochemical Energy Conversion. Moser, C.C., Zhao Z, & Dutton, P.L. ***Nature,*** to be submitted September 2011

2. Guidelines for tunneling in enzymes. Moser, C.C., Anderson, J.L.R. & Dutton, P.L. ***Biochimica et Biophysica Acta-Bioenergetics*** **1797**, 1573-1586 (2010).

3. The Measured and Calculated Affinity of Methyl and Methoxy Substituted Benzoquinones for the QA Site of Bacterial Reaction Centers. Zheng, Z., Dutton, P. L. and Gunner, M. ***Protein-Structure-Function and Bioinformatics*** **78 2638-2654 2010**.

4. Design and Engineering of an O_2 Transport Protein. Koder, R.L., Anderson, J.L.R, Solomon, L.A. Reddy, K.S., Moser, C.C. and Dutton, P.L., ***Nature,*** 458, 305-309, 2009

5. Photo-catalytic Oxidation of a Di-nuclear Manganese Centre **in an E**ngineered Bacterioferritin 'Reaction Centre'. Conlan, B., Cox, N., Su, J., Hillier, W., Messinger, J., Lubitz, W., Dutton, P.L., and Wydrzynski, T. ***Biochimica et Biophysica Acta-Bioenergetics,*** **1787,** 1112-1121, 2009

6. Reversible Proton Coupled Electron Transfer in a Peptide-incorporated Naphthoquinone Amino Acid. Lichtenstein, B.R., Cerda, J.F., Koder, R.L., and Dutton, P.L. ***Chemical Communication,*** **170**, 168-170, 2009.

Other references

7. Moser, C.C., Keske, J.M., Warncke, K., Farid, R.S. & Dutton, P.L. Nature of Biological Electron-Transfer. ***Nature*** **355**, 796-802 (1992).

8. Page, C.C., Moser, C.C., Chen, X.X. & Dutton, P.L. Natural engineering principles of electron tunnelling in biological oxidation-reduction. ***Nature*** **402**, 47-52 (1999).

9. Moser, C.C., Chobot, S.E., Page, C.C. & Dutton, P.L. Distance metrics for heme protein electron tunneling. ***Biochimica et Biophysica Acta-Bioenergetics*** **1777**, 1032-1037 (2008).

Program Title: Directed assembly of hybrid nanostructures using optically resonant nanotweezers

Principle Investigator: David Erickson
Mailing Address: Sibley School of Mechanical Engineering, Cornell University, Ithaca, NY, 14853
E-mail: de54@cornell.edu

Program Scope

In this research I propose to perform a comprehensive theoretical and experimental investigation into the assembly of hybrid nanomaterials and nanostructures using nanophotonically directed optical forces. Recently [1, 2] we have demonstrated how the electromagnetic fields in nanophotonic devices are sufficiently strong that they can be used to physically manipulate biological (nucleic acids & proteins) and non-biological (nanoparticles) materials as small as a few nanometers in size. In fact **we demonstrate the manipulation of the smallest dielectric matter ever** (beating our previous record published earlier this year in Nature [1]).

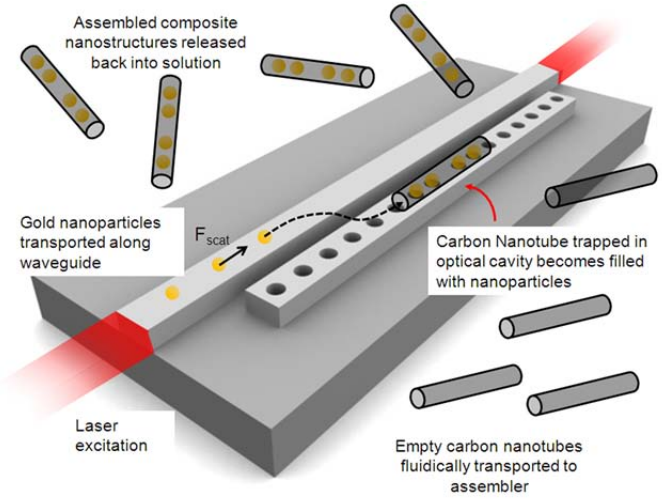

Figure 1: Envisioned Optically Driven Nano-Factories. The ultimate goal of this proposal is to demonstrate the assembly of hybrid nanostructures. Image shows envisioned technique for assembling gold nanoparticles inside a carbon nanotube in an optically resonant trap.

The overarching goal of this work will be to extend this technique to enable the directed assembly of hybrid nanostructures which cannot be manufactured by other means (*e.g.* self-assembly or chemical synthesis). Although we focus our work here on understanding some of the fundamental physics behind this new approach, we envision the ultimate implementation of the technique to look something like the optical nanofactory shown in Figure 1. The image shows how we would eventually use an optically resonant nanotweezer [3] to thread gold nanoparticles inside a single carbon nanotube**.** We envision that structures created with this technique could yield unique high efficiency photo-electric or photo-thermal energy conversion devices and enable more precise studies of the fundamental structure of nanomaterials.

Recent Progress

(1) Demonstration of trapping of nanoparticles, proteins, and other nanoscopic materials.

Our major accomplishment in this project year has been the demonstration of the ability to reversibly trap and directly handle semiconductor quantum dots and individual proteins between 5nm and 10nm in diameter. This is a 10 fold improvement over our previous results [4] (which was 48nm diameter polystyrene spheres) and is, to our knowledge, the smallest

material ever trapped optically. Sample results for quantum dots are shown in Figure 2. This achievement in pushing the trapped size limit to truly nanoscopic and complex materials is a key step towards our goal of demonstrating directed assembly of energetically relevant materials as described in the program scope.

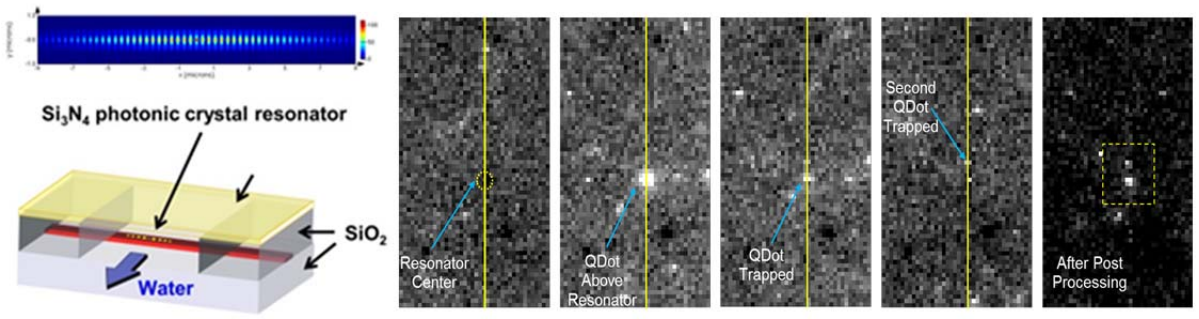

Figure 2: Left Image – Simulation results showing electric field in resonator and diagram showing microfluidic experiment. **Right image** – Demonstration of quantum dot trapping using silicon nitride resonators.

The major technical advancement that led to this breakthrough was the redesign of our trapping devices to use a silicon nitride photonic crystal resonator operating at a wavelength of 1064 nm rather than the standard silicon resonators operating at 1550nm that we used before. Through extensive numerical simulation, we optimized our new devices and showed that using silicon nitride we can tightly confine the electric field to provide trapping stiffness needed for trapping the nanomaterials mentioned above. As we describe in the next section, although our devices were better designed, we believe that this major reason for the improvement is due to the much reduced thermal heating in our device compared to the earlier silicon-based devices. A manuscript is currently being prepared to report these results ***[DOE Paper #1]***.

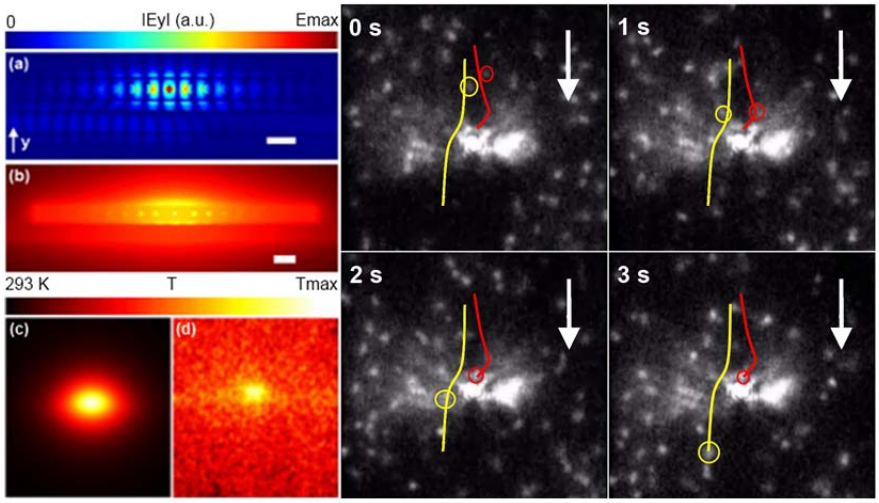

Figure 3: Left image – Theoretical and Experimental results measuring the temperature rise around a silicon photonic crystal resonator. **Right image** – Result deflection and repulsion of DNA from the thermal hotspot resulting from localized thermophoresis.

(2) Examining the coupling between heat generation and transport near optical resonators. In addition to the experimental demonstrations above, we have also performed a comprehensive study on the heat generated from silicon optically resonant nanotweezer operating at a wavelength of 1.5μm (as opposed to the silicon nitride resonators operating at 1μm wavelength described above) and its impact on molecular transport in the vicinity of the resonator. As can be seen in Figure 3 (left image), temperature rises as high as 57K for 10mW of input power were recorded, which were consistent with theoretical predictions. The optical trapping and biomolecular sensing properties of these devices were shown to be strongly affected by the resulting combination of buoyancy driven flow and thermophoresis. As shown in the right image of Figure 3, the region around the electromagnetic hotspot is depleted in biomolecules because of a high free energy barrier. The results of this work, which is currently under review ***[DOE paper #2]***, will provide guidance to the thermal design of optical nanomanipulators but could significantly impact the design of molecular sensors use silicon photonic technology.

Figure 4: Cover for comprehensive review article on nanoscale optical trapping techniques.

(3) Comprehensive Review. With DOE support, in March of this year we published a comprehensive review on "Nanomanipulation using Near Field Photonics" ***[DOE Paper #3]***. This review is the first to cover the subject of this research, expands on the advantages, and describes many of the envisioned potential applications. An image of the cover is shown in Figure 4. It is hoped that this review will draw more attention to the field.

Optofluidics

Figure 5: Logo for start-up company formed to exploit nanotweezer technology.

(4) Formation of a start-up Company to exploit the technology. In January 2011 we formed a start-up company called Optofluidics, Inc. (Figure 5) whose focus is to exploit the nanotweezer technology advanced by this grant. The company currently employs 4 people (including 2 full time Ph.D.'s) in the Philadelphia, PA area. The first product from the company will be a scientific instrument based around the technology. Further information is available at http://www.optofluidicscorp.com.

Future Plans

Over the course of the next year we will focus on three tasks. The first will be to continue to push the limits of size and material complexity, attempting to trap smaller quantum dots and

molecules (hopefully reaching the 2-3nm limit) and carbon nanotubes. The second task will be to begin to work towards the creation of small assemblies. This will first occur at relatively large scales (approximately 100nm particles) and we will move towards smaller materials in the following years. The third task will be to continue to develop the theory and apply it to more complex materials and alternate solutions (in particular heavy water).

References (which acknowledge DOE support)

DOE #1 – Chen, Y-F., Serey, X., Erickson, D., "Optical manipulation of nanoparticles and biomolecules using silicon nitride photonic crystal resonators" (in preparation).

DOE #2 – Serey, X., Mandal, S., Chen, Y-F., Erickson, D., "DNA Delivery and Transport in Thermal gradients near optofluidic resonators" (under review).

DOE #3 - Erickson, D., Serey, X., Chen, Y.-F., Mandal, S., "Review: Nanomanipulation using Near Field Photonics" Lab-on-a-Chip, 11, 995-1009 (2011)

Other References

1. Yang, A.H.J., Moore, S.D., Schmidt, B.S., Klug, M., Lipson, M., and Erickson, D., *Optical manipulation of nanoparticles and biomolecules in sub-wavelength slot waveguides.* Nature, 2009. 457(7225): p. 71-75.
2. Yang, A.H.J., Lerdsuchatawanich, T., and Erickson, D., *Forces and Transport Velocities for a Particle in a Slot Waveguide.* Nano Letters, 2009. 9(3): p. 1182-1188.
3. Mandal, S. and Erickson, D., *Nanoscale optofluidic sensor arrays.* Optics Express, 2008. 16(3): p. 1623-1631.
4. Mandal, S., Serey, X., and Erickson, D., *Nanomanipulation Using Silicon Photonic Crystal Resonators.* Nano Letters, 2010. 10(1): p. 99-104.

Program Title: Material Lessons from Biology: Structure-function studies of protein sequences Involved in inorganic - organic composite material formation.

Principle Investigator: John Spencer Evans

Mailing Address: New York University
Laboratory for Chemical Physics
345 E. 24th Street, New York, NY 10010

E-mail: jse1@nyu.edu

Program Scope

The mollusk shell is a materials Valhalla, a self-repairing composite that combines fracture resistance (inner nacre layer, aragonite) with crack propagation-resistance (outer prismatic layer, calcite). Our DOE research program is focused on the structure-function relationships of nacre proteins that participate in polymorph selection and fracture resistance material properties of the mollusk shell. The goal of this research is to elucidate the mechanisms by which proteins nucleate aragonite and become occluded within it. This data will then translate to the laboratory frame in ways that will benefit the mission of BES: development of novel polymers or proteins for composite construction; routes for single crystal synthesis from amorphous precursors; material remodeling/repair, and selection of crystalline polymorphs for specific applications.

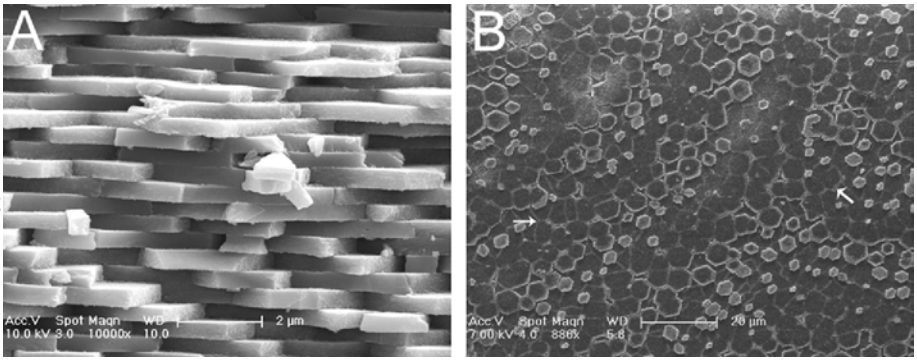

Figure 1: (A) SEM image of nacre layer cross-section, showing lamellar structure. (B) SEM image of lamellae, showing aragonite tablets. Taken from reference 1.

To achieve these goals, we have investigated the structure-function relationships of proteins associated with the nacre layer of the mollusk shell (**Figure 1**). There are two sets of proteins: framework, which are associated with the Lustrin/beta chitin / silk-fibroin insoluble layers which not only nucleate aragonite but also surround and create a elastic, deformable coating around each aragonite tablet,[1-6] and, intracrystalline, which nucleate aragonite and become occluded within the tablets themselves and convey fracture-resistance to these single crystals.[17,8] We initially utilized peptide models based upon important sequence regions of nacre proteins such as intracrystalline AP7[7] and PMFG1,[8] as well as the framework protein n16,[2-6] to determine protein sequence requirements for inhibiting calcite crystal growth and promoting aragonite nucleation. With advances in recombinant protein technology and chemical synthesis, we have now graduated to studies involving full length proteins themselves. Combining these datasets, we have established common molecular requirements for aragonite polymorph selection, namely, that polymorph selection requires the formation of protein supramolecular assemblies which control aragonite synthesis within small volume environments.[2-8]

Recent Progress

The Framework Story. We have created a recombinant version of n16.3, a 108 AA nacre framework protein of the Japanese pearl oyster (*Pinctada fucata*) that is associated with beta-chitin and Pif proteins.[2] In the lab n16.3 forms unusual single-crystal aragonite that is textured and layered in appearance (**Figure 2**). This layered aragonite results from the formation of n16 films which assemble and nucleate aragonite in an interleaved fashion.[6]

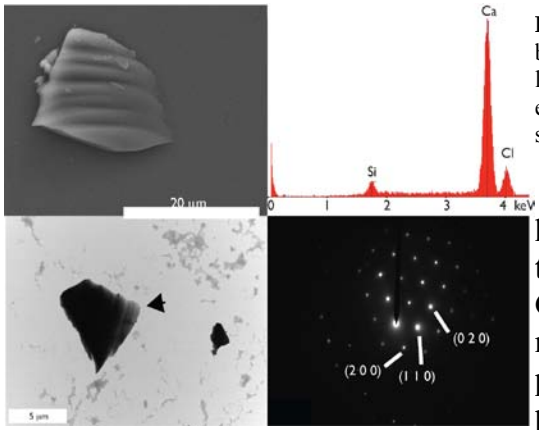

Figure 2: TOP LEFT: Layered single crystal aragonite deposit formed by n16.3; TOP RIGHT: EDS spectra of crystal, showing that it is mineralized; LOWER LEFT: TEM image of similar crystal; LOWER RIGHT: electron diffraction spot pattern obtained from TEM crystal, indexed to single crystal aragonite.

The reason why n16.3 forms nucleating films has to do with the molecular characteristics of this protein. Using sidechain electrostatic interactions (Asp, Glu COO^- with His+, Arg+, Lys+), this protein spontaneously oligomerizes under physiologic conditions and protein particle sizes are enhanced when Ca (II) is present (**Figure 3**). This oligomerization leads to the creation of spheroidal-fibril sub-assemblies that can further assemble into protein films. The driving force for assembly is the intrinsic disorder parameter of the n16.3 sequence, which contains disorder-promoting residues that generate a protein molecule that is 50% random coil, 20% beta strand, 8% alpha helix.[2] This protein undergoes a disorder-to-order transformation when high Ca (II) levels are present, and this transformation may play a role in nacre organic layer assembly and/or aragonite synthesis. The major region responsible for aragonite synthesis and oligomerization appears to be within the 1-30 AA N-terminal domain of n16.3 (n16N).[3-6] This domain also recognizes and binds to beta-chitin polysaccharide, one of the nacre components that surrounds single crystal aragonite tablets.[4,5] We intend to continue our characterization of n16.3 to determine how it assists in aragonite polymorph selection.

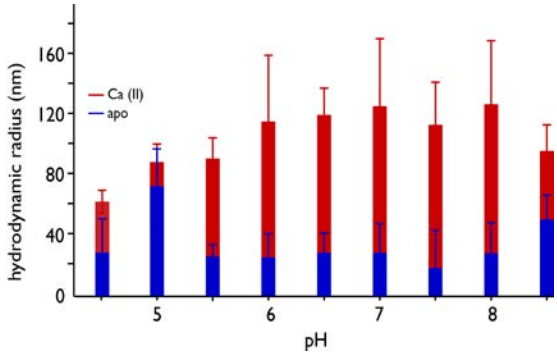

Figure 3: Dynamic light scattering study of n16.3 as a function of pH, demonstrating the oligomerization of this protein over a wide pH range (blue) and in the presence of Ca (II) (red).

The Intracrystalline story. Chemical synthesis has allowed us to recreate the 66 AA AP7 intracrystalline protein that is associated with the nacre layer of the Pacific red abalone, *Haliotis rufescens*.[7] This protein is one of several EDTA soluble proteins that are occluded within aragonite crystals in the nacre layer. This protein is intrinsically disordered and contains residual structure (beta turn, alpha-helix) within the 36 AA C-terminal region (AP7C). The C-terminal region is also noted for its partial homology to the Zn (II) finger C-RING domains that are found in intracellular proteins that form cytoplasmic complexes.[7]

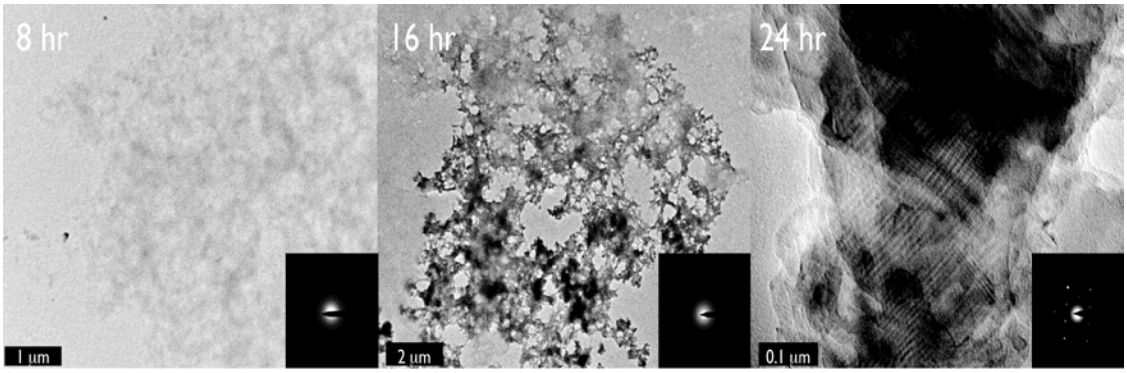

Figure 4: Timeline of AP7 supramolecular assembly formation (TEM) in mineralization assays. At 8 hrs, non-mineralized amorphous AP7 protein assemblies are observed. At 16 hrs, these assemblies develop amorphous-appearing mineral deposits. At 24 hrs, these assemblies have developed single crystal aragonite plates that are semi-organized within the assemblies.[7]

AP7 spontaneously self-assembles in solution to form amorphous-appearing aggregates that form layered single crystal aragonite within the assemblies (**Figure 4**). Like the framework protein family, the intracrystalline AP7 utilizes sidechain electrostatic interactions to stabilize protein oligomers. We found that the C-terminal domain of AP7 also oligomerizes to the same extent that AP7 does, and, nucleates aragonite. This indicates that the C-RING domain of AP7 is largely responsible for oligomeric and polymorph selection activities of AP7.[7]

Figure 5: 4-nitrophenyl acetate hydrolysis assay results obtained for AP7 and other proteins (BSA = bovine serum albumin, Asprich 3 = *A. rigidia* prismatic calcite protein.

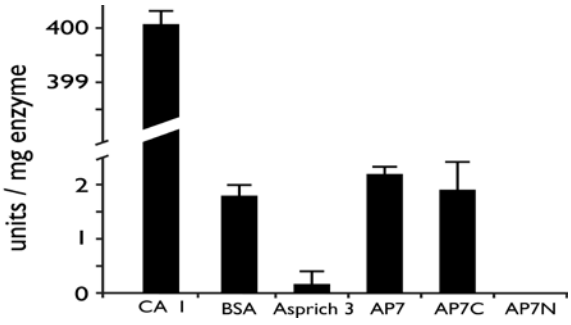

But how does AP7 nucleate aragonite? The key may be that the AP7 protein possesses hydrolytic capabilities that regulate pH, carbonate and/or bicarbonate levels in solution, which would control crystal growth kinetics. Pilot experiments using ester hydrolysis assays indicate that AP7, and its C-RING domain, possess residual hydrolysis activity compared to carbonic anhydrase (CA)(**Figure 5)**.[7] We intend to explore this residual activity further and determine if it has any impact on aragonite nucleation.

Future Plans

(A) We intend to construct a "mini-seashell" system using beta-chitin, silk-fibroin gel protein, AP7, and n16.3. This approach will allow us to examine the kinetics of polymorph formation, the participation of ACC or vaterite as precursor and intermediate phases, respectively, and form fracture-resistant composite crystals that contain occluded proteins.

(B) We will determine the three-dimensional structure of n16.3 in solution and determine which regions are responsible for aragonite formation and beta-chitin interactions. We will also develop site-specific mutants of n16.3 to determine the role of catalytic His and Arg residues in aragonite formation.

(C) Histidine is a catalytic residue found in many enzymes and within several nacre proteins. We will identify the participation of His in mineralization using AP7 and n16.3 proteins possessing His deletions.

(D) Via our collaborations with Helmut Colfen, University of Konstanz, and Fiona Meldrum, University of Leeds, UK, we will investigate the early steps in nucleation and determine if AP7 and n16.3 participate in pre-nucleation cluster assembly or during post-nucleation events as part of the mechanism of aragonite formation.

(E) Using indentation force microscopy, we will determine if protein-occluded aragonite crystals produced by n16.3 and AP7 have developed fracture-resistance relative to unoccluded aragonite.

Other References

1) Gong, N., Shangguan, J., Liu, X., Yan, Z., Maa, Z., Xie, L., Zhang, R. (2008) Immunolocalization of matrix proteins in nacre lamellae and their in vivo effects on aragonitic tablet growth. *J. Struct. Biol.* **164**, 33-40.

Publications which acknowledge DOE support

2) Ponce, C.B., Evans, J.S. (2011) Polymorph crystal selection by n16, an intrinsically disordered nacre framework protein. *Crystal Growth and Design*, submitted.

3) Amos, F.F., Ponce, C.B., Evans, J.S. (2011) Formation of framework nacre polypeptide supramolecular assemblies that nucleate polymorphs. *Biomacromolecules* **12**, 1883-1889.

4) Keene, E.C., Evans, J.S., Estroff, L.A. (2010) Silk fibroin hydrogels coupled with the n16N - beta-chitin complex: An in vitro organic matrix for controlling calcium carbonate mineralization. *Crystal Growth and Design* **10**, 5169-5175.

5) Keene, E.C., Evans, J.S., Estroff, L.A. (2010) Matrix interactions in biomineralization: Aragonite nucleation by an intrinsically disordered nacre polypeptide, n16N, associated with a β-chitin substrate. *Crystal Growth and Design* **10**, 1383-1389.

6) Metzler, R.A., Evans, J.S., Kilian, C.E., Zhou, D., Churchill, T.H., Appathurai, P.,N. Coppersmith, S.N., Gilbert, P.U.P.A. (2010) Lamellar self-assembly and aragonite polymorph selection by a single intrinsically disordered protein fragment. *JACS* **132**, 6329-6334.

7) Amos, F.F., Ponce, C.B., Evans, J.S., (2011) A C-RING-like domain participates in protein self-assembly and mineral nucleation. *Biochemistry*, submitted.

8) Amos, F.F., Destine, E., Ponce, C.B., Evans, J.S. (2010) The N- and C-terminal regions of the pearl-associated EF Hand protein, PFMG1, promote the formation of the aragonite polymorph in vitro. *Crystal Growth and Design* **10**, 4211-4216.

RNA-Mediated Evolution of Catalysts for the Production and Utilization of Alternative Fuels

Dan Feldheim*, Bruce Eaton, Jessica Rouge, Bryan Tienes, Alina Owczarek
Department of Chemistry and Biochemistry
University of Colorado
Boulder, CO 80309
303-492-7907
Daniel.Feldheim@Colorado.edu

Program Scope

We are developing new methods for the discovery of catalyst materials for use in the production and utilization of alternative fuels. The central premise of the project is that biological macromolecules can evolve in response to selection pressures to synthesize materials with desired catalytic activities. The biological macromolecule used in the project is RNA, and RNA containing key chemical modifications that enhance its catalytic activity. Through a process known as RNA in vitro selection, we have shown that RNA sequences can evolve to mediate the formation of new materials. Our primary objective is to apply these methods to the discovery of materials for H_2 production and oxidation and the conversion of CO_2 to hydrocarbon fuels.

RNA in vitro selection as a materials discovery tool. The extraordinary materials found in our biosphere have inspired a growing research effort in which biomolecules are used to synthesize and assemble materials in the laboratory. Peptides, nucleotides, RNA, DNA, and proteins have all been shown to be capable of mediating the formation of nanoscale materials with atypical morphologies, crystal structures, and sizes that have resulted in some instances in unexpected properties. In addition to potentially affording more environmentally benign routes to novel inorganic materials, the highly selective recognition capabilities of biomolecules are proving to be useful in the assembly of nanoscale materials into more complex functional assemblies and devices.

The central premise of this project is that biological macromolecules can evolve in vitro in response to selection pressures to synthesize materials with desired catalytic activities. Prior results from our labs have shown that RNA has the ability to mediate the formation of a variety of inorganic nanoparticles and control nanoparticle size, shape, and physical properties. Our recent work has focused on understanding how the selected sequences function and developing new methods for harnessing the power of biomolecule evolution in the search for novel photocatalyst systems.

RNA In Vitro Selection in Materials Discovery. The RNA in vitro evolution approach to catalyst discovery begins by synthesizing a library of 10^{14} unique RNA sequences (Figure 1). We are not limited to the native RNA bases when generating the RNA library because the Eaton lab has developed novel methods for modifying uridine with >30 different functional groups. When incorporated into RNA these moieties can aid in the formation of inorganic materials. The RNA library is then exposed to an array of different solutions

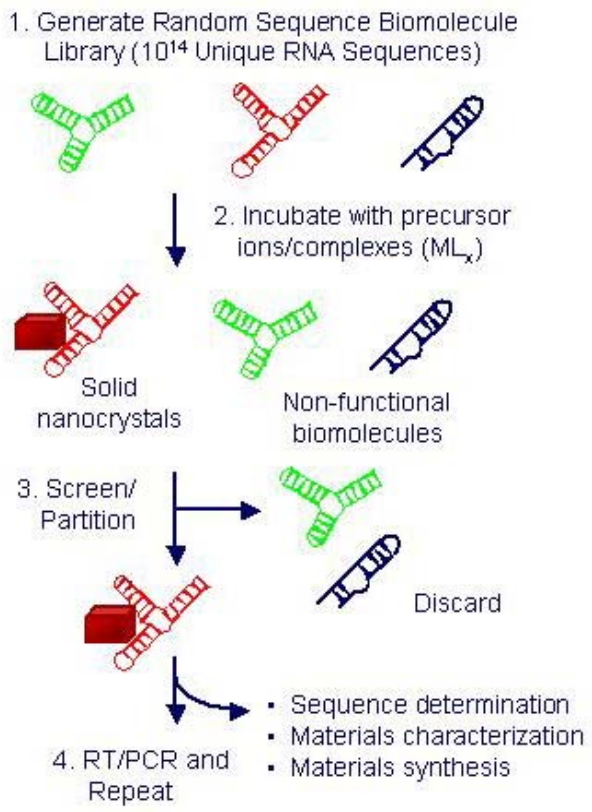

Figure 1. The RNA in vitro selection cycle for discovering new materials.

containing inorganic precursors (e.g., metal salts and organometallic complexes), resulting in nucleation and inorganic cluster growth on the functional RNA sequences. However, because each RNA sequence in the initial mixture differs in primary sequence and 3D structure, many different inorganic crystal types are possible. In fact, our expectation is that different sequences will mediate the formation of nanocrystals that differ in size, shape, or physical properties; of course many of the initial 10^{14} RNA sequences will also be incapable of nucleating a crystal. A separation is then performed to isolate the desired particles. For example, in "selection cycle 1" RNA sequences not bound to a crystal are easily removed by centrifugation. These sequences are said to be "selected" out; that is, only those sequences that grow crystals survive and are carried forward to the second cycle. The RNA that is carried forward may constitute a minor fraction of the overall sample. However, it can be reverse transcribed into cDNA, amplified using the polymerase chain reaction (PCR), and converted back into RNA for the next cycle. In subsequent cycles, more stringent selection pressures may be imposed. It may be possible to select for RNA that grows crystals possessing a certain catalytic, electronic, photophysical, magnetic, etc. property. After several cycles (typically around 10), the initial RNA pool of 10^{14} sequences is narrowed to a much smaller pool (hundreds) containing families of sequences that grow nanoparticles with the desired property.

Recent Progress

RNA in vitro selections have now been performed in our labs to discover unique sequences that can mediate the growth of Pt, Pd, and iron oxide nanoparticles. In studying individual sequences that emerged from these selections we have observed sequence-dependent control over particle size, shape, and composition. In the past year we also made the surprising discovery that the crystallinity of nanoparticles formed from solutions containing RNA depends upon the presence of sequence mixtures. That is, a single sequence selected from the original random RNA sequence library produced very poorly crystalline Pd nanoparticles, while a combination of sequences that emerged from the selection yielded crystalline nanoparticles. To our knowledge this is the first example in which two biomolecules (RNA, DNA, or peptides) selected *in vitro* work together to provide a unique chemical outcome.

Our work to date has shown that RNA sequences can be isolated from large random sequence libraries that mediate the formation of metal nanoparticles with sizes, shapes, and crystal structures that appear to depend upon RNA primary sequence and secondary structure. It was then of interest to determine if RNA in vitro selection could be exploited to synthesize nanoparticles with a desired facet exposed at the surface. Our motivation for this aim is that nearly all metal nanoparticles, regardless of shape, are bound by facets with high coordination numbers and thus are likely not the most catalytically active surfaces. Unfortunately, there is no way currently to predict how one might arrive at a nanoparticle enclosed by high-index, low coordination number facets.

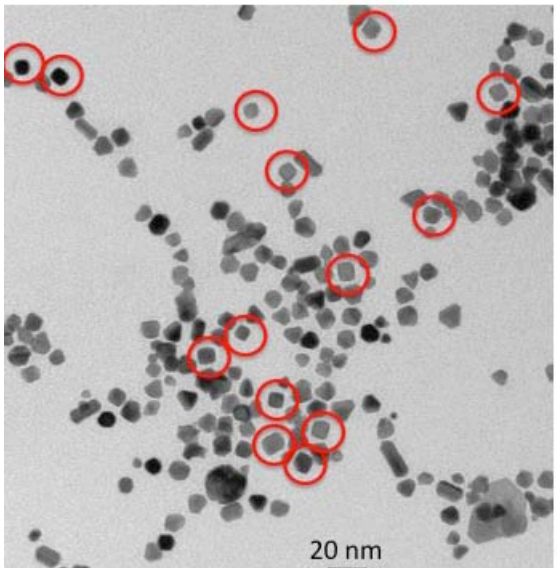

Shape	Count	%
Cube	41	17.8
Tetrahedral	43	18.7
Sphere	19	8.3
Hexagon	37	16.1
Rod	10	4.4
Other	80	34.8

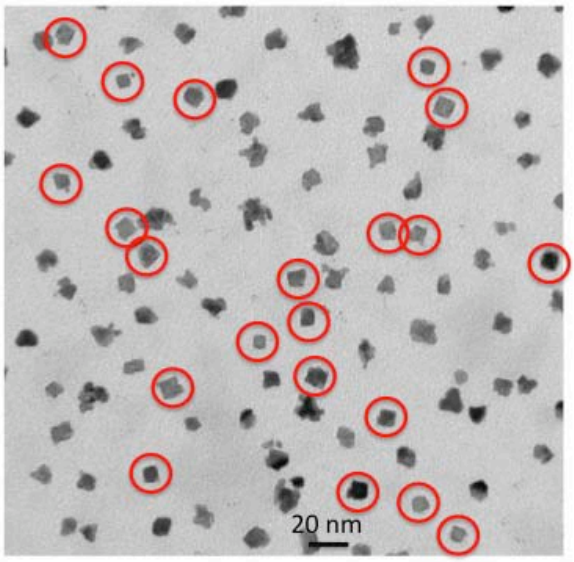

Shape	Count	%
Cube	127	44.8
Tetrahedral	15	5.4
Sphere	1	0.3
Hexagon	0	0
Rod	0	0
Other	141	49.7

Figure 2. Transmission electron microscope images of Pt nanoparticles synthesized in the absence (Top) and presence (Bottom) of RNA sequences selected to bind to a Pt (100) wafer. These preliminary results suggest that the Pt (100)-binding RNA sequences can shift the distribution of nanoparticle shapes observed to cubes, which should possess (100) facets. The true nature of the facets exposed remains to be characterized in detail.

We have thus sought to develop methods by which nanoparticles could be synthesized with any desired facet exposed.

This goal is being pursued by incubating a random sequence RNA library with a Pt wafer that was cut to expose a desired crystallographic plane on the surface. RNA sequences were expected to bind to the surface with a range of affinities and rates. The weakest binders were removed from the surface using temperature as a selection pressure, and the highest affinity binders collected and amplified. The sequences that emerged from eight cycles of binding and amplification were then used as structure-directing reagents during the synthesis of Pt nanoparticles.

Figure 2 shows the outcome of an experiment in which RNA sequences were selected to bind to a Pt (100) wafer and then used in the synthesis of Pt nanoparticles. In the absence of a selected sequence a broad distribution of shapes was observed. Nanoparticles synthesized in the presence of a selected sequence appear to have a shape distribution that was shifted to favor cubes. As cubes should possess (100) facets, these preliminary data suggest that RNA sequences selected to bind to (100) facets may be capable of preserving those facets during nanoparticle synthesis.

Future Directions

Our current work is focused predominantly on further exploring the relationships between the affinity of RNA for a certain crystal facet and the ability of that sequence to direct nanoparticles growth. RNA selections are also in progress in which an RNA library is challenged to evolve sequences capable of assembling metal precursors such as Ni into nanocluster catalysts for H_2 generation.

Publication list (including patents) acknowledging the DOE grant or contract

1. J. Rouge, B. E. Eaton, D. L. Feldheim, "Biomolecules in the Synthesis and Assembly of Materials for Energy Applications", *Energy & Environmental Science*, **2010**.
2. J. Rouge, C. J. Ackerson, B. E. Eaton, Daniel L.Feldeim "Cooperativity Between Two Selected RNA Pdases in the Synthesis of Pd Nanoparticles", *J. Mater. Chem*., **2010**, 20, 8394 - 8398.
3. C. J. Carter, A. Owczarek, D. L. Feldheim "Methods for Isolating RNA Sequences Capable of Binding to or Mediating the Formation of Inorganic Materials" Bionanotechnology Protocols, Edited by Sandra Rosenthal and David Wright, Humana Press Inc. New Jersey, in press.
4. J. D. Vaught, C. Bock, J. Carter, T. Fitzwater, M. Otis, D. Schneider, J. Rolando, S. Waugh, S. K. Wilcox, B. E. Eaton "Expanding the Chemistry of DNA for in Vitro Selection" *J. Am. Chem. Soc.* 2010, *132*, 4141–4151.

Cathode Catalysis in Hydrogen/Oxygen Fuel Cells: New Catalysts, Mechanism, and Characterization

PIs: Andrew A. Gewirth, Paul J.A. Kenis, Ralph G. Nuzzo, and Thomas B. Rauchfuss

Department of Chemistry, Department of Chemical and Biomolecular Engineering, and the Fredrick Seitz Materials Research Laboratory

University of Illinois at Urbana-Champaign, Urbana, IL 61801

Program Scope

In this project, we are engaged in a comprehensive plan of research directed at developing new catalysts and new understandings relevant to the operation of low temperature hydrogen-oxygen fuel cells. The focal point of this work is one centered on the Oxygen Reduction Reaction (ORR), the electrochemical process that most fundamentally limits the technological utility of these environmentally benign energy conversion devices. It is therefore to the single greatest challenge limiting wide-spread implementation of hydrogen-oxygen fuel cells -- providing robust low cost cathodes that efficiently reduce dioxygen to water – that we address the work described in this proposal.

Utilizing support from this project, we developed a new class of ORR catalyst, based on Cu dimers and multimers. These new materials exhibit ORR onsets at potentials higher than any other Cu-based material in neutral and basic environments and are inspired by the three-Cu active site in laccase which has the highest ORR onset potential of any material known. By directly coupling laccase to a Au electrode we showed that this three-Cu active site in laccase is especially competent for the ORR. We also used microfluidic methods to evaluate these catalysts in both the acidic and basic electrochemical environments. We have developed new XAS and microscopy based techniques with which to study the ORR, which provide insight into the ORR active site with unprecedented resolution. These techniques have helped us to develop insights into ORR reaction mechanisms on important electrocatalytic materials. In turn, these insights are providing directions to synthesize new ORR catalytic materials.

Recent Accomplishments

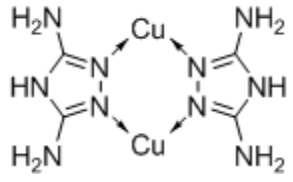

Figure 1: 3,5-diamino-1,2,4-triazole ligands bridging two copper centers. Typical Cu···Cu spacing is 3.5 Å. Counter-ions and ligated water are omitted.

New Catalysts for the Oxygen Reduction Reaction

An important accomplishment was the development of a new class of catalysts for the ORR. [2] We found that direct precipitation of an insoluble copper triazole (Figure 1) coordination complex formed from 3,5 diamino 1,2,4 triazole (DAT) onto a carbon black support leads to the formation of an efficient catalyst for the 4 e^- reduction of O_2 to H_2O . The oxygen reduction activity is reported over a wide pH range from 1 to 13 and the onset of the oxygen reduction reaction occurs at potentials as high as 0.86 V_{RHE}. This potential is the highest ever reported for a Cu complex ORR catalyst. (Figure 2) Ex-situ magnetic susceptibility

measurements confirm the presence of muti-Cu sites, since the on- electrode sample exhibits room temperature antiferromagnetic coupling which can only be explained by the presence of Cu dimer sites. A secondary outcome attendant this work was to develop a new way to entrain molecular materials on carbon electrode surfaces. We discovered that a soluble ligand and soluble metal could be stabilized on an electrode if the complex they formed was insoluble. This precipitation method enables very smooth conformal coatings of molecular catalyst on the electrode.

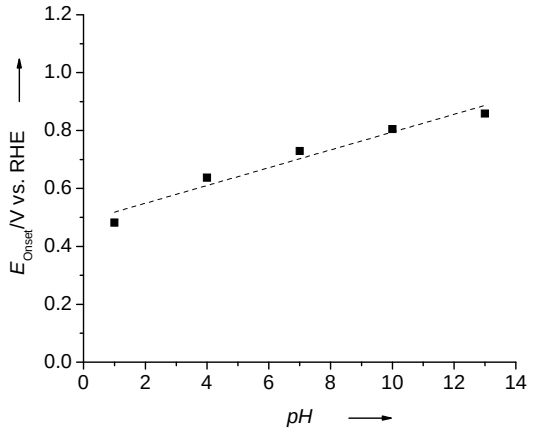

Figure 2 Potentials at which the onset of O_2 reduction occurs at electrodes modified with CuDAT in electrolytes of varying pH and a linear fit (31 ± 4 mV per pH unit slope and 0.49 ± 0.03 V *y*-intercept). Electrodes were rotated at 1600 rpm in 0.1 M $HClO_4$; 0.1 M $NaClO_4$ + 0.04 M Britton-Robinson Buffers (pH 4, 7, 10); or 0.1 N NaOH saturated with O_2. Potential scanned at 5 mV/s. Onset potential chosen as the potential at which the current density reaches -5 μA cm^{-2} which is ca. the most positive potential at which a non-zero current can be visually resolved on a full scale voltammogram.

Cu-containing ORR catalysts are a focus of work since multicoppper oxidases (exemplified by laccase) activate oxygen at a site containing 3 Cu atoms with ca. 3.5 Å spacings and exhibit remarkable ORR activity at potentials approaching 1.2 V RHE. [3,4] A Cu-containing complex entrained on an electrode surface that exhibited this level of reactivity would be highly desirable.

We also examined the effect of DAT substituents on ORR activity. We found that subtle changes in the molecular structure of the catalyst make for profound changes in reactivity. For example, both DAT and the 4-methoxybezylidene diaamino triazole exhibit four electron reduction of oxygen. However, the very similar 4-ethanone diammino triazole, which exhibiting an identical onset potential, shows only a two electron reduction.[5]The origin of this behavior is as yet unknown, although these and similar studies suggest that the degree of stabilization of water hydrogen bonded through the diamino moiety on the DAT ligand to the Cu centers may play an important role in establishing the Cu dimer active site. In particular, Cu dimer materials exhibit ORR activity, while Cu trimers, such as that found in $Cu_3(\mu_3)$-OH structures, with no open coordination site [6] are unreactive.

The focus on coordination of Cu with ligands containing N to form competent ORR catalysts possibly mimicking laccase has led to a reexamination of other such ligands. We recently examined the tris(2-pyridylmethyl)amine (TPA) ligand, recently used in a nonaqueous context for ORR, [7] and showed that this ligand, complexed with Cu, yields the most positive potential onset for the ORR in aqueous acidic solution relative to any Cu-containing complex thus far examined. [8] However, there is little understanding yet developed concerning the nature of the active site in this system.

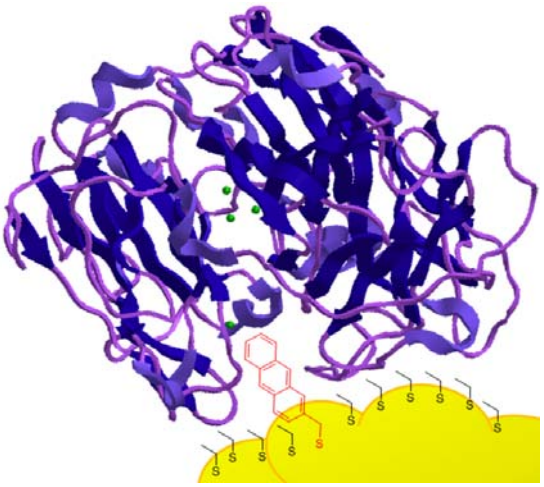

Figure 3. Schematic representation of Lc from *Trametes versicolor* properly oriented for electrocatalytic reduction of O_2 at an electrochemically roughened Au surface modified with a mixture of anthracene-2-methanethiol (AMT) and ethanethiol (ET). The AMT is shown in the hydrophobic pocket where it facilities electron transfer from the electrode surface to the T1 Cu site. After an internal electron transfer, the 4 e^- reduction of O_2 to water occurs at the T2/T3 tricopper cluster near the center of the enzyme. [1]

We also demonstrated that non precious metal catalysts, such as those from Cu DAT, from Fe pthalocyanin, and from pyrolyzed Fe pthalocyanin materials all exhibit poisoning by small molecules added to the electrolyte. In the case of CuDAT, the small molecules included azide and fluoride, molecules identical to those that poison multicopper oxidase enzymes which also perform the ORR. In the case of the Fe-containing materials, we showed that both were poisoned by CN^-, consistent with the presence of metal-centered ORR activity. [9]

The Cu DAT and related complexes are being developed as mimics for the four-Cu active site of laccase, which are highly active for the ORR. In laccase, only three of the Cu atoms form the site at which the ORR occurs, while the fourth Cu acts to transfer electrons from the site of oxidation on the other side of the protein where oxidation occurs. [10] An important question relates to the rate determining step (rds) of the ORR in laccase. In order to address this issue, we recently developed a novel method of immobilizing laccase on a Au surface, using an anthracene thiol, backfilled with a short chain thiol to allow space for the laccase to adsorb with the correct orientation on the Au surface (Figure 3). [11] The stabilized laccase enables direct electron transfer between the enzyme and the Au surface, and direct determination of the Tafel slope for the ORR process. As shown in Fig. 6, the Tafel slope is found to be 140 mV/decade, which can only be consistent with the first electron transfer between the substrate and the electron transfer associated type 1 Cu center being the rate determining step. Consequently, this implies that the 3 Cu active site is in fact kinetically competent and that the ORR occurs quickly there. A Cu-containing complex entrained on an electrode surface that exhibited this level of reactivity would be highly desirable.

Future Plans

In the future we specifically propose to undertake research that has three synergistic program elements. These are: (1) design and synthesis of new advanced solid-state and molecular cathode materials; (2) physico-spectroscopic characterization of the molecular mechanisms of catalysis and the atomistic structures that mediate it; and (3) develop test-bed platforms that facilitate critical performance measurements of catalytic materials, ones integrated at both the sub-cell component and full device levels.

References:

(1) Piontek, K.; Antorini, M.; Choinowski, T. "Crystal structure of a laccase from the fungus Trametes versicolor at 1.90-angstrom resolution containing a full complement of coppers" *Journal of Biological Chemistry* **2002**, *277*, 37663.

(2) Thorum, M. S.; Yadav, J.; Gewirth, A. A. "Oxygen reduction activity of a copper complex of 3,5-diamino-1,2,4-triazole supported on carbon black" *Angew. Chem., Int. Ed.* **2009**, *48*, 165.

(3) Blanford, C. F.; Foster, C. E.; Heath, R. S.; Armstrong, F. A. "Efficient electrocatalytic oxygen reduction by the 'blue' copper oxidase, laccase, directly attached to chemically modified carbons" *Faraday Discuss* **2008**, *140*, 319.

(4) Mano, N.; Soukharev, V.; Heller, A. "A laccase-wiring redox hydrogel for efficient catalysis of O-2 electroreduction" *J. Phys. Chem. B* **2006**, *110*, 11180.

(5) Tornow, C.; Thorum, M. S.; Gewirth, A. A. "in preparation" **2011**.

(6) Ouellette, W.; Yu, M. H.; O'Connor, C. J.; Hagrman, D.; Zubieta, J. "Hydrothermal chemistry of the copper-triazolate system: A microporous metal-organic framework constructed from magnetic {Cu-3(mu(3)-OH)(triazolate)(3)}(2+) building blocks, and related materials" *Angewandte Chemie-International Edition* **2006**, *45*, 3497.

(7) Fukuzumi, S.; Kotani, H.; Lucas, H. R.; Doi, K.; Suenobu, T.; Peterson, R. L.; Karlin, K. D. "Mononuclear Copper Complex-Catalyzed Four-Electron Reduction of Oxygen" *Journal of the American Chemical Society* **2010**, *132*, 6874.

(8) Thorseth, M.; Letko, C. S.; Rauchfuss, T. B.; Gewirth, A. A. " Dioxygen and Hydrogen Peroxide Reduction with a Hemocyanin Model" *Inorg Chem;*. **2011** in press.

(9) Thorum, M. S.; Hankett, J. M.; Gewirth, A. A. "Poisoning the Oxygen Reduction Reaction on Carbon Supported Fe and Cu Electrocatalysts: Evidence for Metal-Centered Activity " *Journal of Physical Chemistry Letters* **2011**, in press.

(10) Solomon, E. I.; Sundaram, U. M.; Machonkin, T. E. "Multicopper Oxidases and Oxygenases" *Chem. Rev* **1996**, *96*, 2563.

(11) Thorum, M. S.; Anderson, C. A.; Hatch, J. J.; Campbell, A. S.; Marshall, N. M.; Zimmerman, S. C.; Lu, Y.; Gewirth, A. A. "Direct, Electrocatalytic Oxygen Reduction by Laccase on Anthracene-2-methanethiol-Modified Gold" *Journal of Physical Chemistry Letters* **2010**, *1*, 2251.

Selected Publications resulting from work supported

1. "Investigation of Pt, Pt_3Co and Pt_3Co/Mo Cathodes for the ORR in a Microfluidic H_2/O_2 Fuel Cell", F.R. Brushett, H.T. Duong, J.W.D. Ng, R.L. Behrens, A. Wieckowski, P.J.A Kenis, *Journal of The Electrochemical Society*, **2010,** *157* (6), B837-B845.

2. "Oxygen Reduction Activity of a Copper Complex with 3,5-Diamino-1,2,4-triazole Supported on Carbon Black" Thorum, M. S.; Yadav, J.; Gewirth, A. A. *Angewandte Chemie* **2009** *48*, 165-7.

3. "Electroreduction of Dioxygen for Fuel Cell Applications: Materials and Challenges" Gewirth, A. A.; Thorum, M. S. *Inorganic Chemistry* **2010** *49*, 3357-66.

4. "Direct, Electrocatalytic Oxygen Reduction by Laccase on Anthracene-2-methanethiol Modified Gold" Matthew S. Thorum, Cyrus A. Anderson, Jeremy J. Hatch, Andrew S. Campbell, Nicholas M. Marshall, Steven C. Zimmerman, Yi Lu, and Andrew A. Gewirth *J. Phys. Chem. Lett.* **2010** *1* (15), 2251–2254.

5. "A Carbon-Supported Copper Complex of 3,5-Diamino-1,2,4-triazole as a Cathode Catalyst for Alkaline Fuel Cell Applications", F.R. Brushett, M.S. Thorum, N.S. Lioutas, M.S. Naughton, C. Tornow, H.R.M. Jhong, A.A. Gewirth, P.J.A. Kenis, *J. Am. Chem. Soc.* **2010** 132(35), 12185-12187.

6. "A Permeation-Based Microfluidic Direct Formic Acid Fuel Cell (DFAFC)" Erickson, E.M.; Mitrovski, S. M.; Gewirth, A. A.; Nuzzo, R. G. *Electrophoresis* **2011** in press.

7. "Poisoning the Oxygen Reduction Reaction on Carbon Supported Fe and Cu Electrocatalysts: Evidence for Metal-Centered Activity" Thorum, M. S.; Hankett, J. M.; Gewirth, A. A. *J. Phys. Chem. Lett.* **2011,** 295–298.

8. "Dioxygen and Hydrogen Peroxide Reduction with a Hemocyanin Model" Matthew A. Thorseth, Christopher S. Letko, Thomas B. Rauchfuss, Andrew A. Gewirth *Inorg Chem;*. **2011** in press.

Program Title: Simulations of Self-Assembly of Tethered Nanoparticle Shape Amphiphiles

Principle Investigator: S.C. Glotzer
Mailing Address: Department of Chemical Engineering, University of Michigan, 2300 Hayward Street, Ann Arbor, MI 48109-2136
Email: sglotzer@umich.edu

Program Scope

Self-assembly of nanoparticle building blocks including nanospheres, nanorods, nanocubes, nanoplates, nanoprisms, etc., may provide a promising means for manipulating these building blocks into functional and useful materials. One increasingly popular method for self-assembly involves functionalizing nanoparticles with "tethers" of organic polymers or biomolecules with specific or nonspecific interactions to facilitate their assembly. However, there is little theory and little understanding of the general principles underlying self-assembly in these complex materials. Using computer simulation to elucidate the principles of self-assembly and develop a predictive theoretical framework is the central goal of this project. Our simulations are providing foundational understanding of the science of assembly of these complex nanomaterial systems.

Under previous funding from this grant, we studied self-assembly and mapped the phase diagram of tethered nanoparticles of several anisotropy classes under various solvent conditions, and discovered many new unexpected nanoscale structured phases. Present simulation studies include reconfigurable TNPs; TNP quasicrystals; TNP telechelics; and, in collaboration with Oleg Gang's group at Brookhaven National Lab, compound DNA-TNPs.

Recent Progress

Reconfigurable TNPs: Reconfigurable nanostructures represent an exciting new direction for materials. Applications of reversible transformations between nanostructures induced by molecular conformations under external fields can be found in a broad range of advanced technologies including smart materials, electromagnetic sensors, and drug delivery. With recent breakthroughs in synthesis and fabrication techniques, shape-changing nanoparticles are now possible. Such novel building blocks provide a conceptually new and exciting approach to self-assembly and phase transformations by providing tunable parameters fundamentally different from the usual thermodynamic parameters. We investigated *via* molecular simulation a transformation between two thermodynamically stable structures self-assembled by laterally tethered nanorods whose rod length is switched between two values. Building blocks with longer rods assemble into a square grid structure, while those with short rods form bilayer sheets with internal smectic A ordering at the same thermodynamic conditions. By shortening or lengthening the rods over a short time

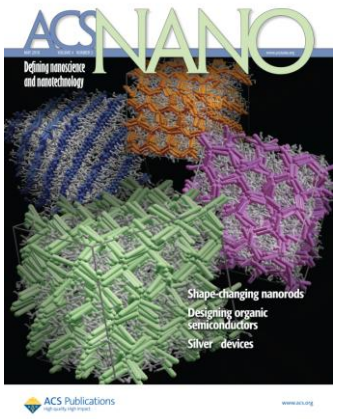

Figure 1. Cover article on self-assembly of shape-changing nanorods.

scale relative to the system equilibration time, we observed a transformation from the square grid structure into bilayer sheets, and *vice versa.* We also observed honeycomb grid and pentagonal grid structures for intermediate rod lengths. The reconfiguration between morphologically distinct nanostructures induced by dynamically switching the building block shape serves to motivate the fabrication of shape-changing nanoscale building blocks as a new approach to the self-assembly of reconfigurable materials.

TNP Quasicrystals: Quasicrystals, or quasi-periodic crystals, are ordered structures that promise compelling material properties on the nano and microscales. Computer simulations have reported the spontaneous self-assembly of dodecagonal quasicrystals and related phases known as Frank-Kasper approximants from systems of spherical particles with specific interaction potentials. However, these potentials have not yet been realized experimentally, even for systems with tailorable interactions, such as colloidal suspen-sions. Here, we use molecular simulation to demonstrate an alternative approach for assembling dodecagonal quasicrystals and their approximants based solely on particle functionaliza- tion and shape. These effects mimic the characteristics of the specialized potentials, thereby replacing complex energetic interactions with simpler-to-achieve bonded and excluded-volume interactions. Our model consists of spherical building blocks functionalized with mobile surface entities to encourage the formation of structures with low surface contact area, including non- close-packed and polytetrahedral structures. The building blocks also posses shape polydispersity, where a subset of the building blocks deviate from the ideal spherical shape, which discourages the formation of close-packed crystals. We show that a model system possessing both mobile surface entities and shape polydispersity consistently assembles complex quasicrystal-like structures. We also report the spontaneous assembly of approximants in two micelle-forming systems of tethered nanoparticle building blocks that possess these key features. We argue that this mechanism can be widely exploited to assemble quasicrystals and approximants on the nano and microscales, and may further elucidate the recent formation of soft matter quasicrystals in experiment. In a broader sense, our study demonstrates how complex interaction potentials can be replicated by packing analogues and serves as a model for future applications involving unique structures.

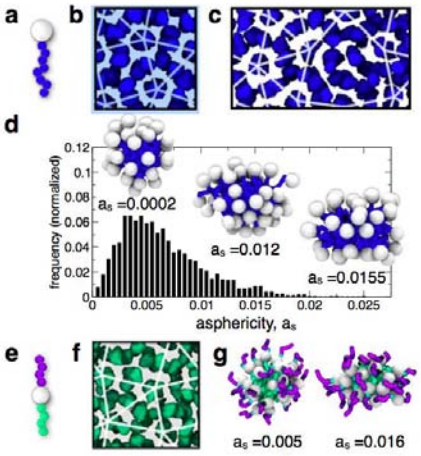

Figure 2. Quasicrystalline assemblies from TNPs. (a) Building block. (b)-(c) QC assemblies. (d) Micelle asphericity. (e) di-TNP building block. (f) QC assembly. (g) Micelle asphericity.

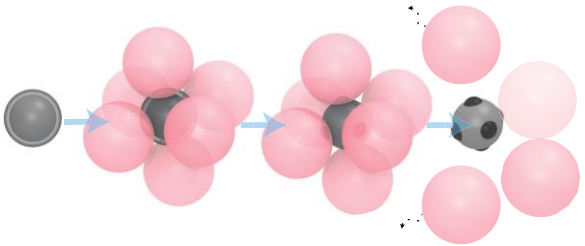

Figure 3. Our simulations predict the thermodyna-mically preferred arrangements of DNA-linked NPs adsorbed from a bath onto a central NP. In this design strategy, releasing of the unlinked DNA and then the "halo" particles would leave behind a patchy particle.

Design of Patchy Particles through DNA-NP Assembly: Particles with attractive patches, also known as "patchy particles," are of great interest in self-assembly because the anisotropy of precisely placed patches can be exploited to drive systems of patchy particles to self-assemble into complex and useful structures. Placing interaction patches on the surface of a sphere,

however, is experimentally challenging. We have demonstrated a strategy to self-assemble the precise placement of four through twelve circular patches of DNA onto the surface of a spherical particle. These arrangements are unique, given a number of patches, and correspond to solutions of a well-studied mathematical optimization problem. Using complementary strands of DNA grafted onto the surfaces of "central" and "halo" particles we demonstrate the binding of halo particles onto central particles in Brownian dynamics simulations accelerated with general purpose graphics processors. These halo particles equilibrate on the surface of the central particle, and we show that free energy minimization via entropy maximization guides their arrangement. We perform free energy calculations predicting the arrangements of particles observed in simulation and explain counterintuitive arrangements.

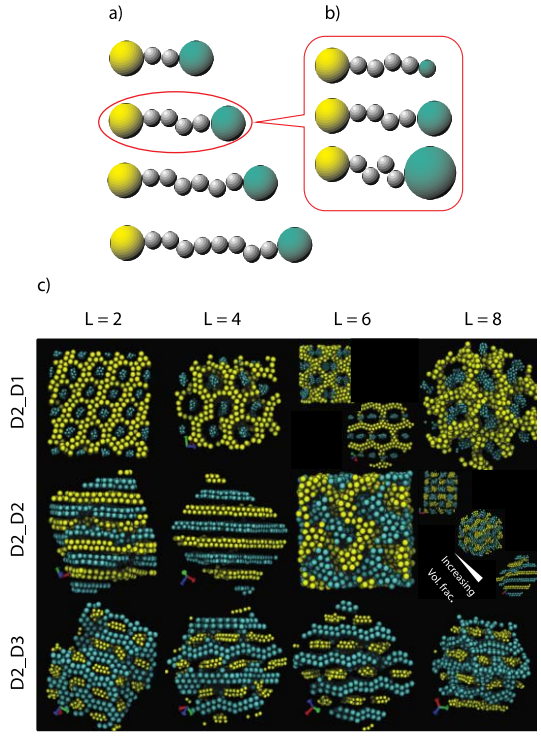

Figure 4. Morphologies predicted for self-assembled TNPTs for various NP sizes, tether lengths, and volume fraction.

Tethered nanoparticle telechelics (TNPTs): Due to their novel NP-flexible tether-NP architecture, TNPTs exhibit a rich diversity of self-assembled structures rivaling those of triblock copolymers, but with novel features arising from the rigidity of the NP "blocks". With a range of possible NP shapes, new functional crystal structures are possible.

Future Plans

We are extending the patchy particle design ideas described above to anisotropic patches.

We have discovered a new spatial subdivision problem relevant to the modeling and simulation of convex and concave polyhedral nanoparticles. We are developing a combination of analyses, heuristics, and optimization algorithms to design solutions for these problems in two and three spatial dimensions.

Publications acknowledging DOE support (last two years)

C.R. Iacovella and S.C. Glotzer, "Complex Crystal Structures Formed by the Self-Assembly of Ditethered Nanospheres," Nano Lett. 9(3) 1206-1211, 2009.

C.R. Iacovella and S.C. Glotzer, "Phase behavior of ditethered nanospheres," Soft Matter, 5(22), 4492-4498 (2009).

A. Santos, C. Singh and S.C. Glotzer, "Coarse-grained models of tethers for fast self-assembly simulations," Phys. Rev. E, 81(1) 011113 (2010).

M.A. Horsch, Z-L Zhang and S.C. Glotzer, “Self-assembly of end-tethered nanorods in a neat system and role of block fractions and aspect ratio,” Soft Matter, DOI: 10.1039/b917403f.

C.L. Phillips, C.R. Iacovella and S.C. Glotzer, “Stability of the double gyroid phase to nanoparticle polydispersity in polymer-tethered nanosphere systems,” Soft Matter, 6, 1693 – 1703, 2010.

T.D. Nguyen and S.C. Glotzer, “Self-assembly and reconfigurability of shape-changing tethered nanorods,” ACS Nano, 4(5), 2585-2594, 2010 (Cover article).

Keys Aaron S.; Iacovella Christopher R.; Glotzer Sharon C., “Characterizing complex particle morphologies through shape matching: Descriptors, applications, and algorithms,” J. Computational Physics, 230(17), 6438-6463, 2011.

C.R. Iacovella and S.C. Glotzer, Assemblies of Polymer-Based Nanoscopic Objects, Comprehensive Polymer Science (2nd Edition), Elsevier, 2011.

C.R. Iacovella, A.S. Keys and S.C. Glotzer, “Self-assembly of soft matter quasicrystals and their approximants,” Proceedings of the National Academy of Science, to be accepted for publication, 2011.

Program Title: A Hybrid Biological/Organic Photochemical Half-Cell for Generating Dihydrogen

Principal Investigator: John H. Golbeck; Co-PI: Donald A. Bryant
Mailing Address: Department of Biochemistry and Molecular Biology, The Pennsylvania State University, University Park, PA 16802
E-mail: jhg5@psu.edu

Program Scope

The goal of this program is to develop a hybrid biological/organic photo-electrochemical half-cell that couples a photochemical module, Photosystem I (PSI), which captures and stores energy derived from sunlight, with a catalytic module, hydrogenase (H_2ase), which catalyzes H_2 evolution with an input of two electrons and two protons. The challenge is to deliver electrons from PSI to the H_2ase rapidly and at high quantum yield, thereby overcoming diffusion-based limits on electron transfer.

The strategy to achieve this goal is to employ molecular wire technology to directly connect PS I with a catalyst. The wire serves to tether the photochemical module to the catalytic module at a fixed distance so that an electron can quantum mechanically tunnel between surface-located [4Fe-4S] clusters of PSI and a H_2ase at a rate faster than the competing charge recombination between P_{700}^+ and F_B^-. To link the photochemical and catalytic modules, a short aliphatic or aromatic dithiol molecule forms a coordination bond with an exposed Fe of the F_B cluster of a PSI variant and with an exposed Fe of the distal [4Fe-4S] cluster of a H_2ase variant. This is practically achieved by changing a ligating Cys residue of the [4Fe-4S] cluster of each protein to a Gly, thereby exposing the Fe atom for chemical rescue by the added dithiolate-containing molecular wire.

Recent Progress

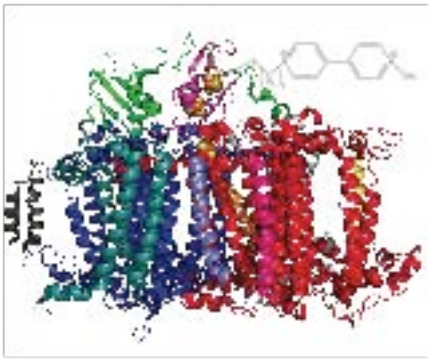

Figure 1. Depiction of the PSI-tethered 1-(3-thiopropyl)-1'-(methyl)-4,4′-bipyridinium cofactor.

Our first objective was to provide spectroscopic evidence that the electron is indeed transferred through the molecular wire by using a bound cofactor, 4,4'-bipyridinium, as a redox marker. Singly reduced 4,4′-bipyridinium absorbs strongly at 600 nm and shows a sharp, derivative EPR signal at $g = 2.002$, whereas doubly reduced 4,4′-bipyridinium absorbs between 370-390 nm and is EPR-silent. For this experiment, we tethered 1-(3-thiopropyl)-1′-(methyl)-4,4′-bipyridinium to the C13G variant of PsaC and measured its reduction by optical and EPR spectroscopy. We first confirmed that the 4,4′-bipyridinium was attached to the isolated PsaC protein by EPR; on chemical reduction, a sharp resonance from the singly reduced bipyridinium was observed at $g = 2.002$ and a typical rhombic spectrum of the F_A cluster was observed at $g =$ 2.05, 1.94 and 1.89 (the chemically rescued F_B cluster is in a S = 3/2 ground spin state and its resonance is seen at $g = 5$ to 6). The PsaC-4,4′-bipyridinium assembly was then bound onto P_{700}-F_X cores in the presence of PsaD and studied after a single-turnover laser flash (**Figure 1**). The

charge recombination kinetics of P_{700}^+ were found to be significantly longer than in the native PSI complex, consistent with a longer distance (and higher redox potential) from the reduced 4,4′-bipyridinium to P_{700}^+. The kinetics at 820 nm from the reduction of P_{700}^+ matched those at 600 nm from the oxidation of the reduced 4,4′-bipyridinium, consistent with the occurrence of charge recombination. Steady-state kinetic studies were carried out in the presence of soluble Cyt c_6, ascorbate and PMS as electron donors. Upon illumination, a steady increase in absorbance at 600 nm was observed, consistent with a one-electron reduction. After the 4,4′-bipyridinium was completely reduced with dithonite, a steady bleaching was observed, consistent with a two-electron reduction. The initial steady-state rates of the single and double reduction were 58.3 µmol and 14 µmol of 4,4′-bipyridinium mg Chl^{-1} h^{-1}, respectively. These rates are comparable to the rate of H_2 evolution in the PSI—molecular wire—[FeFe]-H_2ase construct measured under identical conditions (see below). Because H_2 evolution is a two-electron process, the 30.3 µmol H_2 mg Chl^{-1} h^{-1} evolved in the light corresponds to an electron transfer throughput of 60.6 µmol e^- mg Chl^{-1} h^{-1}, which is in reasonable agreement with the rate of reduction of the PSI—4,4′-bipyridinium cofactor. These results support our hypothesis that an electron can be transferred from the F_B cluster of PSI through a molecular wire to a tethered redox center.

Our second objective was to attach an inorganic catalyst to the end of the molecular wire. When a Pt nanoparticle was attached to the end of the PSI-molecular wire, H_2 was generated at a rate of 49 µmol mg Chl^{-1} h^{-1} when soluble Cyt c_6 was the donor to P_{700}^+. For simplicity, we replaced the 1-(3-thiopropyl)-1′-(methyl)-4,4′-bipyridinium moiety with a simple aliphatic 1,6-hexanedithiol wire, and we retained this wire in all subsequent studies. The maximal rate of light-driven H_2 production occurred at a solution pH of 6.0 when using cross-linked plastocyanin, rebuilt spinach PSI complexes (which contain a larger antenna, and hence, larger optical cross-section than cyanobacterial PSI), and the aromatic wire molecule, 1,4-benzenedithiol, to tether PSI to the Pt nanoparticle. Illumination of this optimized PSI—wire—Pt NP bioconjugate resulted in a rate of 312 µmol H_2 mg Chl^{-1} h^{-1}, a 6.3-fold increase over our initially reported rate.

This study laid the foundation for our third objective, which was to attach a [FeFe]-H_2ase to the end of the molecular wire. Our first attempt at generating the necessary the C97G variant of the *Clostridium acetobutylicum* [Fe-Fe]-hydrogenase *(Ca*HydA*)* involved overexpressing the protein in *Escherichia coli*. Even though the three maturation genes, *hydE, hydF and hydG* were included in the *hydA*-containing plasmid, the wild-type *Ca*HydA and variant H_2ases produced in *E. coli* had low and variable yields and activities (it should be noted that *E. coli* naturally produces only [NiFe]-H_2ases and does not natively produce the required maturation genes.) Nevertheless, we

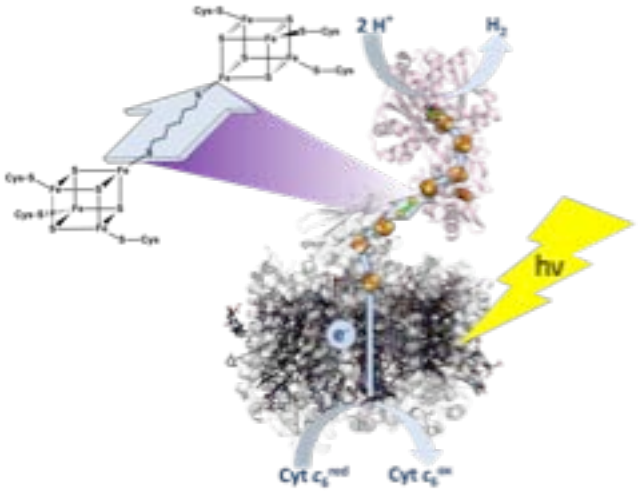

Figure 2. Schematic of the PSI—molecular wire—[FeFe]H_2ase construct. The connecting wire is 1,6-hexanedithiol. Soluble electron donors include Cyt c_6, ascorbate, and PMS. Arrows indicate electron transfer through the system, including reduction of protons to H_2.

were able to attach the C97G variant of the [Fe-Fe]-hydrogenase to the PSI-molecular wire moiety and measure a light-induced rate of 3.7 μmoles H_2 mg Chl^{-1} h^{-1} (**Figure 2**). Seeking a source of higher quality H_2ases, we entered into collaboration with Prof. Thomas Happe (U. Bochum), who has developed a genetic system for natively producing both wild-type and variants of the *Ca*HydA enzyme in *C. acetobutylicum*. The advantage of using this system is that the *Ca* [FeFe]-H_2ase protein is produced in its native organism, and hence the required maturation enzymes for an [FeFe]-H_2ase are already present. When the C97G *Ca*HydA variant was tethered to the PSI—wire, the rate of light-driven H_2 evolution was 30.3 μmol of H_2 mg Chl^{-1} h^{-1}, an order of magnitude higher than our initial report. All control experiments were negative: no H_2 was evolved when the C97G *Ca*HydA variant, the C13G variant of PsaC, or the 1,6-hexanedithiol molecular wire was omitted, or when the complete mixture was incubated in the dark. Similarly, no H_2 was evolved when the C13G variant of PsaC was replaced with either wild-type PsaC or with PSI cores lacking the PsaC subunit, or when the C97G *Ca*HydA variant was replaced with wild-type *Ca*HydA. When fresh ascorbate was added, the PSI—wire—[FeFe]-H_2ase construct showed little or no loss of light-driven H_2 evolution over a period of 64 days. Mechanistically, the molecular wire tethers the two redox centers at a fixed distance so that electrons can quantum mechanically tunnel from PSI to the [FeFe]-H_2ase at a rate faster than the rate of competing charge recombination between P_{700}^+ and F_B^-. The rate of electron tunneling is affected by the nature of the intervening medium, and in this construct, the covalent pathway of σ bonds between the two Fe-S clusters likely affords a more favorable route than more convoluted pathways through H-bonds of the solvent (H_2O). To our best knowledge, this study represents the first instance of an *in vitro* wiring of two enzymes through their physiologically relevant redox centers.

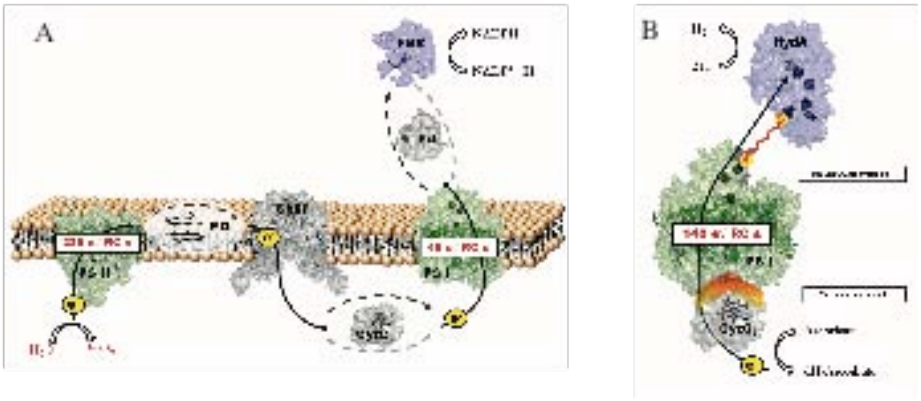

Figure 3. Schematic comparison of electron flow in (A) *in vivo* photosynthesis and (B) the photosynthetic nanoconstructs described here. Rates given indicate the electron throughput through each of the photosynthetic reaction centers in each scenario. Electron transfer is primarily diffusionally governed in (A) and through bonds in (B). Direct electron transfer reactions are indicated as black solid arrows, diffusion-based steps as black dashed arrows.

By optimizing the reaction conditions, we have since improved the rate of light-driven H_2 evolution by an additional factor of ~100. This major increase was due optimization of several factors: (i) use of a highly active H_2ase variant that had been expressed in *C. acetobutylicum* rather than *E. coli*; (ii) the use of phosphate buffer at pH 6.5 instead of Tris-HCl buffer pH 8.3 to increase the concentration of available protons; (iii) the use of 1,8-octanedithiol instead of 1,6-hexanedithiol as the molecular wire; and (iv) using cross-linked Cyt c_6 as the electron donor to minimize the diffusion barrier to P_{700}^+. Our results show that when ascorbate is the sacrificial donor, the PSI—wire—[FeFe]-H_2ase construct evolves H_2 at a rate of 2850 μ moles mg Chl^{-1} h^{-1}, which is equivalent to an electron transfer

throughput of 5700 μmoles mg Chl^{-1} h^{-1}, or 142 μmoles e^- PSI^{-1} s^{-1}. Putting this into perspective, cyanobacteria evolve O_2 at a rate of ~400 μmoles mg Chl^{-1} h^{-1}, which is equivalent to an electron transfer throughput of 1600 μmoles mg Chl^{-1} h^{-1}, or 49 e^- PSI^{-1} s^{-1}, assuming a PSI to PSII ratio of 1.8 a s occurs in the cyanobacterium *Synechococcus* sp. PCC 7002. The above rate is consistent with the assessment that the catalytic module is *not* the rate-limiting step in light-driven H_2 evolution (*Ca*Hyd is capable of evolving 6,000 H_2 $protein^{-1}$ s^{-1}, which is equivalent to 12,000 electrons $protein^{-1}$ s^{-1} when electrons are supplied by reduced methyl viologen.). Because PSI is ultimately capable of transferring ~1000 electrons $protein^{-1}$ s^{-1}, we can anticipate at best another 5-fold improvement may be possible by further adjustment of these and other variables. In conclusion, the significantly greater electron throughput by our hybrid biological/organic nanoconstruct over *in vivo* oxygenic photosynthesis validates the concept of tethering proteins through their physiologically relevant redox cofactors to overcome diffusion-based rate limitations on electron transfer (**Figure 3**).

Future Plans

Now that the goal of reproducibly generating high rates of light-driven H_2 has been realized in the PSI–wire–[FeFe]-H_2ase bioconjugate, we are poised to address a number of technical questions: (1) Are only productive PSI—molecular wire—[FeFe]-H_2ase constructs generated? (2) Is the ratio of PSI to H_2ase in the productive PSI—molecular wire—[FeFe]-H_2ase constructs 1:1 as expected? (3) What is the pattern of H_2 evolved on successive light flashes? (4) What is the quantum yield of light-driven H_2 evolution? (5) Is it possible to increase the rate of H_2 evolution by enlarging the optical cross section of PSI? (6) Is it possible to detect redox changes within the catalytic site of the H_2ase?

References

1) Lubner, C. E., Grimme, R., Bryant, D. A., and Golbeck, J. H. (2010) Wiring photosystem I for direct solar hydrogen production, *Biochemistry 49*, 404-414.

2) Lubner, C. E., Knorzer, P., Silva, P. J., Vincent, K. A., Happe, T., Bryant, D. A., and Golbeck, J. H. (2010) Wiring an [FeFe]-Hydrogenase with Photosystem I for Light-Induced Hydrogen Production, *Biochemistry 49*, 10264-10266.

3) Chauhan, D., Folea, I. M., Jolley, C. C., Kouril, R., Lubner, C. E., Lin, S., Kolber, D., Wolfe-Simon, F., Golbeck, J. H., Boekema, E. J., and Fromme, P. (2010) A Novel Photosynthetic Strategy for Adaptation to Low-Iron Aquatic Environments, *Biochemistry* 50, 686-692.

4) Lubner, C., Heinnickel, M., Bryant, D. A., and Golbeck, J. H. (2011) Wiring Photosystem I for Electron Transfer to a Tethered Redox Dye, *Energy Environ. Science 4,* 2428-2434.

5) Lubner, C., Bryant, D. A., and Golbeck, J. H. (2011) 'Wired Reaction Centers', In *Molecular Solar Fuels* (Hillier, W., and Wydrzynski, T., Eds.), Royal Society of Chemistry, London (in press).

6) Lubner, C., Applegate, A., Knörzer, P., Happe, T., Bryant, D. A., and Golbeck, J. H. (2011) A Solar Hydrogen-Producing Bio-Nanodevice that Outperforms Natural Photosynthesis, *(in review)*.

Program Title: Optical and Electro-optic Modulation of Biomimetically-functionalized Nanotubes

Principal Investigator: Padma Gopalan , Associate Professor, Materials Science and Engineering, University of Wisconsin, 1509 University Ave., Madison, WI 53706; Email: pgopalan@wisc.edu
CO-PI: Mark A. Eriksson Professor, Department of Physics, 5118 Chamberlin Hall, 1150 University Ave, Madison, WI 53706; Email: maeriksson@wisc.edu
Collaborators: Francois Leonard (Sandia National Lab), David Mc Gee (College of New Jersey)

Program Scope

The goals of the program are to develop a fundamental understanding of the light-induced changes on the electronic properties of functionalized carbon nanotubes through a combination of new functionalization chemistry, probing the electrical and optical response of the nanotube/chromophore hybrids, and interpretation of the results with theory/modeling. Nanotube-based electronic and electro-optic devices have long been cited as potentially revolutionary. Despite much initial progress, the promised applications have been slow in coming, due first and foremost to the large diversity in size and chirality of single-wall nanotubes and due to limitations in the strength of interaction with light. In our work, we focus specifically on the development and understanding of functionalization for the optimization of electro-optic properties. And we do so in the context of, and using methods compatible with, the recent important advances in nanotube purification, and leveraging the long-standing understanding and accomplishments in the creation of high-mobility nanotube devices. The project utilizes unique set of expertise covering materials chemistry, physics, and theory.

Recent Progress

BACKGROUND

Light-triggered changes in biological molecules, which enable various functions such as vision, photosynthesis, and heliotropism, have long inspired materials chemists to mimic these phenomena to create new synthetic materials and devices. One example is the molecule retinal undergoing a *cis-trans* isomerization in response to light, creating a cascade of events leading to visual recognition. Synthetic versions of retinal include switchable stilbene, or azo-benzene containing molecules. Azo-benzenes undergo a reversible photoisomerization from a thermally stable *trans* configuration to a meta-stable *cis* form. Dipolar chromophores based on azo-benzene structure are photochemically stable, can be reversibly switched 10^5 to 10^6 times before bleaching, and can be chemically tuned at the donor and acceptor end to alter the magnitude of the dipole moment. The reversible, wavelength-selective isomerization and the accompanying conformational change provide an important handle for optical modulation of electrical and electro-optic properties of nanotubes. Indeed, we recently, demonstrated an optically active nanotube-hybrid material by non-covalent functionalization of SWNT field-effect transistors with an azo-based chromophore. Upon UV illumination, the chromophore undergoes a *trans-cis* isomerization leading to charge redistribution near the nanotube. The resulting change in the local electrostatic environment leads to a shift in the threshold voltage and increased

conductivity of the nanotube. The functionalized transistors showed repeatable switching for many cycles, and the low (100 $\mu W/cm^2$) intensities necessary to optically modulate the transistor are in stark contrast to measurements of intrinsic nanotube photoconductivity, which typically require 1 kW/cm^2 intensity. More recently this approach was used to demonstrate photodetection tunability over the visible range. In order to improve the efficiency, stability, and lifetime of chromophore-functionalized SWNT devices, it is important to understand the na ture of chromophore,/SWNT interaction, including the role of tethers in binding the chromophores to the SWNTs.

FINDINGS

To probe the chromophore/SWNT interface we started with spectroscopic analysis the hybrid systems using complementary experimental techniques and ab initio calculations. For the chromophore, we use Disperse Red 1 (DR1), a w ell-studied and commercially available azobenzene chromophore, with a s eries of three increasing tether strengths: (1) unmodified DR1 with no added tether (DR1U), (2) anthracene-functionalized DR1 (DR1A), and (3) pyrene-functionalized DR1 (DR1P) (see Scheme 1). The first part of our studies on thin-films shows that the binding energy and hence the surface coverage of the chromophores on the nanotubes is strongly influenced by the strength of the tether; we also address the question of the orientation of the molecules on the nanotubes by optical second harmonic generation (SHG) measurements. The second part of our studies focuses on the solution characterization of the hybrids to evaluate the nature of the electronic coupling.

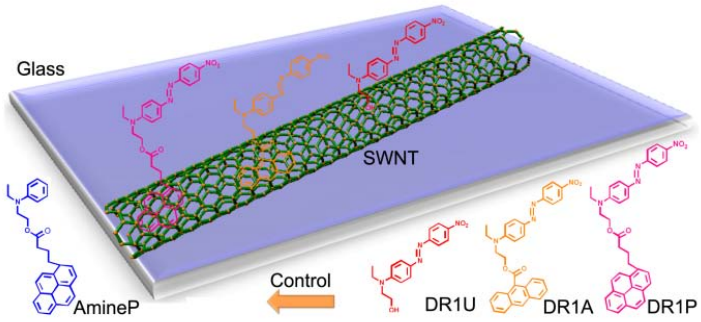

Scheme 1. A depiction of the SWNT hybrid along with the structures of unmodified DR1 (DR1U), DR1 with anthracene tether (DR1A), DR1 with pyrene (DR1P) tether, and the control compound which is a pyrene tether on the donor amine group (Amine P).

(a) Evaluation of strength of binding:

X-ray photoelectron spectroscopy (XPS) provides a route to probe the surface chemical composition and to evaluate the relative surface coverage. After washing with methanol, the decrease in the N (1s) peak intensity (Figure 1) was in the order DR1U/SWNTs > DR1A/SWNTs > DR1P/SWNTs. A shift in the C (1s) peak towards lower binding energy is also observed by the interaction of the chromophores with the SWNTs. The observed shift in the C (1s) peak is 0.12 eV for DR1U, 0.18 eV for DR1A and 0.2 eV for DR1P. A shift of the C (1s) peak toward lower binding energy is associated with a shift in the Fermi level. The calculated coverages are 0.64, 0.67, and 3.12 molecules per 100 nanotube carbon atoms for DR1U/SWNTs, DR1A/SWNTs, and DR1P/SWNTs hybrid, respectively. After washing with methanol, the differences between these three systems are dramatic. The surface coverage of DR1U and DR1A on nanotubes decreased by 78% and 76% respectively, whereas that of DR1P decreased by only 10 %. Complementary experiments by Raman and UV-vis spectroscopy confirm the results from XPS analysis.

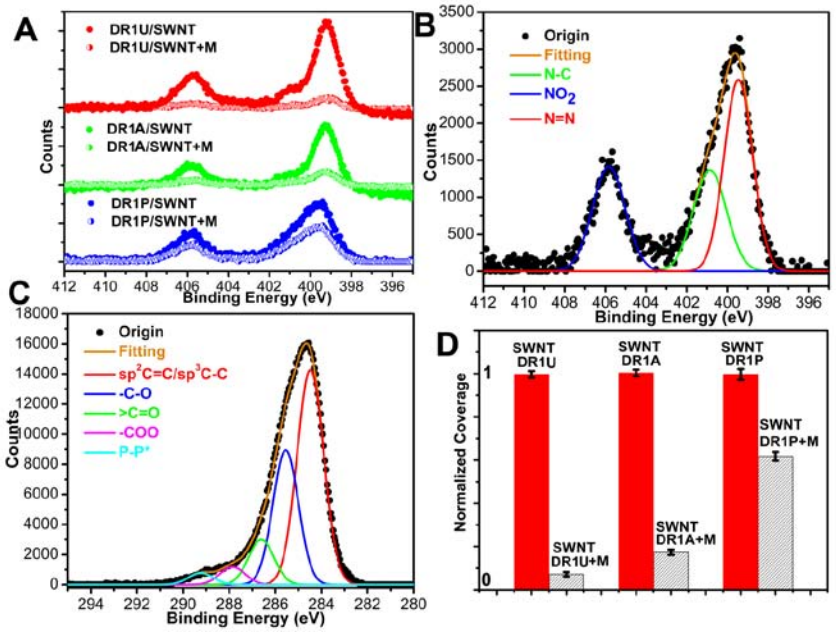

Figure 1 XPS spectra of chromophore-SWNT films showing: (A) XPS core level N (1s) spectra for the three nanohybrid films as cast and after methanol washing, (B) N (1s) spectra of the DR1P/SWNT hybrid with the fitting, (C) C (1s) spectra of DR1P/SWNT hybrid with the fitting, and (D) normalized surface coverage of chromophores on SWNTs calculated by comparison of the area under the N (1s) peak with the area under the C (1s) peak. Red bars correspond to the coverage of the chromophores on the substrate before washing (which is set to 1); and the grey bars correspond to the coverage of the chromophores bound to the nanotubes after methanol rinse.

(b) Fluorescence Quenching upon Binding of Chromophores to Nanotubes

The three chromophore samples showed a strong fluorescence emission when not bound to nanotubes. However, in the presence of nanotubes, the fluorescence intensity (F) drops dramatically compared to the initial fluorescence intensity (F_0). For a given concentration of chromophores, as the concentration of nanotubes increases, the emission from the chromophores decreases. The efficiency of quenching ($1-F/F_0$) for DR1U/SWNTs, DR1A/SWNTs, and DR1P/SWNTs are 84.2%, 92.0%, and 95.6%, respectively. From the Stern-Volmer plots (F_0/F as a function of nanotube concentration), in moving from DR1U to DR1A to DR1P an increasing non-linear plot with a slight upward curvature was observed. The non-linear plot is typically associated with a combination of both static and dynamic quenching, *i.e.*, by both collisions and by complex formation with the chromophores. We measured the PL emission from the nanotubes pumped by absorption of the chromophores. In all three cases no detectable enhancement in the band-gap PL of nanotubes was observed, which points to lack of significant energy transfer from the chromophores to isolated semiconducting nanotubes.

(c) Probing the Orientation of the Molecules on the Nanotube:

Second harmonic generation (SHG) has proven to be a sensitive probe for the determination of acentric molecular ordering in monolayers and thin film, which to our knowledge has not been applied to the study of chromophore functionalized nanotubes. As described below, we have utilized SHG to identify a radial component of chromophore orientation with respect to the SWNT surface. When irradiated by a laser pulse, a collection of weakly interacting chromophores will generate a second-harmonic pulse, with an intensity that depends on the molecular second order hyperpolarizability β and a macroscopic order parameter describing the average orientation of a chromophore with respect to an axis of symmetry (in this case, normal to the SWNT film). Since isomerization of DR1 results in an approximate 5-fold decrease in β in going from the *trans* to the *cis* conformation, monitoring SHG emission from the SWNT-chromophore hybrid during UV exposure should provide insight on the net chromophore

orientation. We observed that the DR1P/SWNT film exhibited SHG immediately following fabrication, indicating a degree of chromophore alignment perpendicular to SWNTs. This SHG signal was not observed for pristine SWNTs. To confirm the role of the chromophores in generation of the SHG signal, further measurements were performed while irradiating the DR1P/SWNT films for 1 minute with 365 nm UV light, followed by 1 minute without UV light (Figure 2). The DR1P/SWNT film shows a clear dependence of the SHG signal on 365 nm UV light. Upon illumination, the SHG drops noticeably, taking 2-4 seconds to reach steady state. Following removal of the UV, the SHG returns to its initial value. These results can be repeated for several cycles. The change that occurred during this process was consistent with the isomerization of DR1P oriented in the perpendicular direction. An AmineP/SWNTs (Scheme 1) film was prepared as a control as it does not have the switchable azo group. No SHG or dependence on the UV light was observed, confirming the importance of the isomerization of DR1P. Collectively, these results suggest that the adsorption of chromophores on the nanotubes is either heterogeneous (in addition to the parallel configuration of DR1P, there are also perpendicular configurations on the SWNTs) or that the adsorption is at an intermediate angle relative to the axis of the nanotube.

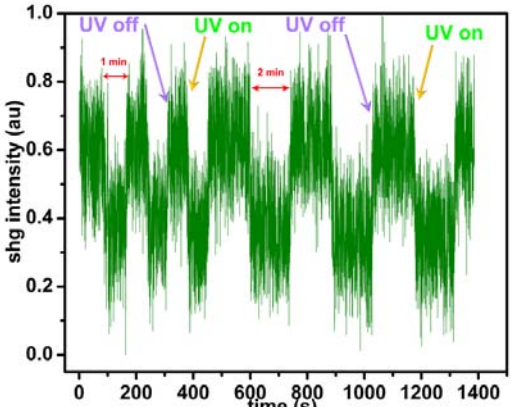

Figure 2 Second harmonic generation (SHG) signal from DR1P/SWNT film subject to cyclic UV irradiation in 1 and 2 minute intervals. For example, UV is on for 100 s < t < 160 s, off for 160 s < t < 220 s. At t = 460 s, the period is increased to 2 minutes.

Future Plans

These studies on the chromophore/SWNT hybrids both in solution and thin-film are relevant for optimizing the photogating of the chromophore/SWNT transistors, and they motivate future work on both tailoring the dipole moment as well as improving the optical activity of the nanotube-hybrid material by selecting specific chiral distributions. The synthetic work will focus not only on tailoring the dipole moment of the chromophores but also expanding the absorptivity of the molecules into the near-IR range.

Building on the chemical characterization described above, we are fabricating carbon nanotube-based transistors to study the effects of optical switching of chromophores adsorbed on those nanotubes. Plans for the coming year include characterization of the photoresponse of such transistors with chromophore functionalization. Parallel studies on how these interactions change in moving to 2D system such as graphene are in progress. Graphene offers all the attractive electronic properties of SWNT but does not have as many of the processing or sample heterogeineity issues.

List of Papers Acknowledging this Grant.

1) "Spectroscopic properties of nanotube-chromophores hybrids" ACS Nano (in Review June 2011).
2) " p-doping of graphene with dipolar chromophores" Nano Letters (to be submitted September 2011).

Phospholipid Vesicles in Materials Science

Steve Granick

University of Illinois
Department of Materials Science and Engineering
1304 West Green St.
Urbana, IL 61801
sgranick@uiuc.edu

Program Scope: It is a grand challenge in material science to form structure that is not frozen in place but instead robustly responds adaptively to its environment. This proposal has the objective to develop the science basis needed to deploy phospholipid bilayers as functional materials in energy contexts. Specifically, we aim to develop: (1) integrated molecular-level understanding of what determines their dynamical shape, phase behavior and spatial organization; and (2) understanding of their diffusion in crowded environments. The methods to do this largely involve fluorescence imaging and other types of fluorescence spectroscopy involved single particles and nanoparticles, vesicles, and liposomes.

Recent Progress: This year, our experiments and reasoning about them led us to conclude that thermal dynamics can be decomposed into a wide set of diffusivities that reflect slowly-varying, heterogeneous microscopic fluctuations. Patterns of non-Gaussian yet Fickian diffusivity, which violate textbook expectations, have now confirmed in 4 distinct experimental systems, the latest being phospholipid vesicle diffusion in not only isotropic but also nematic matrix environments. The identification of non-Gaussian yet Fickian diffusivity with long-lived environmental fluctuations allows us to predict that non-Gaussian diffusivity should characterize much mobility in biomolecular materials systems.

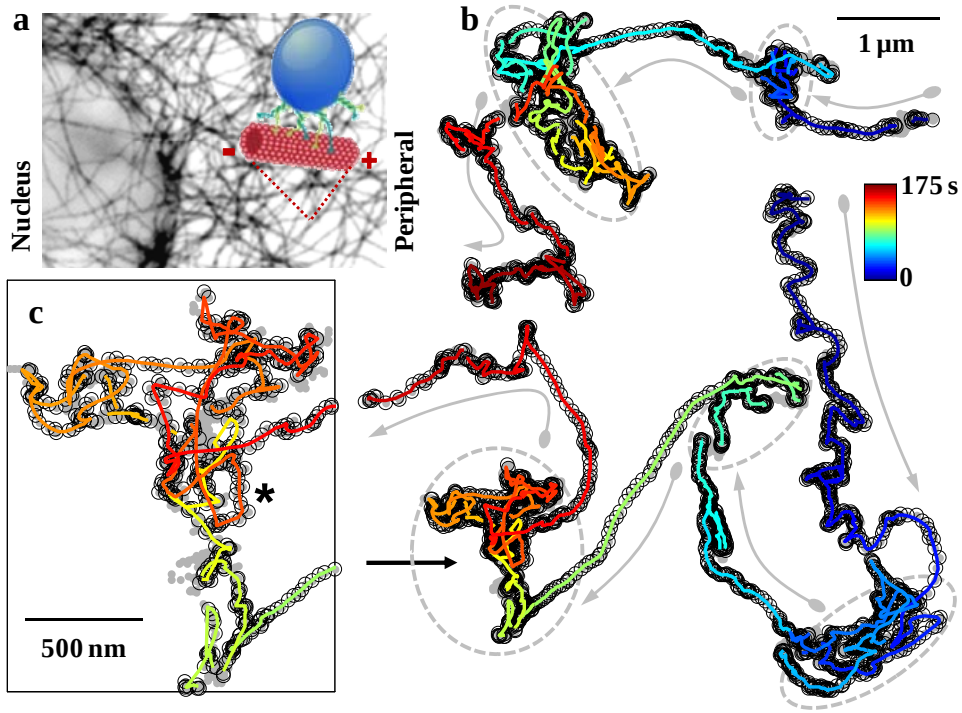

Fig. 1. Active transport of endosomes along

As active transport presents striking contrast to this, we continued with the question how,

microtubules exhibits two phases, persistent transport (T) and local active searching (S). (a) Illustration that cargos are actively transported through microtubule networks in cells with length scale set by mesh size ξ. The inset illustrates a heuristic model of what happens on the molecular scale— cargo is dragged by motor proteins as they walk along the microtubules either to the cell periphery or inwards. (b) Two representative trajectories of individual EGF-containing endosomes in HeLa cells. The smoothened paths of active transport shown as lines with color denoting the elapsed time are overlaid on the original tracked positions (gray dots) with the active portion detected by wavelet analysis highlighted by black open circles (see Methods). The flow of alternating T and S periods is indicated by arrows and dashed circles, respectively. An S period is magnified in (c). The asterisk highlights a closed loop in the trajectory. These data are enabled by novel wavelet-based discrimination of active from passive transport, developed for this study. It is anticipated to generalize readily and to find broad application in quantification of active transport in diverse other systems also.

in biomolecular environments which involve active transport, nature designs target-seeking for maximum efficiency of time and energy cost. Amazingly, target-seeking patterns can explain the rapidity with which vesicle cargo in intracellular active transport can diversify to find the right spots for their biological missions, as illustrated in Fig. 1.

These experiments, based on single-particle tracking, pose the question, can we learn from nature how to transport cargo quickly and efficiently? Active directed motion to pre-determined locations is certainly an attractive ideal, but directionality must diversify according to the needed fate of cargo, which cannot be pre-programmed as to do so would sacrifice adaptability. The polarity of microtubules is inadequate to identify these directions, and no other mechanism is currently known. In this sense, random walks are optimal as the sampling efficiency is $s/R^2 \sim 1$ for random diffusion but $s/R^2 \sim 1/s$ for directed motion (here R^2 is squared displacement and s is traversed distance during a given time), such that efficiency decreases with distance traveled. Unfortunately, objects with the typical size diffuse prohibitively slowly. This is significantly enhanced by biphasic transport as the S phase follows an effective random walk, boosting D to ~0.1 $\mu m^2/s$. This alone is still insufficient to achieve efficacy, as for compartments with size 10-100 μm, ~10^4 s would be needed to explore the body even if the cargo were transported actively all the time. That conundrum is solved by adding the T phase. Recognizing that $D \propto \upsilon\zeta$ where ζ is the directional persistence, the effective diffusivity over long distances further increases by another factor of ~50. These scaling arguments show that this mechanism, with intermittency maintaining the searching efficiency, shifts the time scale into a reasonable range (~10^3 s), which is indeed the typical time for transportation and segregation of cargos.

This research is showing that the paths taken by transport in biomolecular systems are more subtle than anticipated by earlier ensemble-average experiments. The simplest case is where mean-square displacement is proportional to time, which is commonly modeled as resulting from Gaussian statistics as the central limit theorem dictates must hold sway at the very longest times, but there exist many situations in which direct observation finds the distribution of step lengths to deviate from Gaussian – for example, caged diffusion such as in supercooled liquids and biofilament networks, particles close to jamming transitions, and even far-from-equilibrium systems such as tribology, which previously were given system-specific interpretations.

Other recent activities include:

- *Single particle tracking*. We developed a straightforward, automated line tracking method to visualize linear macromolecules as they rearrange shape by Brownian diffusion and under external fields such as electrophoresis. The analysis, implemented with 30 ms time resolution, identifies contour lines from one end of the molecule to the other without attention to structure smaller than the optical resolution. There are three sequential stages of analysis: first, "feature finding" to discriminate signal from noise; second, "line tracking" to approximate those shapes as lines; third, "temporal consistency check" to discriminate reasonable from unreasonable fitted conformations in the time domain. Automation makes it straightforward to accumulate vast quantities of data while excluding the unreliable parts of it. As proof of concept, we implemented this analysis on fluorescence images of λ-DNA molecules in agarose gel to demonstrate its capability to produce large datasets that may also facilitate advances such as real-time quantification of microscopy images.
- *Concentrated liposome suspensions*. Stabilizing liposomes of zwitterionic lipids by the adsorption of cationic nanoparticles, we studied, using single-particle fluorescence tracking, mobility in this distinctively deformable colloid biomolecular system. Liposome motion is diffusive and homogeneous at low volume fractions, but separable fast and slow populations emerge as the volume fraction increases beyond $\varphi \approx 0.45$, the same volume fraction at which hard colloids with sufficiently strong attraction are known to experience gelation. This is reflected not only in scaling of the mean square displacement, but also in the step size distribution (van Hove function) measured by fluorescence imaging. The fast liposomes are observed to follow Brownian motion and the slow ones to follow anomalous diffusion characterized by a 1/3 time scaling of their mean square displacement.
- *Biomolecular models of polymer mobility*. Single-molecule imaging of actin biofilaments, and of DNA when it is heavily entangled within them, are giving rise to an emerging picture of the strengths and limitations of textbook ideas in this field. In one study, using single-molecule fluorescence imaging of actin, we tracked Brownian motion perpendicular to the contour of tightly-entangled F-actin filaments and extracted the confining potential; the implied heterogeneity characterized by a distribution of tube diameter is discussed and quantified. A series of other studies, using single imaging of DNA, tracked its Brownian motion as well as electrophoresis under the action of electric fields. In both systems we find that the mean conceals wide distributions of individual-molecule responses – amazingly, not centered around a single mean. We are seeking to unravel the reasons.

Future Plans: These exciting new developments will be pursued. In the area of phospholipid membrane fluctuations, one problem of intense interest will be to spatially-resolve the power spectrum of thermal fluctuations using a new technique we have finished for this purpose, this data teaching one about local variations in bending stiffness. In the area of biomolecular models of polymer mobility, single-molecule tracking will be combined with computer simulation to separate system-specific from generic aspects of the surprising phenomenological behavior revealed in our preliminary studies of reptation and electrophoresis.

This year's findings regarding the molecular origins of target-seeking efficacy in active transport will be extended and generalized to other phospholipid systems.

Publications 2009-2011:

"Image Analysis with Rapid and Accurate 2D Gaussian Fitting," Stephen M. Anthony, and Steve Granick, ***Langmuir*** 25, 8152 (2009).

"Biomolecular Science of Liposome-Nanoparticle Constructs," Yan Yu, Stephen M. Anthony, Sung Chul Bae, Erik Luijten, and Steve Granick, ***Mol. Cryst. Liq. Cryst.*** 507, 18 (2009).

"Anomalous but Brownian," Bo Wang, Stephen M. Anthony, Sung Chul Bae, and Steve Granick, ***Proc. Nat. Acad. Sci. USA*** 106, 15160 (2009).

"Pearling of Lipid Vesicles Induced by Nanoparticles," Yan Yu and Steve Granick, ***J. Am. Chem. Soc.*** 31, 14158 (2009).

"Long Range Interactions in Nanoscale Science," Roger French et al., ***Rev. Mod. Phys.*** 82, 1887 (2010).

"Vesicle Budding Induced by Pore-Forming Peptide," Yan Yu, Julie A. Vroman, Sung Chul Bae, and Steve Granick, ***J. Am. Chem. Soc.*** 132, 195 (2010). Highlighted: ***Nature*** 463, 439 (2010).

"Confining Potential When a Biopolymer Filament Reptates," Bo Wang, Juan Guan, Stephen M. Anthony, Sung Chul Bae, Kenneth S. Schweizer, and Steve Granick, ***Phys. Rev. Lett.*** 104, 118301 (2010).

"How Liposomes Diffuse in Concentrated Liposome Suspension," Yan Yu, Stephen Anthony, Sung Chul Bae, and Steve Granick, ***J. Phys. Chem. B*** 115, 2748 (2011).

"Automated Single Molecule Tracking of DNA Shape," Juan Guan, Bo Wang, and Steve Granick, ***Langmuir*** 27, 6149 (2011).

"Target-Seeking Efficacy of Active Transport in Living Cells," Bo Wang, Kejia Chen, Sung Chul Bae, and Steve Granick, submitted.

"When Fickian Diffusion is not Gaussian," Bo Wang, Sung Chul Bae, and Steve Granick, ***Nature Materials***, in press.

Program Title: Bioinspired Hydrogen Bonding-Mediated Assembly of Nano-objects toward Adaptive and Dynamic Materials

Principle Investigator: Zhibin Guan, Ph.D.
Mailing Address: 1102 Natural Sciences II, Irvine, CA 92697
Email: zguan@uci.edu

Program Scope

The goal of this project is to develop strong H-bonding-mediated self assembly of nanomaterials having adaptive and dynamic properties for energy relevant applications. Inspired by natural dynamic and adaptive materials, we propose to use strong, reversible H-bonding mediators to achieve dynamic assembly of nano-objects. The dynamic nature of hydrogen bond arrays are proposed to introduce adaptive, autonomically responsive, and self healing properties to the nanomaterials. Compared to other molecular mediators, well-defined hydrogen bonds are stronger and easier to control than other dynamic interactions (e.g., van der Waal, dipole-dipole, ionic, $\pi-\pi$ stacking, etc) while much less expensive to prepare and can be easily scaled up compared to DNAs. Following the design and synthesis of the proposed nanomaterials, we plan to investigate the dynamic assembly of the H-bonding nano-objects. Finally, the adaptive and dynamic mechanical properties of the nano-assembled materials will be investigated in solution, and solid state. Through the proposed study, we want to achieve the follow specific aims:
1. Design and synthesis two categories of H-bonding mediators that can be readily attached to various nano-objects including metallic, carbon-based, and inorganic nano building blocks.
2. Synthesize and investigate H-bonding mediated 1-D linear dynamic assemblies of gold nanoparticles (GNPs) and single wall carbon nanotubes (SWCNTs).
3. Synthesize and investigate H-bonding mediated 3-D dynamic assemblies of C_{60} and silica nanoparticles (SNPs).

The main strategy we use to a achieve our goals is *biomimicry*: copying nature's "bottom-up" approach to *multifunctional* and *mechanically robust* materials synthesis. Nature relies heavily on *weak, non-covalent,* and fundamentally *dynamic* interactions to organize load-bearing network structures over multiple length scales, often using a nano-composite strategy, imbuing natural materials with remarkable toughness, multifunctionality, and self-healing capability. Recently-developed synthetic techniques now enable materials scientists to rapidly and reliably synthesize well-defined polymeric and polymer/nanoparticle hybrid species, with diverse architectures and excellent functional group accessibility. This advance dramatically enhances our ability to translate specific bio-inspired molecular designs into functional polymers and nano-objects, opening up the synthetic space necessary to understand and control assembly of biomimetic materials. In earlier work (including DOE supported work dating back to 2009) we successfully combined the biomimetic design principles of modularity and programmed non-covalent interactions to obtain advanced multifunctional self-assembling polymers[*1, 2, 3*] and materials.[*4, 5, 6*]

The projects involve the custom synthesis of novel dynamically-interacting oligomeric, polymeric, and polymer-grafted-particle nano-objects. The molecular constituents will be tuned to achieve controlled assembly of ordered, multiphase materials with specific emergent bulk properties. The project utilizes the broad spectrum of expertise of the group members in molecular and macromolecular synthesis and characterization, biomimetic self-assembly, X-ray scattering, scanning probe, electron, and optical microscopy characterization techniques.

Recent Progress

Hydrogen-Bonding Brush Polymers and Hybrid Polymer-Grafted Nanoparticles with Tunable Mechanical, Dynamic, and Self-Healing Properties

BACKGROUND

To achieve dynamic and adaptive advanced materials, a common strategy Nature employs is the use of *supramolecular assembly of nano building blocks*. These building blocks are themselves modular assemblies of smaller constituents, such as protein polymers, as in the case of the F-actin cytoskeleton, and inorganic nanoparticles, which form a highly ordered protective superlattice in the case of nacre. Inspired by supramolecular biopolymers and natural nanocomposites, we propose here to synthesize and investigate dynamic and adaptive materials formed by *H-bonding-mediated* assembly of synthetic nano building blocks. This bottom-up nano assembly approach to materials design has several advantages: (a) following Nature's strategy, this may provide an effective method to assemble complex multicomponent materials from simple nano building blocks; (b) it may bridge a fundamental gap between the nanoscopic and macroscopic world for preparing bulk materials; and (c) the overall nano assemblies may have emerging properties that are totally different from their nano components or bulk counterparts. Programmed hydrogen bonding can serve as an ideal assembly mediator for the following reasons (1) the interactions are sufficiently strong to form stable nano assemblies while remaining reversible and dynamic; (2) the interactions are well-defined and have tunable specificity, which provides better system design control; (3) the system is chemically simple, stable, and convenient to prepare and scale up; and (4) the system is versatile in terms of further modification and processing conditions.

Discussion of Findings: We incorporate programmed dynamic interactions (H-bonds, etc.) into different polymer architectures to achieve self-assembled, multi-phase dynamic nanocomposites. The microstructure in bulk is analogous to that of conventional thermoplastic elastomers (TPEs) whose superior mechanical properties result from a self-assembled nanostructure consisting of stiff, glassy domains permanently connected by a flexible matrix. In our design, the covalent connections are replaced by dynamic supramolecular connections based on polyvalent dynamic interactions. Unlike covalent bonds, which rupture irreversibly due to highly reactive fracture intermediates, these dynamic connections can reform quantitatively after damage without external stimuli.

We synthesized a pendant-H-bond monomer which was used to grow polymer grafts from a styrene/ATRP graft initiator scaffold. It was predicted that hydrophobic backbone collapse in polar solvent should lead to a spheroidal bulk nanostructure upon drying. Indeed, the Hydrogen-bonding Brush Polymers self-assemble into dual-phase multiphase materials with tunable mechanical properties that exceed those of specialty commercial elastomers such as Neoprene (Figure 1B), while the same molecular architecture with blocked H-Bonds results in viscous fluids. Most importantly, these materials can self-heal even after catastrophic damage, with quantitative recovery of modulus, yield strength and up to 90% strain recovery after self-healing at r.t. (Figure 1C).

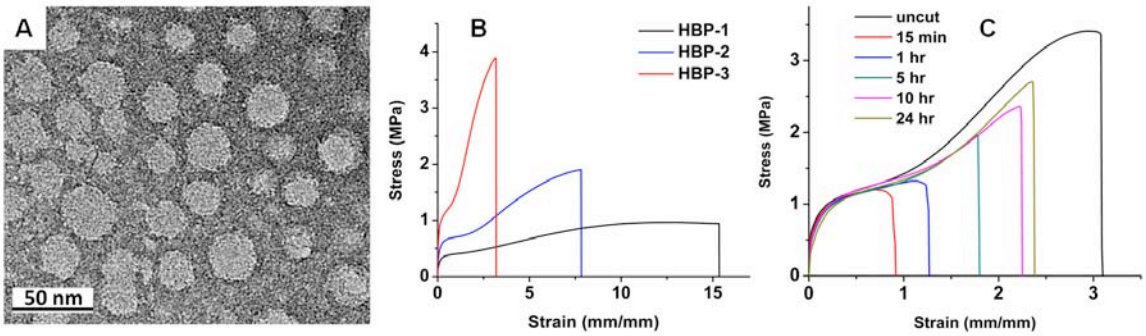

Figure 1. (**A**) A TEM cross-section of an HBP. The dark, continuous phase is the dynamic PHM phase, while the spheroids are composed of polystyrene (**B**) The mechanical properties of our first design are equivalent or better than commercial elastomers such as Neoprene, despite having a purely dynamic, non-covalently-linked nanophase morphology. (**C**) The self-healing properties of this initial system are as good or better than previous spontaneously self-healing elastomers, with *no additives* and with *rational control of nanostructure/mechanical properties*.

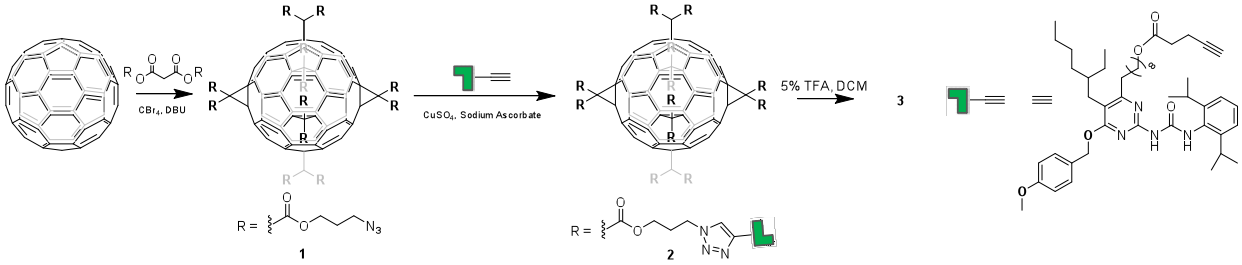

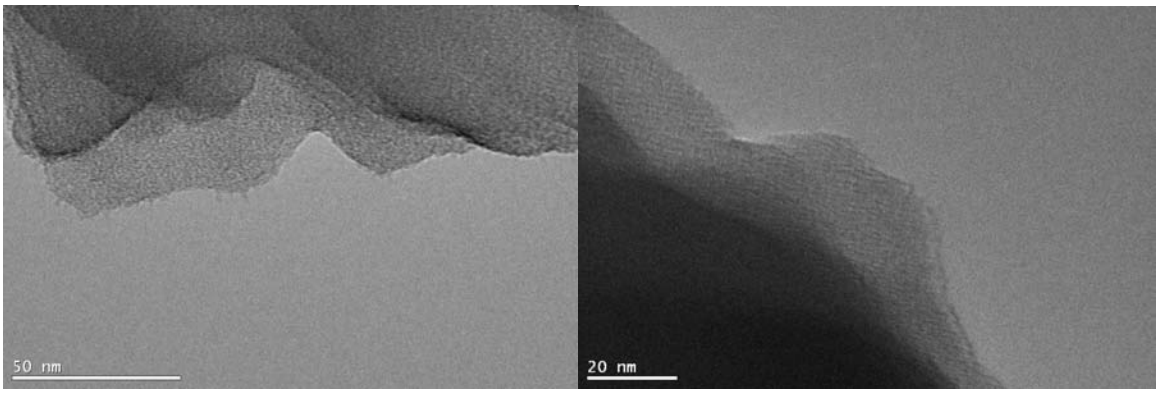

Figure 2. The synthesis of a C_{60}/UPy graft nano-object. After deprotection, the UPy-mediated assembly results in ordered micron scale thin films of C_{60} modules, as observed by TEM.

Assembly of nano-objects into better defined 3-D structures is also of great importance for the "bottom-up" manufacturing of macroscopic materials from nano building blocks. C_{60} is potential ideal for constructing 3-D dynamic assemblies due to its well-defined nanostructure, excellent mechanical properties, and well-developed functionalization methodologies. The assembly dynamics and overall properties of the material can be controlled by the concentration of tethered H-bonding units as well as the length and stiffness of the linker between C_{60} and H-bonding unit. We have synthesized UPy-functionalized C_{60}, and observed their controlled self-assembly into ordered nanosheets (Figure 2). We have also successfully demonstrated the

synthesis of hydrogen-bond-grafted silica SNPs, which self-assemble into mechanically robust, highly ordered bulk materials.

Importance of findings both from experimental and theoretical perspectives: While several groups have reported self-healing systems through the incorporation of encapsulated monomers, reversible or irreversible covalent bonds, and dynamic non-covalent bonding into polymers, these systems either require solvents/plasticizers, healing reagents, or external stimuli, such as heat or light. Our initial biomimetic design success is, to our knowledge, the first example of a material that has the ability to combine excellent self-healing with the desirable and tunable mechanical properties found in commercial thermoplastic elastomers into a multifunctional single-component system which will self-heal spontaneously without the need of any plasticizer, solvent, healing agents, or external stimuli, validating our multiphase dynamic self-assembly approach to advanced energy-relevant materials.

Future Plans

(1) Self-Assembly of Multiphase Self-Healing Elastomers
We will vary the structure our successful multiphase self-healing polymer system, both the backbone and the H-bond assembly mediator functionality, to obtain the structure/property understanding required to tailor these new materials to specific energy-materials applications.

(2) Self-Assembly of Highly-Ordered Nanocomposites
We will explore the self-assembly of C_{60} SNPs into ordered bulk photonic materials, varying the structural parameters of the H-bond assembly-mediator graft.

(3) Self Assembly of Stiff, Strong, and Self-Healing Nanocomposites
We will synthesize various inorganic nanoparticles functionalized with dynamic supramolecular motifs. Furthermore, we will investigate the self-assembly of them into bulk self-healing nanocomposites.

Publications in last two years (which acknowledge DOE support):

1. A.M. Kushner, Z. Guan, Modular Design in Natural and Biomimetic Soft Materials. *Angew. Chem. Int. Ed.*, in press (2011).
2. D. L. Guzman, A. Randall, P. Baldi, Z. Guan, Computational and single-molecule force studies of a macro domain protein reveal a key molecular determinant for mechanical stability. *Proc. Natl. Acad. Sci.* **107**, 1989 (2010).
3. Y.-X. Lu, Z.-M. Shi, Z.-T. Li, Z. Guan, Helical polymers based on intramolecularly hydrogen-bonded aromatic polyamides. *Chem. Comm.* **46**, 9019 (2010).
4. Y.L. Chen, Z. Guan, Bioinspired Modular Synthesis of Elastin-Mimic Polymers To Probe the Mechanism of Elastin Elasticity. *J. Am. Chem. Soc*. **132**, 4577 (2010).
5. A. M. Kushner, J. D. Vossler, G. A. Williams, Z. Guan, A Biomimetic Modular Polymer with Tough and Adaptive Properties. *J. Am. Chem. Soc.* **131**, 8766 (2009).
6. T.B. Yu, Z. Bai, Z. Guan, Cycloaddition-Promoted Self-Assembly of a Polymer into Well-Defined β-Sheet and Hierarchical Nanofibrils. *Angew. Chem., Int. Ed.* **48***,* 1097(2009).

Multicomponent Protein Cage Architectures for Photocatalysis

Arunava Gupta[(a)] and Peter E. Prevelige[(b)]

[(a)] University of Alabama, Tuscaloosa, AL 35487
[(b)] University of Alabama, Birmingham, AL 35294
agupta@mint.ua.edu
prevelig@uab.edu

Program Scope: This is a collaborative project between Drs. A. Gupta (University of Alabama), P. Prevelige (Univ. Alabama Birmingham), T. Douglas (Montana State Univ.), and B. Kohler (Montana State Univ.) The primary goal of the project is to develop protein-templated approaches for the synthesis and directed assembly of semiconductor nanomaterials and dyes that are efficient for visible light absorption and hydrogen production. In general, visible-light-driven photocatalysis reactions exhibit low quantum efficiency for solar energy conversion primarily because of materials-related issues and limitations, such as the control of the band gap, band structure, photochemical stability, and available reactive surface area of the photocatalyst. Synthesis of multicomponent hierarchical nano-architectures, consisting of semiconductor nanoparticles (NPs) and coordination polymers with desired optical properties fabricated to maximize spatial proximity for optimum electron and energy transfer represents an attractive route for addressing the problem.

Virus capsids are highly symmetrical, self-assembling protein cage nanoparticles that exist in a range of sizes and symmetries. Selective deposition of organic or inorganic materials, by design, at specific locations on virus capsids affords precise control over the size, spacing, and assembly of nanomaterials, resulting in uniform and reproducible nano-architectures. We utilize the self-assembling capabilities of the 420 subunit, 60 nm icosahedral, P22 virus capsid to direct the nucleation, growth, and proximity of a range of component materials. Controlled fabrication on the exterior of the temperature stable shell is achieved by genetically encoding specific binding peptides into an externally exposed loop which is displayed on each of the 420 coat protein subunits. Localization of complimentary materials to the interior of the particle is achieved through the use "scaffolding-fusion proteins. The scaffolding domain drives coat protein polymerization resulting in a coat protein shell surrounding a core of approximately 300 scaffolding/fusion molecules. The fusion domain comprises a peptide which specifically binds the semi-conductor material of interest.

Recent Progress: In this funding period we have built on our previous success in nucleating the formation of CdS and ZnS nanocrystals on the exterior of P22 to explore the feasibility of employing scaffolding-fusion proteins to nucleate internal nano-crystal formation. Fusion scaffolding proteins were designed based on the observation that an N-terminally deleted version of the 303 amino acid scaffolding protein spanning residues 141-303 was capable of promoting assembly both *in vivo* and *in vitro*. Using standard molecular biology techniques, coding sequences encoding short peptides reported to bind CdS (amino acid sequence:SLTPLTTSHLRS) or TiO_2 (amino acid sequence:CHKKPSKSC) were introduced at the N-terminus of the coding sequence of the 141-303 scaffolding protein deletion. Based on our observed ability to package large cargos such as green fluorescence protein inside P22 capsids by co-expression a fusion gene encoding the silaffin (rSilC)-141-303 scaffolding protein was also

constructed. rSilC has been reported to induce the formation of both amorphous and rutile TiO_2 in solution.

Synthesis of CdS nanocrystals confined within the procapsids: To exert control over the amount of fusion scaffolding protein within the PCN cage the CdS-scaffolding fusion peptide was cloned into a pET based expression vector and purified using ion exchange chromatography. Previous published data demonstrated that the truncated protein could re-enter preformed shells which had been stripped of their scaffolding protein. We used analytical ultracentrifugation to ascertain that the CdS fusion peptide could similarly re-enter preformed procapsids (Figure 1). The PCNs were treated with for 24 hrs. When examined by transmission electron microscopy after both 2 and 24 hrs, CdS nanocrystals were evident inside the PCNs (Figure 2). The average size of the nanocrystals was 40-50 nm, and the size did not increase between 2 and 24 hrs. Dynamic light scattering measurements (DLS) demonstrated that there was no change in particle diameter upon CdS mineralization.

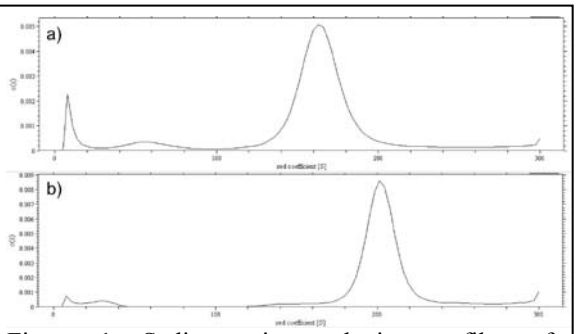

Figure 1: Sedimentation velocity profiles of procapsid shells (a) and re-entry reaction of engineered scaffolds and procapsid shells (b) with sedimentation coefficients of 160 S and 200 S respectively

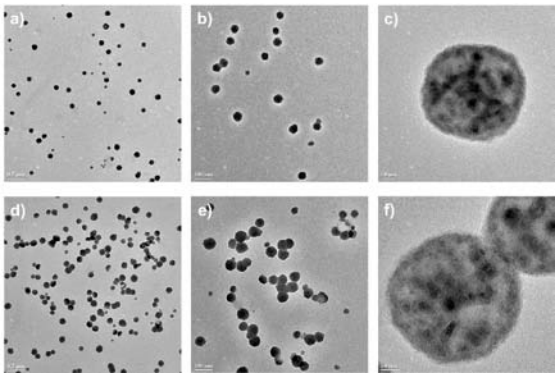

Figure 2: Transmission Electron Microscopy (TEM) images of the CdS nanocrystals synthesized inside the procapsids with CdS binding peptide engineered scaffolds. Micrographs are after 2 hours of the reaction (a-c) and 24 hours of the reaction (d-f). Size of the nanocrystals did not change over the period of 24 hours

Synthesis of TiO_2 nanocrystals confined within the procapsid: We have explored two strategies for synthesizing TiO_2 nanocrystals within the procapsid. In the case of the scaffolding fusion with the nine residue TiO_2 binding peptide we employed a strategy similar to that used for the CdS, re-entry of the fusion protein into preformed shells. In the case of the silaffin fusion protein the size of the silaffin domain (204 amino acids) precludes its re-entry through the pores in the capsid lattice. Therefore, the strategy employed was to clone this gene into the "assembler" plasmid and produce and purify icosahedral particles containing a core of silaffin/scaffolding fusion protein.

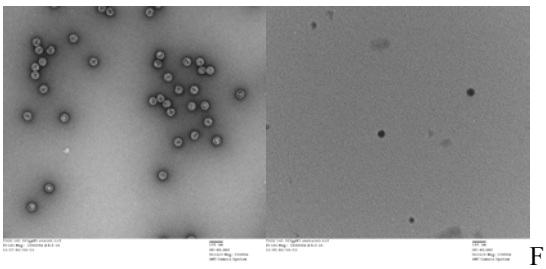

F

Figure 3 T EM of uranyl-acetate stained P22 procapsids containing the TiO_2-fusion scaffolding protein (left) and unstained micrographs of the same particles following TiBALDH treatment (right).

TiO_2-Scaffolding fusion protein: Procapsids containing the TiO_2-scaffolding were purified but were found to pose two problems, (1) the abundance of lysine residues in the sequence resulted in DNA being trapped within the particles, and perhaps related (2) the amount of

TiO_2-scaffold within the procapsids was approximately 50% of the amount seen with the wild type scaffolding protein. Therefore, a re-entry strategy was employed. Empty shells were incubated with TiO_2-scaffold and subsequently purified and characterized by analytical ultracentrifugation and DLS. The observed shift in sedimentation co-efficient and zeta potential indicated that the TiO_2-scaffold efficiently re-enters the shells while the DLS measurements show that this occurs without resulting in an increase in particle size. Treatment of the particles with TiBALDH followed by TEM revealed internal mineralization by TiO_2 (Figure 3).

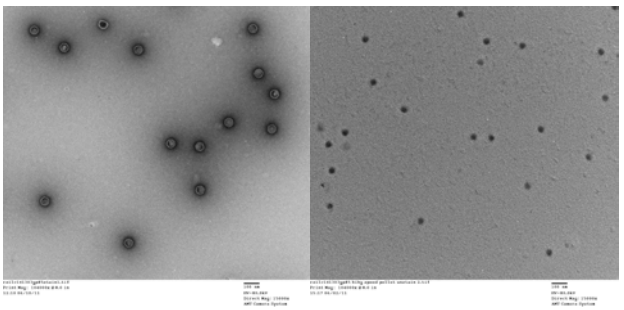

Figure 4 T EM of uranyl-acetate stained P22 procapsids containing the sillafin-scaffolding fusion protein (left) and unstained micrographs of the same particles following TiBALDH treatment (right).

Sillafin-Scaffolding Fusion: A gene encoding rSilC (obtained from N. Kroger) was fused to the 141-303 scaffolding protein truncation. This construct was used for the production of procapsids containing the sillafin-scaffolding fusion in *E. coli*. These particles were characterized by sedimentation and DLS and were seen to have wild type diameters and sedimentation coefficients. Purified procapsids were treated with TiBALDH and examined by TEM (Figure 4). Similar to the results obtained with TiO_2-scaffolding fusion protein these particles also revealed internal mineralization by TiO_2.

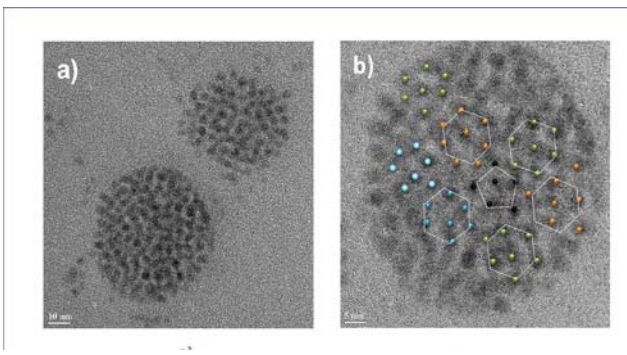

Figure 5 (a) Transmission Electron Microscope (TEM) micrographs showing assembly of 5 nm CdS nanoparticles on P22 procapsid shells. (b) TEM micrograph depicting the hexameric and pentameric patterns of assembly of CdS nanoparticles on a single P22 procapsid shell.

Binding of Preformed CdS Nanoparticles to the Exterior Surface of P22 Procapsids: Building on our success with nucleating CdS nanocrystal formation on the exterior surface of P22 procapsids we tested the ability of wild-type P22 procapsids to bind preformed 6 nm CdS nanocrystals. CdS nanocrystals were reacted with P22 procapsids for 2-24 hours. TEM analysis demonstrated that the CdS nanocrystals had bound to the procapsids in a templated manner reflecting the underlying T=7 pentamer and hexamer driven icosahedral symmetry of the particle (Figure 5). DLS measurements corroborated the TEM observations that the CdS particles were on the exterior surface of the procapsids.

Future Plans:

Formation of CdS/TiO_2 Hybrid Particles: Having demonstrated our ability to mineralize the interior and exterior of the particles in a controlled manner we will now generate hybrid particles with external CdS and internal TiO_2. We will take advantage of two paths towards exterior mineralization with CdS (nucleation and binding preformed CdS particles) and the two paths towards interior TiO_2 mineralization (TiO_2-scaffolding fusion and sillifan-scaffolding fusion).

Hybrid particles produced by these different approaches will be analyzed for integrity, stability, and the amount of each component bound.

Characterization of TiO_2 Containing Particles: Electron and x-ray diffraction studies of the CdS, grown both inside and outside the P22 shell, show that they are crystalline and have the wurtzite (hexagonal) structure. We plan to do similar studies on the TiO_2 particle to determine whether they are crystalline (rutile, anatase) or amorphous. Heat treatment studies will be carried out in order to investigate the phase transformation of the particles.

Photoelectrochemical measurements on the TiO_2 and CdS/TiO_2 hybrid particles will be performed using an electrochemical analyzer in a standard three-electrode configuration with a platinum counter electrode, a saturated Ag/AgCl reference electrode, and semiconductor working electrode. Visible spectrum measurements will be obtained using a Xenon lamp or appropriate LED lamp. This system will also be used to test the properties of a solar cell by studying the photosplitting of water being studied at a potential of 0.50 V (vs. Ag/AgCl). We will also set up a heterogeneous photocatalytic reaction system and measure gas evolution by gas chromatography.

Publication 2010-2011:

L. Shen, N. Bao, A. Kale, P. E. Prevelige, A. Gupta; Bio-templating Synthesis of Nanomaterials using Genetically Engineered Protein Templates, *Journal of Materials Chemistry*, Invited Review (2011), submitted.

A. O'Neil, C. Reichhardt, B. Johnson, P.E. Prevelige, T. Douglas; Genetically programmed in vivo packaging of protein cargo and its controlled release from bacteriophage p22, Angew Chem Int Ed 2011, 50, 7425-7428

C. Reichhardt , M. Uchida M, A. O'Neil, R. Li, P.E. Prevelige, T. Douglas; Templated assembly of organic-inorganic materials using the core shell structure of the P22 bacteriophage, *Chem Commun* 2011, 47, 6326-6328.

Kang, S., M. Uchida, A. O'Neil, R. Li, P.E. Prevelige, and T. Douglas; Implementation of P22 viral capsids as nanoplatforms. *Biomacromolecules.* 2010, 11, 2804-2809.

L. Shen, N. Bao, P. E. Prevelige, A. Gupta; Fabrication of Ordered Nanostructures of Sulfide Nanocrystal Assemblies over Self-Assembled Genetically Engineered P22 Coat Protein, *Journal of the American Chemical Society* 2010, 132, 17354-17357.

L. Shen, N. Bao, P. E. Prevelige; A. Gupta "Escherichia coli Bacteria-Templated Synthesis of Nanoporous Cadmium Sulfide Hollow Microrods for Efficient Photocatalytic Hydrogen Production, *J. Phys. Chem. C* 2010, 114, 2551-2559.

Y. Wang, N. Bao, A. Gupta; Shape-Controlled Synthesis of Semiconducting CuFeS2 Nanocrystals, *Solid State Sciences* 2010, 12, 387-390.

Program Title: Uniform light-activated polymer vesicles for nanoparticle release

Principal Investigator: Daniel A. Hammer, co-PI: Daeyeon Lee
Mailing Address: Chemical and Biolmolecular Engineering, 311A Towne Building, 220 S. 33rd Street, University of Pennsylvania, Philadelphia, PA 19104
E-mail: hammer@seas.upenn.edu

Program Scope

The goal of this project is to design smart, responsive microcapsules that can respond to changes in environmental stimuli and induce collective behavior of other sentinel particles on length-scales well beyond that of the capsule itself. The general principle that will be employed is particle taxis – or directed motion – in response to nanoparticles that are released from a source capsule in response to light or change in pH. Much of the theory for interparticle communication and collective response has been developed by a DOE-funded effort by Dr. Anna Balazs (see, eg, Kolmakov et al., 2010); our goal is to test these predictions experimentally. Central to our design are polymersomes – vesicles whose outer membrane is assembled from block-co-polymers. We have shown that we can make large, uniform populations of polymersomes and have designed these capsules to encapsulate and release active agents such as nanoparticles or molecules in response to stimuli such as light. In the proposed experiments, we will release encapsulated nanoparticles from photo-sensitive or pH-sensitive polymersomes, and induce the motion of target particles through haptokinesis (by making a gradient of particles on a surface) or chemokinesis (making a gradient of particles in solution). Photosensitive polymersomes are constructed by incorporating porphyin dyes (synthesized by Michael J. Therien, Duke University) within the hydrophobic core of the polymersome membrane, and combining an inter-lumenal solute that associates with the membrane's inner leaflet, leading to a differential stress and membrane failure (Kamat et al., 2010). We can use these photo-responsive vesicles to release nanoparticles designed to interact with neighboring sentinel particles. By constructing spatial, ordered arrays of microcapsules using micro-contact printing, and by using nanoparticles and surfaces with tailored adhesiveness, we will endeavor to make a direct test of the principles of collective smart particle motion predicted theoretically. The long-term impact of this work will be to develop autonomous, self-regulating motion of microcapsules that can communicate, mimicking biological activity.

The specific objectives of this work will be:

1. To encapsulate and release nanoparticles from uniform polymersomes in response to light and pH.
2. To use specific adhesion and micro-contact printing to make specific spatial arrays of polymersomes and microparticles.
3. To demonstrate of collective motion of micron-sized particles in response to light and pH. We will adhere particles on printed arrays. We will combine photoresponsive or pH sensitive polymersomes, equipped with nanoparticles, as signaling particles, and vary the density and spacing of target receiving particles. Upon change in stimulus, we will use video microscopy to observe the collective motion of particles on the surface. Collective motions will be catalogued as a function of interparticle spacing, nanoparticle density, and particle size.

a) We will perform experiments with multiple signaling particles, with intervening fields of target particles, to understand how competitive fields of stimuli can induce motion of particles in the field.
b) Additionally, we will compare haptokinesis (in which signaling particles emit nanoparticles that adsorb to substrates) to chemokinesis (in which soluble molecules adsorb to the surface of the surface of the target particles). The latter is potentially more useful, since it is easier to encapsulate and secrete molecules than nanoparticles from signaling vesicles, without any loss of potency.

Recent Progress

Fabrication of uniform polymersomes using microfluidics templating. To perform the proposed work, it is necessary to make large numbers of uniform micron-sized vesicles that encapsulate precise amounts of nanoparticles. One of us (Lee) learned microfluidic templating in David Weitz's laboratory (Utada et al.; 2005), and we have now established methods for making polymer vesicles using this technique, illustrated in Figure 1. A n inner aqueous phase containing a solute is ejected through the center of a pipette filled with organic solvent (toluene and chloroform) and a polymer (in this case, poly(ethylene oxide)-*b*-poly(butadiene); PEO-PBD); these in turn are captured into an outer aqueous phase. We have recently shown that large uniform populations of giant polymersomes (mean diameter ~ 50 m icrons) can be made by this technique, that the organic solvent is removed from the inner membrane after about two weeks, during which the area expansion modulus asymptotically approaches values seen for unilamellar vesicles with single bilayers made by film rehydration (see Figure 1, Kamat et al., 2011).

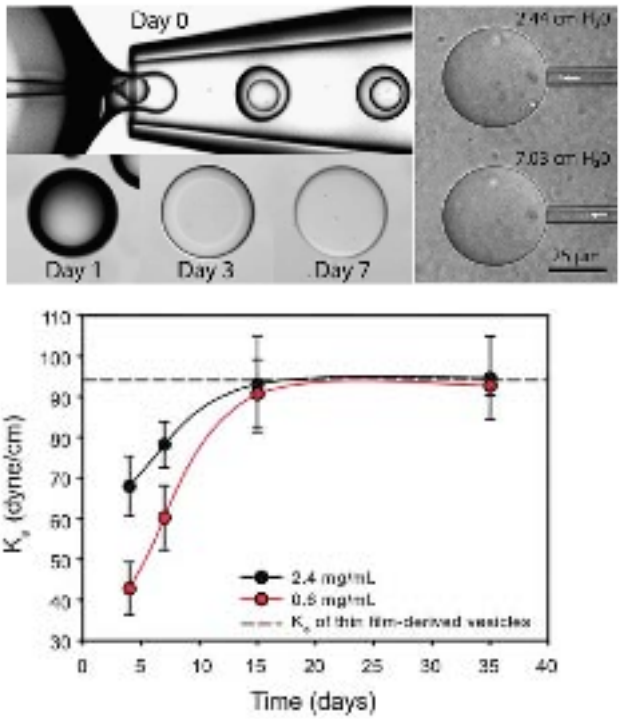

Figure 1. Polymersomes of PEO_{30}-*b*-PBD_{46} were made by microfluidic templating (upper left). Vesicles were progressively annealed through solvent evaporation over two weeks (shown in progression through 7 days). Micropipette aspiration (illustrated upper right) was used to measure the area expansion modulus K_a of the membranes at two different polymer concentrations as a function of time, where K_a asymptotically approaches the value for a rehydrated vesicle. These measurements demonstrate that removal of solvent takes close to two weeks (Kamat et al., 2011).

Photorelease of porphyrin-containing polymersomes. We have recently established the conditions that are required for the photorelease of the contents of a polymersome vesicles in response to light. Polymer vesicles made of PEO-PBD were made by rehydration with porphyrin in the membrane; porphyrin and polymer were co-mixed and dried on a Teflon substrate and

rehydrated in the presence of Dextran at different concentrations and of molecular weights. We found that upon illumination of vesicles at the excitation wavelength of the porphyrin, we see photo-release, as shown in Figure 2. Note, photorelease is not seen in absence of Dextran. We have also shown that prior to release, changes in the optical emission of porphyrin fluorescence due to configurational reordering of the porphyrin allows monitoring the strain of membranes optically; the result is that optical polymersomes can be used as stress sensors (Kamat et al., 2011b).

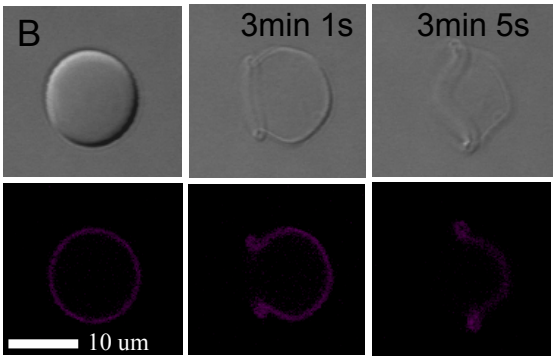

Fig. 2. Polymersomes loaded with Dextran and membrane porphyrin are photoresponsive, and release contents in response to light illumination. We have measured how the degree of release is controlled by the concentration of porphyrin, the molecular weight of the polymer, and the concentration and molecular weight of the Dextran (Kamat et al., 2010). Upper row shows vesicles in DIC; the lower row, in porphyrin fluorescence.

Release of nanoparticles from vesicles in response to optical illumination. We have achieved the goal of encapsulating a controlled number of particles with polymersomes. Polymersomes were made with different numbers of 1 μm amidated beads using microfluidic templating, controlled by changing the density of beads in the inner aqueous core. Figure 3 illustrates the systematic incorporation of different numbers of particles per polymersome.

Optical release of particles from porphyrin-containing polymersomes. We have shown that polymersomes made of PEO-PBD with nanoparticles incorporated in the aqueous lumen and porphyrin in the membrane can be induced to release nanoparticles in response to optical illumination. 800 nm carboxylated beads were entrapped in the center core by microfluidic templating, and a dimeric porphyrin (meso-to-meso ethyne-bridged (porphinato)zinc(II) dimer, PZn_2) was encapsulated within the polymer phase. Optical illumination in excitation band of the porphyrin leads to disruption of the vesicle and release of the particles into the bulk (see Figure 4). Note, previously, the aqueous solute that enabled photorelease was Dextran; however, we have recently found release can be achieved solely with nanoparticles in the core (and porphyrin in the membrane). The origin of the release is then either osmotic pressure or surface interactions between the particles and the inner membrane.

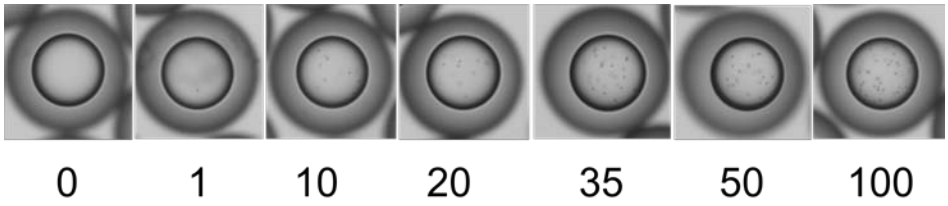

Figure 3. Polymersomes have been made with controlled numbers of 1 micron amidated particles (number indicates the average number of particles per polymersome).

Future Plans

(1). Identifying the design rule and mechanisms for optical release of nanoparticles. We have shown that encapsulating nanoparticles in porphyrin-containing vesicles can lead to optical release, but we have not quantified the relationship between particle density, particle chemistry, porphyrin concentration, and polymer molecular weight and composition that are required for photorelease. A critical question is, what is the minimum density of particles that are required for optical release? Mapping the phase diagram of vesicle failure will ultimately enable elucidation of the mechanism.

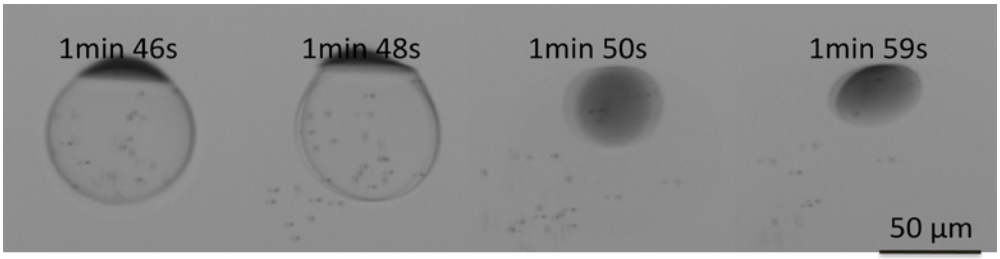

Figure 4. Illumination of polymersomes containing 800 nm carboxylated nano-particles and membrane porphyrin leads to nanoparticle release.

(2). Slow release of nanoparticles. We will make vesicles that can slowly release nanoparticles, using poly(ethylene oxide)-poly(caprolactone) vesicles using that slowly hydrolyze at low pH, and embedding nanoparticles either within the aqueous lumen of the membrane shell.

(3). Making ordered arrays of sentinel particles using microcontact printing. We will employ receptor-ligand binding using weak interactions to place sentinel particles in ordered arrays. This will involve printing avidin, biotin, and protein A/G, and attaching particles with appropriate adhesive chemistry for immobilization. The goal is to weakly tether particles at locations so that gradients of adhesion can lead to significant displacements of the mobile particles.

References (which acknowledge DOE support)

Neha P. Kamat, Myung Han Lee, Daeyeon Lee, and Daniel A. Hammer, (2011), "Micropipette aspiration of double emulsion generated, unilamellar polymersomes", in press, Soft Matter.

Other references

Neha P. Kamat, Gregory P. Robbins, Michael J. Therien, Ivan J. Dmochowski, *and* Daniel A. Hammer, (2010) "A generalized system for photo-responsive membrane rupture in polymersomes," Advanced Functional Materials 20:2588-2596; DOI: 10.1002/adfm.201000659.

Neha P. Kamat, Zhengzheng Liao, Laurel E. Moses, Jeff Rawson, Michael J. Therien, Ivan J. Dmochowski, and Daniel A. Hammer, (2011) "Sensing membrane stress with near IR-emissive porphyrins", in press, Proceedings of the National Academy of Sciences USA.

Kolmakov, G.V., V.V. Yashin, S.P. Levitan, and A.C. Balazs, Designing communicating colonies of biomimetic microcapsules. Proceedings of the National Academy of Sciences of the United States of America, 2010. **107**(28): p. 12417-12422.

Utada, A.S., E. Lorenceau, D.R. Link, P.D. Kaplan, H.A. Stone, and D.A. Weitz, Monodisperse double emulsions generated from a microcapillary device. Science, 2005. **308**(5721): p. 537-541.

Bio-inspired Architectures for Controlled Adhesion, Friction, and Surface Compliance

Anand Jagota* (anj6@lehigh.edu) and Chung-Yuen Hui[&] (ch45@cornell.edu)

* Department of Chemical Engineering & Bioengineering Program, Lehigh University,
[&] Sibley School of Mechanical and Aerospace Engineering, Cornell University, Ithaca,

1. ***Program Scope:*** Our aims are to fabricate, study, and model bio-inspired architectures for controlled surface mechanical properties such as adhesion, friction, and surface compliance. The focus of our current work is on

- *Active control of adhesion and friction* by designing a mechanically bistable surface based on a film-terminated architecture. This surface can be switched repeatedly between an adhesive/high friction and non-adhesive/low friction state.
- *Adhesion Selectivity in Surfaces* by (a) shape, and (b) electrostatic complementarity. We have demonstrated selectivity by shape complementarity using rippled and channel/pillar surface architectures. We have also shown theoretically how surfaces with stripes of charge can lead to highly selectivity of adhesion.

2. ***Recent Progress:*** Our main recent accomplishments are

a. *Active Switching of Adhesion and Friction* [4]:

We demonstrated that the film-terminated fibrillar structure (Figure 1(a)) can be designed such that the surface can be switched between two states, one in which the terminal film is uncollapsed and another one in which it is collapsed [4]. Figure 1 (b) shows qualitatively that the uncollapsed and collapsed states have very different adhesive properties. The region in the background is in the uncollapsed state while the region in the foreground is in the collapsed, apparently rough, state. Particles adhere to the uncollapsed region but are easily removed from the collapsed region.

Figure 1(c) shows results of indentation experiments. In the uncollapsed state, the surface is highly adhesive with a pull-off load of about 10 mN. In the collapsed state adhesion is negligible. We can switch the surface between the collapsed and uncollapsed state repeatedly without any significant change in properties. The switch in adhesive properties is mirrored by frictional properties, i.e., the uncollapsed state has much higher friction than the collapsed state. We are working on

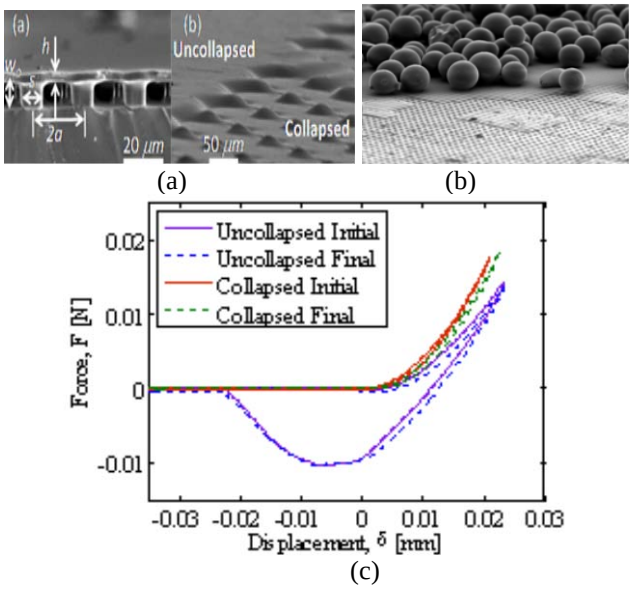

Figure 1 (a) A film-terminated structure can exist in one of two metastable states, flat and bumpy. (b) Qualitative demonstration that the two metastable states have very different adhesive properties. Particles remain stuck to the region in the uncollapsed state (towards the back/upper end of the micrograph), whereas they are easily removed from the collapsed region (foreground of the micrograph). (c) Indentation experiment to measure compliance and adhesion shows strong adhesion in the uncollapsed state (blue plots) and negligible adhesion in the collapsed state (red and green plots).

detailed quantitative models for the mechanics of collapse and conditions for bistability.

b. *Adhesion Selectivity Using Surfaces with Ripples and Pillar/Grooves*

A common motif in nature is that of selective adhesion by shape or inter-surface force complementarity. We have begun to study these two approaches to achieving selective adhesion. In collaboration with Prof. Shu Yang of the University of Pennsylvania, we have shown that highly selective adhesion can be achieved by using rippled surfaces (Figure 2(a)). Two specimens with matched amplitude and wavelength adhere well to each other and have poor adhesion to others. Figure (2(b)) shows measured crack velocity as a function of applied energy release rate. We find that adhesion of complementary surfaces is actually enhanced compared to that of flat controls whereas that of non-complementary surfaces is immeasurably small. Our quantitative model for crack-trapping based enhancement of adhesion matches experimental measurements very well.

Figure 2(c) shows a pillar-channel surface architecture which we are currently investigating as another method to achieve selectivity of adhesion. Figure 2(d) shows that such complementary surfaces can be brought into contact and that small misorientation or relative shear is accommodated by dislocation lines. We find very significant enhancement of adhesion, by up to a factor of 40.

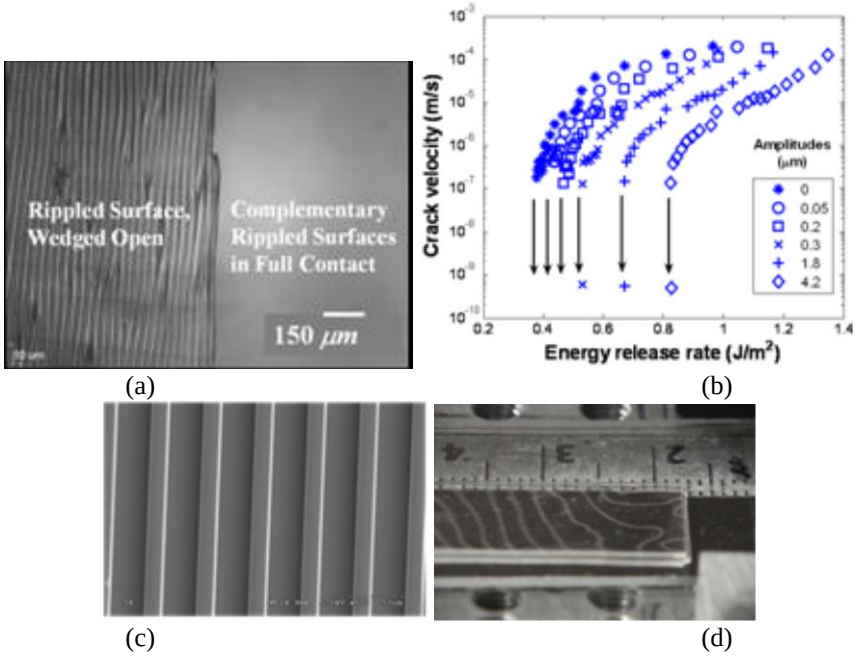

Figure 2 (a) Optical micrograph of two complementary surfaces in intimate conformal contact (to the right of the crack tip). The sample is being wedged open from the left. (b) Crack velocity as a function of energy release rate for conformal rippled surfaces. Adhesion between conformal surfaces increases with increasing ripple amplitude. Adhesion between surfaces with mismatched amplitude or wavelength is very poor. (c) Pillar-channel structure (d) Surfaces with complementary pillar-channel structures adhere well to each other with small misorientation or relative shear accommodated by dislocations that appear as lines.

c. *Adhesion Selectivity by Electrostatic Complementarity* [7,8].

To begin our study of adhesion selectivity by electrostatic complementarity we have considered surfaces patterned with strips of charge. We show that pairs of such surfaces have strong recognition and that this recognition is modulated by elasticity (Figure 3).

d. *Other work supported by this grant.* We wrote an extensive review of the growing and active field of biomimetic and bioinspired structured interfaces [9]. It is our hope that this paper will not only provide a detailed exposition and critique of the state of the art, but also help to promote its future growth. A number of problems related to structured surfaces require analysis of their contact mechanics and extraction of properties from indentation experiments. We have worked on both the theoretical and experimental aspects of this problem. On the theoretical side, we have developed a new technique that allows general and powerful analyses of the contact mechanics of structured surfaces [10]. We have additionally shown how indentation experiments can be designed so that they can be used to extract works of adhesion for arbitrarily large elastic deformations [12]. Friction testing of fibrillar interfaces by our group and others has shown that fibrils can buckle under combined compression and shear, for which we have developed mathematical models [14,15]. In collaboration with Ronsin and Baumberger, we have studied some basic mechanisms of friction [11]. A fundamental problem closely related to our DOE project is how to model adhesion and slip along interfaces. The standard approach is to use a cohesive zone model which assumes that the interfacial tractions are potential functions of interfacial displacements. We have published an extensive analysis and review of cohesive zone models for adhesion and fracture [5] where we discussed the limitation of various approaches and developed a damage based interface model. Our previous DOE-supported work on crack-trapping, it turns out, can be used to understand the resistance of barnacles to interfacial failure. Barnacles are small marine invertebrates that foul structures such as the hulls of ships. In collaboration with Dr. Kathryn Wahl of US Naval Research lab, we have shown that barnacles resist removal by a crack trapping mechanism [13].

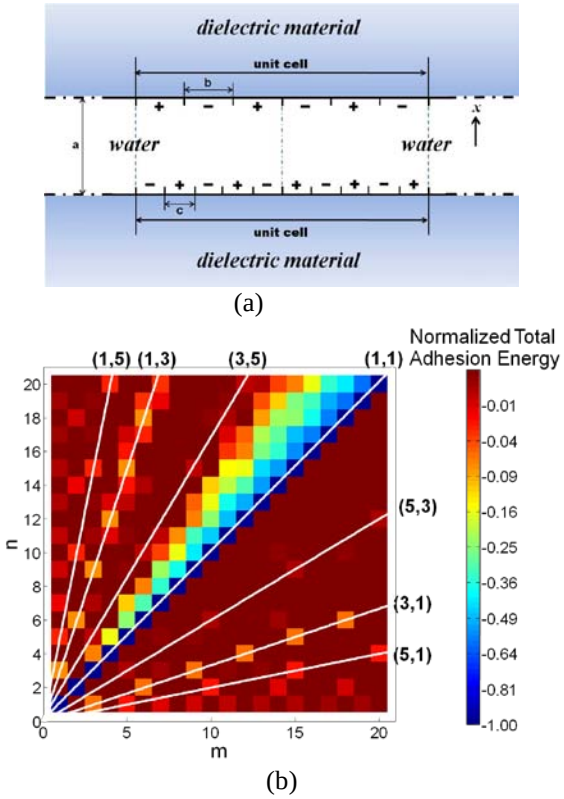

Figure 3 (a) Schematic diagram of surfaces patterned with stripes of charge (*mb=nc,* in this case, *3b=5c*). Two infinitely large surfaces with striped patterns of alternating positive and negative charges on a dielectric material face each other in aqueous medium. (b) Plots of interaction energy between two patterned surfaces for different *m* and *n*. (Negative values represent adhesion.) Each square represents a single (*m,n*) combination and is colored using the (non-linear) scale shown to the right of the figure. Results below the diagonal, i.e., for *m>n,* are for two rigid surfaces; those above the diagonal (*m<n*) are for a deformable surface

3. Future Plans

- *Active Control of Adhesion and Friction.*

We are following up on our initial demonstration of active control by bistability to develop a quantitative understanding of (a) conditions under which the collapsed and uncollapsed states are bistable and (b) pressure needed to initiate initial collapse.

- *Channel-Pillar Complementary Surfaces*.

Our work on channel-pillar complementary surfaces is ongoing. We will study what architectural parameters are optimal and will develop a quantitative understanding of the novel dislocation-like defects, their effect on adhesion and friction, and how to reduce it.

- *Selectivity by Electrostatic Complementarity.*

We will work to realize experimentally the prediction that surfaces with appropriately designed stripes of charge can be made to exhibit strong selectivity.

4. ***Publications resulting from DOE support (August 2009- August 2011)***

1. Jingzhou Liu, C.Y. Hui, A. Jagota, L. Shen, "A model for static friction in a film-terminated micro-fibril array," *Journal of Applied Physics*, **106** [5] 053520 (2009).
2. Jingzhou Liu, C-Y. Hui, A. Jagota, "Effect of fibril arrangement on crack trapping in a film-terminated fibrillar interface," *Journal of Polymer Science Part B: Polymer Physics* **47** [23] 2368-2384 (2009).
3. Shilpi Vajpayee, Anand Jagota, Chung-Yuen Hui , "Adhesion of a Fibrillar Interface on Wet and Rough Surfaces," *Journal of Adhesion*, **86** [1] 39-61 (2010).
4. Nichole Nadermann, Jing Ning, Anand Jagota, C-Y. Hui, "Active Switching of Adhesion in a Film-Terminated Fibrillar Structure," *Langmuir*, **26** (19) 15464-15471 (2010).
5. C.Y. Hui, A. Ruina, R. Long, A. Jagota, "Cohesive Zone Models and Fracture", *Journal of Adhesion*, **87** [1] 1-52 (2011).
6. Shilpi Vajpayee, Krishnacharya Khare, Shu Yang, Chung-Yuen Hui, Anand Jagota, "Adhesion Selectivity Using Rippled Surfaces", *Advanced Functional Materials*, **21** [3] 547-555 (2011).
7. Ying Bai, Congrui Jin, Anand Jagota, C-Y. Hui, "Adhesion Selectivity by Electrostatic Complementarity: Part I, One-dimensional stripes of charge," *Journal of Applied Physics*, in the press (2011).
8. Congrui Jin, Ying Bai, Anand Jagota, and Chung-Yuen Hui, "Adhesion Selectivity by Electrostatic Complementarity: Part II, Two dimensional Analysis," *Journal of Applied Physics*, in the press (2011).
9. Anand Jagota and C-Y. Hui, "Adhesion, Friction, and Compliance of Bio-mimetic and Bio-inspired Structured Interfaces*," Materials Science and Engineering – Reviews*, accepted (2011).
10. C. Jin, A. Jagota, C-Y. Hui, "An easy-to-implement numerical simulation on adhesive contact problems involving complex geometries," under review (2011).
11. O. Ronsin, T. Baumberger, C.Y. Hui, "Nucleation and propagation of quasi-static interfacial slip pulses," *Journal of Adhesion*, 87,504-531 (2011).
12. C.Y. Hui and R. Long, "A Compliance based, Model Independent Method to determine the Work of Adhesion in Contact Experiments: Generalization of JKR Theory to Flexible Structures and Large Deformation." *Journal of Adhesion,* accepted for publication, (2011).
13. C.Y. Hui, Rong Long, K. J. Wahl, R. K. Everett, Barnacle resist removal by crack trapping, *Royal Soc. Interface*, 6, 8(59):868-79 (2011)
14. N. Nadermann, A. Kumar, S. Goyal and C.Y. Hui, "Buckling of sheared and compressed microfibrils", *Royal Soc. Interface*, 7, 1581-1589(2010)
15. Kumar and C.Y. Hui, "Numerical study of shearing of a microfiber during friction testing of a microfiber array", Proc. R. Soc. A, 467, 1362-1389, (2011)

Engineering the Interface Between Inorganic Materials and Cells

PIs: Ravi Kane, Rensselaer Polytechnic Institute and David Schaffer, University of California, Berkeley
kaner@rpi.edu, schaffer@berkeley.edu

i) Program Scope

This new project is motivated by the goal of interfacing biological and non-biological components to create "living materials". Our proposed work will focus on cellular engineering efforts to endow cells with the capability to respond to novel signals and to integrate cells with pristine inorganic materials. To further optimize cell function in hybrid "living materials", it would be advantageous to render cells responsive to novel "orthogonal" cues, i.e. signals they would not ordinarily respond to but that can be engineered to feed into defined intracellular signaling pathways. To that end, we are pursuing a protein engineering approach to endow cells with the ability to respond to light as a novel signal. To complement efforts based on engineering the surface chemistry of materials, we will also explore cellular engineering efforts to promote cell adhesion on inorganic materials.

ii) Recent Progress

Our initial focus has been to design a system to mediate "light-initiated protein degradation". The ability to degrade a protein of interest in a controlled fashion would provide a useful handle to control many cellular functions. Our approach makes use of the photoreactive PHR domain from the cryptochrome 2 protein (Figure 1), which upon photoexcitation heterodimerizes with the protein CIB. This property has recently been harnessed to inducibly recruit proteins to the cell surface membrane [2], a result we were able to reproduce (Figure 2).

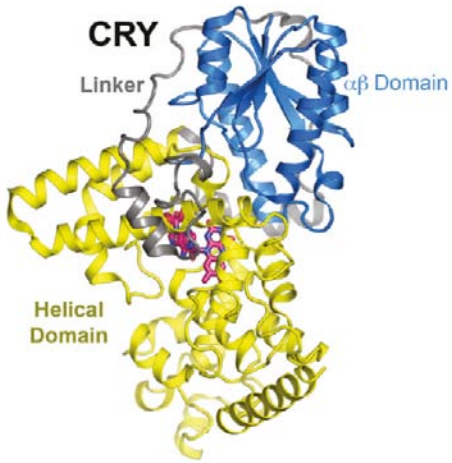

Figure 1. The *Arabidopsis thaliana* CRY2 domain, a member of the cryptochrome family of light-responsive proteins (structure shown [1]), is an important regulator of the circadian rhythm. The CRY2 PHR domain contains a flavin mononucleotide (FMN, present in all cells) as the light responsive moiety. Upon blue light stimulation, the C-terminus undergoes a conformational change that apparently helps actuate alterations in protein function [3].

Building upon this capacity, we are designing a fusion protein wherein the CRY2 PHR domain is fused to a peptide linker that can mediate degradation via the cellular protein degradation machinery. We hypothesize that upon photoactivation, this domain can recruit CIB fused to a protein of interest to the proteasome, thereby inducing light-responsive protein degradation.

As a first step towards this goal, we have screened a number of peptides for their ability to mediate the degradation of the fluorescent protein Venus. Specifically, we designed a number of constructs that express Venus-degradation-peptide fusion proteins. We hypothesized that some of the selected "degradation-peptides" would mediate degradation by recruiting ubiquitin ligases, whereas other peptides were expected to be "ubiquitin-independent". We expressed these fusion proteins in mammalian cells and monitored the intensity of Venus

fluorescence in the presence and absence of a proteasomal inhibitor. As seen in Figure 3, a number of these peptides enhanced the degradation of Venus. We are currently fusing these peptides to CRY2-PHR and testing the ability to induce the degradation of target proteins fused to CIB.

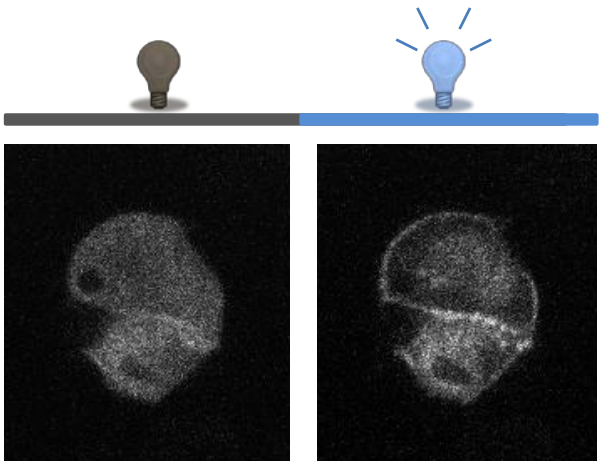

Figure 2. CRY2-PHR fused to mCherry and CIBN fused to a prenylated variant of GFP were expressed in 293 cells, using constructs that are a kind gift of C. Tucker [2]. Exposure to blue light induces the heterodimerization of CRY2 and CIBN, thereby inducing relocalization of the CRY2-mCherry to the cell membrane.

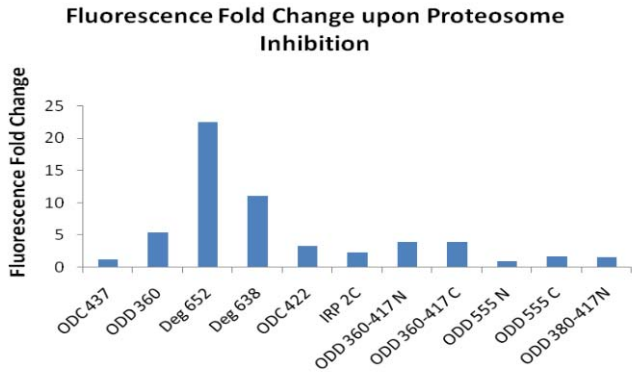

Figure 3. 293Ts were infected with retrovirus encoding a fusion of Venus to 11 different degradation peptides. To assess degradation efficiency, cells were treated with 10 μM of proteosomal inhibitor MG132 for 6 hrs, and the resultant fluorescence intensity was compared to infected but untreated cells via flow cytometry. Graph shows median fluorescence of Venus fused to each peptide.

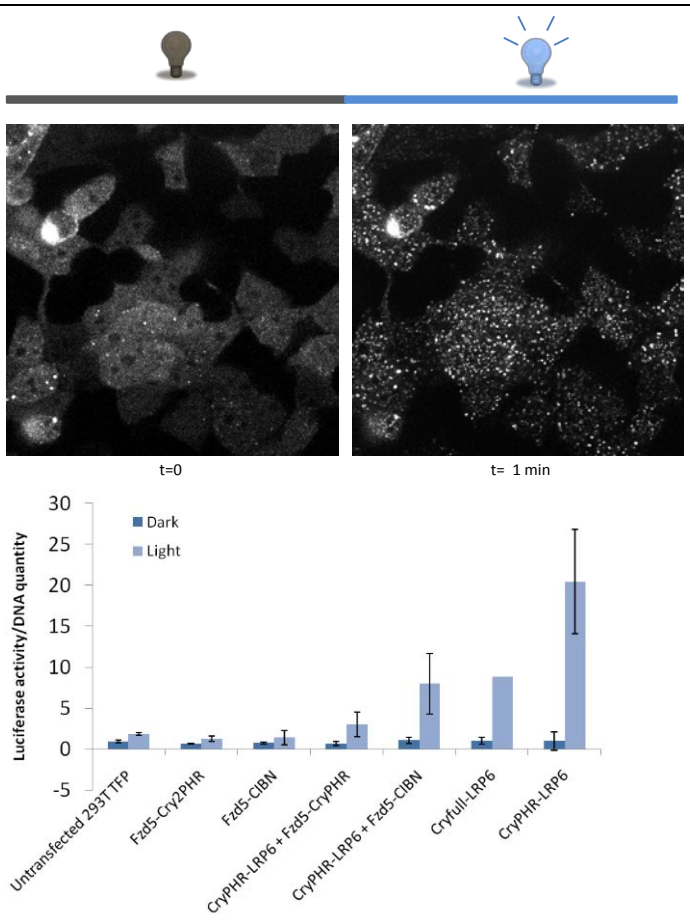

Figure 4. 293 cells were transfected with a construct to express the CRY2-PHR domain fused to the C-terminus of LRP6 and the fluorescent protein mCherry. Exposure to blue light strongly induced protein oligomerization (top). 293 cells were infected with a lentiviral vector carrying a β-catenin responsive promoter driving luciferase expression. Subsequent transfection with the CRY2-LRP6 construct led to potent activation of β-catenin dependent gene expression in response to light, compared to either untransfected cells or cells not exposed to light. Other variants of the system, including fusion of the LRP6 co-receptor Frizzled5 to CRY2 or CIB, induced a weaker response.

In addition to inducing heterodimerization, it has been shown that the CRY2-PHR can under some circumstances homo-oligomerize in response to light [4]. A number of cellular signal transduction events involve protein oligomerization. For example, in the Wnt signaling pathway the oligomerization of the Wnt co-receptor LRP6 appears to be important for the downstream activation of β-catenin [5]. We anticipated that fusion of CRY2 to the LRP6 C-terminus may yield a system in which light induced the activation of this signaling pathway. As we hypothesized, exposure of CRY2-LRP6-mCherry to blue light induced the oligomerization of the protein. In addition, when a β-catenin responsive promoter driving expression of firefly luciferase was introduced into these cells, blue light potently activated β-catenin dependent gene expression (Figure 4).

We will continue our efforts to engineer cells to recognize and interface with inorganic systems, including light-inducible control of protein degradation and signal transduction.

iii) Future Plans

In the next year, we plan to continue our efforts to engineer cells to respond to light. For numerous applications, it would be desirable to channel novel signals into defined intracellular signaling pathways and thereby gain enhanced control over cell function. We will focus on two thrusts. One effort will involve the engineering of proteins that recognize light as a signal; our preliminary efforts in this regard have been summarized above. We will also attempt to design light-sensitive riboswitches and initiate cellular engineering efforts to promote the adhesion of cells to inorganic substrates.

iv) References:

1. Zoltowski, B.D. and K.H. Gardner, *Tripping the Light Fantastic: Blue-Light Photoreceptors as Examples of Environmentally Modulated Protein-Protein Interactions.* Biochemistry, 2010. **50**(1): p. 4-16.
2. Kennedy, M.J., et al., *Rapid blue-light-mediated induction of protein interactions in living cells.* Nat Methods, 2010. **7**(12): p. 973-5.
3. Partch, C.L., et al., *Role of Structural Plasticity in Signal Transduction by the Cryptochrome Blue-Light Photoreceptorâ€* Biochemistry, 2005. **44**(10): p. 3795-3805.
4. Yu, X., et al., *Formation of Nuclear Bodies of Arabidopsis CRY2 in Response to Blue Light Is Associated with Its Blue Light-Dependent Degradation.* The Plant Cell Online, 2009. **21**(1): p. 118-130.
5. Metcalfe, C., et al., *Stability elements in the LRP6 cytoplasmic tail confer efficient signalling upon DIX-dependent polymerization.* J Cell Sci, 2010. **123**(Pt 9): p. 1588-99.

Program Title: **(Bio)Chemical Tailoring of Biogenic 3-D Nanopatterned Templates with Energy-relevant Functionalities**

Principle Investigator: **Nils Kröger; Co-PI: Kenneth H. Sandhage**
Mailing Address: **School of Chemistry and Biochemistry, Georgia Institute of Technology, 901 Atlantic Dr. NW, Atlanta, GA 30332**
E-mail: **nils.kroger@chemistry.gatech.edu**

Program Scope: This project is aimed at obtaining fundamental understanding of methodologies for (bio)chemical functionalization of biosilica structures (frustules) produced by diatoms, a large group of unicellular microalgae. The well-controlled hierarchical (micro-to-nanopatterned) 3-D morphologies of diatom frustules endow such structures with attractive characteristics (e.g., mechanical, mass transport) for certain applications including filters/supports for macro-molecular separations or catalysis.[7] However, the native biochemistry and inorganic chemistry of diatom frustules have severely limited the range of applications for such structures. The PI and co-PI of this effort have developed critical new capabilities for (bio)chemical tailoring of diatom frustules for energy-related applications. Two different methodologies are under investigation:

- *In vivo* functionalization of diatom biosilica through molecular genetic engineering, and
- *In vitro* functionalization onto high surface area inorganic replicas (Si, C, Au) of diatom silica.

Emerging basic understanding of these methodologies is being used to establish methods for incorporating energy-relevant enzymes into diatom biosilica and onto inorganic diatom replicas.

(1) The first methodology ("***li***ve ***d***iatom ***s***ilica ***i***mmobilization" or LiDSI) is based on a recent discovery, by the Kröger group, that expression in the diatom *T. pseudonana* of recombinant proteins containing the silaffin tpSil3 results in incorporation of the fusion proteins into the biosilica *in vivo*.[9] Silaffin tpSil3 is a natural component of *T. pseudonana* biosilica, and serves two functions in such fusion proteins: (i) it acts as an "address tag" to mediate intracellular transport of the fusion protein to the silica deposition vesicle (SDV); (ii) it binds tightly to silica, thus immobilizing the fusion protein in biosilica. Previously, LiDSI has only been demonstrated for GFP and the "simple" small (164 amino acid) enzyme HabB[9] which does not require co-factors or post-translational modifications for activity.[8] More complex enzymes, such as those for biomass degradation (e.g., hydrolases, oxidoreductases), require oligomerization, co-factors, and post-translational modifications for activity.[6] In order to allow optimized LiDSI-enabled enzyme immobilization, two main questions are under investigation by the Kröger group:

- ▶ Which energy-relevant enzymes are compatible with LiDSI?
- ▶ What cellular factors limit the amount of enzyme incorporated in diatom silica via LiDSI?

(2) The second methodology ("***b***iological ***a***ssembly and ***s***hape-preserving ***i***norganic ***c***onversion" or BASIC), established and patented by the Sandhage group, involves reaction-based methods for the shape-preserving conversion of diatom silica into other inorganic materials, including highly porous replicas.[1] Such high surface area replicas are highly attractive as substrates for *in vitro* enzyme immobilization, as such templates can utilize the 3-D open hierarchical nature of diatom silica while allowing for new surface chemistries and appreciably higher surface areas for enzyme attachment. While the BASIC process for diatom conversion has been demonstrated, mechanisms associated with such structural evolution and shape preservation were not previously well understood. Such knowledge can allow for enhanced control of surface areas and pore size distributions of frustule replicas, which, in turn, can enable a high degree of enzyme loading for energy applications. Key questions being addressed by the Sandhage group include:

- What mechanism(s) control the chemical/structural evolution during SiO_2 conversion, and how can such conversion be used to tailor replica surface areas and pore sizes?
- How can porous replica surfaces be tailored for optimal enzyme loading and enzyme activity?

Recent Progress: Progress has been made in all aspects of the project. Regarding *in vivo* enzyme immobilization, we have focused on **(a)** investigating the scope of the LiDSI method for enzymes that require oligomerization, cofactors and posttranslational modifications for activity, and **(b)** identifying and functionally analyzing a targeting signal for intracellular delivery of proteins to the SDV (i.e., the silica-forming organelle). Regarding *in vitro* enzyme immobilization, our efforts have been directed towards **(c)** understanding the mechanism(s) of BASIC conversion and **(d)** developing methods to generate high surface area C and Au replicas for subsequent attachment of energy-relevant enzyme glucose oxidase (GOx).

We have examined the use of LiDSI for multimeric and co-factor dependent enzymes, and found that β-glucuronidase (GUS), glucose oxidase (GOx), galactose oxidase (GAOx), and horseradish peroxidase (HRP) can be functionally incorporated in diatom silica *in vivo* (Table 1).[4] To facilitate assembly of multimeric enzymes, we have modified the LiDSI procedure by using a drastically shortened silaffin fragment, coined T8 (37 amino acid residues), instead of the previous tpSil3 (205 amino acid residues). T8 proved to be functional as an intracellular "address tag" for delivery of enzyme fusion proteins to the SDV, and for anchoring enzymes in diatom biosilica.[4] The insight that T8 may be suitable for LiDS was obtained from our studies to identify the SDV targeting signal of silaffins (see below). The successful *in vivo* immobilization of GUS, GOx, HRP, and GOAx demonstrated that the redox cofactors FAD, heme, and $Cu^{+1/+2}$ are available during intracellular maturation and transport of the T8-enzyme fusion proteins, which suggests that other enzymes with similar co-factor requirements may also be applicable for LiDSI.

Table 1. Complex enzymes functionally immobilized in diatom silica through LiDSI.

Enzyme	Reaction type	Structure	Cofactor
Glucuronidase (GUS)	Acetal hydrolysis	homotetramer, 272 kDa	none
Glucose oxidase (GOx)	Redox	homodimer, 128 kDa, glycosylated	FAD
Horseradish peroxidase (HRP)	Redox	monomer, 44 kDa, 2 Ca^{2+}	heme
Galactose oxidase (GAOx)	Redox	monomer, 68 kDa, His-Cys cross-link	Cu-center

We hypothesize that intracellular transport path of silaffin-enzyme fusion proteins proceeds from the endoplasmic reticulum (ER), via the Golgi apparatus to the SDV[9], and requires a specific peptide-based targeting signal To identify the SDV targeting signal in silaffins, GFP fusion proteins containing different fragments of the silaffin tpSil3 were expressed in *T. pseudonana*, and their location in live cells and isolated biosilica was analyzed by fluorescence microscopy. The 19 amino acid peptide T10 (sequence: ESSMPSSKAAKIFKGKSG) was found to be the shortest peptide that mediates efficient targeting of GFP to the SDV (note: the silaffin fragment T8 used for LiDSI of enzymes discussed above contained an additional 12 amino acid residues).[5] Site directed mutagenesis of the T10 peptide in combination of GFP fusion protein expression demonstrated that the post-translational modifications on the lysine residues rather than just the positive charges, and the presence of negative charges on the serine residues (possibly phosphorylation) are essential for SDV targeting. The amino acid sequence of the targeting signal is also important, as a scrambled T10 sequence was incapable to mediate SDV targeting. Such information about the structural requirements of an SDV targeting peptide will now be used in attempts to design an artificial SDV targeting signal that exhibits better targeting efficacy than the natural one.

New BASIC approaches have been developed for converting SiO_2 diatom frustules into high surface area C and Au replicas. A magnesiothermic reduction process[12] was first used to convert

Aulacoseira diatom SiO_2 frustules into porous Si. These replicas were then exposed to heated methane to allow for C deposition and then reaction with Si to yield SiC.[2] The SiC replicas were, in turn, converted into highly-porous C replicas via selective Si removal by reaction with $Cl_2(g)$.[2,13] The C replicas were exposed to a heated HNO_3 solution to generate surface carboxyl groups. These frustule replicas were then immersed in a $SnCl_2$ solution to allow for the binding of tin cations to replica surfaces. Such sensitized replicas were exposed to a $AgNO_3$ solution to allow for electroless Ag deposition. After removing the C by oxidation, the freestanding Ag replicas were converted into porous Au replicas by displacement with a $HAuCl_4$ solution. The specific surface areas of the resulting Au and C replicas were 70 and 700 times higher, respectively, than for the starting SiO_2 frustules (Table 2).

In vitro methods to attach glucose oxidase (GOx, a model enzyme for biofuel cells) to these high surface area C and Au replicas, and to diatom SiO_2, have also been developed. Research from another program (using GOx in anti-microbial coatings; BIONIC Air Force Center of Excellence) demonstrated that chemical cross-linking of the polycationic peptide protamine (PA) to GOx yielded a catalytically active derivative, GOx-PA, that binds strongly to silica and titania.[10] In this DoE effort, GOx-PA has been found to bind well to carboxyl-bearing C and Au replicas (formed in the latter case by exposure to mercaptopropanoic acid). In each case, the binding was due to negative charges (at pH 7.0) on the substrate surfaces. As expected, the amount of bound enzyme increased significantly with an increase in the substrate surface area (Table 2). Pore size distribution analyses are underway to determine, for each substrate, the surface area of pores with diameters comparable to or larger than the effective GOx-PA diameter (hydrodynamic dia.: 22 nm). Understanding how the substrate pore size distribution is correlated to enzyme loading would provide important information for tailoring of the substrate porosity.

Table 2. Attachment of GOx-PA to diatom silica and to diatom replicas with different surface characteristics.

Substrate	Specific surface area (m^2 per g substrate)	Surface groups	Specific enzyme loading (mg GOx-PA/g substrate)
Aulacoseira diatom SiO_2 frustules	1.8 ± 0.2	-Si-OH/Si-O^-	1.9 ± 0.4
C frustule replicas	1,290 ± 88	-CO_2^-	45.3 ± 1.6
Au frustule replicas	127*	-CO_2^-	15.7 ± 1.1

*only one measurement made to date (more analyses underway)

The magnesiothermic conversion of 1 mole of amorphous, quartz, or cristobalite SiO_2 into 2 moles of MgO and 1 mole of Si (the initial reaction step preceding steps leading to porous Si, C, and Au replicas) results in large increases in molar volume ($\geq$27%). Indeed, residual stress analyses of MgO/Si product layers formed on partially-reacted quartz single crystals, obtained in this effort via the $\sin^2\psi$ x-ray diffraction method, has yielded extremely high states of compression (>1 GPa) after partial magnesiothermic reaction at 650-750^{o}C. Post-reaction annealing at 650-750^{o}C resulted in sharp relaxation of this stress. TEM analyses revealed the surprising formation of a MgO-rich layer on top of the MgO/Si product layer during such annealing, which suggested that this layer was associated with the observed stress relaxation.

Future Plans: The following aims will be addressed in future research:

(i) LiDSI. The targeting efficacy of native and engineered SDV targeting signals will be compared. This will be analyzed by both expression of GFP fusion proteins, GOx fusion proteins. The aim is to maximize GFP fluorescence intensity and GOx activity per g silica. LiDSI will be attempted with glucan degrading enzymes CelB (β-glucosidase), EglA (endoglucanase), both from the hypothermophilic archaea *Pyrococcus furiosus*, and CfEg3a

(endoglucanase) from the termite *Coptotermes formosanus*. All three enzymes are co-factor independent, and only active in the homooligomeric state.

(ii) *In vitro* enzyme immobilization. The same glucanases as above will be recombinantly expressed in *E. coli* carrying "protamine-like" peptide tags. These tags will be optimized for high affinity binding to diatom silica and appropriately prepared diatom derived C and Au replicas. Surface functionalization protocols to amplify the density of surface carboxyl groups present on the high surface area C and Au replicas will also be explored. The influence of reactive conversion conditions, and of post-reaction annealing, on the pore size distributions of these replicas will also be examined (i.e., to increase the extent of mesoporosity, which can accommodate the desired enzymes, at the expense of microporosity).

(iii) Activities and stabilities of immobilized enzymes. The specific enzyme activities, and the stabilities against elevated temperatures (60-100^{o}C) of *in vivo* and *in vitro* immobilized enzymes will be compared. We will aim to improve enzyme stabilities by applying nanoscale silica coatings through the previously established method of Layer-by-Layer (LbL) mineralization.[11]

(iv) Mechanism(s) of stress relaxation during reactive conversion. TEM analyses of ion-milled cross-sections of partially-reacted (MgO/Si-bearing) SiO_2 specimens after post-reaction annealing for varied times will be used to evaluate the extent of surface MgO formation during such annealing. Inert markers placed on the surfaces of as-reacted specimens will be used to determine whether such MgO formation is the result of the outward migration of magnesium cations and oxygen anions, or to the loss of Si from the underlying MgO/Si product layer. Thermogravimetric analyses will be used to evaluate weight changes during such annealing.

References (acknowledging DOE support)

1. Sandhage, K. H., Materials "Alchemy": Shape-Preserving Chemical Transformation of Micro-to-Macroscopic 3-D Structures. *JOM* **62**, 32-43 (2010).
2. Bao, Z., Song, M.-K., Davis, S., Cai, Y., Liu, M., Sandhage, K. H. High Surface Area, Micro/Mesoporous Carbon Particles with Selectable 3-D Biogenic Morphologies for Tailored Catalysis, Filtration, or Adsorption. *Energy & Environ. Sci.* **accepted, in press**.
3. Kim, S., Bastani, Y., Lu, H., King, W., Marder, S.R., Sandhage, K.H., Gruverman, A., Riedo, E., Bassiri-Gharb, N. Direct Patterning of Arbitrary-Shaped Ferroelectric Nanostructures on Platinized Si and Glass Substrates. *Adv. Mater.* **Accepted** (published online July 16, 2011).
4. Sheppard, V. C., Scheffel, A., Poulsen, N., Kröger, N. Live Diatom Silica Immobilization (LiDSI) of Multimeric and Redox-active Enzymes. **Submitted**.
5. Poulsen, N., Scheffel, A., Kröger, N. Intracellular Targeting of Silaffins to the Silica Deposition Vesicle (SDV) in the Diatom *Thalassiosira pseudonana*. **In preparation**.

Other References

6. Bommarius, A., Riebel, B.R., *Introduction to Biocatalysis*, Wiley-VCH, Weinheim (2004).
7. Yang, W., Lopez, P.J., Rosengarten, G., *Analyst* **136**, 42 (2011).
8. Davis, J.K., Paoli, G.C., He, Z., Nadeau, L.J., Sommerville, C.C., Spain, J.C., *Appl. Environ. Microbiol.* **66**, 2965 (2000).
9. Kröger, N., Poulsen, N., *Annu. Rev. Genet.* **42**, 83 (2008).
10. Haase, N.R., Shian, S., Sandhage, K.H., Kröger, N., *Adv. Funct. Mater.* **in press**.
11. Fang, Y., Wu, Q., Dickerson, M.B., Cai, Y., Shian, S., Berrigan, J., Poulsen, N., Kröger, N., Sandhage, K.H., *Chem. Mater.* **21**, 5704 (2009).
12. Bao, Z., Weatherspoon, M.R., Cai, Y., Shian, S., Graham, P.D., Allan, S.M., Ahmad, G., Dickerson, M.B., Church, B.C., Kang, Z., Summers, C.J., Abernathy, H.W., Liu, M., Sandhage, K.H., *Nature*, **446** [3] 172 (2007).
13. Gogotsi, Y., Welz, S., Ersoy, D.A., McNallan, M.J., *Nature* **411**, 283 (2001).

Program Title: Stability of Proteins inside a Hydrophobic Cavity

PI: Sanat Kumar, Columbia University

Email: sk2794@columbia.edu

Program Scope

We come across many instances where proteins are confined to a small space (a 'cage'). Examples of such spaces might include pores within chromatographic columns, the Anfinsen cage in chaperonins, the interiors of ribosomes or regions of steric occlusion inside cells. Theoretically it's a known fact that an athermal confinement stabilizes the protein against reversible unfolding since the unfolded state loses more entropy upon confinement compared to the folded state [1]. When the surface interacts with the protein we have complex process because, the interactions between the protein and the surface contribute to the enthalpic term of the free energy. It is imperative to better our understanding on this aspect as they play a vital role in biological functioning like receptor binding, cell response and cell adhesion [2]. The field has gained more interest recently as a result of industrial applications like immobilization of enzymes, biosensors and chromatographic separations [3, 4]. The main goal of the current project is to investigate the effect of interactions between the confining surface and the protein on its stability under different degrees of confinement and protein surface interaction strengths.

Recent Progress

We chose a coarse grained Hydrophobic-Polar lattice model commonly known as the HP model for modeling proteins introduced by Dill [5]. In our study we have considered a 64mer and 42mer as model proteins both designed by Yue et al [6]. These sequences have shown to exhibit protein like characteristics. A spherical cavity is created in a cubical lattice. Canonical Monte Carlo simulations were carried out at different temperatures, surface hydrophobicities and degree of confinement.

Our results indicate that, for an athermal cavity, the melting temperature of protein increased with increase in the degree of confinement indicating stabilization. Figure 1 and Figure 2 shows the specific heat curves for the 64mer and 42mer at different degree of confinement. The peak of the curves indicates the melting transition. Now the interaction between the cavity and protein is turned on. The parameter λ, which is the surface hydrophobicity of the cavity relative

to the interaction between the hydrophobic groups of the protein, can be varied from zero (athermal) to larger values. For low surface hydrophobicity (λ <0.1) we see that the melting temperature almost remains the same. As λ is increased, the melting temperature of the proteins drops indicating destabilization. This can be explained by the fact that the protein wants to unfold and hence expose more hydrophobic groups to interact with the surface as surface hydrophobicity increased. This tendency to unfold increases with increase in the degree of confinement as the number of surface sites available and the strength of interaction per site increases. In our own previous study, we have shown the on a flat surface, the protein is stabilized at low surface hydrophobicities owing to fact that, the entropic loss for a folded protein upon adsorption is small compared to that for an unfolded protein. So on a flat surface, the protein adsorbs onto the surface in its folded state and gets stabilized unlike inside a cavity where it unfolds. Figure 3 shows the folding free energy (G_{folded}-$G_{unfolded}$) for different degree of confinement at their respective melting temperatures.

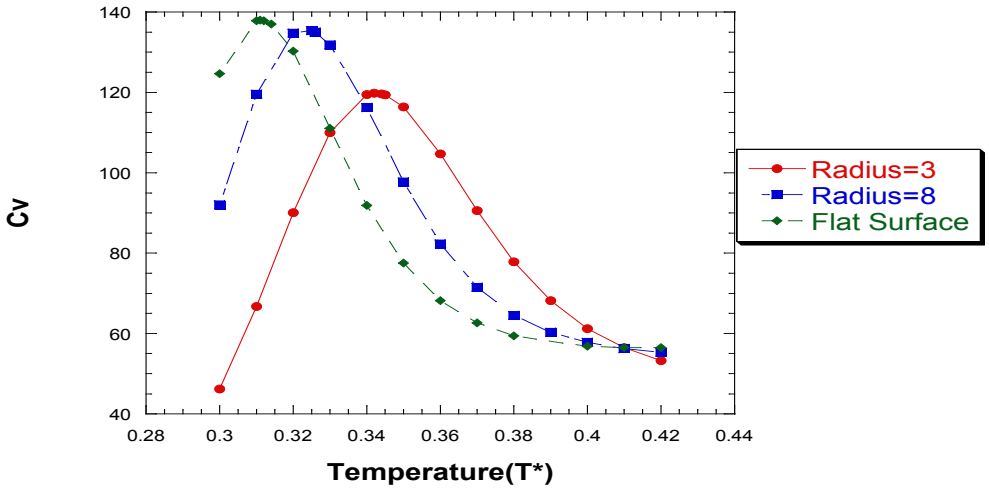

Figure 1: Specific heat curve of 64mer HP under different degree of confinement with a thermal surface

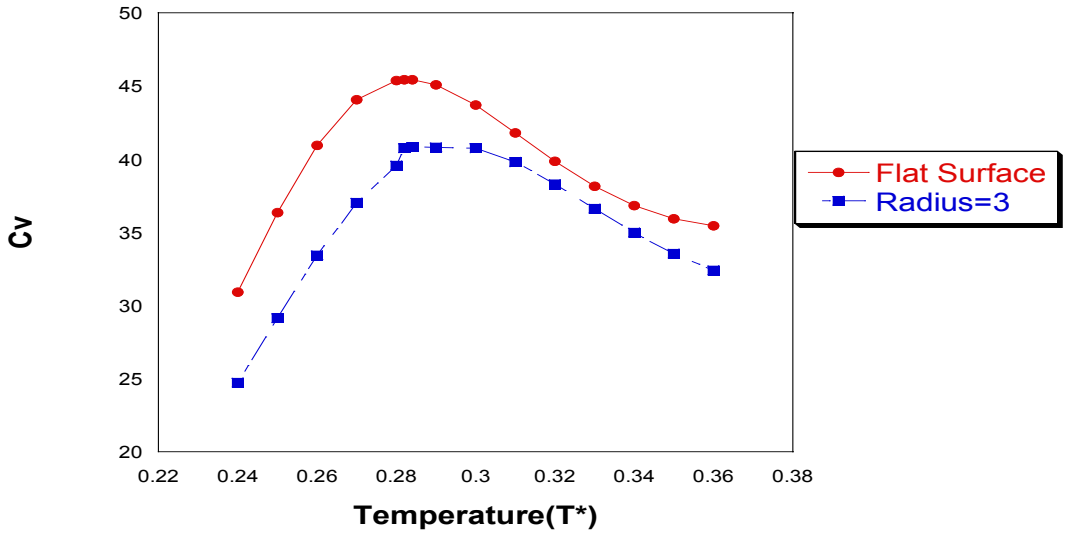

Figure 2 : Specific heat curve for a 42mer HP protein under different degree of confinement with a thermal surface

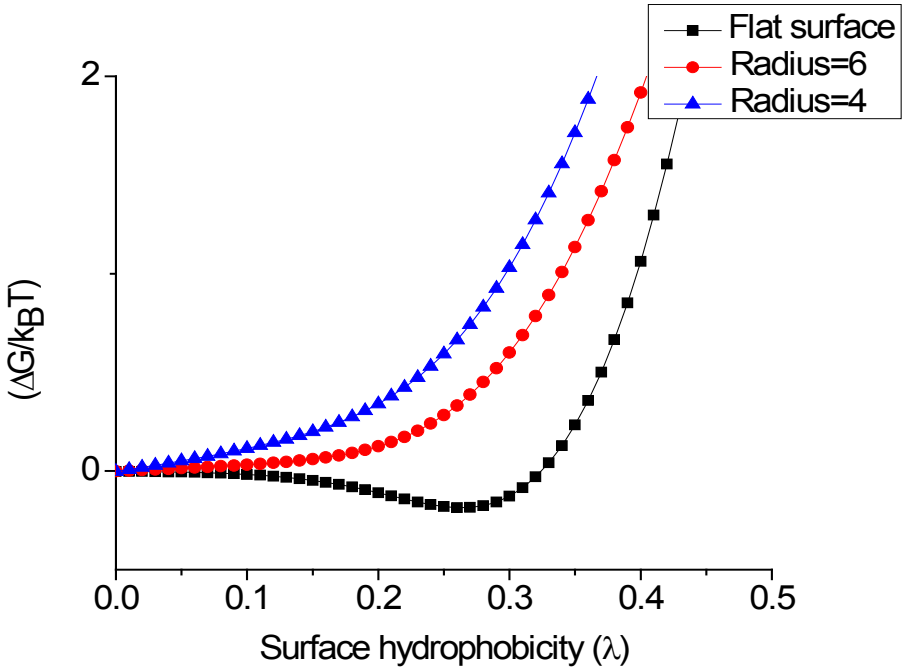

Figure 3: Folding free energy of 64mer HP protein under different degree of confinement at their respective melting temperatures when λ=0

Future Plan

We seek to investigate adsorption of protein using an explicit solvent model. We have started working with off lattice proteins with the solvent interacting via Jagla Potential. The amino acids residues are modeled as hard spheres or Jagla particles depending on whether they are hydrophobic or polar respectively.

Publications

1)"Enhanced Wang Landau sampling of adsorbed protein conformations", Radhakrishna M, Sharma S, Kumar S K (To be submitted to Journal of Chemical Physics)

References

[1] H. X. Zhou, and K. A. Dill, Biochemistry **40**, 11289 (2001).
[2] J. J. Gray, Curr. Opin. Struct. Biol. **14**, 110 (2004).
[3] C. A. Haynes, and W. Norde, Colloids and Surfaces B: Biointerfaces **2**, 517 (1994).
[4] M. Malmsten, J. Colloid Interface Sci. **207**, 186 (1998).
[5] K. A. Dill, Biochemistry **24**, 1501 (1985).
[6] K. Yue *et al.*, Proc. Natl. Acad. Sci. U. S. A. **92**, 325 (1995).

Programmed Nanomaterial Assemblies in Large-Scale 3D Structures: Applications of Synthetic and Genetically-Engineered Peptides to Bridge Nano-Assemblies and Macro-Assemblies

PI: Hiroshi Matsui

Department of Chemistry and Biochemistry, City University of New York, Hunter College, 695 Park Avenue, New York, NY 10065, e-mail: hmatsui@hunter.cuny.edu

i) Program Scope

Recent trends in the complexity of device design demand the fabrication of three-dimensional (3D) superstructures assembled from multi-nanomaterial components in precise configurations; homogeneous distribution in a long-range order, tailored packing distance with precise periodicity, and defined shape of resulting 3D superlattices. Biomimetic assembly is an emerging technology in such pursuits since organisms are efficient, inexpensive, and environmentally benign material factories allowing low temperature fabrication. The main objective in this proposal is to establish a new peptide-assisted material assembling technology for the generation of 3D macroscale multi-component materials that still retain superior nanoscale properties (i.e., a new technology to bridge between nano- and macro-assemblies). To achieve this goal, we propose to develop novel biomimetic material fabrication technology that can program directed assemblies of materials in the tailored shape and superstructure in large volumes (μm^3 - mm^3) from multi-nanomaterials, metal/semiconductor nanoparticles (NPs) and peptides. The overall hypothesis is that robust assemblies of synthetic or genetically-engineered peptides can form large-scale frames in targeted shapes by co-assembling NPs as joints and these NPs are aligned in the resulting 3D hybrid superlattices precisely in remarkable long-range order. The outcome of proposed researches will have broad impacts in basic sciences and applied engineering because this peptide-templated material synthesis technology has potential to create new materials possessing novel physical, structural, and catalytic properties with no synthetic counterparts via large-scale directed-assemblies of nanomaterials. This proposed work could also impact cost-effective assembly of solar cells with superior power conversion efficiency and microelectronics capable of processing at unprecedented speeds and low power consumption. Development of such efficient technologies will usher in the next generation of energy conversion technologies, data storages, computing, optical communications, and sensing, which will benefit the principal mission of the Department of Energy greatly.

ii) Recent Progress

(a) Large-scale collagen peptide assembly into 2D film with structural reinforcement via biomolecular recognition-based cross-linking of proteins

Collagen provides outstanding mechanical property to various bone tissues as it co-assembles with mineral particles of hydroxyapatite as joints because collagen can dissipate external forces and energies through molecular unfolding and intermolecular shear in the composite assembly[1]. Here we mimic the superstructure of bone tissues to develop large-scale rigid 2D peptide assembly from the engineered collagen-mimetic peptide B877B, a triple helical molecule containing a segment of the α1 chain of type I collagen and displaying biotin on both C- and N-terminus. To reinforce this fragile biomolecular assembly for the practical applications, free-standing collagen films are reinforced by cross-linking the collagen peptide ends with streptavidin. Nanoindentation experiments indicate that the mechanical strength of as-prepared collagen peptide film is remarkably enhanced after the biomolecular cross-inking reinforcement, and Young's modulus of peptide-QD assembled films could reach to 16 GPa, comparable with osteon bone tissues of 22 GPa [1].

(b) Large-scale & reconfigurable 3D structures of precise nanoparticle assemblies in self-assembled collagen peptide grids

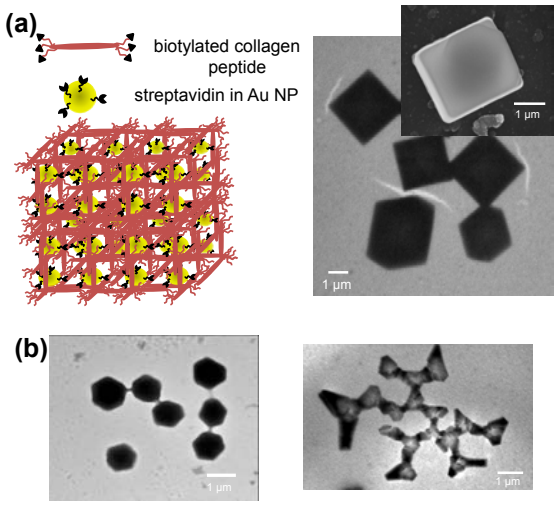

Figure 1. (a) Structure (left) and TEM image (right) of 3D superlattice microcubes assembled from collagen peptides and streptavidin-conjugated Au NPs (ϕ=10 nm). Inset is SEM image. (b) Structural transformation of 3D collagen peptide-AuNP superlattice assembly with (left) 30 nm-Au NPs (right) and 5 nm-Au NPs in TEM images.

The ability to control self-assembly of complex 3D architectures from functional building blocks could allow further development of complex device configurations. Here our goal is to develop peptide-based assembly technology enabling the precise 3D superlattice assembly of metal nanoparticles in defined 3D shapes as shown by DNA origami but in much larger scale (from μm^3 to mm^3), the higher yield, and the higher reproducibility. In this work, nanoscale peptides and ligand-functionalized nanoparticle joints were self-assembled into micron scale 3D cube-shaped crystals, creating a physical framework for the proposed biomimetic assembly strategy[2]. In this approach we took advantage of the naturally robust assembly of collagen triple helix peptides and used them as nanowire building blocks for the 3D crystal generation. Using streptavidin-functionalized Au nanoparticles and the α1 chain of type I wild type collagen specifically modified with a biotin moiety *in vivo*, we created micro-sized 3D superlattice cubes with peptide nanowires as grids and Au NPs as joints (Fig. 1-a). SAXS spectra indicate that Au NPs are arranged in b.c.c structure in the collagen peptide grids. This simple, rapid fabrication protocol can assemble 3D superlattice materials in different shapes such as hexagons and triangles (Fig. 1-b), dependent on the design of the NP junctions, in extremely high yields, promising ease and flexibility in manufacturing future functional devices. Furthermore, under optimized assembling conditions, the ratio of the numbers of collagen peptides and NPs sensitively influences the density of Au NPs in 3D superstructures. The reconfigurability of the 3D directed assembly was also demonstrated by incorporating salt bridge in the collagen peptide sequence. Due to this salt bridge insertion, the conformation change of peptide building blocks can be induced by pH and this dynamic conformational transformation triggers the disassembly of the hybrid NP-peptide cube, following the reassembly of reconfigured peptides into different shapes such as rod and rhombus. Further evolution for more dynamic and versatile reconfigurability will upgrade this system toward more practical applications.

(c) Application of evolution approaches to find novel catalytic peptides for new material syntheses and biomolecular reactions

To achieve the high performance in proposed nanoparticle-assembled devices, the quality of these building blocks of metal/semiconductor nanoparticles is critical since low crystallinity with many defects in nanoparticles degrades their conductivity and the charge mobility. The low temperature catalytic growth process is not only effective for the reduction of energy consumption in manufacturing processes but also very beneficial to grow higher crystalline materials because the slow crystal growth process reduces the local thermal stresses and the number of resulting defect sites. Nature finds the easiest way to grow and assemble materials,

and thus biomimetic approach is a potential path to break through this challenge because biocatalytic function of enzymes exhibits high efficiency and accuracy in the material growth at room temperature. However, it is difficult to design enzymes to catalyze specific reactions and predict their activity from their complex structures.

If peptides can replace enzymes to catalyze chemical reactions and material growth, these catalytic peptides will be more versatile because of their simpler structures and the ease of their syntheses. To effectively discover the novel peptides that can catalyze targeted reactions such as amide bond formation or semiconductor growth at room temperature, we developed a new evolutionary peptide screening method. Biopanning system using bacteriophage viruses has been widely used to discover new signal-transducing peptides, metal-binding peptides, and antibodies but it was limited to simply identify peptides that bind the target surfaces[3]. The novelty of our combinatory approach is to use the genetic evolution of viruses directly for the screening of peptide sequences that can catalyze target reactions (Fig. 2). To accomplish this biopanning process phage viruses are directly incubated into precursor solutions where no reactions are expected to occur without catalysts. The product is observed only when there are phages in the solution which display the peptides to catalyze the target reactions. As a proof-of-concept, we discovered a catalytic peptide, ZP-1, to grow ZnO single crystals at room temperature from this new phage peptide library. The outstanding catalytic activity of ZP-1 peptide for the single crystalline semiconductor growth is due to crystalline face recognition of the peptide which effectively accelerates the fusion of randomly-oriented crystal domains into the single crystal phase *via* non-classical crystallization process on (100) and (110) faces at room temperature.

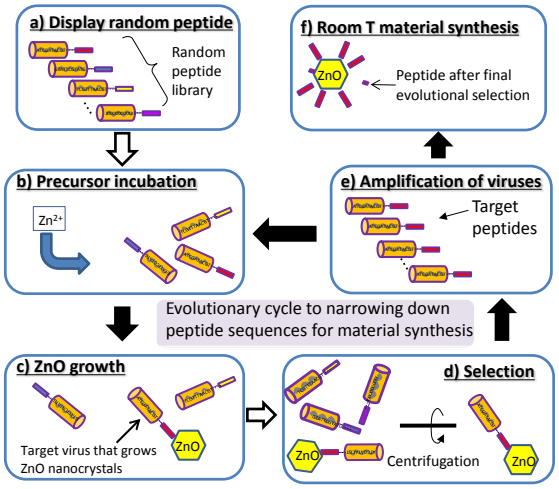

Figure 2. Scheme of new evolutionary peptide screening protocol to discover catalytic peptides that can grow oxide semiconductors at room temperature.

iii) Future Plans

Recently, we discovered the optimized assembling condition that the ratio of the numbers of collagen peptides and NPs can sensitively change the coordination of peptides around NP joint which ultimately tune the electronic coupling between Au NPs in 3D cube structure. On the basis of this new knowledge, a variety of 3D superstructures of Au NPs and QDs in varied NP coordination and spacing will be created in the collagen peptide grids and their optical and electric properties will be explored. For the reconfiguration of 3D superstructures, in addition to further exploring the collagen assembling systems with salt bridges, we will introduce calmodulin proteins into the 3D assembling systems because calmodulin can modulate its conformation more dynamically than collagen with Ca ion concentration and this transformation is expected to trigger more robust reconfiguration of 3D superlattice assembly. By using the newly developed evolutionary peptide screening method, we are currently screening peptides that catalytically form or break amide bonds and ester bonds just like enzymes do. This finding will have significant impact on synthesis, conjugation, and functionalization of biological molecules and more efficient polymerizations. We are also targeting the room temperature-growths of various metal and semiconductor NPs such as lithium iron phosphates, indium

arsenate, cobalt oxide, barium titanate, and potassium niobate with catalytic peptides discovered by the new phage display library, and then these NPs and QDs will be co-assembled with collagen peptides and calmodulin proteins for the generations of 3D superstructures and reconfigurable assembly systems.

iv) References

1. Rho, J-Y.; Kuhn-Spearing,A L.; Zioupos, P.: Mechanical properties and the hierarchical structure of bone. *Med. Eng. Phys*., **20**, 92-102 (1998).
2. Kaur, P.; Maeda, Y.; Mutter, A.C.; Matsunaga, Y.; Xu, Y.; Matsui, H.: 3D Self-Assembly of Peptide Nanowires into Micron-Sized Crystalline Cubes with Nanoparticle Joints. *Angew. Chem. Intl. Ed.*, **49**, 8375-8378 (2010). (selected as a highlight paper in 2010)
3. a) Lee, Y.J.; Yi, H.; Kim, W.-J.; Kang, K.;Yun, D.S.; Strano, M.S.; Ceder, G.; Belcher, A.M.: Fabricating Genetically Engineered High-Power Lithium-Ion Batteries Using Multiple Virus Genes. *Science* **2009**, *324*, 1051-1055.

v) Publications resulting from work supported by the DOE project over the last two years.

1. "Assemblies of functional peptides and their applications in building blocks for biosensors", R. de la Rica, C. Pejoux, H. Matsui, *Adv. Func. Mater*. **21**, 1018 (2011).
2. "Electrical transport properties of peptide nanotubes coated with gold nanoparticles via peptide-induced biomineralization", S. Shekhar, L. Anjia, H. Matsui, S.I. Khondaker, *Nanotechnology*, **22,** 095202 (2011).
3. "3D Self-Assembly of Peptide Nanowires into Micron-Sized Crystalline Cubes with Nanoparticle Joints", P. Kaur, Y. Maeda, A.C. Mutter, T. Matsunaga, Y. Xu, and H. Matsui, *Angew. Chem. Intl. Ed.*, **49**, 8375-8378 (2010).
4. "Applications of peptide and protein-based materials in bionanotechnology", R. de la Rica, H. Matsui, *Chem. Soc. Rev*., **39**, 3499 - 3509 (2010).
5. "Bio-inspired Target-specific Crystallization on Peptide Nanotubes for Ultra-Sensitive Pb Ion Detection", R. de la Rica, E. Mendoza, H. Matsui, *Small*, **6**, 1753-1756 (2010).
6. "Biomimetic crystallization nanolithography; Simultaneous nanopatterning and crystallization", R. de la Rica, K.I. Fabijanic, A. Baldi, and H. Matsui, *Angew. Chem. Intl. Ed*., **49,** 1447 (2010).
7. "PbSe nanocrystal growth as nanocubes and nanorods on peptide nanotubes via different directed-assembly pathways", M. Shi, W. Su, and H. Matsui, *Nanoscale*, **2**, 2373-2376 (2010).
8. "Biomimetic crystallization of sulfide semiconductor nanoparticles in aqueous solution", C. Pejoux, R. de la Rica, and H. Matsui, *Small*, **6**, 999 (2010).
9. "Biomimetic conformation-specific assembly of proteins at artificial binding sites nano-patterned on silicon", R. de la Rica, H. Matsui, *J. Am. Chem. Soc*., **131**, 14180 (2009).
10. "Long Electron-Hole Separation of ZnO-CdS Core-Shell Quantum Dots", F. Xu, V. Volkov, Y. Zhu, H. Bai, A. Rea, N.V. Valappil, X. Gao, I.L Kuskovsky, and H. Matsui, *J. Phys. Chem. C*, **113**, 19419 (2009).
11. "Biomineralization Nanolithography: Combination of Bottom-Up and Top-Down Fabrications to Grow Arrays of Monodisperse Au Nanoparticles along Peptide Lines on Substrates", N. Nuraje, S. Mohammed, L. Yang, and H. Matsui, *Angew. Chem. Intl. Ed*., **48,** 2546 (2009).
12. "Low temperature synthesis of ZnO nanowire by using a genetically modified collagen-like triple helix as a catalytic template", H. Bai, F. Xu, L. Anjia, and H. Matsui, *Soft Matter*, **5**, 966 (2009).

Biological and Biomimetic Low-Temperature Routes to Materials for Energy Applications

Daniel E. Morse
California NanoSystems Institute, Univ. of California, Santa Barbara, CA 93106-5100;
d_morse@lifesci.ucsb.edu

I. Program Scope:

New materials are needed to radically transform the efficiencies of energy harnessing, transduction, storage and delivery. To help address this need, we are investigating the mechanism and usefulness of a new, biologically inspired, low cost, low temperature method we developed for the kinetically controlled catalytic synthesis of nanostructured materials optimized for energy applications. This biologically inspired materials synthesis method is low-cost, low temperature, and uses no polluting chemicals. In addition to the near-term application of the results of these studies for the improvement of batteries and related energy technologies, the broader impact of this research includes a deeper fundamental understanding of the factors governing the control of synthesis, assembly and performance of a wide range of semiconductors and other valuable inorganic materials.

II. Recent Progress:

A. Kinetically controlled catalytic nanofabrication: We translated the biomolecular mechanism of synthesis of silica and related metal oxides that we discovered (described above) to a robust new methodology, without the use of organic molecules, capable of producing nanostructurally controlled metalloid and metal oxide semiconductors and related materials for improved efficiency of energy generation, transduction, storage and use. This method uses vapor diffusion of a catalyst through a gas-liquid interface to provide ***kinetically and vectorially controlled catalysis***, at low-temperature, of synthesis from molecular precursors that require hydrolysis. The result is a novel low-temperature and environmentally benign method for the nanofabrication of a wide range of metal oxide, metal hydroxide and metal phosphate semiconductors (and the corresponding metals) in unique and potentially useful nanocrystalline morphologies - some of which could never have been made before - with significantly enhanced electronic performance (Schwenzer et al., 2996; Brutchey & Morse, 2006; Schwenzer & Morse, 2008). The method relies on the integrated tuning of molecular precursors and vectorially controlled catalysis, utilizing only chemical physics and highly purifiable inorganic components, *with no biochemicals, biologicals or organic materials.* The use of the molecular precursor and its vectorially controlled catalytic hydrolysis provide coordinate kinetic and directional control of semiconductor growth that is not available using conventional high-temperature approaches. This bio-inspired, kinetically controlled catalytic synthesis method is highly generic, yielding both free (unsupported) and supported nanostructured thin films and nanoparticles of more than 50 different metal hydroxides, oxides, phosphates and perovskites - many in morphologies that had not been achievable before. We demonstrated that the range of products can be further expanded by facile post-synthesis conversion to the nitrides and sulfides, with preservation of the nanostructured thin-film morphology. Direct reduction to the pure nanocrystalline metal also is possible. Because no organics or biochemicals are used, the method produces very high purity materials that are fully integrable with MOCVD and CMOS fabrication.

B. <u>Kinetically controlled catalytic synthesis of nanocomposite anodes and cathodes for high-power lithium ion batteries</u>: We have used the kinetically controlled catalytic synthesis method described above to inexpensively produce a nanocomposite anode for high-power lithium ion batteries consisting of nanocrystals of Sn grown by a 2-step catalytic process *in situ* within the pores of compliant and conductive microparticles of graphite (Fig. 1; Zhang and Morse, 2009). This composite exhibits higher energy capacity than the graphite alone, as a result of the contribution to lithium ion capacity of the metal. Exceptionally high power-density (nearly 50 % retention of capacity, with full recovery, after discharge at 50C) and stability (cyclability) are the result of the compliance of the graphite, which provides a resilient host that can accommodate the swelling and shrinking of the metal with each cycle of lithiation (alloying) and de-lithiation that accompanies each discharge and charge cycle (Zhang and Morse, 2009).

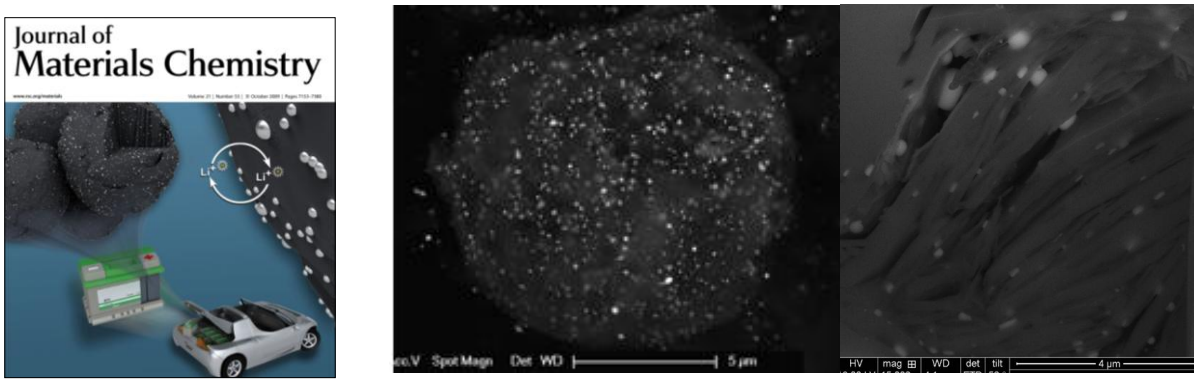

Figure 1. High power tin-in-graphite nanocomposite anode. (center) Back-scattered electron image and EDX (energy-dispersive X-ray mapping - not shown) reveal uniform dispersion of Sn nanoparticles throughout the graphite matrix. X-ray diffraction and BET measurements (not shown) confirm that the gentle, low-temperature method preserves the essential crystallinity and high porosity of the graphite. (right) FIB cross-section and TEM show nanocrystals of tin grown in situ within the interstices of the graphite. (Zhang and Morse, 2009)

Smaller Sn nanocrystals can be obtained by replacing the graphite matrix with a comparably conductive and compliant carbon matrix of inexpensive, mass-produced, bulk multi-wall carbon nanotubes (MW-CNTs) (Zhang and Morse, 2011, submitted). Preliminary and as-yet unoptimized results demonstrate that use of the CNT matrix yields lower heterogeneity and smaller average size (ca. 120 nm) of the final Sn nanocrystals than formed in the graphite, with nearly 50% higher energy capacity of the composite than obtained with the graphite matrix:

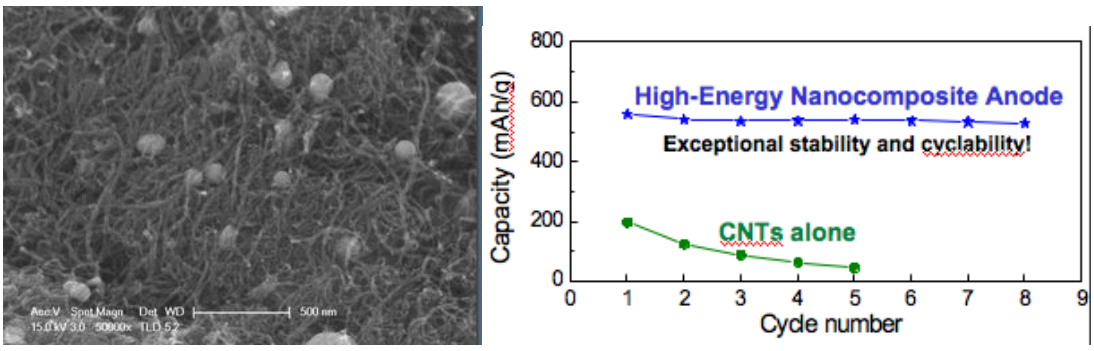

Figure 2. Higher energy-density anode consisting of Sn nanocrystals grown catalytically in a compliant and conductive matrix of MW-CNTs. Highly agglomerated bulk-produced MW-CNTs are readily dispersed by ultrasonication. *In situ* catalytic growth of Sn nanocrystals in the dispersed microparticles (ca. 10 micron diam.) produces more uniform Sn nanocrystals (ca. 120 nm diam.) (left). XRD confirms purity and high crystallinity of the Sn particles. Higher energy capacity and good stability are shown for this first, unoptimized Sn-CNT nanocomposite (upper rt.). (Zhang and Morse, submitted for publication, 2011)

We extended the use of bio-inspired, kinetically controlled, catalytic synthesis to produce a **high-power, relatively high-voltage, nanocomposite cathode** for rechargeable Li-ion batteries (Fold et al., submitted, 2011). This cathode consists of nanocrystalline (spinel) $LiMnO_4$ grown *in situ* and intimately mixed with well-dispersed, inexpensive multiwall carbon nanotubes) (Fig. 3). This cathode operates at an average voltage of 3.9 v and exhibits exceptionally stable cyclability. It retains 96% of its original capacity after discharge at 10C, >80% capacity after discharge at the exceptionally high rate of 20C, and shows complete recovery to 100% capacity after full discharge at 50C (indicating that it suffers no damage after this exceptionally high rate of discharge) (Fig. 4).

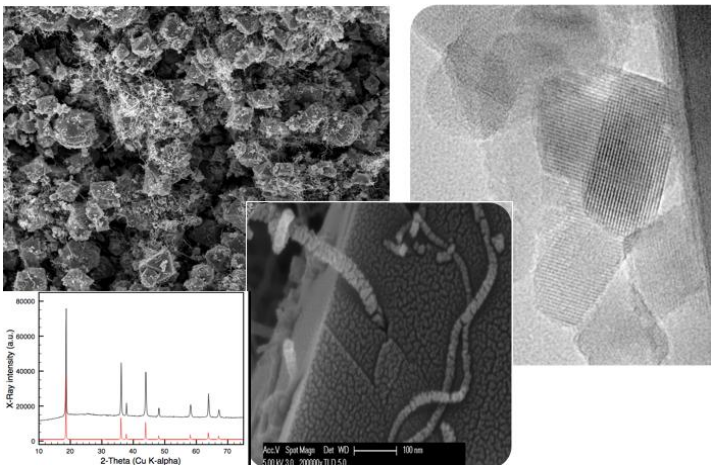

Figure 3. Hi-power cathode consisting of $LiMnO_4$ catalytically grown *in situ* and intimately mixed with well-dispersed, inexpensive multiwall carbon nanotubes). X-ray diffraction (lower left shows high-purity of the spinel nanocrystallites. Scanning electron micrographs (upper left and center) show highly faceted crystals intimately mixed and connected with CNTs. High-resolution TEM (right) shows atomic lattices of uniform, highly faceted nanocrystallites.

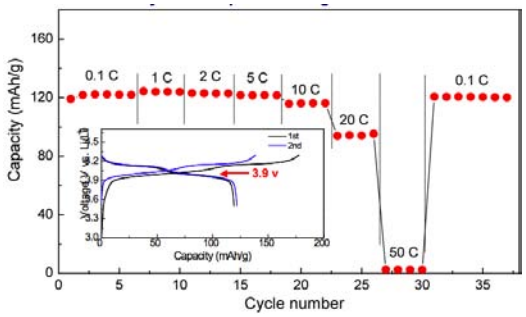

Figure 4. High power performance of catalytically fabricated nanocomposite cathode shown in Fig. 1. Note 96% capacity after discharge at 10C, >80% capacity after discharge at 20C, and complete recovery after complete discharge at 50C. Inset shows capacity as a function of voltage, indicating 3.9 v average voltage of this cathode.

III Future Plans:

Future plans include dynamic analyses during cycling of the electrodes described above by *in situ* measurements using NMR and synchrotron XRD to analyze the mechanisms of ionic and electronic entrance, storage and exit, with the aim of identifying kinetic barriers to these processes that can be addressed by further improvements in design and synthesis.

IV References (work supported by this DOE project):

Schwenzer, B., K.M. Roth, J. R. Gomm, Meredith Murr & D. E. Morse. 2006. Kinetically controlled vapor-diffusion synthesis of novel nanostructured metal hydroxide and phosphate films using no organic reagents. J.Mater. Chem. 16: 401 - 407

Brutchey, R.L. and D.E. Morse. 2006. Template-free, low-temperature synthesis of crystalline barium titanate nanoparticles under bio-inspired conditions. Angewandte Chemie Intl. Ed. 45: 6564-6566.

Schwenzer, B. and D. E. Morse, 2008. Biologically inspired synthesis route to three-dimensionally structured inorganic thin films. Journal of Nanomaterials, vol. 2008, Article ID 352871, 6 pages, 2008. doi:10.1155/2008/352871.

Zhang, H.-L. and D.E. Morse. 2009. Vapor-diffusion catalysis and *in situ* carbothermal reduction yields high performance Sn@C anode materials for lithium ion batteries. J. Mater. Chem. 19: 9006 – 9011.

(DOI: 10.1039/b914554k)
Zhang H.L., J. R. Neilson and D. E. Morse. 2010. Kinetically controlled sol-gel synthesis of flaky lithium vanadium oxide and its electrochemical behavior. J. Phys. Chem. C 114 (45), 19550–19555,

V. Other publications from work supported by the DOE project over the last two years:

Neilson, J.R., B. Schwenzer, R. Seshadri and D.E. Morse. 2009. Kinetic control of intralayer cobalt coordination in layered double hydroxides: $Co^{oct}_{1-0.5x}Co^{tet}_{x}(OH)_2(Cl)_x(H_2O)_n$. Inorg. Chem. 48: 11017-11023.
Schwenzer, B., L. Pop, J. Neilson, T. B. Sbardellati and D.E. Morse. 2009. Nanostructured ZnS and CdS films synthesized using layered double hydroxide films as precursor and template. Inorganic Chemistry 48(4), 1542-1550.
Schwenzer, B., J.R. Neilson, K. Sivula, C. Woo, J. M. J. Fréchet and D. E. 2009. Nanostructured *p*-type cobalt hydroxide thin film infilled with a conductive polymer yields an inexpensive bulk heterojunction photovoltaic cell. Thin Solid Films 517: 5722-5727.
Qian, F., M. Baum, Q. Gu and D. E. Morse. 2009. A 1.5 mL microbial fuel cell for on-chip bioelectricity generation. Lab on a Chip 9: 3076 - 3081.
O'Leary, P., C.A. v.-Walree, N. C. Mehendale, J. Sumerel, D. E. Morse, W. C. Kaska,* G. v.-Koten and R. J.M. K. Gebbink. 2009. Enzymatic immobilization of organometallic species: Biosilification of NCN- and PCP-pincer metal species using demosponge axial filaments. Dalton Transactions 22: 4289-4291
Niesz, K. and D. E. Morse. 2010. Sonication-accelerated catalytic synthesis of oxide nanoparticles. Nano Today 5: 99-105.
Neilson, J. R., J. A. Kurzman, R. Seshadri and D. E. Morse, 2010. Cobalt coordination and clustering in alpha-Co(OH)2 revealed by synchrotron X-ray total scattering. Chem. Eur. J. 16 (33), 9998-10006.
Tao, A.R., K. Niesz And D.E. Morse. 2010. Bio-Inspired nanofabrication of barium titanate. J. Mater. Chem., 20: 7916-7923
Niesz, K., C. Reji, J. Neilson, R.C. Vargas, C. and D.E. Morse. 2010. Unusual evolution of ceria nanocrystal morphologies promoted by a low-temperature vapor diffusion-based process. Crystal Growth and Design, DOI: 10.1021/cg100708q
Schwenzer, B., J. R. Neilson, S.e M. Jeffries and D.l E. Morse. 2010. $Cd_{1-x}Zn_xO$ [$0.05 \leq x \leq 0.26$] synthesized by vapor-diffusion induced co-nucleation from aqueous metal salt solution. Dalton Trans. 2011, 40 (6), 1295 - 1301.
Niesz, K, T.Ould-Ely, H.Tsukamoto and D. E. Morse. 2011. Engineering grain size and electrical properties of donor-doped barium titanate ceramics. Cermics Internatnl. doi:10.1016/j.ceramint.2010.08.040 (in press).
Ould-Ely, T., K. Niesz , M. Luger , l. Kaplan-Reinig, K. Niesz, M. Doherty and D. E. Morse. 2011. First large-scale engineered synthesis of $BaTiO_3$ nanoparticles using low temperature bioinspired principles. Nature Protocols 6: 97-104.
Qian, F. and D.E. Morse. 2011. Miniaturizing microbial fuel cells. Trends in Biotechnol (in press).
Schwenzer, B., J. Hu, and D. E. Morse. 2011. Correlated compositions, structures, and photoluminescence properties of GaN nanoparticles. Adv. Mater. (in press).
Neilson. J.R. J.A. Kurzman, R. Seshadri[2], and D.E. Morse. 2011. Ordering double perovskite hydroxides by kinetically controlled aqueous hydrolysis. Inorg. Chem. (in press)
Neilson, J.R., D,E. Morse, B. C. Melot, D. P. Shoemaker, J. A. Kurzman, and R. Seshadri. 2011. Understanding complex magnetic order in disordered cobalt hydroxides through analysis of the local structure. Phys. Rev. B (in press).

Electrostatic Driven Self-Assembly Design of Functional Nanostructures

PI: Monica Olvera de la Cruz[1,2,3]. Co_PIs: Michael J. Bedzyk[1,4] and Graziano Vernizzi[5]

Participants: R. Sknepnek[1] and C. Y. Leung.[4]

Collaborators: S. I. Stupp,[1,3] L. Palmer[3] and J. W. Zwanikken.[1]

Departments of (1) Materials Science and Engineering, (2) Chemical and Biological engineering, (3) Chemistry and (4) Physics, Northwestern University, Evanston Il, and (5) Physics and Astronomy Department, Siena College, Albany, NY.

Program Scope: The project aim is to understand how to control the functionality of charged molecules by modifying the environment conditions like salt concentration and pH as well as by designing molecules with specific ionization states and charge density configurations. Such approach offers the possibility to design complex multifunctional structures with the ability to control properties with the nanoscale resolution. Due to their long-range nature, electrostatic interactions lead to complex correlation patterns and are able to drive the spontaneous formation of highly organized structures. By using biocompatible cationic and anionic amphiphiles we are able to generate closed shapes such as spheres, polyhedrons, and cylindrical assemblies with a tunable distribution of surface heterogeneities, which provides such shapes with a wide range of functionalities.

Moreover, ionic materials are particularly suitable for a fine control of the shape and structure as they can assemble and disassemble by modifying the pH of the solution or by including an electric field. In addition to its dependence on electrostatic interactions, the global structure of the co-assembly intricately depends on the microscopic architecture of the cationic and anionic amphiphiles, specific short-range interactions, charged densities and concentrations. In this proposal we explore molecular structure and external conditions to design the co-assembly of cationic and anionic peptide amphiphiles, into vesicles, which can from a wide range of regular and irregular polyhedral shapes. The outcomes of the proposed work are:

1. The guidelines to design amphiphilic molecules of opposite charges that will co-assemble into vesicles of different shapes and sizes
2. The analysis of the shape of the aggregates, and in particular, the parameters that determine the buckling of vesicles into different polyhedrons.
3. The understanding of the stability of the aggregates in different ionic conditions and the characterization of the structures.

Recent progress: We have developed a sophisticated multipurpose Monte Carlo code which allows us to rapidly generate and analyze shapes and patterns of multicomponent elastic shells that arise as a result of the self-assembly of ionic amphipiles with different charge ratios. The shells are assumed to be made of a thin solid membrane. Thus, next to the consideration of the bending contributions to the free energy a proper description of these quasi two-dimensional systems requires introduction of the elastic terms which penalize stretching. The coupling between bending and stretching necessarily present in the spherical topology leads to a rich set of phenomena even in our minimal coarse-grained model. We have explored in details[1] the gallery of shapes of a two-component elastic shell assembled of two elastic materials with substantially different elastic properties like bending rigidity and Young's modulus, i.e., one

component is set to be very stiff and therefore hard to bend, while the other is soft and easily accommodates large deformations. Such soft regions are believed to naturally arise at the contacts of the crystalline domains present on the surface of an ionic vesicle. In contrast to similar techniques used in the literature to study optimal shapes of various elastic sheets and shells, our approach makes no assumptions on either shape or component distribution, but uses simulated annealing method so concomitantly optimize the shape and the distribution of the components.

The observed buckling mechanism is very different than the commonly reported icosahedral deformation located at the twelve topological disclination defects responsible for the transition from a spherical shape for small shell radii to an icosahedron for larger shells, e.g., as observed when studying shapes of various viruses. In the case of a two-component system there is a separate pathway for the shell to relieve some of its stress. Instead of buckling at the effects, such shell can form very sharp ridges of the soft component. Those ridges are substantially bent with most of the curvature concentrated along them. As a result nearly flat facets of the hard component are formed and the shell takes a polyhedral shape. The exact number of facets as well as the optimal shell shape is determined by the relative fraction of the two components and the ratio of their elastic constants. It is worth noting that while vast majority of obtained shapes are irregular with a carefully tuned set of elastic parameters and component fractions one can obtain regular Platonic and Archimedean solids. Typical optimal shell shapes for a various fractions of the soft component are shown in Fig. 1 (a).

Despite a very rich variety of observed polyhedral shapes, including highly symmetric Platonic structures, the model used in Ref. [1] does not include energy penalty for mixing of the components, i.e., no line tension is associated with the boundary between the soft and hard domains. As such domains in principle can arise by mixing chemically different amphiphiles, it is natural to expect a certain degree of mixing penalty. In Ref. [2], we extend our model to include line tension between soft and hard components. The gallery of the resulting optimal shapes is even richer than with no line tension, with various polyhedral and Janus-like shell structures. A small subset of those shapes is shown in Fig. 1 (b).

In addition to the crystallization of the lipid molecules for very small shells (diameter ~20nm) the electrostatic interaction can lead to a reversible collapse of the structure. In Ref. [3] we explore this phenomenon in detail and show that for weak electrostatic interactions the elastic energy wins and electrostatics only slightly perturbs the shell shape. As the strength of the electrostatic interaction is increased, e.g., by tuning pH or the salt concentration of the surrounding, the shell can undergo a full collapse on completely. A series of such transitions is shown in Fig. 1(c) for a range of stoichiometric charge ratios on the shell surface.

We have also recently generated a large variety of shell geometries, either fully faceted polyhedral or mixed Janus-like vesicles with faceted and curved domains that resemble cellular shells by co-assembling a water-insoluble anionic (–1) amphiphile with cationic (+2 and +3) amphiphiles (by extending our previous work funded by this program to various non-polymerized amphiphiles mixtures: M. A. Greenfield, L. C. Palmer, G. Vernizzi, M. Olvera de la Cruz, and S. I. Stupp J. Am. Chem. Soc., 131 (34), 12030–12031 (2009)). Our electron microscopy, X-ray scattering, theory and simulations works demonstrate that the resulting faceted ionic shells are crystalline, and stable at high salt concentrations [4]. Elastic inhomogeneities resulting from the competition of ionic correlations with charge-regulation

explain the unusual shapes. This work promotes the design of faceted shells for various applications and improves our understanding of the origin of polyhedral shells other than icosahedra in nature.

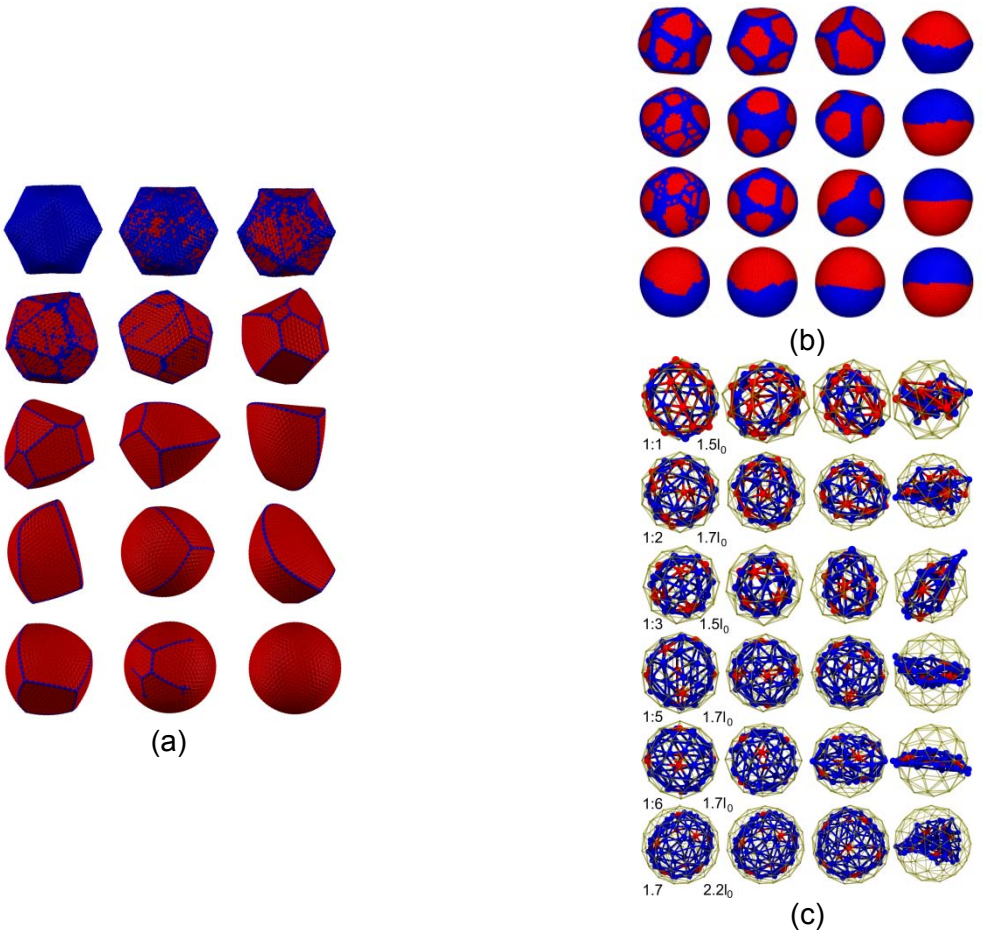

Fig. 1: (a) Gallery of optimal shapes of a two component elastic shell with hard (red) and soft (blue) components as a function of the relative ration of the two components; (b) variety of shapes is even richer if we introduce line tension between the components as shown for the 50% soft to hard component ratio; (c) electrostatic collapse of charged elastic nanocages for different stoichiometric surface charge ratios (indicated on the left side of each row).

Future plans: With the dependence of the shape on the elastic properties of its constitutive components firmly established, the following new developments will be pursued:

1. It is necessary to establish a more refined microscopic understanding of the origin of the elastic heterogeneity. In other words, it is desirable to build an atomistic or a particle based coarse grained description of the underlying amphiphilic system which would

provide a tool to accurately determine the elastic parameters in our coarse-grained elastic model;

2. Our calculation based on the continuum elasticity assumed the presence of regular crystalline lattices. It is necessary to see how much of the described physics applies to an amorphous solid membranes that would arise, e.g., in non-charged lipid membranes cooled below gelation temperature.
3. We will also describe the adsorption of ions at membranes separating liquids with different permittivity and the assembly of cationic-anionic molecules at liquid interfaces including dielectric heterogeneities.

Publications 2010-2011:

[1] G. Vernizzi, R. Sknepnek, M. Olvera de la Cruz, *Proc. Natl. Acad. Sci. U. S. A.* **108**, 4292-4296 (2011).
[2] R. Sknepnek, G. Vernizzi, M. Olvera de la Cruz, *Soft Matter*, accepted (2011).
[3] R. Sknepnek, G. Vernizzi, M. Olvera de la Cruz, *Phys. Rev. Lett.* (2011).
[4] L. C. Palmer, C. Y. Leung, R. Sknepnek, G. Vernizzi, S. I. Stupp, M. J. Bedzyk and M. Olvera de la Cruz (submitted).

Program Title: Dynamic Self-Assembly: Structure, dynamics, and function relations in lipid membranes (DE-FG02-04ER46173).

Principal Investigator: Atul N. Parikh, University of California, Davis, CA 95616, anparikh@ucdavis.edu Co-PI: Sunil K. Sinha, University of California, La Jolla CA 92093, ssinha@physics.ucsd.edu (sub-contract).

Program Scope. Cellular lipidome consists of about 9600 di stinct species of glycerosphingolipids, more than 100,000 species of sphingolipids, and many fatty acids and sterol based components. This enormous compositional complexity naturally raises a fundamental question: how are membrane components organized? A simple application of Gibb's phase rule predicts an unusually large number of co-existing independent phases within the equilibrated membrane medium. Experimentally, however, the number of co-existing phases in cellular membranes is almost invariably limited. A meaningful hypothesis, in this regard, is that the membrane's compositional heterogeneity is effectively reduced because many membrane components do not exist as chemically independent species and exhibit preferential associations forming structural (e.g., curvature-dependent) and compositional (e.g., micro-domains) complexes and assemblages. T hese compositional and structural biases or organized heterogeneities in membranes then couples with in-plane and out-of-plane dynamics (itself spanning a broad range of length- and time scales) to produce a spectacular array of spatially and temporally distinct membrane functionalities (e.g., molecular recognition, energy transduction, and transport) conferring the living system with a significant evolutionary advantage in placing function before structure. From the vantage of fundamentals of materials science, these notions of spatially and temporally organized heterogeneity or **dynamic and hierarchical self-assembly** embodied by domain structure and curvature-dependent organization suggest a major shift in fundamental emphasis from thermodynamic to kinetic regimes. H ere, equilibrium structures (global minima) are replaced by higher-order organizational states (e.g., transitions between various local metastable minima of different structures). Current program seeks to develop a fundamental understanding of the formation and organization of composition- and curvature-dependent sub-membrane assemblie us ing (1) well-defined membrane models in which molecular composition and ambient properties can be manipulated and (2) development of complementary spatially-and temporally resolved characterization methods.

Recent Progress. We have made considerable progress along each of the three objectives (as reflected in the publication list). Below, we highlight three of the most recent findings.

First, multilamellar lyotropic phases of stacked lipid bilayers exhibiting smectic liquid-crystalline order (or membrane multilamellae) are spontaneously produced primarily via hydrophobic forces of lipid-water interactions. A unique feature of such smectic mesophases of stacked-membrane systems is that while the constituent lipids exhibit in-plane translational degrees of freedom, their out-of-plane incoherent undulation fluctuations are severely restricted because of the steric spatial confinement they experience with the neighboring layers. In recent experiments, using membrane multilayers, consisting of phase-separating multi-component lipid mixtures, we have shown the existence of an additional order parameter, which propagates across hundreds of lamellae, producing long-range alignment of phase-separated domains in three dimensions. We also probed the dynamics of this smectic self-assembly. Our quantitative analysis of the real-time dynamical experiments reveals a unique interplay between the intra-layer domain growth and the inter-layer smectic coupling, suggesting a remarkably co-operative multilayer epitaxy. We postulate that this long range epitaxy is solvent-assisted, originating from the differences in the network of H-bonded water molecules at the aqueous interfaces of the domains and the surrounding phase. These results suggest new self-assembly based strategies for three-dimensional registration of functional domains toward designing biomolecular devices for applications spanning energy harvesting, photonics, sensing, and DNA delivery.

Second, our work with synchrotron x-ray and neutron scattering has been focused on determining the nanostructures of mixed lipid systems with various concentrations of cholesterol as model systems in order to understand the underlying physics of "raft" formation in real biological membranes. Nanophase separation is known to lead to the formation of domains of ordered phases co-existing with fluid phase at physiological temperatures. Such in-plane structure may have important consequences in many membrane-mediated biological functions including protein trafficking, cell surface signaling, and membrane fusion. We have completed our analysis of synchrotron X-ray reflectivity studies of a mixed silicon-supported, wet lipid bilayer consisting of equimolar DPPC, DOPC, and cholesterol (CH) concentrations.

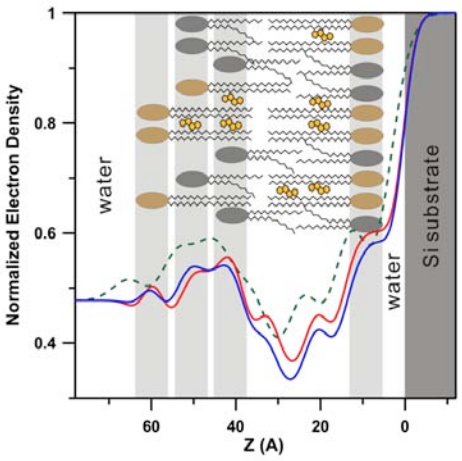

Figure 2.| Electron density profile for a raft-forming single supported bilayer consisting of 1:1:1 mixture of DOPC, sphingomyelin, and cholesterol. (Chen et al, in review).

We find an unusual consequence of a physical property of the membrane/ substrate interface in influencing phase separation in supported bilayers. The planarity of the interface constrains the head-groups of the inner leaflet to organize in a single topologically-defined plane within the roughness of the substrate. As a consequence, we find that the topology of the outer leaflet becomes strongly corrugated in multicomponent bilayers. This bilayer asymmetry causes phase separation in mixed bilayers on substrates to be modified from that exhibited in giant unilamellar vesicles (GUV's) which have been the subject of several studies, mainly using optical fluorescence microscopy.

Third, Mechanochemical coupling in cells represents a dynamic means by which membrane components are spatially organized. An extra-ordinary example of such coupling involves curvature-dependent polar localization of chemically-distinct lipid domains at bacterial poles, which also undergo dramatic reequilibration upon subtle changes in their interfacial environment such as during sporulation. This year, we demonstrated that such interfacially-triggered mechanochemical coupling can be recapitulated in synthetic systems by real-time introduction of mechanically-generated periodic curvatures and attendant strain-induced lateral forces in lipid bilayers supported on elastomeric substrates.

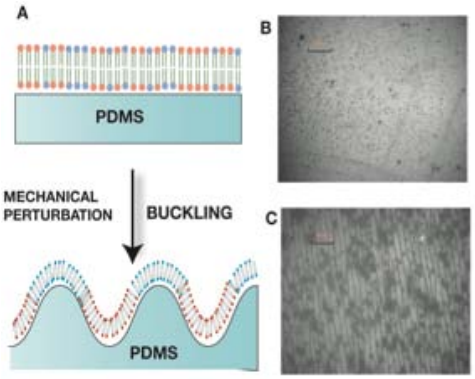

Fig. 3| Dynamic reorganization of membrane components [cholesterol /DOPC/sphingomyelin]. (A) Introduction of interfacial buckling permits (B→C) dynamic re-equilibration, sorting cholesterol-enriched domains in regions of low curvature.

In particular, we demonstrated that real-time wrinkling of an elastomeric substrate, following membrane deposition prompts a dynamic domain reorganization within the adhering phase-separation bilayer (Fig.3), producing large, oriented liquid-ordered domains enriched in cholesterol and sphingomyelin in regions of low curvature. Our results suggest a mechanism in which interfacial forces generated during surface wrinkling and the topographical deformation of the bilayer facilitate dynamic reequilibration prompting the observed domain reorganization. We anticipate this model system will prove to be a simple and versatile tool for a broad range of studies of curvature-dependent dynamic reorganizations under dynamic and elastic constraints (e.g., actin cytoskeleton).

Future Work. In addition to continuing our work on composition and curvature-dependent organization above, we will study how variations in interfacial hydration allows for dynamic reorganization of membrane components. As seen in our recent exploratory measurements using single lipids (See above), simple hydration of dry lipid plaques by bulk water produces non-equilibrium transient mesostructures characterized by their appearance and growth, coiling, uncoiling, and retraction. Building on these initial studies, we will ***first*** characterize the phase separation in tubular myelins formed during lipid hydration. ***Second***, we plan to develop systematic experimental correlations between protrusion properties (shapes, average maximum length, average diameter, and life times) as a function of key molecular properties of lipids (e.g., spontaneous curvature, chain saturation, and head-group charge) and ambient aqueous phase properties (e.g., pH and ionic strengths).

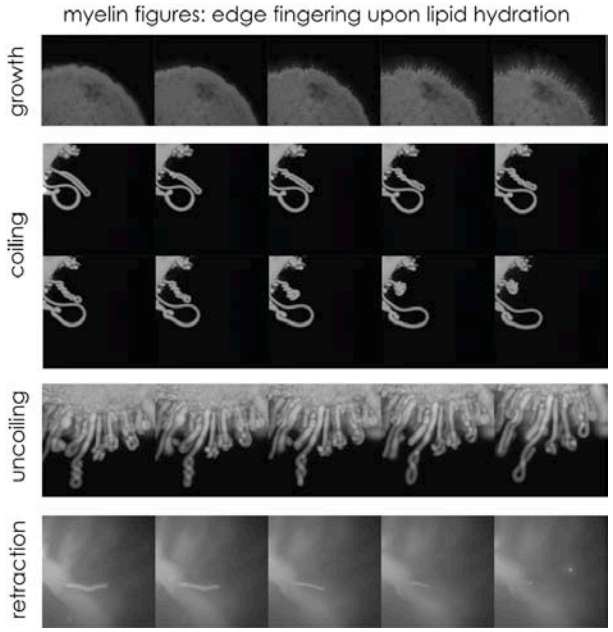

Fig. 4. Time-lapse fluorescence images obtained during hydration of a dry plaque of POPC by water. The four regimes observed reveal driven dynamic organization of tubular protrusions from the lipid front.

Together, these experiments furnish an elemental "phase diagram" for finger formation in terms of membrane molecular properties, ambient conditions, and the hydration differential force. Taken together, these studies help provide a clearer picture of mechanisms of this distinct class of interfacially driven self-assembly process.

Next, we study enzyme-induced reaction-diffusion processes that modulate membrane self-assembly. A dominant class of organized compositional heterogeneity, which sequesters saturated lipids with cholesterol, termed lipid rafts are believed to represent dynamic self-assemblies "activated" to coalesce into larger micro-domains by specific lipid-lipid, protein-lipid, and protein-protein interactions. Domains in these "activated" or coalesced states constitute a distinct ordered environment for many raft-dependent signaling functions. In addition to cytoskeleton activity, an important pathway for the "activation" of lipid rafts involves selective chemical transformation of raft-partitioning molecules. Such raft-specific chemistries then can be envisaged to set the stage reaction-diffusion mechanisms to modulate both the domain morphology and raft compositions. In this vein, an elegant example is the enzymatic action of sphingomyelinase (SMase) on raft-partitioning sphingomyelin (SM), which producing membrane-soluble ceramide. To explore the link between membrane morphology and real-time ceramide generation via SMase activity - specifically in order to dissect the roles of in-plane phase separation and out-of-plane membrane destabilization - we are devising a simple, model-membrane-based experimental strategy. Our model system is based on a supported lipid membrane configuration, with an added feature that complete bilayers and half-bilayers (or monolayers) can be juxtaposed on single samples, and their responses to enzyme activity probed simultaneously. We plan to characterize morphological and dynamical changes in terms of a mechanistic picture in which intra-leaflet fluidity, lateral phase separation, and inter-leaflet cooperativity act in concert to produce the gross reorganization of the membrane in response to SMase action.

At the Synchrotron, we continue our investigations of the dynamical fluctuations of these systems, using X-ray Photon Correlation Spectroscopy (XPCS) with coherent X-ray beams. Our experimental results on off-specular scattering and our calculations show that the scattering

should be observable provided we can focus the X-ray beam onto the sample. We have procured a focusing lens suitable for this purpose at the 8-ID beam line. These experiments should provide the first results using X-ray scattering on the slow dynamical fluctuations of pure and mixed lipid bilayers and we hope to use this to study properties such as the viscosity of the different fluid regions, and related properties also related to the static diffuse scattering such as the surface tension and the bending modulus of the bilayers. We will also study the difference in the dynamics of bilayers deposited directly on the substrate and on cushioned bilayers deposited on polymer or surfactant cushions on the substrate to see how interaction with the substrates affects the dynamics.

Publications (acknowledging current grant)

1. Structural and Compositional Asymmetry in Supported Lipid Bilayers, Gang Chen, Mrinmay K. Mukhopadhyay, Zhang Jiang, Yicong Ma, Curt M. DeCaro, Justin D. Berry, Adrian M. Brozell, Atul N. Parikh, Laurence B. Lurio, and Sunil K. Sinha, submitted, 2011
2. Structural characterization of a multiple stacked supported bilayer system, Curt. M. DeCaro, Justin. D. Berry, Laurence B. Lurio, Yicong Ma, Gang Chen, Sunil Sinha, Lobat Tayebi, Atul Parikh, Zhang Jiang and Alec R. Sandy, in revision, 2011
3. .pH Responsive Polymer Cushions for Probing Membrane Environment Interactions, Rita J. El-khouri, Daniel A. Bricarello, Erik B. Watkins, Caroline Y. Kim, Chad E. Miller, Timothy E. Patten, Atul N. Parikh, and Tonya L. Kuhl, **Nano Letters**, in press **2011**
4. In vivo lipidomics using single-cell Raman spectroscopy, Huawen Wu, Joanne V. Volponia, Ann E. Oliver, Atul N. Parikh, Blake Simmons, and Seema Singh, **PNAS**, 108, 3809-3814 **2011**.
5. Reconstituted lipoprotein: a versatile class of biologically-inspired nanostructures", Daniel A. Bricarello, Jennifer T. Smilowitz, Angela M. Zivkovic, J. Bruce German, Atul N. Parikh **ACS Nano**, 5, 42-57 **2011.**
6. "A Stripe-to-Droplet Transition Driven by Conformational Transitions in a Binary Lipid-Lipopolymer Mixture at the Air-Water Interface", Rita El-khouri, Shelli L. Frey, Alan W. Szmodis, Emily Hall, Karlina Kauffman, Timothy Patten, Ka Yee Lee, Atul N. Parikh, **Langmuir**, 27, 1900-1906, **2011**.
7. "Liposil-Supported Lipid Bilayers as a Hybrid Platform for Drug Delivery", Shukun Shen, Eric Kendall, Ann Oliver, Viviane Ngassam, Daodao Hu, and Atul N. Parikh **Soft Matter**, 7, 1001-1005, **2011**.
8. "Thermally induced phase separation in supported bilayers of glycosphingolipid and phospholipid mixtures", Alan Szmodis, Craig D. Blanchette, Margie L. Longo, Christine Orme, Atul N. Parikh **Biointerphases**, 5, 120-128, **2010**.
9. "A comparison of lateral diffusion in supported lipid monolayers and bilayers", Christopher B. Babayco, Sennur Turgut, Andreia Michelle Smith, Babak Sanii, Donald Landa, Atul N. Parikh, **Soft Matter** 6, 5877-5881 **2010**.
10. "Biosynthetic Decoys: Ganglioside embedded in reconstituted lipoprotein binds cholera toxin with elevated affinity", Daniel A Bricarello1, Emily J. Mills, Jitka Petrlova, John C. Voss, Atul N. Parikh, **J. Lipid Research**, 51, 2731-2738, **2010**.
11. Order at the Edge of the Bilayer: Membrane Remodeling at the Edge of a Planar Supported Bilayer is Accompanied by a L ocalized Phase Change, Andreia Michelle Smith, Madhuri Vinchurkar, Niels Gronbech-Jensen, Atul N. Parikh, **J. Amer. Chem. Soc.**, 132, 9320-9327, **2010.**
12. "Lipid Bilayers on Topochemically Structured Planar Colloidal Crystals: A Versatile Platform for Optical Recording of Membrane-mediated Ion Transport", Adrian M. Brozell, Sean Inaba, A. N. Parikh, **Soft Matter** 6, 5334-5341 **2010.**
13. Salt-induced lipid transfer between colloidal supported lipid bilayers, E. L. Kendall, E. Mills, J. Liu, X. Jiang, C. J. Brinker and A. N. Parikh, **Soft Matter,** 6, 2628-2632, **2010**
14. Templating Membrane Assembly, Structure, and Dynamics Using Engineered Interfaces, A. Oliver and A. N. Parikh, **Biochimica et Biophysica Acta**, 1798, 839-850, **2010.**

Program Title: Hyperbranched Conjugated Polymers and Their Nanodot Composites as Universal Bioinspired Architectures

Principle Investigator: Uwe Bunz[§,‡]; Co-PIs: Vincent Rotello,[#] Laren Tolbert [§]

Mailing Address: ‡ Department of Chemistry, University of Heidelberg, Heidelberg Germany.§ Department of Chemistry, Georgia Institute of Technology, Atlanta GA. # Department of Chemistry, University of Massachusetts, Amherst, MA

Program Scope

The goals of this program are to interface the structural and physical properties of polymers, proteins and nanoparticles. For polymer scaffolds we have explored both linear and hyperbranched conjugated polymers. These materials have been interfaced with gold nanoparticles (AuNPs) and quantum dots (QDs), generating supramolecular and covalent assemblies that synergistically combine the physical properties of the disparate materials. In our ongoing research we have added proteins to our toolkit, integrating their structural and catalytic properties to our systems.

Our research integrates the polymer expertise of **Bunz** with the nanoparticle and nanobiology experience of **Rotello**. The recent move of **Bunz** from Georgia Tech to Heidelberg has resulted in the addition of **Tolbert** as a co-PI, adding photophysical expertise to our program.

Recent Progress

Our research has successfully developed strategies for both covalent and non-covalent polymer-particle assembly. As our research progresses, we have increased our emphasis on the dynamic biomimetic opportunities provided by supramolecular assembly.

I) Particle-polymer self-assembly

In our research we have studied the interaction of rigid poly(phenylene ethynylenes) (PPEs) with AuNPs. This research has focused on both the fundamental understanding of the interactions as well as the applications of these systems for sensing.

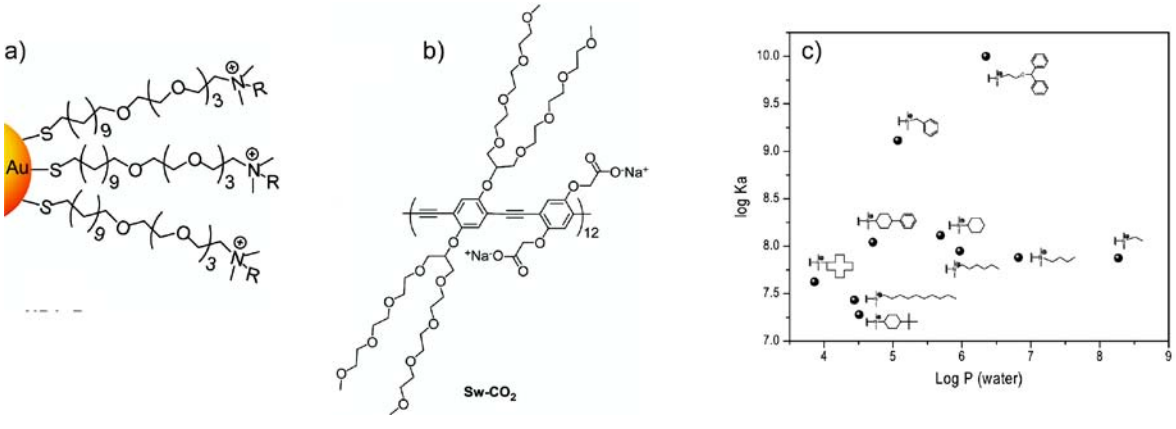

Figure 1. Interactions of nanoparticles and PPE polymers. a) Parent nanoparticle structure. b) PPE polymer. c) plot of particle-PPE affinity as a function of calculated headgroup hydrophobicity.

In fundamental studies, **Rotello** and **Bunz** have quantified the interaction of an anionic PPE with cationic AuNPs featuring a wide range of headgroups.[2] The water-oil log P values for these headgroups were estimated computationally, and binding affinity plotted versus the headgroup log P. Interestingly, particle-polymer binding was essentially independent of hydrophobicity. There was, however a strong correlation between aromatic surface area and accessibility and affinity,

indicating the importance of aromatic stacking in determining PPE-nanoparticle interactions.

II) Particle-Polymer sensing

Building on our fundamental studies of particle polymer interactions, **Rotello** and **Bunz** have developed sensing strategies for biosystems. In these studies we have demonstrated that non-covalent nanoparticle-polymer complexes can be used to differentiate between cell types as well as cell states. We have developed an array-based system for identification of normal and cancer cells (Figure 2a,b).[4] Using this sensing strategy we could rapidly (minutes/seconds) and effectively distinguish: 1) different cell types; 2) normal, cancerous and metastatic human breast cells; 3) *isogenic* normal, cancerous and metastatic murine epithelial cell lines (Figure 2c,d). The particles used for this study were chosen from a small library through screening using stepwise analysis with different polymer set(s) (i.e. jackknifed classification) to determine which NP set best differentiates between the cells (Figure 2e), a technique that provides insight into clustering of properties as well as utility in sensing. More recently, we have demonstrated effective cell differentiation using differentially-modified polymers.[6]

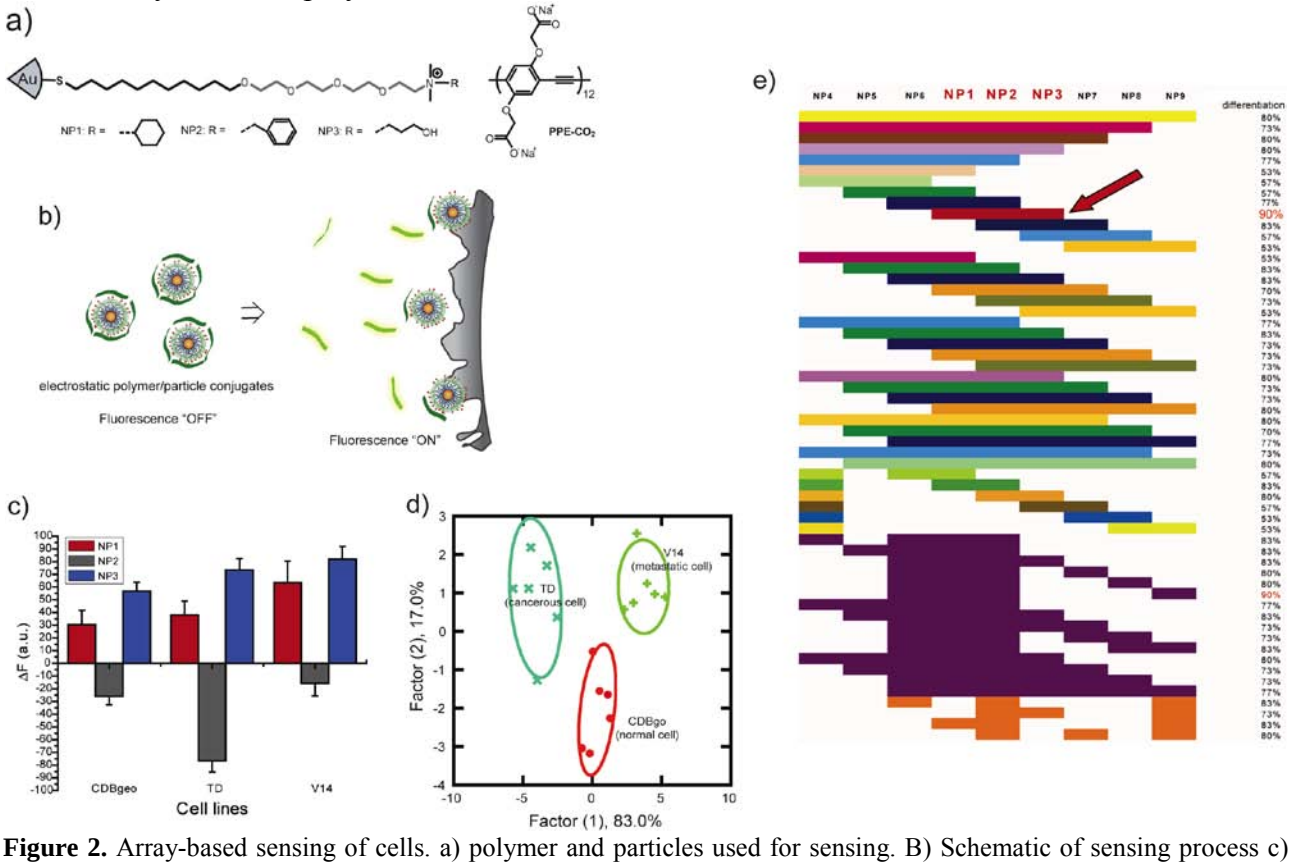

Figure 2. Array-based sensing of cells. a) polymer and particles used for sensing. B) Schematic of sensing process c) Fluorescence response for conjugates using three isogenic breast cell lines derived from BALB/c mouse. D) Canonical score plot for the first two factors of simplified fluorescence response patterns obtained with NP-PPE assembly arrays (95% confidence ellipses shown). e) Jackknifed classification matrix of the fluorescence data corresponding to different nanoparticle-polymer combinations for our particle-polymer cell sensing research, indicating maximal differentiation with only three particles of the nine tested. This strategy will be used to screen nanoparticles for our proposed protein and cell sensing.

Future Plans

Sensing is only one potential avenue of development for "smart" materials. In our future studies we will explore the creation of environmentally responsive materials using nanoparticles

developed by **Rotello** and polymers synthesized by **Bunz**. One particularly interesting architectural motif is self-assembly at the oil-water interface. For these studies, we will use charged linear and hyperbranched polymers to assemble complementarily-charged quantum dots at the surface of microemulsions. The structure of these assemblies will be established using optical and electron microscopy, while the dynamics will be determined by Tolbert using time-resolved spectroscopy.

Another area we will pursue is the integration of GFP chromophore analogs developed by **Tolbert** with polymer and nanoparticle architectures. We are exploring direct covalent attachment of these GFP-based systems through both conjugated and unconjugated linkages. We are also exploring the use of these chromophores for non-covalent self-assembly strategies. Once fabricated, we will determine the photophysical properties of these systems, with the expectation that both direct conjugation and energy transfer processes will result in novel behavior.

Publications acknowledging DOE support 2009-2011

12) Moyano, D. F.; Rana, S.; Bunz, U. H. F.; Rotello, V. M. "Gold Nanoparticle-Polymer/Biopolymer Complexes for Protein Sensing" *Faraday Disc*., in press.

11) Miranda, O. R.; Li, X. N.; Garcia-Gonzalez, L.; Zhu, Z. J.; Yan, B.; Bunz, U. H. F.; Rotello, V. M. "Colorimetric Bacteria Sensing Using a Supramolecular Enzyme-Nanoparticle Biosensor" *J. Am. Chem. Soc.* **2011**, *133*, 9650-9653.

10) McGrier, P. L.; Solntsev, K. M.; Zucchero, A. J.; Miranda, O. R.; Rotello, V. M.; Tolbert, L. M.; Bunz, U. H. F. "Hydroxydialkylamino Cruciforms: Amphoteric Materials with Unique Photophysical Properties" *Chem.-Eur. J.* **2011**, *17*, 3112-3119.

9) Yeh, Y. C.; Patra, D.; Yan, B.; Saha, K.; Miranda, O. R.; Kim, C. K.; Rotello, V. M. "Synthesis of cationic quantum dots via a two-step ligand exchange process" *Chem. Commun.* **2011**, *47*, 3069-3071.

8) Bunz, U. H. F.; Rotello, V. M. "Gold Nanoparticle-Fluorophore Complexes: Sensitive and Discerning "Noses" for Biosystems Sensing" *Angew. Chem. Int. Edit.* **2010**, *49*, 3268-3279.

7) Miranda, O. R.; Chen, H. T.; You, C. C.; Mortenson, D. E.; Yang, X. C.; Bunz, U. H. F.; Rotello, V. M. "Enzyme-Amplified Array Sensing of Proteins in Solution and in Biofluids" *J. Am. Chem. Soc.* **2010**, *132*, 5285-5289.

6) Bajaj, A.; Miranda, O. R.; Phillips, R.; Kim, I. B.; Jerry, D. J.; Bunz, U. H. F.; Rotello, V. M. "Array-Based Sensing of Normal, Cancerous, and Metastatic Cells Using Conjugated Fluorescent Polymers" *J. Am. Chem. Soc.* **2010**, *132*, 1018-1022.

5) Kub, C.; Tolosa, J.; Zucchero, A. J.; McGrier, P. L.; Subramani, C.; Khorasani, A.; Rotello, V. M.; Bunz, U. H. F. "Hyperbranched Conjugated Polymers: Postfunctionalization" *Macromolecules* **2010**, *43*, 2124-2129.

4) Bajaj, A.; Miranda, O. R.; Kim, I. B.; Phillips, R. L.; Jerry, D. J.; Bunz, U. H. F.; Rotello, V. M. "Detection and differentiation of normal, cancerous, and metastatic cells using nanoparticle-polymer sensor arrays" *Proc. Natl. Acad. Sci. U. S. A.* **2009**, *106*, 10912-10916.

3) Tolosa, J.; Kub, C.; Bunz, U. H. F. "Hyperbranched: A Universal Conjugated Polymer Platform" *Angew. Chem. Int. Edit.* **2009**, *48*, 4610-4612.

2) Phillips, R. L.; Miranda, O. R.; Mortenson, D. E.; Subramani, C.; Rotello, V. M.; Bunz, U. H. F. "Gold nanoparticle-PPE constructs as biomolecular material mimics: understanding the electrostatic and hydrophobic interactions" *Soft Matter* **2009**, *5*, 607-612.

1) Kim, I. B.; Han, M. H.; Phillips, R. L.; Samanta, B.; Rotello, V. M.; Zhang, Z. J.; Bunz, U. H. F. "Nano-Conjugate Fluorescence Probe for the Discrimination of Phosphate and Pyrophosphate" *Chem.-Eur. J.* **2009**, *15*, 449-456.

Program Title: Miniaturized Hybrid Materials Inspired by Nature

Principle Investigator: C. R. Safinya; Co-PIs: Y. Li and K. Ewert
Mailing Address: Materials Department, University of California at Santa Barbara
Santa Barbara, CA 93111
E-mail: safinya@mrl.ucsb.edu

Program Scope

The objectives of the program are to develop a fundamental understanding of the interactions and mechanisms underlying lipid- and protein-based assembly, which lead to hierarchical structures with distinct shapes and morphologies. The physicochemical approach used in the projects combined with custom synthesis, are designed to lead to biomolecular materials with scientific and technological interest. Nanoscale tubules and rods and their assemblies are of interest in a range of applications, including as templates for hierarchical nanostructures, enzyme encapsulation systems and biosensors, and vehicles for chemical delivery.

Much of our work is inspired by, and directed at, understanding the formation of novel structures (both relatively static and highly dynamic) observed in biological systems in vivo. A recent series of studies have focused on understanding network and bundle formation of biological polyampholytes (derived from cell cytoskeletal proteins) resulting from competing long-range repulsion and short-range attractions. We have discovered a novel neurofilament (NF) gel-expanded to gel-condensed transition mediated by the polyampholyte nature of the sidearms of NFs, which give rise to short-range attractions overwhelming long-range repulsions [1,2]. The interpenetration of the unstructured sidearms, which leads to the distinctly different mechanical properties of the two gel states with implications in cytoskeletal mechanical stability, is a unique finding not expected for brush-like polyelectrolyte materials. Counterion directed bundling of microtubules (MTs) is another important model system for studies of competing interactions [3,11]. Unexpectedly the studies revealed a transition from 3D to 2D bundles with decreasing counterion charge, which is not predicted by any of the current theories of polyelectrolytes. A separate series of studies on bioassemblies exhibiting “molecularly-triggered” dynamical shape changes (as occurs often in vivo), has led to the discovery of protein and lipid based nanotubule formation. The specific systems include (i) curvature stabilizing multivalent lipids forming nanotubes and nanorods [4-6] (mimicking membrane curvature generating proteins [12]) and (ii) invertible protein nanotubes from two-state tubulin building blocks [manuscript in preparation].

The projects involve purification of proteins [1,2] and custom synthesis of novel multivalent lipids [13,14], PEG-lipids with or without functional end groups, and environmentally responsive degradable lipids [7]. The projects utilize the broad spectrum of expertise of the group members in biomolecular self-assembling methods, synchrotron x-ray scattering and diffraction, and electron and optical microscopy characterization techniques.

Recent Progress

(1) Competing Long-Range Repulsion and Short-Range Attractions Microtubules (MTs) are nanometer scale hollow cylinders derived from the eukaryotic cell cytoskeleton. In vivo, MTs and their assembled structures (e.g. bundles resulting from interactions between MTs and microtubule-associated-proteins) are critical components in a range of cell functions from providing tracks for the transport of cargo (organelles, vesicles, neurotransmitters) to forming the spindle structure in cell division. Thus, while supramolecular structures of MTs are ubiquitous in vivo the mechanisms leading to their assembly remain poorly understood. In earlier work we reported on a novel new type of counterion-induced higher-order assembly of MTs [11]. Large sized, tri-, tetra-, and penta-valent cations, exhibit tight 3D hexagonal bundles. Unexpectedly, small, spherical divalent cations cause MTs to assemble into a 2D bundled structure where TEM revealed topologically distinct linear, branched, and loop morphologies not predicted by current theories of polyelectrolytes. The 3D to 2D bundle transition my be understood in terms of competing short-range attractions (tunable with changes in the counterion charge) and longer-ranged repulsions due to the unstructured C-terminus tail of tubulin [3].

Higher Order Assembly in Neurofilament Gels In recent BES supported work we used the synchrotron SAXS-osmotic pressure technique to directly measure forces, which stabilize the gel-like network of neurofilaments (NFs, Fig. 1) [1]. NFs are charged heteropolymers consisting of three distinct molecular-weight subunits (NF-L, NF-M, and NF-H). NF subunits spontaneously assemble to form a core filamentous protein and long sidearms extending away from the core NF filament. Our studies aim to understand the nature of the sidearm interactions and its role in stabilizing the NF-network, which is important to the axon cytoskeleton stability.

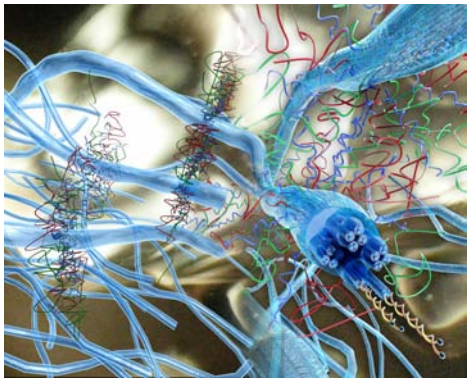

Fig. 1 Illustration of an interacting neurofilaments (NF) network including an end-view of one NF. NFs consist of three molecular weight subunits (NF-L, NF-M, NF-H), which self-assemble to form the mature neurofilament (NF). Each subunit protein is composed of an unstructured head, an alpha-helical body, and an unstructured charged sidearm domain of variable length extending radially from the filament core (red, green, blue). The alpha-helical domains of the NF subunits assemble through coiled-coil interactions to form the filament core. The interfilament side-arm attractions from adjacent NFs result from the (cationic/anionic) polyampholytic nature of the sidearm residues. Here, the end view of one neurofilament shows the hierarchical structure comprised of assemblies of coiled-coil alpha-helical dimers. Protruding sidearms (red, green, blue) mediate inter-filament interactions leading to mechanically stable axons (examples of two such interpenetrating sidearms are shown). Related to [1,2].

A significant finding was that for NF gels comprised of all three subunits (NF-LMH), the pressure-distance curves revealed an initial long-range repulsion followed by an abrupt gel expanded to gel condensed transition indicative of short-ranged inter-filament attractions between interpenetrating sidearms of neighboring NFs (examples of two such interpenetrating sidearms are shown schematically in Fig. 1). The interpenetration of the sidearms, which leads to the different mechanical properties of the gel state, is a unique finding not expected for brush-like polyelectrolytes (which lack both cationic and anionic charged residues). Similar attractions between sidearms on a single NF were also observed in recent AFM studies [2].

(2) Nanotubes and Nanorods from Curvature Stabilizing Charged Lipids Recently, we reported the formation of a new class of chain-melted liposomes, termed block liposomes (BLs) [4,5], in

mixtures of the charged curvature-stabilizing multivalent lipid MVLBG2 [13] (+16 e) and neutral lipid DOPC. Hallmarks of BLs are linked liposome shapes such as vesicles and micelles. In a BL, liposome shapes are comprised of lipid bilayers such as spheres and tubes, but also micellar rod comprised of a lipid monolayer, are connected into one object. Characterization of BLs led to a model for their formation that suggests an interplay of membrane undulations and concentration fluctuations of the two lipid components [4]. These lead to phase separation of MVLBG2 and DOPC, with MVLBG2 grouping into nanotube and nanorod regions of high curvature, and DOPC in locally flat bilayer spheres attached to the ends of nanotubes/nanorods.

Most recently we presented a cryo-TEM study on the formation of block liposomes [6] from membranes containing multivalent lipids MVL3 (+3e) or MVL5 (+5e) [14]. Both MVL3/DOPC and MVL5/DOPC lipid mixtures in water exhibit a regime of BL-formation with pronounced nanotube formation at Φ_{MVL3} = 0.1 to 0.3 and Φ_{MVL5} = 0.1 (Fig. 2). Our experiments show that formation of BLs is a general phenomenon in membranes containing multivalent charged lipids. BLs are candidates for templating of nanostructures such as wires and needles.

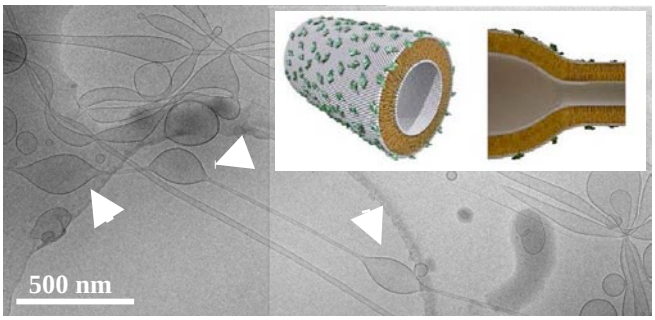

Fig. 2 Block Liposome and Nanotube Formation is a General Phenomenon of Membranes Containing Multivalent Lipids. Cryo-TEM image of MVL3/DOPC BLs (Φ_{MVL3}=0.1 (mole fraction)). White solid arrows point to the pearling instability occurring in this system. Enlarged insets (left) and (right) show an illustration of the molecular arrangement of the charged (green) and neutral (white) lipid. Adapted from [6] (see also [4]).

In a recent self-consistent field theory Greenall and Gompper have indeed found that mixtures of amphiphiles with different molecular shapes may form equilibrium block liposome phases [15]. The Greenall-Gompper model is the starting point for a revised model where the charge of the curvature generating lipid and counter-ions are explicitly taken into account.

(3) Invertible Protein Nanotubes We have recently discovered that microtubule bundles may be "molecularly-triggered" to undergo a dynamical shape change resulting from a configurational transition, from straight to curved, in the two-state tubulin building blocks of the MT walls [manuscript in preparation]. The result of this conformation transition is a "peeling" off of the tubulin oligomers, which then re-assemble in their curved conformation state to produce a novel "inverted" nanotube state where the original tubule outer surface now forms the inner surface.

Future Plans

(1) 2-Dimensional Ordering of Short-DNA Adsorbed on Cationic Membranes: Directed Assembly due to End-to-End Stacking Interactions Modulated Via Non-Sticky Overhangs

We are currently studying the conditions required for short double-stranded DNA (sDNA) to spontaneously assemble into ordered structures when confined in two dimensions [8]. Short nucleic acid (double stranded DNA or RNA) rods electrostatically adsorbed to oppositely charged cationic membranes are ideal macromolecules for such studies because of the ability to readily tune their anisotropic shape (L/D) with varying number of base-pairs. We are studying sDNA molecules, which contain varying length non-sticky ends in order to modulate the DNA end-end stacking interactions. The studies will have important implications in DNA-based

directed assembly on a 2D substrate platform where now the end-to-end stacking interactions may bond together building blocks, which contain short base-pairs tethered to their surfaces.
(2) Lipid nanotubues and Nanorods We will continue our studies, which use custom synthesized lipids with systematic variations in the headgroup steric size and charge of the curvature-stabilizing lipid. The experiments will distinguish between and clarify the separate contributions of key membrane parameters such as headgroup size, charge to the formation of block liposomes. The studies should also lead to optimal control of physical parameters, such as the conditions of nanorod versus nanotube formation and the nanotube diameter distribution.

References (which acknowledge DOE support)

1. Beck, R., et al.: Gel Expanded–Gel Condensed Transition in Neurofilament Networks Revealed by Direct Force Measurements. *Nature Materials* **2010**, 9, 40-46.
2. Beck, R., et al.:Unconventional Salt-Switch from Soft to Stiff in Single Neurofilament Biopolymers. *Langmuir* **2010**, *26*, 18595-18599.
3. Safinya, C. R. et al.: Nanoscale Assembly in Biological Systems: From Neuronal Cytoskeletal Proteins to Curvature Stabilizing Lipids. *Adv. Mater.* **2011**, 23, 2260-2270.
4. Zidovska, A. et al.: Block Liposomes from Curvature-Stabilizing Lipids: Connected Nanotubes, –rods or –spheres. *Langmuir* **2009**, 25, 2979–2985.
5. Zidovska, A. et al.: The effect of salt and pH on block liposomes studied by cryogenic transmission electron microscopy. *BBA - Biomembranes* **2009**, 1788, 1869–1876.
6. Zidovska, A., et al.: Block Liposome and Nanotube Formation is a General Phenomenon of Membranes Containing Multivalent Lipids. *Soft Matter* **2011** (published online 20 June).
7. Shirazi, R. S., et al.: Synthesis and Characterization of Degradable Multivalent Cationic Lipids with Disulfide-Bond Spacers for Gene Delivery. *BBA-Biomembranes* **2011**, 1808, 2156–2166.
8. Bouxsein, N. F., et al.:Two-Dimensional Packing of Short DNA with Non-Pairing Overhangs in Cationic Liposome–DNA Complexes: From Onsager Nematics to Columnar Nematics. *J. Am. Chem. Soc.* **2011**, 133, 7585–7595.
9. Leal, C., et al.: Highly efficient gene silencing activity of siRNA embedded in a nanostructured gyroid cubic lipid matrix. *JACS* **2010**, 132, 16841–16847.
10. Leal, C., et al.: Nanogyroids Incorporating Multivalent Lipids: Enhanced Membrane Charge Density and Pore Forming Ability for Gene Silencing. *Langmuir* **2011**, 27, 7691–7697.

Other References

11. Needleman, D. J., et al.: Higher-order assembly of microtubules by counterions: From hexagonal bundles to living necklaces. *PNAS* **2004**, *101*, 16099-16103.
12. McMahon, H. T. & Gallop, J. L. Membrane curvature and mechanisms of dynamic cell membrane remodelling. *Nature* **438**, 590-596 (2005).
13. Ewert, K., et al.: A columnar phase of dendritic lipid-based cationic liposome-DNA complexes for gene delivery: Hexagonally ordered cylindrical micelles embedded in a DNA honeycomb lattice. *J. Am. Chem. Soc.* **2006**, *128*, 3998-4006.9.
14. Ewert, K. K., et al.: Dendritic cationic lipids with highly charged headgroups for efficient gene delivery. *Bioconjugate Chem.* **2006**, *17*, 877-888.
15. Greenall, M. J.; Gompper, G.: Bilayers Connected by Threadlike Micelles in Amphiphilic Mixtures: A Self-Consistent Field Theory Study, *Langmuir*, **2011**, **27**, 3416-3423.

Electronic Interfacing Between a Living Cell and a Nanodevice: A Bio-Nano Hybrid System

Principle Investigator: Ravi F. Saraf
Chemical & Biomolecular Engineering; University of Nebraska – Lincoln; Lincoln NE 68588
rsaraf2@unl.edu

Program Scope

At nanoscale dimension the electronic and optical properties can be modulated by regulating size and shape of the material. The goal of the program is to develop and study fundamental electronic, electrochemical and structural characteristics of self-assembled nanoparticle in shape of necklaces, and explore their electronic interface with cells. Recent studies in this program have shown that these novel structures are sensitive to local charging by single electron making them sensitive to cellular activitiy.[1] A deeper understanding of the physics of these non-linear electronic systems will lead to a better structure-property relationship to tailor nanoparticle necklace material for catalytic electrodes and gating devices with impact on applications, such as, fuel cells and biosensors. The cell/necklace electrochemical coupling mediated by, (local) potential modulation or catalytic redox of cell products is considered.

The nanoparticle necklace deposited on a silica substrate, between Au electrodes form a two dimensional (2D) network that is sensitive to small modulation in the electrochemical environment and can be easily coupled to cell. The 1D chain of necklaces are made from 10 nm Au particles where, the adjacent particles are either bonded by an ionic bridge[1] or cemented with a salt.[2] High electronic sensitivity is obtained due to the small capacitance of the nanoparticles that create a substantial local Coulomb blockade barrier on charging by a single electron. Although, the barrier created by an electron in a single 10 nm particle is only ~50 eV, due to the local 1D topology of the network the single electron effect is greatly enhanced to affect a blockade with energy well above 500 eV. This makes them highly sensitive systems operable at room temperature.[1-3] Thus, the novelty of the necklace network structure is that it combines single electron sensitivity of nanoparticles and macro-scale integrability to circuits similar to CNT and nanowires. In a sense, similar to nature, the concept of the program is to translate phenomenon at small scale to build larger functional structures that are easy to integrate.

The overall strategy of the program is twofold: (a) Develop self-assembly processes to synthesize nanoparticle necklaces with tailored interfacial tunneling barrier structure between the nanoparticles, and deposition process to control the overall morphology/topology of the necklace network array. (b) Study their electronic and electrochemical behavior to understand the underlining guidelines to optimize their characteristics for proper electronic coupling to cells.

In the program, novel necklace self-assembly strategies, and (patterned) deposition method are developed to make precise electrical and electrochemical measurements. Because the necklace structures for testing will be small, typically 100 by 100 μm, a sensitive optical instrument is developed to measure *local* electrochemistry and electrochemical potential/charging.[4]

Recent Progress

Fabrication of Nanoparticle Necklaces in solution. Nanoparticle necklace fabrication has been reported.[1-3] Briefly, negatively charged Au nanoparticles are coated with a monolayer of mobile, cations in solution. As the particles come close to each other during Brownian motion, the cation monolayer rearranges leading to polarization of the particles. The local polarization cause the particles to bind forming a linear chain with the electric dipoles aligned. The formation is readily realized as change in the color of the solution from red to blue due to delocalization of surface plasmons. The electronic property of the network is studied by depositing them on SiO_2/Si chip with Au electrodes 10 to 100 μm apart.

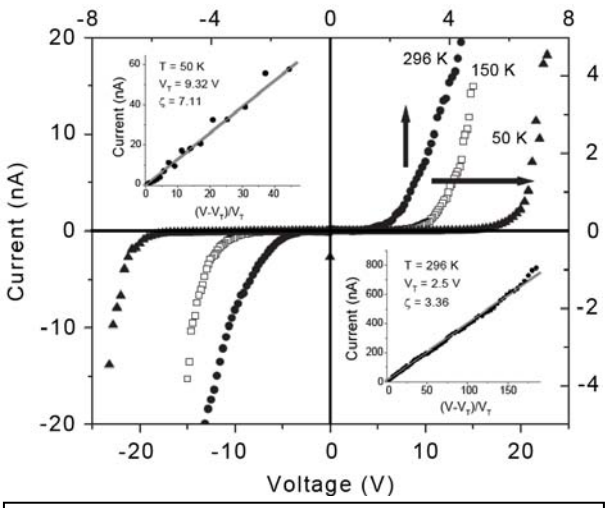

Fig. 1: I-V behavior of Au nanoparticle necklace cemented with CdS (….).

Electronic Property of 2D Nanoparticle Necklace Array: The current, I through the nanoparticle array as a function of applied bias, V is given as, $I \sim [(V-V_T)/V_T]^{\xi}$, where ξ is a critical exponent and V_T is the threshold bias needed to overcome the charge in the system. The strong non-Ohmic behavior is a signature of single electron behavior due local (single electron) charge storage called the quenched charge distribution that does not alter with applied bias. Typically, $\xi \sim 2$ for random 2D array of nanoparticles and the threshold is observed at sub-ambient temperatures. However, for the necklace network, ξ can be as large as 3.4 with $V_T \sim 2.5$ V (Fig. 1). The high V_T and large ξ is attributed to "efficient" single electron charge storage due to local quasi 1D morphology. <u>The high V_T and ξ will improve the sensitivity of coupling to cells.</u>

Electrochemical Property of the 2D Necklace Network Array. As a metallic electrode is immersed in an electrolyte solution, ions are spontaneously attracted towards the metal due to image charge. The sign of the charge depends on the difference in the Fermi Levels (i.e., electrochemical potential), $\Delta\varphi$ between the solution and the electrode. For example, if the Fermi Level of the electrode is lower (i.e., $\Delta\varphi > 0$) than the solution, anions will be attracted towards the electrode to bring the system in equilibrium. The result is a formation of an electrical double layer (EDL) with an accumulation of anions in the interfacial layer of nominal thickness given by the Debye length, ζ. The charge on the electrode will be $\sim -\Delta\varphi A/\zeta$, A is the electrode area. For a homogeneous, planar

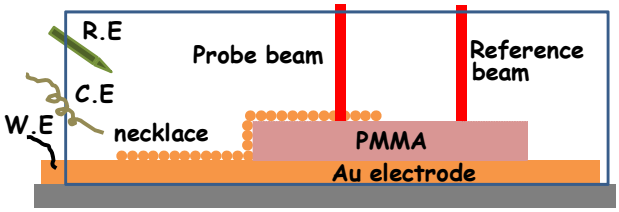

Fig. 2: Electrochemical set up with three electrode system to optically measure PZC.

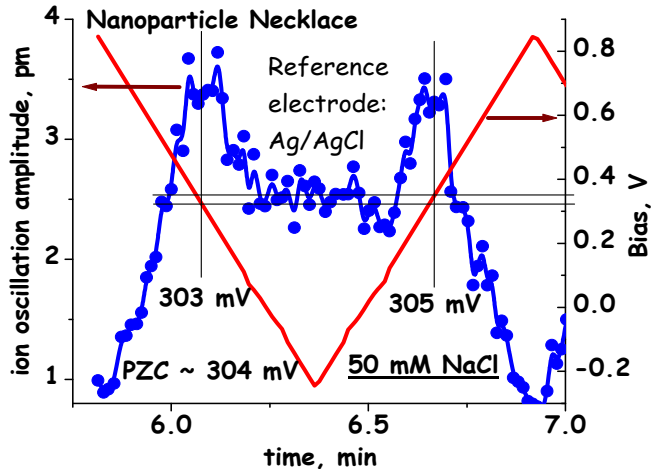

Fig. 3: Ion oscillation measured by interferometer for nanoparticle necklace electrode in contact with NaCl solution. (pm = picometer)

electrode, at potential of V with respect to the solution, the change density, $\sigma \sim (V-\Delta\varphi)/\zeta$. Thus, at $V = V_O$ (= $\Delta\varphi$), the charge in the EDL (and on the electrode vanishes) completely vanishes, and the EDL is completely discharged (i.e., it is removed). The potential, V_O is called the potential of zero charge (PZC). In a method partially developed in this program, for the first time, the PZC or Fermi Level distribution of an electrode relative to the electrolyte solution can be directly mapped. Briefly, a differential interferometer is designed to measure the amplitude of ion oscillation in the vicinity of the EDL at sensitivity of picometer.[4] For this study the necklace is deposited on a 30 nm thick polymer film and an electrode (Fig. 2). For non-Faradic ions in the solution (i.e., NaCl), the oscillation exhibits a maxima at PZC (Fig. 3). The PZC of the necklace is 304 mV (Fig. 3) which, is consistent with planar Au electrode at 310 mV (not shown).

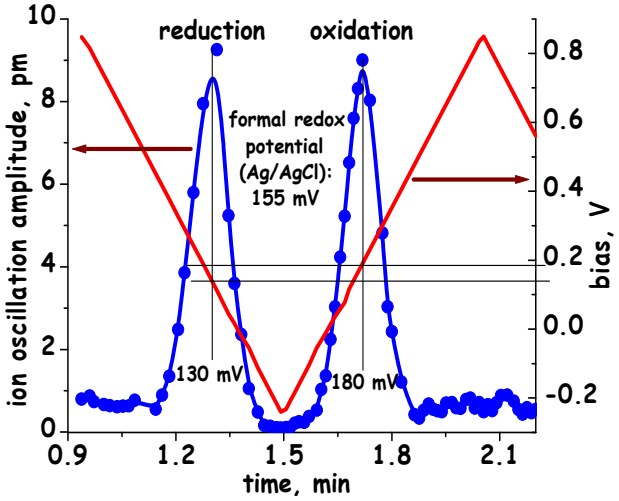

Fig. 4: Ion oscillation measured by interferometer for nanoparticle necklace electrode in contact with 50 mM $K_4[Fe(CN)_6]$ solution.

Interestingly, the nanoparticle necklace electrode is catalytic. The catalytic electrode property of nanoparticle necklace is studied by measuring local redox of $[Fe(CN)_6]^{4-/3-}$ using the same differential interferometer. The ion oscillation is highest at the redox potential (Fig. 4). Thus, the redox of $[Fe(CN)_6]^{4-/3-}$ occurs at 155 mV (with respect to Ag/AgCl) which is close to thermodynamic value (~140 mV) but about 60 mV below the formal redox potential for bare Au electrode also measured by interferometer (not shown). The redox currents are also significantly larger than that measured for bare Au electrode.

Electrochemical gating. The necklace network has the capability to store charge in the electrolyte media. Thus, the change in necklace potential with respect to the surrounding solution will modulate the quenched charge distribution leading change in the differential conductance of the necklace network (i.e., gating). A structure was designed and fabricated, where the source and drain Au electrodes are insulated by an organic photoresist film of SU-8 except for two ~100 μm holes called the "via" (Fig. 5, inset). The holes were fabricated using a standard lithographic

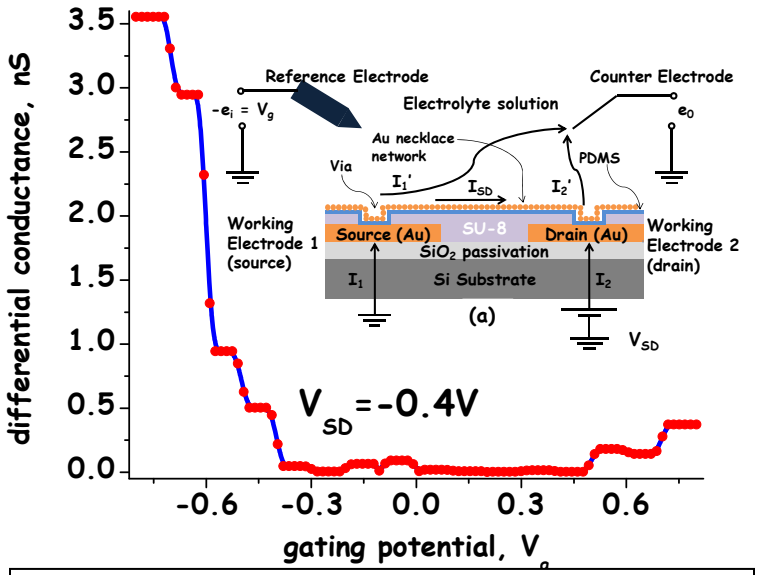

Fig. 5: Electrochemical gating (inset) using a four electrode bipotentiostat shows the change in differential conductance at a bias of V_{SD} = -0.4 V. The steep rise in conductance from -0.4 to 0.7V is remarkable compared to other nanostructures.

method. The nanoparticle necklace is deposited between the two via on the source and the drain using soft lithography based on a poly(dimethyl siloxane) (PDMS) stamp to make 100 µm line of necklace network. On modulating the potential between the solution and the necklace (i.e., V_g), the current modulates leading to a change in differential conductance (Fig. 5). Significant electrochemical gating of necklace is successfully achieved.

Future Plans

Sensitive electrochemical gating will lead to strong electronic coupling with mammalian cells. As the local pH, solution potential and ion concentration modulate the quenched charge distribution will modulate affecting the differential conductance. Such modulations occur in mammalian cells during to activities such as, respiration, action potential transport, and metabolism. The study would focus on understanding effect of parameters, such as, cementing, on gating sensitivity.

Catalytic activity of necklace electrode. Secretion of Superoxide flux from macrophages on exposure to lipopolysaccharides and formaldehyde from pichia pastoris in response methanol are two products that can undergo redox on catalytic electrode. Sensitivity of necklace electrode as a function structure will be studied to maximize its catalytic activity to propagate redox reaction.

Coupling to mammalian cell. The H^+/K^+-adenosine triphosphatase (ATPase) is the primary pump for acid secretion in gastric cells to maintain the pH in the stomach. The extracellular pH will be modulated by stimulating human gastric adenocarcinoma (AGS) cell in response to histamine to gate the necklace network electrode. Similar attempt with neurons due to action potential will be attempted and studied.

References (1 and 3 acknowledge DOE)

1. Kane, J; Inan, M.; Saraf, R.F., "Self-assembled Nanoparticle Necklaces Network Showing Single-Electron Switching at Room Temperature and Bio-Gating Current by Living Microorganisms," *ACS Nano*, **2010**, *4*, 317-323.
2. Maheshwari, V., Kane, Jennifer, and Ravi F. Saraf, *Adv. Materials*, **2008**, *20* (2), 284-287.
3. Kane, J; Ong, J; Saraf, R.F., "Chemistry, physics, and engineering of electrically percolating arrays of nanoparticles: a mini review", Feature article, *J. Material Chem.*, **2011**, accepted.
4. Singh, G.; Moore, D.; R.F. Saraf, *Analytical Chemistry*, **2009**, *81*, 6055-6060.

Program Title: Biopolymers Containing Unnatural Building Blocks
Principle Investigator: Peter G. Schultz
Mailing Address: The Scripps Research Institute, 10550 N. Torrey Pines Rd. SR202, La Jolla, CA 92037
Email: schultz@scripps.edu

Program Scope

Chemists have exquisite control over the structures of small molecules. However, our ability to control the structures of biological polymers such as proteins and nucleic acids is far more limited. Although it is possible to manipulate protein structures by selective chemical modification and by site directed mutagenesis, we are in general limited by the chemical functionality contained within the canonical twenty amino acid building blocks. For many applications of proteins to problems in energy, the environment or materials science, additional building blocks would be desirable and in many cases may be essential. To overcome this biological limitation we have developed a method that allows unnatural amino acids, beyond the common twenty, to be genetically encoded in bacteria, yeast and mammalian cells with high fidelity and good yields. Previously, a large number of amino acids with novel chemical and photochemical properties were genetically encoded. We are now exploring the use of these new building blocks to selectively modify the structures of protein to generate new functions, and to begin to create new classes of templated unnatural biopolymers of defined length and sequence. Specifically, we will: (1) develop methods for engineering and/or evolving metal ion binding sites in proteins and peptides to generate catalytic, redox active or structural elements; and (2) begin to develop the ability to generate templated biopolymers consisting of three or more distinct unnatural amino acids to ultimately biosynthesize defined length and sequence abiological polymers. This work should provide the scientific community powerful new tools to manipulate the properties of proteins in ways currently not possible for energy and materials related applications.

Recent Progress

A. *Development of mutually orthogonal tRNA/aminoacyl-tRNA synthetase (aaRS) pairs to incorporate multiple unnatural amino acids into biopolymers.*

The ability to simultaneously incorporate multiple unnatural amino acids into proteins should allow the synthesis of new structural and functional biopolymers. To achieve this goal we need to develop new tRNA/aaRS pairs which are mutually orthogonal to each other; the new pairs must be able to suppress a variety of mutually orthogonal at different sites in the same open reading frame; and the active sites of the new aaRSs need to be engineered toallow the incorporation of new unnatural amino acids. In addition to the two mutually orthogonal archaebacteria derived pairs in hand, we have focused on developing new pairs from seryl, prolyl and tryptophan tRNA/aaRS pairs. Screening of all possible combination of 6 tRNASer and 6 SerRS from archaea provided several efficient amber suppressors. The heterologous pair MmSRS/AftRNASer showed the highest activity. Since SerRS lacks an anticodon binding domain, a broad anticodon-tolerance for this pair was expected. Accordingly, efficient suppression of AGGA, CTAG, CCCT and TGA using this pair was verified. An acceptor-stem library of the tRNA has been generated to identify a more active, yet orthogonal hit. Screening of all possible combinations of six different archaeal tRNA and ProRS (chosen to represent the natural diversity) revealed only one heterologous pair (AfPtRNAPro/PhPRS) that showed amber suppression activity. To improve the efficiency of ProRS for tRNAProCUA, six residues in the anticodon binding pocket of PhPRS were randomized to generate a (NNK) 6 library which was screened for enhanced amber suppression efficiency. We then randomized 5 base pairs in the A-stem of the proline tRNA and screened the library to find a

considerably more active variant. Interestingly, most of the amber suppressing PhPRS mutants were specific for tRNACUA and did not charge tRNAAGGG (CCCT). Engineering of the anticodon loop of the tRNAAGGG created a significantly improved suppressor of CCCT. Thus, two efficient, mutually orthogonal Pro-pairs were evolved that could suppress TAG or CCCT. Finally, a yeast Trp pair was cloned into our vectors and was shown to be very weak. Using a combination of rational engineering and evolution, two tRNA hits were identified with considerably higher activity. To improve the interaction between ScWRS to SctRNACUA, a four-residue anticodon-binding library of ScWRS was constructed and is being screened.

B. *Improvements in protein yield and methodology*

We have developed a new expression system, pEVOL, for the incorporation of unnatural amino acids into proteins in *E. coli* using evolved *M. jannaschii* aminoacyl-tRNA synthetase(s) (aaRS)/suppressor tRNA pairs. This new system affords higher yields of mutant proteins through the use of both constitutive and inducible promoters to drive the transcription of two copies of the *M. jannaschii* aaRS gene. Yields were further increased by coupling the dual-aaRS promoter system with a newly optimized suppressor tRNA(CUA)(opt) in a single-vector construct. The optimized suppressor tRNA(CUA) afforded increased plasmid stability compared with previously reported vectors for unnatural amino acid mutagenesis. To demonstrate the utility of this new system, we introduced 14 mutant aaRS into pEVOL and compared their ability to insert unnatural amino acids in response to three independent amber nonsense codons in sperm whale myoglobin or green fluorescent protein. When cultured in rich media in shake flasks, pEVOL was capable of producing more than 100 mg/L mutant GroEL protein. These yields are transferring to multiple grams/liter in fermentation systems. The versatility, increased yields, and increased stability of the pEVOL vector will further facilitate the expression of proteins with unnatural amino acids. We have also generated aminoacyl-tRNA synthetases with broad specificity to facilitate the incorporation of a wide variety of building blocks into proteins. We employed a rapid fluorescence-based screen to assess the polyspecificity of several aminoacyl-tRNA synthetases (aaRSs) against an array of unnatural amino acids. We discovered that p-cyanophenylalanine (pCNF-RS) and coumarin (pCouRS) specific aminoacyl-tRNA synthetases have high substrate permissivity for unnatural amino acids, while maintaining their ability to discriminate against the 20 canonical amino acids. The orthogonal pCNF-RS, together with its cognate amber nonsense suppressor tRNA, is able to selectively incorporate 18 unnatural amino acids into proteins, including trifluoroketone-, alkynyl-, and halogen-substituted amino acids. In an attempt to improve our understanding of this polyspecificity, the X-ray crystal structure of the aaRS-p-cyanophenylalanine complex was determined. A comparison of this structure with those of other mutant aaRSs showed that both binding site size and other more subtle features control substrate polyspecificity.

C. *Engineering new protein structures and functions*

i) *Metal ion binding sites.* Reengineering the existing structure and function of a naturally occurring protein with unnatural amino acids (UAAs) offers the opportunity to answer some basic biochemical questions, and may also provide guiding principles to design and create artificial proteins with new structures and functions. Recent progress has enabled the efficient screening of protein libraries containing the metal-chelating amino acid residue, (2,2′-bipyridin-5-yl)alanine

(Bpy) for new structures and functions. We chose the zinc finger DNA-binding protein zif268 as our model system. Zif268 contains three domains whose folded structures are individually stabilized by bound zinc ions. Each domain recognizes a corresponding tri-nucleotide DNA sequence. A library targeting the residues of the first domain was constructed. Five sequential residues located on the α helix of this domain (His125, Ile126, Arg127, Ile128 and His129) were randomized. The codons of residues 125 and 129 were mutated to DNK (coding Bpy and all canonical amino acids except for His, Pro and Gln), and the codon of residues 126, 127 and 128 were mutated to NNK (encoding Bpy and all 20 canonical amino acids). Mutant sequences of zif268 were fused upstream of the filamentous phage pIII gene. The library was used to cotransform E. coli Top10F' cells harboring another plasmid expressing the orthogonal pair of tRNA and aminoacyl-tRNA synthetase (aaRS) that encodes Bpy in response to the amber TAG codon. The mutant zif268-pIII fusion proteins and other phage components encoded by the hyperphage, assembled in E. coli to form phage particles whose surfaces display mutant zif268 proteins. The selection was carried out by mixing phage with biotin-labeled dsDNA containing the GCGTGGGCG binding sequence and unlabeled competitive dsDNA containing the GCGTGGTAT sequence. Five rounds of selection enriched phages specifically bound to the target dsDNA. Three converged mutants were purified as MBP fusions. Gel mobility assay was used to confirm the binding and determine the binding constants to the corresponding dsDNA. The binding constants of these three mutants were determined (10.2 nM, 14.3 nM and 5.4 nM, respectively), comparable to the Kd of the wild-type zif268 (6.2 nM). EPR and UV-Vis spectroscopy indicate we have generated new Fe(II) binding site in places of natural Zn(II) sites. This work should pave the way to the creation of new metal ion binding sites in proteins for catalytic, sensor and structural applications.

ii) *Nanomolding.* We have begun a new effort to use unnatural amino acids to direct polymerization reactions in naturally occurring biological nanostructures. Bromoisobutyryl bromide is a widely used ATRP initiator which can trigger controlled polymerization reactions. We have evolved a *Methanosarcina barkeri* pyrrolysine tRNA and synthetase pair to site-specifically incorporate this ATRP initiator into proteins. We are now attempting to genetically introduce this unnatural amino acid within the interior of various biotemplates, to selectively initiate ATRP polymerization and synthesize polymeric nanoparticles. Bacteriophage HK97 prohead is a well-characterized capsid structure, which has a 60nm icosahedral cavity surrounded by a 0.2 nm-thick wall of protein. Based on the crystal structure of the gp5 subunit, we have chosen cavity-oriented residues to introduce the ATRP inhibitor. After expression in *E. coli*, the purified mutant particles containing the ATRP initiator will be equilibrated with the monomer solution through the ~10 A size pores between capsomer junctions. Copper (I) will be added to trigger polymerization; the reaction will be monitored by native agarose gel analysis and the shape of particle will be determined by TEM imaging. Upon completion of the polymerization, proteolytic removal of capid proteins will be carried out by the treatment with proteinase K. To verify that the ATRP initiator amino acid can be stably incorporated into proteins**,** we first expressed myoglobin as a model system. The incorporation of the unnatural amino acid was confirmed by both SDS-PAGE gel and mass spectrometry.

Future Plans

In the next year we will focus on the following three efforts: (1) genetically encoding multiple unnatural amino acids through the development of multiple, orthogonal UAA specific tRNA/aaRS pairs; (2) building additional synthetic metal ion binding sites into proteins; and (3) using UAAs to carry out polymerization reactions in biological templates to create novel nanoscale architectures. Specifically we will further optimize the orthogonal serine, proline and tryptophan pairs. We will at the same time build active site libraries in an attempt to evolve these aaRSs to accept novel backbone (cyclic amino acids, N-Me amino acids, β-amino acids) and side chain structures. We will then attempt to substitute 2-4 distinct UAAs into a single polypeptide chain. On a second front we will continue the characterization of the synthetic Zif268 Fe(II) site using a combination of x-ray crystallography, magnetic circular dichroism spectroscopy and resonance raman techniques. We will then attempt to replace the remaining Cys residues by a similar in vitro evolution approach. At the same time we will attempt to broaden this approach to the generation of metal ion dependent catalytic sites in proteins. Here we have begun to generate libraries of a noncatayltic E. coli protein in the attempt to create a Zn or Fe dependent acyl transfer catalyst. These libraries will be selected using a scheme that depends on hydrolysis of a toxic substrate. We are also attempting to use metal ion binding amino acids to mediate the homodimerization of coiled coil proteins in an effort to template the self-assembly of biomolecules with metal ions. On a third front we will continue our efforts to utilize ATRP initiating UAAs to create novel nanopolymers. We are currently attempting to develop efficient, O_2 free conditions for carrying out polymerization reactions with our myoglobin model system. At the same time we are characterizing our gp5 mutants with regard to mutant particle expression levels and stability. We expect high yields of protein containing UAA, but if stability proves a problem then we can chemically crosslink the phage proheads prior to polymerization. The next step will be to attempt polymerization reactions under a variety of conditions (monomer concentrations, scavengers, etc.) and characterize the resulting particles (in collaboration with the Johnson lab at TSRI) both in the presence and absence of protease treatment.

Publications (2009 – 2011)

1. Lee, H.S., Spraggon, G., Schultz, P.G., Wang, F. "Genetic Incorporation of a Metal-ion Chelating Amino Acid into Proteins as a Biophysical Probe." *J. Am. Chem. Soc.*,131(7):2481-2483*,* **2009**.
2. Young, T.S., Ahmad, I., Brock, A., Schultz, P.G. "Expanding the Genetic Repertoire of the Methylotrophic Yeast, *Pichia pastoris*." *Biochemistry,* 48(12):2643-2653, **2009**.
3. Chen, P.R., Groff, D., Guo, J., Ou, W., Geierstanger, B., Schultz, P.G. "A Facile System for Encoding Unnatural Amino Acids in Mammalian Cells." *Angew. Chem.,* 48(22):4052-4055*,* **2009**.
4. Ai, H., Shen, W., Brustad, E.M., Schultz, P.G. "Genetically Encoded Alkenes in Yeast." *Angew. Chem.,* 49(5):935-7, **2010**.
5. Liu, C.C., Schultz, P.G. "Adding new chemistries to the genetic code." *Ann. Rev Biochem*, 79:413-44, **2010**.
6. Young, D.D., Young, T.S., Jahnz, M., Ahmad, I., Spraggon, G., Schultz, P.G. "An evolved aminoacyl-tRNA synthetase with atypical polysubstrate specificity" *Biochem.,* 50(11):1894-900, **2011**.
7. Young, D.D., Jockush, S., Turro, N.J., Schultz, P.G., "Synthetase polyspecificity as a tool to modulate protein function." *Bioorg. Med. Chem. Lett., in press,* **2011.**

Program Title: Theoretical Research Program on Bio-inspired Inorganic Hydrogen Generating Catalysts and Electrodes.

Principal Investigator : Annabella Selloni; Co-PI: Roberto Car
Mailing Address: Department of Chemistry, Princeton University, Princeton, NJ 08544
E-mail: aselloni@princeton.edu

Program Scope

The overall goal of the program is the theoretical design of a model electrocatalytic or photo-electrocatalytic system for economical production of hydrogen from water and sunlight via the hydrogen evolution reaction. A feasible system for production from sunlight and water must be made of earth abundant materials and contain a catalyst active enough to utilize efficiently electrons generated from the solar flux. The system we focus on is an FeS_2 (100) surface (the electrode) decorated with a cluster derived from the active site of the di-iron hydrogenase enzyme (the catalyst). The di-iron hydrogenases found in hydrogen-producing microorganisms have a turnover frequency of over 9000 H_2 molecules per second at room temperature, almost an order of magnitude faster than Pt. Their catalytically active site, the $[FeFe]_H$ cluster, could be an attractive candidate for a catalyst for hydrogen production from water by electro- or photo-catalysis. It is composed of abundant elements and is small enough to pack densely. The pyrite surface is chosen because its atomic structure is compatible with that of the $[FeFe]_H$ cluster and *a priori* suggests the possibility of stable linkage and easy electron transfer to the cluster.

The hydrogen production cycle of the $[FeFe]_H$ cluster and its coupling to a pyrite electrode have been explored in earlier work funded under this program.[1-3] We found that $[FeFe]_H$ does not remain structurally stable in contact with acidified water during the course of the hydrogen evolution reaction.[3] The cluster has to be redesigned in order to be stably attached to the electrode surface and retain its catalytic activity outside the enzyme. This goal has been achieved in more recent work based on ab-initio molecular dynamics simulations. We have designed a catalytic cluster, $[FeFe]_P$, obtained by modification of the $[FeFe]_H$ cluster of the di-iron hydrogenase, and functionalized the pyrite (100) surface with it.[4] Remaining stable throughout, the $[FeFe]_P$ cluster produces hydrogen from acidified water with a free-energy barrier of less than 8.2 kcal/mol in room temperature simulations. The rate-limiting step in the cycle is the first protonation, subsequent steps are barrier free and fast. A detailed mechanistic analysis of the oxidation-state changes and electron flow during that step has been carried out.[5]

It is known that di-iron hydrogenases are inactivated by oxygen[9,10] and pyrite decomposes in the presence of oxygen and water.[11] Our preliminary studies of the O_2 sensitivities of $[FeFe]_P$ and FeS_2(100) indicate that dissolved oxygen, which is inevitably present in the electrochemical cell, can attack and inactivate the $[FeFe]_P$ / FeS_2 system as well. Our next goal is then to design a protective structure which inhibits the attack of the clusters and the exposed FeS_2 sites by dissolved O_2. At question are the optimal composition and internal structure of suitable overlayer molecules as well as the nanoscale structure of the overlayer into which those molecules pack. This hydrophobic overlayer should form densely in the interstices between the clusters but leave open above each cluster nanoscale water channels with hydrophobic walls.

The last part of our project will be devoted to the challenging task of characterizing the properties of the H_2-evolving catalyst inside the water-filled channels of the protecting overlayer

on FeS_2(100). The main questions that need to be addressed concern the influence of the confining channel, including its length, on the structure and stability of the supported cluster, its sensitivity to O_2, and finally its ability to produce H_2.

Recent Progress

The achievements to date are: 1. design of the $[FeFe]_P$ catalytic cluster; 2. demonstration of hydrogen production from acidified water; 3. demonstration of structural stability of the functionalized surface throughout the production cycle; 4. identification of the first protonation of the catalyst as the rate-limiting step in the cycle, with an upper bound of 8.2 kcal/mol for its free-energy barrier; 5. detailed mechanistic analysis of the bond switching, oxidation-state changes, and electron flow during the first protonation; 6. study of O_2 sensitivity of $[FeFe]_P$ and pyrite.

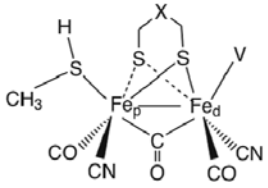

Figure 1. The active μ-CO isomer (after Ref. [1]).

Design of $[FeFe]_P$: We studied the hydrogen production cycle of the unsupported $[FeFe]_H$ cluster in vacuo[1] and in acidified water.[2] In the di-iron $[FeFe]_H$ cluster, two iron atoms are coordinated to CO and CN ligands and bridged by a chelating group, S-CH_2-X-CH_2-S where X is an NH (DTMA) or CH_2 (PDT) group, Figure 1. One iron atom, Fe_p, is 6-fold coordinated, the other, Fe_d, 5-fold with a vacant coordination site V at which the reaction occurs in the active isomer.

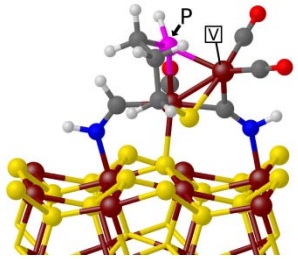

Figure 2. Side view of the $[FeFe]_P$ cluster linked to the FeS_2 (100) surface.

We made several critical modifications to $[FeFe]_H$ (with PDT) to obtain a stable and functional pyrite-supported catalyst.[3] To form $[FeFe]_P$, Figure 2, we 1. stripped off the thiol from Fe_p and connected it directly to a surface sulfur atom; 2. linked a surface Fe atom to the N atom of the CN ligand of Fe_p; 3. interchanged the CO bridging group with the CN ligand of Fe_d to form a third link between the N atom and a surface Fe atom, locking the cluster into the bridging configuration; and 4. changed the outer S in the chelating group to an isoelectronic PH group to stabilize the Fe_d-chelating group bond.

Demonstration of structural stability and H_2 production: Both the cluster-electrode linkage and the cluster structure remain stable throughout the H_2 production cycle,[4] which starts with the $[FeFe]_P^{-1}$ state. Both proton additions take place at the vacant coordination site V on Fe_d. The structural and compositional modifications leading to $[FeFe]_P$ eliminate other protonation sites and structural lability and simplify the reaction mechanism.

In water, the first proton moves towards Fe_d by a complex pathway over a free-energy barrier. We simulated the reaction by constrained FPMD, obtaining a barrier of $\leq$8.2 kcal/mol (0.36 eV) .[4]

Electron flow and oxidation-state changes: The rate-limiting step in room-temperature simulation of hydrogen production from acidified water is first protonation . Second protonation and H_2 desorption occur spontaneously during picosecond-scale simulations. We studied the mechanism of 1st protonation in Ref. [5] by computing densities of maximally-localized Wannier functions (WD) and their centers of gravity (WC) for several states along the reaction pathway of Ref. [4].

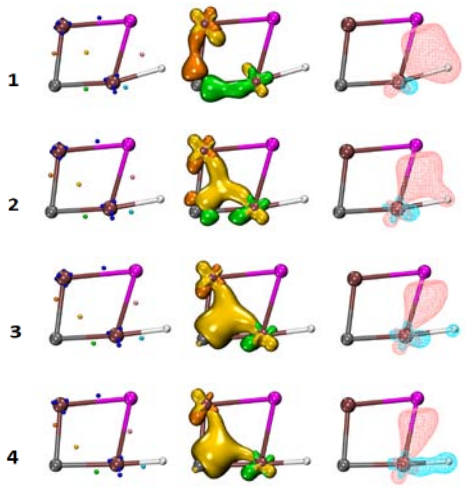

Figure 3. Four stages in the evolution of the relevant MLWF density and WC's as the first protonation proceeds. Fe atoms are brown; S atoms are yellow; the P atom is violet; C atoms are gray; N atoms are blue; O atoms are red; and H atoms are white. The isosurfaces are at 20% of their maximum values.

The locations and forms of the WD and the locations and movements of the WC established that only the Fe_p, Fe_d, μ-C, and P atoms as well as the added H play significant roles in the reaction. We determined the nature of their bonds, their oxidation states (OS), and t he electron flow responsible for the OS changes and bond switching. The P atom acts as the initial proton attractor, the μC-Fe_d pair act as the redox center, and the Fe_p acts to facilitate bond switching from two 2-center μC-to-Fe bonds to one 3-center bond upon protonation. These features of the reaction mechanism are displayed in Figure 3. This novel method of OS determination should be of broad use for the analysis of redox reactions; we illustrated it in [5] for the superoxide reductase enzyme as well.

O_2 sensitivity of pyrite and the catalyst: Undesirable oxidation of catalytic active centers is a common problem in catalyst design. To address these issues, we performed FPMD simulations of the reaction of O_2 with the catalytic center in water. The O_2 molecule was initially attached to the Fe_d of the $[FeFe]_p^{-1}$ cluster with the system solvated in water. O_2 binds stably on the Fe_d and rapidly abstracts a proton from a water molecule. The resulting OH^- in turn takes up a proton from a water molecule physisorbed on the pyrite surface via an H-bond chain. Two protons were added, one goes to the surface OH^- which had lost a proton to the O_2, the other the distal O of the O_2. The O-O bond breaks shortly after the 2nd protonation. A water molecule forms from the distal O and its two protons. The proximal O then forms a CO_2 molecule with the nearby terminal CO ligand which forms a ligand bond with the Fe_d.
Thus O_2 binding and its subsequent protonation poisons the catalyst, which must be protected from ambient oxidation.

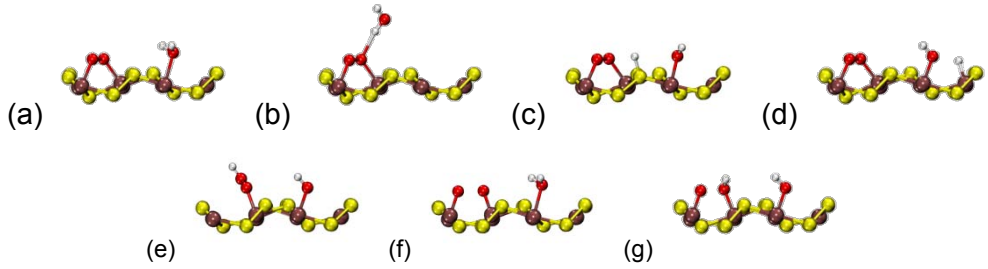

Figure 4. Representative configurations of O2 and H2O coadsorbed on the pyrite (100) surface.

The coadsorption of O_2 and H_2O on the pyrite surface was studied; representative configurations are shown in Figure 4. The most stable physisorption structure for O_2 is side-on where the two O atoms are linked two Fe atoms (configurations (a) and (b)). Proton transfer from H_2O to the surface S, to the surface Fe atoms, or to O_2 in end-on binding conformation (configurations (c), (d) and (e)) is energetically less favorable. A large gain in energy from configuration (a) is observed when the O-O bond breaks (configuration (f)), and the energy decreases further when one of the O atoms acquires a proton from H_2O (configuration (g)). This

agrees with the experiments suggesting that pyrite oxidation in the presence of O_2 is faster when water is present. Nudged-elastic band calculations give an energy barrier for O-O bond breaking of 6.1 kcal/mol. The two Fe to which the O_2 binds are oxidized from Fe(II) to Fe(IV) upon O-O bond breaking according to our new OS determination methods [5,7].

Future Plans

Reactions of the catalytic center and the pristine pyrite surface with molecular oxygen and water. Simulations are underway to obtain the free-energy profiles for O_2 binding on the $[FeFe]_P$ cluster and for the successive protonation steps on the O_2. Preliminary results indicate that while O_2 binds only metastably to the Fe_d of the $[FeFe]_p^{-1}$ cluster, the abstraction of a proton from the water proceeds too rapidly for the O_2 to desorb, thereby initiating the poisoning of the catalyst. The calculations of O_2/H_2O absorption on pyrite in vacuo allow us to plan full-scale FPMD simulations in water to reveal the detailed reaction pathways and free-energy changes of pyrite oxidation.

Design of a protective overlayer permitting nanochannel access of water and protons to the active sites and H_2 egress. We have found that phosphonic acid forms a strong bidentate bond with the bare FeS_2 (100) surface after one OH is removed, making akylphosphonates promising candidates for the hydrophobic channel walls.The interaction of that end group with the decorated FeS_2 (100) surface will be studied in vacuo and in water with full quantum mechanical methods, but, when the alkyl chains are added, the increased complexity will require recourse to classical MD or QM/MM. The chain configuration in the protective overlayer will be studied with and without the cluster present and with and without water to build up the information needed for subsequent studies of the motion of H_2 and hydronium ions into and through the channels and of the inhibition of oxygen penetration.

References (which acknowledge DOE support)

[1] C. Sbraccia, F. Zipoli, R. Car, M. H. Cohen, G. C. Dismukes, A. Selloni, Mechanisms of H_2 production by the $[FeFe]_H$ Subcluster of Di-iron hydrogenases: implications for abiotic catalysts J. Phys. Chem. B **2008,** *112* 13381-13390.

[2] F. Zipoli, R. Car, M. H. Cohen, A. Selloni, Hydrogen Production by the Naked Active Site of the Di-Iron Hydrogenases in Water, J. Phys. Chem. B **2009,** *113* 13096-13106.

[3] F. Zipoli, R. Car, M. H. Cohen, and A. Selloni, Theoretical design by first principles molecular dynamics of a bio-inspired electrode-catalyst system for electrocatalytic hydrogen production from acidified water, J.Chem. Th. Comp., **2010**, 6, 3490-3502

[4] F. Zipoli, R. Car, M. H. Cohen, and A. Selloni, Simulation of Electrocatalytic Hydrogen Production by a Bio-inspired Catalyst Anchored to a Pyrite Electrode, J. Am. Chem. Soc., **2010,** 132 (25), 8593–8601

[5] P. H.-L. Sit, F. Zipoli, J. Chen, R. Car, M. H. Cohen, and A. Selloni, Oxidation state changes, bond switching, and electron flow in enzymatic and electro-catalysis via Wannier function analysis, Chemistry – A European Journal (in press)

[6] F. Zipoli, R. Car, M. H. Cohen, and A. Selloni, Electrocatalyst design from first principles: a hydrogen-production catalyst inspired by Nature, Catalysis Today, **2011**, 165(1), 160-170.

[7] P. H.-L. Sit, R. Car, M. H. Cohen, and A. Selloni, A simple, unambiguous theoretical approach to oxidation state determination via first-principles calculations, (submitted)

[8] P. H.-L. Sit, F. Zipoli, R. Car, M. H. Cohen, and A. Selloni, Redox chemistry of a model of the active site of the di-iron hydrogenases; H_2-production and O_2-binding mechanisms, (in preparation)

Other References

[9] M. T. Stiebritz, M. Reiher, Inorg. Chem. **2009,** *48* 7127-7140.

[10] J. A. Rodriguez, I. A. Abreu, J. Phys. Chem. B **2005,** *109* 2754-2762.

[11] K. M. Rosso, U. Becker, M. F. Hochella, Am. Mineral. **1999,** *84* 1549-1561.

Program Title: Self-assembly and self-repair of novel photovoltaic complexes – synthetic analogs of natural processes

Principle Investigator: Michael S. Strano
Mailing Address: Chemical Engineering Department, Massachusetts Institute of Technology
Cambridge, MA 02139
E-mail: strano@mit.edu

Program Scope

The goal of the program is to develop a fundamental understanding behind the regenerative, self-repair processes used in plants to create bio-inspired constructs that interface with synthetic nanomaterials. This understanding is essential for the development of regenerative materials including biomimetic photovoltaics with enhanced efficiencies and self-repairing polymeric constructs with indefinite lifetimes. The application of dynamic, self-repairing mechanisms to traditionally static constructs would allow high-efficiency photovoltaic devices that lack stability to become more economically viable solutions to the energy problem.

The primary strategy used to realize this goal consists of learning from, and building upon, natural processes that utilize regenerative mechanisms for light-harvesting applications. In the natural self-repair cycle that occurs in plants (Figure 1),[1] incident light is partially absorbed by photosystem II (PSII) within the chloroplast of the plant cell. Subsequent electron-hole formation and separation, which drives photosynthesis, occurs within the D1 protein. Over time, the D1 protein becomes photodamaged due to radical oxygen formation (Figure 1, right). Upon photodamage, PSII spontaneously disassembles, releasing the denatured D1 protein for subsequent protein digestion. Newly synthesized D1 protein concomitantly diffuses towards the disassembled PSII complex (Figure 1, bottom). Introduction of the new protein triggers the autonomous self-assembly (Figure 1, left) of the PSII to regenerate a fully functional PSII.[2-4] The incorporation of this self-repair cycle in the plant results not only in the indefinite prolongation of lifetime, but also a 2000% increase in the photosynthetic yield of the plant cell.[5] To further enhance photosynthetic productivity, the PSII is surrounded by light-harvesting antenna, which harvest light at an extended range of wavelengths and shuttles this extra energy to the D1 protein of the PSII.

Recent Progress

In our recent work,[6] we interfaced plant-derived components with nanostructured complexes to synthesize the first photoelectrochemical complex capable of mimicking key aspects of the plant self-repair cycle (Figure 2). In this setup, a solution consisting of photosynthetic reaction centers, phospholipids, scaffold proteins, single-walled carbon nanotubes (SWNTs) and surfactant is dialyzed to remove surfactant. The remaining components spontaneously self-assemble into a photoactive complex, wherein the reaction centers are each embedded into a lipid bilayer.[7] These lipid bilayers align along the length of a SWNT to create a unidirectional densely packed array of photoactive proteins. Like plant-based self-assembly, this self-assembly process is completely reversible; the re-addition of surfactant to the reaction solution results in the reversible

disassembly of the photoactive complex. This reversibility was applied to demonstrate a regeneration cycle wherein photoactivity of the assembled complex is monitored under continuous illumination. Upon photodamage, the complex is disassembled. The photodamaged proteins are replaced, and the complex is once more reassembled via surfactant removal. Application of this biomimetic regeneration cycle results in a 300% increase in photo-efficiency over 168 hours (Figure 3).

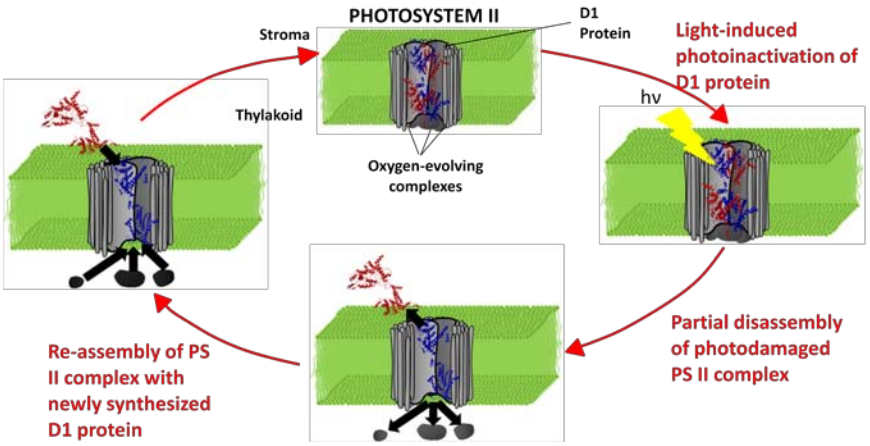

Figure 1| Self-repair of Photosystem II in Plants. Self-repair process in plants is driven by the molecular recognition of parts as the system transitions through a series of meta-stable states. [1] (Adapted from reference 1, A. Boghossian; Ham, M.H.; et al. *Energy Environ. Sci*., 2011).

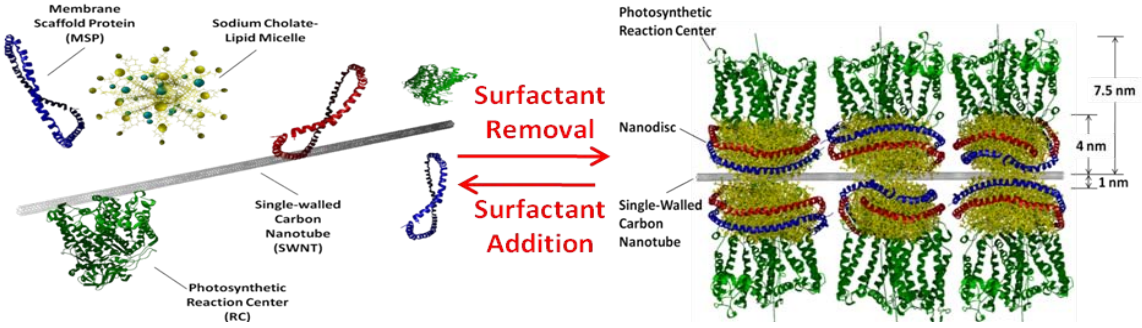

Figure 2| Self-assembly of RC-ND-SWNT complexes. Dialysis of the surfactant (sodium cholate) results in the self-assembly of the complex shown on the right, where lipid bilayer discs (nanodiscs) housing RCs align along the nanotube. (Adapted from reference 6, Ham, M.H.; Choi, J.H.; Boghossian, A.A.*; Nature Chemistry*, 2011).

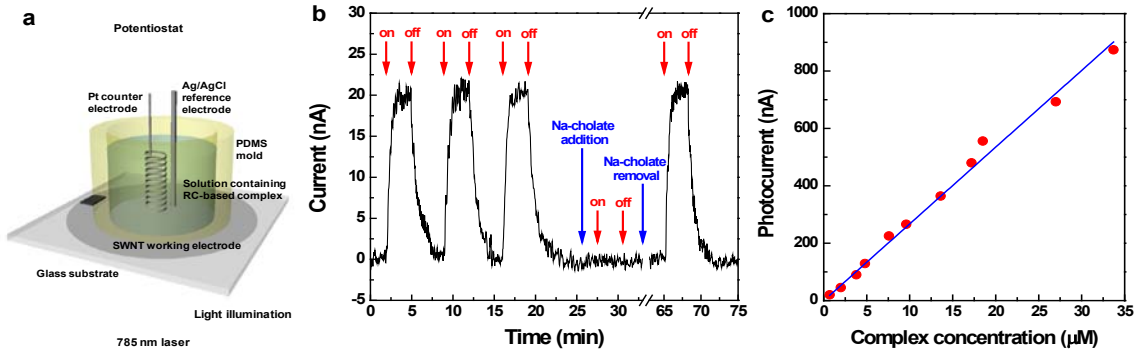

Figure 3| Measuring RC-ND-SWNT Photoactivity. a, The photoelectrochemical measurement apparatus includes a potentiostat in a three-electrode configuration and 785 nm illumination. **b,** 700 nM RC-ND-SWNT complex solution shows photoelectrochemical activity only in the absence of surfactant (in the assembled state). **c,** The photocurrent increases linearly with complex concentration. (Adapted from reference 6, Ham, M.H.; Choi, J.H.; Boghossian, A.A.; *et al. Nature Chemistry*, 2011).

In an alternative study,[8] we synthesized synthetic, light-harvesting antennas reminiscent of those surrounding the PSII used to enhance photo-conversion. The core-shell constructs consists of large band-gap nanotubes in an outer shell and small, band-gap nanotubes within the fiber core (Figure 4). Broad band absorption in the ultraviolet (UV)–near-infrared (nIR) wavelength regime provides quasi singular photoemission at the smallest band gap SWNT. Thus, the optical antenna behaves as a solar funnel wherein photon absorption in the outer shell results in the concentration of excitons within the core.

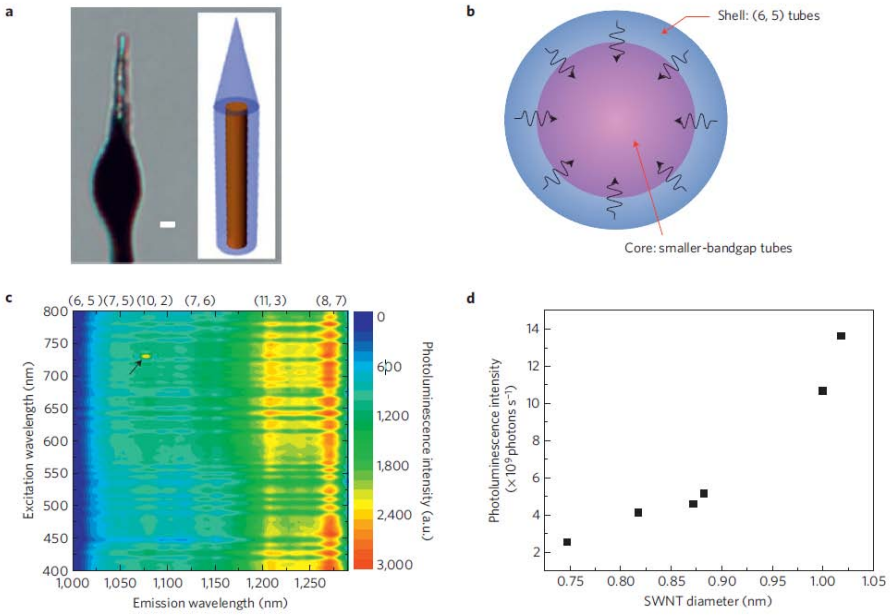

Figure 4| Development of an exciton antenna from a core–shell carbon nanotube structure. a, An optical image of the exciton antenna (scale bar, 2 μm) with a schematic. **b**, A top view of the antenna structure, where the curved black arrows indicate the inward energy transfer. **c**, The resulting excitation profile, demonstrating the dominant emission produced from the smallest-bandgap element . **d**, Experimental data showing the photoluminescence intensity for each type of SWNT in the exciton antenna for excitation at 570nm and at room temperature. (Adapted from reference 8, Han, J.H.; Paulus, G.L.C.; *et al. Nature Chemistry*, 2011).

As an extension of this work, recent progress has focused on the development of constructs wherein biologically derived components are interfaced with nanomaterials to enhance biomimetic processes for energy application purposes. In our most recent development, we have interfaced chloroplasts, which consist of densely packed arrays of photosystems surrounded by naturally-derived light-harvesting antennas, with dextran-wrapped nanoceria. The nanoceria, which behave as radical oxygen scavengers, has been shown to effectively reduce the formation of oxygen radicals in the presence of chloroplasts (Figure 5). This is hypothesized to enhance the regeneration properties of the chloroplast and prolong photoactivity for subsequent energy extraction.

Future Plans

Device Fabrication via the Interfacing of Biologically-derived Components with Nanostructures

Our future plans includes the extension of our work in the development of synthetic, nanostructured devices that mimick various aspects of the light-harvesting processes used in plants. Specifically, we are interested in (1) complexing our RC-ND-SWNT platform with our synthetic optical antenna to create a regenerative device with enhanced photo-efficiencies.

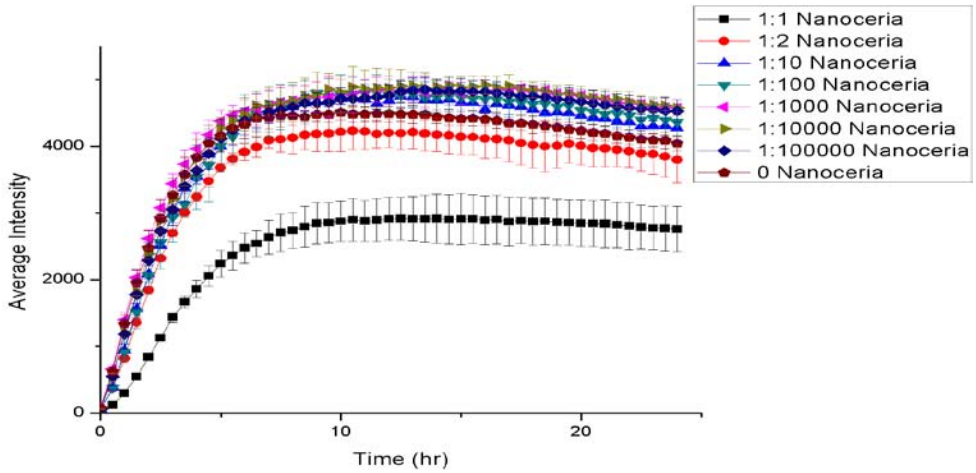

Figure 5| Effect of Nanoceria Concentration on Reactive Oxygen Concentration. In the presence of reactive oxygen species, fluorescein dye becomes oxidized, fluorescing at 520 nm with 485 nm excitation. Increasing concentrations of dextran-wrapped nanoceria decreases fluorescence intensity, decreasing in reactive oxygen concentration. (Unpublished)

We are also interested in (2) interfacing additional biologically derived components, such as chloroplasts which consist of densely packed arrays of reaction centers and antennas, with nanostructures that enhance photo-regeneration. In addition to dextran-wrapped nanoceria, we are also interested in interfacing chloroplasts with other radical oxygen scavengers, including hydroxylated fullerenes. With the effective scavenging of photo-damaging reactive oxygen species, we plan to monitor the photoactivity of the chloroplast directly. Enhanced photoactivity of the chloroplast will result in the development of biomimetic light-harvesting devices with enhanced regenerative properties and prolonged lifetimes.

References

(1) Boghossian, A. A.; Ham, M.-H.; Choi, J. H.; Strano, M. S. *Energy & Environmental Science* (2011).
(2) Aro, E. M.; Virgin, I.; Andersson, B. *Biochimica Et Biophysica Acta* (1993).
(3) Constant, S.; Perewoska, I.; Alfonso, M.; Kirilovsky, D. *Plant Mol.Biol.* (1997).
(4) Melis, A.; Nemson, J. A.; Harrison, M. A. *Biochimica Et Biophysica Acta* (1992).
(5) Melis, A. *Trends Plant Sci.* (1999).
(6) Ham, M. H.; Choi, J. H.; Boghossian, A. A.; Jeng, E. S.; Graff, R. A.; Heller, D. A.; Chang, A. C.; Mattis, A.; Bayburt, T. H.; Grinkova, Y. V.; Zeiger, A. S.; Van Vliet, K. J.; Hobbie, E. K.; Sligar, S. G.; Wraight, C. A.; Strano, M. S. *Nat. Chem.* (2010).
(7) Boghossian, A. A., Choi, J.H, Ham, M.H., Strano, M.S. *Langmuir* (2011).
(8) Strano, M. S.; Han, J. H.; Paulus, G. L. C.; Maruyama, R.; Heller, D. A.; Kim, W. J.; Barone, P. W.; Lee, C. Y.; Choi, J. H.; Ham, M. H.; Song, C.; Fantini, C. *Nat. Mater.* (2010).

Publications

- Boghossian, A. A.; Ham, M.-H.; Choi, J. H.; Strano, M. S. *Energy & Environmental Science* (2011).
- Boghossian, A. A., Choi, J.H, Ham, M.H., Strano, M.S. *Langmuir* (2011).
- Ham, M. H.; Choi, J. H.; Boghossian, A. A.; Jeng, E. S.; Graff, R. A.; Heller, D. A.; Chang, A. C.; Mattis, A.; Bayburt, T. H.; Grinkova, Y. V.; Zeiger, A. S.; Van Vliet, K. J.; Hobbie, E. K.; Sligar, S. G.; Wraight, C. A.; Strano, M. S. *Nat. Chem.* (2010).
- Han, J. H.; Paulus, G. L. C.; Maruyama, R.; Heller, D. A.; Kim, W. J.; Barone, P. W.; Lee, C. Y.; Choi, J. H.; Ham, M. H.; Song, C.; Fantini, C.; Strano, M.S. *Nat. Mater.* (2010).

Program Title: Membranes and Cell-Like Microcapsules through Hierarchical Self-Assembly

Principle Investigator: S. I. Stupp; **Co-PIs**: Y. S. Velichko, D. I. Rozkiewicz, and R. Bitton

Mailing Address: Departments of Chemistry, Materials Science and Engineering, and Medicine, Northwestern University, 2220 Campus Drive, Evanston, IL 60208-3108

Email: s-stupp@northwestern.edu

Program Scope: The goal of this program is to develop self-assembling supramolecular materials and organic-inorganic hybrids using biomimetic strategies with functions that are relevant to energy. These functions include photovoltaic properties, catalysis, and designed interactions with bacteria and other cells.

Background: Biological membranes play important roles as physical barriers, as well as functional interfaces between cell compartments and between cells. The variety of morphologies and compositional arrangements of biological membranes reflect a great diversity of functions. For that reason such membranes have attracted significant attention given their relevance in the preparation of chemically defined surfaces and interfaces. Among all synthetic strategies, self-assembly represents one of the most promising directions to create nanostructured and multifunctional materials leading to a much richer structural diversity compared to equilibrium processed materials.

Our laboratory has demonstrated several examples of nanoscale design of bioactive self-assembled peptide materials[1-8]. These materials utilize an extensive family of peptide amphiphiles (PAs) developed in our laboratory[9, 10]. These PAs contain a charged amino acid sequence covalently bound to an alkyl segment and upon electrostatic screening create cylindrical nanofibers through the formation of β-sheets and hydrophobic collapse of alkyl chains.[11-13]. The peptide sequences of PA molecules can be used effectively to control the mechanical properties of the resulting nanofiber networks they form over orders of magnitude[14].

Recent Progress: Recently we discovered that contact of a water droplet containing the negatively charged hyaluronic acid (HA) with an aqueous solution of positively charged peptide amphiphiles $C_{16}V_3A_3K_3$ (Fig. 1 A-C) can form a highly ordered membrane with millisecond speed (Fig. 1 D). Initial membrane of planar filaments that completely encapsulates the droplet and prevents the two liquids from mixing[15, 16]. After the planar filaments seal the liquid-liquid interface, the ionic osmotic pressure difference between the two liquids causes diffusion and

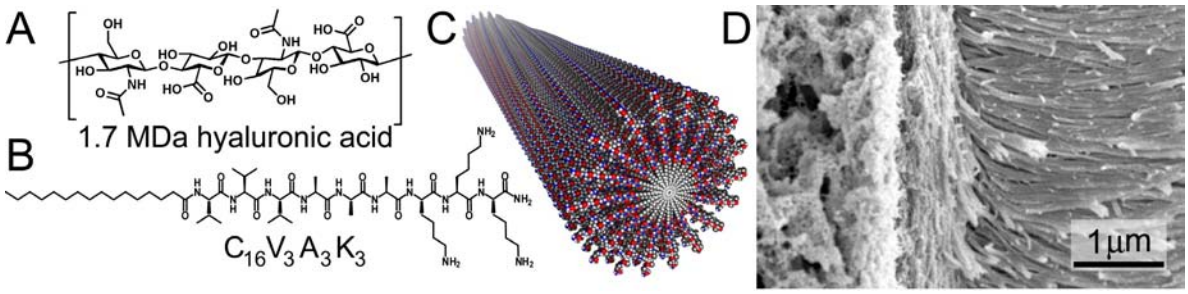

Figure 1: Chemical structures of (A) hyaluronic acid and (B) the positively charged peptide amphiphile used to create the hierarchically structured sac membrane. (C) Molecular graphics representation of self-assembled PA nanofibers. (D) SEM image of the PA-HA membrane cross section revealing three distinct zones of the hierarchical structure (from left to right, (1) amorphous, (2) parallel nanofibers, and (3) perpendicular nanofibers).

stretching of the biopolymer chains as they diffuse through interstices in the diffusion barrier. It is this event that triggers the formation of filaments oriented perpendicular to those in the original membrane. The key feature of the sac membranes is their permeability to proteins or high molecular weight polymers, as well as, ability to self-heal large defects by contact with oppositely charged small molecules.

We developed strategies to create microcapsules in the size range from the few microns to few millimiters in diameter. The diameter of the microcapsules will determine to a large extent their potential applications. Using a spraying technique,[17] we obtained PA-alginate microcapsules with a mean diameter of 25 µm (Fig. 2 A-B). We built a spray-based device, which enables production of droplets with diameters as small as 5 µm by nebulizing the stream of alginate solution using a high-velocity flow of nitrogen[17]. The microdroplets of the biopolymer solution were directly ejected into an aqueous solution of $C_{16}V_3A_3K_3$ PA to induce the membrane-forming self-assembly. Using this technique, we obtained PA-alginate microcapsules with a mean diameter of 25 µm (Fig. 2A-B). Also, using a microfluidic method (Fig. 2C) microcapsules in the size range of 50-200 µm were successfully created, with the water droplet templating the size and shape of the final membrane.

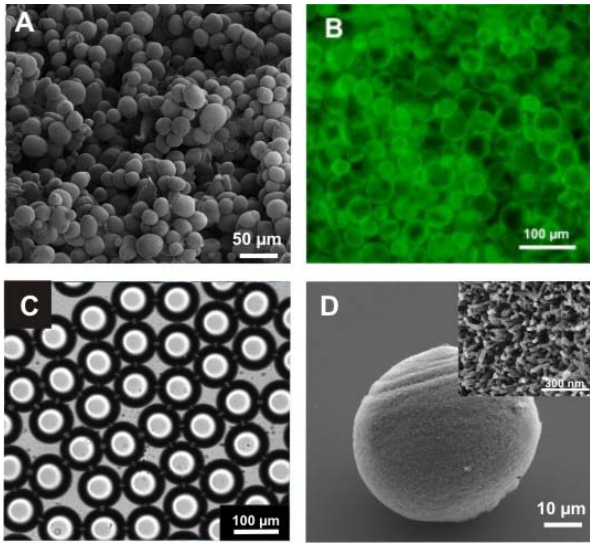

Figure 2: PA-alginate microcapsules made by (A, B, D) spraying or (C) micro-fluidics techniques, imaged by (A, C) optical, (B) fluorescence, and (D) SEM microscopy.

In order to increase functionality of microcapsules, we developed different strategies to control the structural organization and complexity of the self-assembled membranes. We studied membrane formation from various mixtures of the same charge PAs and polyelectrolytes. This multi-component system has more degrees of freedom than the cannonical two-component

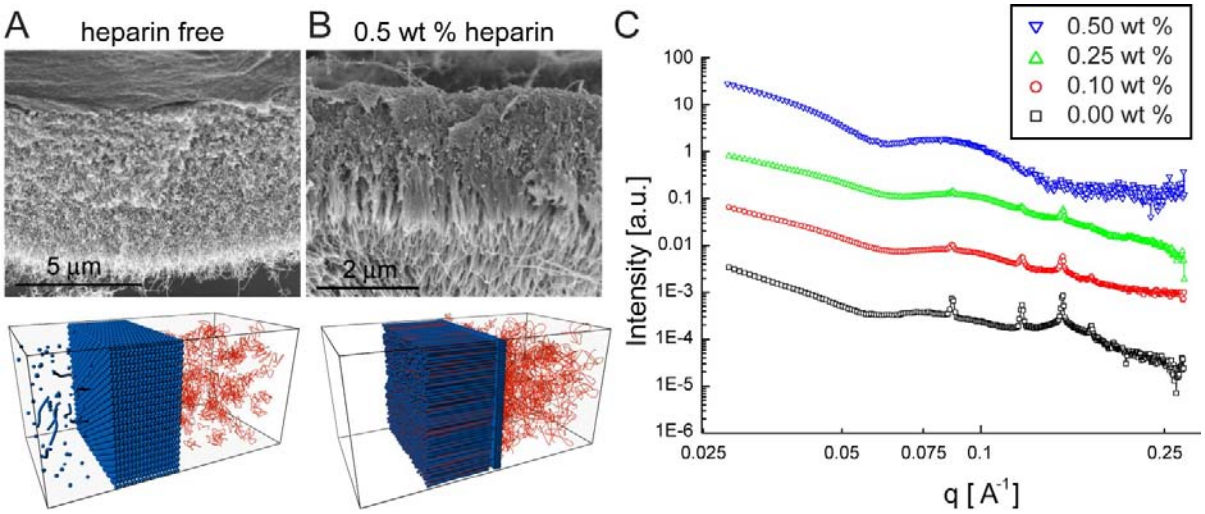

Figure 3: Scanning electron micrographs of the cross-section of the (A) heparin free and (B) 0.5 wt % heparin containing membrane. (C) Small angle X-ray scattering (SAXS) of HA/HBPA sac with (▼) 0.5 wt %, (▲) 0.25 wt %, (○) 0.1 wt %, and (o) 0 wt % heparin. Curves were shifted vertically for visual convenience.

system[15] in terms of molecular composition, concentration, and molecular weight. One system to be described involves self-assembly between positively charged PAs with the heparin binding sequence LRKKLGKA and a mixture of negatively charged biopolymers, HA and heparin. In the absence of the heparin, the sac was found to be opaque, but becomes more transparent with increasing heparin concentration. SEM micrographs show that the 0.5 wt% heparin membrane exhibits the parallel and perpendicular fiber morphology. However, heparin-free membranes and membranes made with 0.1 wt% and 0.25 wt% heparin appear to be thicker and denser than the one with 0.5 wt% and lack the hierarchical features (Fig. 3 A and B). On the other hand, small-angle X-ray scattering (SAXS) pattern of the heparin-free membranes shows narrow peaks characteristic of a bicontinuous cubic phase such as Pm3n or Ia3d (Fig. 3 C) indicating an ordered structure. Our work demonstrates that this hierarchical structure is directly linked to the rapid assembly of the diffusion barrier, and that its formation requires the presence of pre-existing nanofibers and strong introduced introduced here through the use of the heparin and a peptide amphiphile designed to specifically bind these macromolecules.

Another area of interest in our work self-assembly of the PA-HA membranes in the presence of external electric fields. Superimposing local intermolecular forces with external forces can significantly alter the self-assembly thus providing greater degrees of freedom to control the structure and properties of self-assembling materials. Depending on the strength and orientation of the field we observe a significant increase or decrease of up to nearly 100% in membrane thickness, as well as the controlled rotation of nanofiber growth direction by 90 degrees, resulting in a significant increase in mechanical stiffness.

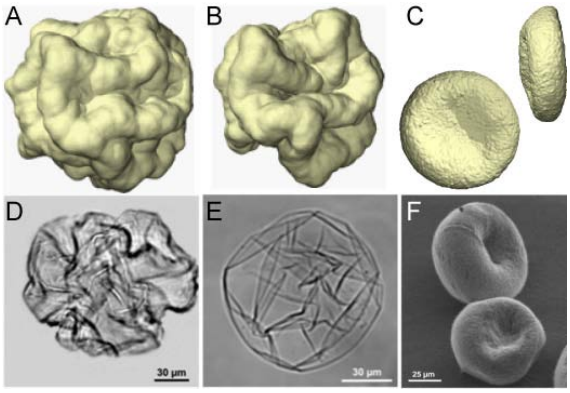

Figure 4: (A-C) Snapshots of microcapsules from the molecular simulation. (D-F) Partially folded spherical and biconcave PA-alginate microcapsules.

Inspired by the structural functionality of the human red blood cell (RBC) we investigated the folding of self-assembled microcapsules. The large surface to volume ratio and structural flexibility of RBCs are necessary to achieve oxygen transfer and transport through the microvasculature. We studied physical mechanisms underlying the folding of the microcapsules, i.e. shape deformations and formation of surface stress patterns. Our contribution discusses the results of computational (Fig. 4A-C) and experimental (Fig. 4 D-F) studies of microcapsule folding. For example, Fig. 4D shows alginate-based microcapsules which was incubated in high concentration of a K3-PA solution (≥1 wt %) for more than 30 min., and Figure 4E shows alginate-based microcapsules incubated for more than 30 min. in ≥0.5 wt % iso$C_{18}V_3A_3K_3$-PA in geraniol. Figure 8F shows a biconcave disc-shaped microcapsules obtained from alginate and K3-PA. Our study indicates a good match between the type of microcapsules folding predicted by the simulations and that observed in experiments.

Future Plans: Future plans in this program include the crafting of increasingly complex cell-like microcapsules using self-assembly strategies that utilize both small molecules and macromolecules. The objective is to develop cell mimics with novel catalytic functions and dynamic behavior. Future plans also include the development of lamellar hybrids with photovoltaic and other electronic properties in which two-dimensional inorganic structures are

templated by supramolecular assemblies, as well as the development of bioactive matrices for bacterial cells.

References

1. Chow, L. W.; Wang, L. J.; Kaufman, D. B.; Stupp, S. I. *Biomaterials* **2010,** 31, (24), 6154.
2. Mata, A.; Geng, Y. B.; Henrikson, K. J.; Aparicio, C.; Stock, S. R.; Satcher, R. L.; Stupp, S. I. *Biomaterials* **2010,** 31, (23), 6004-6012.
3. Huang, Z.; Newcomb, C. J.; Bringas, P.; Stupp, S. I.; Snead, M. L. *Biomaterials* **2010,** 31, (35), 9202.
4. Shah, R. N.; Shah, N. A.; Lim, M. M. D.; Hsieh, C.; Nuber, G.; Stupp, S. I. *Proc. Natl. Acad. Sci. U. S. A.* **2010,** 107, (8), 3293-3298.
5. Webber, M. J.; Tongers, J.; Renault, M. A.; Roncalli, J. G.; Losordo, D. W.; Stupp, S. I. *Acta Biomater.* **2010,** 6, (1), 3-11.
6. Chow, L. W.; Bitton, R.; Webber, M. J.; Carvajal, D.; Shull, K. R.; Sharma, A. K.; Stupp, S. I. *Biomaterials* **2011,** 32, (6), 1574-1582.
7. Webber, M. J.; Newcomb, C. J.; Bitton, R.; Stupp, S. I. *Soft Matter* **2011**.
8. Zhang, S.; Greenfield, M. A.; Mata, A.; Palmer, L. C.; Bitton, R.; Mantei, J. R.; Aparicio, C.; de la Cruz, M. O.; Stupp, S. I. *Nature Materials* **2010,** 9, (7), 594-601.
9. Hartgerink, J. D.; Beniash, E.; Stupp, S. I. *Science* **2001,** 294, (5547), 1684-1688.
10. Hartgerink, J. D.; Beniash, E.; Stupp, S. I. *Proc. Natl. Acad. Sci. U. S. A.* **2002,** 99, (8), 5133.
11. Jiang, H. Z.; Guler, M. O.; Stupp, S. I. *Soft Matter* **2007,** 3, (4), 454-462.
12. Velichko, Y. S.; Stupp, S. I.; de la Cruz, M. O. *J. Phys. Chem. B* **2008,** 112, (8), 2326.
13. Cui, H.; Pashuck, E. T.; Velichko, Y. S.; Weigand, S. J.; Cheetham, A. G.; Newcomb, C. J.; Stupp, S. I. *Science* **2010,** 327, (5965), 555-559.
14. Pashuck, E. T.; Cui, H.; Stupp, S. I. *J Am Chem Soc* 132, (17), 6041-6.
15. Capito, R. M.; Azevedo, H. S.; Velichko, Y. S.; Mata, A.; Stupp, S. I. *Science* **2008,** 319, (5871), 1812-1816.
16. Carvajal, D.; Bitton, R.; Mantei, J. R.; Velichko, Y. S.; Stupp, S. I.; Shull, K. R. *Soft Matter* **2010** 6, (8), 1816-1823.
17. Rozkiewicz, D. I.; Myers, B. D.; Stupp, S. I. *Angew. Chem. Int. Ed.* **2011**.

Selected References (which acknowledge DOE support)

1. Muraoka, T.; Koh, C.-Y.; Cui, H.; Stupp, S. I. *Angewandte Chemie-International Edition* **2009,** 48, (32), 5946-5949.
2. Greenfield, M. A.; Palmer, L. C.; Vernizzi, G.; de la Cruz, M. O.; Stupp, S. I. "Buckled Membranes in Mixed-Valence Ionic Amphiphile Vesicles" J. Am. Chem. Soc. **2009**, 131(34), 12030-12031.
3. Greenfield, M. A.; Hoffman, J. R.; de la Cruz, M. O.; Stupp, S. I. *Langmuir* **2010,** 26, (5), 3641-3647.
4. Cui, H.; Webber, M. J.; Stupp, S. I. *Biopolymers* **2010,** 94, (1), 1-18.
5. Stupp, S. I. *Nano Letters* **2010,** 10, (12), 4783-4786.
6. Zhang, S.; Greenfield, M. A.; Mata, A.; Palmer, L. C.; Bitton, R.; Mantei, J. R.; Aparicio, C.; de la Cruz, M. O.; Stupp, S. I. *Nature Materials* **2010,** 9, (7), 594-601.
7. Cui, H.; Pashuck, E. T.; Velichko, Y. S.; Weigand, S. J.; Cheetham, A. G.; Newcomb, C. J.; Stupp, S. I. *Science* **2010,** 327, (5965), 555-559.
8. Tsai, W.-W.; Tevis, I. D.; Tayi, A. S.; Cui, H.; Stupp, S. I. *J. Phys. Chem. B* **2010,** 114, (45), 14778.
9. Stone, D. A.; Tayi, A. S.; Goldberger, J. E.; Palmer, L. C.; Stupp, S. I. *Chemical Communications* **2011,** 47, (20), 5702-5704.
10. Tung, V. C.; Huang, J-H.; Tevis, I.; Kim, F.; Chu, C-W.; Stupp, S. I.; Huang, J. "Surfactant-free Water-processable Photoconductive All-carbon Composite" J. Am. Chem. Soc. **2011**, 133(13), 4940.
11. Sone, E. D.; Stupp, S. I. *Chemistry of Materials* **2011,** 23, (8), 2005-2007.
12. Herman, D. J.; Goldberger, J. E.; Chao, S.; Martin, D. T.; Stupp, S. I. *Acs Nano* **2011,** 5, (1), 565.
13. Tevis, I. D.; Stupp, S. I. *Nanoscale* **2011**, 3, 2162-2165.
14. Rozkiewicz, D. I.; Myers, B. D.; Stupp, S. I. *Angew. Chem. Int. Ed.* **2011**.

Project Title

SISGR: Using *In vitro* Maturation and Cell-free Evolution to Understand [Fe-Fe]hydrogenase Activation and Active Site Constraints

James Swartz[1,2] * (PI), Alyssa Bingham[1], Phillip Smith[1], Simon J. George[3], and Stephen P. Cramer[3,4]
[1]Department of Chemical Engineering, [2]Department of Bioengineering, Stanford University
[3]Department of Applied Science, University of California, Davis, CA
[4]Physical Sciences Division, Lawrence Berkeley National Laboratory, Berkeley, CA
*Presenter's Address:
Stauffer III, Room 113
Stanford, CA 94305-5025
650-723-5398 (office); 650-725-0555 (fax); *jswartz@stanford.edu*

DOE Program Manager: Michael Markowitz
[301-903-6779; *Mike.markowitz@science.doe.gov*]

Objectives

With this project, we seek increased understanding of the mechanisms for assembly and activation of [FeFe] hydrogenases as well as the structural role that the polypeptide scaffolding plays in forming and stabilizing this complex enzyme's active site. We are developing in vitro maturation methods to enable detailed study of the biochemical reactions required to provide precursors and to assemble the catalytic H-cluster as well as to install it into the apoenzyme. We are also searching for enzyme mutations that will reveal the role of the polypeptide structure. To accomplish these objectives and to help advance this important field of research, we are also developing improved methods for producing these complex enzymes and for evaluating various functional characteristics.

Technical Barriers

This project is designed to provide information relative to the maturation and structure function relationships of [FeFe] hydrogenases. Since these are nature's most prolific hydrogen producers, this information will facilitate the design, assembly and cost-effective production of improved biological and biomimetic catalysts for the production of hydrogen and for hydrogen based fuel cells. The project will also deliver improved methods for the evolution, evaluation, and production of improved hydrogen producing catalysts. Since the most plentiful proton source for producing hydrogen is water and oxygen is a side product, the project will also search for oxygen tolerant hydrogenase mutants and seek to understand the structure function relationships relative to oxygen tolerance.

Abstract

The first project objective is to elucidate the substrates and mechanisms for assembly and maturation of the 6Fe-6S active site of [FeFe] hydrogenases. An early *in vitro* maturation method was developed using an *E.coli* cell extract in which the three required maturases had been expressed and activated. The extract was also dialyzed to remove small molecules. We showed, for the first time, that activation of the purified apoenzyme was significantly enhanced by incubating this extract in the presence of S-adenosyl methionine, Fe(II), sulfide, and 20 amino acids. A design of experiment (DOE) investigation then showed that tyrosine was required and

cysteine was beneficial for maturation. Further investigation showed that the para-hydroxyl substituent of tyrosine was required for efficient activation. An improved maturation procedure was then developed in which the three maturase proteins were expressed separately to avoid *in vivo* maturase interactions. Such interactions were thought to be important for function, and we sought to gain control over this portion of the maturation mechanism. In contrast to previous inferences, efficient apoenzyme activation was observed using the separately produced maturases. This new system enabled the production of much larger quantities of *in vitro* activated [FeFe] hydrogenase. This, in turn, enabled high resolution FTIR (Fourier transform infrared spectroscopy) analysis of the C-O and C-N stretches associated with the cyanide and carbon monoxide adducts in the 6Fe-6S active site. Isotopic labeling of tyrosine then conclusively showed that all three of the CO and both of the CN moieties in the active site are derived from tyrosine. Further evaluation has shown, for the first time, catalytic function; i.e., multiple turnovers, for each of the maturases when functioning in the *in vitro* maturation system.

The second project objective is to gain better understanding of the impact of the polypeptide scaffolding on hydrogenase activity. The expression gene for the CpI [FeFe] hydrogenase from *Clostridium pasteurianum* was extensively mutated using nucleotide analogs, and isolates were identified that retained at least partial activity and also displayed increased stability during oxygen exposure. The most interesting isolate contained 13 mutations and was extensively analyzed. When two of the amino acid changes were reversed, full activity was restored. Three different mutations increased oxygen tolerance. Unexpectedly, none of these mutations are near the active site 6Fe-6S H-cluster, but four of the five mutations are close to the proximal 4Fe-4S center that either donates electrons to the active site H-cluster or receives them, depending on the direction of catalysis. These results suggest that the function of this ancillary iron-sulfur center has a stronger than expected influence on enzyme function. During this work, we also observed that oxygen inactivation of [FeFe] hydrogenases can be substantially reversed in contrast to general belief. The reversibility also appears to be influenced by the ancillary Fe-S center. A mutational library is now being constructed to assess the function of the amino acids surrounding this ancillary center as well as those that support the active site.

During the course of these investigations, a number of methods were developed of general utility to this field of research. These include: the *in vitro* hydrogenase maturation protocols, a procedure for producing high levels of maturases and hydrogenases in *E.coli* cultures, improved methods for producing and screening hydrogenase mutants, and a new method for assessing sustained hydrogen production activity while using a reduced ferredoxin protein as the electron donor. In particular, the last method is very important as it will now allow us to screen for mutants with increased oxygen stability while they are actively making hydrogen. In addition, this method suggests the feasibility for cost-effectively producing hydrogen from biomass hydrolysates. A new research program has now been initiated to develop technology for the large scale production of hydrogen from biomass hydrolysates.

Progress Report

Taking our lessons from the investigation of another important and complex enzyme, nitrogenase, we first sought to develop methods for the *in vitro* maturation of the [FeFe] hydrogenases. Although early work from the Peters lab at U. of Montana had achieved *in vitro* activation (although with very low yields), that system was not suitable for investigating the effects of small molecular weight substrates. Based on our success with cell-free protein synthesis of the hydrogenases (Boyer et al, 2008), we developed an *in vitro* maturation protocol that achieved substantial activation of the *C. rheinhardtii* HydA1 [FeFe] hydrogenase using cell extracts in which the three maturases, HydE, HydF, and HydG, had been expressed. These maturases were expressed from the relevant genes taken from *Shewanella oneidensis* and were produced under anaerobic conditions at 20°C to encourage proper folding. For convenience, the extracts were then prepared under aerobic conditions and were frozen for storage. The extracts

were then dialyzed just before use to remove small molecules, and the maturases were reconstituted (reactivated) by anaerobic incubation with Fe(II) and S^{-2}. The apoenzyme was produced in *E.coli* cultures lacking the maturases and had no activity after purification. As expected, S-adenosyl methionine, Fe(II), and S^{-2} were necessary for activation. However, full activation was only achieved with the additional presence of a mixture of the 20 natural amino acids. A design of experiment (DOE) protocol then indicated that tyrosine was essential and cysteine was beneficial for hydrogenase activation.

A previous report had suggested that co-expression of the maturases was necessary for their activation. However, we reasoned that more information about hydrogenase maturation could be gained if the maturases could be expressed in separate *E.coli* cultures. This would then require that nearly all maturation related reactions take place during the *in vitro* activation. This protocol would also have a higher likelihood of enabling complete incorporation of isotopically labeled precursors into the H-cluster active site. Again, the apoenzyme was produced in cultures lacking the maturases and had no activity. At this point in the project, we had discovered that an *E. coli* strain with a Δ*iscR* deletion (Akhtar & Jones, 2008) produced more of the maturases as well as more apoenzyme. By mixing three extracts, each containing high levels of an individual maturase, effective apoenzyme activation was achieved. This protocol also efficiently matured the more complex CpI hydrogenase from *Clostridium pasteurianum.* After isotopically labeled tyrosine was added to the maturation reactions**,** the activated and purified hydrogenase samples were analyzed by FTIR. Distincitive shifts in the C-O and C-N stretches were observed as shown in Figure 1. These shifts indicated that all of the CN^- adducts in the active site H-cluster derived from the alpha carbon and amino nitrogen of tyrosine and all of the CO adducts derived from the carboxylate group of tyrosine. Recent work had shown that CO and CN could be extracted from the HydG maturase and that these species derived from tyrosine, but these recent publications had not shown that all of the adducts in the active enzyme derived from tyrosine. Conitnued work with this maturation system has now also established, for the first time, that full CpI activity can be obtained with substoichiometric quantities of the maturases, in other words, that they are functioning catalytically.

Fig. 1

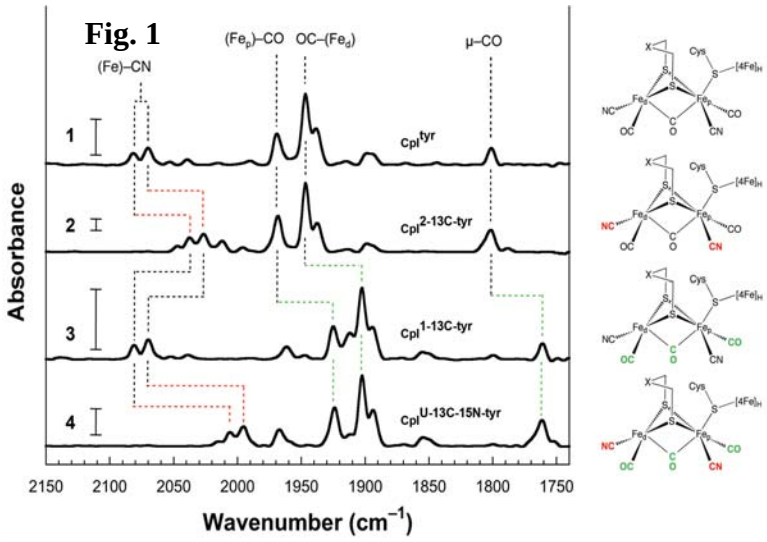

Fig 2

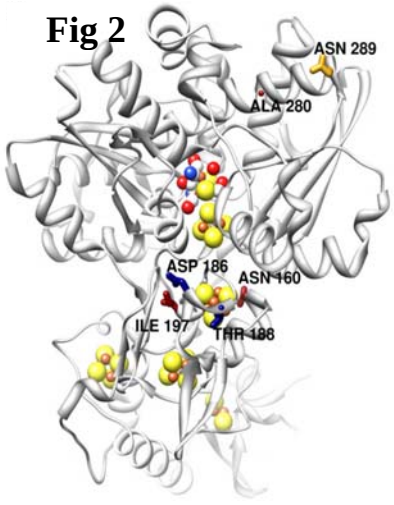

The work to characterize the role of the polypeptide structure began with a mutant of the *C. pasteurianum* CpI hydrogenase that was isolated with 13 amino acid changes that conferred lower activity and improved oxygen tolerance. When the wild type amino acids were restored at positions 186 and 188, full activity was also restored. (See Figure 2) Interestingly, these mutations were not near the active site, but rather adjacent to the electron conducting 4Fe-4S center proximal to the active site. It also turned out that the most

influential mutation for conferring oxygen tolerance was at position 197, an amino acid that is adjacent to the same 4Fe-4S center. Amino acid position 160 was also influential for oxygen tolerance and was adjacent to the same cluster. It thus became clear that this 4Fe-4S cluster proximal to the catalytic center has strong influences on functional properties. The influences of the other amino acids surrounding this cluster will now be further characterized in addition to those surrounding the catalytic center.

Perhaps even more important than these specific discoveries is the collection of methods that have been developed. For example, paper no. 2 in our publication list describes a new production protocol that increases volumetric hydrogenase yields by 10 to 30 fold when produced by an rDNA *E.coli* culture. We have also established the ability to continually transfer electrons from NADPH to the hydrogenase to assess oxygen tolerance while the enzyme is making hydrogen. Unfortunately, this new technique showed that our oxygen tolerant mutant was only tolerant when in the resting state and not when it is producing hydrogen. This is a totally unexpected observation. It will be investigated further, but it also suggests that we need to adjust our screening assays. The new pathway from NADPH will form the basis for a high throughput screening assay that assesses oxygen tolerance for the active enzyme. This new method also forms the basis for a new pathway to convert biomass hydrolysates to hydrogen and this is now being pursued by a new project.

Future Directions

We have accumulated a large variety of enzyme production and assessment methods and we can now enter a more active period to generate many new mutants that differ in functional characteristics. We will assess the effects of 89 amino acid residues near the active site and the proximal Fe-S center. In order to obtain more accurate assessments, we will use lessons learned from the *in vitro* maturation studies to improve CpI activation during the cell-free protein synthesis procedures. This will allow rapid assessment of the site directed mutants and will also provide improved technology for hydrogenase evolution. We will also continue to work with our spectroscopy experts to gain a fuller understanding of the relationship between structural and functional changes and will most likely also begin a collaboration with X-ray structural experts to gain more detailed information about the impact of individual mutations.

References

1. Boyer ME …. Swartz JR. (2008) Cell-free synthesis and maturation of [FeFe] hydrogenases. Biotech. and Bioeng. **99**: 59-67.
2. Akhtar MK and Jones PR (2008) Deletion of iscR stimulates recombinant clostridial Fe-Fe hydrogenase activity and H2-accumulation in *Escherichia coli* BL21(DE3). Appl. Microbiol. and Biotechnol. **78**(5): 853-62.

Publication list (including patents) acknowledging the DOE grant or contract

1. Kuchenreuther JM, Stapleton JA, Swartz JR. (2009) Tyrosine, Cysteine and S-Adenosyl Methionine Stimulate *In Vitro* [FeFe] Hydrogenase Activation. PLoS ONE4(10): e7565.
2. Kuchenreuther JM, Grady-Smith CS, Bingham AS, George SJ, Cramer SP, Swartz JR. (2010) High-Yield Expression of Heterologous [FeFe] Hydrogenases in *E coli*. PLoS One 5(11): e15491.
3. Kuchenreuther JM, George SJ, Grady-Smith CS, Cramer SP, Swartz JR. (2011) Cell-free H-cluster synthesis and [FeFe] hydrogenase activation: all five CO and CN^- ligands derive from tyrosine. PLoS ONE 6(5): e20346.
4. Bingham AS, Smith PR, Swartz JR. (2011) Evolution of an [FeFe] hydrogenase with decreased oxygen sensitivity. International Journal of Hydrogen Energy; In Press, Available on-line 22 March 2011.
5. Swartz JR, Smith PR (2010). A General Enzymatic Pathway for Hydrogen Production. Provisional Patent Application filed 9/3/2010.

Inorganic Control of Biological Self-Assembly: Engineering Novel Biological Architectures and Redox-Active Protein Assemblies

Principle Investigator: F. Akif Tezcan
Mailing Address: University of California, San Diego, Department of Chemistry and Biochemistry, 9500 Gilman Drive, La Jolla, CA 92093-0356
E-mail: tezcan@ucsd.edu

i) Project Scope

The goals of this project are:

1) to utilize combined inorganic and protein engineering approaches we have developed (Metal-Directed Protein Self-Assembly (MDPSA)[1] and Metal-Templated Interface Redesign (MeTIR)[2]) for the construction of discrete or 1- 2- and 3-D protein superstructures and frameworks, using folded proteins as building blocks and metals as interfacial joints; and

2) to exploit the extensive non-covalent interactions formed around the interfacial metal sites within these protein frameworks to control the metal reactivity in ways not accessible in current synthetic inorganic and bioinorganic methodologies.

These goals combined will lead to the chemically controllable self-assembly of well-ordered superstructures under ambient conditions that will be used for light-harvesting and redox catalysis. These structures also will provide a framework for a fundamental understanding of protein self-assembly as well as crystal nucleation and growth.

The significance of the ability to understand and control protein self-assembly cannot be overstated: proteins represent the functionally and structurally most versatile molecular building blocks available to an organism or to a chemist;[3] their self-assembly provides a direct access to the "nanoscale" (2-100 nm) not accessible by top-down approaches and not easily achieved by bottom-up approaches using other types of building blocks;[3] their assembly into periodic arrays is an absolute necessity for diffraction-based structure determination methods and therefore a driving force for all biosciences. Nevertheless, the mastery/control over the self-assembly of proteins (or even polypeptides) has not yet reached a level where *discrete (closed) or 1-, 2- and 3-dimensional* architectures with long-range order can be engineered, especially when compared to DNA/RNA-based materials.[4, 5]

Our goals of using metal coordination chemistry to direct protein self-assembly and then to tune the reactivity of interfacial metals are approached at several different levels: these include the design and synthesis of natural and non-natural metal-chelating motifs on protein surfaces to control metal coordination, protein engineering and computational design, structural characterization of superprotein assemblies through crystallography, electron, fluorescence and atomic force microscopy, and the characterization of metal reactivity and photophysics through an armament of static and time-resolved spectroscopic methods.

ii) Recent Progress

ii.1) New Metal Coordinating Motifs and Protein Oligomerization Motifs:

The prerequisite to MDPSA is the ability to control the strength, kinetics, valency and the geometry of metal coordination on the protein surface. In addition to the genetically encoded *i*,*i*+4 bis-His coordination motifs on helical surfaces, we have now synthesized a number of non-natural bi- and tri-dentate ligands (phenanthroline, 8-hydroxyquinolate, terpyridine) that can be site-specifically attached to surface cysteine residues. Using these Cys-labeled groups in combination with a His at *i*+7 position leads to tri- and tetradentate metal coordination platforms, which we have termed hybrid

coordination motifs (HCMs).[6-8] HCMs provide a) nano- to femtomolar binding affinities for late-first-row transition metals, b) stabilize the α-helical scaffold and the overall protein stability, c) and allow the formation of C_2-symmetrical protein dimers and micromolar dissociation constants. The construction of such stable, discrete dimers is an important component of engineering larger supramolecular architectures that require the proper combination of two-fold symmetry with other symmetry elements.

ii.2) *De Novo* Design of Interfacial Metal Binding Sites with Catalytic Activity:

An inspection of nature's most sophisticated metalloenzymes, including the two globally most significant ones (Photosystem II and Nitrogenase), reveals that their active site metal centers have evolved in the interfaces between proteins or protein subunits. While reengineering existing metal active sites or the introduction of extraneous metal complexes into natural protein scaffolds has resulted in impressive catalytic activities, these approaches are limited by the fact that these protein scaffolds have already evolved for a certain function. One of the goals of our project is to internalize metal centers in completely unbiased/uniformed protein interfaces and design metal-based functions, particularly redox catalysis, from first principles. Using our approach of Metal-Templated Interface Redesign (MeTIR), we have constructed a stable, tetrameric assembly of cytochrome cb562 monomers that were templated by tetrahedral Zn^{2+} coordination. The engineered hydrophobic interactions and disulfide bonds around the Zn templates result in an assembly that is one of the most stable protein complexes ever engineered (K_d ~ 50 nM), and binds Zn^{2+} more selectively over other divalent metal ions than any small molecule ligand platform (Figures 1a and b).[9] In its interfaces, this tetrameric scaffold can stably house Cu in +1 and +2 oxidation states as well as in a dinuclear arrangement (Figure 1c), which is highly reminiscent of Cu-enzymes involved in dioxygen binding and activation. Using MeTIR-stabilized dimers and tetramer, we have also constructed coordinatively unsaturated, interfacial Zn- and Mn-centers that show hydrolase activities. These proof-of-principle experiments show that such metal centers, which have been challenging targets for de novo de sign, can be readily accessed through MeTIR, and set the stage for directed evolution studies for targeted catalytic reactions.

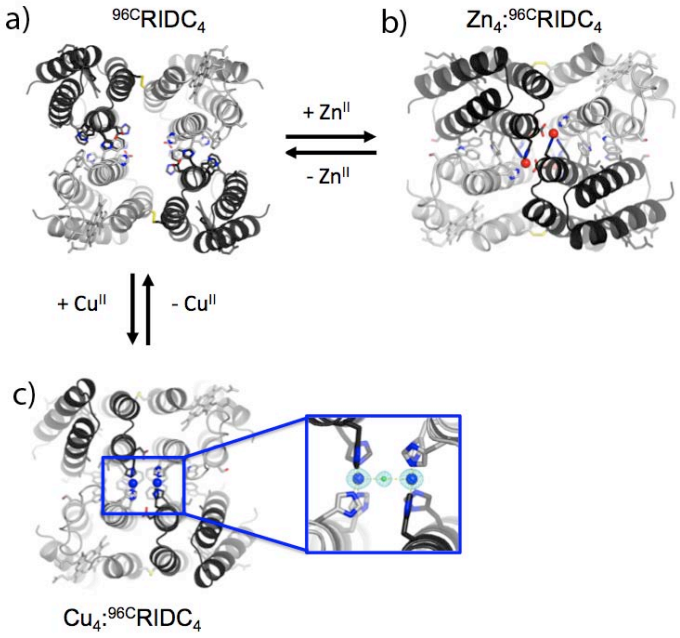

Figure 1. a) The Zn-templated tetrameric assembly, ^{96C}RIDC1$_4$, and its structural transformations upon binding Zn^{2+} (b), and Cu^{2+} (c). One of the two dinuclear Cu centers in the Cu$_4$:^{96C}RIDC1$_4$ complex is shown in detail, highlighting the bridging chloride ligand. The internuclear Cu-Cu distance is 5 Å, indicating that it can accommodate O_2 binding.

ii. 3) Closed, Symmetrical Protein Superstructures Assembled through Metal Coordination:

Symmetrical, homooligomeric protein assemblies are highly prevalent in nature. For a major fraction of these proteins, their homooligomeric nature (and thus their shape) are intimately linked to their function, such as iris-like proteins involved in ion and substrate transport across membranes, hollow-cylinder shaped chaperonins involved in protein refolding and cage-like ferritins or bacterial

microcompartments that contain insoluble or toxic cargo. Using MDPSA, we were able assemble cyt cb562 derivatives into open pentagonal (Figure 2a) or closed, tetrahedral architectures (Figure 2b) via directed Zn coordination, and thoroughly characterize their structures. We were further able to trap flexible and thus crystallographically unwieldy species (a heme microperoxidase) on the inside of the tetrahedral cage, which allowed its atomic structure to be resolved for the first time (Figure 2c).[10] We believe that this methodology will be readily applicable to other transient species like catalytic reaction intermediates, whose reaction coordinates may be captured by crystallography through immobilization on the interior wall of a protein cage.

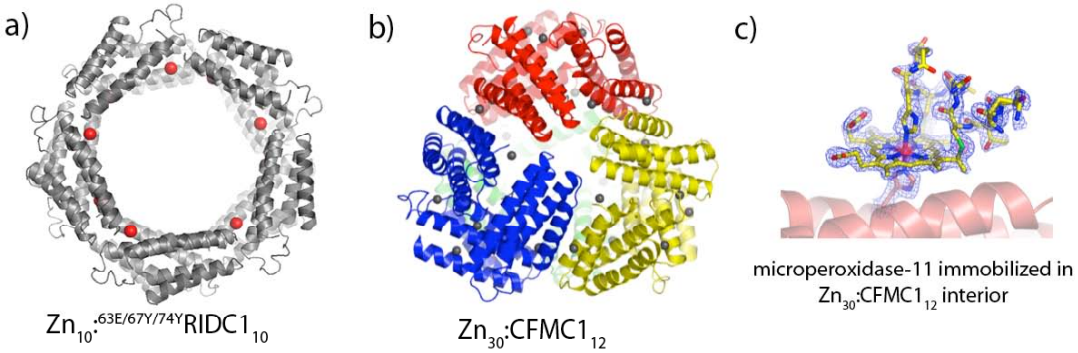

Figure 2. Closed pentagonal (a) or tetrahedral (b) assemblies of cytochrome cb562 variants directed by Zn coordination. (c) The $2F_o$-F_c electron density map (1.1 σ) around a microperoxidase-11 molecule immobilized on the interior wall of Zn_{30}:CFMC1$_{12}$.

ii.4) Chemically-Controlled Assembly of 1-, 2-and 3-D Protein Arrays with Crystalline Order:

In the field of Supramolecular Coordination Chemistry, inorganic chemists have been particularly successful in exploiting the directionality and reversibility of metal coordination to construct stable 1-, 2- and 3-D coordination polymers through careful ligand design. Inspired by these efforts, we have designed a dimeric cyt cb562 derivative (termed RIDC3) that presents a pair of three-coordinate Zn-binding sites, whose coordination vectors are orthogonally oriented (Figure 3a). Using the Zn_2:RIDC3$_2$ dimer as a corner-like building block allows the Zn-dependent formation of uniform 1-D nanotubes (60 nm width, several microns long) (Figures 3b and c), and 2- and 3-D sheets (microns long/wide, nanometers thick) with crystalline order (Figure 3d and e). The full structural characterization of these architectures through X-ray crystallography, transmission electron microscopy and cryo-electron microscopy has allowed a detailed structural understanding of how these various architectures form through Zn coordination and interconvert amongst themselves. This study, to our knowledge, represents the first example where a monomeric protein can be designed to yield (with 2-D constraints or templating) crystalline nanotubes and 2-D sheets. Significantly, these structures not only mimic biological assemblies like the tobacco mosaic virus or microtubules, but also capture their stimulus-(in particular metal-stimulus) responsive nature. Finally, our study also represents the first case where the crystallization of a protein can be fully chemically controlled in all three dimensions.

iii) Future Directions

Our work in the near future will use as a springboard the advances we made in controlling the self-assembly of proteins through metal coordination chemistry, and focus on creating new functional materials. Of particular interest to us are 1) interfacial Cu sites for catalytic O_2 activation and long-range electron transfer, 2) the structural capture of catalytic reaction intermediates in cage-immobilized metal-clusters and 3) functionalization of 1-, 2- and 3-D protein arrays discussed in ii.4 with photosensitizers and catalytic sites for light-harvesting and photo-driven redox catalysis.

Especially based on our results described in ii.4, we are aiming to impart further control on protein crystal nucleation and growth through coordination chemistry, and pursue light-mediated temporal control over crystal growth in different dimensions.

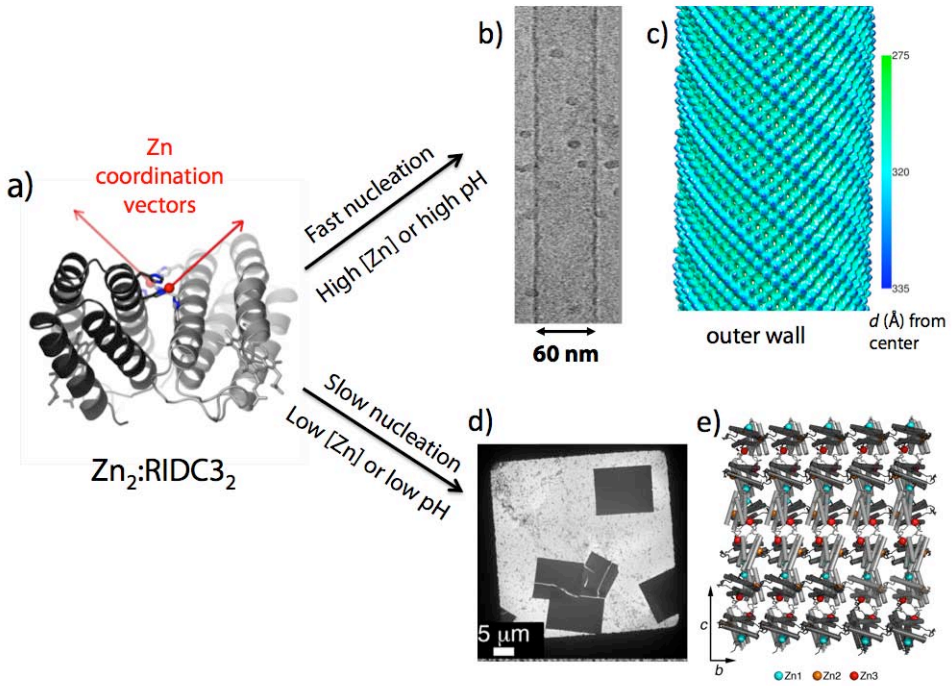

Figure 3. (a) The designed dimer Zn_2:RIDC3_2 and the coordination vectors that originate from the two His_3-coordinated Zn sites. As shown in the cryo-EM image (b) and the helical reconstruction (c) obtained at 8.4 Å, Zn_2:RIDC3_2 assembles into uniform, crystalline nanotubes under fast nucleation conditions, and into 2- and 3-D sheets (d) under slow nucleation conditions. Figure 3 shows the atomic structure of the underlying 2-D array mediated by three different types of Zn coordination environments.

iv) Publications Resulting from DOE-support (7 total)

2. Salgado, E. N.; Ambroggio, X. I.; Brodin, J. D.; Lewis, R. A.; Kuhlman, B.; Tezcan, F. A., **Proc. Natl. Acad. Sci. USA** 2010, *107*, 1827-1832.

6. Radford, R. J.; Nguyen, P. C.; Ditri, T. B.; Figueroa, J. S.; Tezcan, F. A., **Inorg. Chem**. 2010, *49*, 4362-4369.

7. Radford, R. J.; Nguyen, P. C.; Tezcan, F. A., **Inorg. Chem**. 2010, *49*, 7106-7115.

8. Radford, R. J.; Brodin, J. D.; Salgado, E. N.; Tezcan, F. A., **Coord. Chem. Rev**. 2011, *255*, 790.

9. Brodin, J. D.; Medina-Morales, A.; Ni, T.; Salgado, E. N.; Ambroggio, X. I.; Tezcan, F. A., **J. Am. Chem. Soc.** 2010, *132*, 8610-8617.

10. Ni, T. W.; Tezcan, F. A., **Angew. Chem. Int. Ed. Eng.** 2010**,** *49*, 7014-7018.

11. Radford, R. J.; Lawrenz, M.; Nguyen, P. C.; McCammon, J. A.; Tezcan, F. A., **Chem. Comm.** 2011, *47*, 313-315.

v) Other Cited References

1. Salgado, E. N.; Radford, R. J.; Tezcan, F. A., ***Acc. Chem. Res.*** 2010, 43, 661-672.

3. Bromley, E. H. C.; Channon, K.; Moutevelis, E.; Woolfson, D. N., ***ACS Chem. Biol.*** 2008, 3, 38.

4. Seeman, N. C., Nanomaterials Based on DNA. In Annual Review of Biochemistry, Vol 79, Annual Reviews: Palo Alto, Vol. 79, pp 65-87.

5. Delebecque, C. J.; Lindner, A. B.; Silver, P. A.; Aldaye, F. A., ***Science*** 2011, 333, 470-474.

Self-Assembly of Pi-Conjugated Peptides in Aqueous Environments Leading to Energy-Transporting Bioelectronic Nanostructures

PI: John D. Tovar
Johns Hopkins University, Department of Chemistry, Department of Materials Science and Engineering, and Institute for NanoBioTechnology, NCB 316, Baltimore, MD 21218
Email: tovar@jhu.edu
Group webpage: http://www.jhu.edu/~chem/tovar/index.html

Program Scope: Peptide-based nanomaterials have attracted increasing attention in both biomedical and energy sciences. Supramolecular interactions can be engineered to encourage the self-association of molecular components into discrete nanostructures, and peptide residues can be chosen to control solubility or biological interaction. The design of electronically relevant biomaterials capable of energy migration and interaction with the biotic interface would be the first step towards the transduction of artificial and natural energy currencies for harvesting or transport. This DOE program is concerned with our efforts to synthesize and understand pi-conjugated self-assembling peptides that form one-dimensional electronically delocalized materials under completely aqueous conditions. In the context of peptide-based electronic materials, this poses several challenges. First, the pi-conjugated entities tend to be very insoluble in aqueous environments so careful peptide design must be capable of providing molecular solubility. Second, the cofacial pi-stacking recognized as optimal for energy migration suffers from electrostatic quadrupolar repulsion among the pi-electron clouds and must be compensated for by design with other more enthalpically favorable electrostatic interactions among the peptide hydrogen-bonding arrays.

We developed two synthetic methods to prepare a broad family of self-assembling peptides bearing a diverse range of pi-electron structures spanning p-type semiconductors (oligothiophenes), n-type semiconductors (rylene diimides), fluorophores (oligo phenylene vinylenes) etc. These electronic structures are incorporated directly into the backbone of the peptides as opposed to side-chain modifications commonly used for protein labeling. During molecular association and aggregation into the supramolecular nanostructures (Figure 1), the peptide sequences undergo hydrogen bonding and force the pi-electron units into close pi-stacked orientations. With proper choice of peptide residues, purification and characterization is straightforward. The initiation of molecular self-assembly into discrete 1-D nanostructures is achieved through changing solution pH or even in the presence of cell culture media and physiologically relevant calcium ion concentrations.

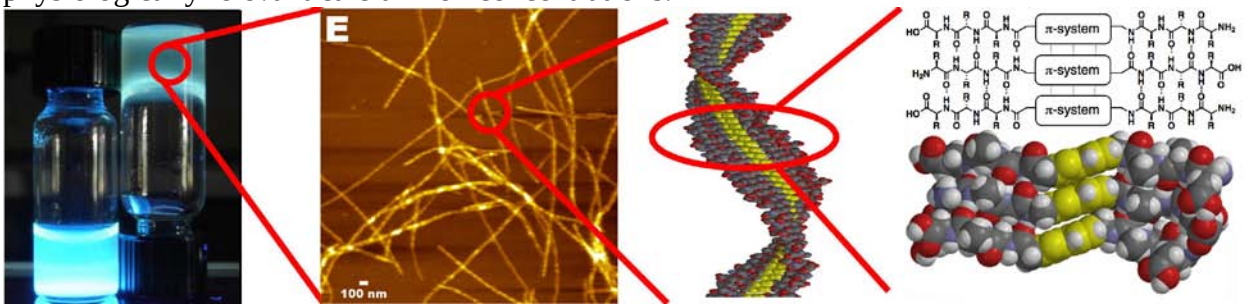

Figure 1: A solution of pi-conjugated (bithiophene) peptides (fluorescent at far left) is triggered to assemble resulting in a macroscopic self-supporting hydrogel comprised of random networks of 1-D nanostructures (center left) that form as molecular components (far right) self-associate into pi-stacked aggregates (center right).

These materials were characterized photophysically using steady-state and time-resolved UV-vis, photoluminescence and circular dichroism. Nanomaterial morphologies were visualized using atomic force, scanning electron and transmission electron microscopies. Our collective spectroscopic and morphological examinations led us to propose a working mechanism for the nanomaterial assembly whereby peptide molecules form b-sheet hydrogen bonding networks that force the pi-conjugated units into H-like aggregates that involve cofacial electronic interactions. These aggregates could be envisioned to consist of tape-like structures, coil-like structures, or higher-order aggregates derived from extended assembly modes. This is quite common for amyloid-like materials, where very complex but shallow energy landscapes exist among different self-assembled material morphologies. Regardless, the end structures are under 10 nm in diameter and extend microns in length. This ability to fashion pi-conjugated structures from aqueous environments at this length scale is unprecedented and opens up many possibilities for future research as discussed below.

Recent progress. Critical advances over the first year of the program include (1) the development of a new synthesis strategy to incorporate even more pi-electron complexity into the peptide frameworks, (2) the exploration of a novel patterning process to prepare globally aligned macroscopic structures (as opposed to the random networks shown above), (3) the synthesis of reactive peptides that undergo intermolecular crosslinking to form conjugated polymer nanostructures, and (4) photophysical and electrical measurements within individual nanostructures and within globally aligned macrostructures. All of this work is unpublished: one manuscript as been submitted, and at least three are in various stages of preparation but with anticipated submission dates within the next three months.

(1) New synthesis techniques. Our prior synthetic approaches required difficult syntheses of amino acid or diacid containing pi-electron units. We devised a strategy that minimizes the need for complex synthetic chromophores and at the same time allows for a much greater diversity of electronic structures (Ref 2). Using this new strategy we prepared some of the longest pi-conjugated oligomer sequences yet reported within completely water soluble oligopeptides which will be important for encouraging more effective energy migration through the resulting supramolecular nanostructures, particularly in contexts that may require gate-modulated conductance variation necessary for transistor behavior.

(2) Macroscopic alignment of peptide nanostructures. The Stupp lab at Northwestern recently described a simple yet powerful method to prepare globally aligned hydrogels comprised of self-assembling peptide amphiphile nanostructures. The technique in brief involves injecting a solution of molecularly dissolved amphiphiles (with an added blue dye in Figure 2) into a solution with high ionic strength that would ordinarily provoke nanostructure assembly. If done in the bulk, (e.g. adding the "trigger solution" to the molecular peptide solution at once) one would ordinarily obtain a hydrogel made up of randomly aligned nanostructures. However, by injecting the solution through a fine pipette tip into the ionic

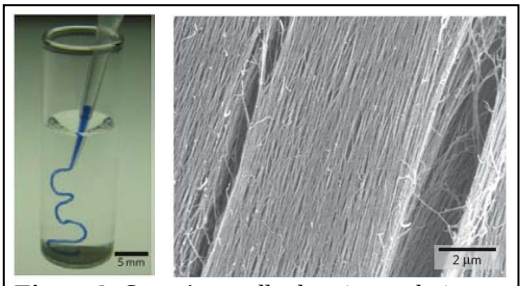

Figure 2: Stupp's noodle drawing technique (left) leads to aligned bundles of 1-D peptide amphiphile nanostructures (right). Taken from Nature Materials **2010**. *9*. 594-601.

solution, the shear forces present at the point of delivery guided the formation of a hydrogel "noodle" that could be physically manipulated into complex structures such as knots without rupture or damage. SEM revealed that this noodle was made up of aligned bundles of peptide amphiphile nanostructures (Figure 2, right).

We were able to employ this technique to prepare noodles of several pi-conjugated self-assembling peptides (Figure 3). The chromic properties of the internal pi-conjugated group can be used in lieu of an external dye and at the same time can impart new functions to the macroscopic noodle structures. The individual aligned features observed in the SEM are on the order of 30-40 nm, suggesting that they are made up of several bundled peptide amphiphile nanostructures whose long axes are coincident with the noodle long axis (or, the direction of solution extrusion). Similar features are found among our noodles, where they can be envisioned to form from bundles of amyloid-like peptides. The nature of the molecular aggregation event enforces cofacial interactions among the pi-electron units with the axis of intermolecular delocalization running coincident with the nanomaterial long-axis and subsequently along the noodle long axis, leading to anisotropic electrical properties in the macrostructire. We believe these optoelectronic matrices offer a unique environment to achieve cell adhesion within a 3-D hydrogel material that offers at the same time the ability for external optical or electrical stimulation and will be the subject of our future work. A communication describing this research has been provisionally accepted to *Advanced Materials*.

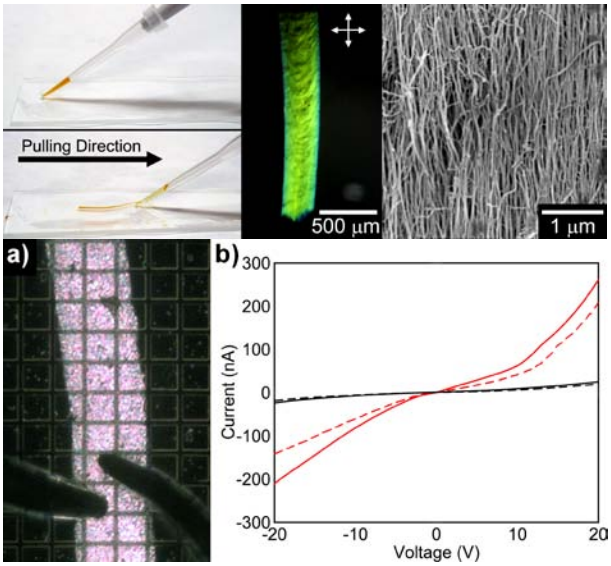

Figure 3: A solution of optoelectronic peptides is drawn into a noodle hydrogel comprised of aligned nanostructures (top). These materials show anisotropic hole mobilities when measured parallel (red) or perpendicular (black) to the alignment axis (bottom).

(3) Conjugated polymer nanostructures. We found that if reactive pi-conjugated linkers were incorporated into the peptide molecules prior to the nanostructure assembly, external triggers such as light or heat could provoke an intermolecular reaction that ultimately resulted in the formation of a conjugated polymer covalently captured within the supramolecular structure. In some cases, the resulting structures were made up of *single conjugated polymers* but in other cases bundles of multiple chains were observed on account of the amyloid-like energetics of the assembly process depicted in Figure 1. Using the noodle technique described in part (2), we prepared aligned precursor materials for global or spatially controlled polymerization. Beyond the importance of bio-based conjugated polymers, the ability to macroscopically align polymers without the application of harsh electrical or magnetic fields is a significant advance. We will present the sensory responses of these nanomaterials in the presence of different chemical stimuli as well as the carrier transport properties of the individual nanostructures and the collectively aligned domains within the noodle macrostructures. This work is currently in the final stages of manuscript preparation (Ref 4).

(4) Photophysical and electrical characterization. Our recent efforts for continued optoelectronic characterization are concerned with solution characterization of nanostructures up through the interrogation of macroscopic noodles. We prepared a series of peptides with different degrees of steric bulk and are establishing a structure-function relationship regarding the extent of intermolecular pi-electron interaction and the resulting influence on photophysical observables (Ref 5). These studies rely on steady-state and time-resolved photoluminescence and circular dichroism measurements in-house as well as one- and two-photon confocal microscopy at the JHU Integrated Imaging Center. We have explored the ramifications of the uniform alignment on noodle photophysics and on carrier transport anisotropy when source and drain electrodes are probed parallel and perpendicular to the noodle alignment long axis, in collaboration with William Wilson and Howard Katz at JHU. We are also employing a variant of electrostatic force microscopy with Nina Markovic at JHU that allows us to observe the presence of charge carriers in a transistor-like operating environment but without the formal need to deposit electrodes on the nanomaterials. Although we succeeded in overcoming the contact resistance expected for depositing electrodes on the insulating peptides on the periphery of the nanostructures, this technique simply examines the inherent ability for the conductances of these materials once doped to screen the field from the underlying gate electrode. Our collective results show quite dramatically how subtle molecular designs can impact energy migration.

Future plans. In addition to our continuing photophysical, electrical and morphological characterization, we will examine the incorporation of new types of "2-D" conjugated electronic structures into the peptide backbones, using cruciform-type molecules as well as looking at polyvalent peptide attachment to defined graphene subunits. Our intentions are to prepare new materials with delocalized electronics and at the same time use the geometric properties of certain 2-D electronic motifs as a way to arrest the hierarchical amyloid-like assembly process in early stages. Finally, the inclusion of bioactive peptide sequences will be addressed thus leading to more explorations of the surface chemistry presented by the nanomaterial periphery.

List of papers to acknowledge DOE support: 2011

1) J. D. Tovar, "Organic halogenation chemistry as a vital tool for the construction of functional pi-conjugated materials" invited by Synthesis (special issue on "organic halogenation," Erick M. Carreira, editor), 2011, 2387-2391. (DOI: 10.1055/s-0030-1260086)

2) A. M. Sanders, S. R. Diegelmann and J. D. Tovar, *communication evolving*: New synthesis techniques

3) B. D. Wall, S. R. Diegelmann, S. Zhang, T. J. Dawidczyk, W. L. Wilson, H. E. Katz, H.-Q. Mao and J. D. Tovar, *"*Aligned macroscopic domains of optoelectronic nanostructures prepared via the shear flow assembly of peptide hydrogels," provisionally accepted in *Advanced Materials*

4) S. R. Diegelmann, N. Hartmann, N. Markovic and J. D. Tovar, *communication in preparation:* Conjugated polymer nanostructures

5) B. D. Wall and J. D. Tovar, *full paper in preparation:* Photophysical characterization

Self Assembling Biological Springs:

Force Transducers on the Micron and Nanoscale

Ying Wang[a], Aleksey Lomakin[a], and George B. Benedek[a,b]

[a]Materials Processing Center, [b]Department of Physics, Massachusetts Institute of Technology, 77 Massachusetts Avenue, Cambridge, MA 02139

PI: George B. Benedek

Program Scope:

We have discovered that helical ribbons with a fixed pitch angle self assemble in a variety of quaternary solutions containing the sterol, a mixture of surfactants and water [1]. Our X-ray studies have shown that the cholesterol helical ribbons are single crystal strips wrapped into a helical form [2]. The overall goal of this project is to utilize these novel biomolecular objects as mesoscopic springs and deformation gauges.

We are developing new methods to use these helical ribbons for measuring and applying forces in the pico- and nano-newton range. These are forces characteristic of macromolecular interactions in biological systems. Cholesterol helical ribbons can serve as very soft mesoscopic springs. Depending on their dimensions, they have spring constants ranging from 0.5 t o 500 pN /m [3]. The spring constants of all cholesterol helical ribbons can be calculated from their observable geometrical features: width w, contour length s, and radius R [4]. A helical ribbon with a spring constant appropriate for a particular application can be readily selected from a polydisperse ensemble of ribbons formed in solution.

To be used for force measurements and force transduction, the ribbon must be attached to the objects under investigation. Direct tethering of cholesterol ribbons is difficult because of its delicacy and absence of chemically active groups on its surface. Various means to modify the surface of the helical ribbons have been explored, and we have found that polydopamine surface coating provides the desired adhesion. In addition, this coating renders the helical ribbons more robust, and also enables further surface modifications such as metal plating. Our helical ribbons are soft and have the same pitch angle in their unstrained form independent of external solution conditions, but can change in response to a local strain. These properties suggest the use of helical ribbons as strain detectors and indicators to measure plastic and elastic deformation in hydro gels.

Recent Progress:

We have made significant progress towards achieving the goal of this project. The results are summarized as follows.

(1) *The relation between the elastic moduli and the geometry of ribbon thickness.*

We have established a quantitative relationship between the spring constant of any low-pitch cholesterol helical ribbon and its readily observable external dimensions,

namely width, radius, and length. We have measured the thickness, t, of a large number of helical ribbons of different radii, R, using quantitative phase microscopy [4, 5]. These results suggest a quadratic relationship between R and t namely: $R = ct^2$. Here, c is a coefficient which is determined to be equal to $(3.56 \pm 0.11) \times 10^3$ μm^{-1} for low-pitch cholesterol helical ribbons.

We have previously shown in [3], that the spring constant K_{spring} of a cholesterol crystalline helical ribbon is determined by its width, w, its contour length, s, and its radius, R, according to: $K_{spring} = 8wK_\alpha/R^2s$, where the effective bending modulus K_α is proportional to the cube of the thickness t, $K_\alpha \propto t^3$. Since we now find that $t \propto R^{1/2}$, it follows that $K_\alpha \propto R^{3/2}$. Thus we may express the spring constant entirely in terms of the external dimensions which can be measured with an optical microscope, viz:

$$K_{spring} = \kappa \frac{w}{R^{1/2}s}$$

where κ is a constant. Using the previously measured value of K_{spring} of a single low-pitch cholesterol helical ribbon [3] and the geometrical parameters w, R, s directly measured by optical microscope, we have determined the value of κ to be equal to 1.37×10^{-6} $N/m^{1/2}$.

By this means we have established a calibration of all low pitch helical ribbons in terms of their external dimensions. This relationship is important because the helices which self-assemble in multi-component solutions containing sterols and appropriate surfactants are widely polydisperse in length, width, and radius.

(2) *Growing helical ribbons with high yield in small volume of solution.*

In the previous studies, we have shown that formation of sterol helical ribbons can be observed in a variety of sterol-surfactant-fatty acid-water quaternary system [1]. The previously reported procedure to grow sterol helical ribbons was based on dilution of the quaternary sterol solution [1]. This dilution approach produced high overall yield of helical ribbons, but the number of ribbons per unit volume of solution is small.

In order to increase the feasibility of further processing such as chemical modification and tethering, we designed a novel thermal quenching approach to obtain high yield of ribbons in small volume of solution. Specifically, we solubilized cholesterol at 35 overnight. We then quenched the solution to a lower temperature (20˚C). Because the CMCs of surfactants (Pluronic F-68) increase as the temperature decreases, the surfactant concentration became below the CMC at the low temperature and sterol helical ribbons grew from the supersaturated solution. A large number of long helical ribbons were found in this cholesterol saturated solution after one week.

(3) *New method for tethering helical ribbons to functionalized polystyrene beads and glass capillaries.*

In order to use cholesterol helical ribbons as mesoscopic springs, we want to tether the helical ribbons to functionalized polystyrene beads. This bead will serve as the biologically active binding tip of one end of the helical ribbon spring. We also wish to tether the other end of the helix to a glass capillary, which will serve as a suspension post.

The reproducibility of our current tethering method, which uses Devcon Epoxy, is limited by the absence of active surface functional groups on cholesterol helical ribbons. In the last two years, we have developed three methods for tethering the cholesterol helical ribbons. First, after trying a large number of different chemical polymerization systems, we developed an adhesive system based on the UV induced copolymerization of HEMA (Hydroxyethyl Methacrylate) and EGDMA (Ethylene glycol). By adjusting the concentrations of the monomer HEMA and the cross-linker EGDMA, we optimized the conditions for polymerization, which produces a transparent gel joining the capillary and helical ribbon together. Secondly, we have coated helical ribbons with polyvinyl alcohol, which makes it easier to tether ribbons to glass capillaries with Epoxy. Finally, we have developed a tethering technique which takes advantage of combining polydopamine coating and amine cross-linking (with glutaraldehyde). We have used this technique to tether the helical ribbons to both polystyrene spheres and glass capillaries. Of these three methods, the last one proves to be the best. This tethering method is easy to perform and produces the most reliable and reproducible results (Fig. 1).

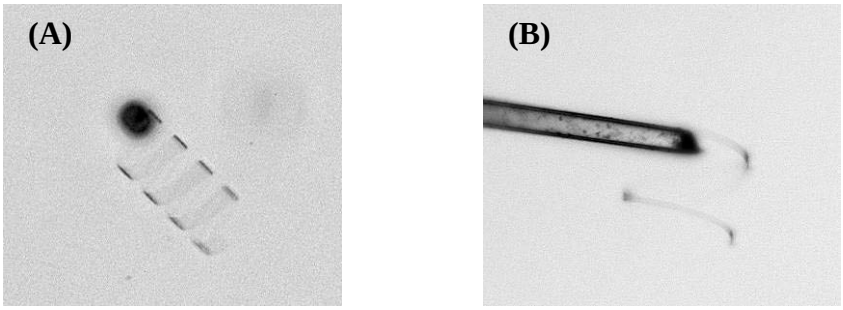

Fig. 1. Using polydopamine coating and glutaraldehyde cross-linking, we have attached the cholesterol helical ribbons to the polystyrene sphere (A) and the tip of the glass capillary (B).

(4) *To use the helical ribbons as mesoscopic rulers to measure the internal deformations of hydro gels, and other continuous media.*

We have prepared hydro gels (polyacrylamide gel and collagen gel), which contains embedded cholesterol helical ribbons (Fig. 2).

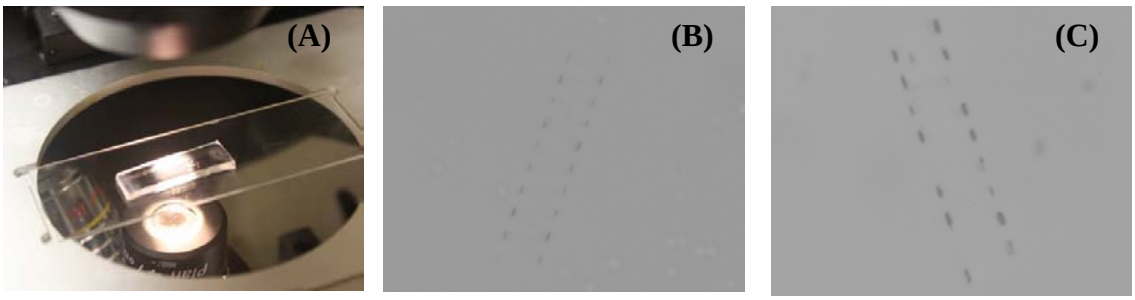

Fig. 2. (A) A polyacrylamide gel which contains immobilized cholesterol helical ribbons. (B) A helical ribbon immobilized in the gel. (C) An immobilized helical ribbon remains undamaged after drying and re-hydration of the gel.

The immobilized helical ribbons are very robust. Upon drying the gel and subsequently rehydrating it, we observed that most of the helical ribbons remained undamaged (Fig. 2C). Interestingly, we have also observed even in the rehydrated gel that ribbons have altered pitch angles (Fig. 2C). This likely reflects residual local plastic deformation in the rehydrated gel. T hese experiments demonstrate how the helical ribbons may be used as a measure of the local deformation in a h ydro gel subjected to external stress.

Several unique characteristics make these embedded helical ribbons good gauges of the local strains in the gel under external stresses. The helical ribbons are stable in the gel, and can be easily handled and used under different solution conditions. All the low pitch cholesterol helical ribbons have the same pitch angles 11° i n solution. Under external forces, the pitch angle change, $\Delta\psi$, permits a measure of the length change, Δl, in the axial direction, viz. $\Delta l = s[\sin(11° + \Delta\psi) - \sin(\Delta\psi)]$, where s is the contour length of the helical ribbon. Moreover, these helical ribbons are very soft compared to the gel. Their stiffness (~0.01-1 kPa) is lower than that of most biological gels in tissues (~0.1-17 kPa) [6]. Therefore, the deformation of the helical ribbons themselves will not generate significant internal stresses in the biological gels.

Future plans:

The progresses summarized above enable us to explore and optimize the utility of sterol helical ribbons as mesoscopic springs and rulers. We are designing experimental set up to measure the internal deformations of collagen gels using the helical ribbons. We also plan to set up experiments to measure quantitatively the forces between macromolecules and other microscopic biological entities using the helical ribbons and the polydopamine coating techniques followed by further surface modifications.

.

References:

[1] Y. V. Zastavker, N. Asherie, A. Lomakin, J. Pande, J. M. Donovan, J.M. Schnur, G. B. Benedek "Self-assembly of helical ribbons", *Proc. Natl. Acad. Sci. USA* **96**, pp. 7883 (1999).

[2] B. Khaykovich, C. Hossain, J. J. McManus, A. Lomakin, D. E. Moncton, and G. B. Benedek, "Structure of cholesterol helical ribbons and self-assembling biological springs", *Proc. Natl. Acad. Sci.* USA. **104**, pp 9656 (2007).

[3] B. Smith, Y.V. Zastavker, G.B. Benedek, "Tension-induced straightening transition of self-assembled helical ribbons", *Phys. Rev. Lett.* **87,** pp. 278101 (2001).

[4] Khaykovich B, Kozlova N, Choi W, Lomakin A, Hossain C, Sung Y, Dasari RR, Feld MS, Benedek GB. Thickness-radius relationship and spring constants of cholesterol helical ribbons. *P Natl Acad Sci* USA. 2009;106(37):15663-6.

[5] W. Choi, C. Fang-Yen, K. Badizadegan, S. Oh, N. Lue, R. R. Dasari, M. S. Feld "Tomographic phase microscopy", *Nature Methods*, **4**, pp. 717, (2007).

[6] Sen S, Engler AJ, Discher DE. Matrix Strains Induced by Cells: Computing How Far Cells Can Feel. *Cell Mol Bioeng*. 2(1):39-48, (2009).

DOE Sponsored Publications in 2009-2011:

Khaykovich B, Kozlova N, Choi W, Lomakin A, Hossain C, Sung Y, Dasari RR, Feld MS, Benedek GB. Thickness-radius relationship and spring constants of cholesterol helical ribbons. *P Natl Acad Sci* USA.;106(37):15663-6, (2009).

Dynamic Self-assembly, Emergence, and Complexity

Principal investigator: George M. Whitesides
Department of Chemistry and Chemical Biology
Harvard University
Cambridge MA 02138
Gwhitesides@gmwgroup.harvard.edu

i. PROGRAM SCOPE.

General Description. The focus of this research program is the study of complex systems, and especially complex systems whose properties manifest themselves in terms of patterns or regular structures. (We define a complex system – following the definition common in physics – as one comprising "components" "interacting" dissipatively. Components and interactions can be virtually anything; the "dissipative" constraint ensures that the system is out of equilibrium, and almost certainly shows – for some number of components – the influences of nonlinear effects.) Complex systems characteristically display unexpected (often called "emergent") behaviors. These emergent characteristics point to the properties of the system that were *not* considered in the first-order analyses, and suggest new phenomena to study and exploit in applications.

The program has four general goals. i) To build (e.g., in chemical terms, to "synthesize") complex systems, by selecting and characterizing individual components, adding them to the system one at a time, and observing the appearance of unexpected behaviors and phenomena. ii) To rationalize – in so far as possible – these behaviors/phenomena, and to build quantitative or semi-quantitative analytical models for them that reveal the underlying nonlinearities and the physical processes that give rise to them. iii) To develop a mechanistic understanding (which will often combine analytical, physics-based approaches with more physical-organic, chemically based approaches) of the systems to the point where it is possible to use it to design and build new systems, and to control them rationally, by design. iv) To identify areas and problems where these systems might be applied, and to prototype (but not fully develop) these applications. It also aims to understand important phenomena (for example, crystallization of droplets of supercooled water, a subject basic to understanding atmospheric phenomena.

Subprograms, short description. This program has focused on five types of self-assembly involving both static and dissipative systems: **i) Meso-Scale Self-Assembly of Coulombic Crystals.** Contact electrification has been used to form arrays (in 2D) of charged spherical particles, and the assembly of these particles studied as a function of relative charge, shape, and other parameters. This work provides a physics-based model for crystallization and phase-change. **ii) "Entropic" Self-assembly.** Meso-scale particles—even when uncharged—self-assemble when agitated. The mechanism of this self-assembly is not entirely obvious, but is probably related to some of the types of entropic mechanisms for self-organization observed with colloids and macromolecules. **iii) Nucleation and Crystallization of Ice from Supercooled Water.** The formation of ice is a rich field, with importance in subjects ranging from weather to the theory of molecular self-assembly in crystallization. Microfluidic systems provide a powerful

method of studying these behaviors. i**v) Self-organization of Flamelets and Plasmas.** Flames are prototypical dissipative systems, and systems of flamelets show a variety of self-organizing structures. **v) Complex Self-Organization on Bubbles in Microfluidic Channels.** When a bubble moves through a microchannel—within a range of dimensions for the bubble and the channel—it changes the fluidic resistance of the channel. This change is communicated to other bubbles in the system in terms of changes in pressure drops, and emerges as complex and non-intuitive behaviors, with potential relations to subjects such as traffic.

Significance. This research is important for four reasons:

i) It is clarifying the characteristics of complexity: that is, the relations between interactions and properties in physical (e.g., not theoretical or computer-based) systems that are tractably simple (relatively small numbers of simple components) but still show emergent behaviors.

ii) It has proved successful in generating new phenomena and materials that can be developed to understand materials, and to solve problems in chemical, materials, and biological science. Examples include systems of bubbles in microchannels, electrets and electrostatically charged matter, flames, and others.

iii) It is developing physical systems that can provide tests of theory in fields such as self-assembly: "electrostatic matter" based on electrets is the most advanced of these systems.

iv) It is focusing attention on dissipative and out-of-equilibrium systems. Much of science is based on the study of systems at equilibrium or at steady state, but many of the most interesting phenomena in nature are dissipative. This work is contributing to building an intellectual bridge between the two.

ii. RESEARCH PROGRESS

We summarize the major advances in the project in work published in this period; some of the work was executed in part in the preceding period.

Electrets. We have developed a system comprising a rolling metal sphere and a flat polymer sheet that makes it possible to follow the detailed kinetics of charging (a process following first-order kinetics) and discharging (a rapid event that involves either a spark or a brief corona discharge. We have also extended studies of self-assembly in oppositely charging systems of polymer spheres (and other shapes). During this work, we have also discovered an unexpected new type of self-assembly, in which the components (meso-scale shapes) self-assemble in a dynamic system (a shake-table) apparently without an electrostatic component. We are trying to understand the mechanism of this system now.

Droplets and Bubbles in Microchannels. We are exploring systems of droplets and bubbles in microchannels. These systems show very complex patterns of movement through the microsystems, based on the fact that each bubble (assuming that its size is bigger than the size of the channel) modifies the fluidic resistance in the channel, and thus communicates its position (within a channel segment) to droplets both ahead of it and behind it). These types of behaviors provide a perfect opportunity to explore classically complex behavior. They also offer the change to consider the potential of these systems as analog computers for phenomena such as "traffic" and "logistics transport", and to understand the flow of capillaries in blood vessels.

Nucleation of Ice. In a distinct major application, we have used these kinds of microfluidic systems in an effort to study the nucleation of ice from supercooled water, a subject of great

importance in understanding clouds. Our major interest was to explore whether particles (silica, carbon, etc) included in supercooled water would nucleate the formation of ice. Silver iodide did; nothing else showed significant activity. Barring an unforeseen opportunity, we consider this project essentially completed.

Flames. We have worked on this subject for two years, and have developed a range of remarkable observations, but have still not published papers: it is a very complex subject with an interplay between ionic winds, charged streams of particles, a charge flame, the rate of propagation of the flame in the gas mixture, and so on. We will begin publishing papers in the coming year.

iii. FUTURE PLANS

Contact Electrification.

Studies of Mechanisms. We have made substantial qualitative progress in understanding many of the mechanisms of contact electrification involving organic insulators. We are now involved in quantitative studies of rates of charging. These studies are demonstrating that some of the processes that we considered to be single, seem, in fact, to be multiple: that is, there are indications of multiples competing processes. We will continue to disentangle these complex processes (which probably involve competing reactions that lead to charging and discharging).

Self-Assembly and Phase Separation. The development of rational methods for using contact electrification to charge polymers has led to a rich new field of electrostatic self-assembly. We will continue to examine and define the processes that occur in this type of "electrostatic matter," with an emphasis on understanding phenomena that mimic—in 2D—the processes of phase separation that occur at a molecular level.

"Non-charging Surfaces". We are now in the position to *design* materials that do not charge electrostatically. Demonstrating appropriate strategies will be a substantial step the development of systems that can suppress or eliminate the damage and loss that occurs due to idiosyncratic spark discharges (in electronics, in handling flammable liquids, and in systems that involve contact of different materials).

"Entropic Self-Assembly". In the course of studies of electrostatic self-assembly, we have discovered an entirely new type of self-assembly, which occurs on agitation of meso-scale particles, but does not involve electrostatics. We believe that this system has some similarity to the entropically driven processes encountered in suspensions of colloids and polymers, but have not established the mechanisms yet.

Bubbles in Channels. We have a variety of phenomena that we have discovered in systems of bubbles in microchannels. These systems are relevant to microfluidics and bioanalysis, to the flow of dispersed phased in channels (e.g., oil in rock, erythrocytes in capillaries), and to analog computation. We will continue to develop a description of these systems, with the objective of being able to predict the complex behaviors that we observe.

Flamelets. The study of systems of small, interacting flames has been difficult experimentally. We believe that we finally have a reproducible system, and will begin to examine the behavior of this prototypic dissipative system.

PUBLISHED (since 2/1/2009)

1. "Independent Control of Drop Size and Velocity in Microfluidic Flow-Focusing Generators Using Variable Temperature and Flow Rate", Stan, C. A., Tang, S. K. Y., Whitesides, G. M., *Analytical Chemistry,* 2009, *81,* 2399-2402
2. "Phase Separation of 2D Coulombic Crystals of Meso-scale Dipolar Particles from Meso-scale Polarizable "Solvent"", Kaufman, G. K., Reches, M., Thomas, S. W., Feng, J., Shaw, B. F.,Whitesides, G. M., *applied Physics Letters,* 2009, *94,* 4, 044102-1 - 3
3. "Phase Separation of 2D Meso-Scale Coulombic Crystals from Meso-Scale Polarizable "Solvent"", Kaufman, G. K., Thomas, S. W. R., M, Shaw, B. F., Feng, J.,Whitesides, G. M., *Soft Matter,* 2009, *5,* 1188-1191 PMCID: PMC2755486
4. "Propulsion of Flexible Polymer Structures in a Rotating Magnetic Field", Garstecki, P., Teirno, P., Weibel, D. B., Sagués, F.,Whitesides, G. M., *J. Phys.: Condens. Matter,* 2009, *21,* 204110+ 0
5. "Preparation of Monodisperse Biodegradable Polymer Microparticles Using a Microfluidic Flow-Focusing Device Controlled Drug-Delivery", Xu, Q., Hashimoto, M., Dang, T. T., Hoare, T., Kohane, D. S., Whitesides, G. M., Langer, R.,Anderson, D. G., *Small,* 2009, *5,* 13, 1575-1581
6. "Controlling the Kinetics of Contact Electrification with Patterned Surfaces", Thomas, S. W., Vella, S. J., Dickey, M. D., Kaufman, G. K.,Whitesides, G. M., *Journal of American Chemical Society,* 2009, *131,* 8746-8747
7. "A Microfluidic Apparatus for the Study of Ice Nucleation in Supercooled Water Drops", Stan, C. A., Schneider, G. F., Shevkoplyas, S. S., Hashimoto, M., Ibanescu, M., Wiley, B. J.,Whitesides, G. M., *Lab on a Chip,* 2009, *9,* 16, 2293-2305
8. "Folding of Electrostatically Charged Beads-on-a-String: An Experimental Realization of a Theoretical Model", Reches, M., Snyder, P. W.,Whitesides, G. M., *Proc. Natl. Acad. Sci. USA,* 2009, *106,* 42, 17644-17649 PMCID: PMC2764904
9. "Green Nanofabrication: Unconventional Approaches for the Conservation Use of Energy", Lipomi, D. J., Weiss, E.,Whitesides, G. M., *Nanotechnology for the Energy Challenge,* 2010, *ch. 10,* 231-280
10. "Formation of Bubbles in a Multi-section Flow-focusing Junctions", Hashimoto, M.,Whitesides, G. M., *Small,* 2010, *6,* 9, 1051-1059
11. "The Determination of the Location of Contact Electrification-Induced Discharge Events", Vella, S. J., Chen, X., Thomas, S. W., Zhao, X., Suo, Z.,Whitesides, G. M., *Journal of Physical Chemistry C,* 2010, *114,* 20885-20895
12. "Externally Applied Electric Fields up to $1.6x10^5$ V/m Do Not Affect the Homogenous Nucleation of Ice in Supercooled Water", Stan, C. A., Tang, S. K. Y., Bishop, K. J. M.,Whitesides, G. M., *Journal of Physical Chemistry B,* 2011, *115,* 1089-1097
13. "Chemistry and the Worm: *Caenorhabditis elegans* as a Platform for Integrating Chemical and Biological Research", Hulme, S. E.,Whitesides, G. M., *Angewandte Chemie International Edition,* 2011, *50,* 4774-4807
14. "Sheathless Hydrodynamic Positioning of Buoyant Drops and Bubbles inside Microchannels", Stan, C. A., Guglielmini, L., Ellerbee, A. K., Caviezel, D., Stone, H. A.,Whitesides, G. M., *Physical Review E,* in press 2011,

Multi-Responsive Polyelectrolyte Brush Interfaces:
Coupling of Brush Nanostructures and Interfacial Dynamics

PI: Y. Elaine Zhu
Department of Chemical and Biomolecular Engineering
182 Fitzpatrick Hall, University of Notre Dame,
Notre Dame, IN 46556
Email: yzhu3@nd.edu

Program Scope

The overall goal of this project is to understand and effectively control the dynamics of probe molecules, neutral or charged, at polyelectrolyte (PE) brush surfaces of tunable brush chain nanostructures and interfacial interactions under varied external stimuli. The long-term goal is to establish a new paradigm in molecular design of polyelectrolyte based multi-responsive polymer thin films for biolubrication, non-fouling coating, and efficient ion and molecular transport for energy storage and microfluidic applications. The experimental methods involve integrated single-molecule imaging and spectroscopic measurements in a microfluidic platform. The project also involves the expertise in the PI's group in polymer brush synthesis and surface modification to molecular design and synthesis of smooth and homogeneous polyelectrolyte thin films for single-molecule experiments.

Recent Progress

The focus of our latest activity is to manipulate and understand the conformational structure of polyelectrolytes in solution and at surface under external stimuli, including pH, added ions and applied ac-electric fields, which leads to the field-controlled macromolecular assembly and interfacial molecular transport.

In this project, we have examined the coil-to-globule conformational transition (CGT) and electric potential of a model weak PE, poly(2-vinyl pyridine) (P2VP) of varied molecular weight (Mn) in aqueous solutions at a single molecule level by fluorescence correlation spectroscopy (FCS) and photon counts histogram (PCH). Upon increasing solution pH, a CGT is evidently observed with P2VP and exhibits strong Mn-dependent characteristics as shown in Fig. 1: a gradual and continuous CGT at low Mn is in sharp contrast to the first-order and abrupt transition at high Mn, which agrees well with recent theoretical and computer simulation results. Decreased pH_{CGT} with increased P2VP Mn indicates an enlarged difference between local and bulk pH, suggesting overall stronger electric repulsion of local protons with longer P2VP chains in the

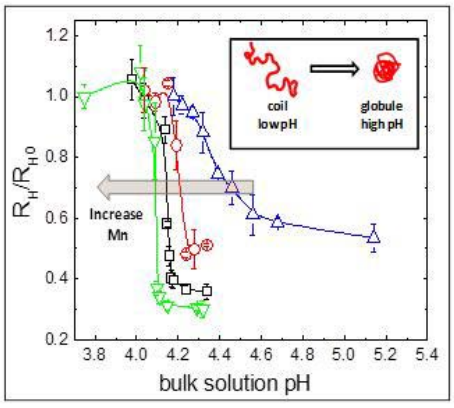

Fig.1. Mn-dependent CGT of a single weak P2VP chain in dilute aqueous solution: a gradual transition at low Mn versus a 1st-order transition at high Mn.

expanded coil conformation state. To further elucidate the effect of Mn on CGT and local electrostatic interaction, PCH is employed with pH-sensitive fluorophore probes attached to a P2VP chain to determine the local pH, *i.e.* the local proton concentration immediately adjacent to an expanded P2VP coil. The electric potential, φ for a P2VP chain is thereby estimated from the difference between local and bulk pHs, exhibiting a scaling with P2VP polymerization degree, N as $\varphi \sim N^{0.1}$. The increase in φ with increasing Mn suggests an enhanced electrostatic repulsion between local protons and a longer P2VP backbone, leading to the lowering of pH_{CGT}.

In further studies, we have strived for not only understanding the structural dynamics of P2VP chains in dilute solution, but also actively and effectively modifying their dynamic nanostructures of PE brushes under applied ac-filed to improve their functionality with optimized structures. Recently we have experimentally demonstrated that ac-electric fields over an ac-frequency range of 5 kH z-10 MHz can produce dynamically penetrating ionic currents to polarize the ions within the double layer around a P2VP chain and consequently induce the CGT of P2VPs in bulk aqueous solution at applied ac-field strength exceeding a cr itical value as shown in Fig. 2a-b. To further achieve a mechanistic understanding of the ac-field induced CGT in dilute PE solution, we have conducted a coarse-grained molecular dynamics simulation of a flexible PE chain in an explicit salt solution of varied valence under an ac-field. Our simulation results in Fig. 2c have found that a PE chain can breathe with applied ac-frequency and becomes dynamically stretched, only when applied field strength exceeds the critical field strength and applied ac-frequency is comparable to or less than the intrinsic relaxation frequency of the PE chain, which qualitatively agree with our experimental findings.

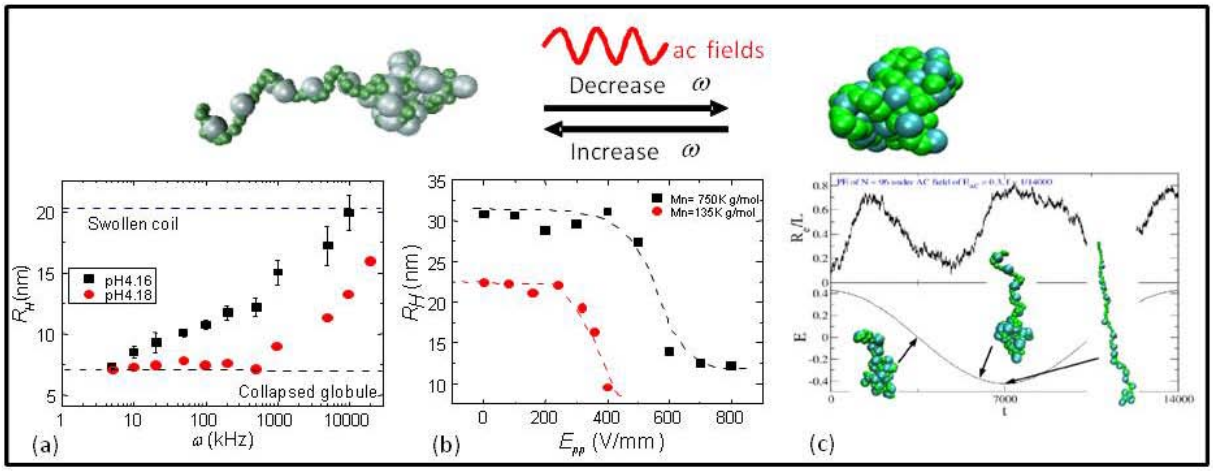

Fig.2. (a) Applied ac-electric field-induced gradual CGT of single P2VP chains in dilute aqueous solutions, showing a strong dependence of P2VP chain size on ac-frequency, when applied ac-field strength, E exceeds a critical value, E_r that is of Mn-dependence, as shown in (b). (c) MD simulation shows the breathing of a PE chain with applied ac-frequency at $E \geq Er$, which confirms our experimental observation in (a)-(b).

Other recent activities include:

- *Molecular surface diffusion on hard, soft and fluid surfaces.* We have investigated the surface diffusions of small fluorescent probe molecules hard, soft and fluid surfaces of distinct dynamic characteristics by FCS. It is surprising to find that the surface diffusion of probe molecule on neutral polymer brushes or fluid α-PC lipid bilayer appears much slower than on hard methyl-terminated monolayer, despite stronger interaction with hydrophobic monolayer, suggesting the coupling of thermal activated molecular hopping and interfacial dynamics of surface coating films. On neutral poly(N-isopropylacrylamide) (PNIPAM) brush surfaces, the coupling effect is further examined with PNIPAM brushes of varied brush thickness, h and grafting density, σ. At very low σ or very high h, surface inhomogeneity, which arises from polymer mushroom conformation and low polymer end-segment density, respectively, results in the slowing-down of interfacial dynamics of PNIPAM chains. The presence of optimal σ and h is detected to facilitate interfacial transport of small probe molecules at neutral polymer brush interface. Such optical brush structural parameters will be further examined with PE brushes in our future work.

- *Nanocolloidal interactions with lipid bilayers.* The interaction of semi-hydrophobic nanoparticles (NP) on supported lipid bilayers (SLBs) and resulting morphological re-organization of disrupted SLBs are investigated by combined fluorescence spectroscopy and imaging measurement. We have observed that *semi-hydrophobic* NPs can readily adsorbed on SLBs and drag lipids from SLBs to NP surfaces. Above a critical NP concentration, the disruption of SLBs is observed, accompanied with the formation and rapid growth of lipid-poor regions on NP-adsorbed SLBs. In the study of the effect of solution ionic strength on NP surface hydrophobicity and the growth of lipid-poor regions, we have concluded that the hydrophobic interaction enhanced by screened electrostatic interaction underlies the envelopment of NPs by lipids as illustrated in Fig. 3. The formation and growth of lipid-poor regions, or vaguely referred as "pores" or "holes", can be controlled by NP concentration, size and surface hydrophobicity, which is critical to design functional nanomaterials and filtration membranes of controllable pore size and transport selectivity.

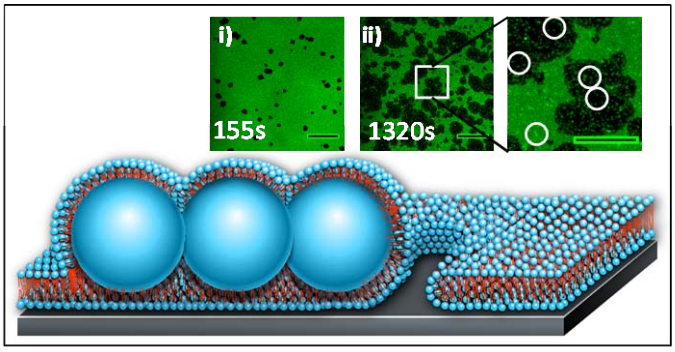

Fig.3. Schematic of the disruption and "pore" formation of SLBs by adsorbed NPs based on fluorescence microscopic observation of the morphology of SLBs in (i)-(ii).

Future plan:

This renewal project just started this year. The focus will be on investigating the conformational structure of P2VP chains grafted to a solid surface as well as the diffusion of probe molecules at P2VP brush interfaces. Specifically,

1) We will investigate the coupling of brush conformations and local counterion concentration of PE brushes of varied grafting density and thickness in response to solution pH and added salts. The shift of critical conformational transition pH of P2VP brushes will be examined against brush grafting density, and a scaling of P2VP brush thickness with grafting density at varied pH will be explored.

2) To actively tuning the nanostructures of weak PE brushes, microfluidic devices embedded with arrays of interdigitated microelectrodes will be designed and fabricated. With the application of ac-electric fields to P2VP brushes, the brush conformations and interfacial probe dynamics on P2VP brush thin films will be locally and dynamically controlled and examined.

3) Interfacial diffusive dynamics of single probe molecules on P2VP brushes will be studied by FCS. Both neutral and charged fluorescence probes will be selected, and their diffusive behaviors on P 2VP brushes of varied grafting density and thickness will be compared. The resulting *optimal brush structural* for efficient interfacial molecular transport will lead to the molecular design of PE thin films of tunable interfacial electrostatic interaction for superlubricious coatings or energy charge storage membranes

DoE sponsored publications in 2009-2011

1) S. Wang and Y. Zhu, Conformation transition and electric potential of single weak polyelectrolyte: Molecular weight dependence, *Soft Matter* 7, 7410-7415 (2011).

2) B. Jing and Y. Zhu, Disruption of supported lipid bilayers by semihydrophobic nanoparticles, *J. Am. Chem. Soc.* 133, 10983-10989 (2011).

3) V. E. Froude, J. I. Godfroy, S. Wang, H. Dombek and Y. Zhu, Anomalous dielectrophoresis of nanoparticles: A rapid and sensitive characterization by single-particle laser spectroscopy, *J. Phys. Chem. C* 114, 18880-18885 (2010).

4) S. Wang and Y. Zhu, Hysteretic conformational transition of single flexible polyelectrolyte under resonance ac-electric polarization, *Macromolecules,* 43, 7402-7405 (2010).

5) S. Wang and Y. Zhu, Molecular diffusion on surface-tethered polymer layers: coupling of molecular thermal fluctuation and polymer chain dynamics, *Soft Matter* 6, 4661-4665 (2010).

6) H. Liu, Y. Zhu and E. Maginn, Polyelectrolyte breathing under ac-electric fields, *Macromolecules* 43, 4805-4813 (2010).

7) L. Zhang and Y. Zhu, Dielectrophoresis of Janus particles under high frequency AC-electric fields. *Appl. Phys. Lett.* 96, 141902 (2010).

8) T. J. Politano, V. E. Froude and Y. Zhu, AC-electric field dependent electroformation of giant lipid vesicles, *Colloids & Surfaces B: Biointerfaces* 79, 75-82 (2010).

9) S. Wang and Y. Zhu, Facile method to prepare smooth and homogeneous polymer brush surfaces of varied brush thickness and grafting density, *Langmuir* 25, 13448-13455 (2009).

10) L. Zhang and Y. Zhu, Electrostatically tuned DNA adsorption on like-charged colloids and resultant colloidal clustering, *Soft Matter* 5, 4290-4296 (2009).

11) V. Froude and Y. Zhu, Dielectrophoresis of lipid unilamellar vesicles (liposomes) of contrasting surface constructs, *J. Phys. Chem. B* 113, 1552-1558 (2009).

INVITED TALKS

Phase Behavior and Self-Assembly in Polyelectrolyte Complexes

Matthew Tirrell
Institute for Molecular Engineering
University of Chicago and Argonne National Laboratory
Searle Chemistry Laboratory, Room 402
5735 South Ellis Avenue
Chicago, IL 60637

Highly charged polymers, natural or synthetic polyelectrolytes, and their assemblies, possess unique capabilities for structure determination and manipulation. Electrostatic interactions are among the most important non-covalent interactions employed in nature. They are very responsive to easily deployable signals (salt, pH). Charge-based interactions can drive macromolecular chains into either sparse, highly extended states (polyelectrolyte brushes at low ionic strength) or compact, dense states (globular proteins, complex coacervates or multi-valent ionic media). Even dense states remain highly hydrated, leading to high fluidity and facile ionic charge transport within them, and to useful properties such as ultralow interfacial tension with water and unusual underwater adhesiveness. The objective of our work is to create and study model systems that will enable the development of a fundamental understanding of the factors that govern self-assembly of ion-containing, multi-component polymers, and that produce a range of new and interesting properties. This talk will focus on observations and interpretations of coacervate phase behavior and their self-assembly into coatings, micelles and gels. A particular emphasis is placed on polypeptide-based materials, connecting observations in nature with phenomena observable in well-controlled synthetic polymers.

From Basic Science to Attempts at Combating Antibiotics

Ada Yonath

Department of Structural Biology, Weizmann Institute, Rehovot 76100, Israel

Ribosomes are the universal cellular machines that translate the genetic code into proteins. Composed of proteins and RNA, among which the RNA moieties perform almost all functional tasks, they posses spectacular architecture accompanied by inherent mobility that facilitate their smooth performance in decoding, peptide bond formation and nascent protein elongation. Of particular interest is the site of peptide bond formation, as it is located within a semi symmetric conserved region that seems to be a remnant of a prebiotic bonding apparatus that is still functioning in the contemporary ribosome.

Owing to their fundamental role, ribosomes are targeted by many antibiotics that paralyze the ribosomes by binding to their functional sites. Their binding modes, inhibitory action and synergism pathways, will be demonstrated. Issues concerning their ability to differentiate between patients and pathogens, and mechanism leading to bacterial resistance to antibiotics will be discussed.

Key words: ribosomes, antibiotics, resistance, synergism, selectivity, RNA

Poster Sessions

Biomolecular Materials
Principal Investigators' Meeting

Poster Session I

Monday, October 24, 3:30pm & 8:30pm

1. Toward Capturing Soft Molecular Material Dynamics
Paul Ashby, Lawrence Berkeley National Laboratory

2. Three Dimensional Ordering in Multicomponent Mixed Lipid Multilayers
Yicong Ma, Lobat Tayebi, Daryoosh Vashaee, Sunil K. Sinha, Atul N. Parikh, University of California, Davis

3. Program Bending Reveals Dynamic Mechanochemical Coupling in Phospholipid Bilayers
Sean Gilmore, Harika Nanduri, Atul N. Parikh, *University of California, Davis*

4. Dynamic Self-Assembly, Emergence, and Complexity
George Whitesides, Harvard University

5. Modeling the Dynamic Self-Assembly of Communicating Microcapsules
Anna Balazs, University of Pittsburgh

6. Uniform Optical Polymer Vesicles for Nanoparticle Release and Stress Sensing
Daniel Hammer, University of Pennsylvania

7. Self-Assembling Biological Springs: Force Transducers on the Micron and Nanoscale
Ying Wang and George Benedek, Massachusetts Institute of Technology

8. Dynamic Self-Assembly of Composite Nanomaterials
George Bachand, Sandia National Laboratories

9. Multicomponent Protein Cage Architectures for Photocatalysis
Peter E. Prevelige and Arunava Gupta, University of Alabama

10. Self-Assembly and Self-Repair of Novel Photovoltaic Complexes--Synthetic Analogs of Natural Processes
*Michael S. Strano***,** *Massachusetts Institute of Technology*

11. A Kinetic Monte Carlo Analysis for the Production of Singularly Tethered Carbon Nanotubes
Andrew J. Hilmer, Nitish Nair, and Michael S. Strano, Massachusetts Institute of Technology

12. Biomimetic Light-Harvesting Complexes Capable of Autonomous Regeneration
Ardemis Boghossian and Michael S. Strano, Massachusetts Institute of Technology

13. Exploring the Interface between Single-Walled Carbon Nanotubes and Silica Nanocomposite Materials
Gautam G. Gupta, Juan Duque, Stephen K. Doorn and Andrew M. Dattelbaum, Los Alamos National Laboratory

14. Electroactive Liquid-Crystalline Polymers for Constructing Bioelectronic Interfaces
Sungwon Lee, Scott M. Brombosz, Millicent A. Firestone, Argonne National Laboratory

15. Repairable Artificial Cell Architectures
Scott M. Brombosz, Millicent A. Firestone, Argonne National Laboratory

16. Molecular Nanocomposites: Biotic/Abiotic Interfaces, Materials, and Architectures
Bryan Kaehr, C. Jeffrey Brinker, Jason Townson, Eric C. Carnes, and Carlee Ashley, Sandia National Laboratories and University of New Mexico

17. Graphene Directed Nucleation and Self-Assembly
Jun Liu, Pacific Northwest National Laboratory

18. Building Metamaterials Bottom-Up with Biological Templates
Marit Nilsen-Hamilton, Ames Laboratory

19. Quaternary Structure and Functional Studies of Mms6: A Biomineralization Protein that Promotes the Formation of Magnetic Nanoparticles
Lijun Wang, Shuren Feng, Tanya Prozorov, Pierre E. Palo, Xunpei Liu, Bruce Fulton, David Vaknin, Ruslan Prozorov, Surya Mallapragada and Marit Nilsen-Hamilton, Ames Laboratory

20. Controlled Synthesis of Platinum Nanostructures from Biomolecules and Polymers
Jennifer Cha, University of California, San Diego

21. Towards the Direct Visualization of In-Situ Bio-templated Magnetic Particle Formation
Tanya Prozorov, Ames Laboratory

22. Nanobioelectronic Devices with Light-Harvesting Protein Channels
R. Tunuguntla, K. Kim, M. Bangar, C. Grigoropoulos, P. Stroeve, C. Ajo-Franklin, A. Noy, University of California, Merced, and Lawrence Berkeley Laboratory

23. Organization of Photoactive Virus-DNA Heterostructures Using Nanoscale Templates
Debin Wang, Jolene Lau, Stacy Capehart, Suchetan Pal, Minghui Liu, Hao Yan, Matthew B. Francis, James J. De Yoreo, Lawrence Berkeley Laboratory

Biomolecular Materials
Principal Investigators' Meeting

Poster Session 2

Tuesday, October 25, 3:30pm & 8:30pm

1. Kinetically Controlled Catalytic Synthesis of Nanocomposite Anodes and Cathodes for High-Power Lithium Ion Batteries
Hong-Li Zhang and Daniel E. Morse, University of California, Santa Barbara

2. Cooperative Binary Ionic Solids, Nanostructures, and Nanocomposites for Solar Hydrogen Evolution
John Shelnutt, Sandia National Laboratories

3. Tailored Structure-Property Relationships of Novel Conjugated Polymers and Their Assemblies
H.H. Tsai, C.C. Wang, Y. Gao, D. Williams, A. Dattelbaum, A.P. Shreve, L. Wang, Z. Zhu, M. Cotlet, H.-L. Wang, Los Alamos National Laboratory

4. Development and Characterization of Fluorescent Noble Metal Nanoclusters
H. Yoo, M.L. Neidig, S. Sinha, A.P. Shreve, J.S. Martinez, Los Alamos National Laboratory

5. PPV Organization in Membrane Assemblies
F. Zendejas, M.A.A. Sanchez, P. Narasimmaraj, S. Iyer, H.-L. Wang, A. Shreve, S. Gilmore, A. Parikh, D. Sasaki, Los Alamos National Laboratory

6. Interfacial Control of Membrane Organization
D. Bricarello, S. Gilmore, A. Oliver, V. Ngassam, J. Brozik, M. Howland, B. Sanii, D. Sasaki, A.P. Shreve, A.N. Parikh, Los Alamos National Laboratory

7. Lipid-Mediated Assembly of Icosahedral Viruses at Liquid Interfaces
Masafumi Fukuto and Ben Ocko, Brookhaven National Laboratory

8. Mechanics of 2-D Clathrin Assembly
Jules VanDersarl, Shafigh Mehraeen, Alia Schoen, Sarah Heilshorn, Andrew Spakowitz, and Nick Melosh, SLAC National Accelerator Laboratory

9. Self-Assembly on Fluctuating Membranes and Interfaces
Andy Spakowitz, SLAC National Accelerator Laboratory

10. Clathrin Self-Assembled Biotemplates
Alia Schoen and Sarah Heilshorn, SLAC National Accelerator Laboratory

11. Shaken Not Stirred: New Mechanisms for the Production of 2D Nanomaterials
Ron Zuckermann, Lawrence Berkeley Laboratory

12. RNA-Mediated Assembly of Nanoscale Photocatalysts
Jessica Rouge, Bruce Eaton and Daniel Feldheim, University of Colorado

13. Regular and Irregular Polyhedral Ionic Shells
Monica Olvera de la Cruz, Northwestern University

14. Membranes and Cell-Like Microcapsules through Hierarchical Self-Assembly
Samuel Stupp, Northwestern University

15. Nanomaterial Synthesis with Catalytic Peptides Discovered by New Combinatorial Phage Display Approach and Programmed Nanomaterial Assemblies in Large-Scale 3D Structure
Hiroshi Matsui, CUNY, Hunter College

16. Simulations of Self-Assembly of Tethered Nanoparticle Shape Amphiphiles
Sharon Glotzer, University of Michigan

17. Supramolecular Assembly to Dynamic Materials
Zhibin Guan, University of California, Irvine

18. Multi-responsive Polymeric Interfaces for Controlled Surface Diffusion and Supramolecular Assembly
Y. Elaine Zhu, University of Notre Dame

19. Bio-inspired Design of Hydrogel-Actuated Integrated Responsive Systems (HAIRS) for Dynamic and Multi-functional Materials
Philseok Kim, Lauren Zarzar, Joanna Aizenberg, Harvard University

20. Optimizing Immobilized Enzyme Performance in Cell-Free Environments to Produce Liquid Fuels
Joseph J. Grimaldi, Cynthia H. Collins and Georges Belfort, Rensselaer Polytechnic Institute

Author Index and List of Participants

Author Index

Participant List

Last Name	First Name	Organization	E-Mail Address
Abbott	Nicholas	University of Wisconsin-Madison	abbott@engr.wisc.edu
Aizenberg	Joanna	Harvard University	jaiz@seas.harvard.edu
Aronson	Igor	Argonne National Laboratory	aronson@anl.gov
Ashby	Paul	Molecular Foundry, Lawrence Berkeley National Laboratory	pdashby@lbl.gov
Bachand	George	Sandia National Laboratories	gdbacha@sandia.gov
Bai	Ying (Richard)	Lehigh University	yib308@lehigh.edu
Balazs	Anna	University of Pittsburgh	balazs@pitt.edu
Baldo	Marc	Massachusetts Institute of Technology	baldo@mit.edu
Bangar	Mangesh	Molecular Foundry, Lawrence Berkeley National Laboratory	mabangar@lbl.gov
Belfort	Georges	Rensselaer Polytechnic Institute	belfog@rpi.edu
Boghossian	Arde	Massachusetts Institute of Technology	arde@mit.edu
Bouxsein	Nathan	Sandia National Laboratories	nfbouxs@sandia.gov
Braatz	Richard	Massachusetts Institute of Technology	braatz@mit.edu
Brinker	C. Jeffrey	Sandia National Laboratories	cjbrink@sandia.gov
Brombosz	Scott	Argonne National Laboratory	sbrombosz@anl.gov
Bunker	Bruce	Sandia National Laboratories	bcbunke@sandia.gov
Cha	Jennifer	University of California, San Diego	jencha@ucsd.edu
Christen	Hans	Oak Ridge National Laboratory	christenhm@ornl.gov
Crockett	Teresa	DOE, Basic Energy Sciences	teresa.crockett@science.doe.gov
Cui	Honggang	Johns Hopkins University	hcui6@jhu.edu
Dattelbaum	Andrew	Los Alamos National Laboratory	amdattel@lanl.gov
de Pablo	Juan	University of Wisconsin-Madison	depablo@engr.wisc.edu
De Yoreo	Jim	Lawrence Berkeley National Laboratory	jjdeyoreo@lbl.gov
Doniach	Sebastian	Stanford University	sxdwc@slac.stanford.edu
Douglas	Trevor	Montana State University	tdouglas@chemistry.montana.edu
Dutton	P. Leslie	University of Pennsylvania	dutton@mail.med.upenn.edu
Erickson	David	Cornell University	de54@cornell.edu
Eriksson	Mark	University of Wisconsin-Madison	maeriksson@wisc.edu
Evans	John	New York University	jse1@nyu.edu
Feldheim	Dan	University of Colorado	Daniel.Feldheim@Colorado.edu
Firestone	Millicent	Argonne National Laboratory	firestone@anl.gov
Francis	Matthew	Lawrence Berkeley National Laboratory	francis@cchem.berkeley.edu
Fukuto	Masafumi	DOE, Basic Energy Sciences	fukuto@bnl.gov
Gersten	Bonnie	Brookhaven National Laboratory	Bonnie.Gersten@science.doe.gov
Gewirth	Andrew	University of Illinois	agewirth@illinois.edu
Ghosh	Sajal Kumar	University of California, San Diego	skghosh@physics.ucsd.edu
Gilmer	George	Lawrence Livermore National Laboratory / Colorado School of Mines	gilmer1@llnl.gov

Gilmore	Sean	University of California, Davis	sfgilmore@ucdavis.edu
Glotzer	Sharon	University of Michigan	sglotzer@umich.edu
Golbeck	John	The Pennsylvania State University	jhg5@psu.edu
Gopalan	Padma	University of Wisconsin-Madison	pgopalan@wisc.edu
Gough	Dara	Sandia National Laboratories	dgough@sandia.gov
Granick	Steve	University of Illinois	sgranick@uiuc.edu
Grimaldi	Joseph	Rensselaer Polytechnic Institute	grimaj@rpi.edu
Guan	Zhibin	University of California, Irvine	zguan@uci.edu
Guo	Hongyu	University of California, San Diego	hguo@physics.ucsd.edu
Gupta	Arunava	University of Alabama	agupta@mint.ua.edu
Hammer	Daniel	University of Pennsylvania	hammer@seas.upenn.edu
Heilshorn	Sarah	Stanford University / SLAC	heilshorn@stanford.edu
Hilmer	Andrew	Massachusetts Institute of Technology	ahilmer@mit.edu
Horton	Linda	DOE, Basic Energy Sciences	linda.horton@science.doe.gov
Huber	Dale	Sandia National Laboratories	dlhuber@sandia.gov
Hui	Chung Yuen	Cornell University	ch45@cornell.edu
Jagota	Anand	Lehigh University	anj6@lehigh.edu
Kaehr	Bryan	Sandia National Laboratories	bjkaehr@sandia.gov
Kane	Ravindra	Rensselaer Polytechnic Institute	kaner@rpi.edu
Kim	Kyunghoon	Molecular Foundry, Lawrence Berkeley National Laboratory	kenkim@berkeley.edu
Kim	Philseok	Wyss Institute/Harvard University	philseok.kim@wyss.harvard.edu
Kini	Aravinda	DOE, Basic Energy Sciences	a.kini@science.doe.gov
Kröger	Nils	Georgia Institute of Technology	nils.kroger@chemistry.gatech.edu
Kuksenok	Olga	University of Pittsburgh	olk2@pitt.edu
Kumar	Sanat	Columbia University	sk2794@columbia.edu
Lau	Jolene	Lawrence Berkeley National Laboratory	jllau@lbl.gov
Lee	Sungwon	Argonne National Laboratory	sungwonlee@anl.gov
Liu	Jun	Pacific Northwest National Laboratory	jun.liu@pnnl.gov
Mallapragada	Surya	Ames Laboratory	suryakm@iastate.edu
Markowitz	Michael	DOE, Basic Energy Sciences	mike.markowitz@science.doe.gov
Martinez	Jennifer	Los Alamos National Laboratory	jenm@lanl.gov
Matsui	Hiroshi	City University of New York - Hunter College	hmatsui@hunter.cuny.edu
Melosh	Nick	Stanford Institute for Materials & Energy Science (SIMES)	nmelosh@stanford.edu
Morse	Daniel	University of California, Santa Barbara	d_morse@lifesci.ucsb.edu
Nilsen-Hamilton	Marit	Ames Laboratory	marit@iastate.edu
Noy	Aleksandr	University of California, Merced	anoy@ucmerced.edu
Ocko	Ben	Brookhaven National Laboratory	ocko@bnl.gov
Olvera de la Cruz	Monica	Northwestern University	m-olvera@northwestern.edu
Parikh	Atul	University of California, Davis	anparikh@ucdavis.edu
Prevelige	Peter	University of Alabama, Birmingham	prevelig@uab.edu
Prozorov	Tatiana	Ames Laboratory	tprozoro@ameslab.gov
Radhakrishna	Mithun	Columbia University	mr2972@columbia.edu

Rana	Subinoy	University of Massachusetts, Amherst	srana@chem.umass.edu
Rotello	Vincent	University of Massachusetts, Amherst	rotello@chem.umass.edu
Rouge	Jessica	University of California	jessica.rouge@colorado.edu
Safinya	Cyrus	University of California, Santa Barbara	safinya@mrl.ucsb.edu
Sandhage	Ken	Georgia Institute of Technology	ken.sandhage@mse.gatech.edu
Saraf	Ravi	University of Nebraska-Lincoln	rsaraf2@unl.edu
Sasaki	Darryl	Sandia National Laboratories	dysasak@sandia.gov
Schaffer	David	University of California, Berkeley	schaffer@berkeley.edu
Schmidt-Rohr	Klaus	Ames Laboratory	srohr@iastate.edu
Schoen	Alia	Stanford University	aliapm@stanford.edu
Selloni	Annabella	Princeton University	aselloni@princeton.edu
Sennett	Michael	DOE, Basic Energy Sciences	michael.sennett@science.doe.gov
Shelnutt	John	Sandia National Laboratories	jasheln@unm.edu
Shreve	Andrew	Los Alamos National Laboratory	shreve@lanl.gov
Sinha	Sunil	University of California, San Diego	ssinha@physics.ucsd.edu
Sit	Hoi Land	Princeton University	hsit@princeton.edu
Sknepnek	Rastko	Northwestern University	r-sknepnek@northwestern.edu
Snezhko	Alexey	Argonne National Laboratory	snezhko@anl.gov
Spakowitz	Andrew	Stanford University	ajspakow@stanford.edu
Spoerke	Erik	Sandia National Laboratories	edspoer@sandia.gov
Strano	Michael	Massachusetts Institute of Technology	strano@mit.edu
Stupp	Samuel	Northwestern University	s-stupp@northwestern.edu
Subramani	Chandra	University of Massachusetts, Amherst	csubrama@chem.umass.edu
Swartz	James	Stanford University	jswartz@stanford.edu
Talley	Lee-Ann	Oak Ridge Institute for Science and Education	lee-ann.talley@orise.orau.gov
Tezcan	F. Akif	University of California, San Diego	tezcan@ucsd.edu
Thiyagarajan	Pappannan	DOE, Basic Energy Sciences	P.Thiyagarajan@science.doe.gov
Tirrell	Matthew	University of Chicago	mtirrell@uchicago.edu
Tovar	John	Johns Hopkins University	tovar@jhu.edu
Travesset	Alex	Ames Laboratory / Iowa State University	trvsst@ameslab.gov
van Buuren	Anthony	Lawrence Livermore National Laboratory	vanbuuren1@llnl.gov
Van Voorhis	Troy	Massachusetts Institute of Technology	tvan@mit.edu
Velichko	Yuri	Northwestern University	y-velichko@northwestern.edu
Voigt	James	Sandia National Laboratories	javoigt@sandia.gov
Wang	Debin	Lawrence Berkeley National Laboratory	debinwang@lbl.gov
Wang	Hsing-Lin	Los Alamos National Laboratory	hwang@lanl.gov
Wang	Lijun	Ames Laboratory	wlj@iastate.edu
Wang	Ying	Massachusetts Institute of Technology	ywang09@mit.edu
Whitesides	George	Harvard University	gwhitesides@gmwgroup.harvard.edu
Yonath	Ada	Weizmann Institute of Science	ada.yonath@weizmann.ac.il
Zhu	Yingxi	University of Notre Dame	yzhu3@nd.edu
Zuckermann	Ronald	Lawrence Berkeley National Laboratory	rnzuckermann@lbl.gov